

Appendices for Determining Pavement Design Criteria for Recycled Aggregate Base and Large Stone Subbase



NRRA GEOTECHNICAL TEAM

Authors: Bora Cetin (Michigan State University), Haluk Sinan Coban (Michigan State University), Tuncer B. Edil (University of Wisconsin-Madison), Halil Ceylan (Iowa State University), William Likos (University of Wisconsin-Madison), Junxing Zheng (Iowa State University), Ashley Buss (Iowa State University)

A pooled fund project administered by the Minnesota Department of Transportation

Report No. NRRA202103A

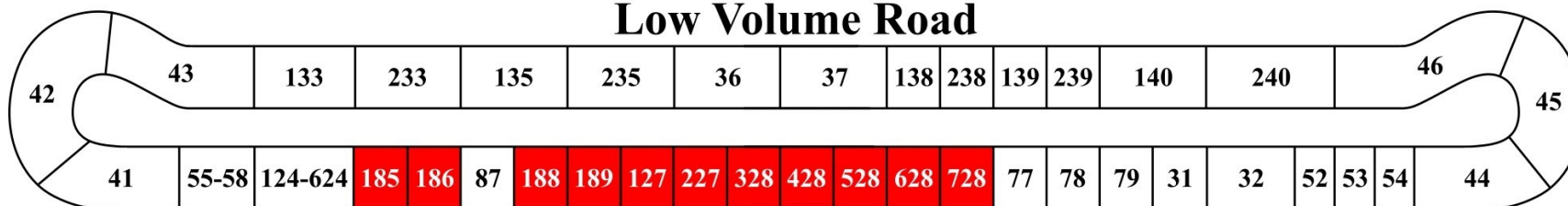
APPENDICES

APPENDIX A

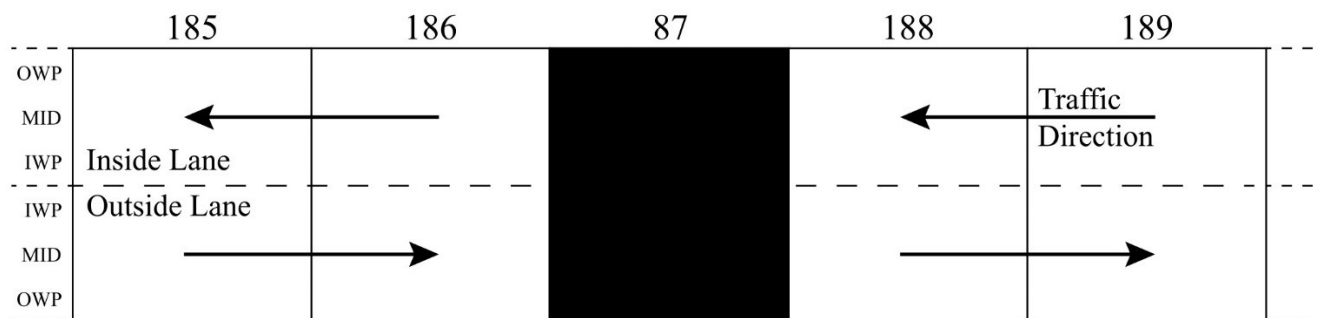
TEST CELLS ON MINNESOTA ROAD RESEARCH PROJECT (MNROAD) LOW VOLUME ROAD (LVR) AND ROAD LANES

MnROAD

Low Volume Road



NOTE: Test cells shown in red are related to this project.

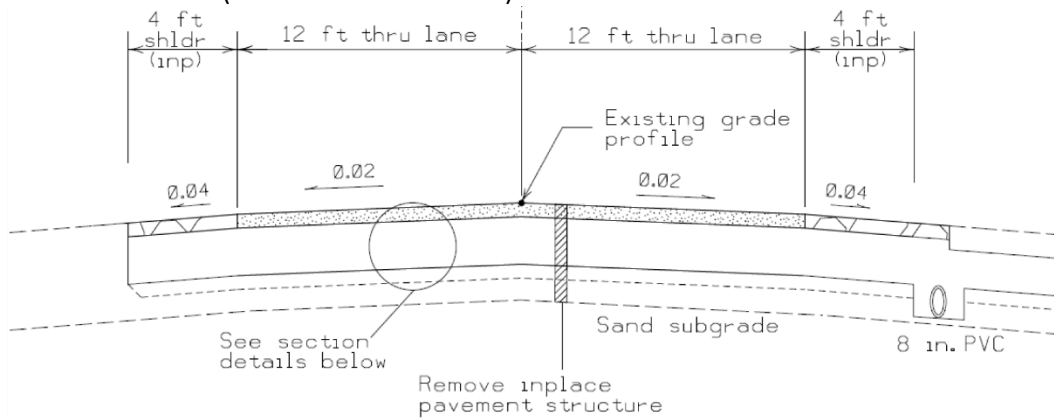


NOTE: OWP: outer wheel path, MID: midline, IWP: inner wheel path

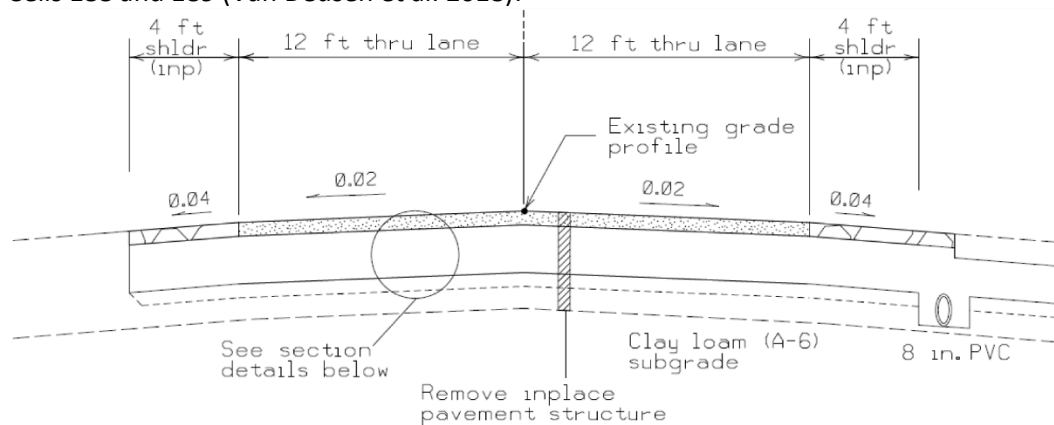
APPENDIX B

CROSS-SECTIONAL ELEMENTS OF TEST CELLS

Cells 185 and 186 (Van Deusen et al. 2018):

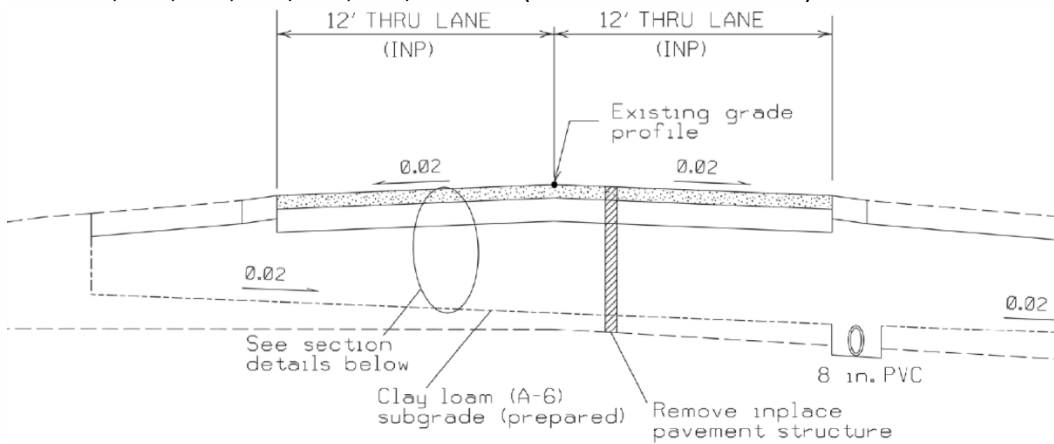


Cells 188 and 189 (Van Deusen et al. 2018):



Recycled Aggregate Base (RAB) Group			
185	186	188	189
3.5 in Asphalt	3.5 in Asphalt	3.5 in Asphalt	3.5 in Asphalt
12 in Coarse RCA	12 in Fine RCA	12 in Limestone	12 in RCA+RAP
3.5 in S. Granular Borrow	3.5 in S. Granular Borrow	3.5 in S. Granular Borrow	3.5 in S. Granular Borrow
Sand	Sand	Clay Loam	Clay Loam

Cells 127, 227, 328, 428, 528, 628, and 728 (Van Deusen et al. 2018):



Large Stone Subbase (LSSB) Group		LSSB with Geosynthetics Group				
127	227	328	428	528	628	728
3.5 in Asphalt	3.5 in Asphalt	3.5 in Asphalt	3.5 in Asphalt	3.5 in Asphalt	3.5 in Asphalt	3.5 in Asphalt
6 in Class 6 Aggregate	6 in Class 6 Aggregate	6 in Class 5Q Aggregate	6 in Class 5Q Aggregate	6 in Class 5Q Aggregate	6 in Class 5Q Aggregate	6 in Class 5Q Aggregate
18 in LSSB	18 in LSSB	9 in LSSB	9 in LSSB	9 in LSSB	9 in LSSB	9 in LSSB
		TX	TX+GT	BX+GT	BX	
		Clay Loam	Clay Loam	Clay Loam	Clay Loam	Clay Loam
Clay Loam	Clay Loam					

APPENDIX C

START AND END STATIONS OF TEST CELLS

	Cell Number	Position	Station	Length (ft)
Recycled Aggregate Base (RAB) Group	185	Start	16368	201
		End	16569	
	186	Start	16619	201
		End	16820	
	188	Start	17046	201
		End	17247	
	189	Start	17297	200
		End	17497	
Large Stone Subbase (LSSB) Group	127	Start	17498	258
		End	17756	
	227	Start	17805	260
		End	18065	
LSSB with Geosynthetics Group	328	Start	18065	109
		End	18174	
	428	Start	18174	109
		End	18283	
	528	Start	18283	108
		End	18391	
	628	Start	18391	113
		End	18504	
	728	Start	18504	131
		End	18635	

APPENDIX D

CONSTRUCTION TIMELINE OF TEST CELLS

Cells 185, 186, 188, and 189 (Van Deusen et al. 2018):

Activity \ Date	June				July					August				September			
	5	12	19	26	3	10	17	24	31	7	14	21	28	4	11	18	25
Erosion Control	X																
Strip Topsoil																	
Pavement Removal		X	X			X											
Common Excavation						X	X										
Subsurface Drain							X										
Place Conduits and Handholes							X										
Place Risers and Sensors							X			X							
Place Aggregate Base									X								
HMA Paving												X				X	

Cells 127, 227, 128, 228, 328, 428, 528, 628, 728 (Van Deusen et al. 2018):

Activity \ Date	June				July					August				September			
	5	12	19	26	3	10	17	24	31	7	14	21	28	4	11	18	25
Erosion Control	X																
Strip Topsoil							X										
Pavement Removal							X										
Common Excavation								X	X	X							
Subsurface Drain										X							
Place Conduits and Handholes																	
Subgrade Preparation											X						
Place Large Aggregate Subbase											X						
Place Risers and Sensors																	
Place Aggregate Base											X						
HMA Paving												X					
Remove Failed Cells (128-228)													X				
Reconstruct Cells (328-628)													X	X			
Final HMA Paving																X	

NOTE: Cells 128 and 228 failed and Cells 328, 428, 528, and 628 were reconstructed in place of them.
Cell 728 is a remnant from Cell 228.

Construction Dates of Each Cell (Van Deusen et al. 2018):

Cell Number \ Layer	Subgrade	Base	HMA (1st Layer)	HMA (2nd Layer)
185	7/14/2017	8/10/2017	8/21/2017	9/19/2017
186				
188				
189				
127	8/15/2017	8/19/2017	8/21/2017	9/19/2017
227				
128 (Failed)				
228 (Failed)				
328 (Reconst.)	8/28/2017	8/31/2017	9/19/2017	9/19/2017
428 (Reconst.)				
528 (Reconst.)				
628 (Reconst.)				
728 (Remnant)	8/15/2017	8/19/2017	8/21/2017	9/19/2017

NOTE: Cells 128 and 228 failed and Cells 328, 428, 528, and 628 were reconstructed in place of them.
Cell 728 is a remnant from Cell 228.

APPENDIX E

CONSTRUCTION OF CELLS 128 (9-IN LSSB) AND 228 (9-IN LSSB)

Rutting on LSSB layer and subgrade soil pumping under construction traffic (White and Vennapusa 2017):



Rutting on LSSB layer and subgrade soil pumping under construction traffic (White and Vennapusa 2017):



Aggregate base layer rutting (White and Vennapusa 2017):



APPENDIX F

GEOSYNTHETICS AND CONSTRUCTION OF CELLS 328 (9-IN LSSB - TX), 428 (9-IN LSSB - TX+GT), 528 (9-IN LSSB - BX+GT), AND 628 (9-IN LSSB - BX)

Properties of geosynthetics (as reported by manufacturers)

Geosynthetic Type	Property	Test Method	Values
Tensor TriAx TX190L (Triaxial Geogrid)	Rib Pitch ^{a, b}	NA	2.4 in (60 mm)
	Junction Efficiency ^c	ASTM D7737	93%
	Isotropic Stiffness Ratio ^d	NA	0.6
	Radial Stiffness at 0.5% Strain	ASTM D6637	23,989 lb/ft (350 kN/m)
Tensor BX1300 (Biaxial Geogrid)	Aperture Dimensions ^{a, e}	NA	1.8 in (46 mm)
	Minimum Rib Thickness ^{a, e}	NA	0.05 in (1.27 mm)
	Tensile Strength at 5% Strain ^e	ASTM D6637	720 lb/ft (10.5 kN/m)
	Ultimate Tensile Strength ^e	ASTM D6637	1,100 lb/ft (16 kN/m)
SKAPS GT-116 (Needle-Punched Nonwoven Geotextile)	Junction Efficiency ^c	ASTM D7737	93%
	Grab Tensile Strength	ASTM D4632	380 lb (1.690 kN)
	Grab Elongation	ASTM D4632	50%
	Trapezoid Tear Strength	ASTM D4533	145 lb (0.644 kN)
	CBR Puncture Resistance	ASTM D6241	1,080 lb (4.804 kN)
	Permittivity ^f	ASTM D4491	0.7 sec ⁻¹
	Apparent Opening Size ^{f, g}	ASTM D4751	0.0059 in (0.150 mm)

NOTE: NA = not available.

^aNominal dimensions

^bLongitudinal and diagonal

^cLoad transfer capability expressed as a percentage of ultimate tensile strength

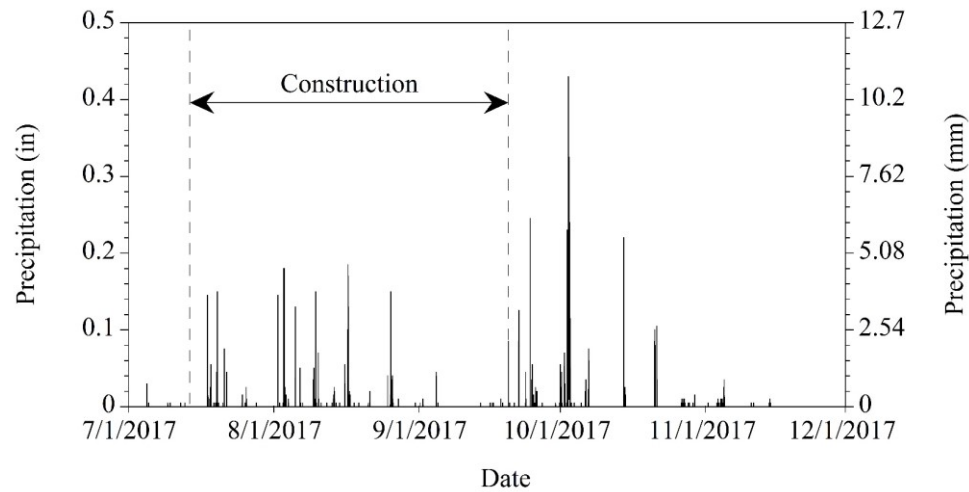
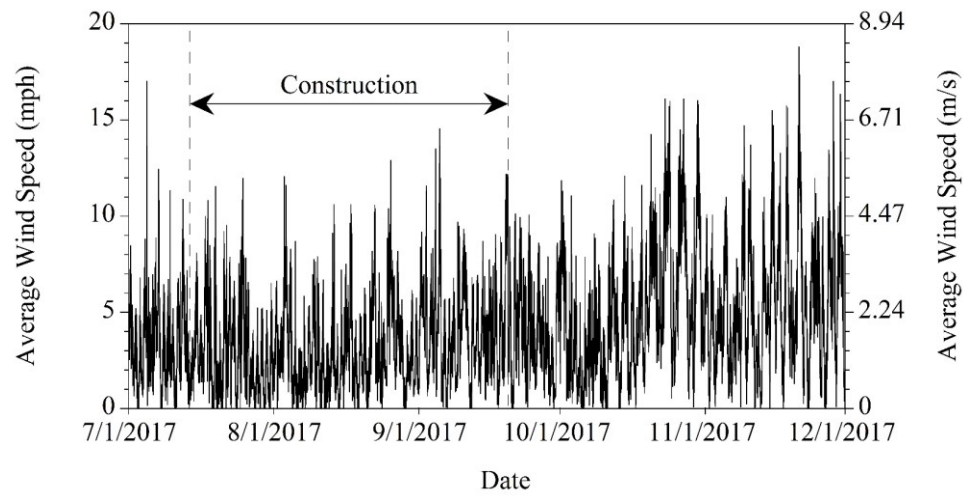
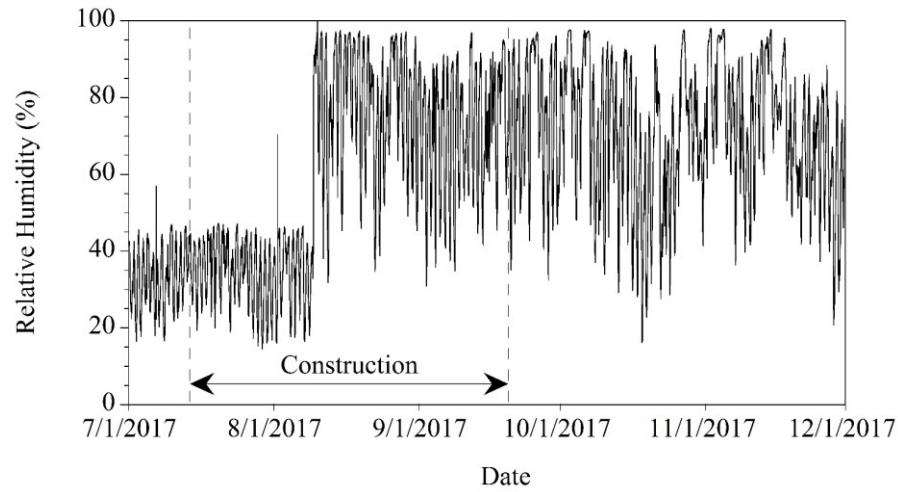
^dRatio between the minimum and maximum radial stiffness values at 0.5% strain

^eMachine direction

^fAt time of manufacturing. Results may change after handling.

^gMinimum average roll value.

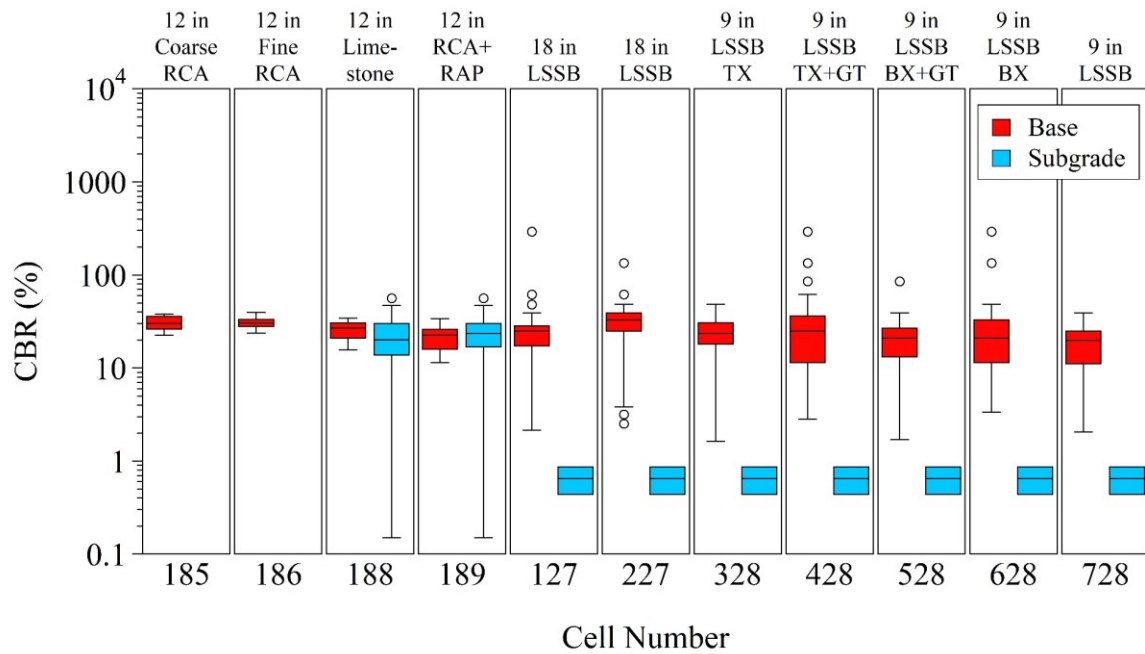
APPENDIX G
RELATIVE HUMIDITY, AVERAGE WIND SPEED, AND
PRECIPITATION DATA DURING AND SHORTLY AFTER
CONSTRUCTION



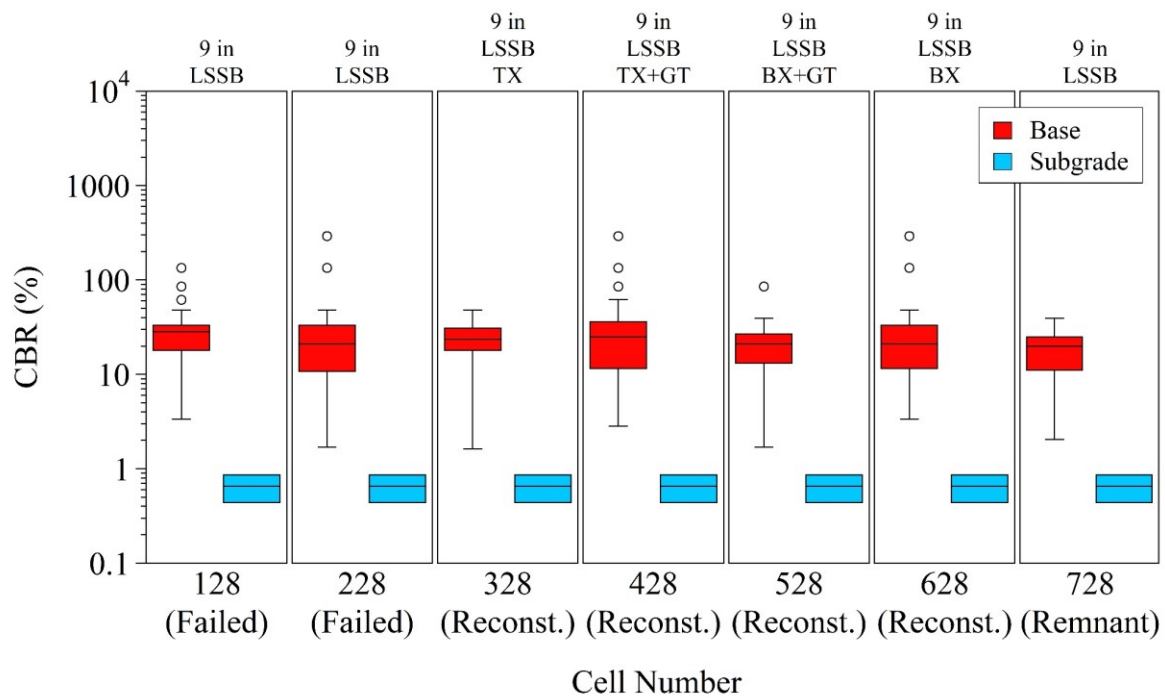
APPENDIX H

CALIFORNIA BEARING RATIO (CBR) VALUES ESTIMATED FROM DYNAMIC CONE PENETRATION (DCP) TEST DATA

CBR values of all test cells:



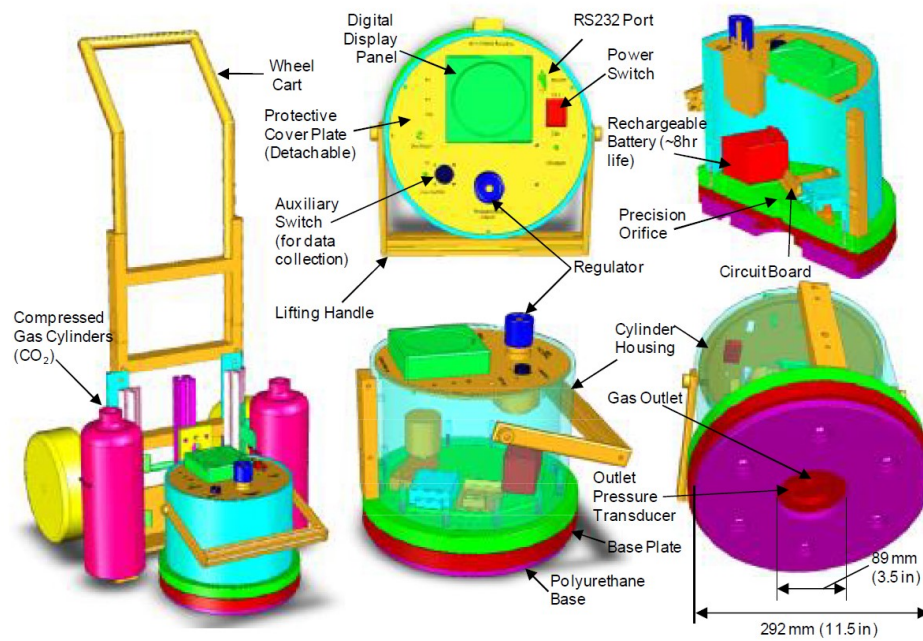
CBR values of failed (Cells 128 and 228) and reconstructed (Cells 328 to 628) test cells:



APPENDIX I

GAS PERMEAMETER TEST (GPT) EQUIPMENT AND TEST SURFACE TEXTURES

GPT equipment (White et al. 2010):



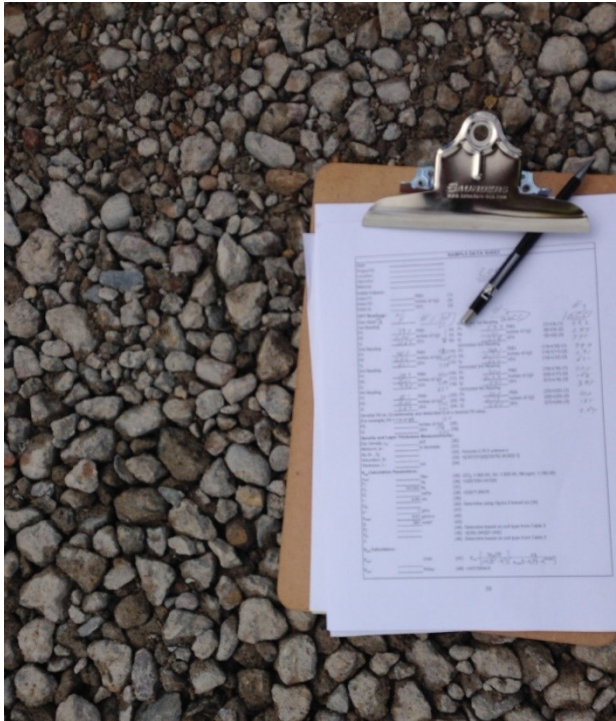
Fine surface texture



Medium surface texture



Coarse surface texture



APPENDIX J

INTELLIGENT COMPACTION (IC) AND ITS CALIBRATION

APLT test system at the MnROAD LVR (White and Vennapusa 2017):



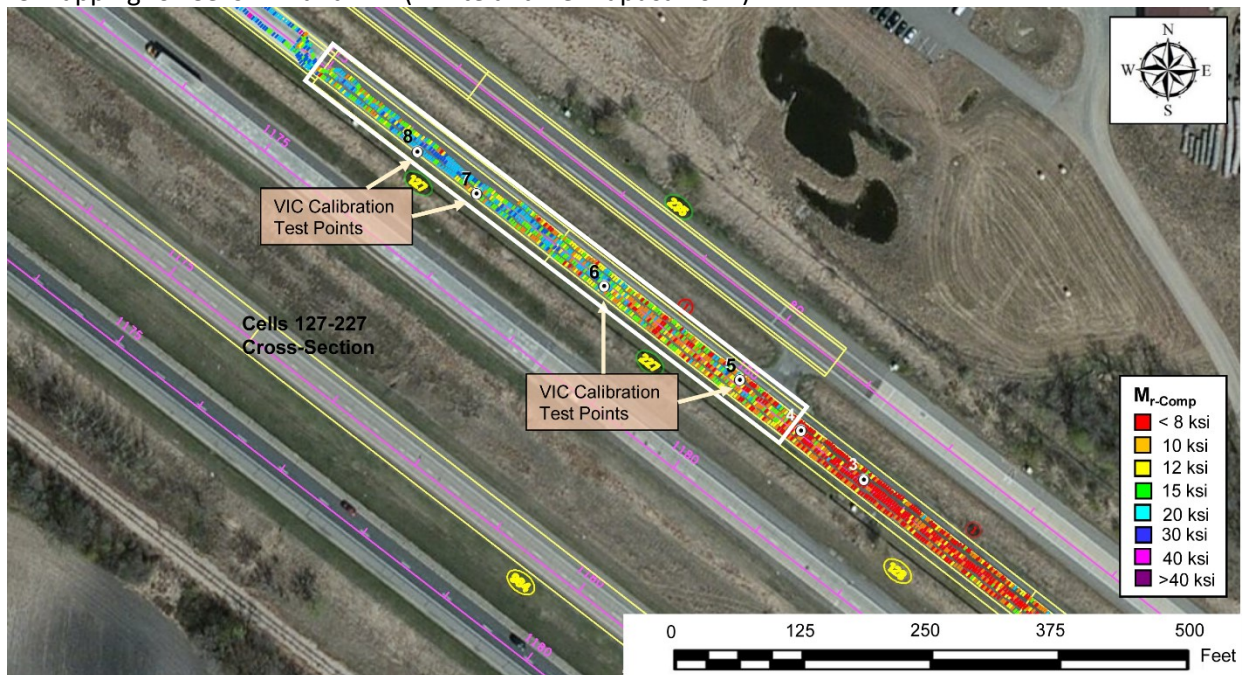
APLT test setup and deflection basin measurement kit with center plate (White and Vennapusa 2017):



Caterpillar CS56 vibratory smooth drum roller outfitted with Ingios VIC system and RTK-GPS (White and Vennapusa 2017):



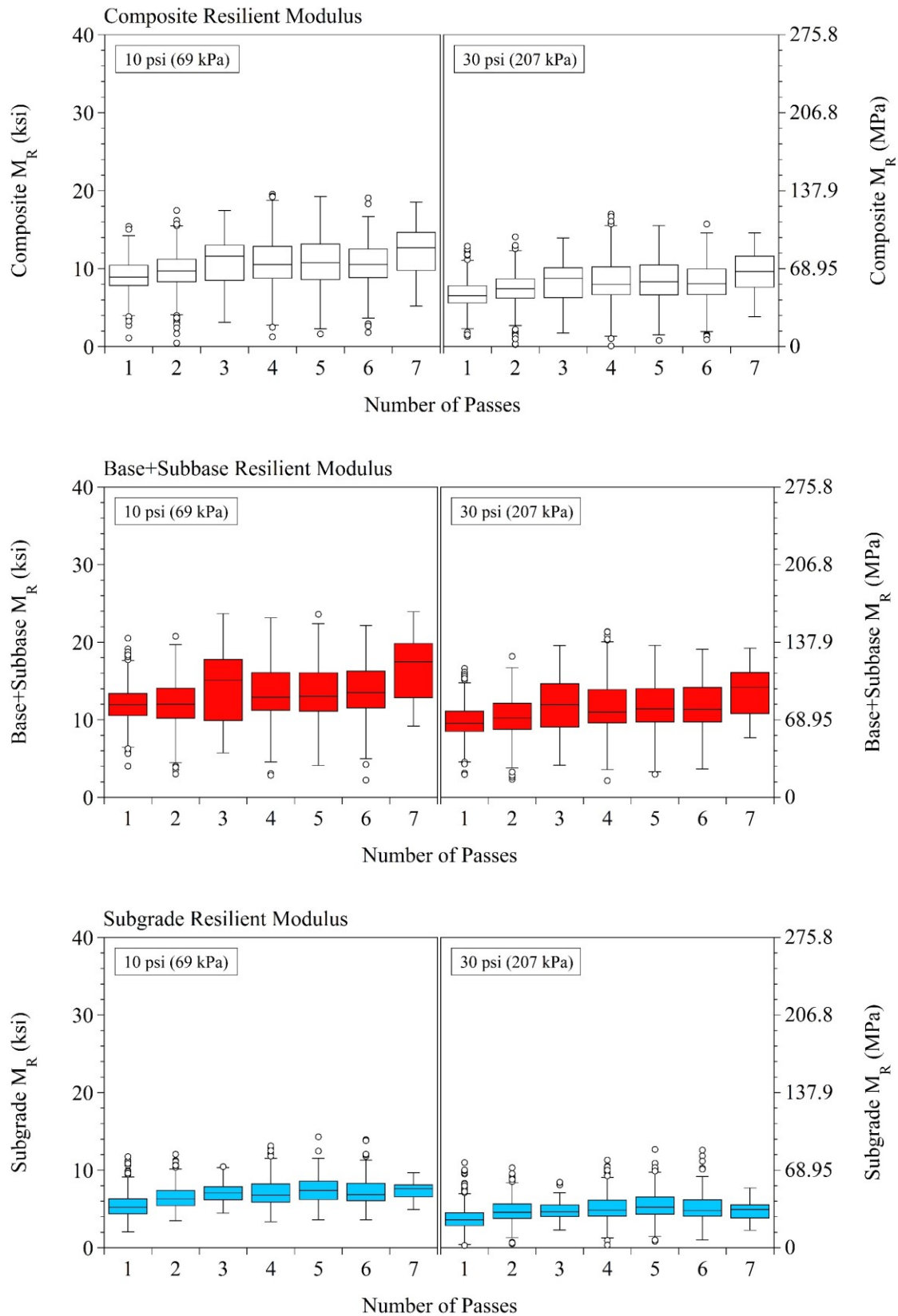
IC mapping for Cells 127 and 227 (White and Vennapusa 2017):



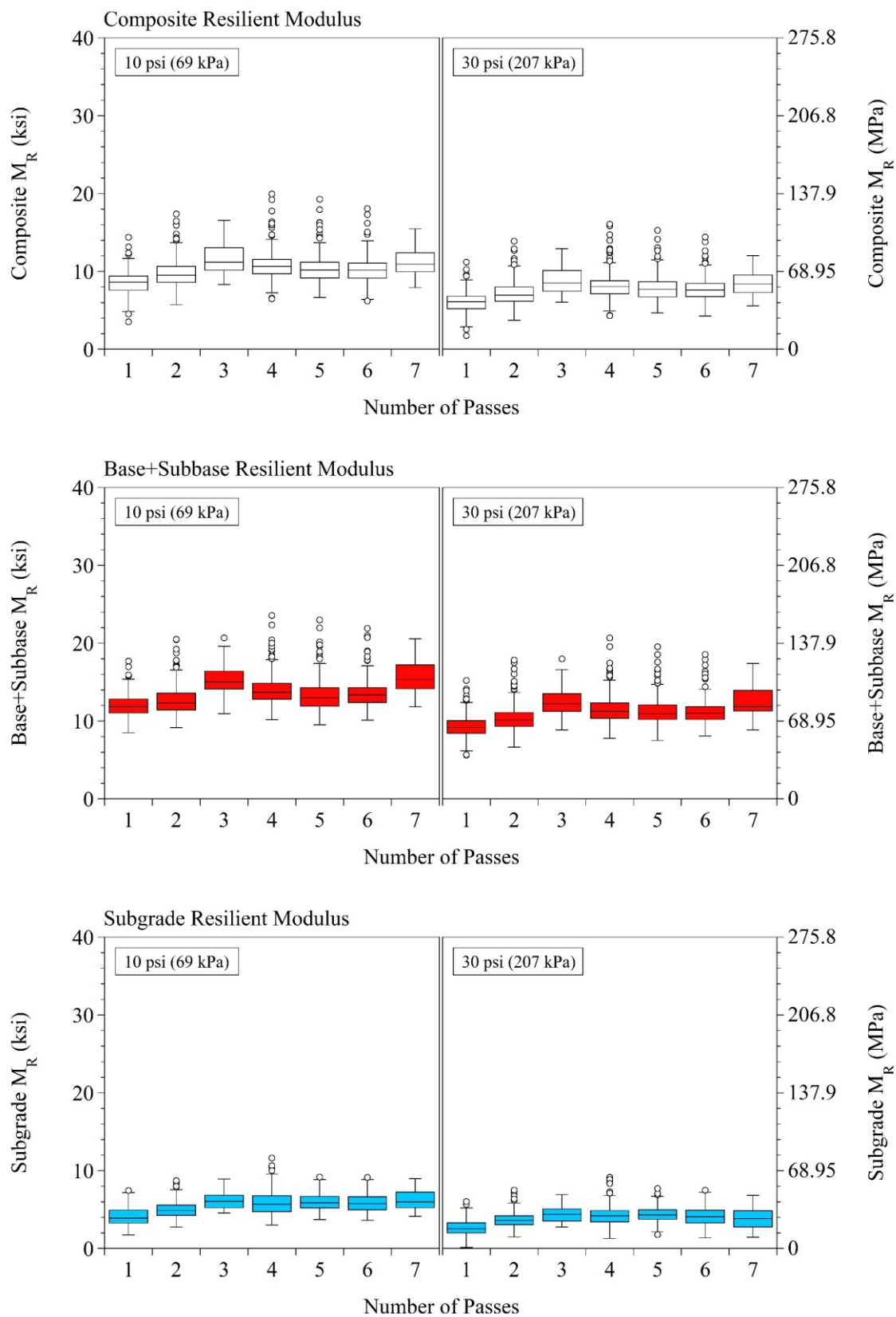
APPENDIX K

RESILIENT MODULUS (M_R) OF RECONSTRUCTED CELLS AT EACH PASS

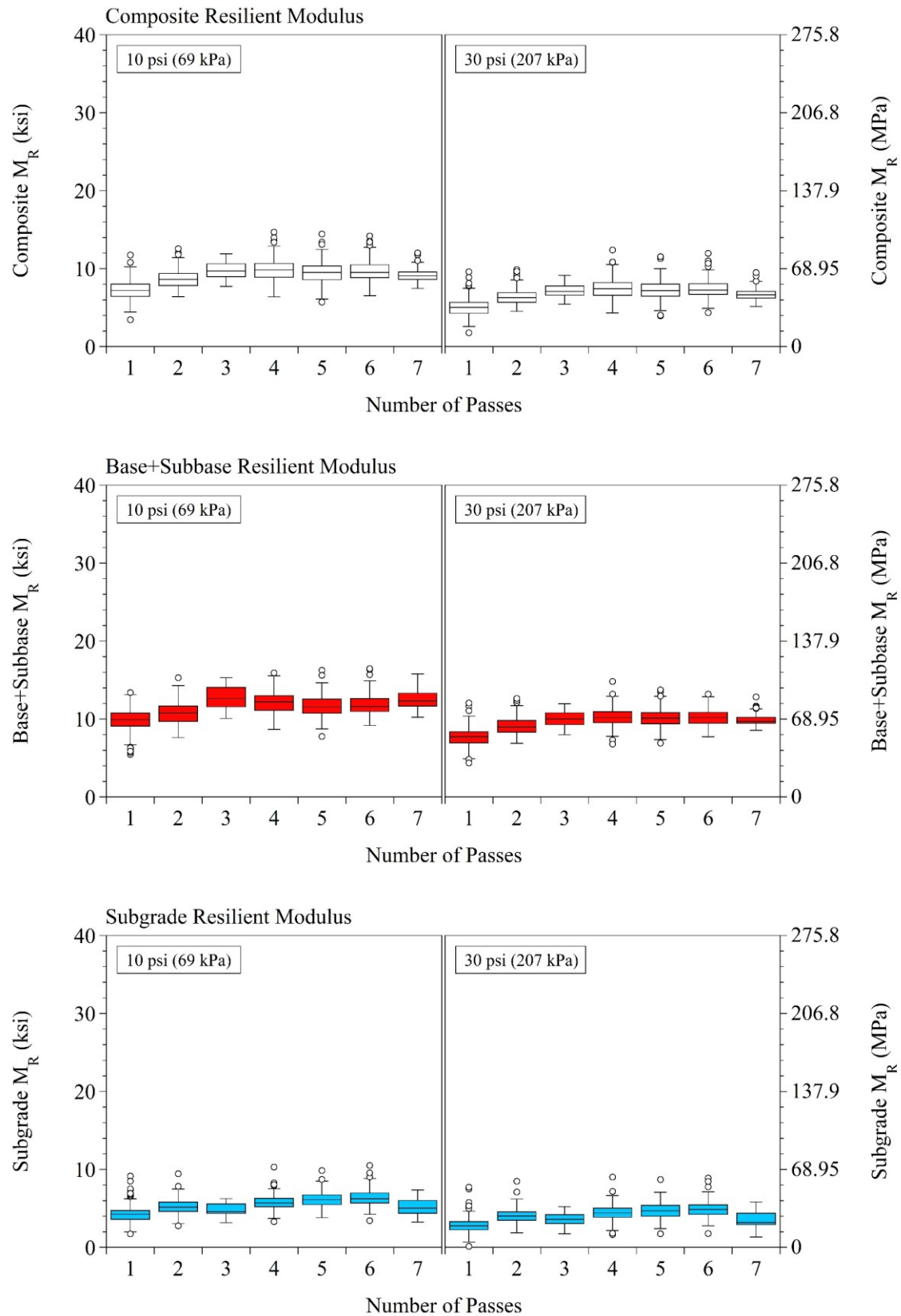
Cell 328:



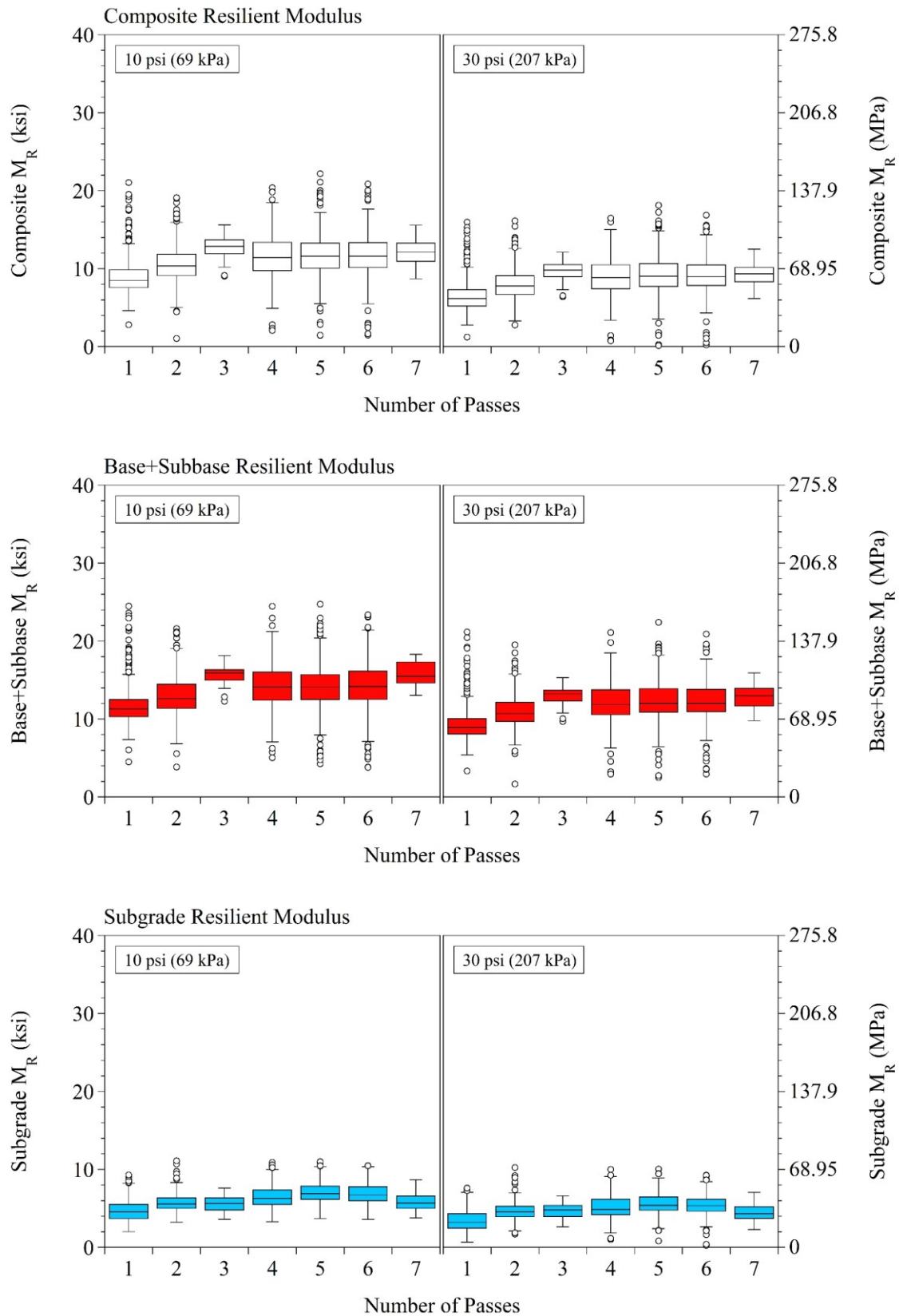
Cell 428:



Cell 528:



Cell 628:



APPENDIX L

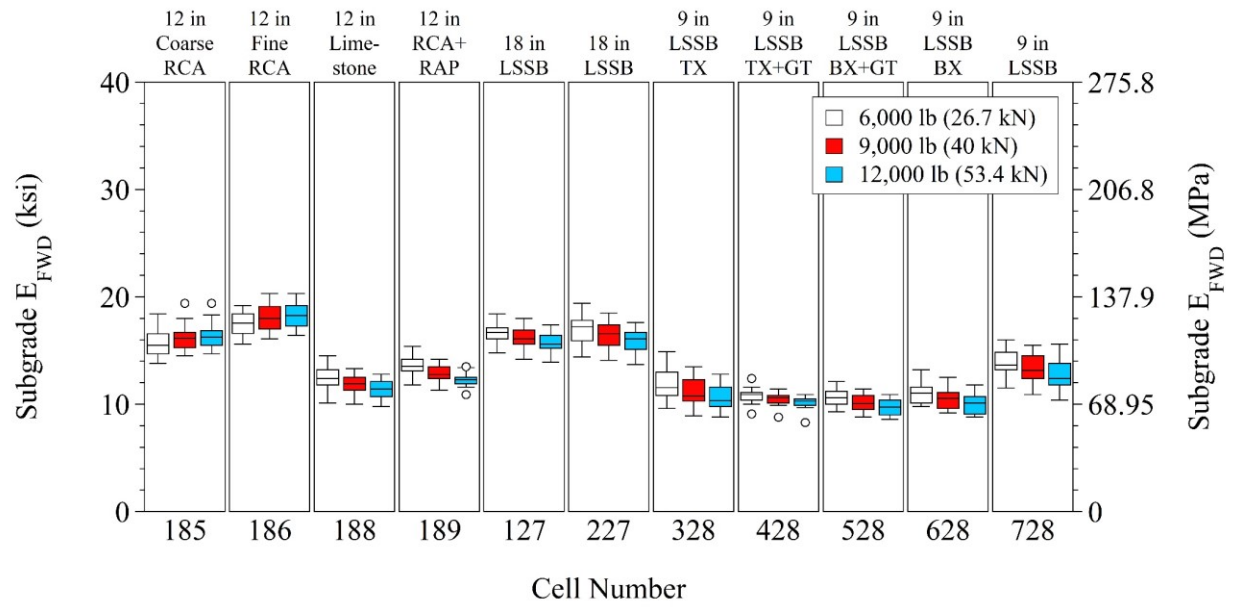
FALLING WEIGHT DEFLECTOMETER (FWD) TESTING EQUIPMENT

Trailer-mounted Dynatest Model 8002 FWD device:

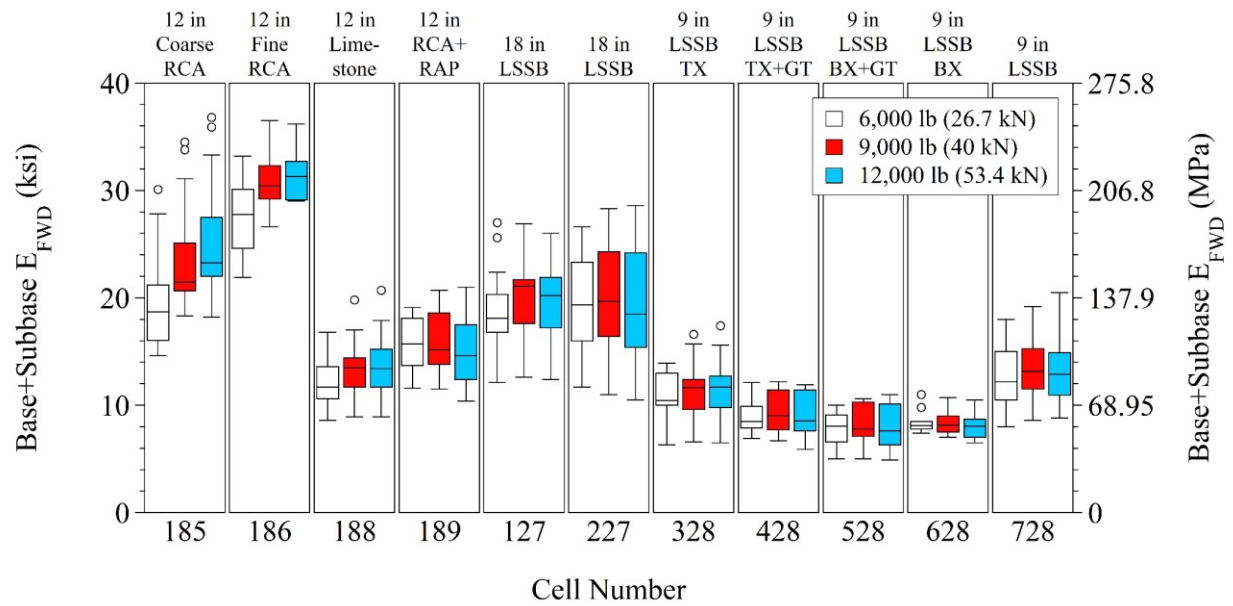


APPENDIX M
FALLING WEIGHT DEFLECTOMETER (FWD) TEST RESULTS OF
CELLS AFTER PAVING

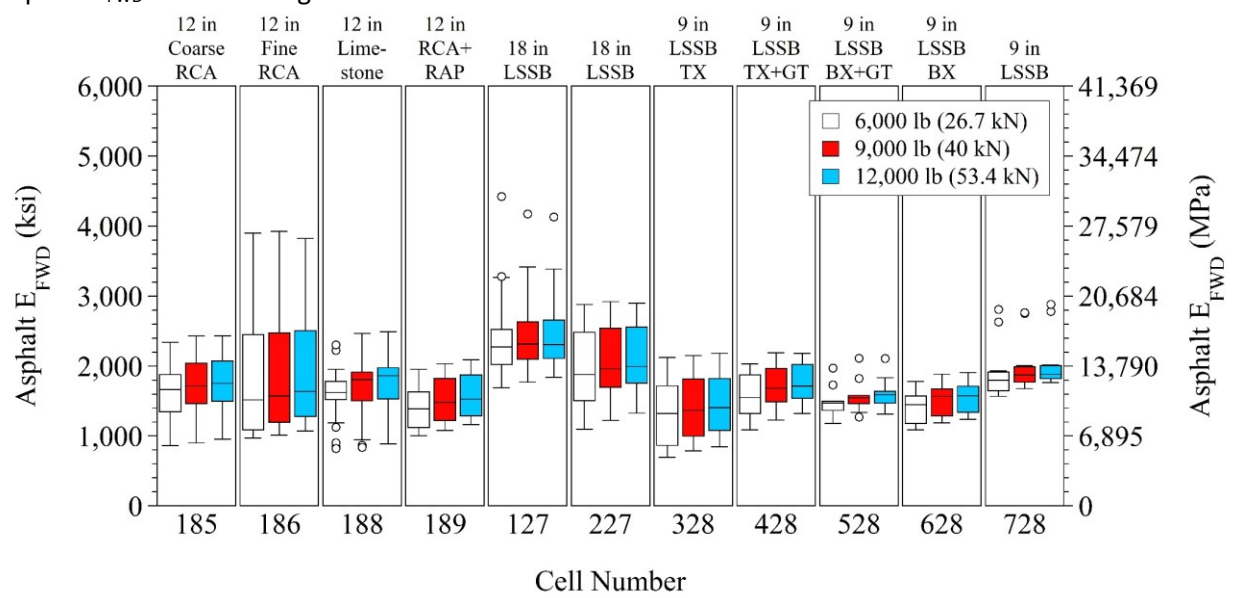
Subgrade E_{FWD} - After Paving



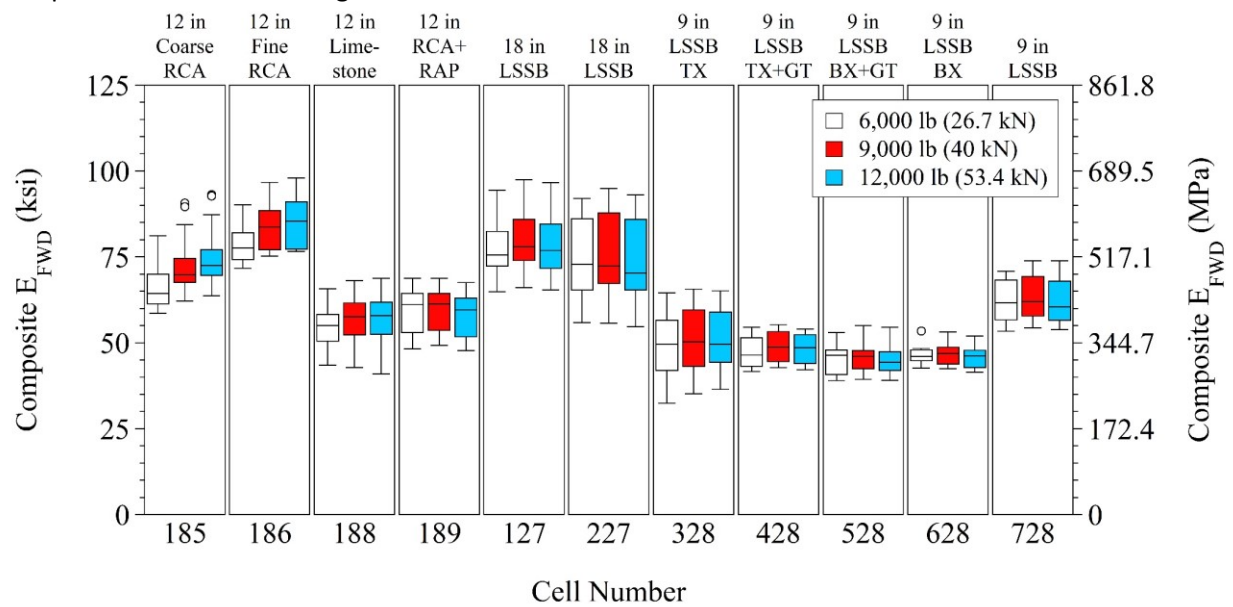
Base+Subbase E_{FWD} - After Paving



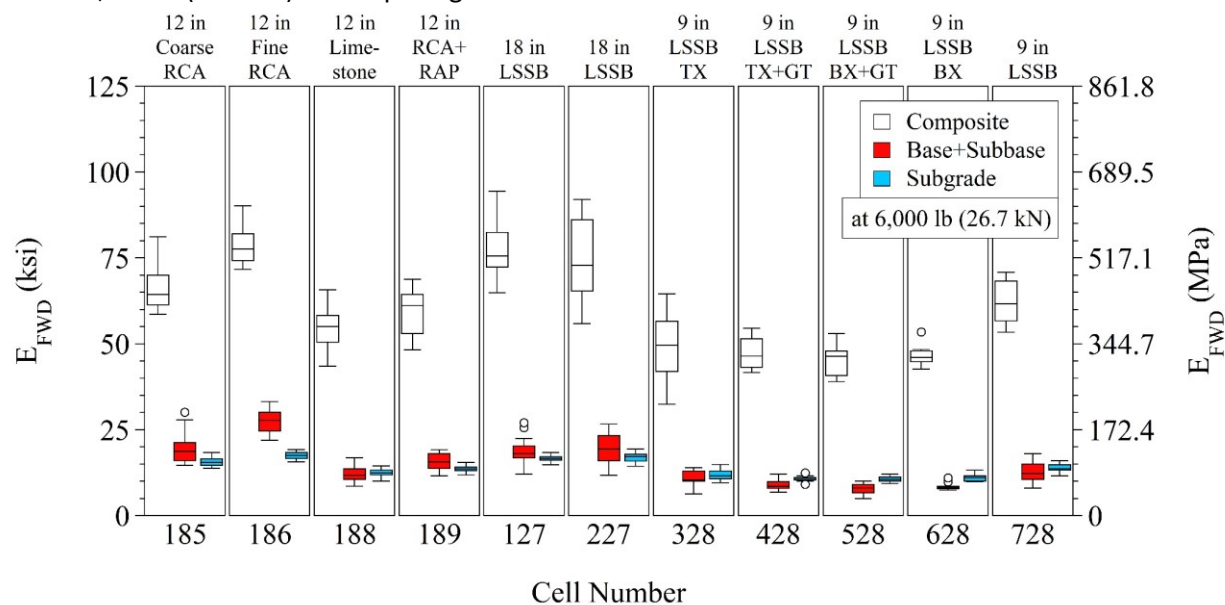
Asphalt E_{FWD} - After Paving



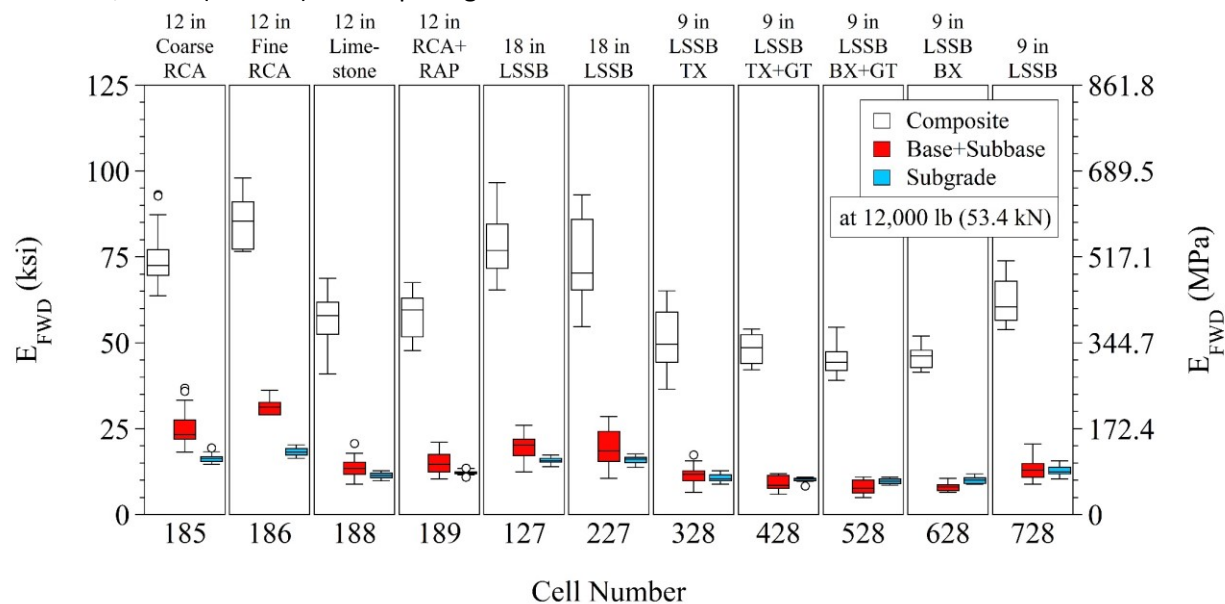
Composite E_{FWD} - After Paving



E_{FWD} at 6,000 lb (26.7 kN) - After paving

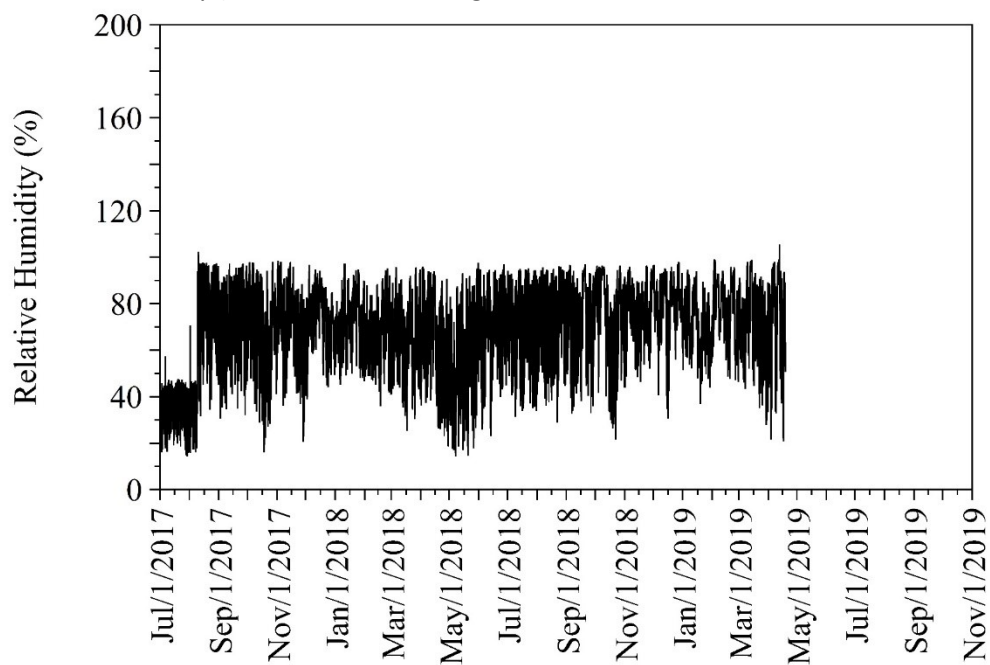


E_{FWD} at 12,000 lb (53.4 kN) - After paving

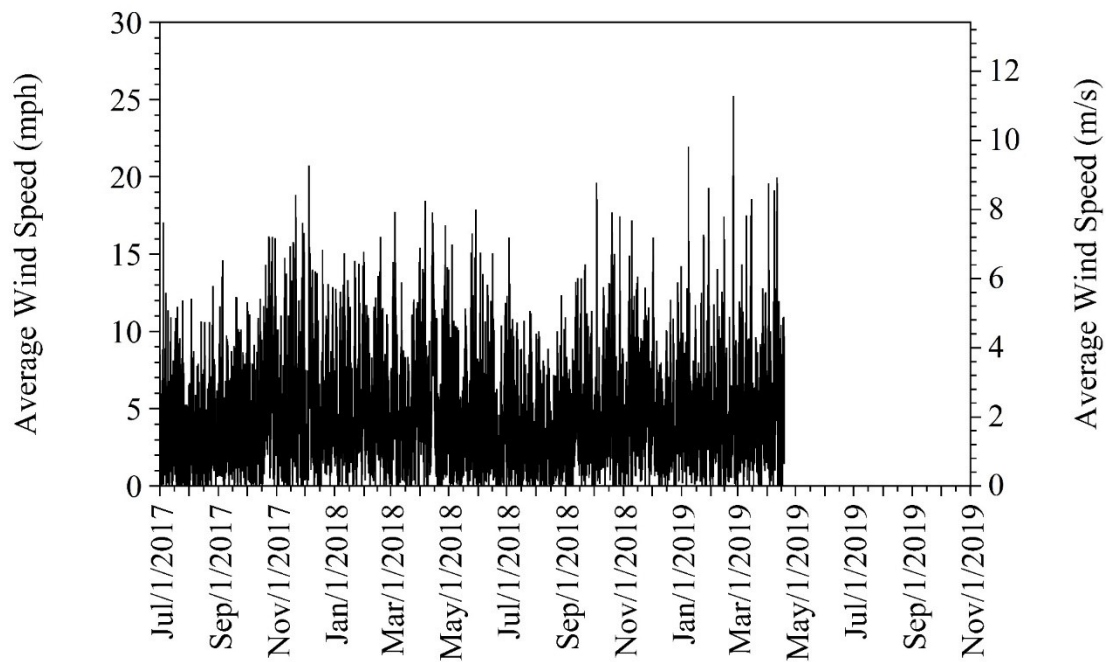


APPENDIX N
RELATIVE HUMIDITY AND AVERAGE WIND SPEED DATA IN THE
LONG-TERM

Relative humidity (results are the average of the data collected from the two weather stations):



Average wind speed (results are the average of the data collected from the two weather stations):



APPENDIX O

LOCATIONS OF EMBEDDED SENSORS

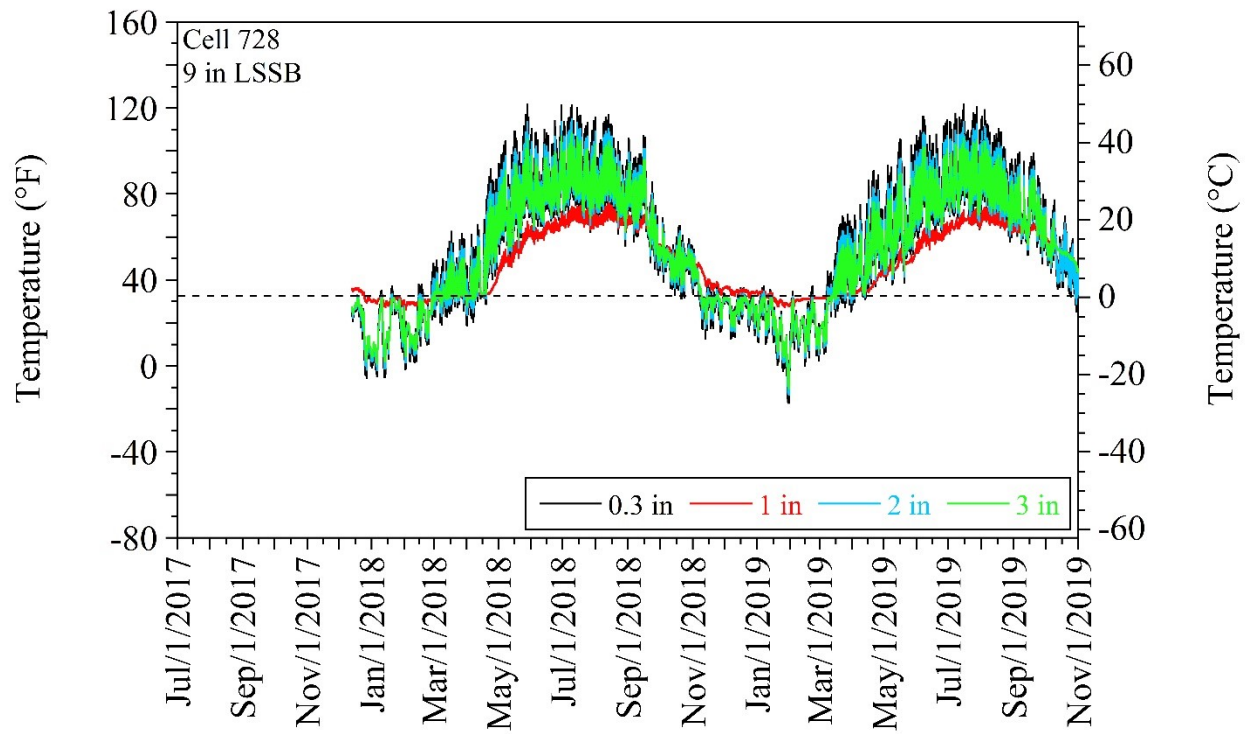
Cell Number	Cell Description	Sensor	Number	Station	Offset (ft)	Depth from Surface (in)
185	12 in Coarse RCA	Thermocouple (TC)	1	16538.51	-6.4	2.8
			2	16538.51	-6.4	3.8
			3	16538.51	-6.4	9.3
			4	16538.51	-6.4	14.8
			5	16538.51	-6.4	15.8
			6	16538.51	-6.4	18.3
			7	16538.51	-6.4	19.3
			8	16538.51	-6.4	23.8
			9	16538.51	-6.4	35.8
			10	16538.51	-6.4	47.8
			11	16538.51	-6.4	59.8
			12	16538.51	-6.4	71.8
		Moisture Probe (EC)	1	16538.81	-5.8	5
			2	16538.81	-5.8	14
			3	16538.81	-5.8	17
			4	16538.81	-5.8	20.5
186	12 in Fine RCA	Thermocouple (TC)	1	16678.52	-6.3	3
			2	16678.52	-6.3	4
			3	16678.52	-6.3	9.5
			4	16678.52	-6.3	15
			5	16678.52	-6.3	16
			6	16678.52	-6.3	18.5
			7	16678.52	-6.3	19.5
			8	16678.52	-6.3	24
			9	16678.52	-6.3	36
			10	16678.52	-6.3	48
			11	16678.52	-6.3	60
			12	16678.52	-6.3	72
		Moisture Probe (EC)	1	16678.91	-5.6	5
			2	16678.91	-5.6	14
			3	16678.91	-5.6	17
			4	16678.91	-5.6	20.5

Cell Number	Cell Description	Sensor	Number	Station	Offset (ft)	Depth from Surface (in)
188	12 in Limestone	Thermocouple (TC)	1	17111.5	-5.5	3
			2	17111.5	-5.5	4
			3	17111.5	-5.5	9.5
			4	17111.5	-5.5	15
			5	17111.5	-5.5	16
			6	17111.5	-5.5	18.5
			7	17111.5	-5.5	19.5
			8	17111.5	-5.5	24
			9	17111.5	-5.5	36
			10	17111.5	-5.5	48
			11	17111.5	-5.5	60
			12	17111.5	-5.5	72
		Moisture Probe (EC)	1	17111.8	-4.8	5
			2	17111.8	-4.8	14
			3	17111.8	-4.8	17
			4	17111.8	-4.8	20.5
189	12 in RCA+RAP	Thermocouple (TC)	1	17306.1	-5.3	3
			2	17306.1	-5.3	4
			3	17306.1	-5.3	9.5
			4	17306.1	-5.3	15
			5	17306.1	-5.3	16
			6	17306.1	-5.3	18.5
			7	17306.1	-5.3	19.5
			8	17306.1	-5.3	24
			9	17306.1	-5.3	36
			10	17306.1	-5.3	48
			11	17306.1	-5.3	60
			12	17306.1	-5.3	72
		Moisture Probe (EC)	1	17306.2	-4.7	5
			2	17306.2	-4.7	14
			3	17306.2	-4.7	17
			4	17306.2	-4.7	20.5

Cell Number	Cell Description	Sensor	Number	Station	Offset (ft)	Depth from Surface (in)
127	18 in LSSB	Thermocouple (TC)	1	17569	-11.5	3
			2	17569	-11.5	4
			3	17569	-11.5	6.5
			4	17569	-11.5	9
			5	17569	-11.5	10
			6	17569	-11.5	12
			7	17569	-11.5	18
			8	17569	-11.5	24
			9	17569	-11.5	36
			10	17569	-11.5	48
			11	17569	-11.5	60
			12	17569	-11.5	72
		Moisture Probe (EC)	1	17569	-11	6.5
			2	17569	-11	29
			3	17569	-11	36
728	9 in LSSB	Thermocouple (TC)	1	18544.1	-11.6	3
			2	18544.1	-11.6	4
			3	18544.1	-11.6	6.5
			4	18544.1	-11.6	9
			5	18544.1	-11.6	10
			6	18544.1	-11.6	14
			7	18544.1	-11.6	18.5
			8	18544.1	-11.6	24
			9	18544.1	-11.6	36
			10	18544.1	-11.6	48
			11	18544.1	-11.6	60
			12	18544.1	-11.6	72
			13	18544.1	-11.9	0.3
			14	18544.1	-11.9	1
			15	18544.1	-11.9	2
			16	18544.1	-11.9	3
		Moisture Probe (EC)	1	18544	-11	8.5
			2	18544	-11	19.5
			3	18544	-11	24
			4	18544	-11	36

APPENDIX P

CHANGE IN TEMPERATURE OF ASPHALT LAYER IN CELL 728 (9-IN LSSB)



APPENDIX Q

CALIBRATION EQUATIONS TO ESTIMATE VOLUMETRIC WATER CONTENT (VWC) AND DEGREE OF SATURATION (DOS) VALUES

Calibration equations:

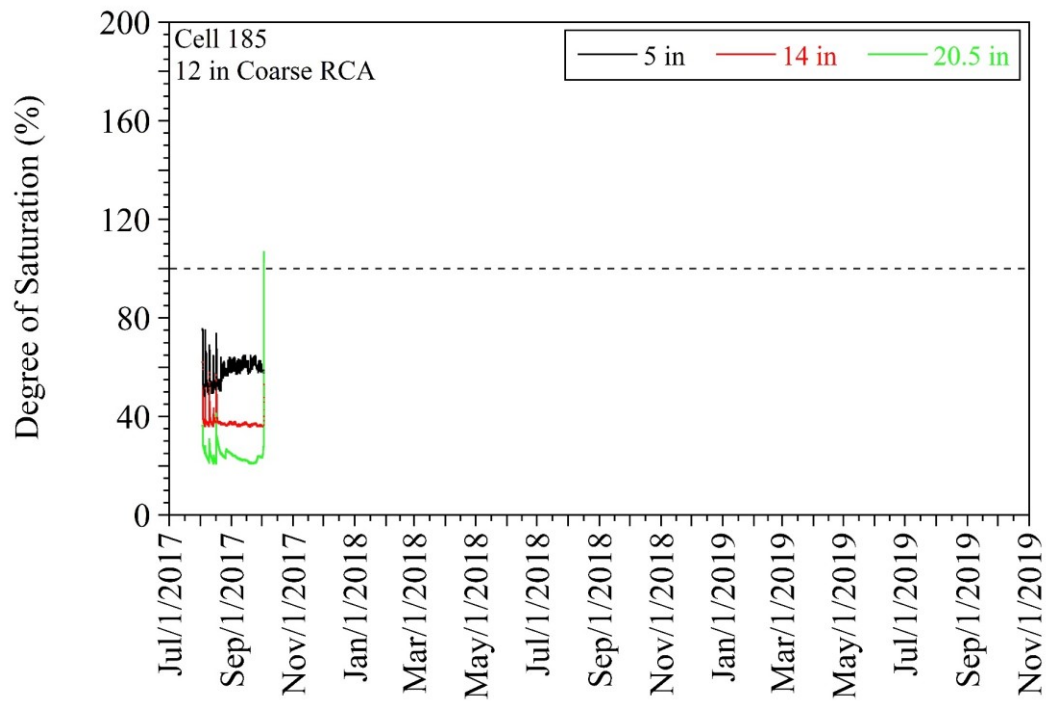
Cell/Instrument	Layer	Calibration Equation
185-186		
EC 1	RCA (-5")	$-0.0000004 * RAW^2 + 0.0007 * RAW - 0.0409$
EC 2	RCA (-14")	$-0.0000004 * RAW^2 + 0.0007 * RAW - 0.0409$
EC 3	S. Granular (-17")	$0.0005 * RAW - 0.0908$
EC 4	Sand (-20.5")	$0.0004 * RAW - 0.078$
188		
EC 1	Cl-6 Limestone (-5")	$0.0003 * RAW - 0.0437$
EC 2	Cl-6 Limestone (-14")	$0.0003 * RAW - 0.0437$
EC 3	S. Granular (-17")	$0.0005 * RAW - 0.0908$
EC 4	Clay (-20.5")	$0.0003 * RAW - 0.0021$
189		
EC 1	Cl-6 Recycled (-5")	$0.0006 * RAW - 0.1358$
EC 2	Cl-6 Recycled (-14")	$0.0006 * RAW - 0.1358$
EC 3	S. Granular (-17")	$0.0005 * RAW - 0.0908$
EC 4	Clay (-20.5")	$0.0003 * RAW - 0.0021$
127		
EC 1	Cl-6 (-6.5")	$0.0006 * RAW - 0.1358$
EC 2	Clay (-29")	$0.0003 * RAW - 0.0021$
EC 3	Clay (-36")	$0.0003 * RAW - 0.0021$
728		
EC 1	Cl-5Q (-8.5")	$-0.0000004 * RAW^2 + 0.0007 * RAW - 0.0409$
EC 2	Clay (-19")	$0.0003 * RAW - 0.0021$
EC 3	Clay (-24")	$0.0003 * RAW - 0.0021$
EC 4	Clay (-36")	$0.0003 * RAW - 0.0021$

Degree of Saturation (DOS) Values

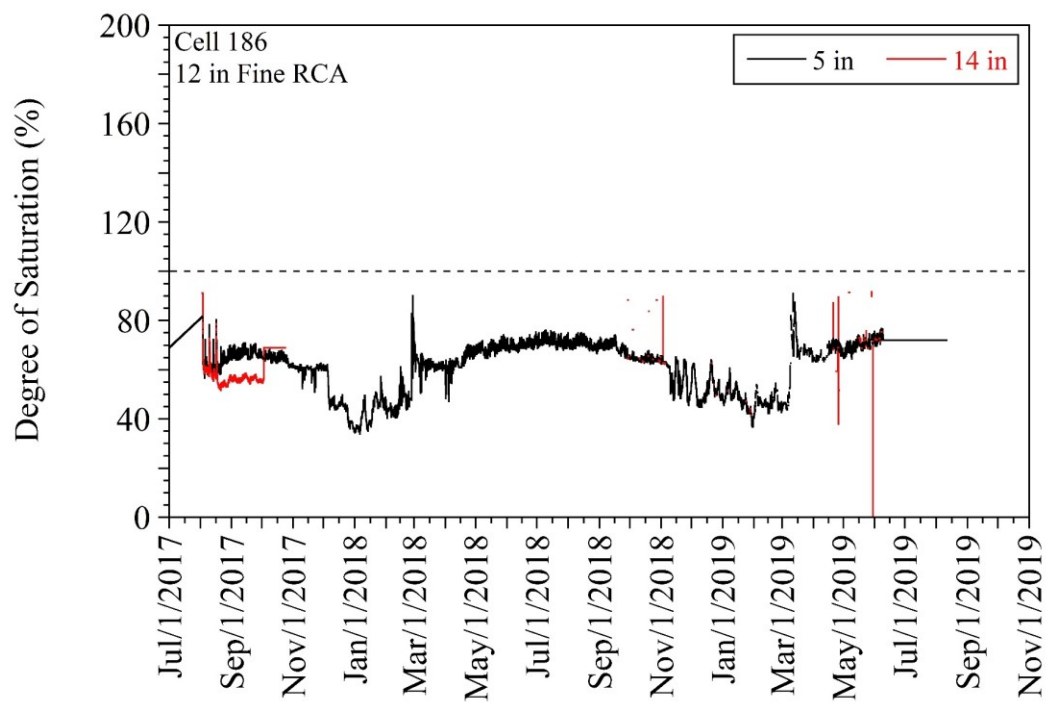
The following equation was used to calculate the degree of saturation (DOS). The median dry unit weight (γ_{dry}) values of the materials were determined from the nuclear density gauge (NDG) measurements taken from the outside lanes of the test cells during construction. The specific gravity (G_s) values of the materials were taken from laboratory test results. To calculate the moisture content (gravimetric) of the materials (ω), the WVC values were divided by γ_{dry} ($\gamma_{water} = 1 \text{ g/cm}^3$). Overall, it was concluded that slight increases in the DOS values were observed due to precipitation in the rainy periods.

$$DOS (\%) = \frac{\gamma_{dry} * G_s * \omega}{\gamma_{water} * G_s - \gamma_{dry}} * 100$$

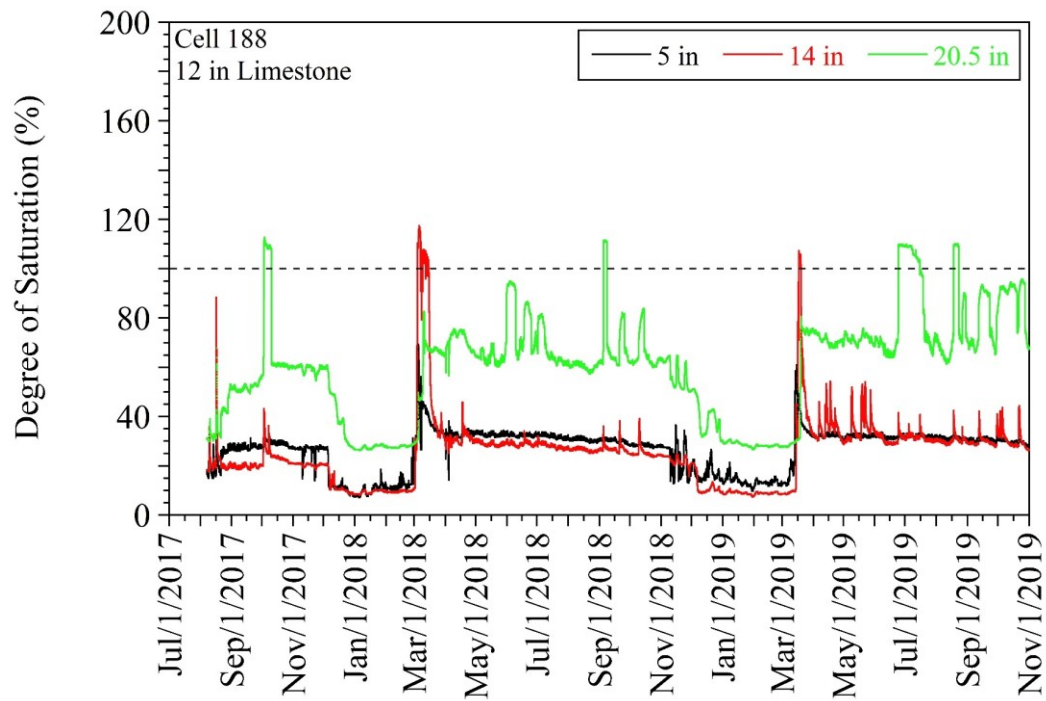
Cell 185 (12-in Coarse RCA)



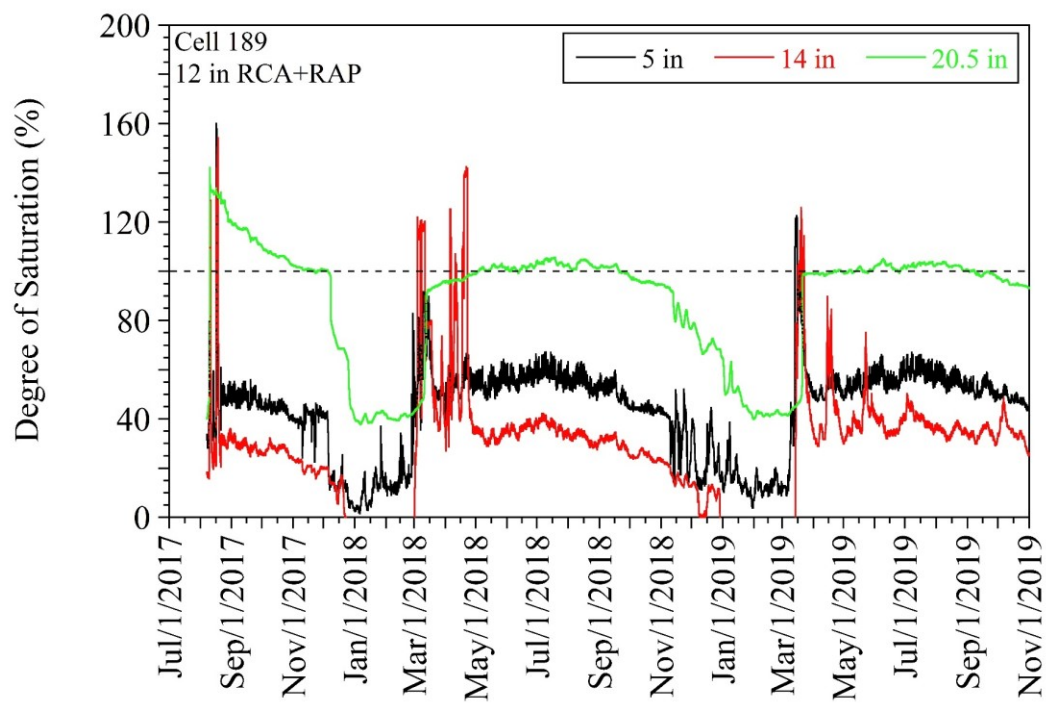
Cell 186 (12-in Fine RCA)



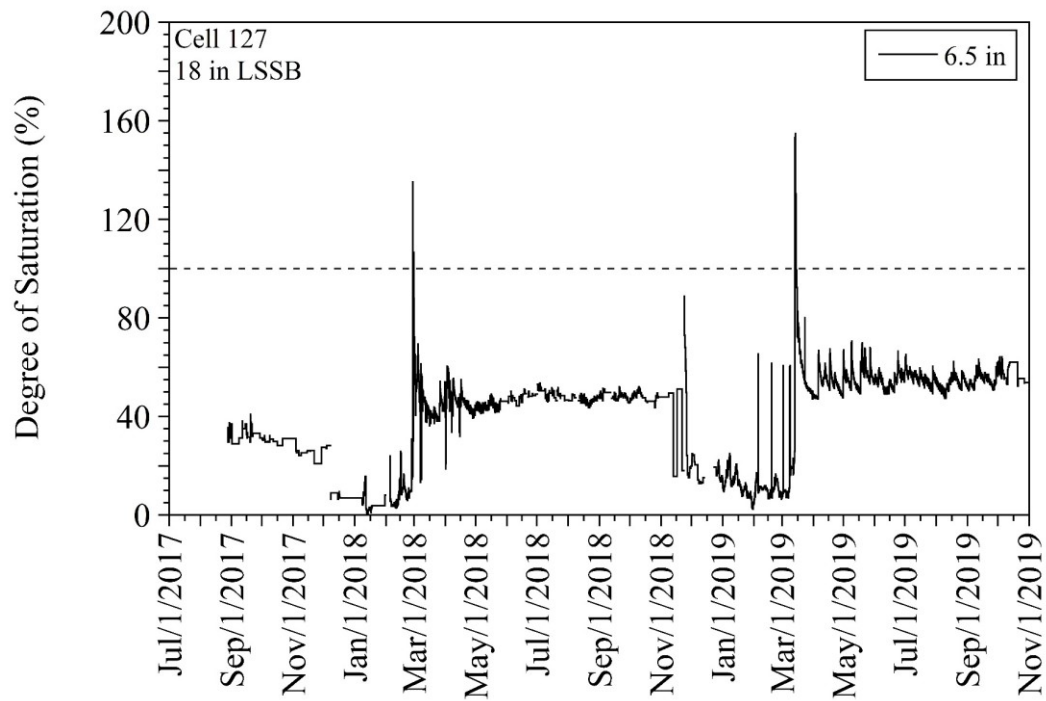
Cell 188 (12-in Limestone)



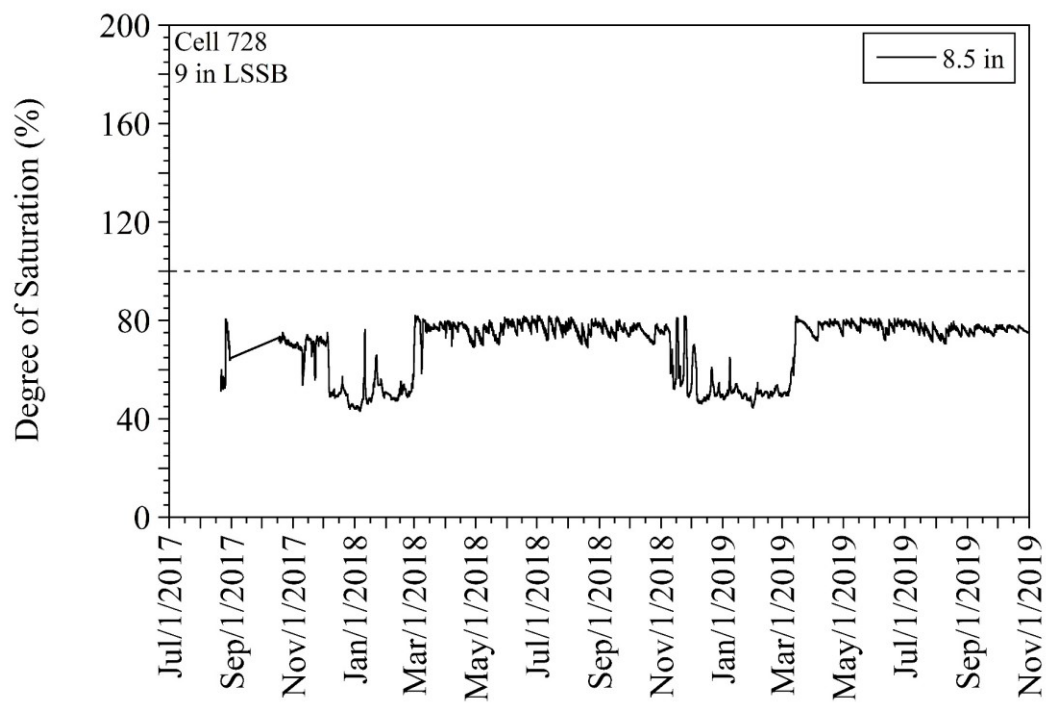
Cell 189 (12-in RCA+RAP)



Cell 127 (18-in LSSB)



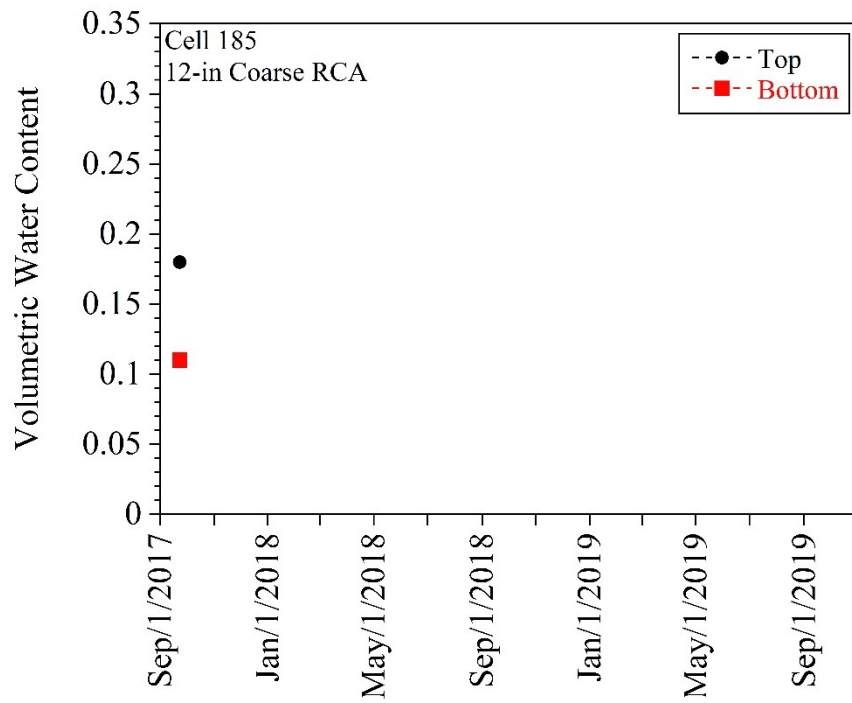
Cell 728 (9-in LSSB)



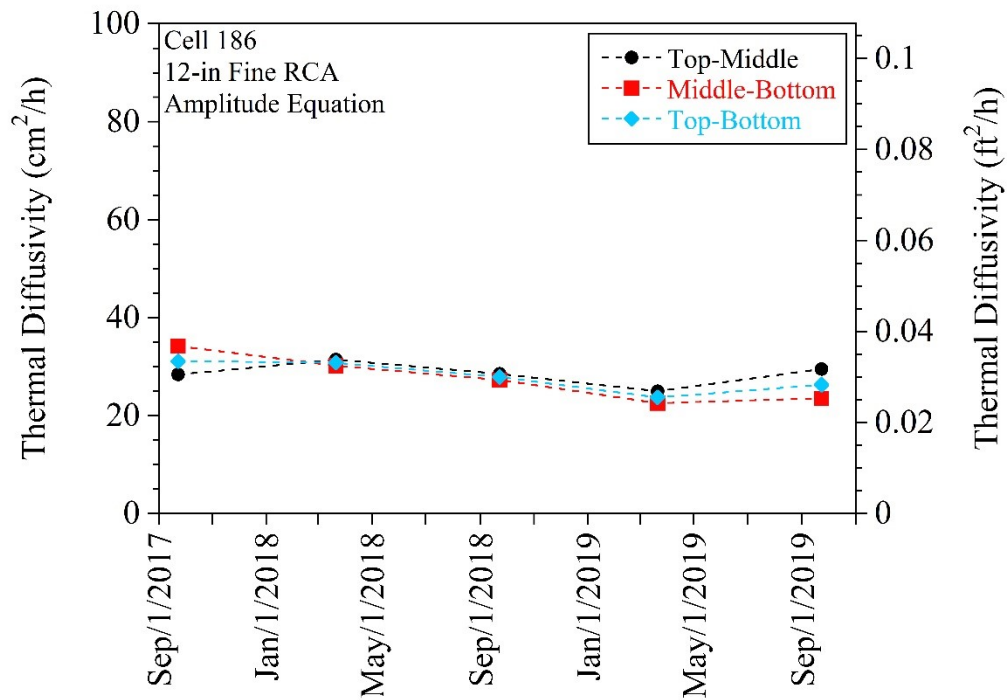
APPENDIX R

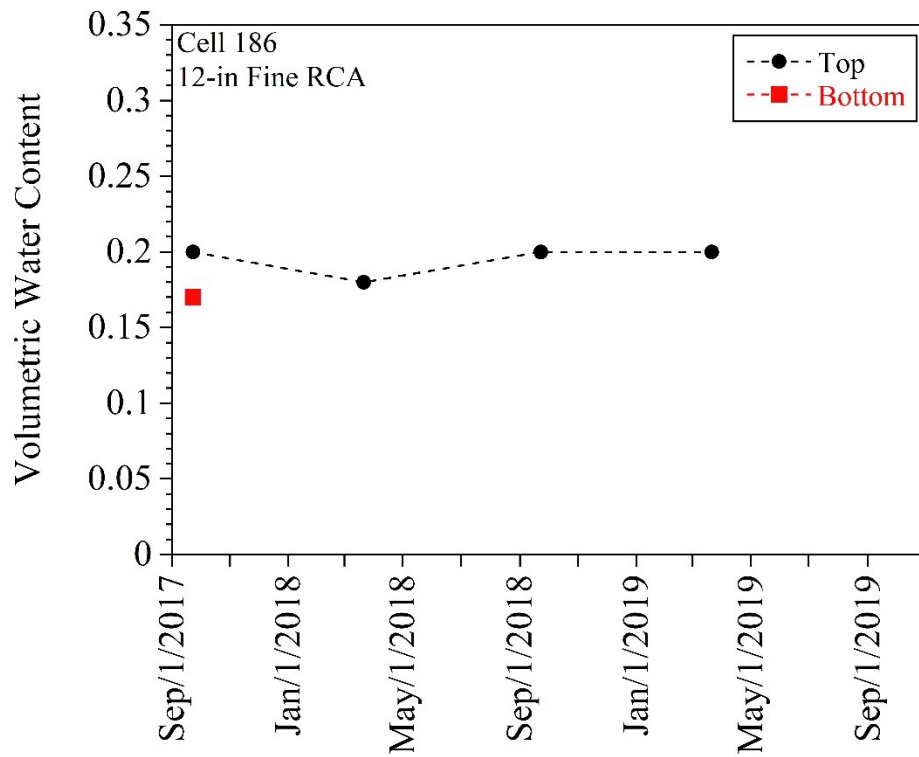
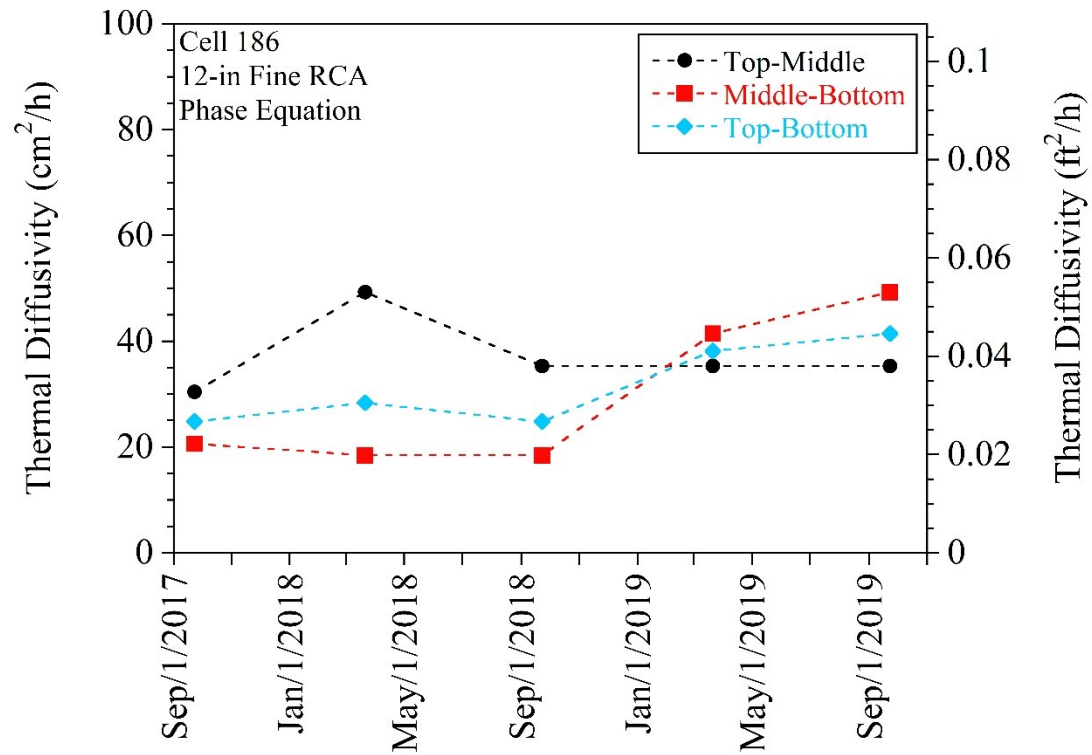
THERMAL DIFFUSIVITY (α) AND VOLUMETRIC WATER CONTENT (VWC) VALUES DETERMINED FOR 12-IN COARSE RCA (CELL 185), FINE RCA (CELL 186), LIMESTONE (CELL 188), AND RCA+RAP (CELL 189) BASE LAYERS

For 12-in Coarse RCA (Cell 185):

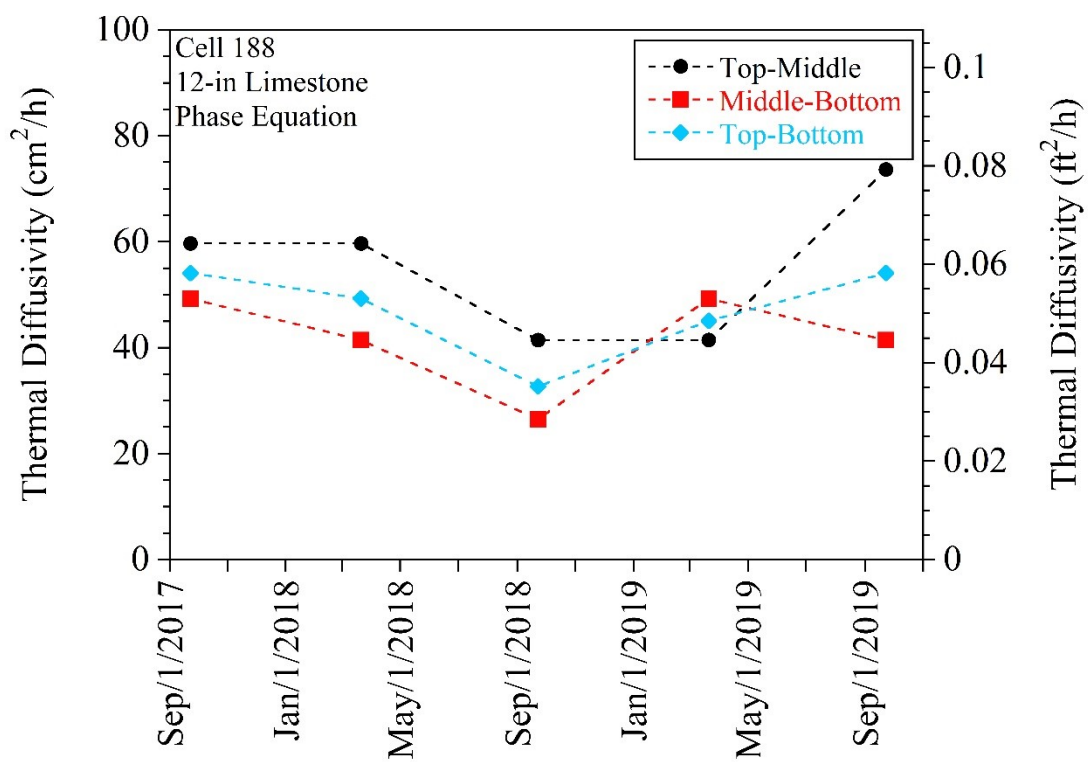
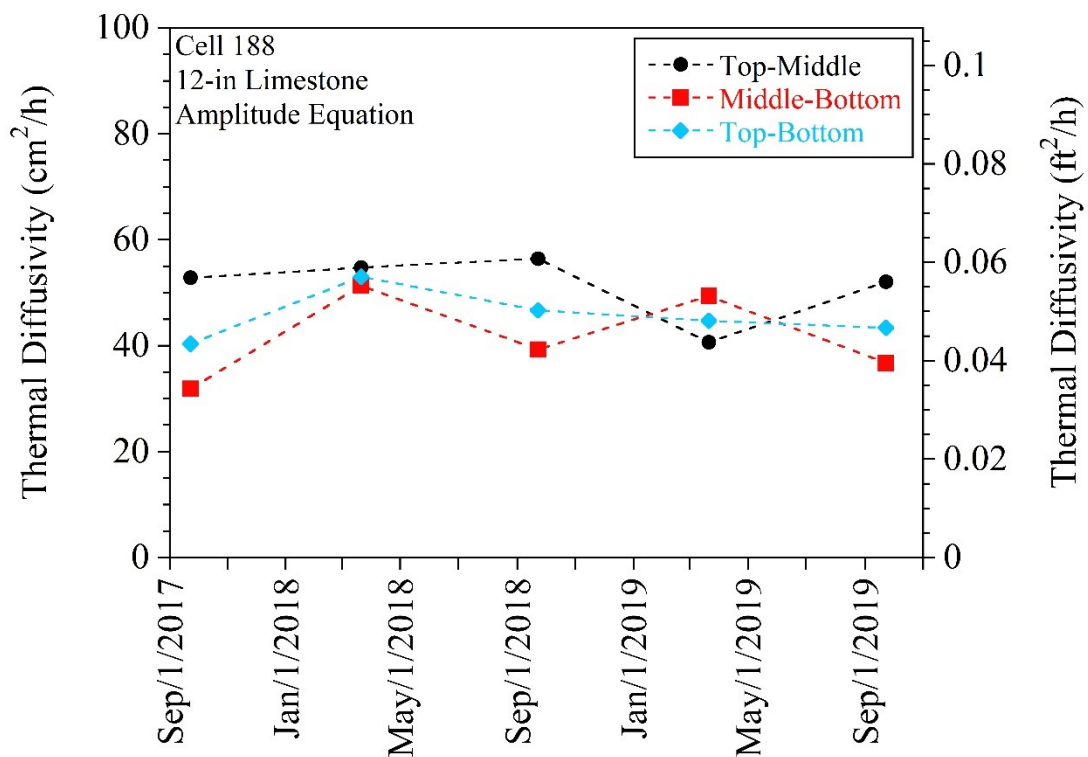


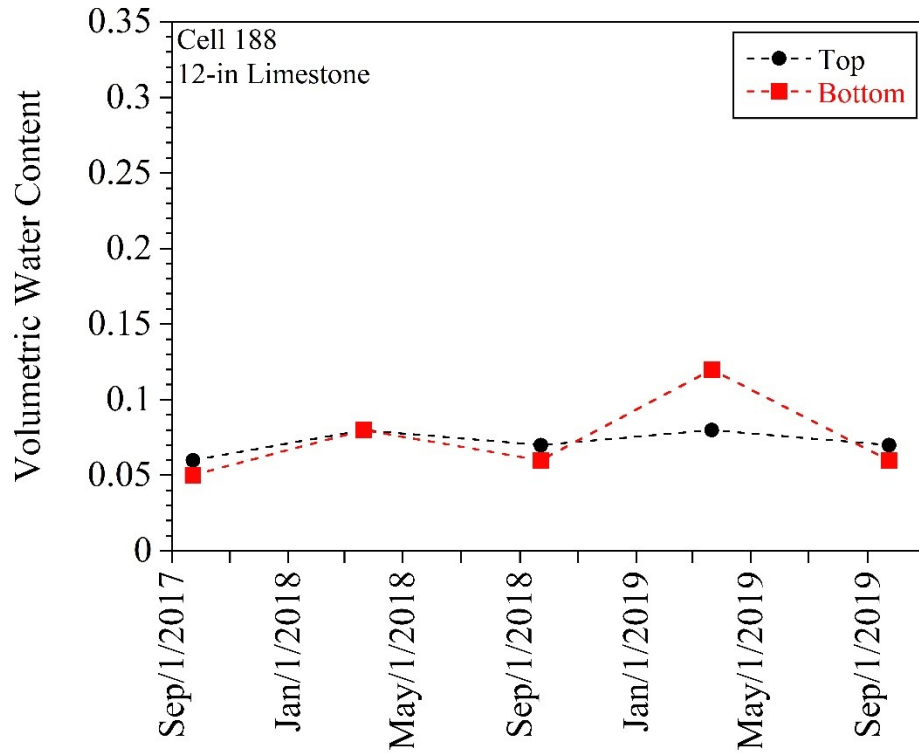
For 12-in Fine RCA (Cell 186):



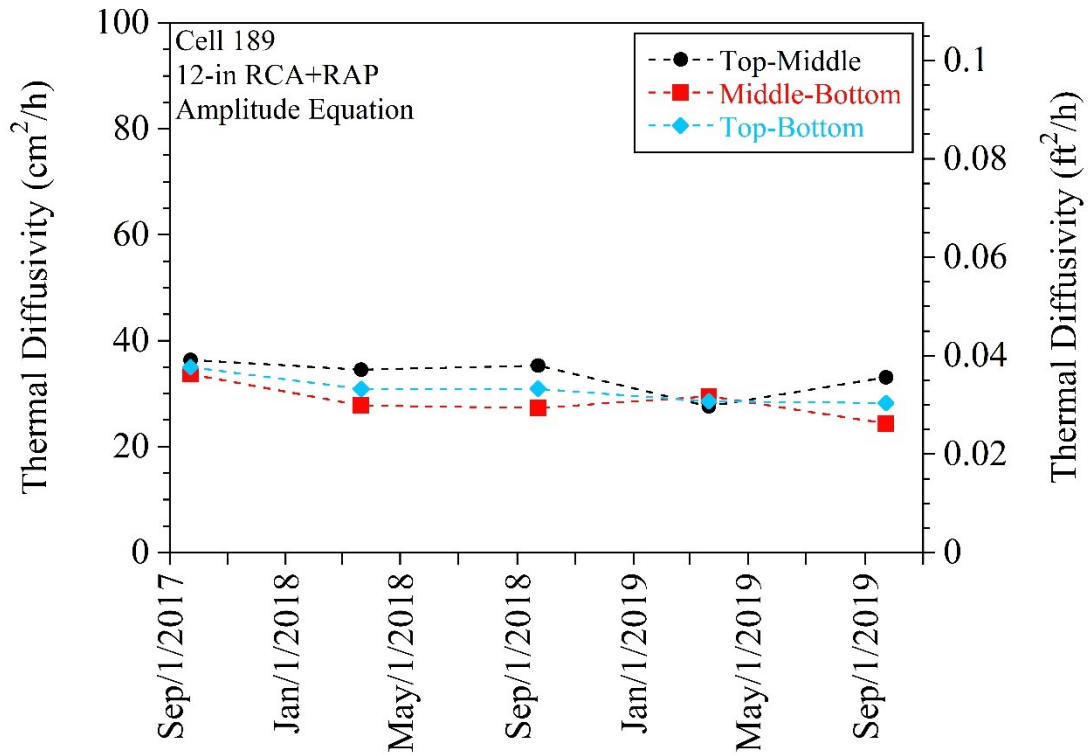


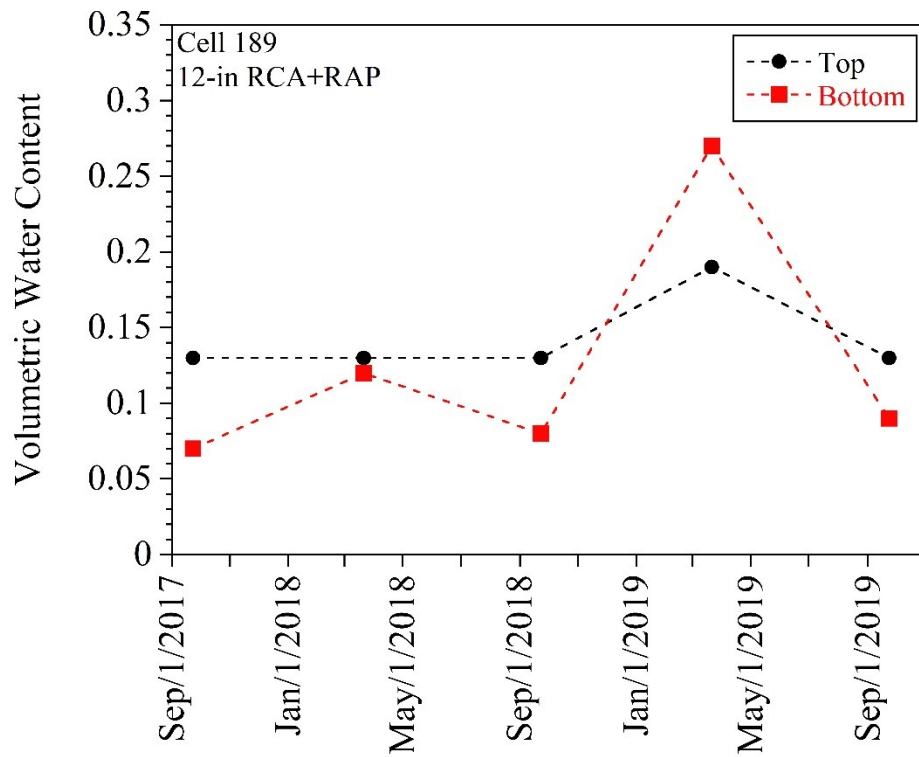
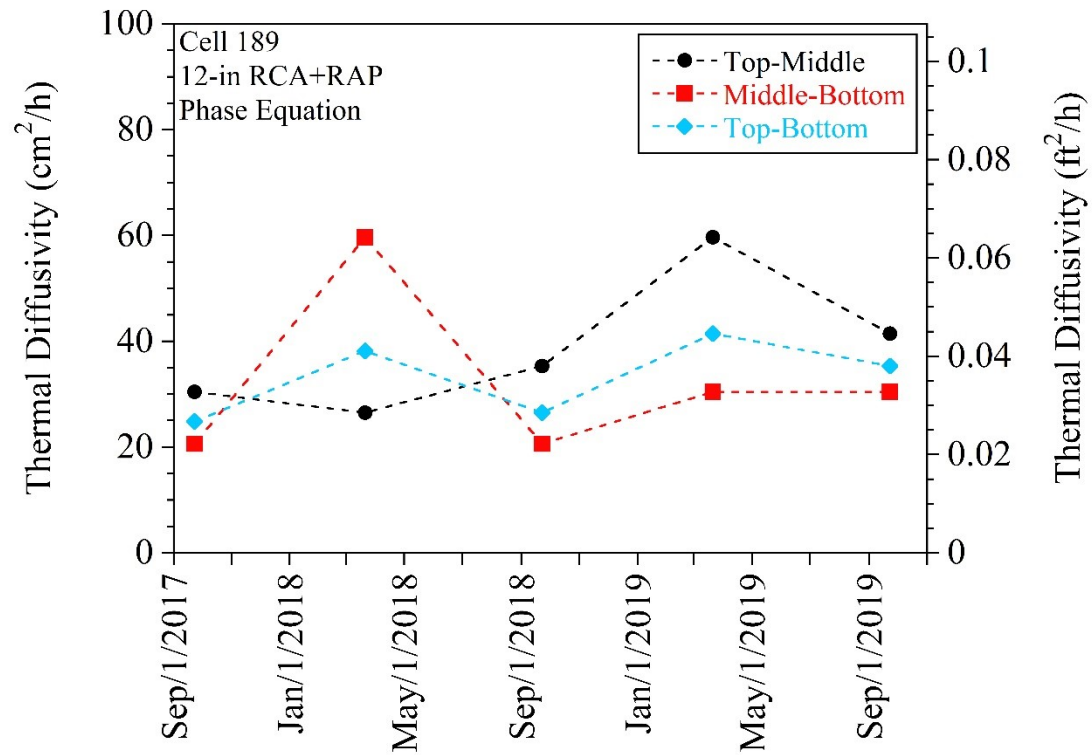
For 12-in Limestone (Cell 188):





For 12-in RCA+RAP (Cell 189):

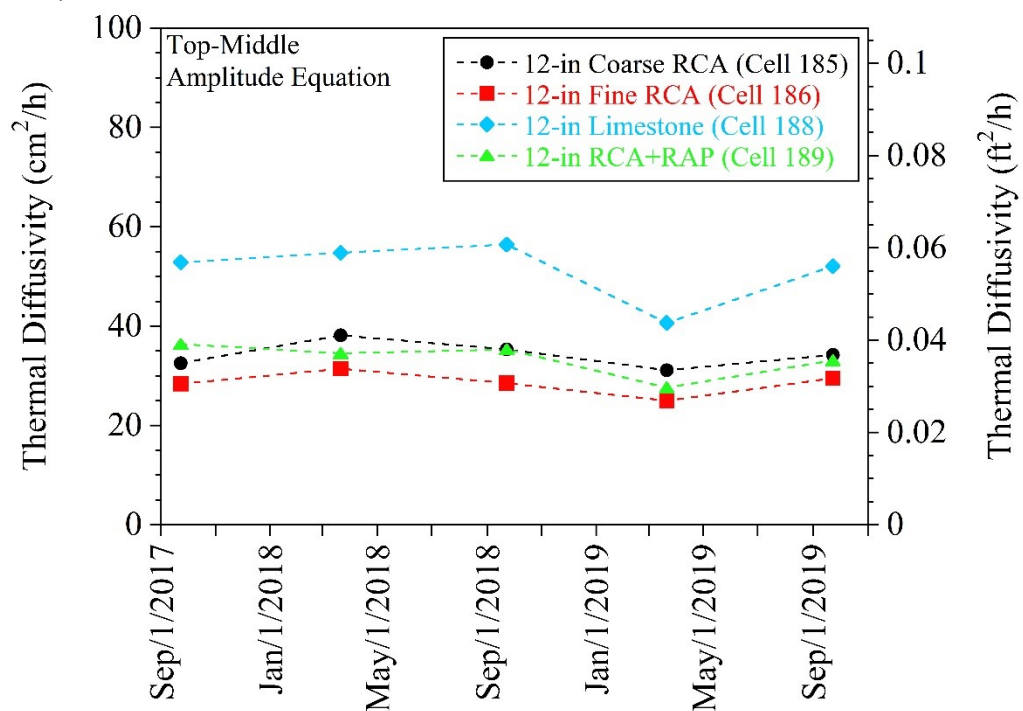




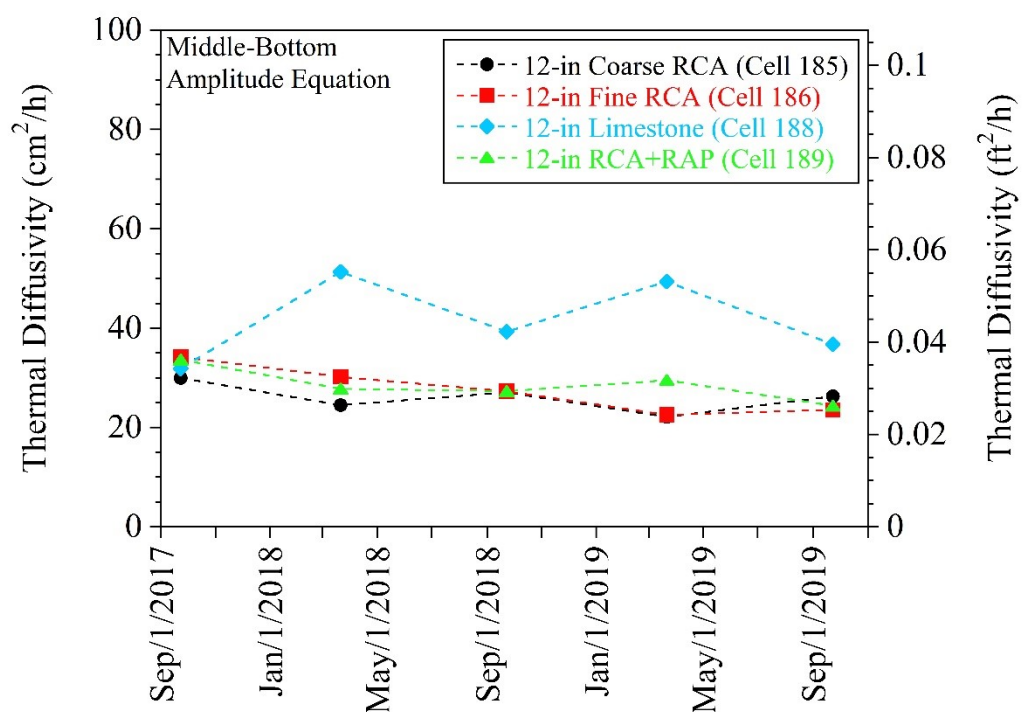
APPENDIX S

COMPARISONS BETWEEN TOP-MIDDLE AND MIDDLE- BOTTOM THERMOCOUPLES (TCS) IN 12-IN AGGREGATE BASE LAYERS

For top-middle TC sensors:

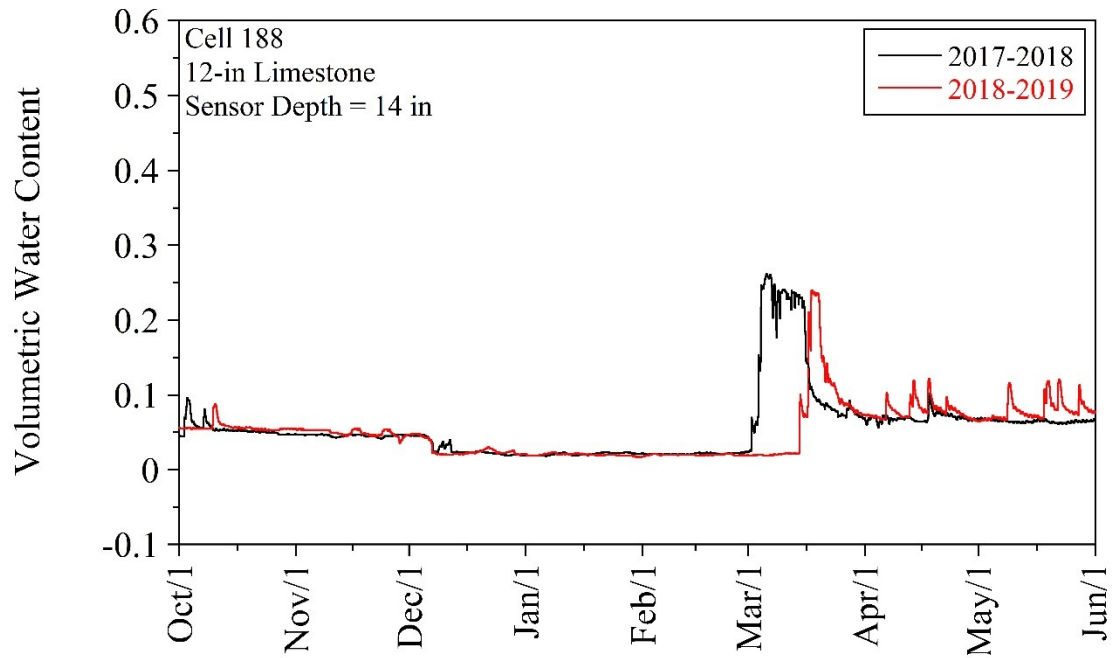


For middle-bottom TC sensors:

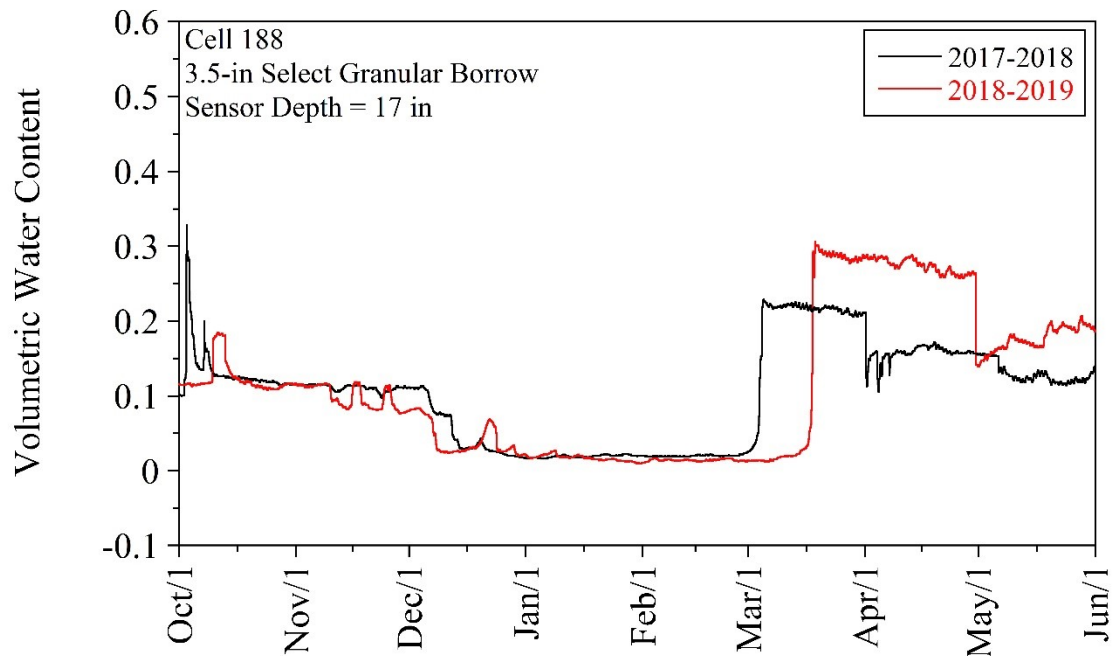


APPENDIX T
COMPARISONS BETWEEN VOLUMETRIC WATER CONTENT (VWC)
VALUES IN FIRST (2017-2018) AND SECOND (2018-2019)
FREEZING AND THAWING PERIODS

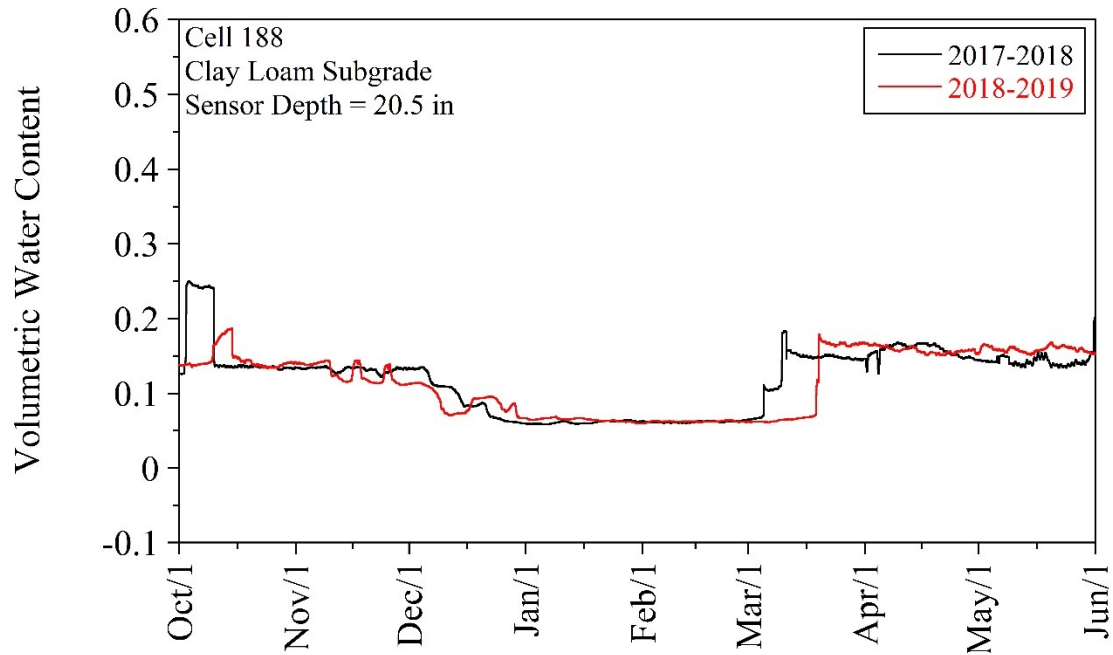
For Cell 188:



(the dates on the x-axis represent the time periods for both 2017-2018 and 2018-2019 years)

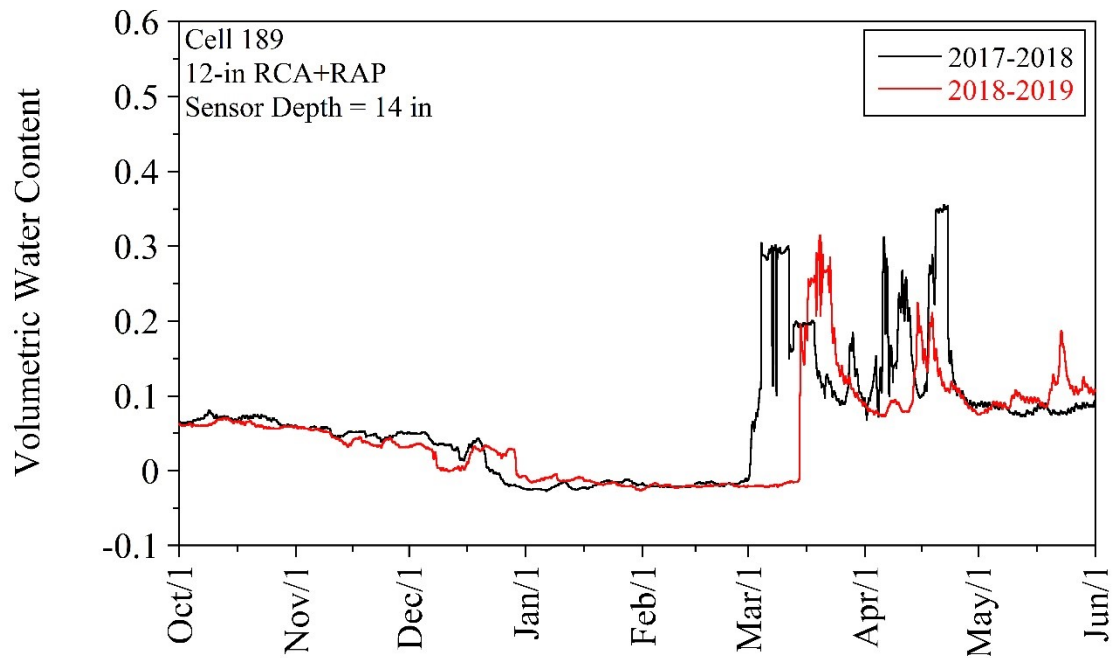


(the dates on the x-axis represent the time periods for both 2017-2018 and 2018-2019 years)

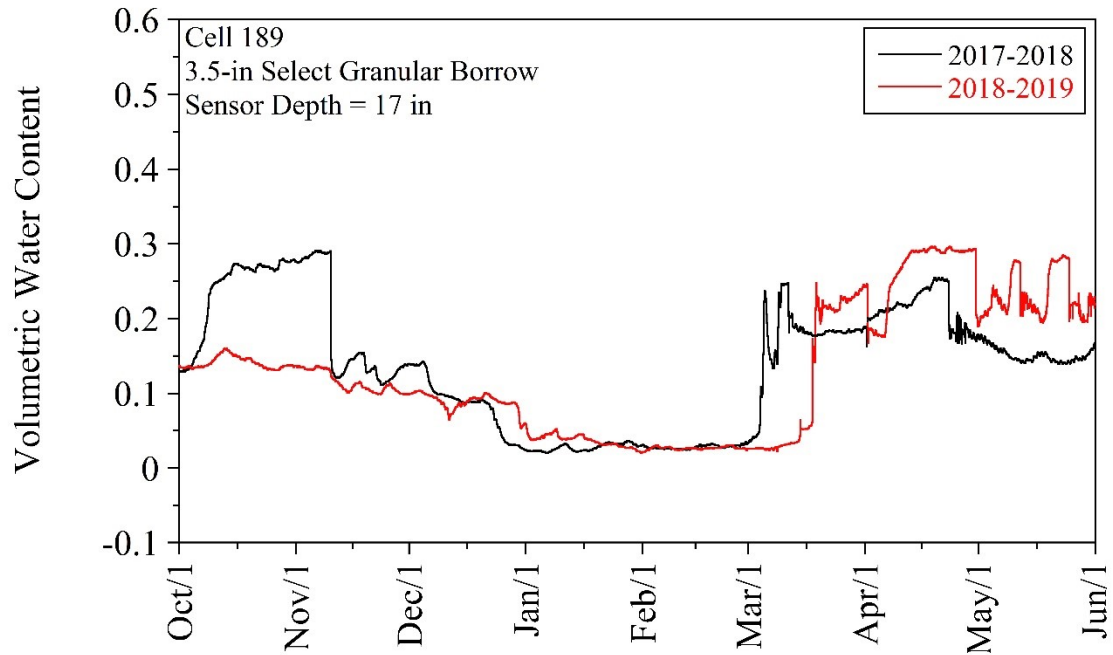


(the dates on the x-axis represent the time periods for both 2017-2018 and 2018-2019 years)

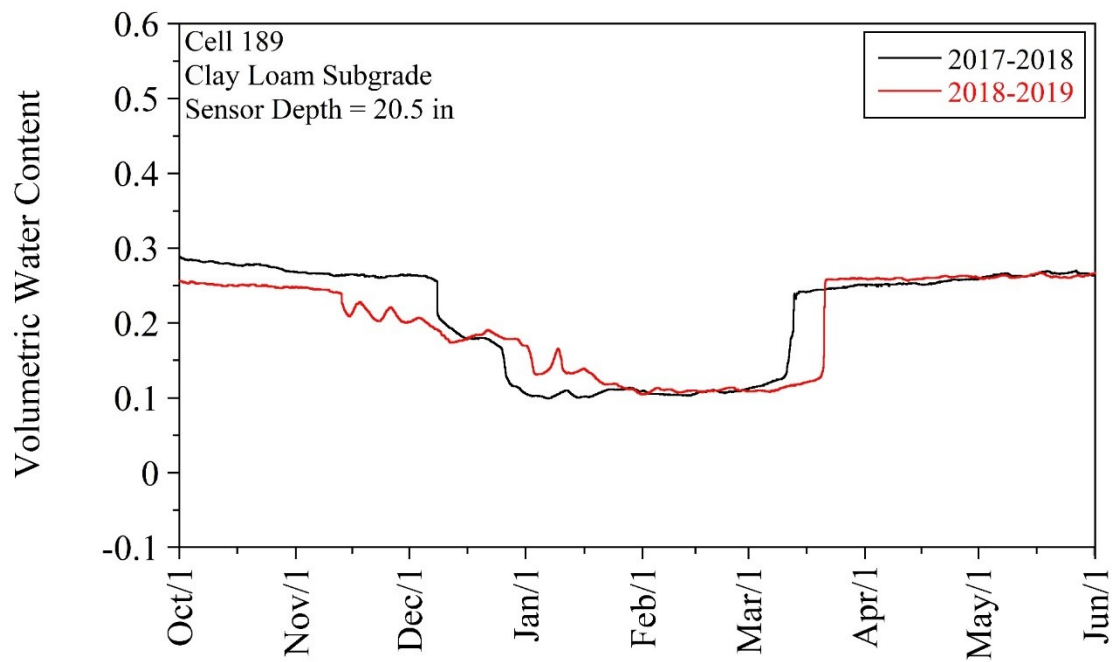
For Cell 189:



(the dates on the x-axis represent the time periods for both 2017-2018 and 2018-2019 years)

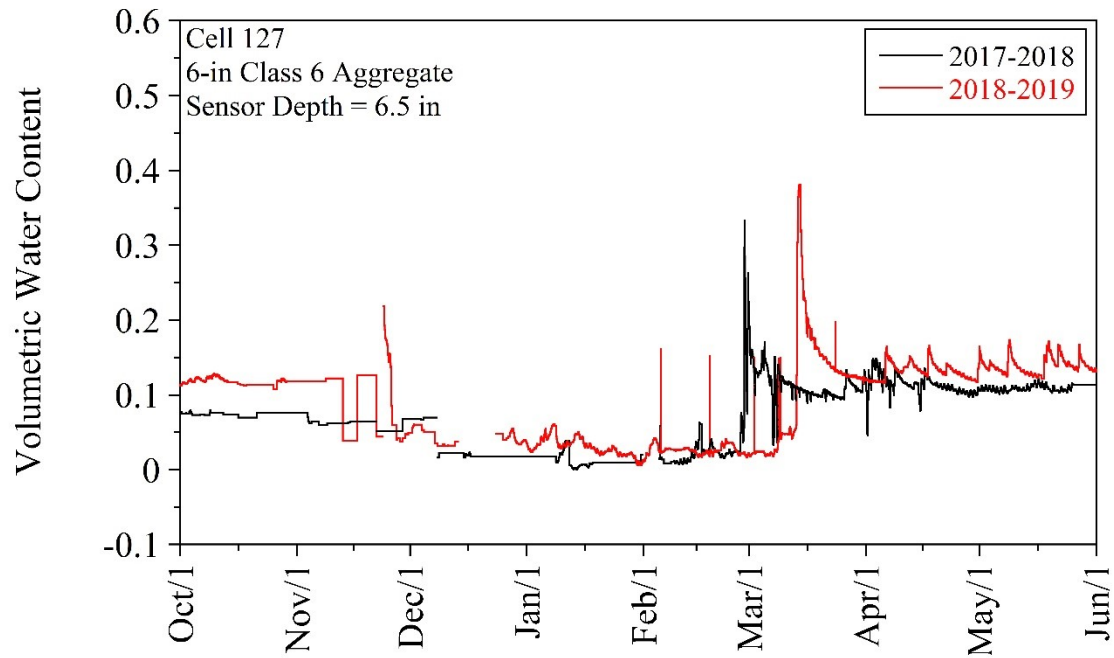


(the dates on the x-axis represent the time periods for both 2017-2018 and 2018-2019 years)

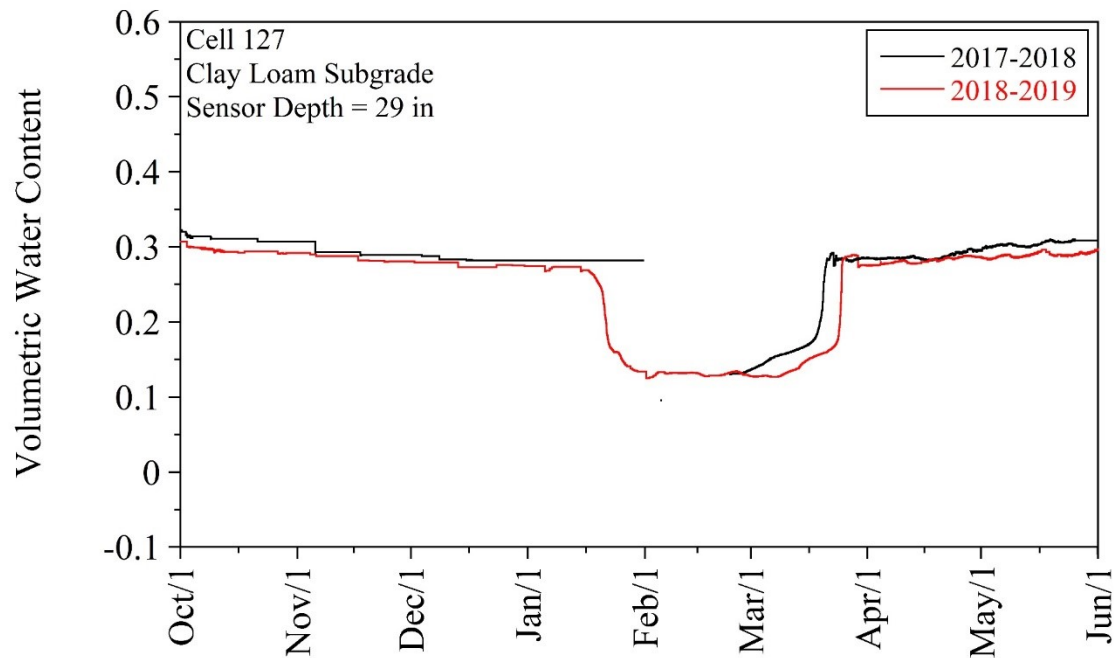


(the dates on the x-axis represent the time periods for both 2017-2018 and 2018-2019 years)

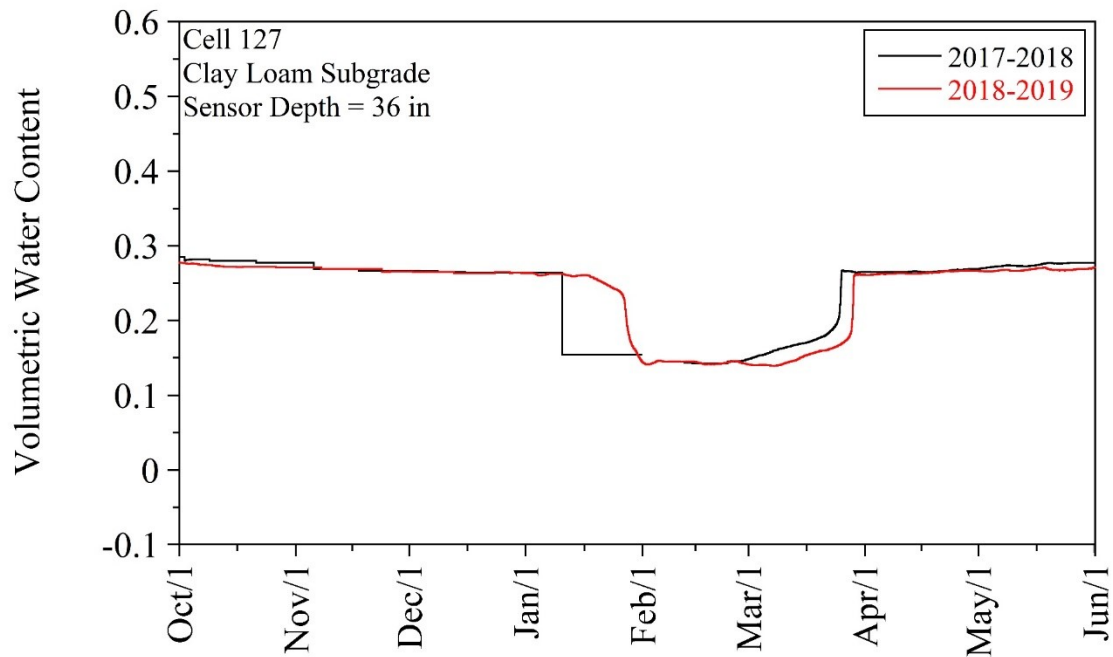
For Cell 127:



(the dates on the x-axis represent the time periods for both 2017-2018 and 2018-2019 years)

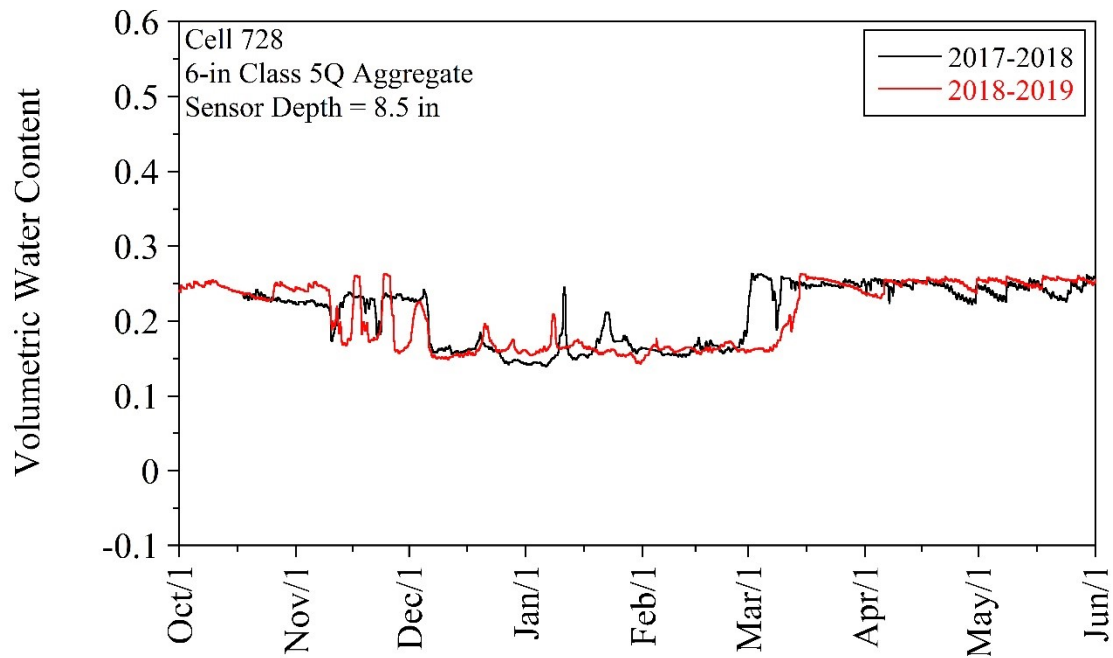


(the dates on the x-axis represent the time periods for both 2017-2018 and 2018-2019 years)

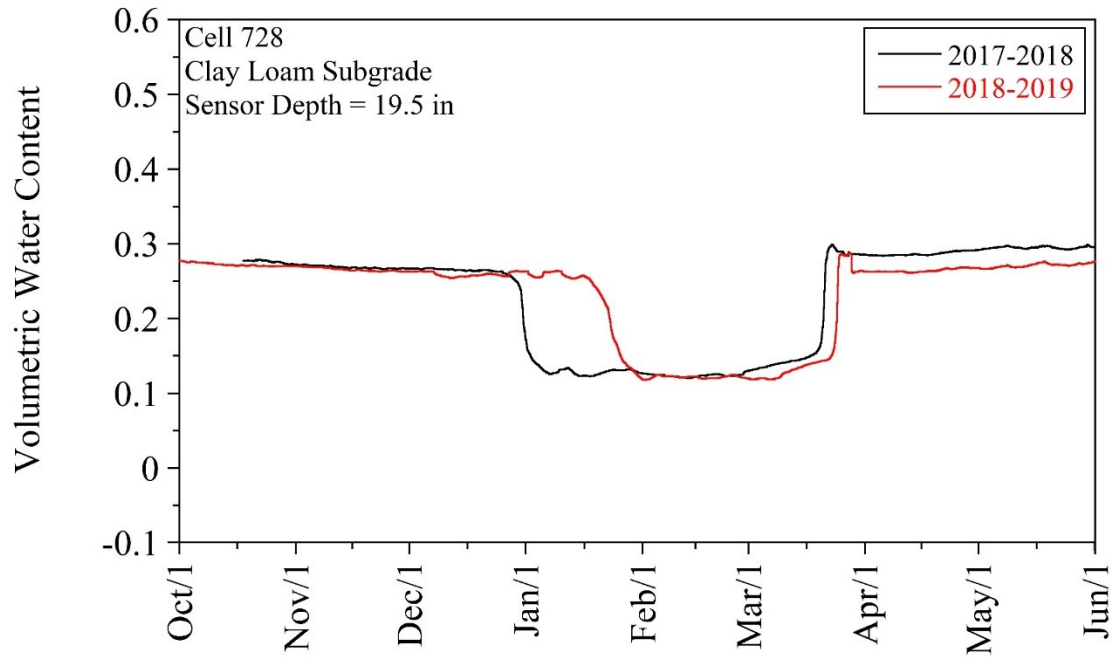


(the dates on the x-axis represent the time periods for both 2017-2018 and 2018-2019 years)

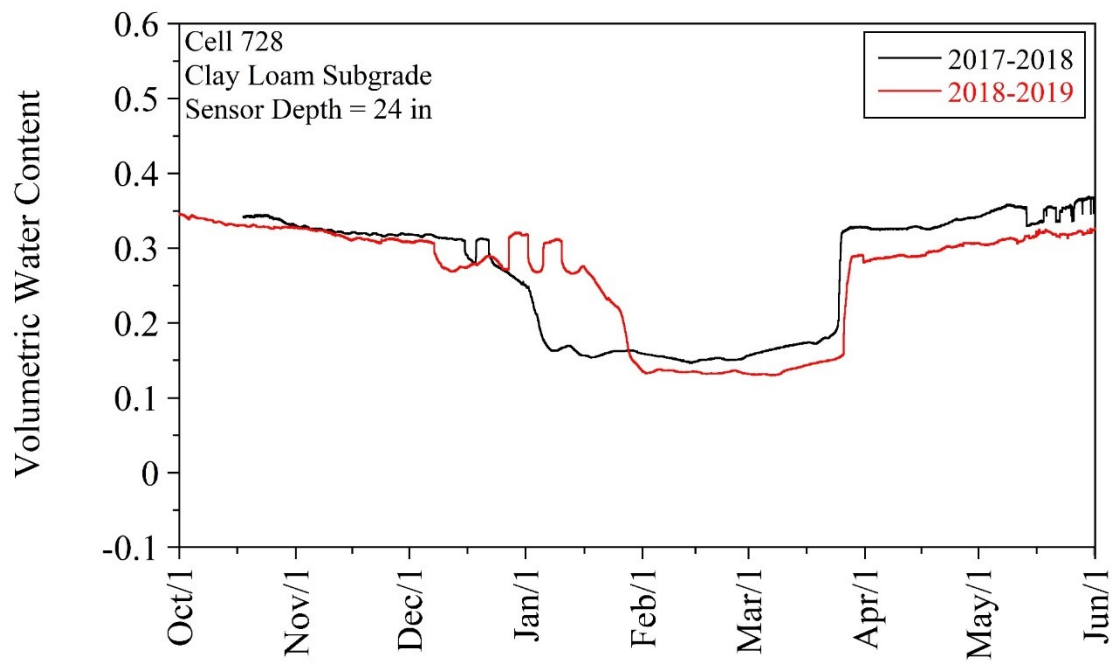
For Cell 728:



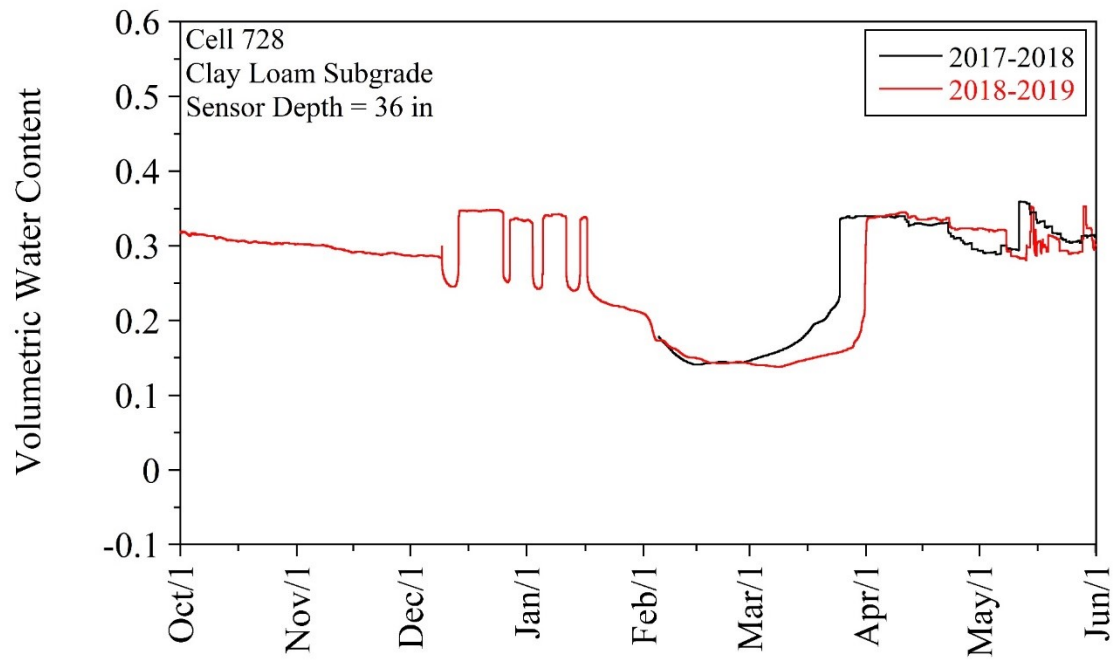
(the dates on the x-axis represent the time periods for both 2017-2018 and 2018-2019 years)



(the dates on the x-axis represent the time periods for both 2017-2018 and 2018-2019 years)



(the dates on the x-axis represent the time periods for both 2017-2018 and 2018-2019 years)

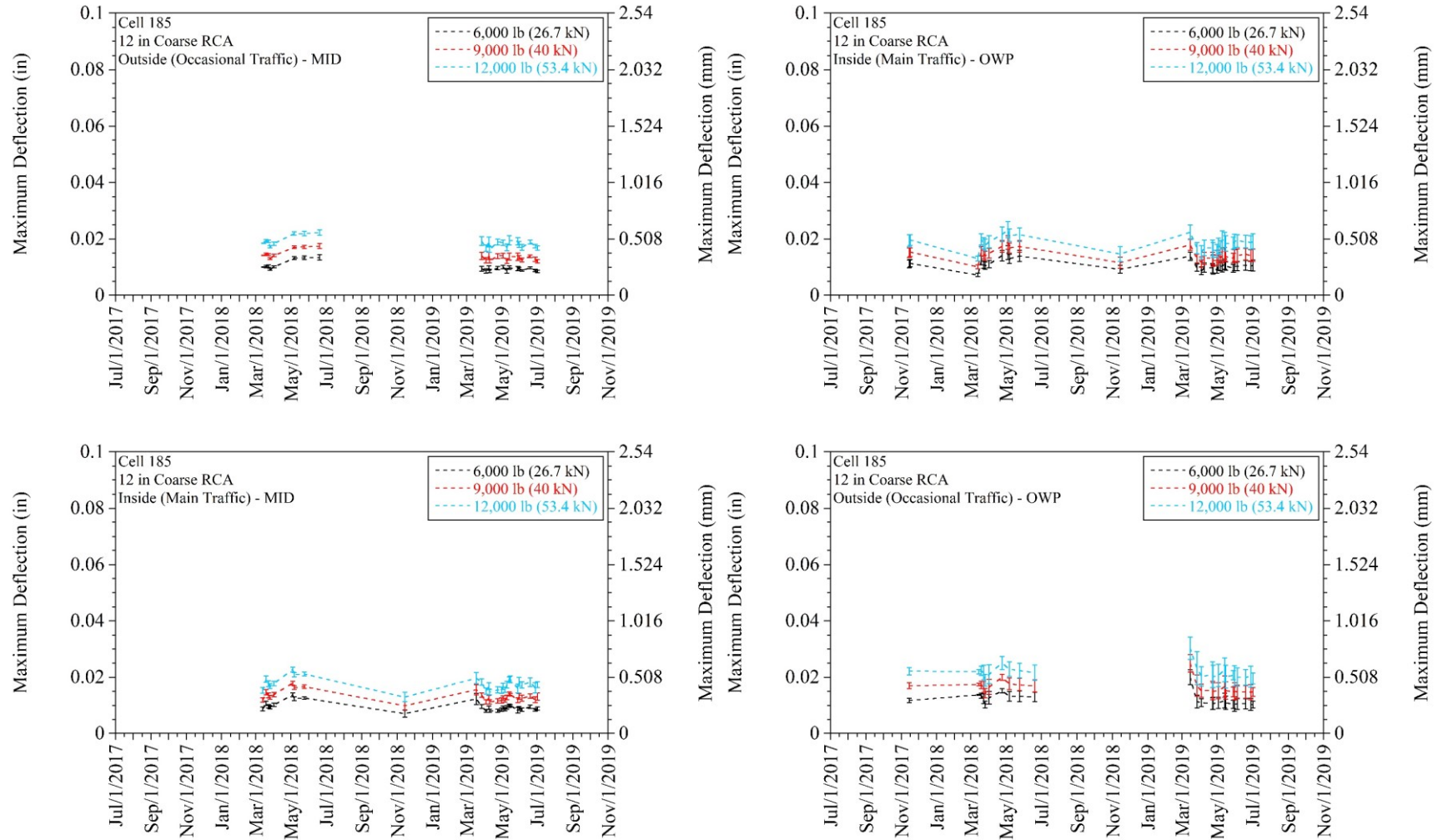


(the dates on the x-axis represent the time periods for both 2017-2018 and 2018-2019 years)

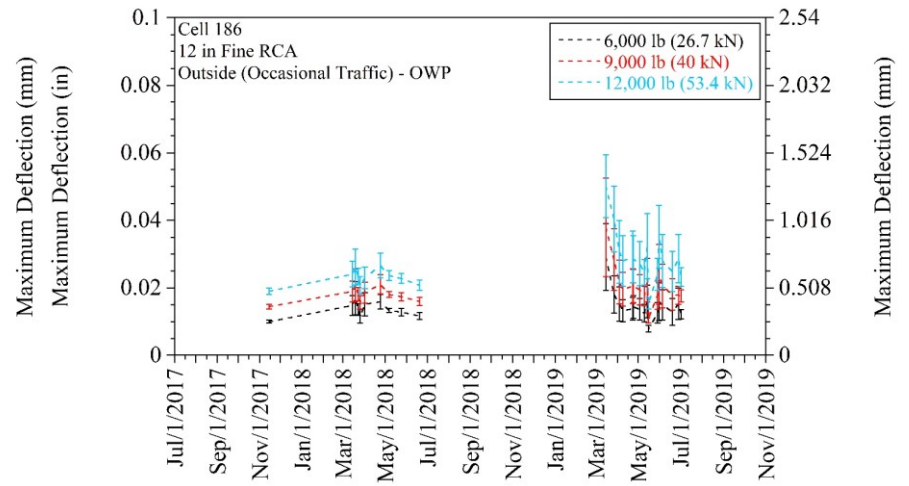
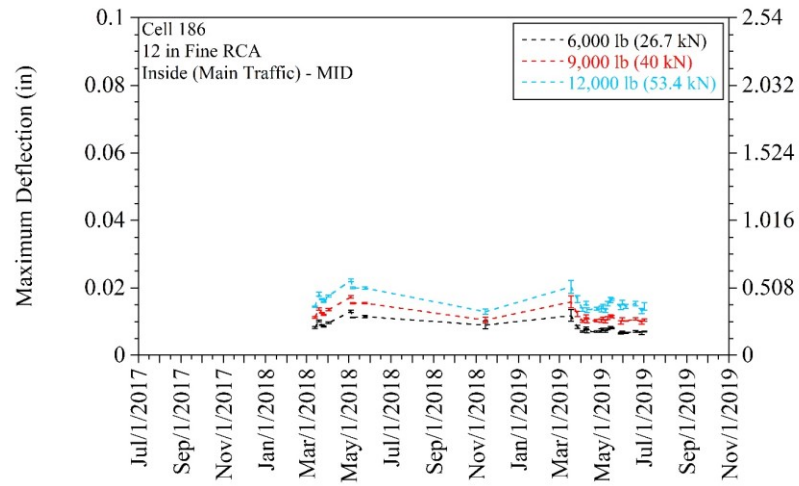
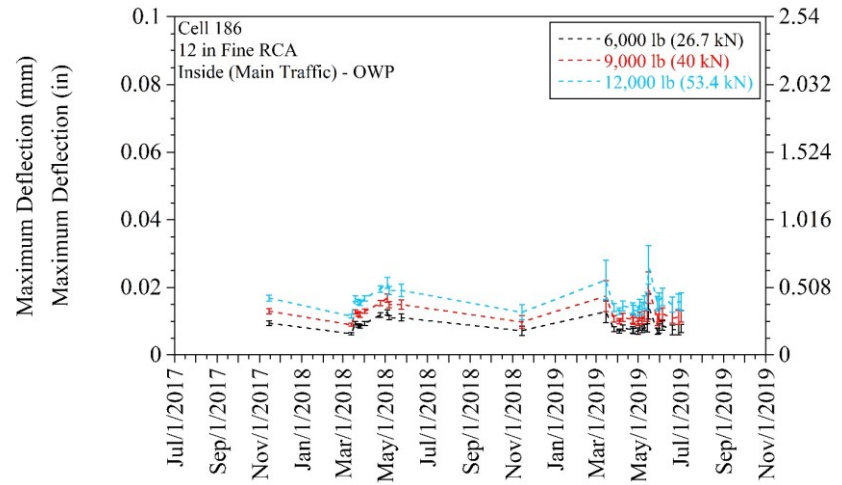
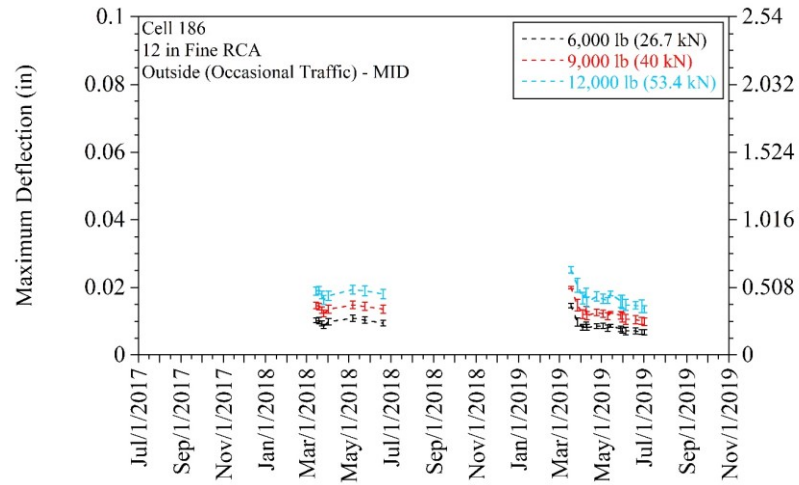
APPENDIX U

MAXIMUM DEFLECTION VALUES AT 6,000 LB (26.7 KN), 9,000 LB (40 KN), AND 12,000 LB (53.4 KN) FOR EACH CELL

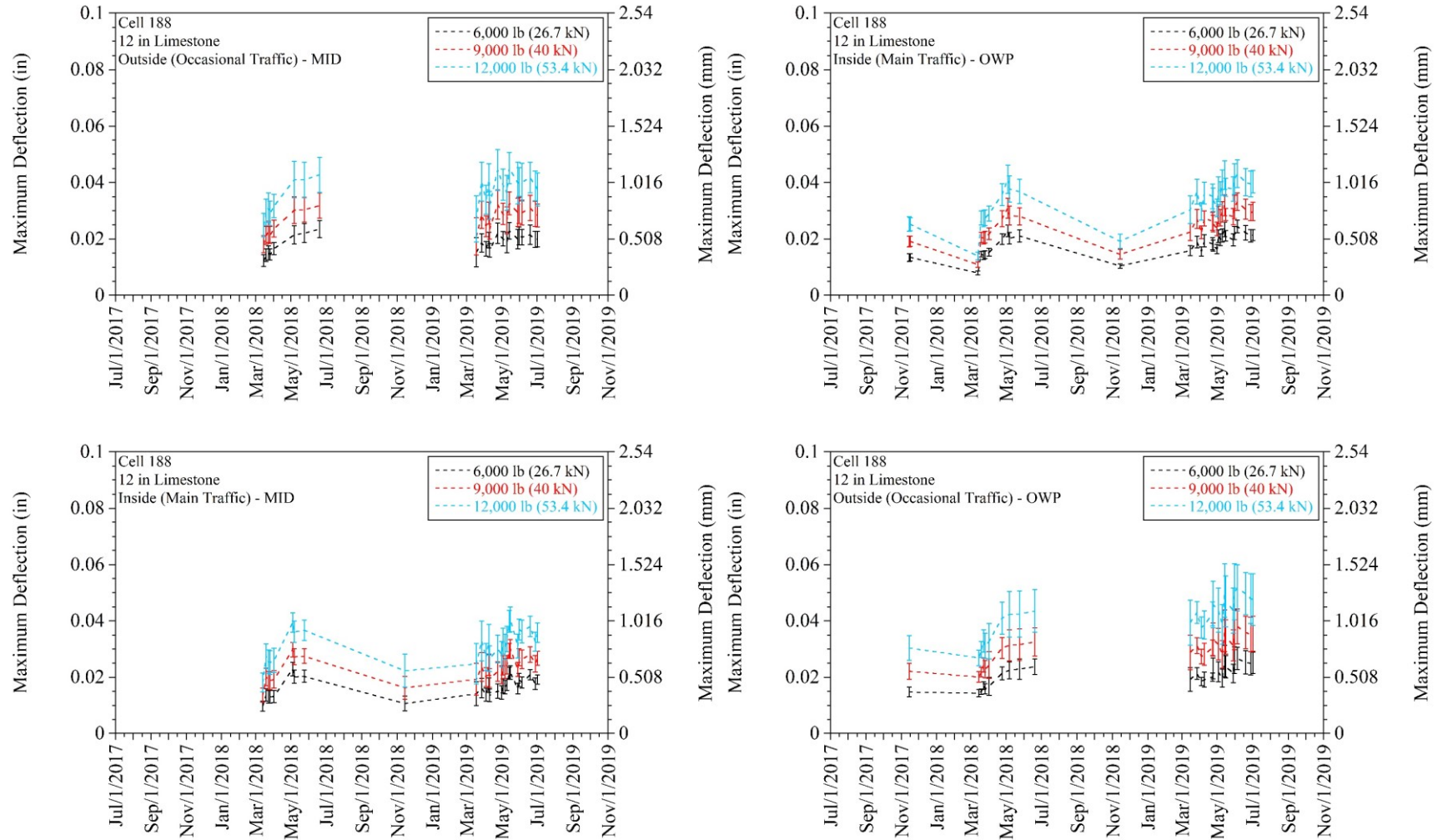
Cell 185 (12-in Coarse RCA) - maximum deflection (error bars represent one standard deviation of the data):



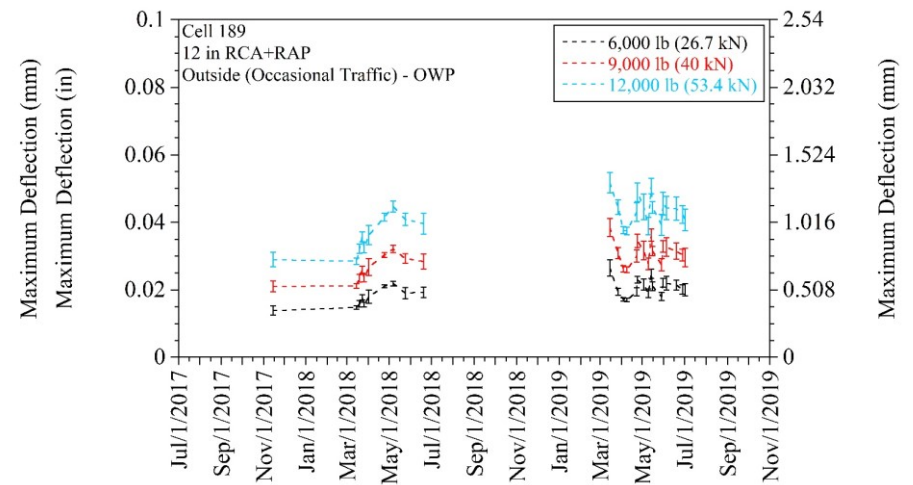
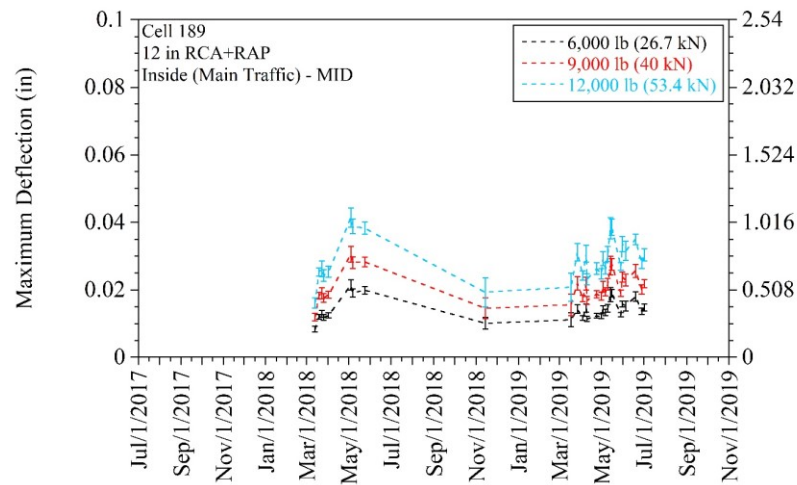
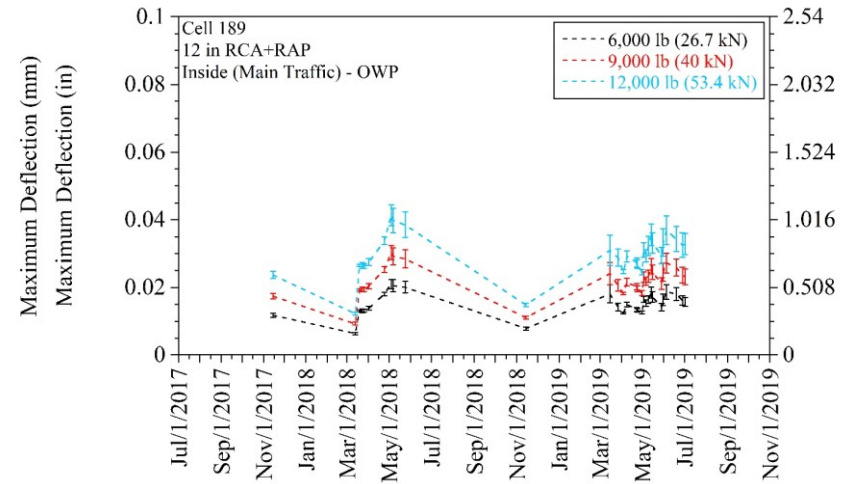
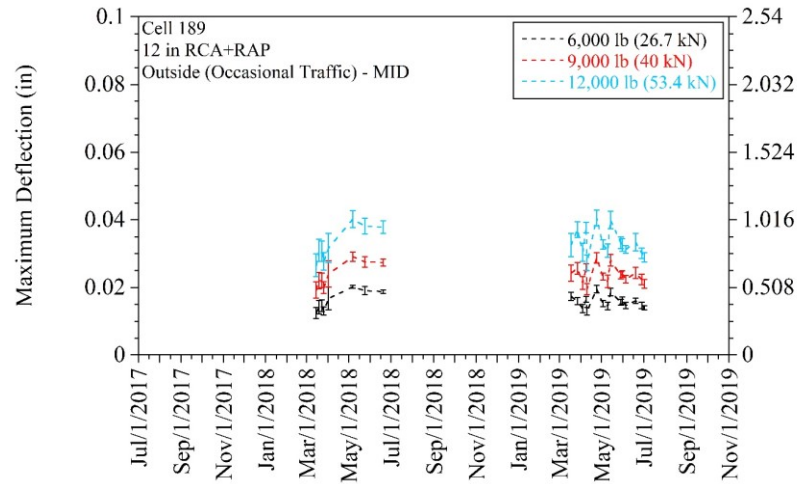
Cell 186 (12-in Fine RCA) - maximum deflection (error bars represent one standard deviation of the data):



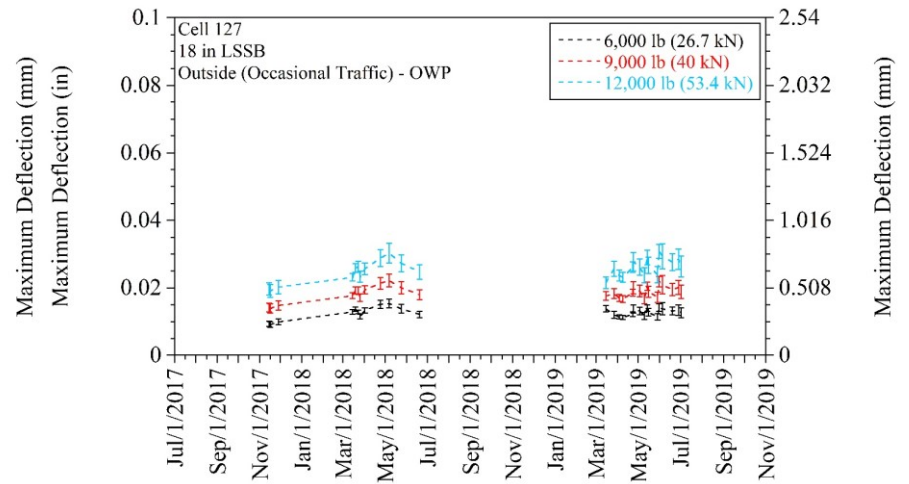
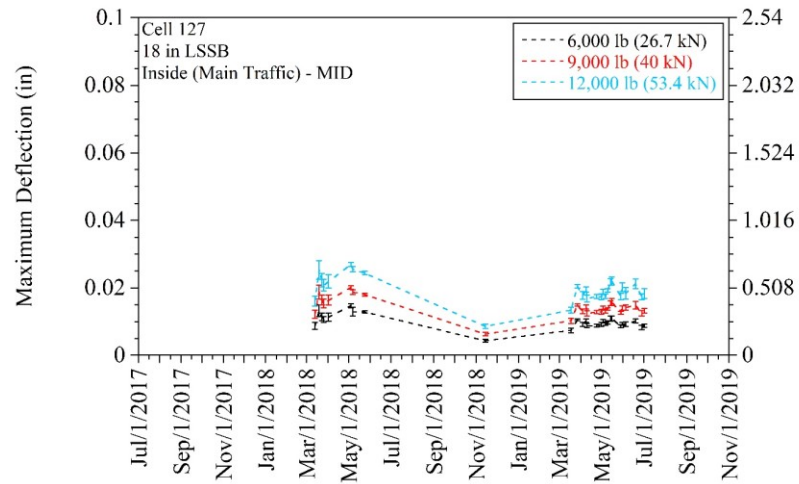
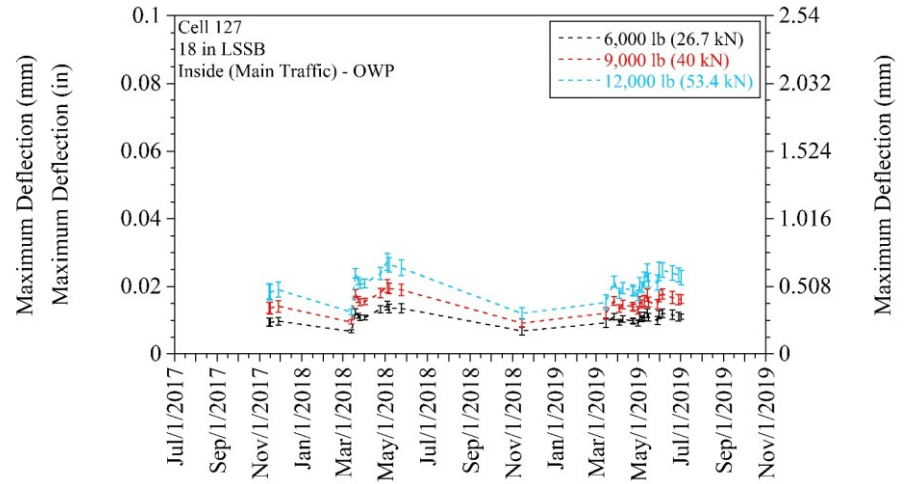
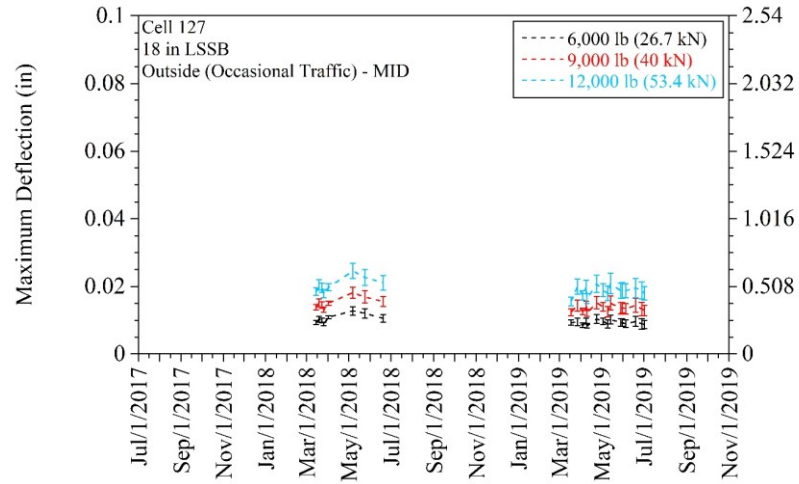
Cell 188 (12-in Limestone) - maximum deflection (error bars represent one standard deviation of the data):



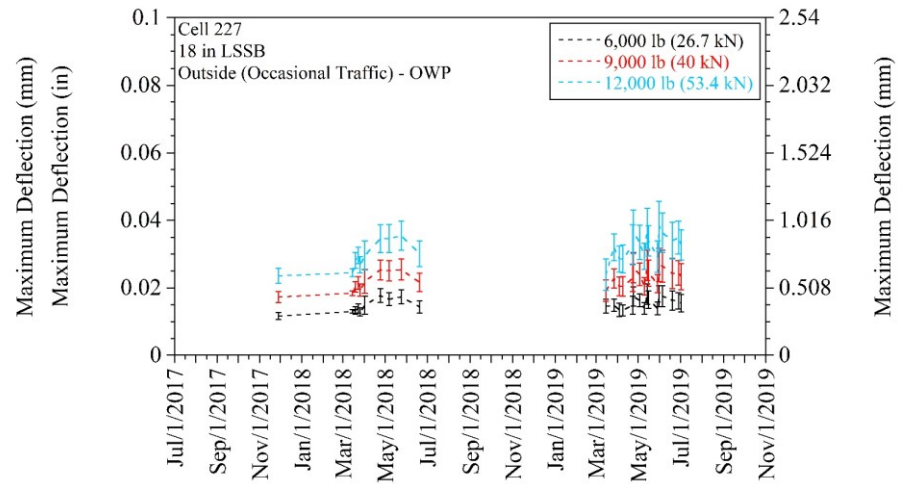
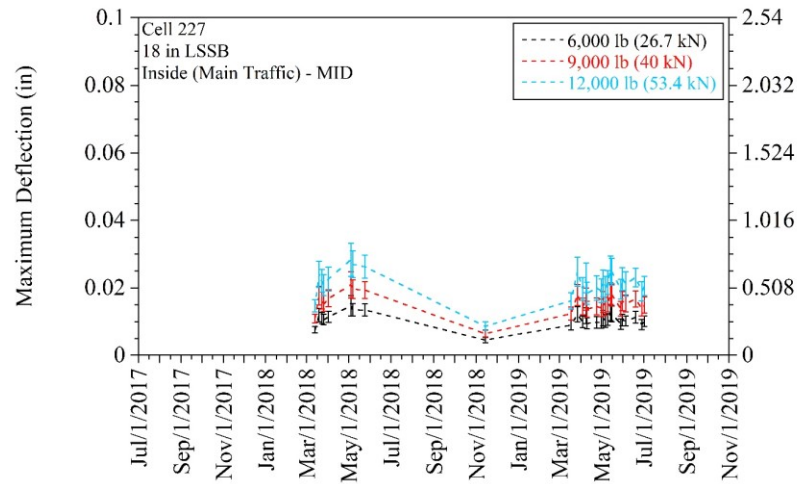
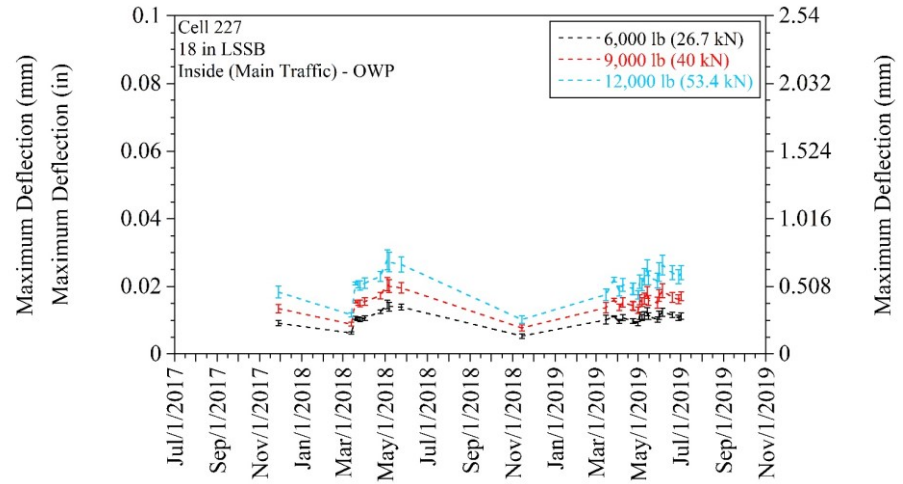
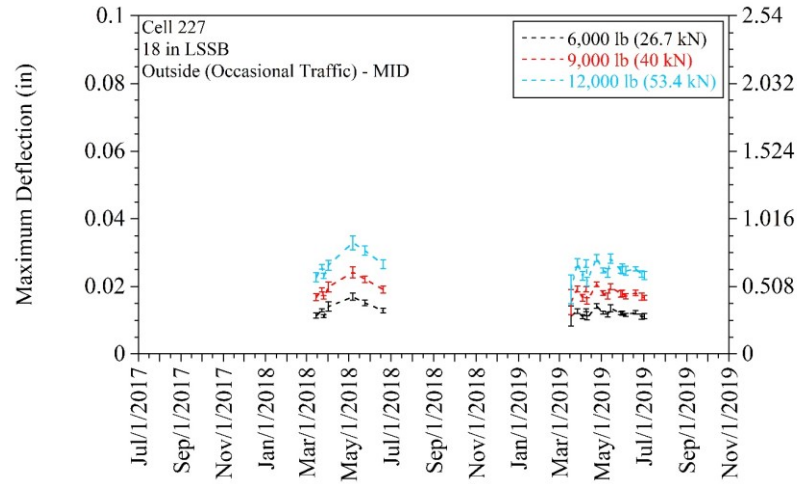
Cell 189 (12-in RCA+RAP) - maximum deflection (error bars represent one standard deviation of the data):



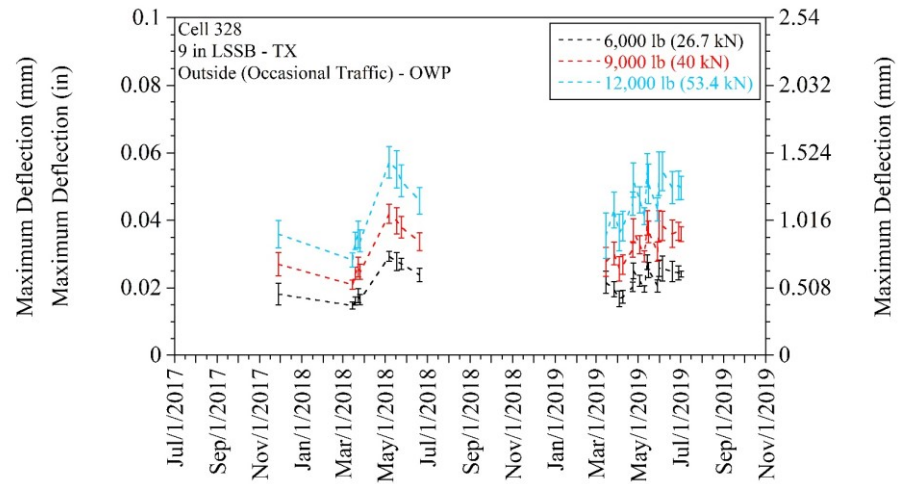
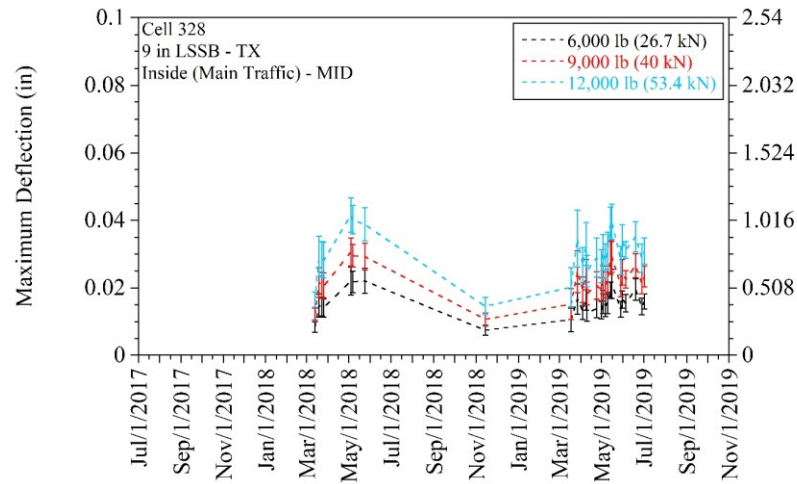
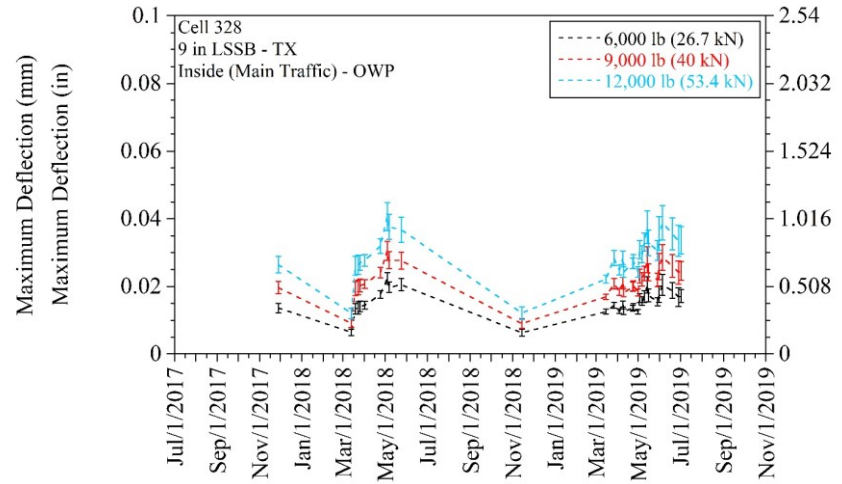
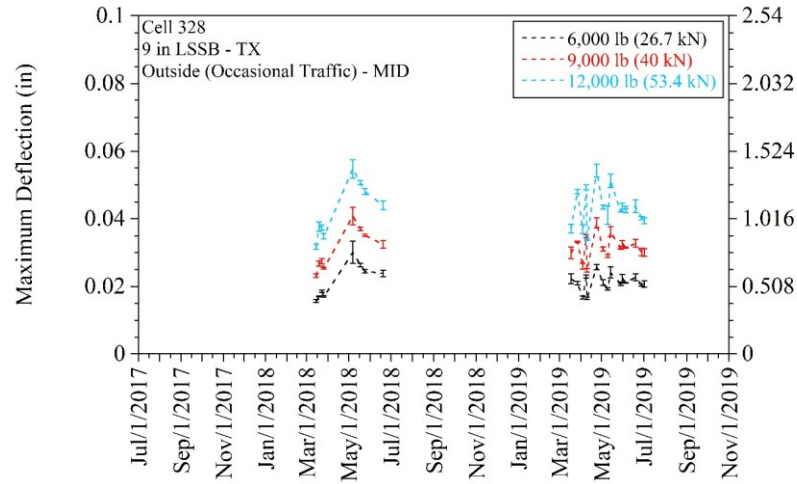
Cell 127 (18-in LSSB) - maximum deflection (error bars represent one standard deviation of the data):



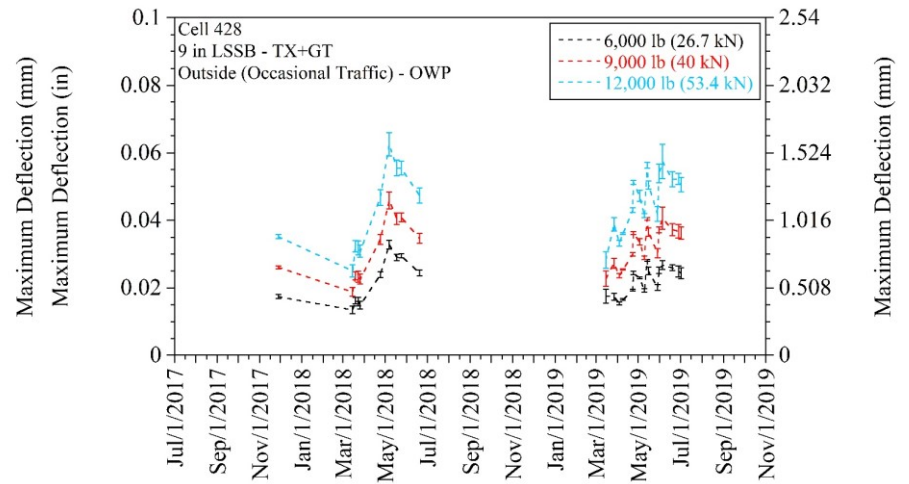
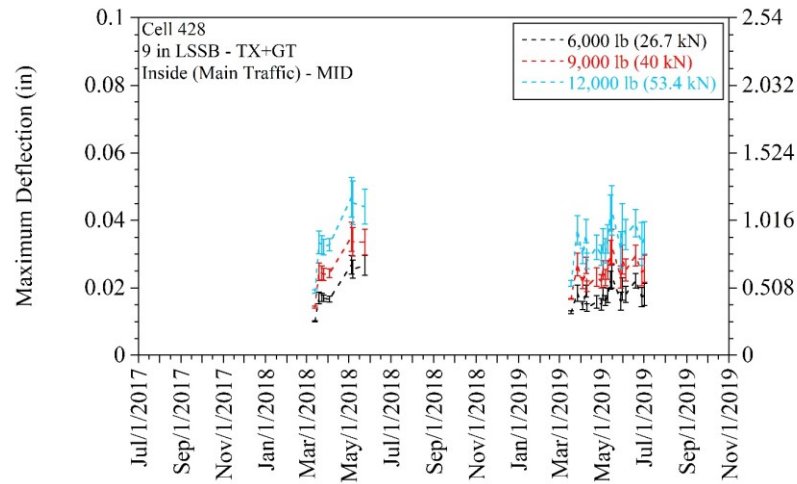
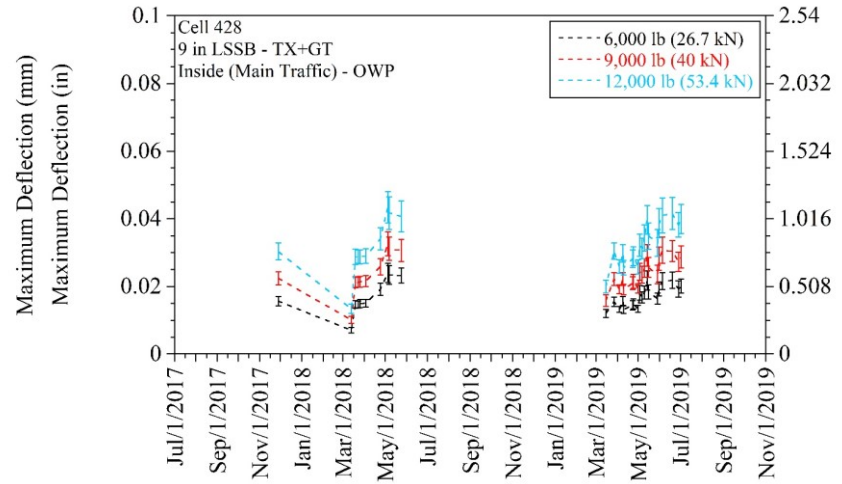
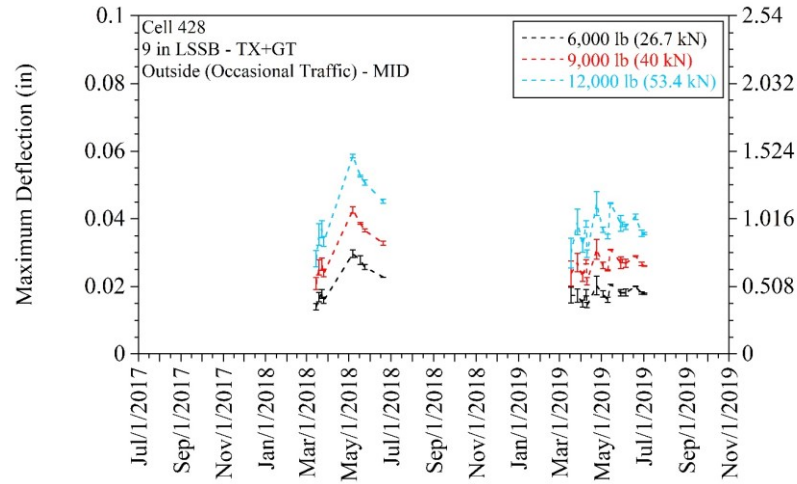
Cell 227 (18-in LSSB) - maximum deflection (error bars represent one standard deviation of the data):



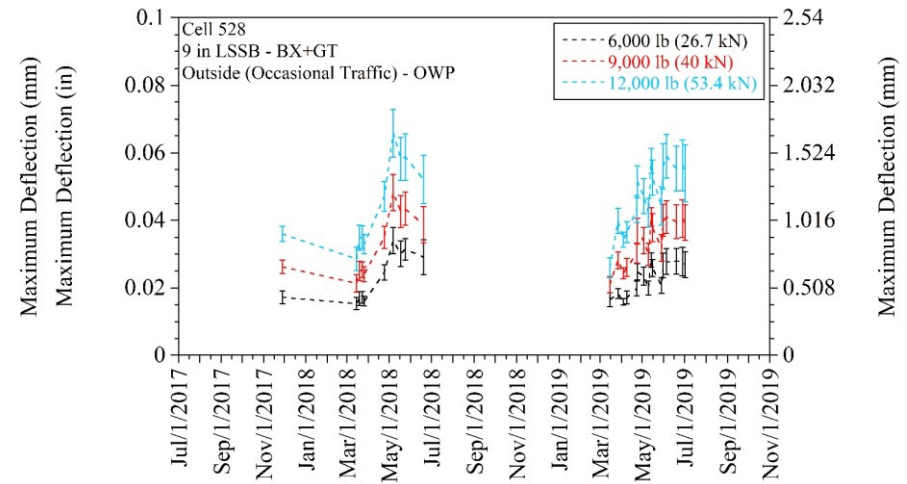
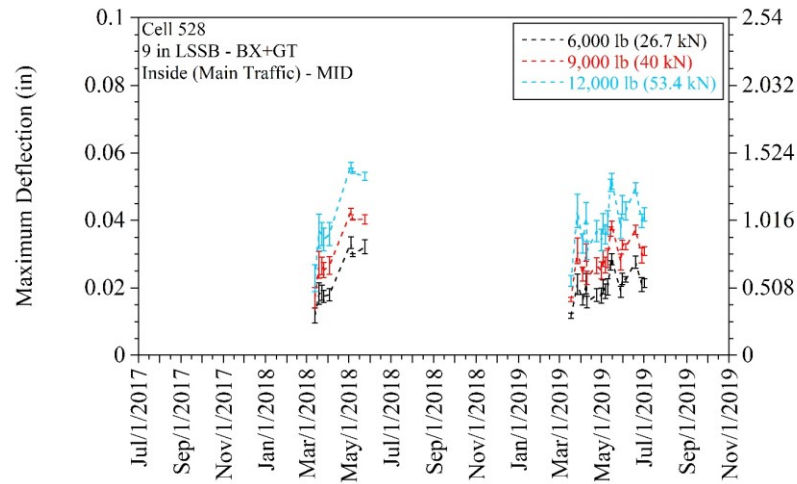
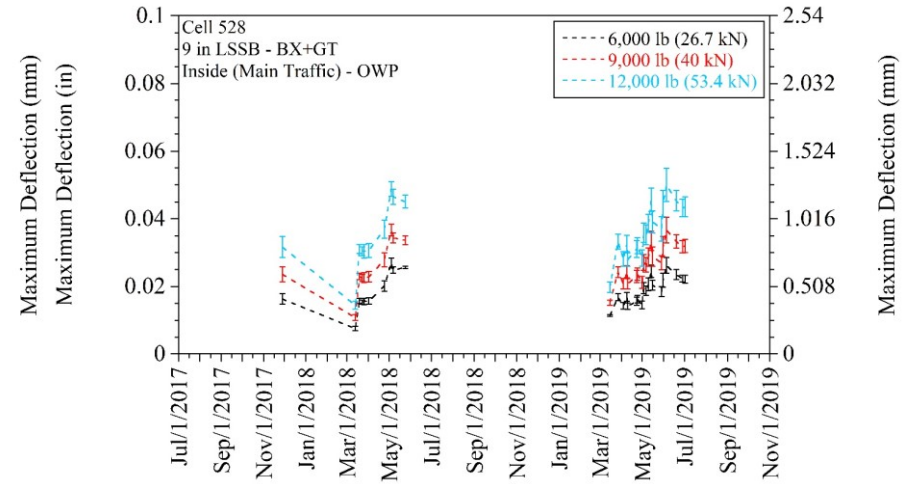
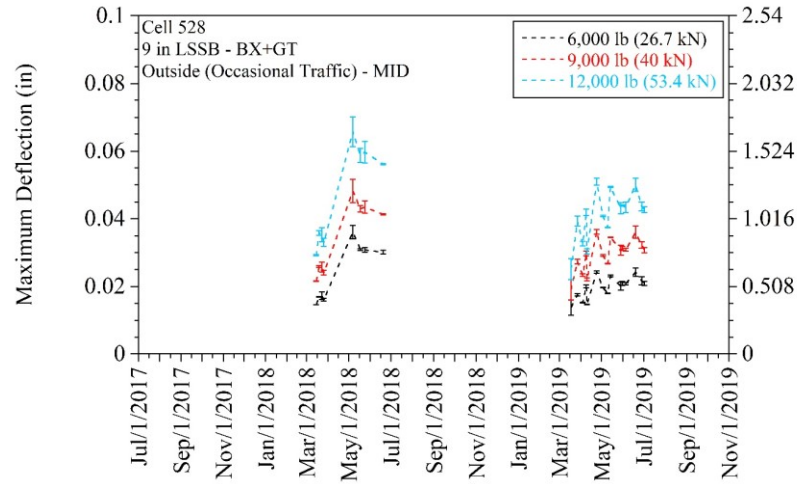
Cell 328 (9-in LSSB - TX) - maximum deflection (error bars represent one standard deviation of the data):



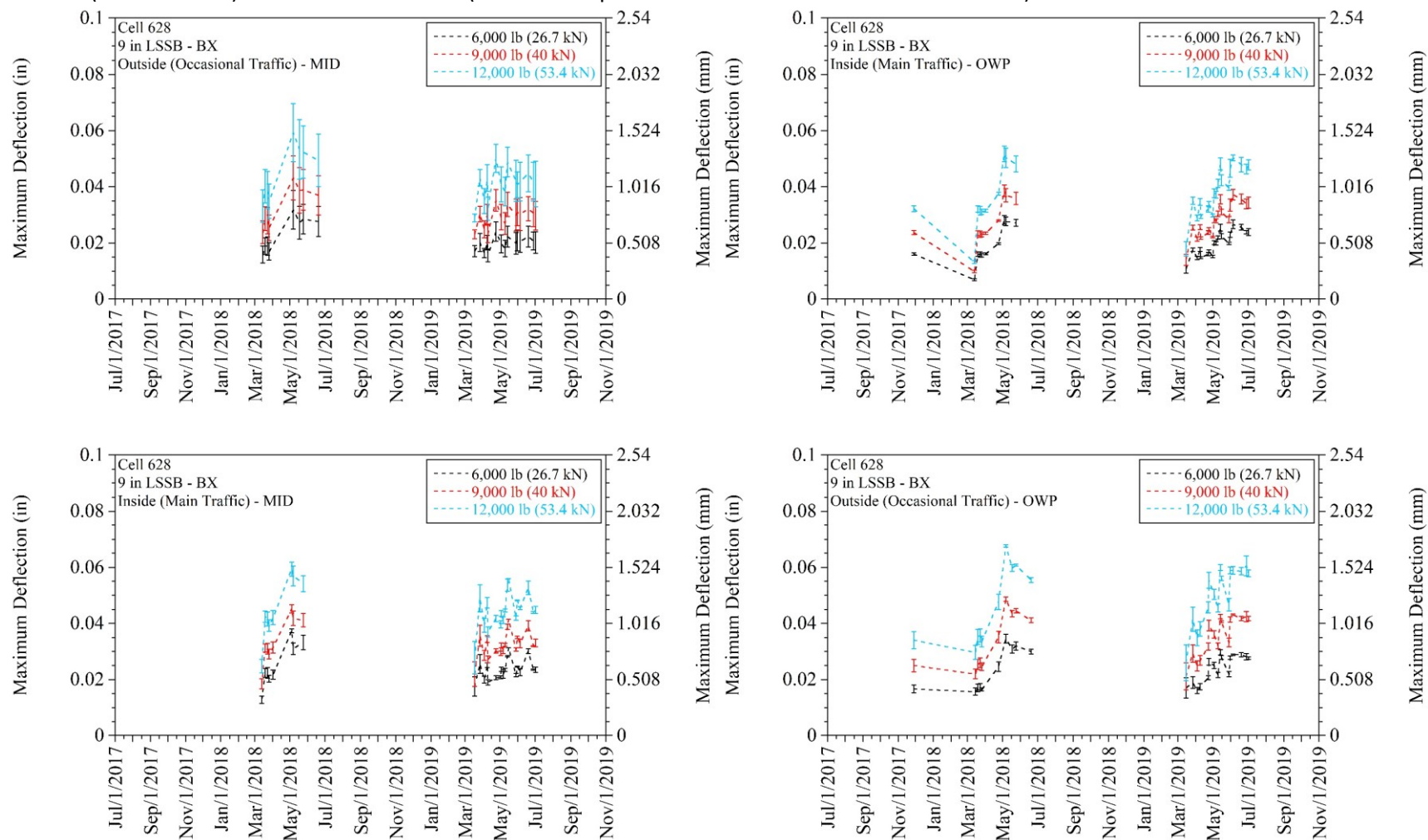
Cell 428 (9-in LSSB - TX+GT) - maximum deflection (error bars represent one standard deviation of the data):



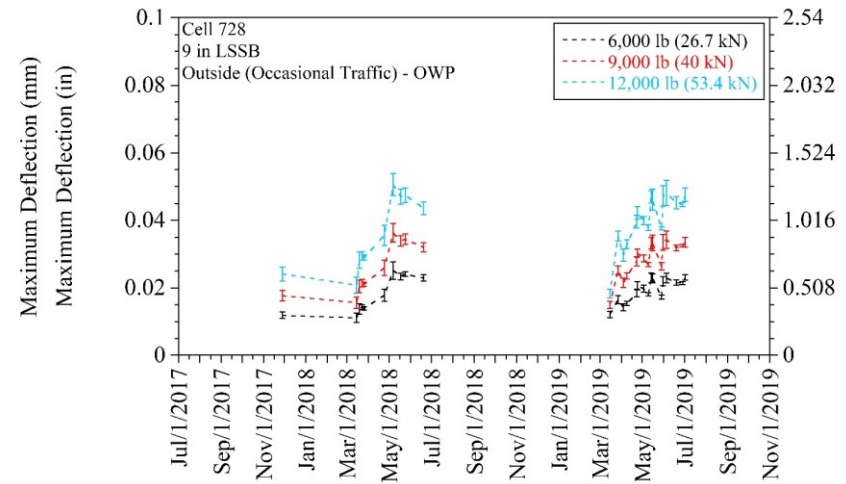
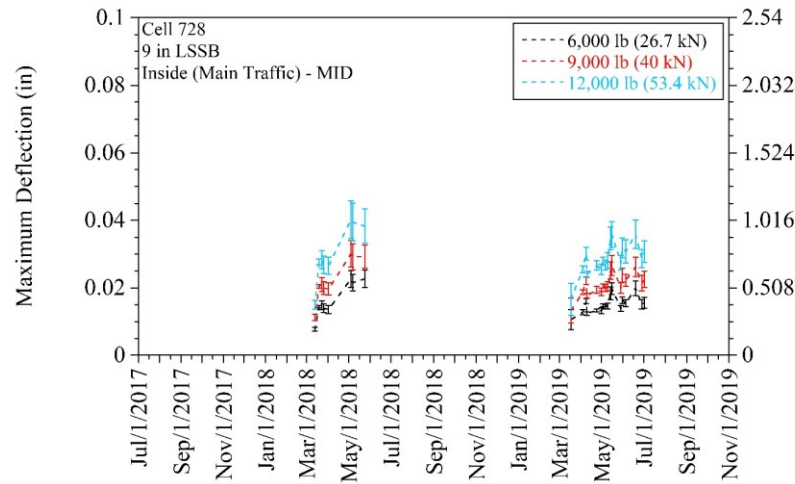
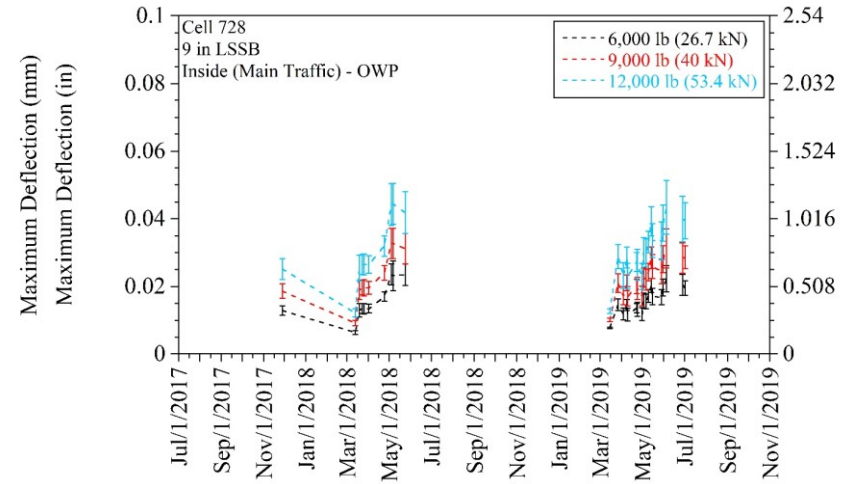
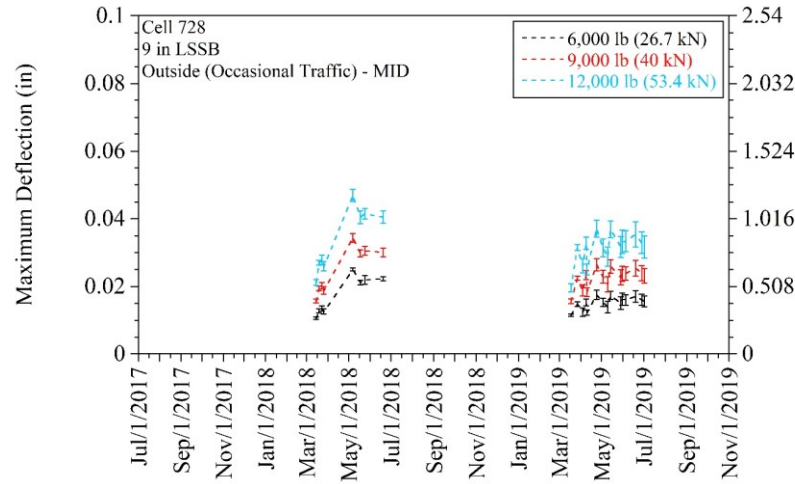
Cell 528 (9-in LSSB - BX+GT) - maximum deflection (error bars represent one standard deviation of the data):



Cell 628 (9-in LSSB - BX) - maximum deflection (error bars represent one standard deviation of the data):



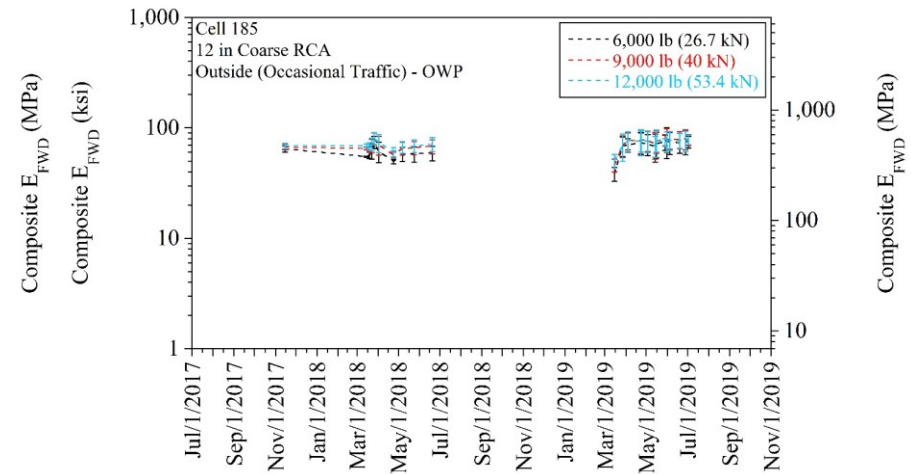
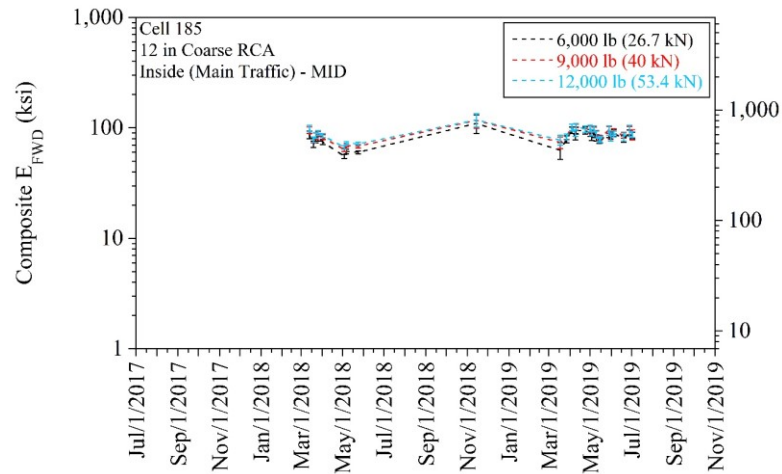
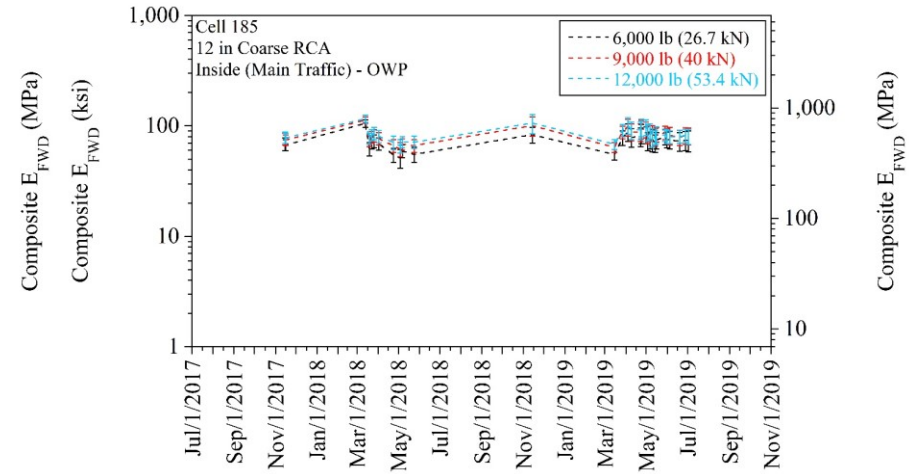
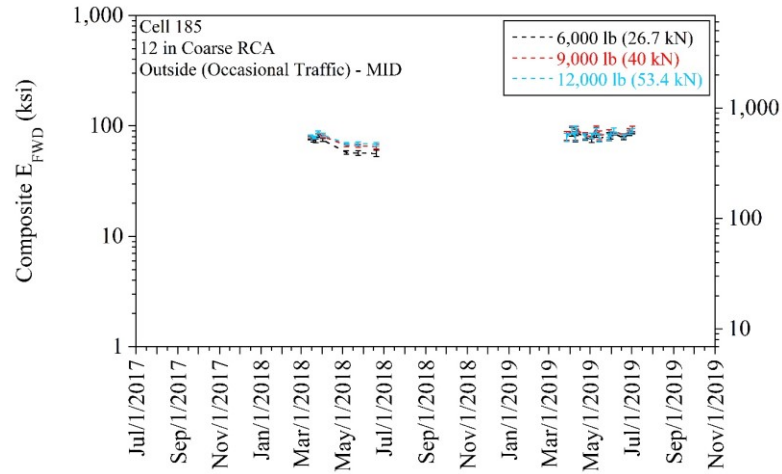
Cell 728 (9-in LSSB) - maximum deflection (error bars represent one standard deviation of the data):



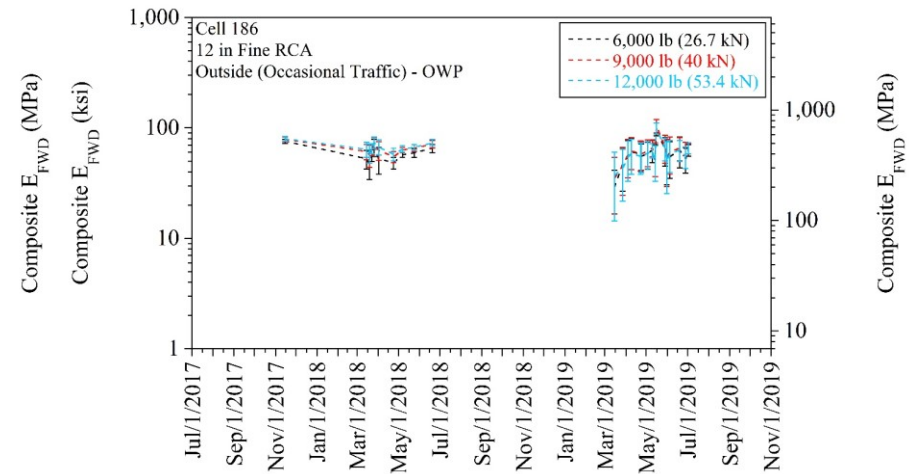
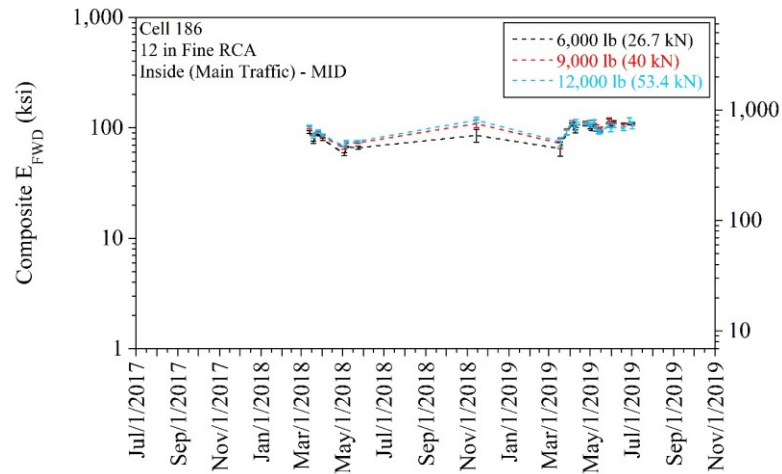
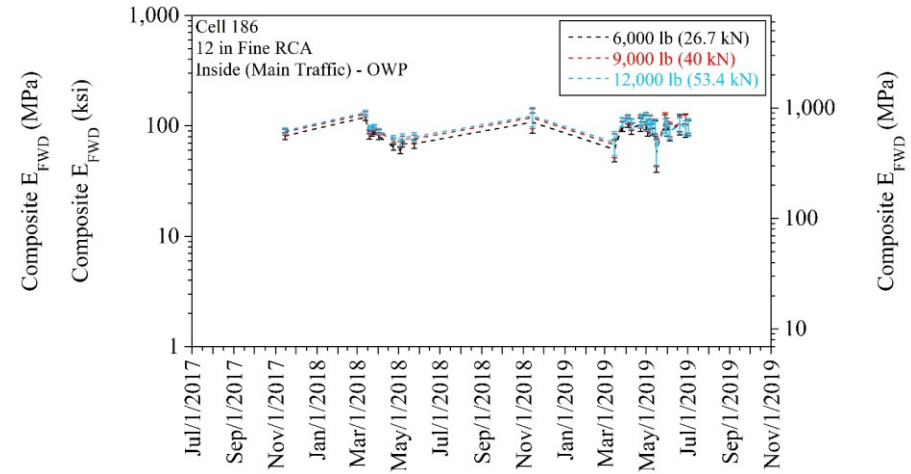
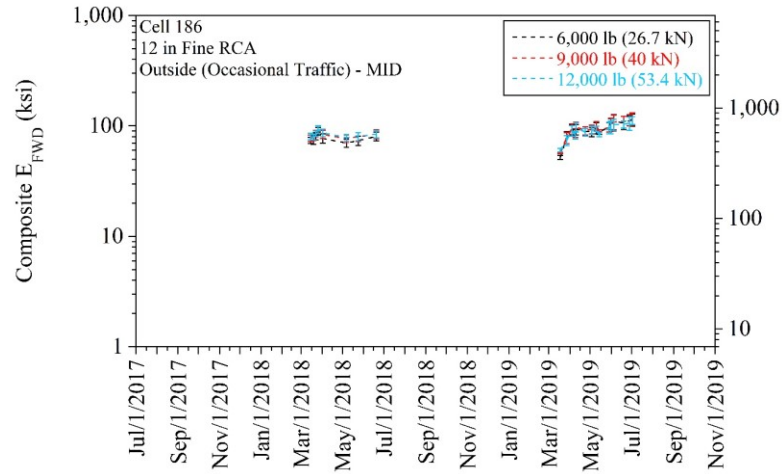
APPENDIX V

COMPOSITE FALLING WEIGHT DEFLECTOMETER (FWD) ELASTIC MODULUS (E_{FWD}) VALUES AT 6,000 LB (26.7 KN), 9,000 LB (40 KN), AND 12,000 LB (53.4 KN) FOR EACH CELL

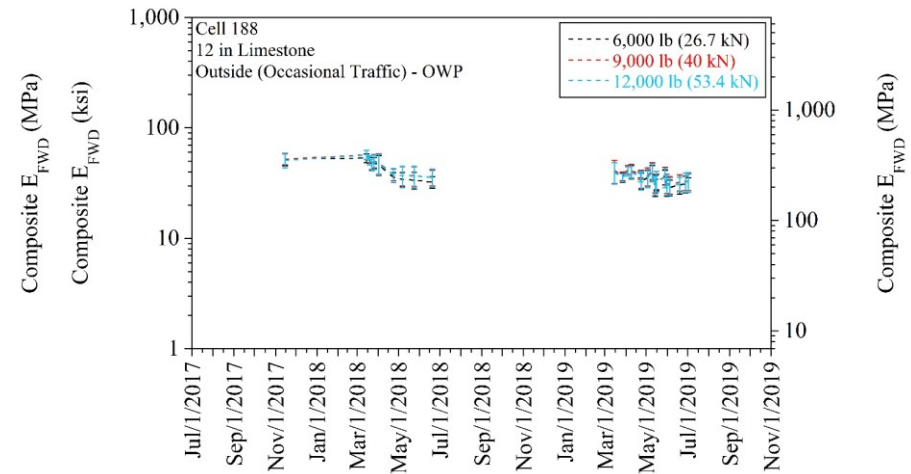
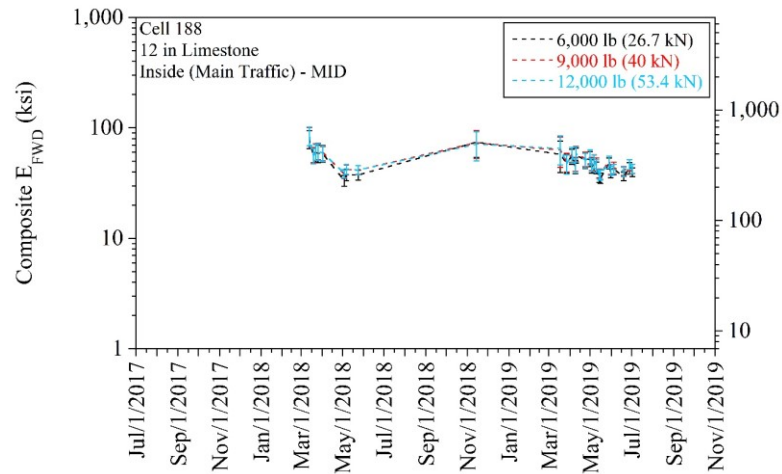
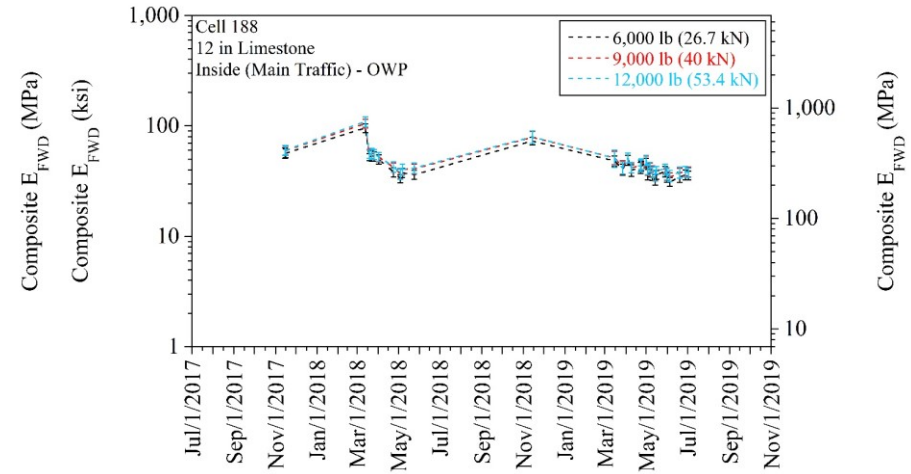
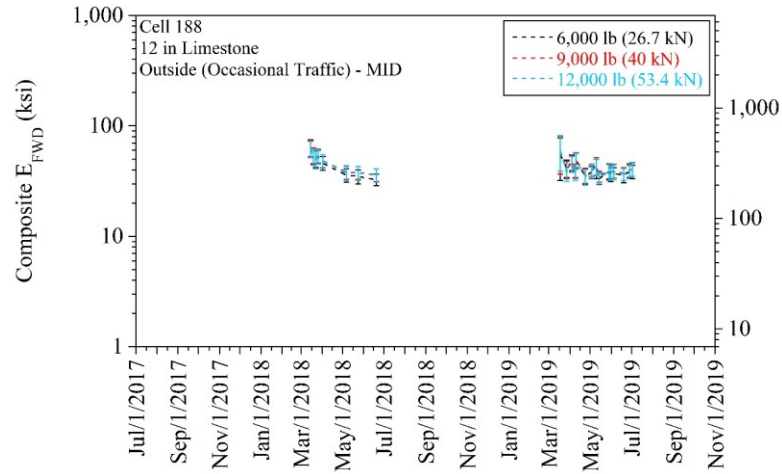
Cell 185 (12-in Coarse RCA) - composite E_{FWD} (error bars represent one standard deviation of the data):



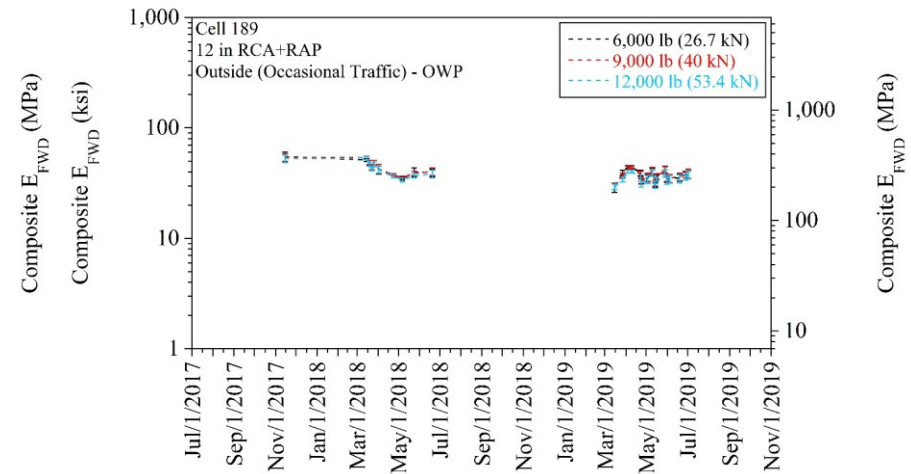
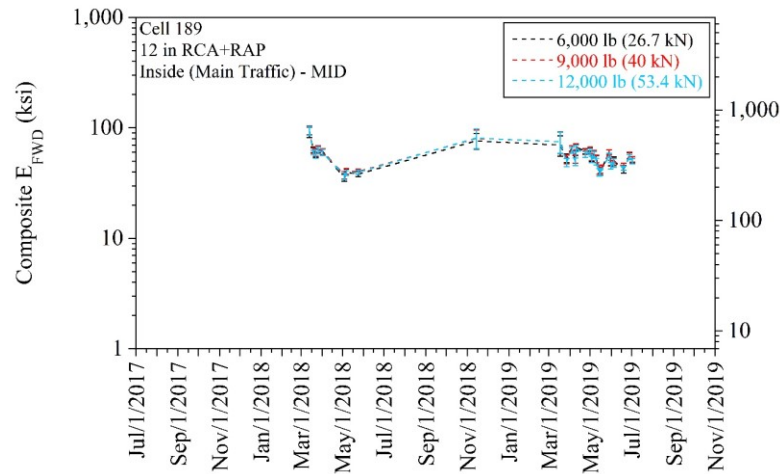
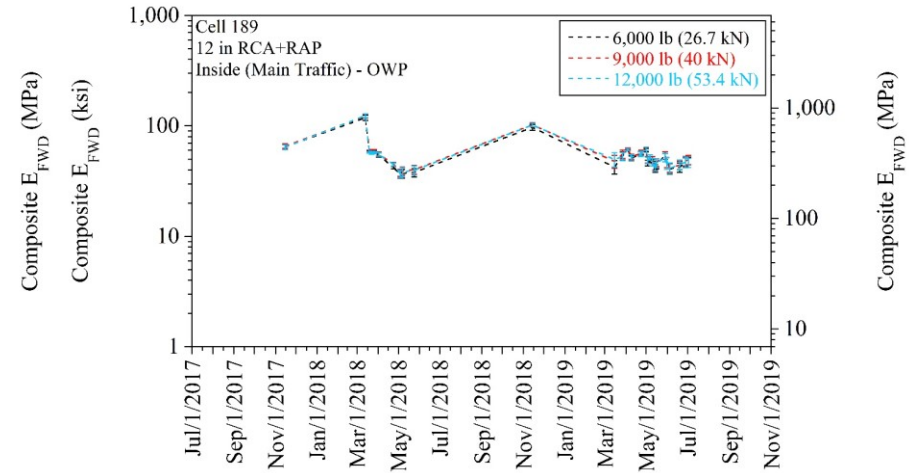
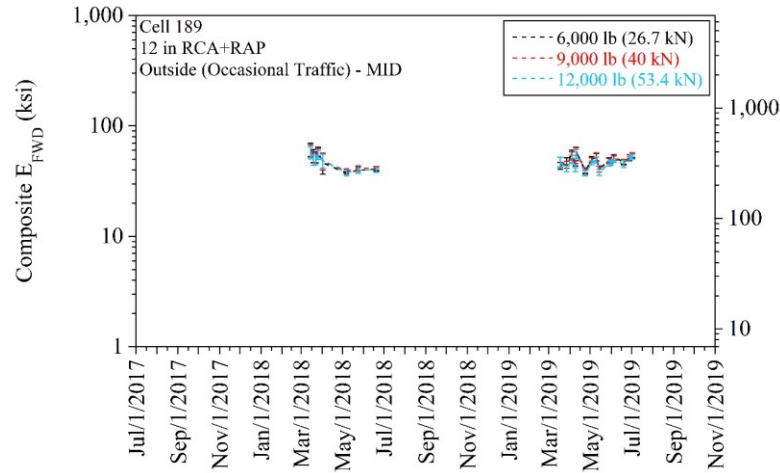
Cell 186 (12-in Fine RCA) - composite E_{FWD} (error bars represent one standard deviation of the data):



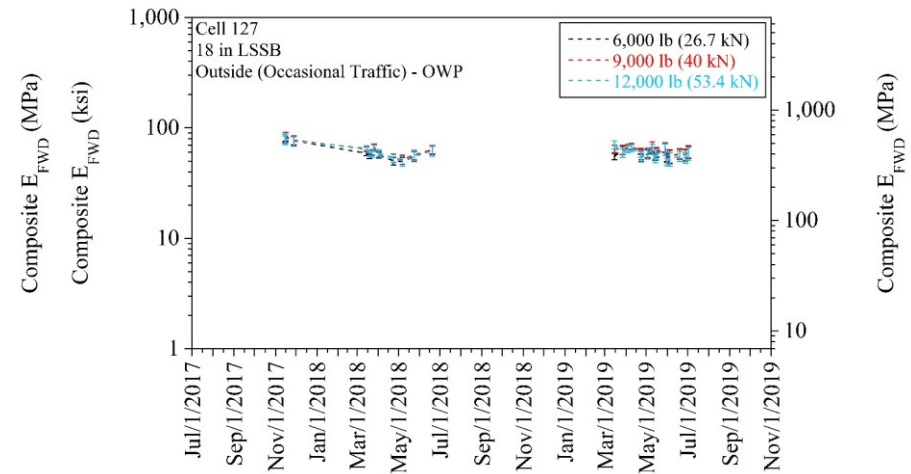
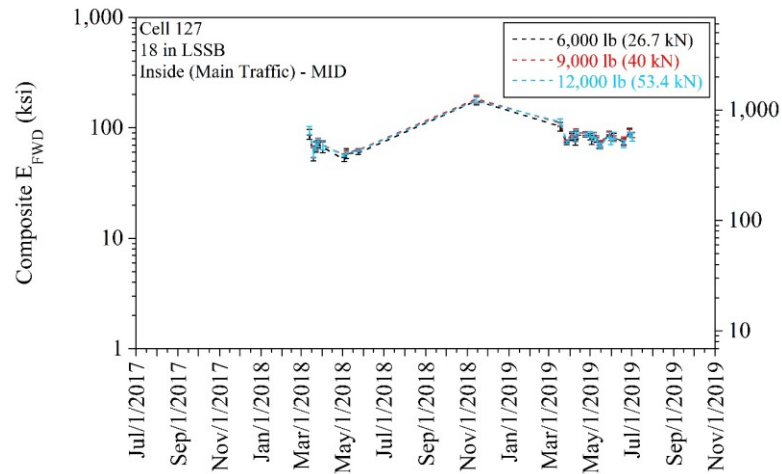
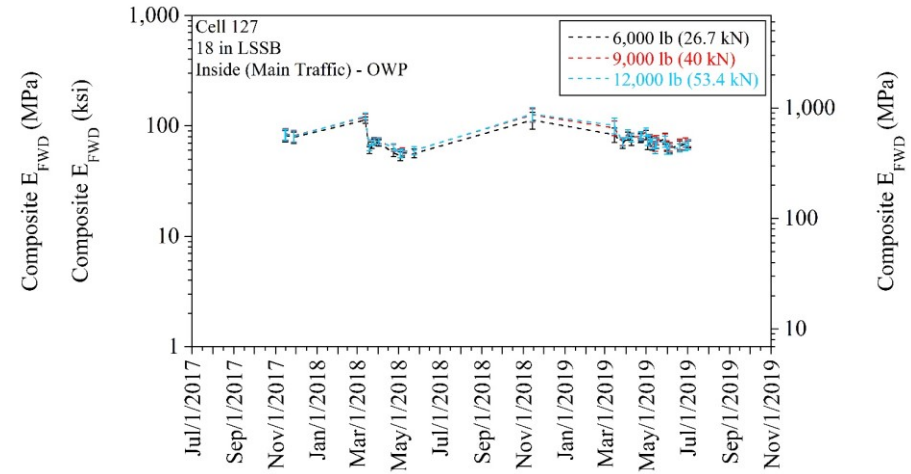
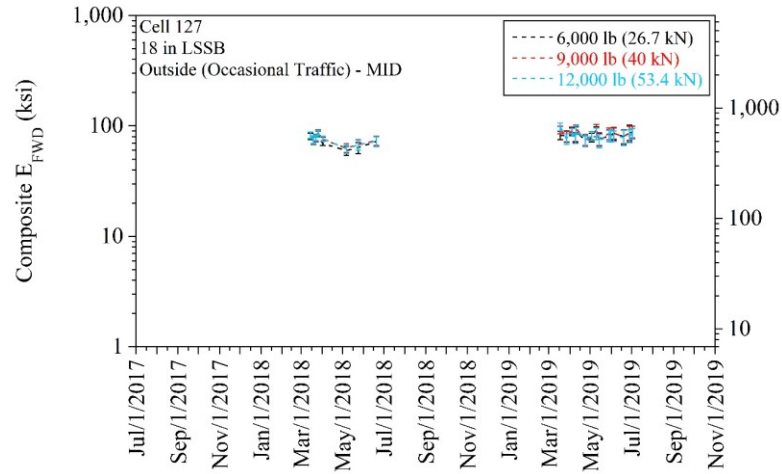
Cell 188 (12-in Limestone) - composite E_{FWD} (error bars represent one standard deviation of the data):



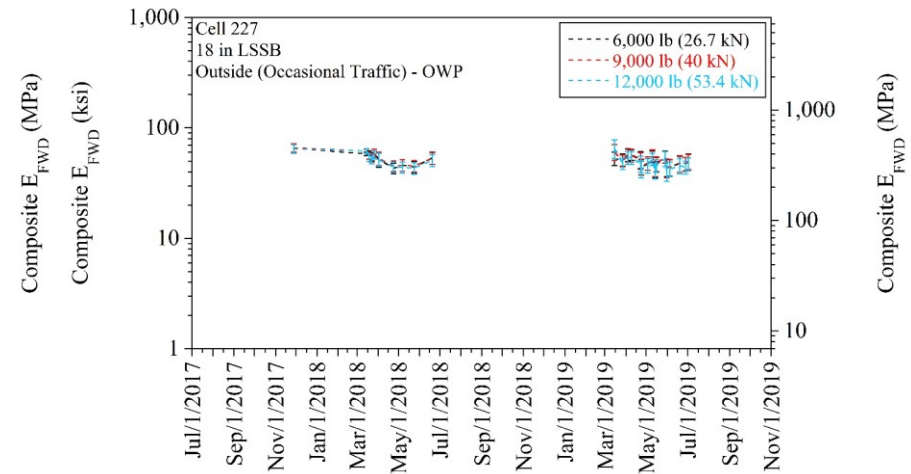
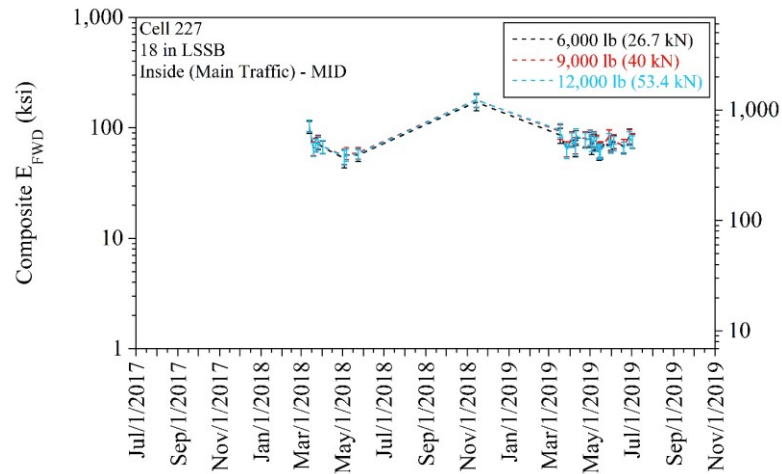
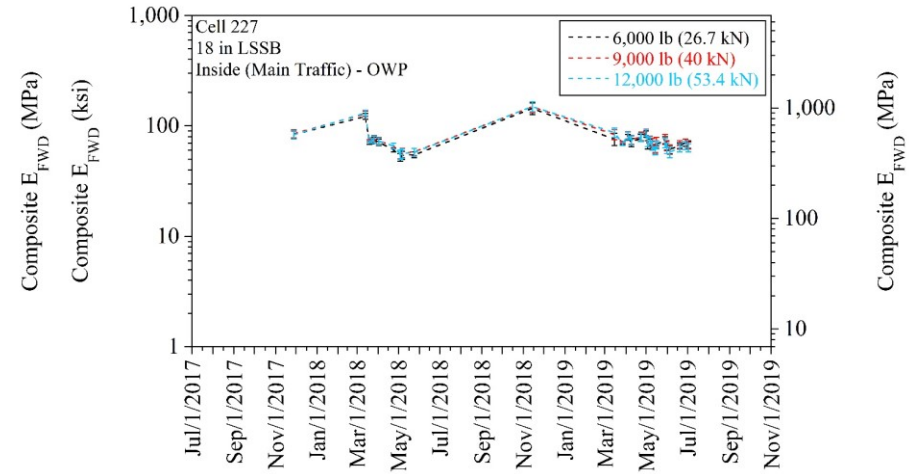
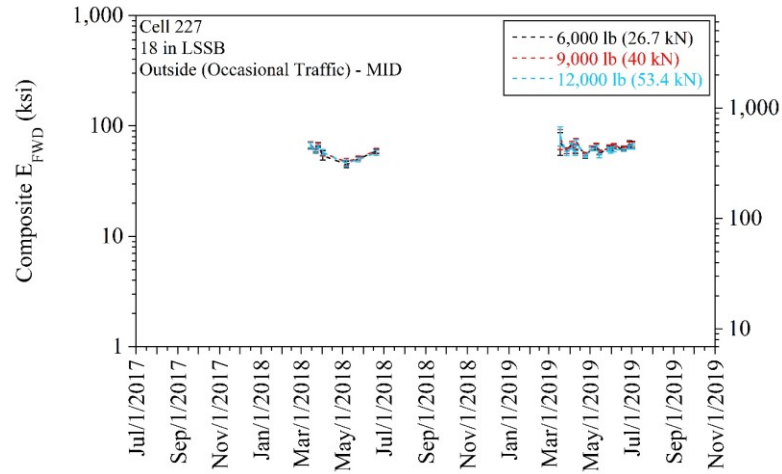
Cell 189 (12-in RCA+RAP) - composite E_{FWD} (error bars represent one standard deviation of the data):



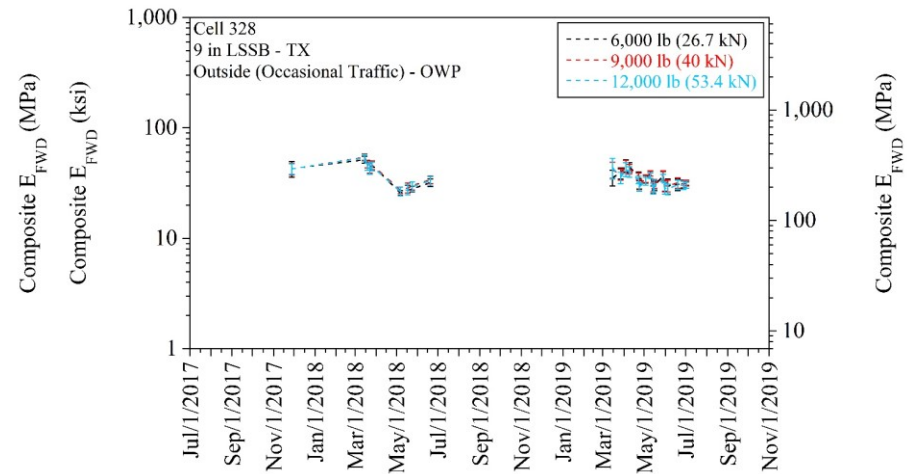
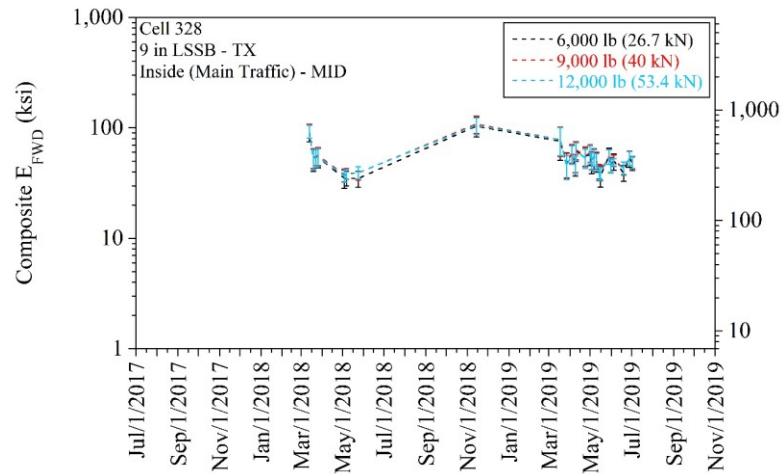
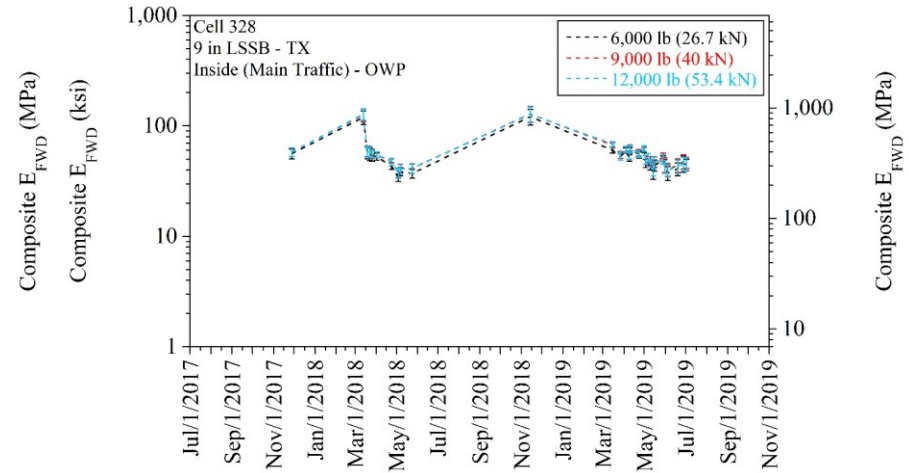
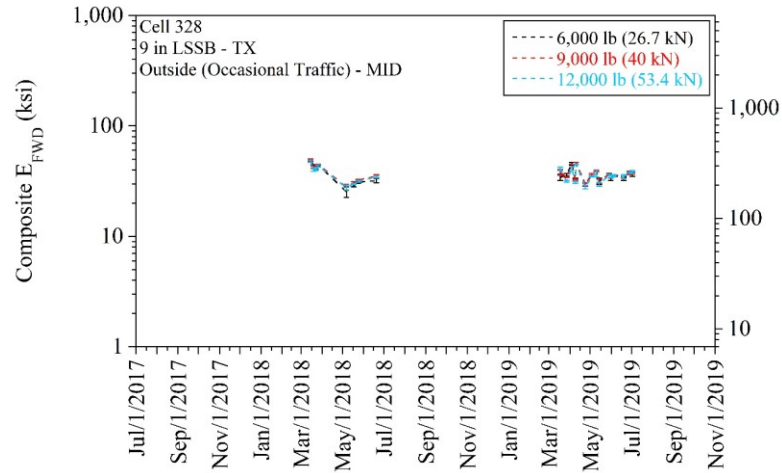
Cell 127 (18-in LSSB) - composite E_{FWD} (error bars represent one standard deviation of the data):



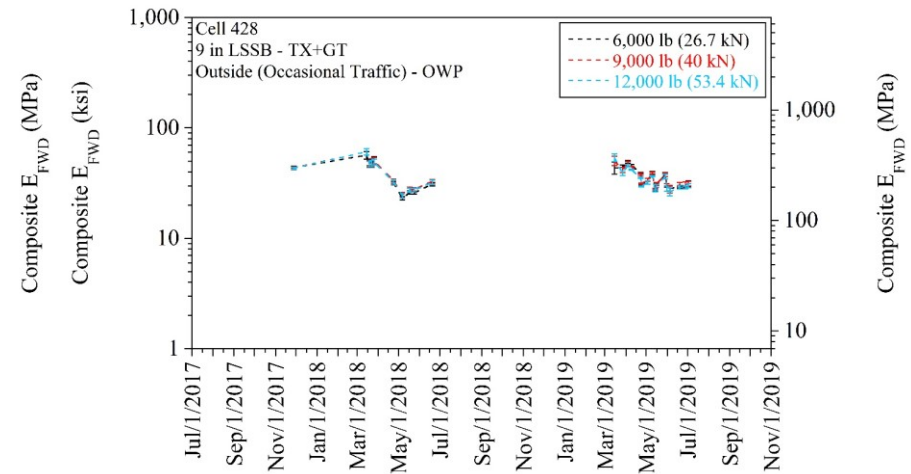
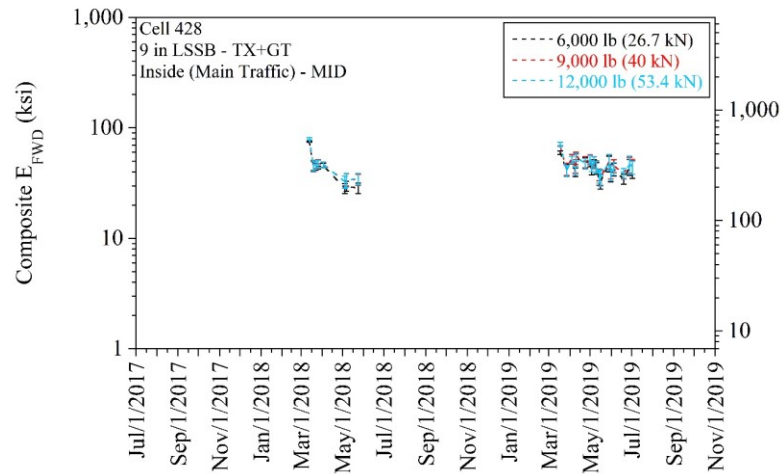
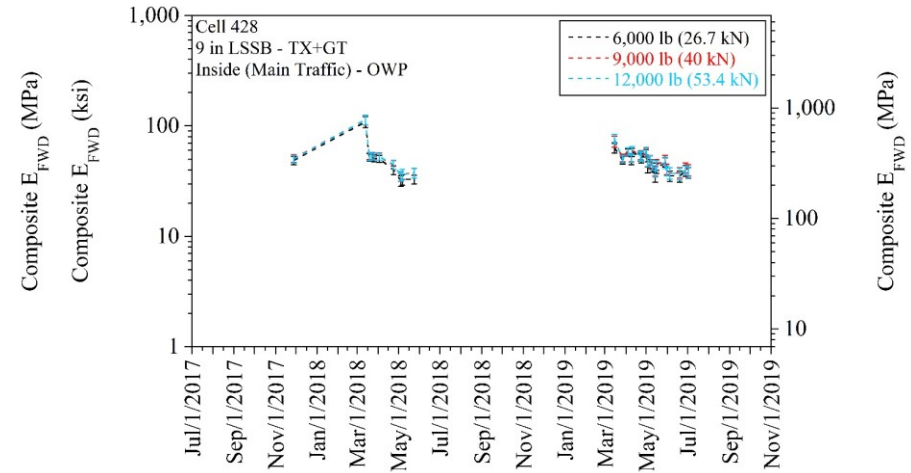
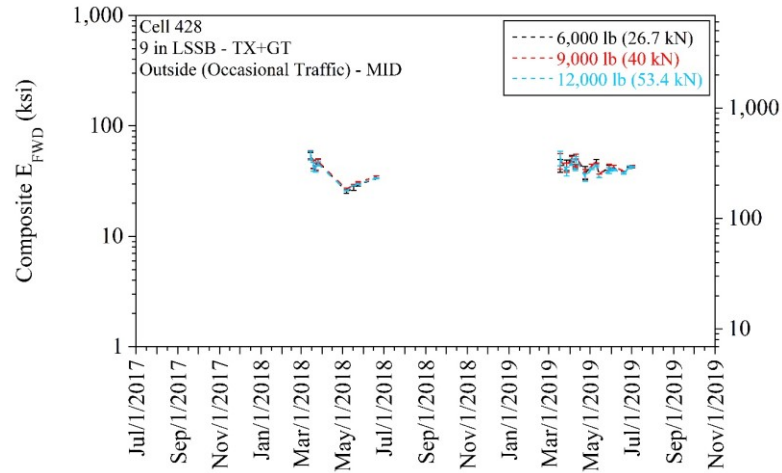
Cell 227 (18-in LSSB) - composite E_{FWD} (error bars represent one standard deviation of the data):



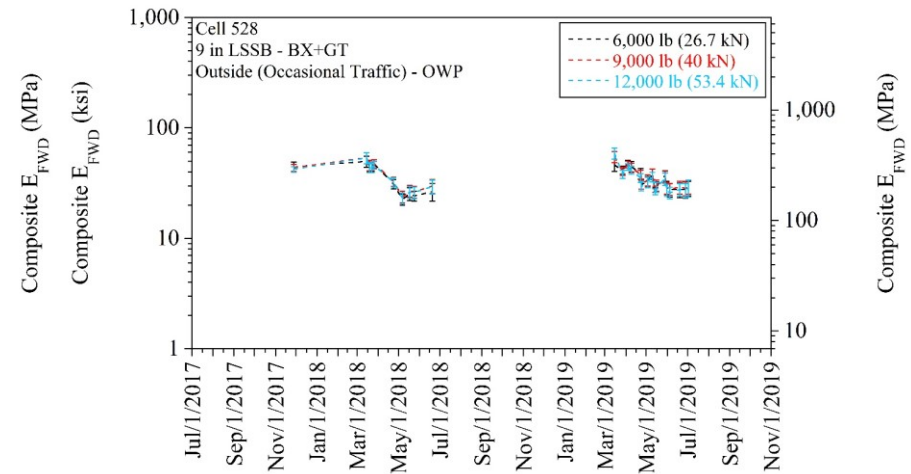
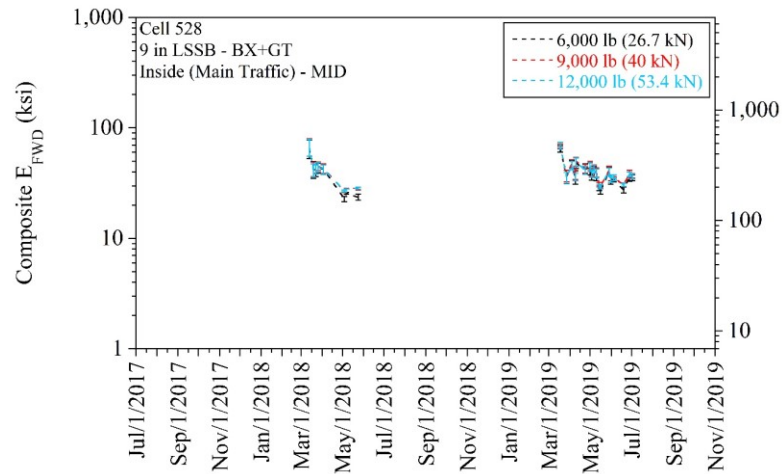
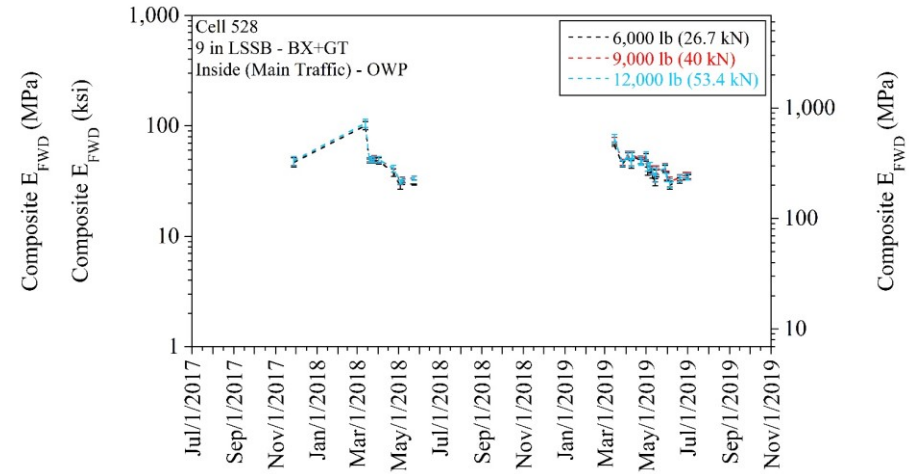
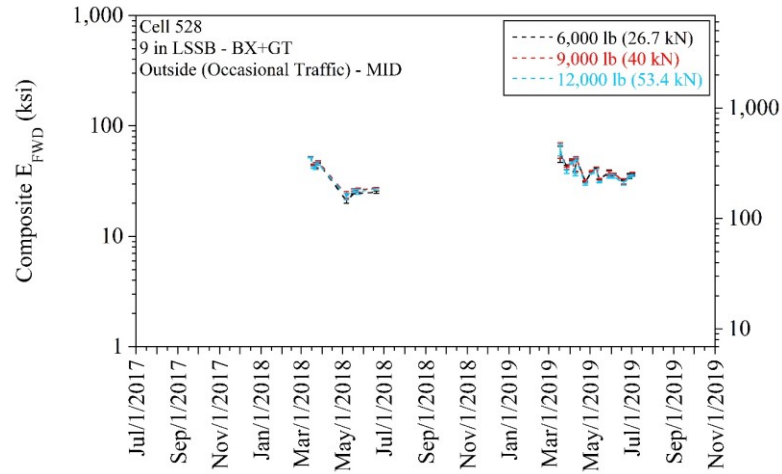
Cell 328 (9-in LSSB - TX) - composite E_{FWD} (error bars represent one standard deviation of the data):



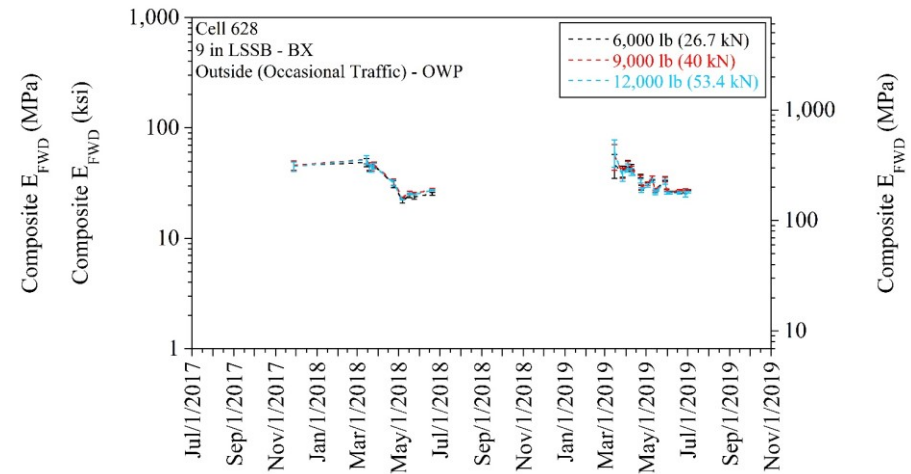
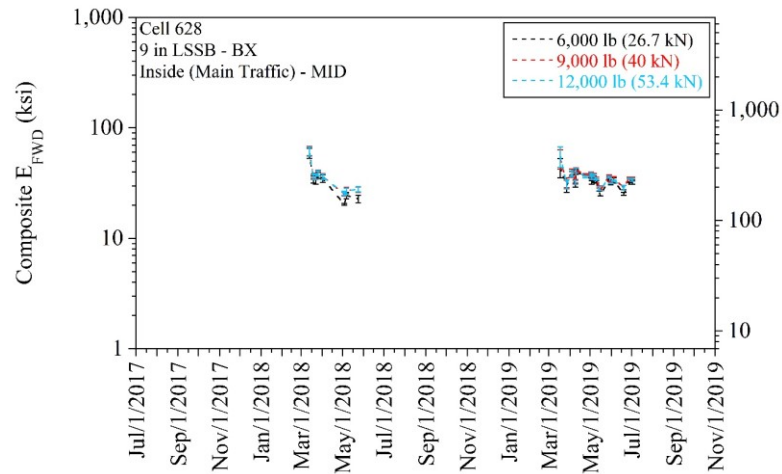
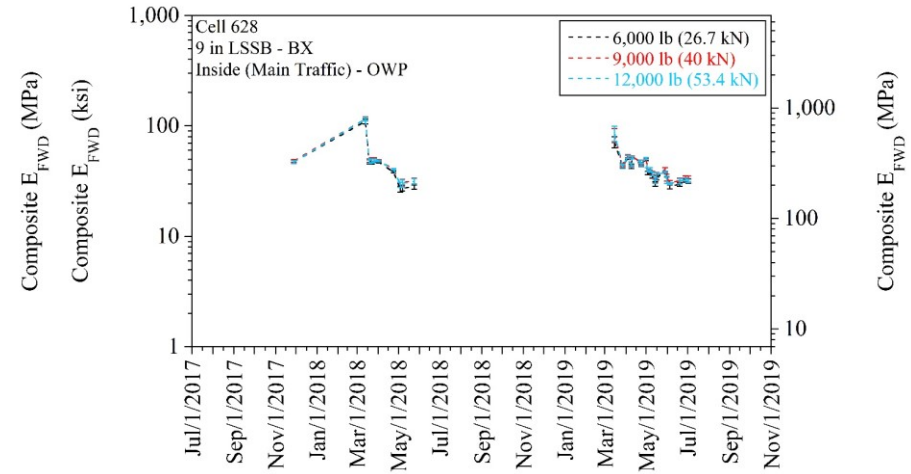
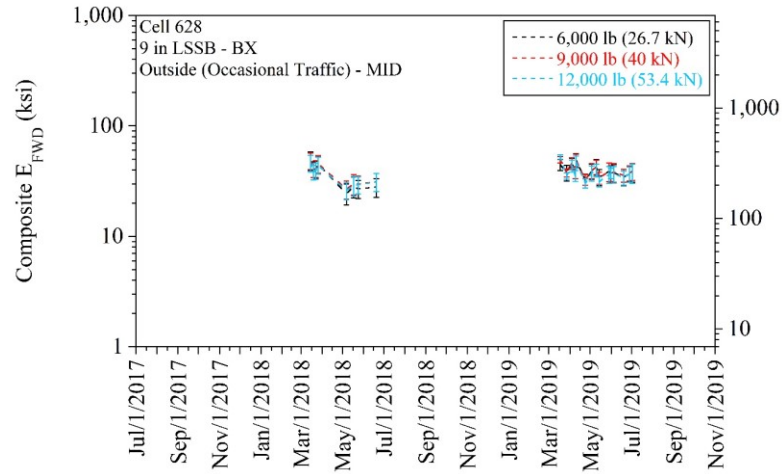
Cell 428 (9-in LSSB - TX+GT) - composite E_{FWD} (error bars represent one standard deviation of the data):



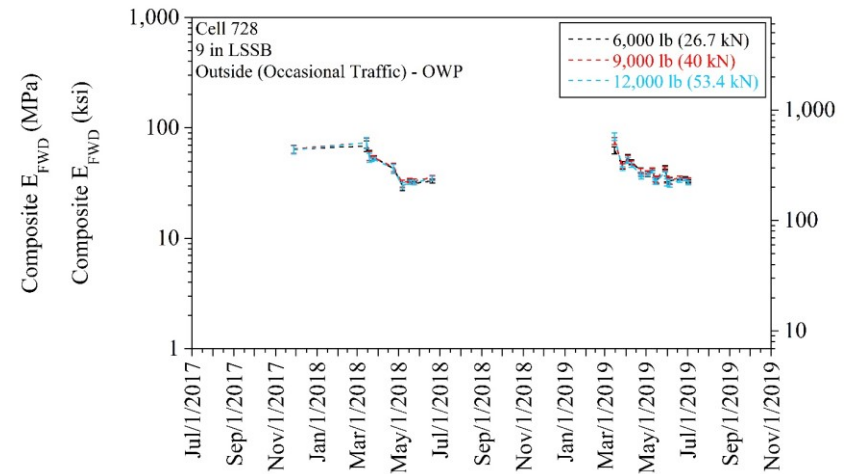
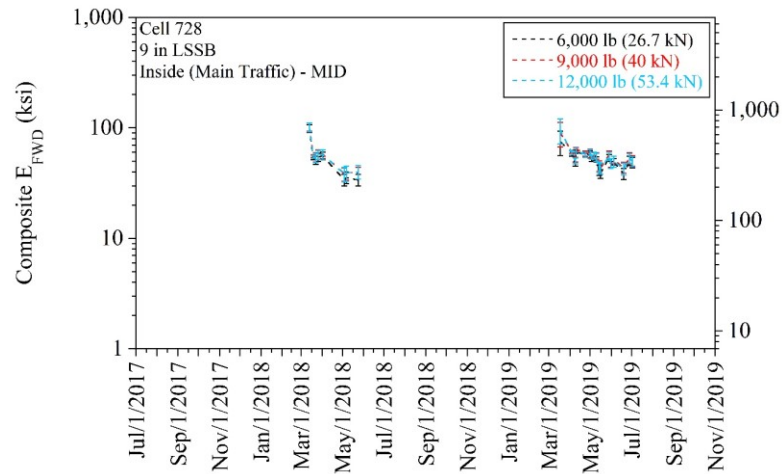
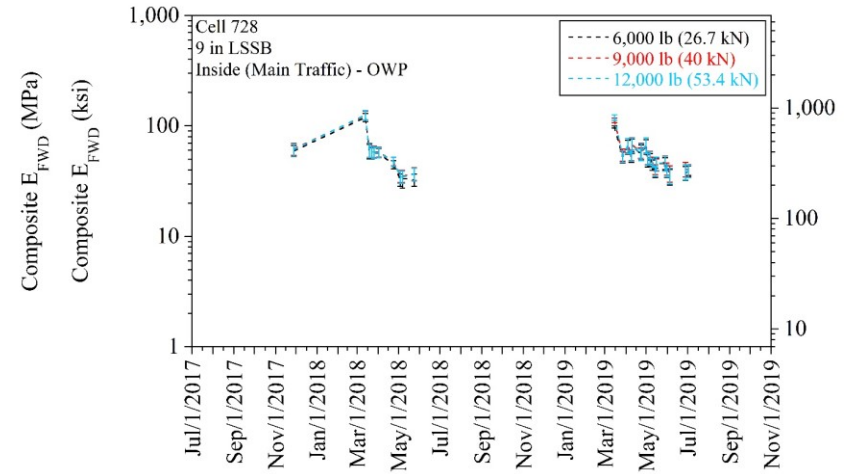
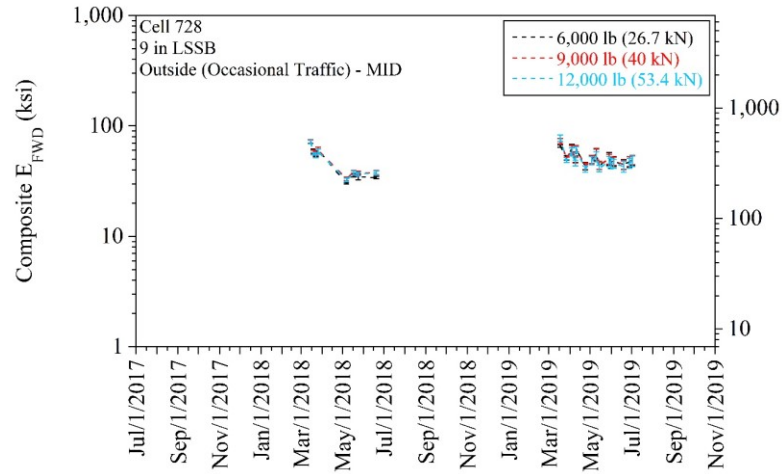
Cell 528 (9-in LSSB - BX+GT) - composite E_{FWD} (error bars represent one standard deviation of the data):



Cell 628 (9-in LSSB - BX) - composite E_{FWD} (error bars represent one standard deviation of the data):



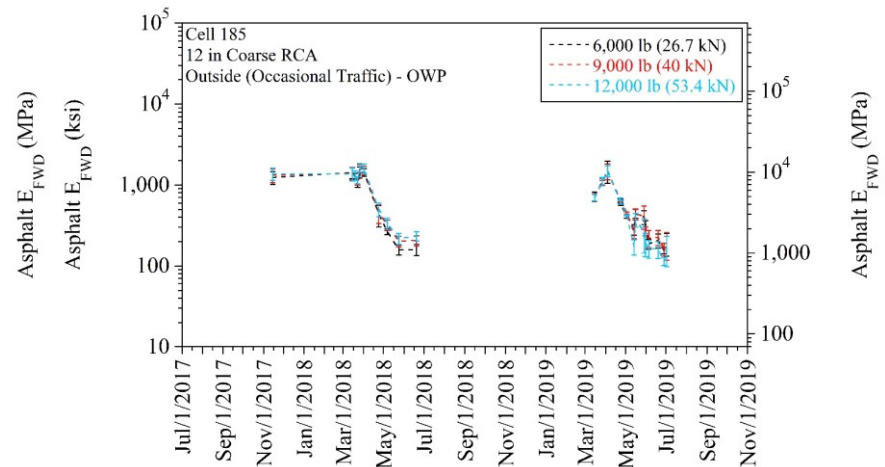
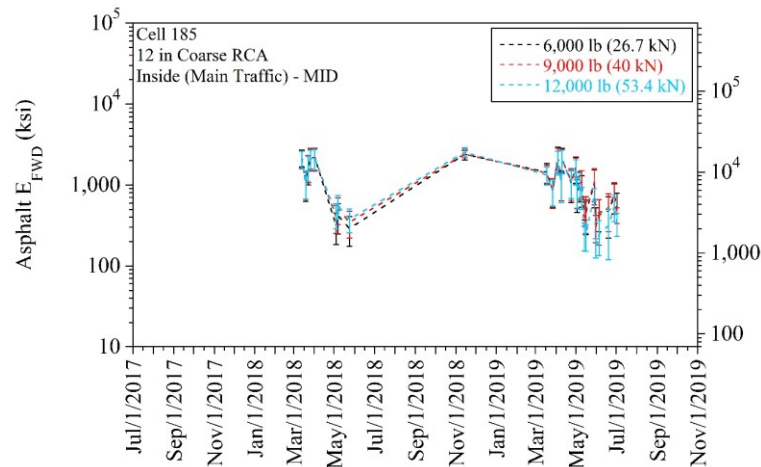
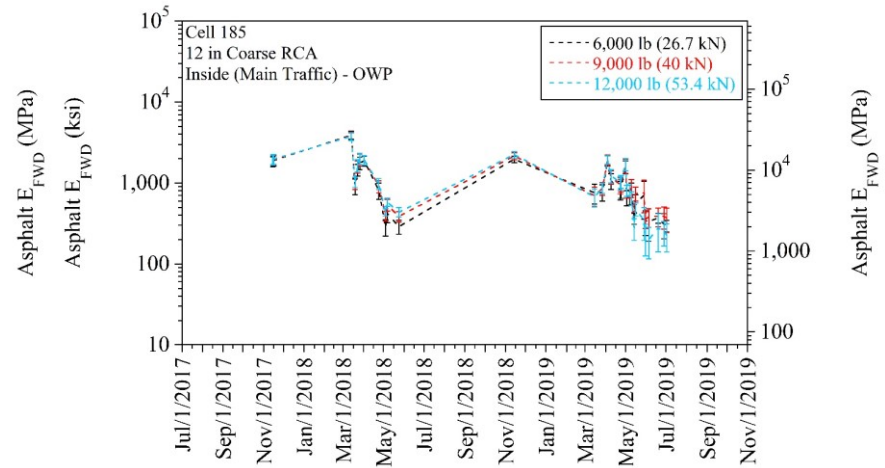
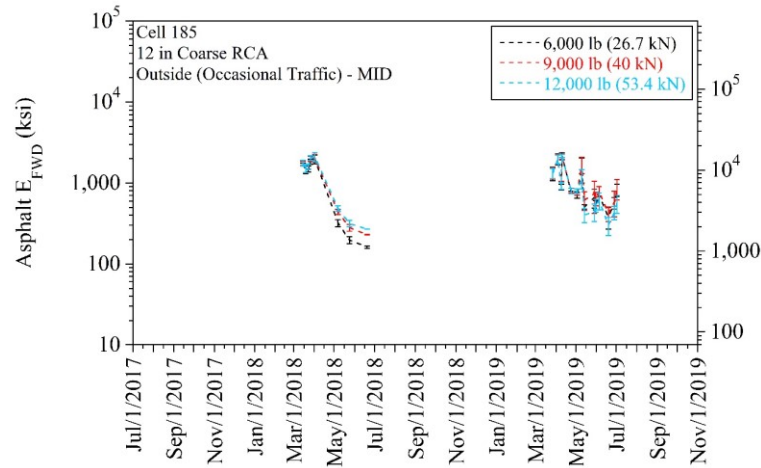
Cell 728 (9-in LSSB) - composite E_{FWD} (error bars represent one standard deviation of the data):



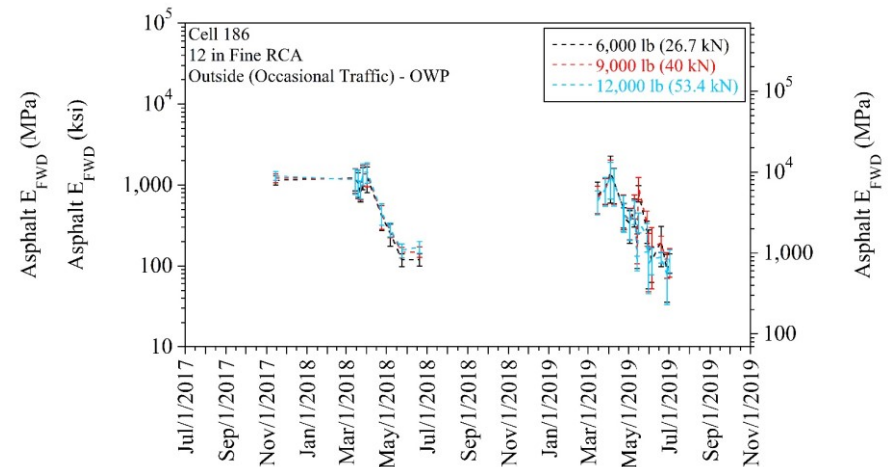
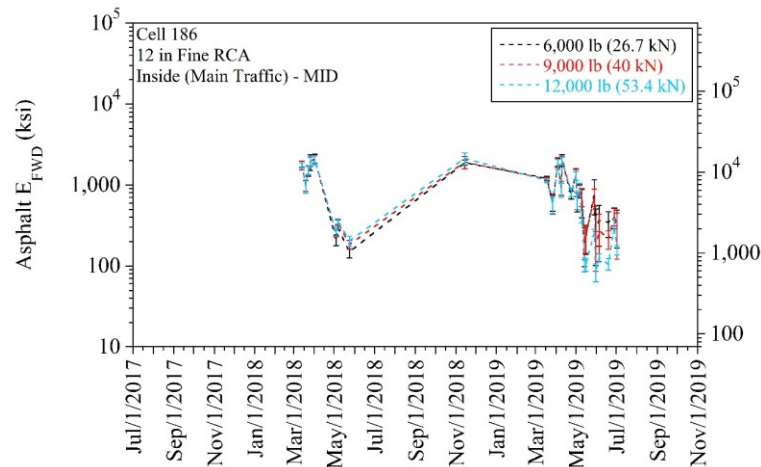
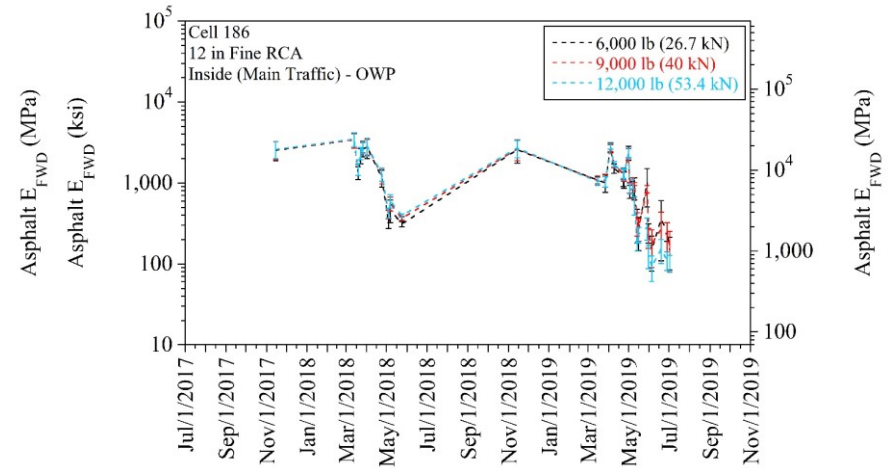
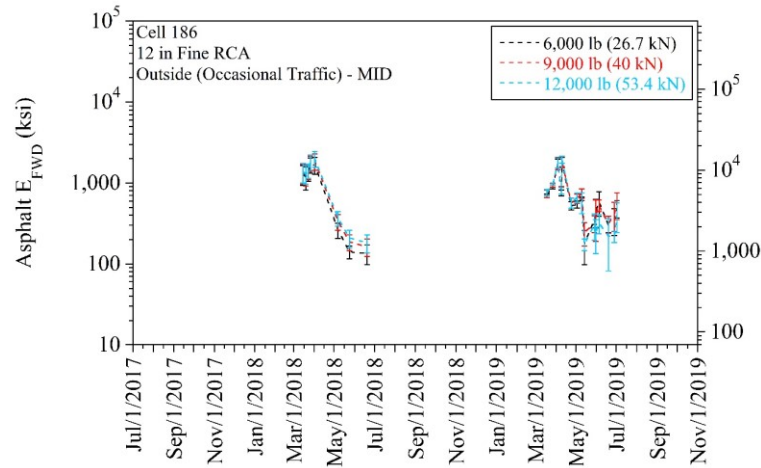
APPENDIX W

**ASPHALT FALLING WEIGHT DEFLECTOMETER (FWD) ELASTIC
MODULUS (E_{FWD}) AT 6,000 LB (26.7 KN), 9,000 LB (40 KN), AND
12,000 LB (53.4 KN) FOR EACH CELL**

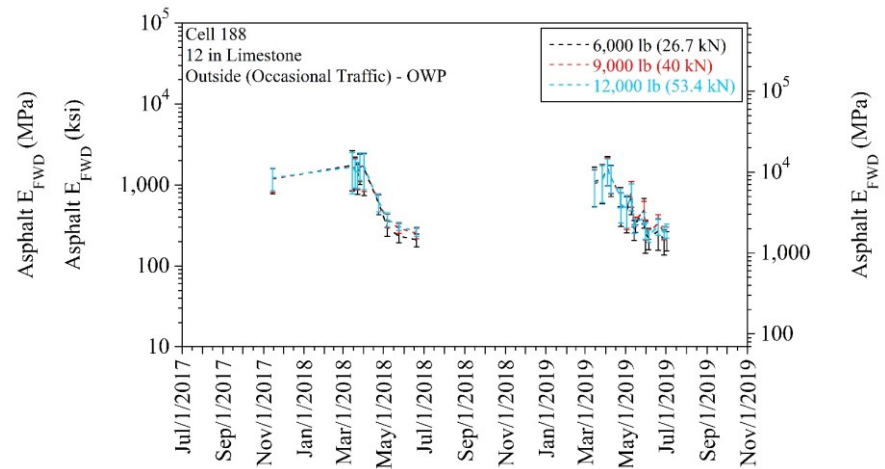
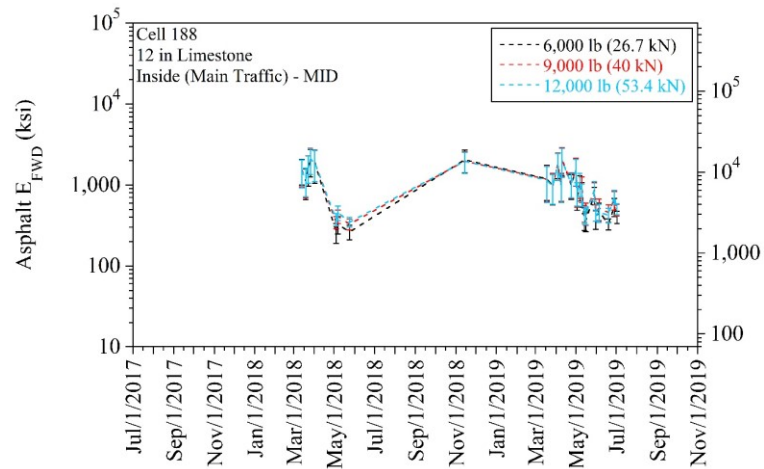
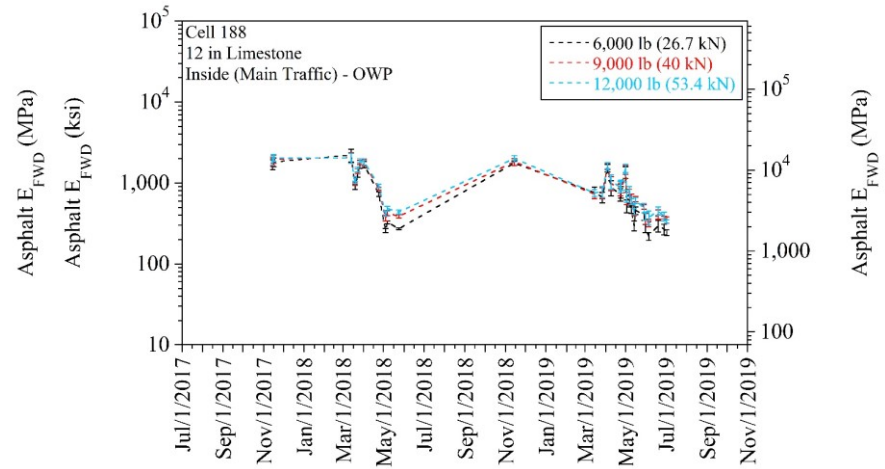
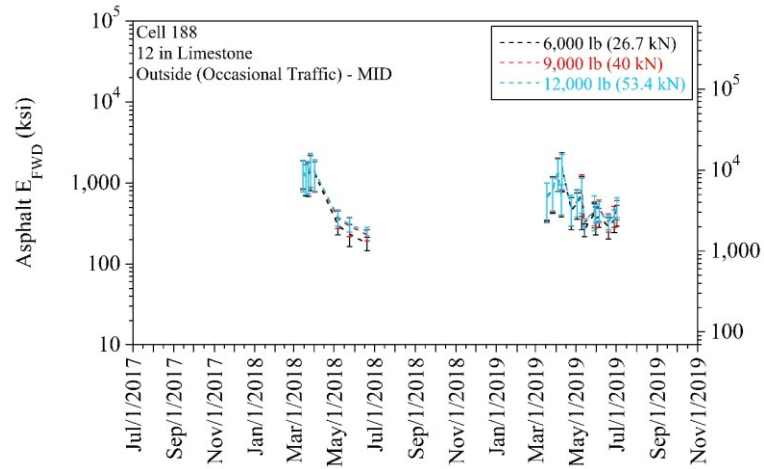
Cell 185 (12-in Coarse RCA) - asphalt E_{FWD} (error bars represent one standard deviation of the data):



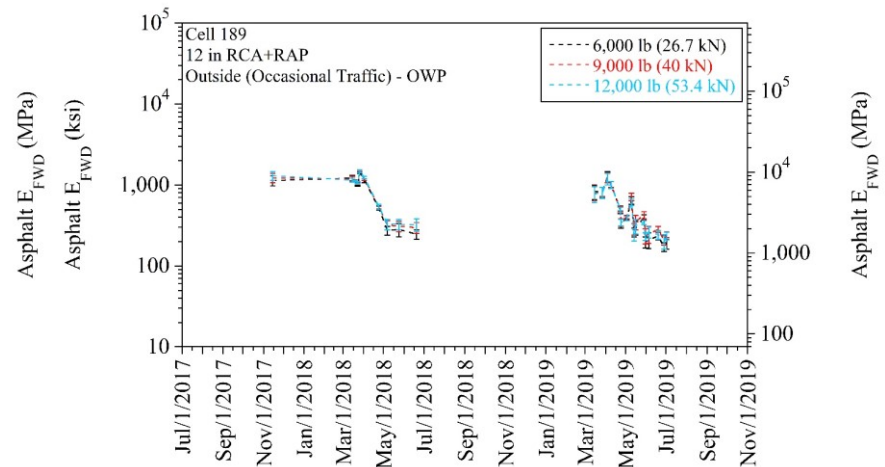
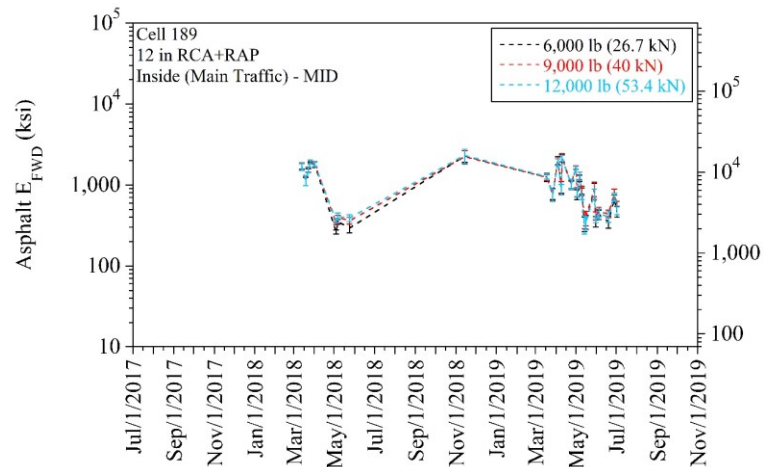
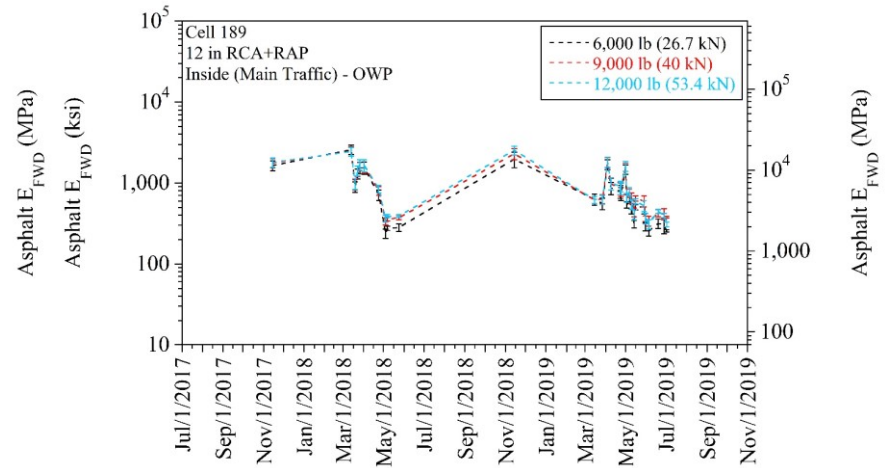
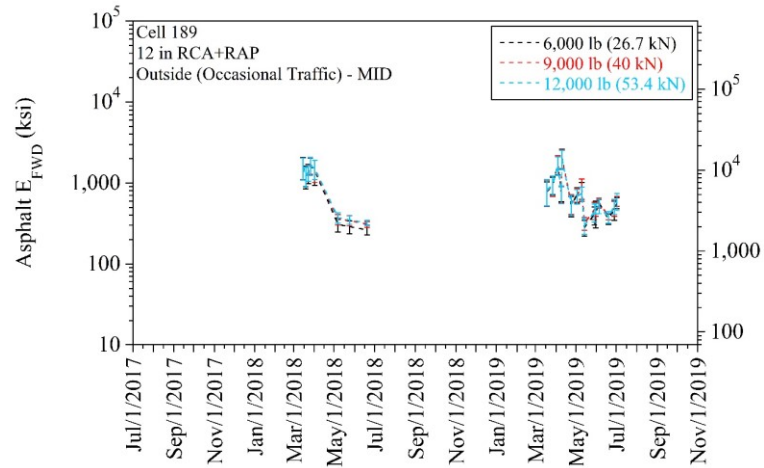
Cell 186 (12-in Fine RCA) - asphalt E_{FWD} (error bars represent one standard deviation of the data):



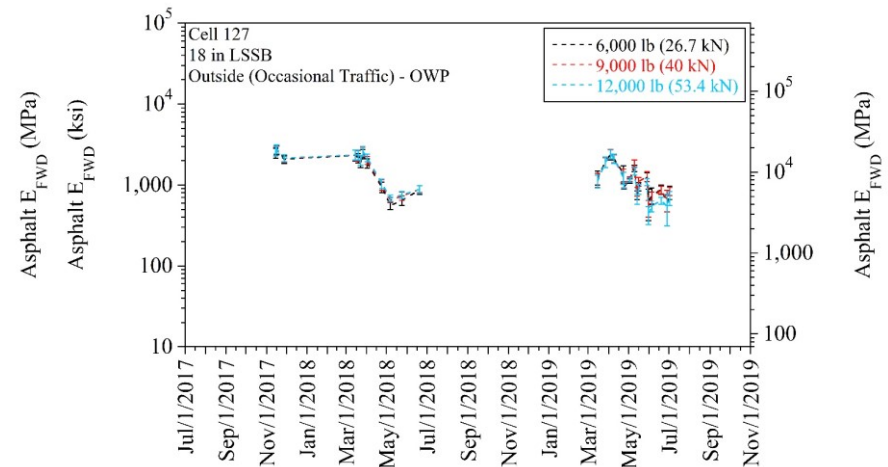
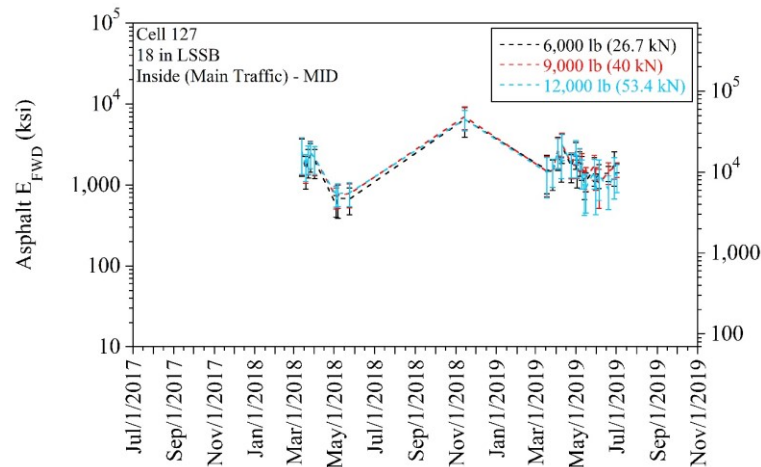
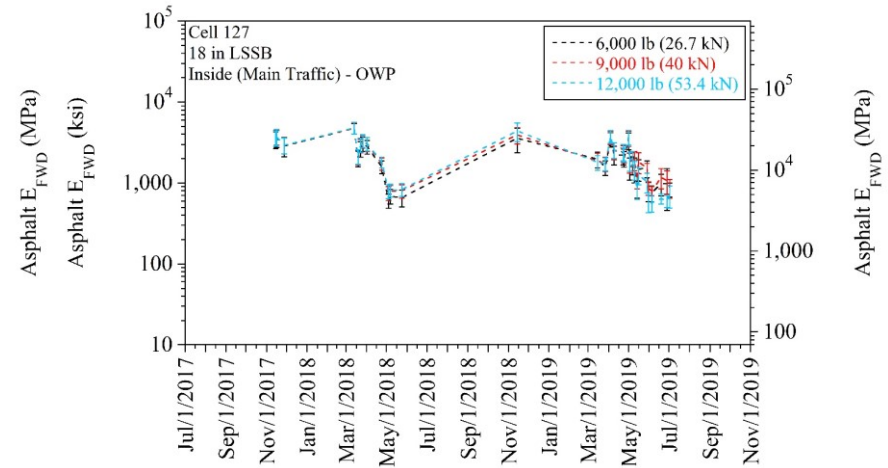
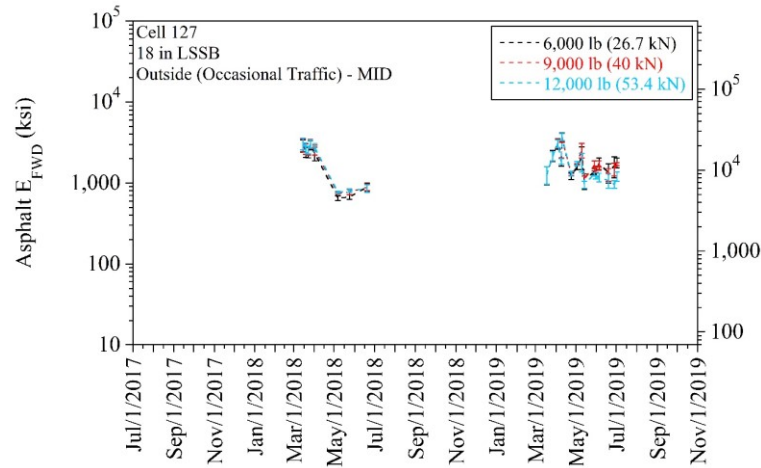
Cell 188 (12-in Limestone) - asphalt E_{FWD} (error bars represent one standard deviation of the data):



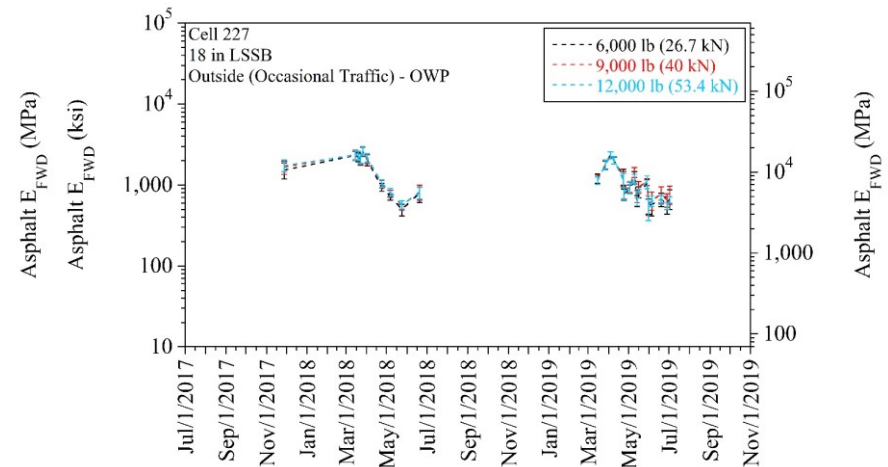
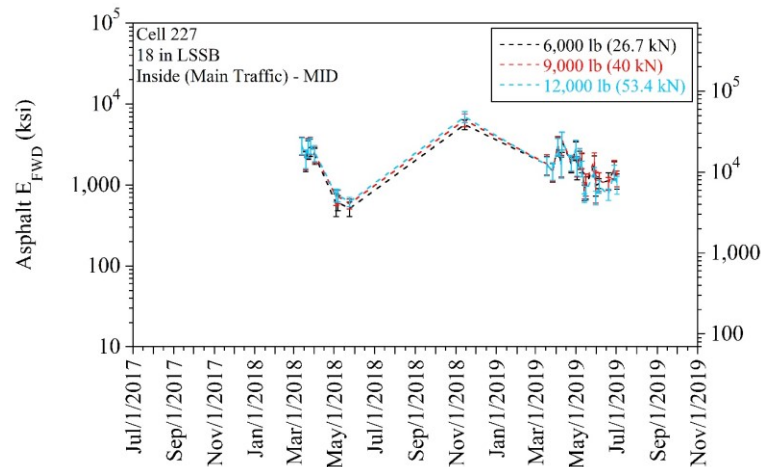
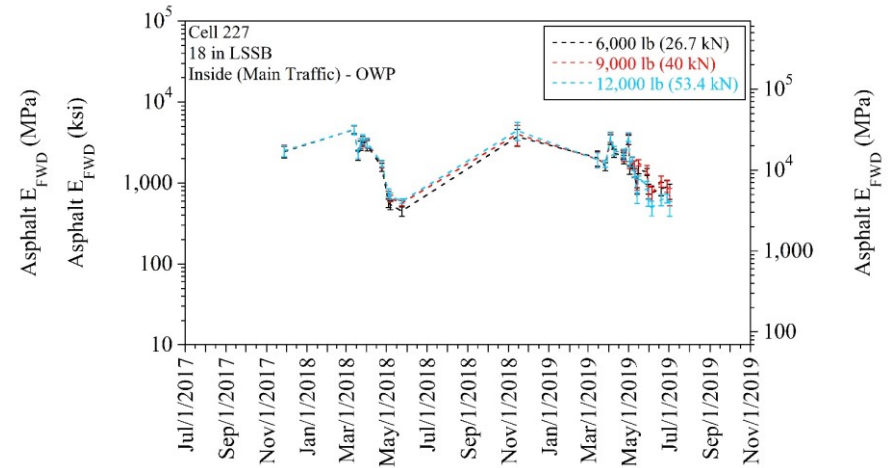
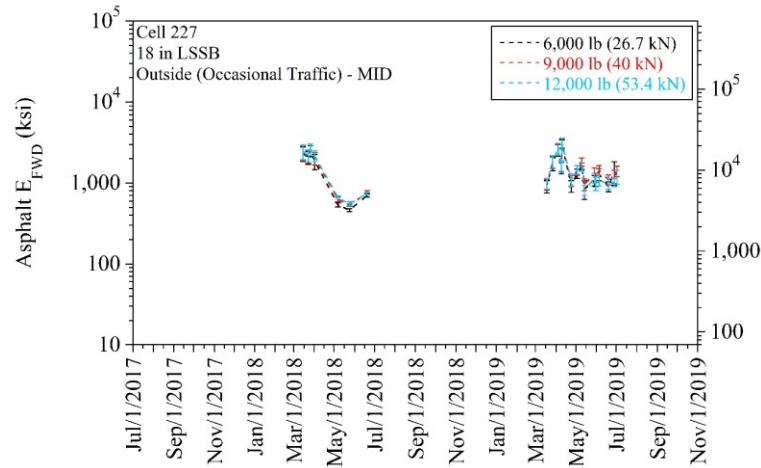
Cell 189 (12-in RCA+RAP) - asphalt E_{FWD} (error bars represent one standard deviation of the data):



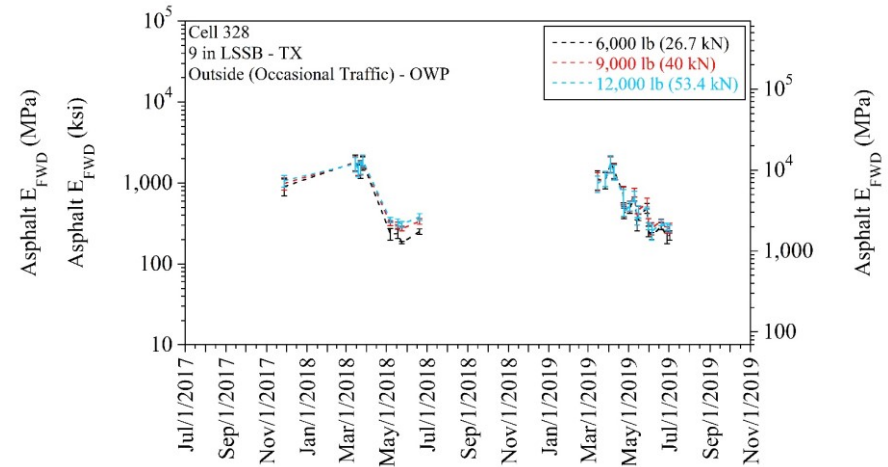
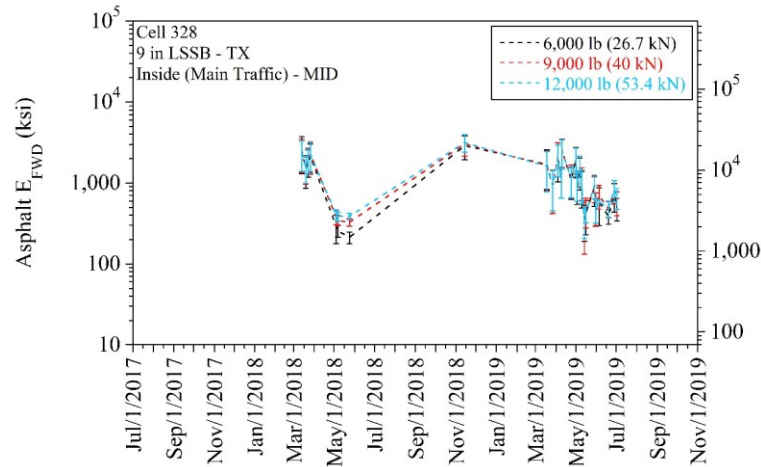
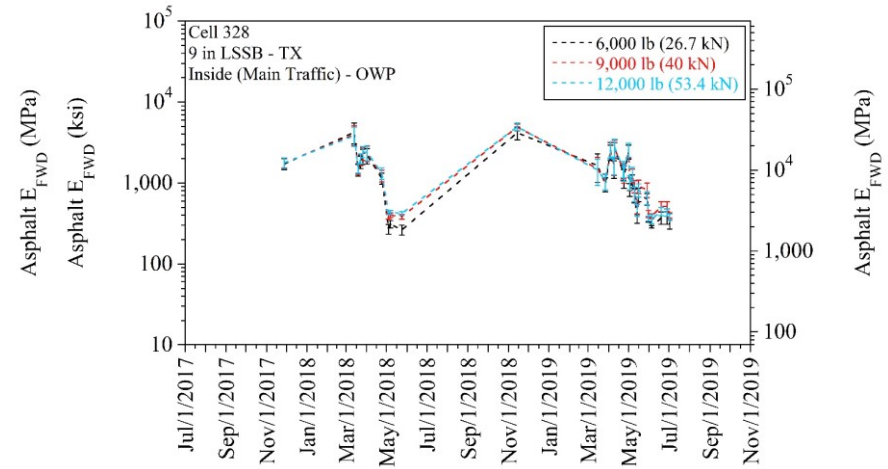
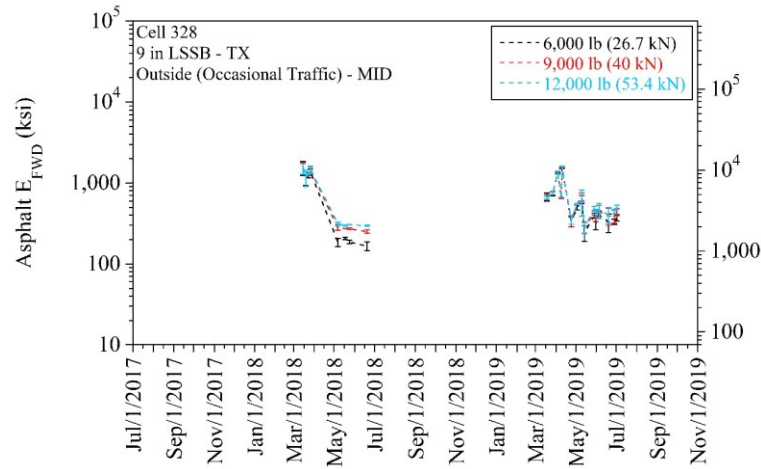
Cell 127 (18-in LSSB) - asphalt E_{FWD} (error bars represent one standard deviation of the data):



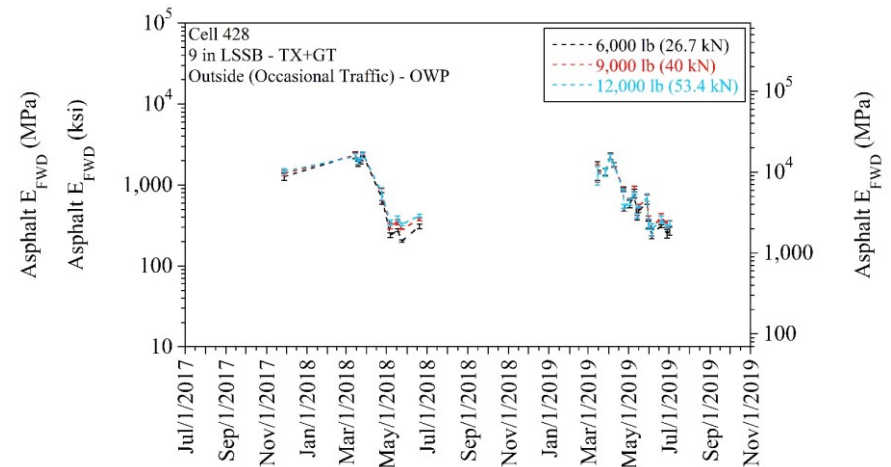
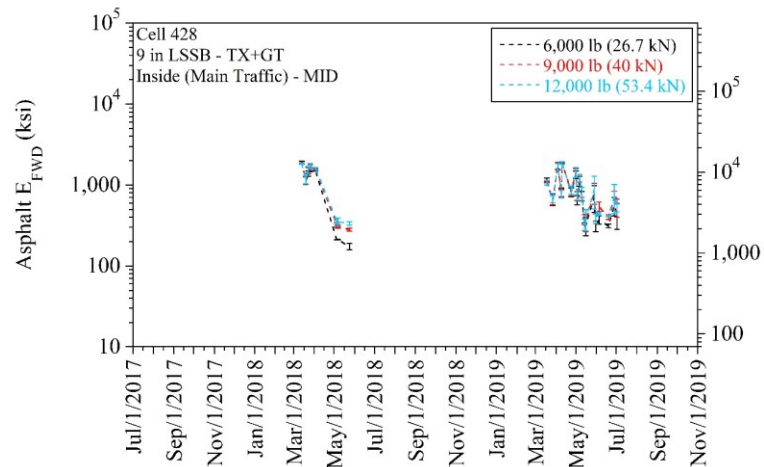
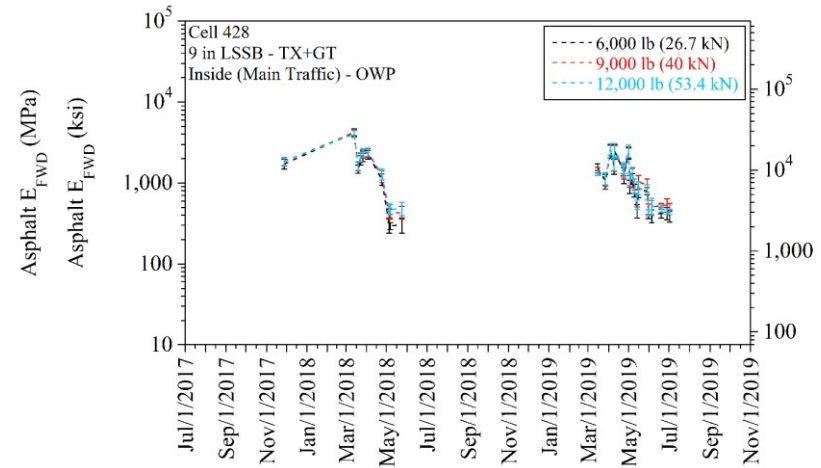
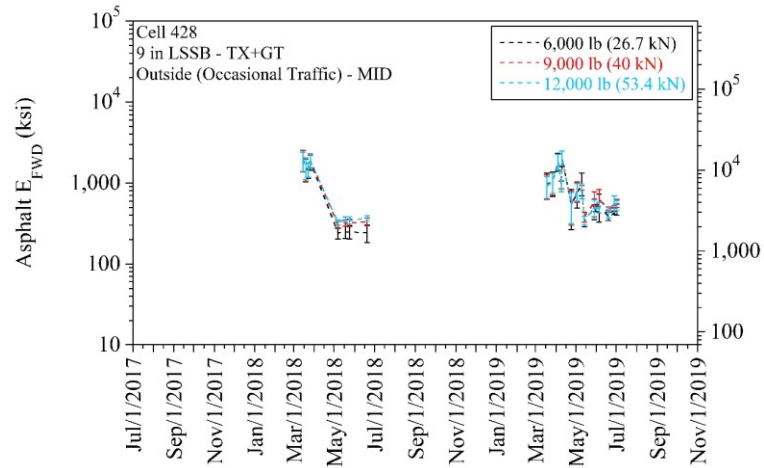
Cell 227 (18-in LSSB) - asphalt E_{FWD} (error bars represent one standard deviation of the data):



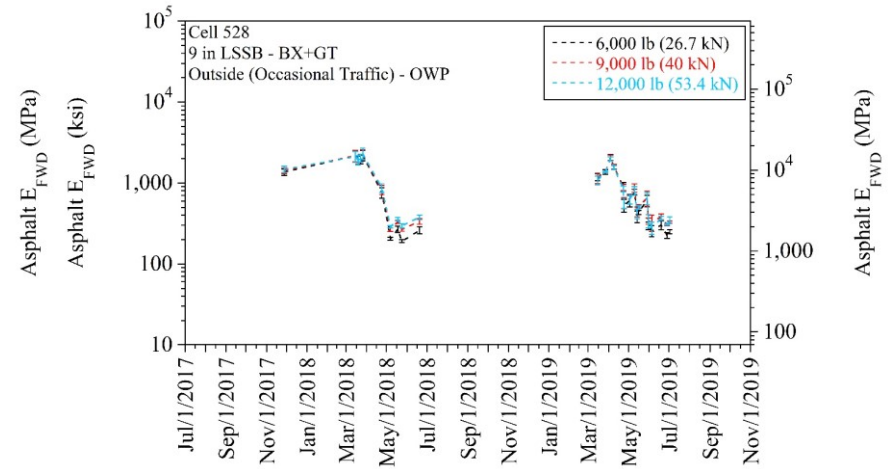
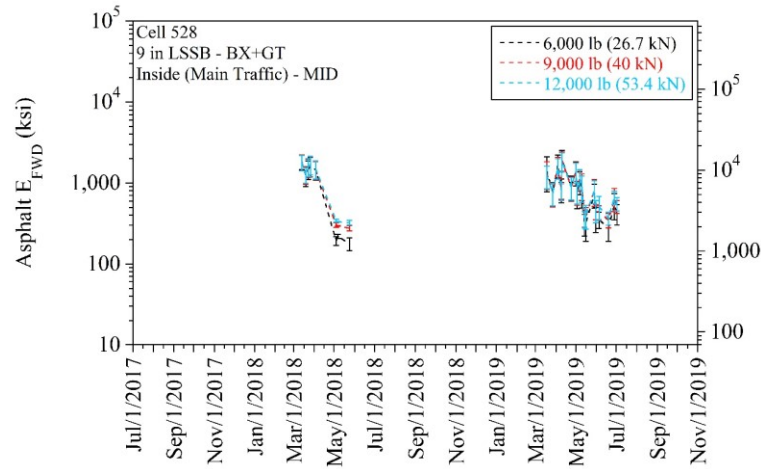
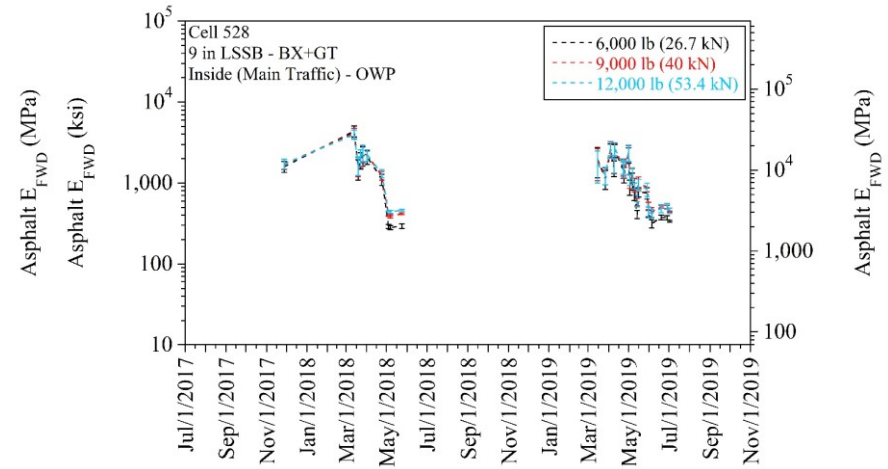
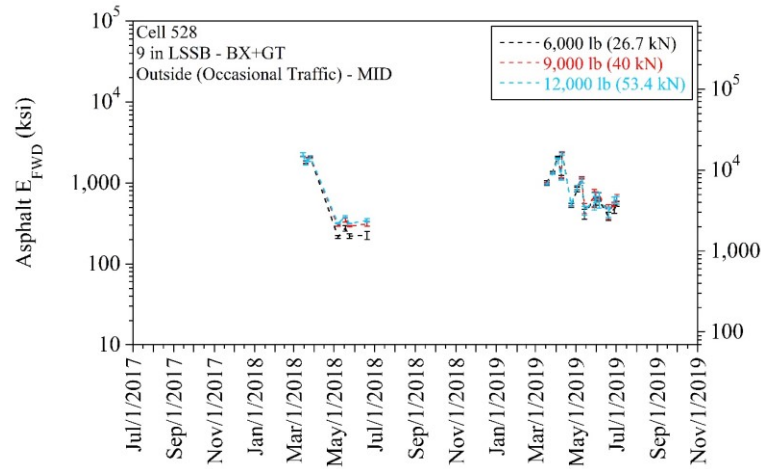
Cell 328 (9-in LSSB - TX) - asphalt E_{FWD} (error bars represent one standard deviation of the data):



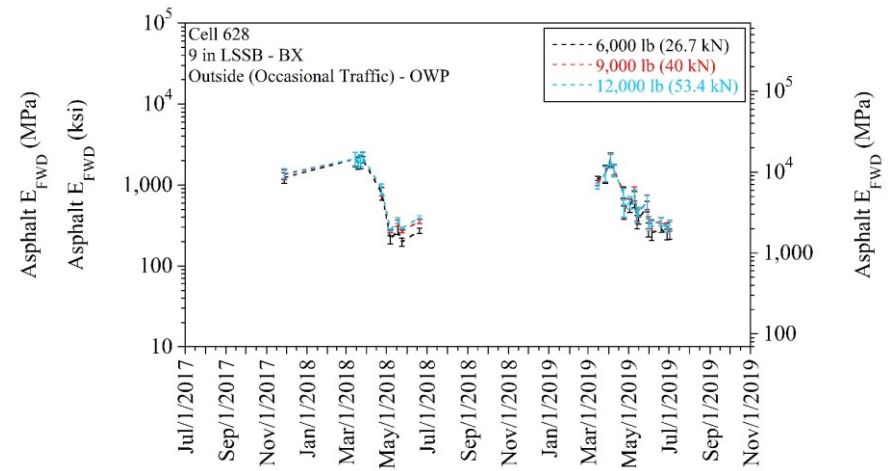
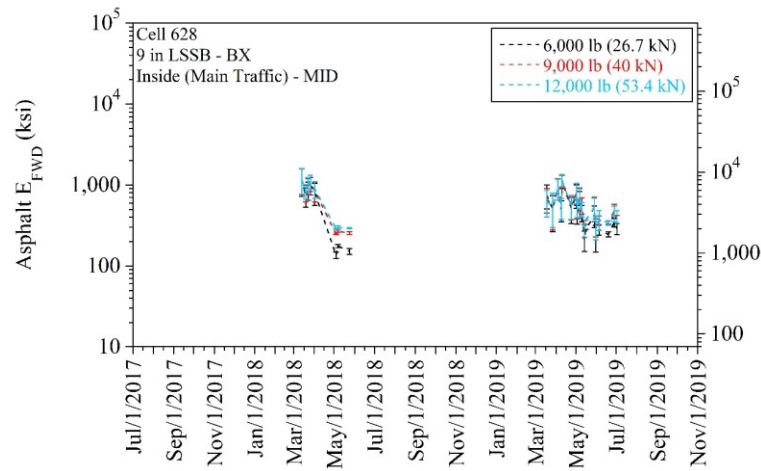
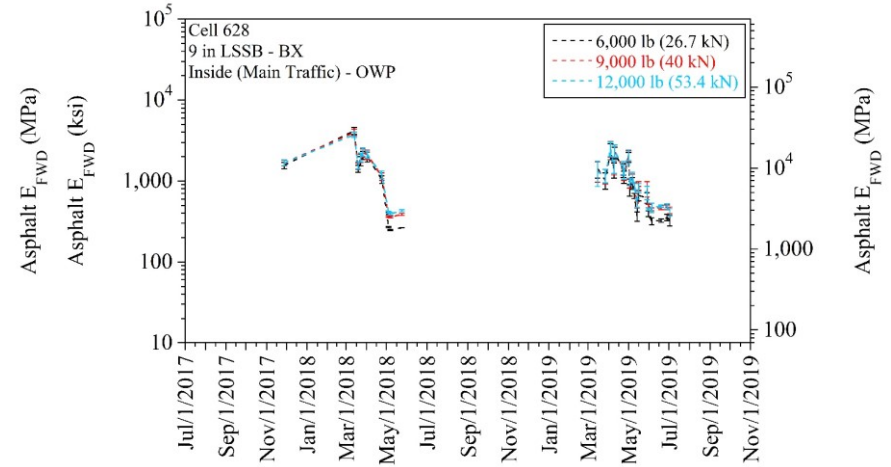
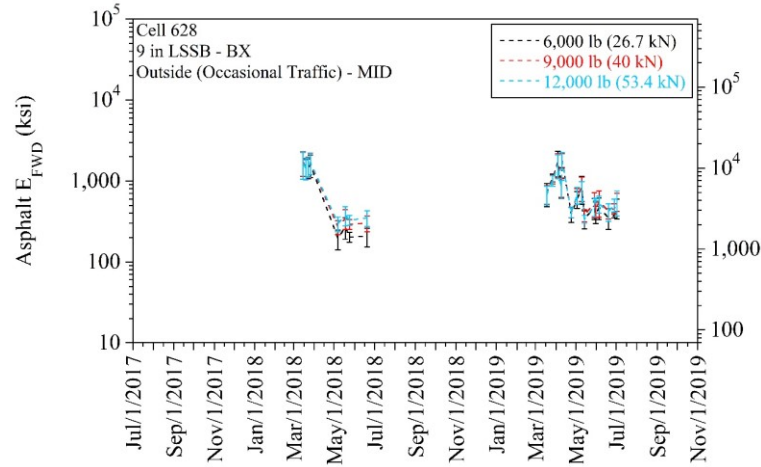
Cell 428 (9-in LSSB - TX+GT) - asphalt E_{FWD} (error bars represent one standard deviation of the data):



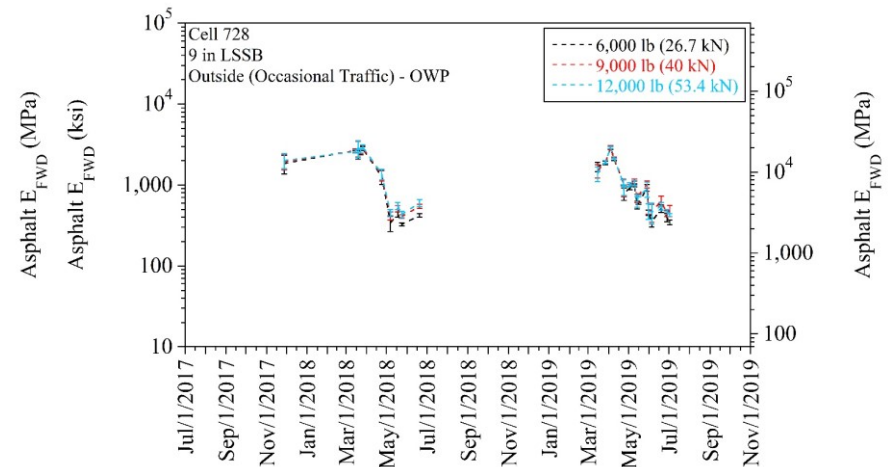
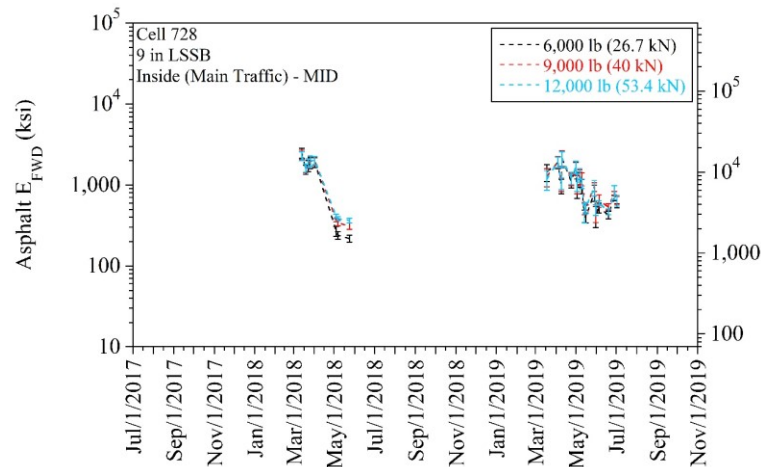
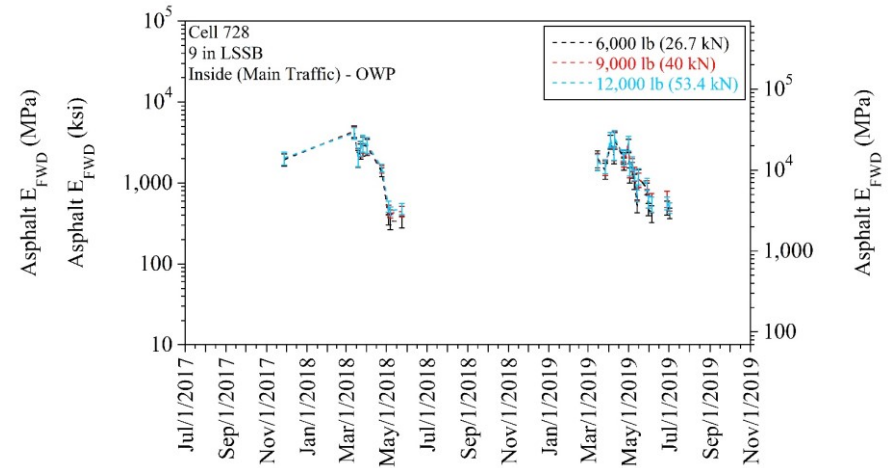
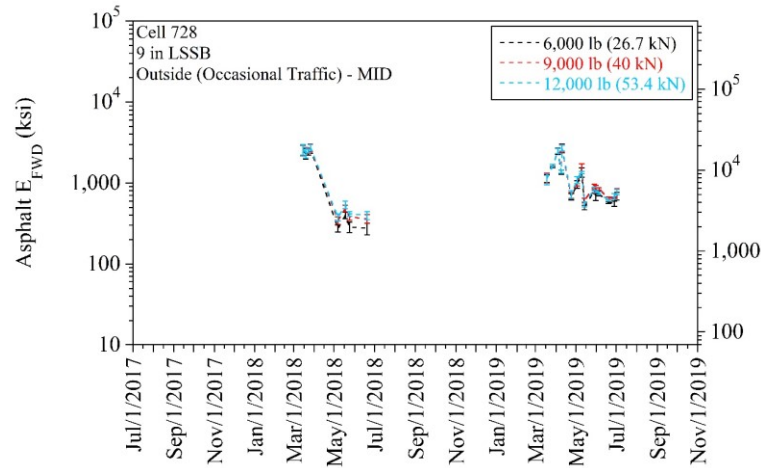
Cell 528 (9-in LSSB - BX+GT) - asphalt E_{FWD} (error bars represent one standard deviation of the data):



Cell 628 (9-in LSSB - BX) - asphalt E_{FWD} (error bars represent one standard deviation of the data):



Cell 728 (9-in LSSB) - asphalt E_{FWD} (error bars represent one standard deviation of the data):

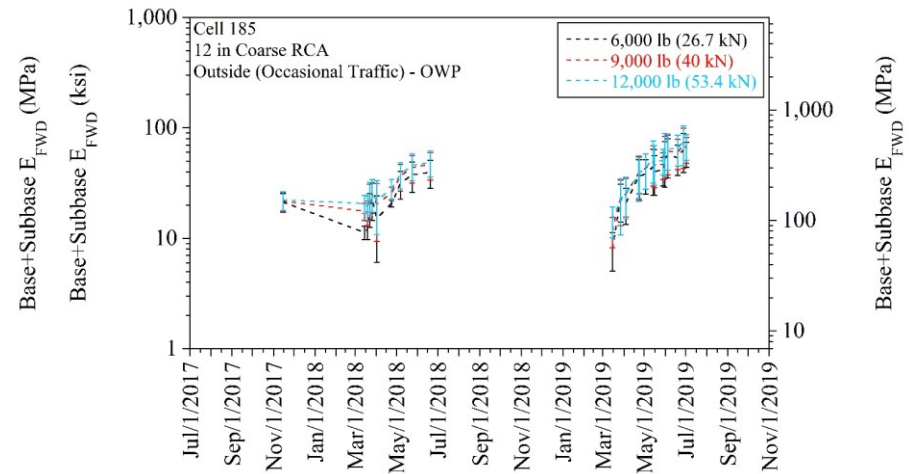
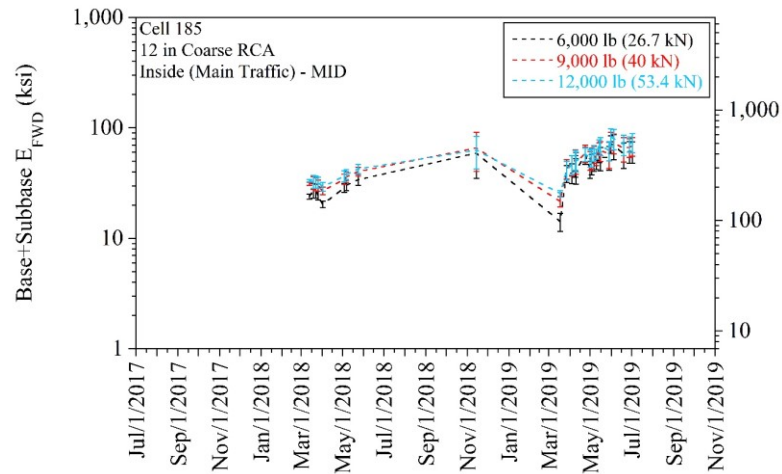
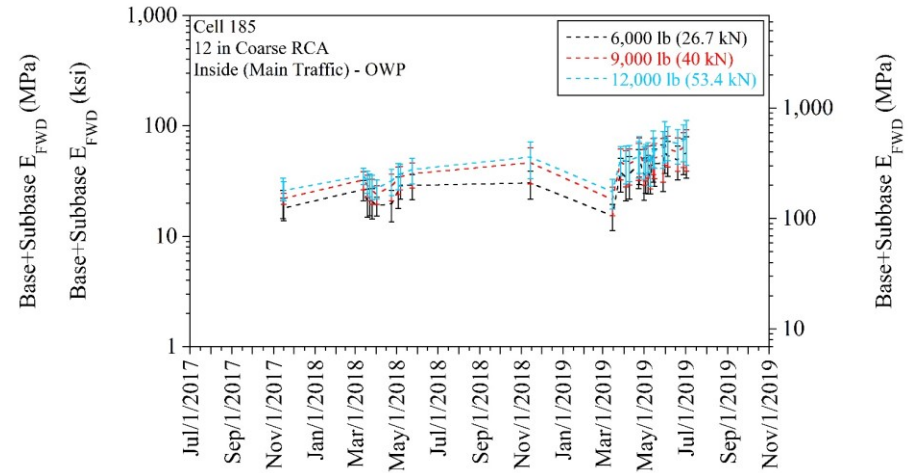
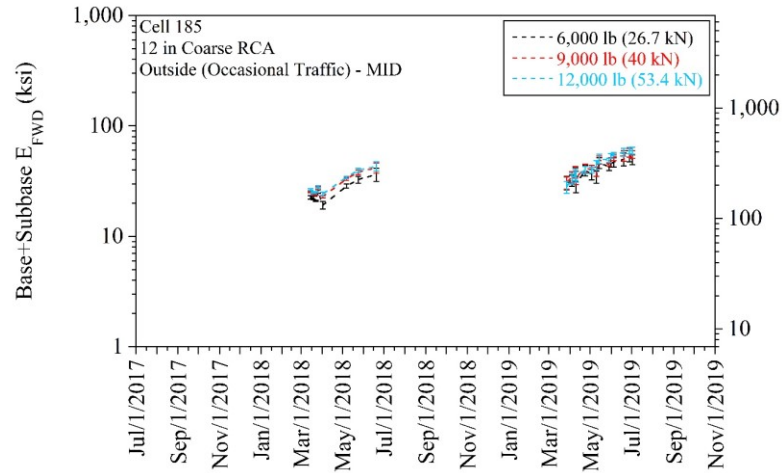


APPENDIX X

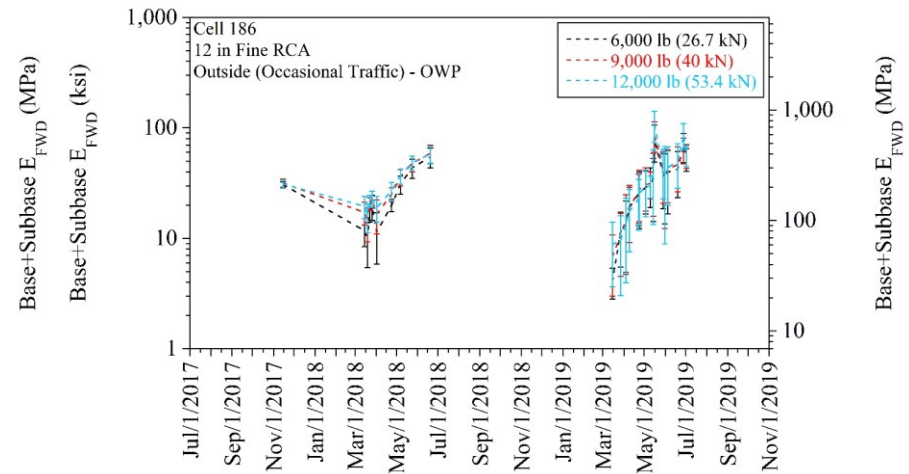
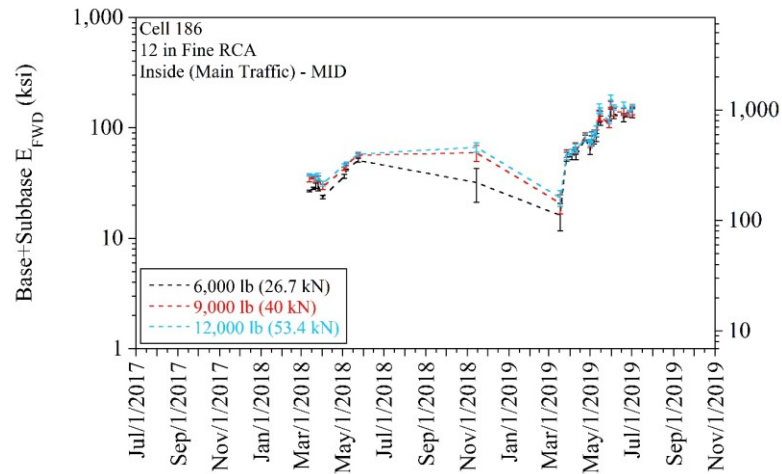
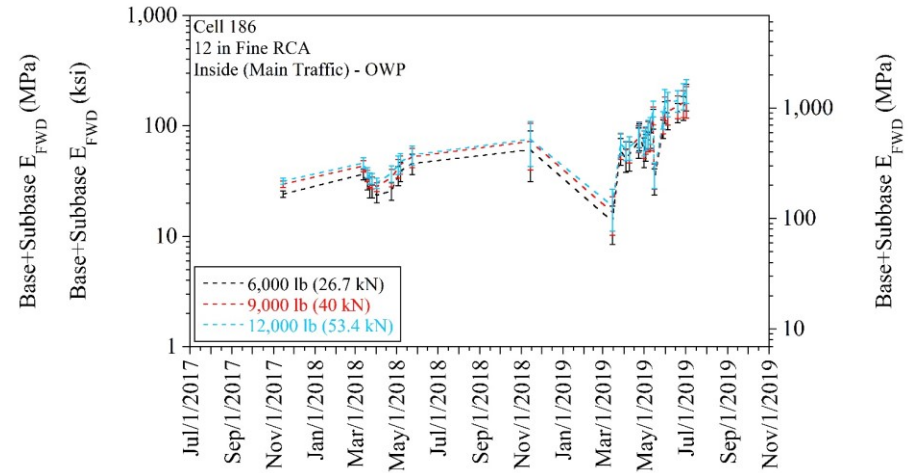
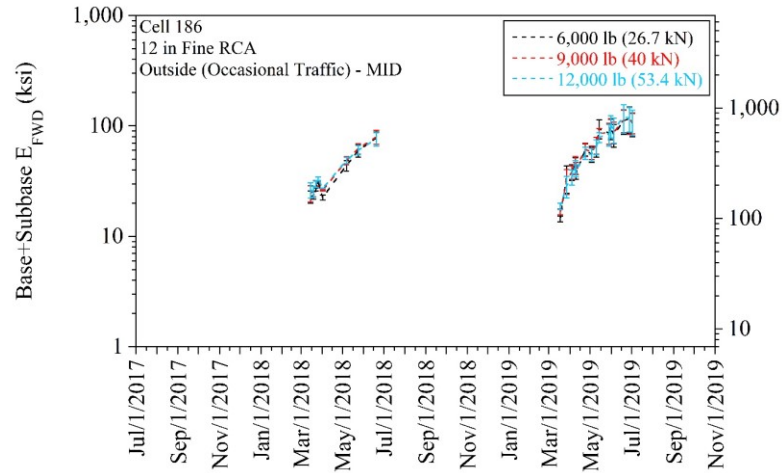
BASE+SUBBASE FALLING WEIGHT DEFLECTOMETER (FWD)

ELASTIC MODULUS (E_{FWD}) AT 6,000 LB (26.7 KN), 9,000 LB (40 KN), AND 12,000 LB (53.4 KN) FOR EACH CELL

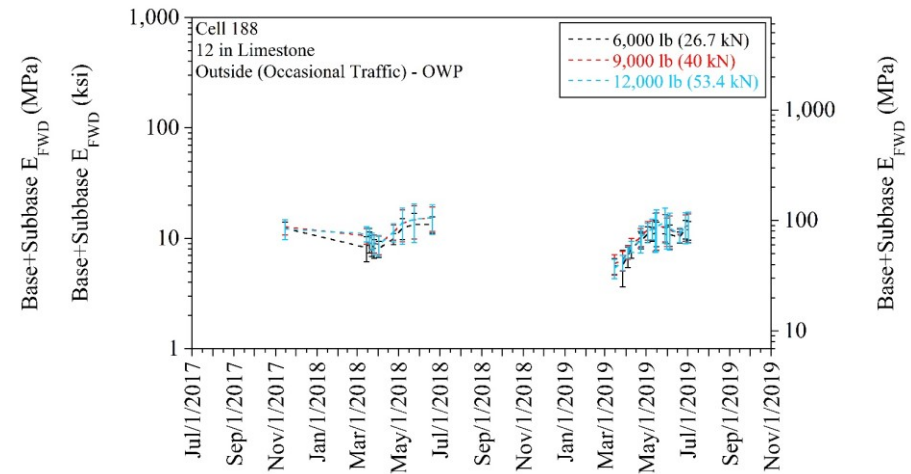
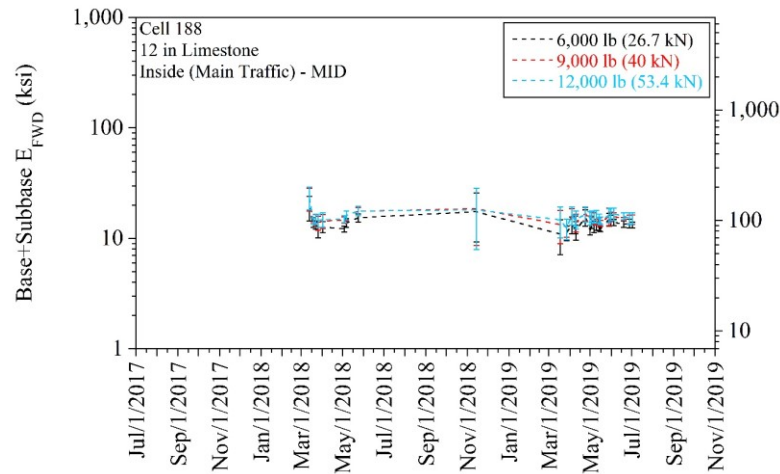
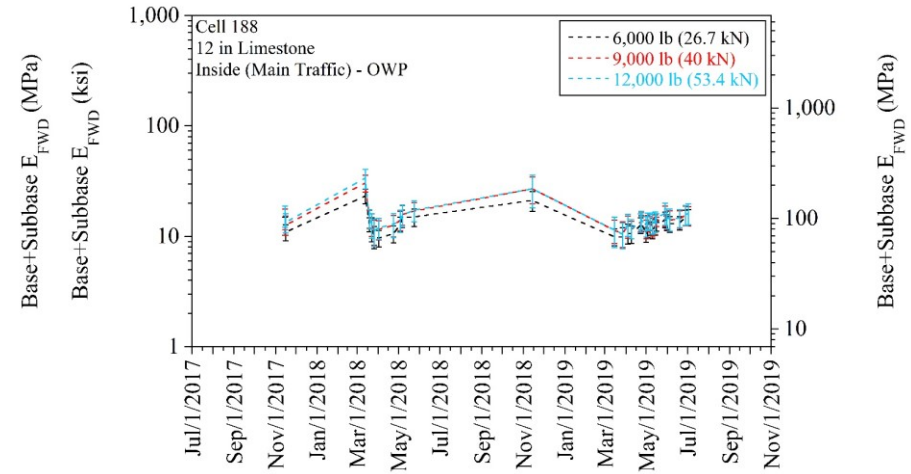
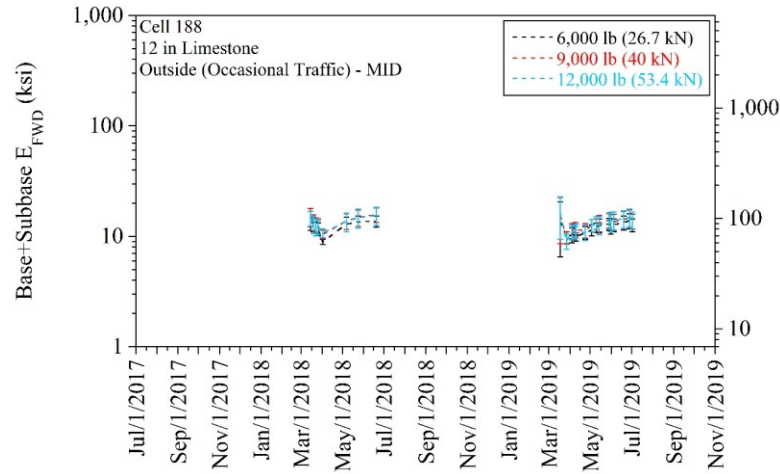
Cell 185 (12-in Coarse RCA) - base+subbase E_{FWD} (error bars represent one standard deviation of the data):



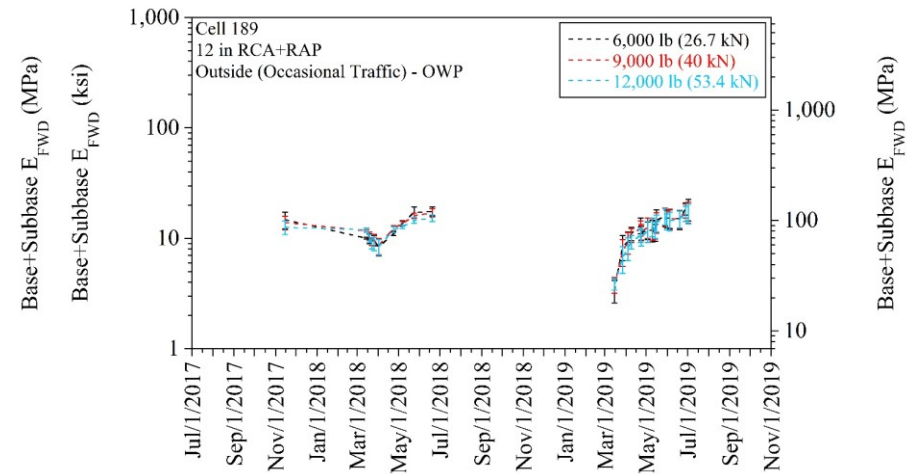
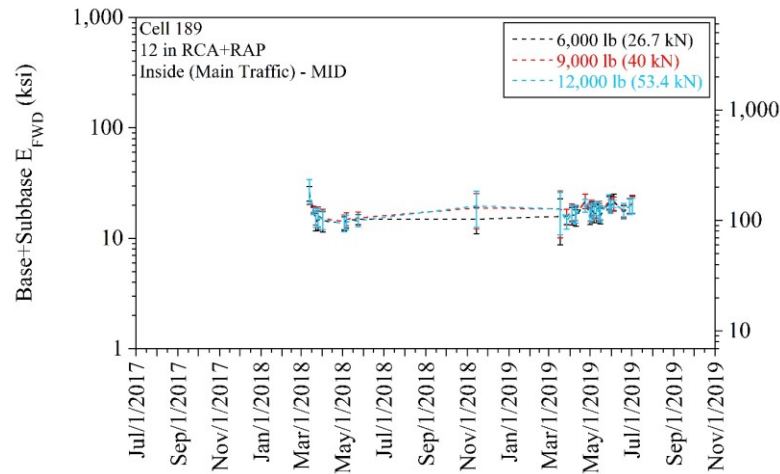
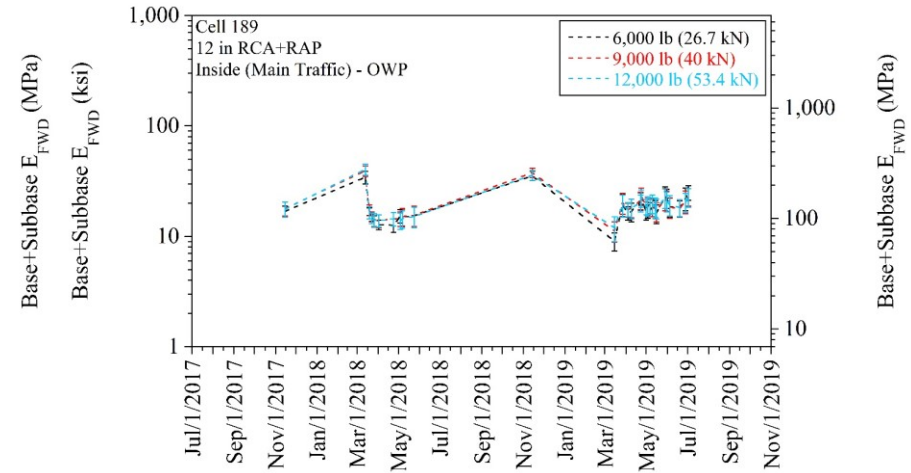
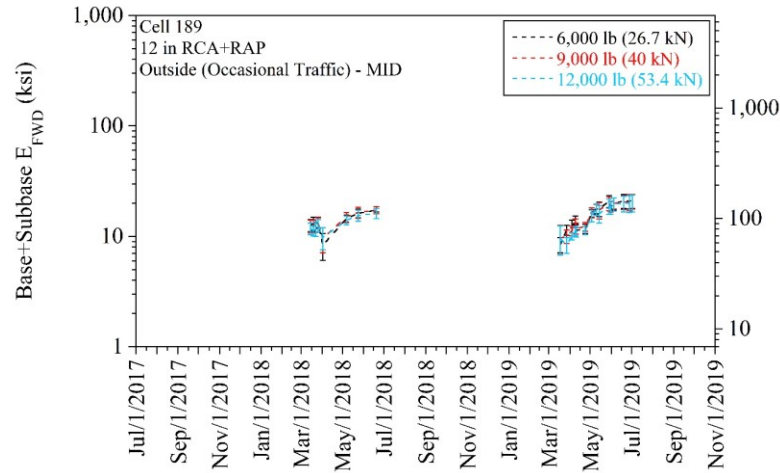
Cell 186 (12-in Fine RCA) - base+subbase E_{FWD} (error bars represent one standard deviation of the data):



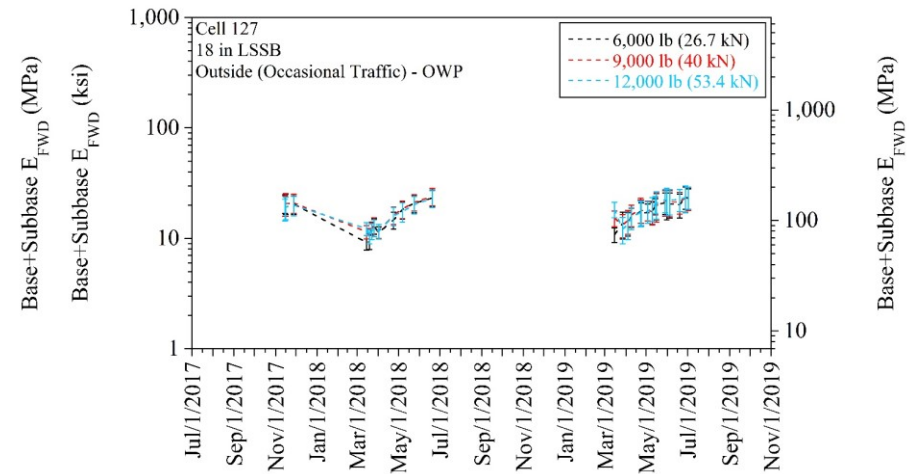
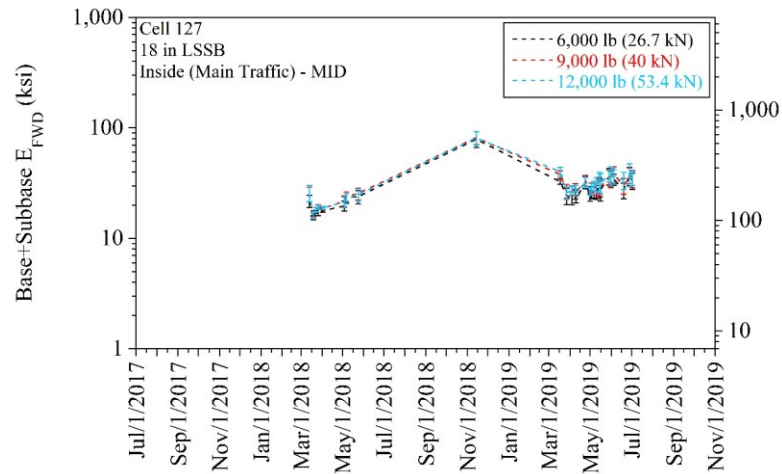
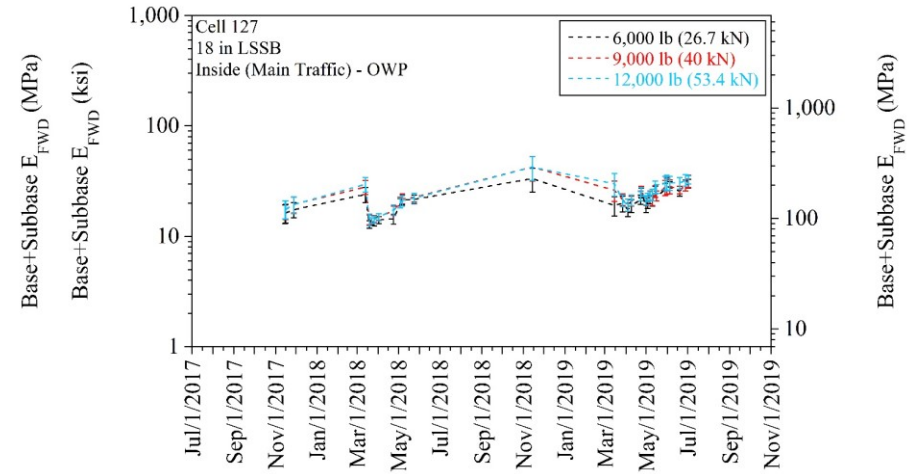
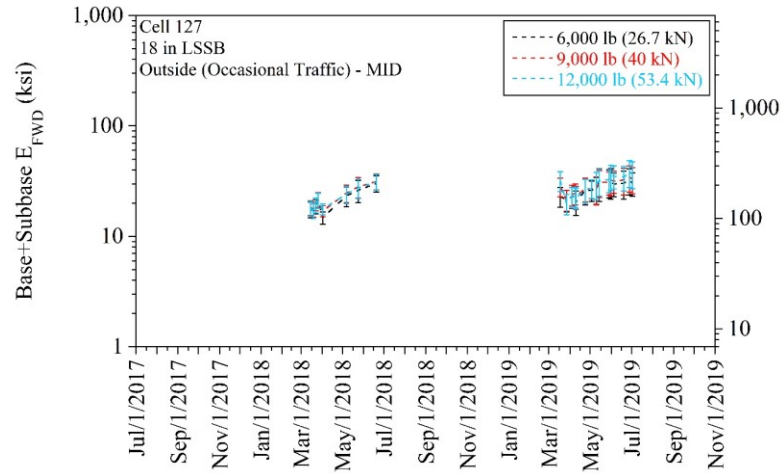
Cell 188 (12-in Limestone) - base+subbase E_{FWD} (error bars represent one standard deviation of the data):



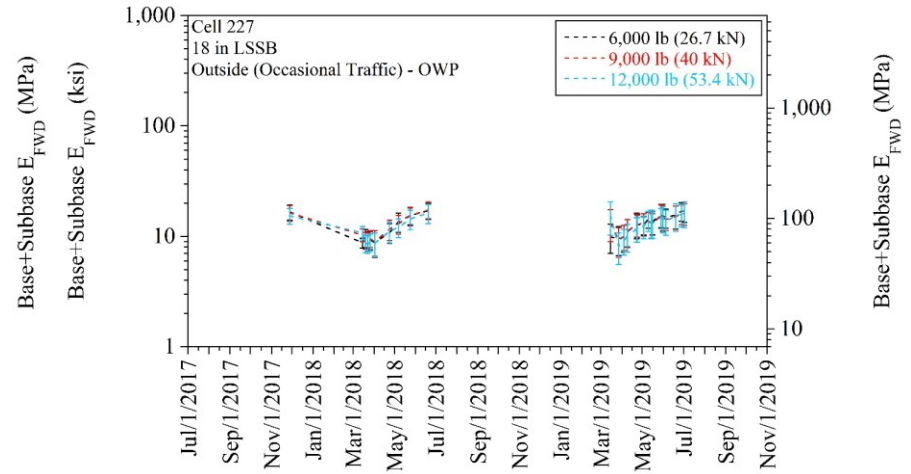
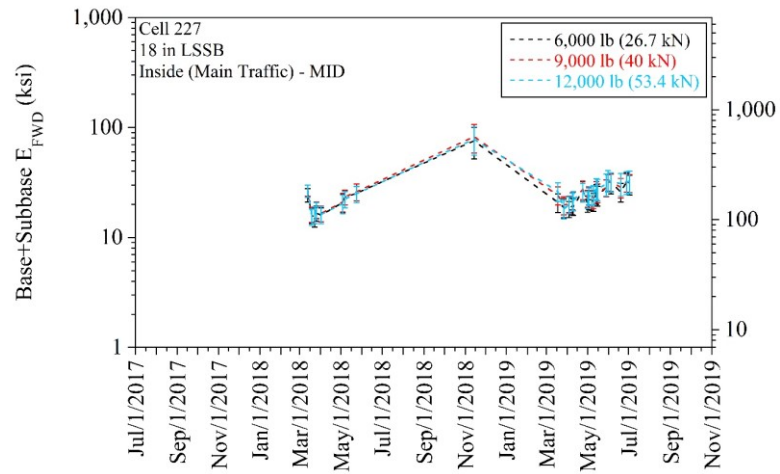
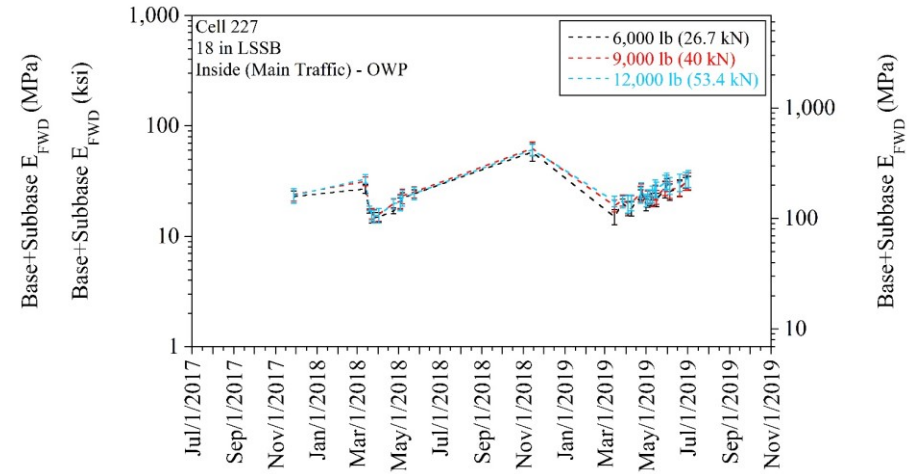
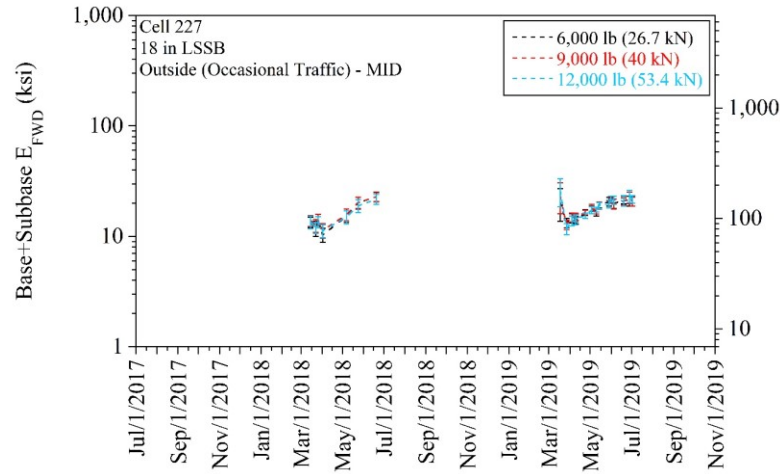
Cell 189 (12-in RCA+RAP) - base+subbase E_{FWD} (error bars represent one standard deviation of the data):



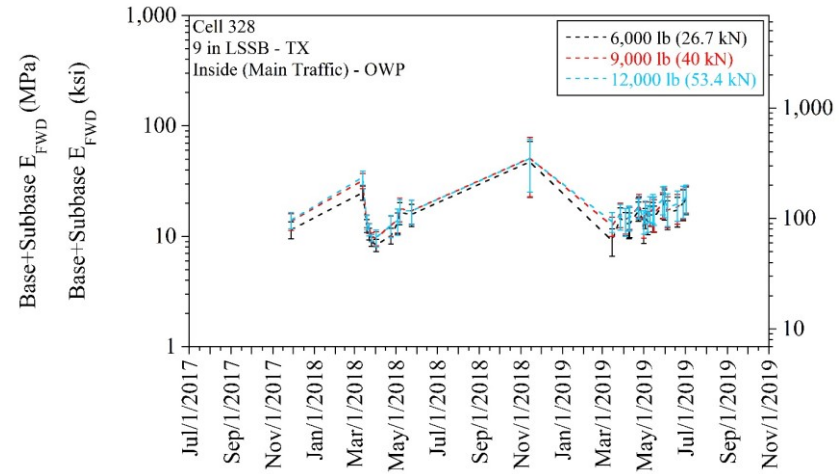
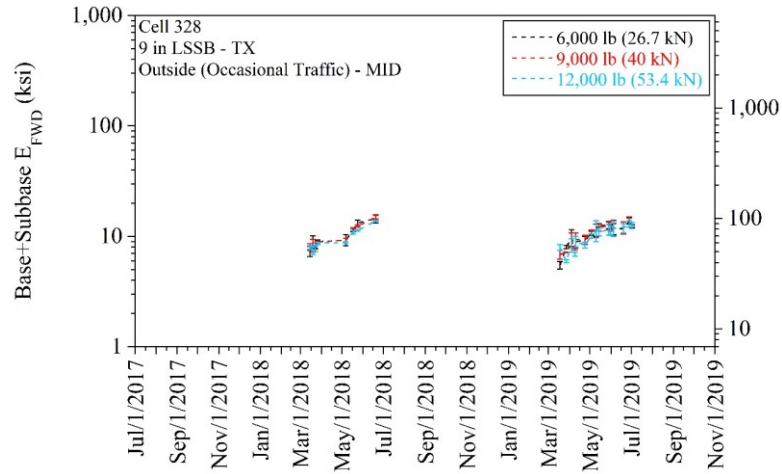
Cell 127 (18-in LSSB) - base+subbase E_{FWD} (error bars represent one standard deviation of the data):



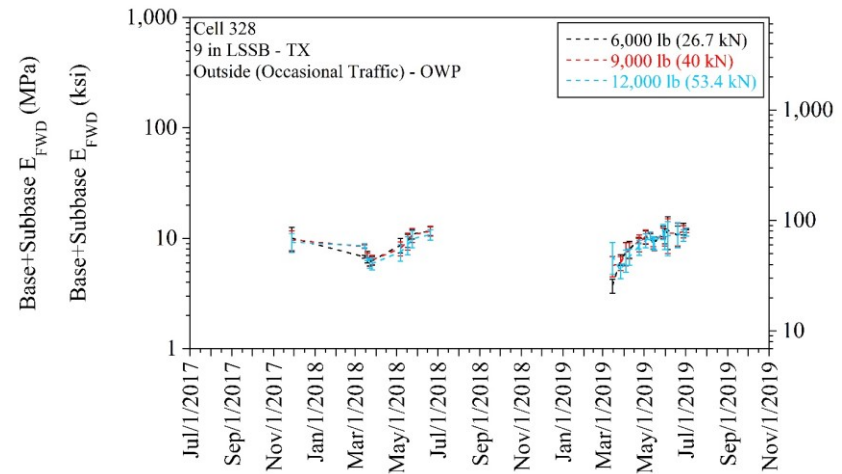
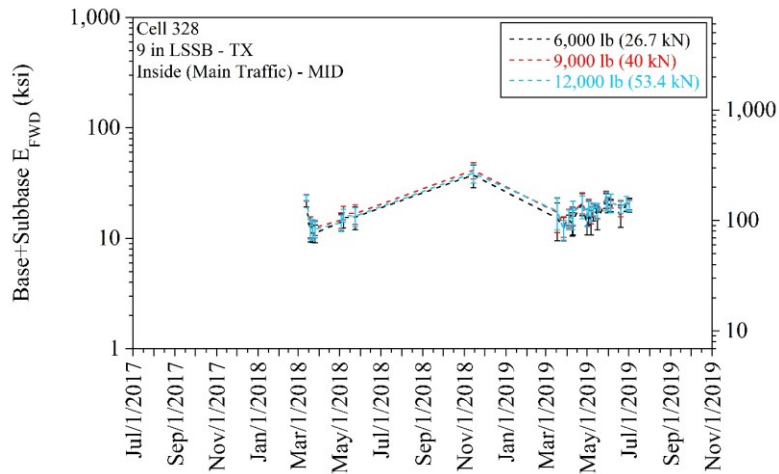
Cell 227 (18-in LSSB) - base+subbase E_{FWD} (error bars represent one standard deviation of the data):



Cell 328 (9-in LSSB - TX) - base+subbase E_{FWD} (error bars represent one standard deviation of the data):

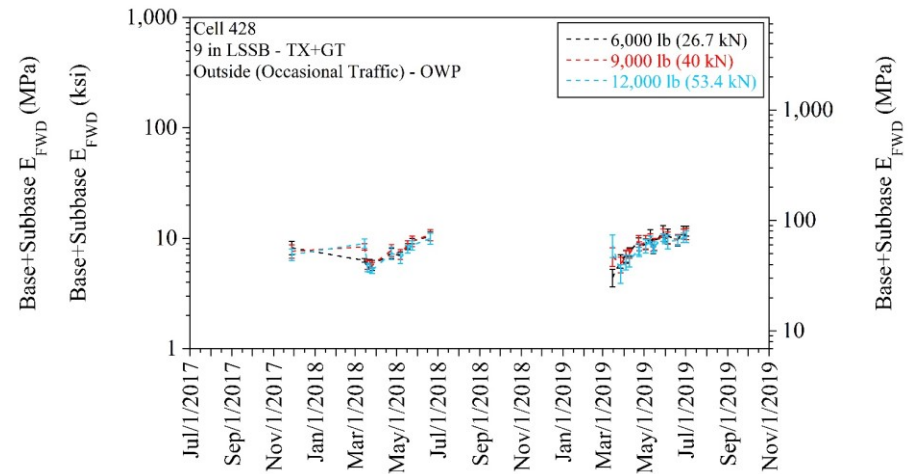
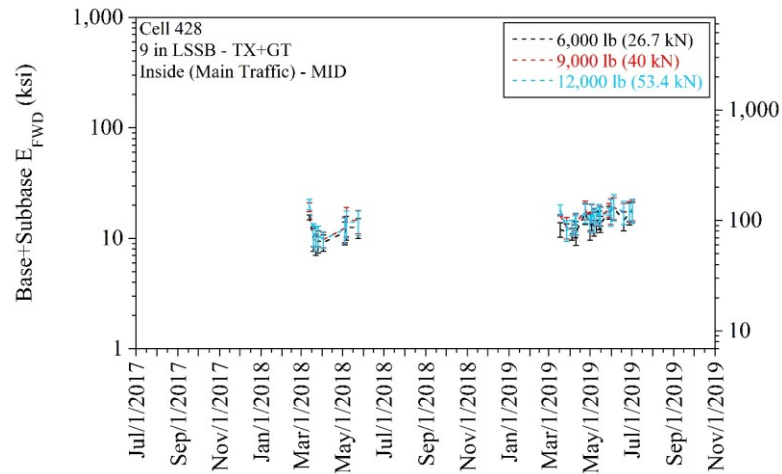
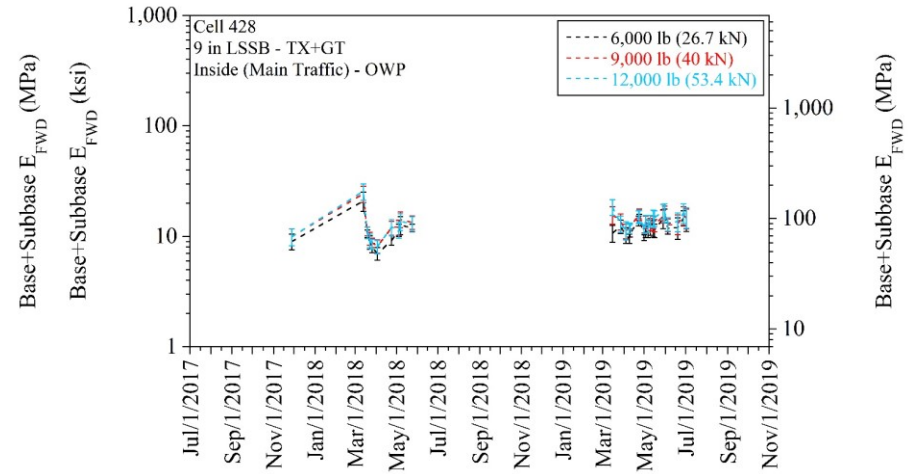
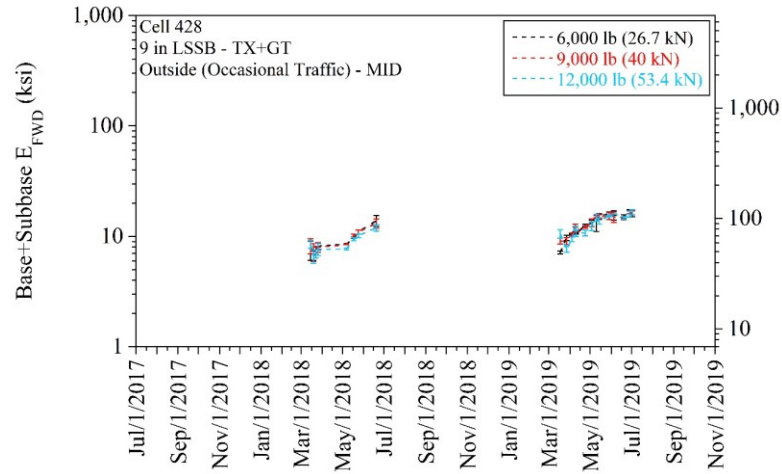


Base+Subbase E_{FWD} (MPa)

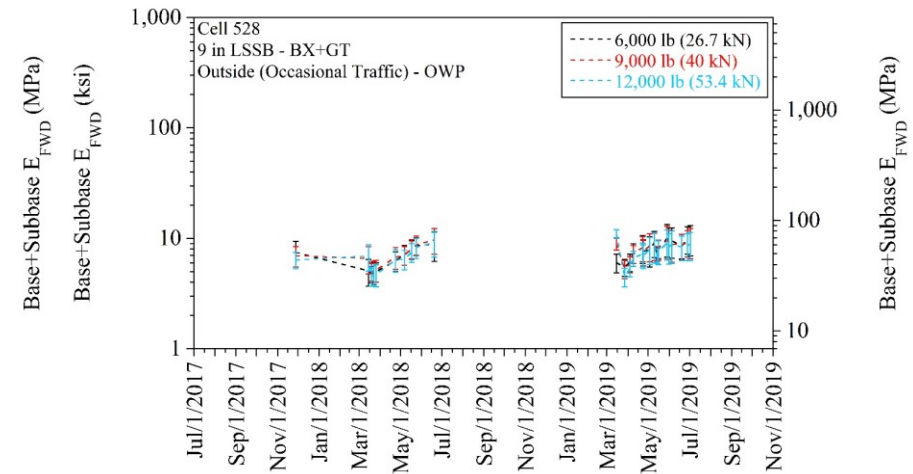
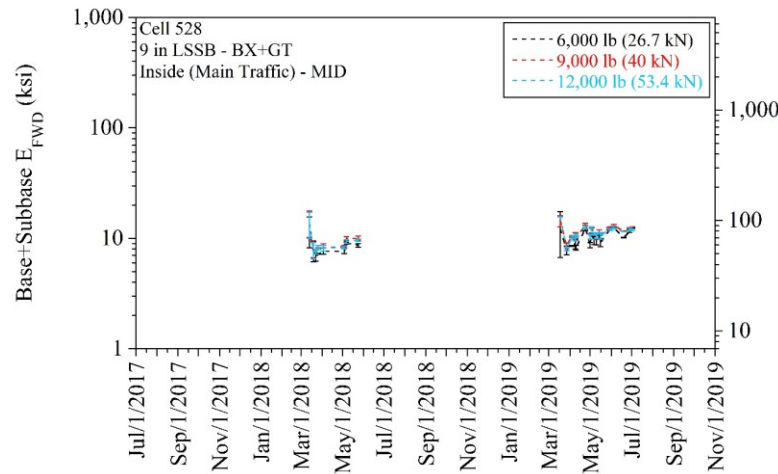
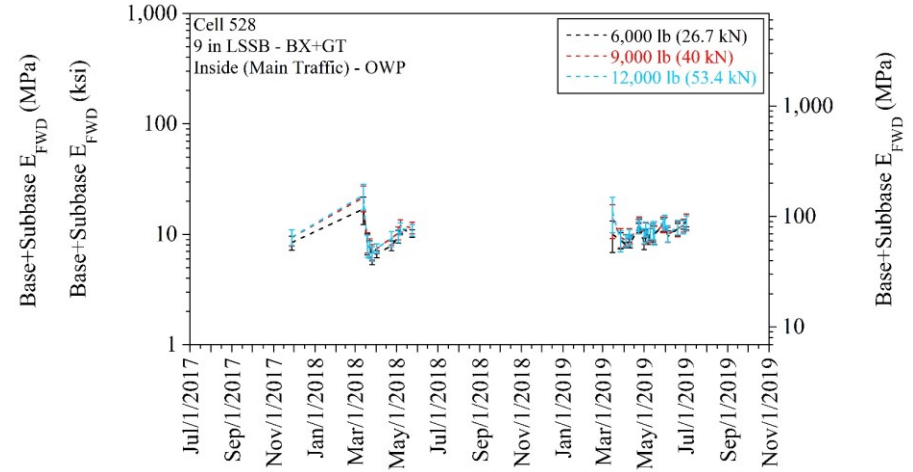
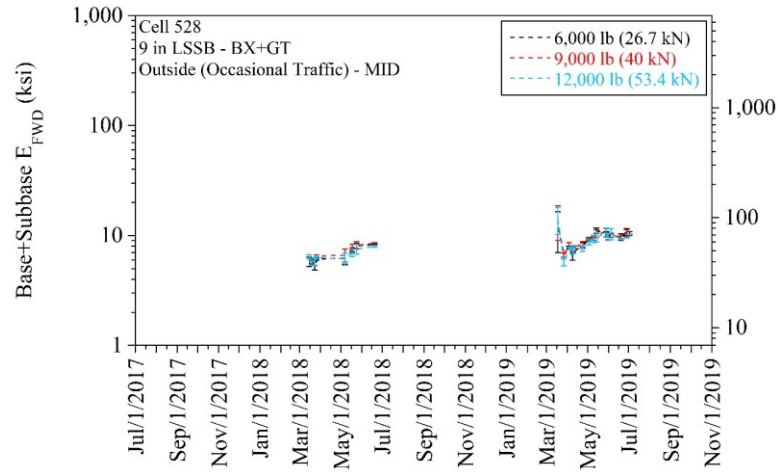


Base+Subbase E_{FWD} (MPa)

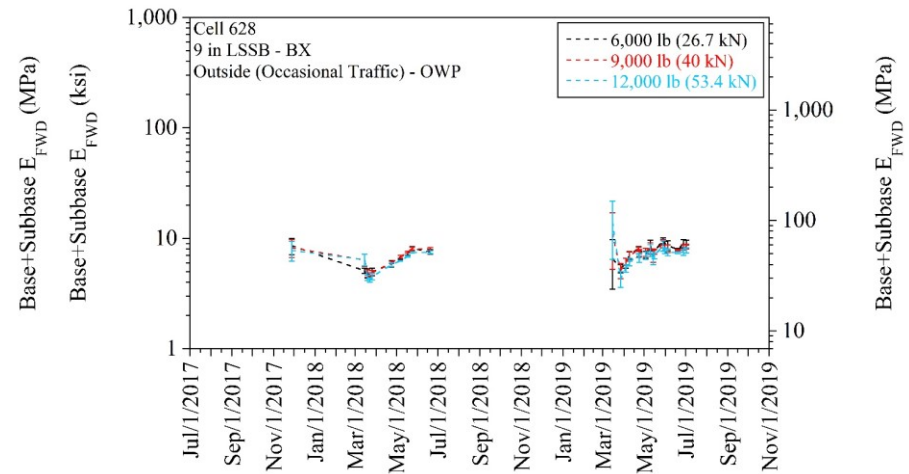
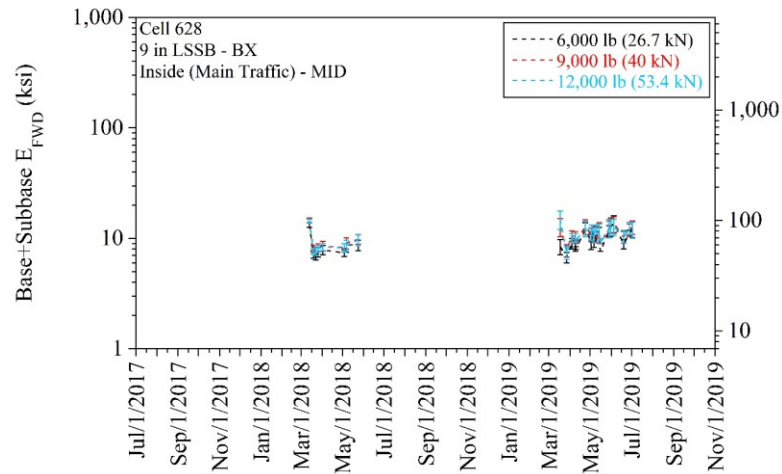
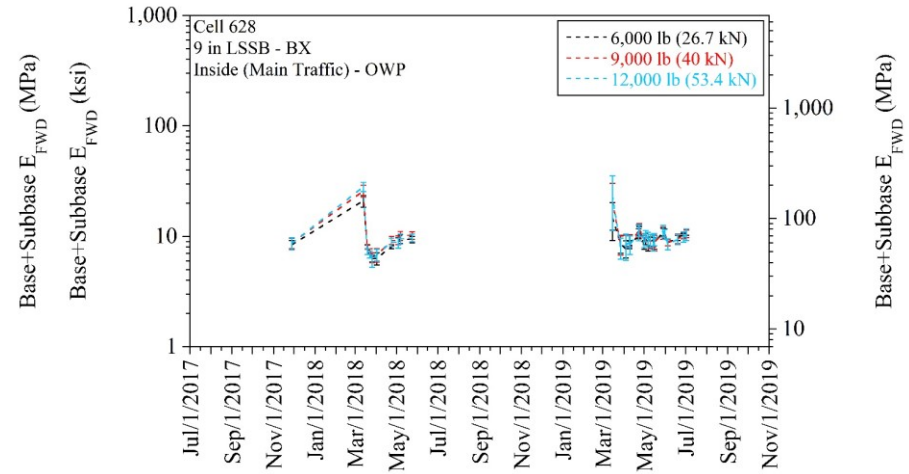
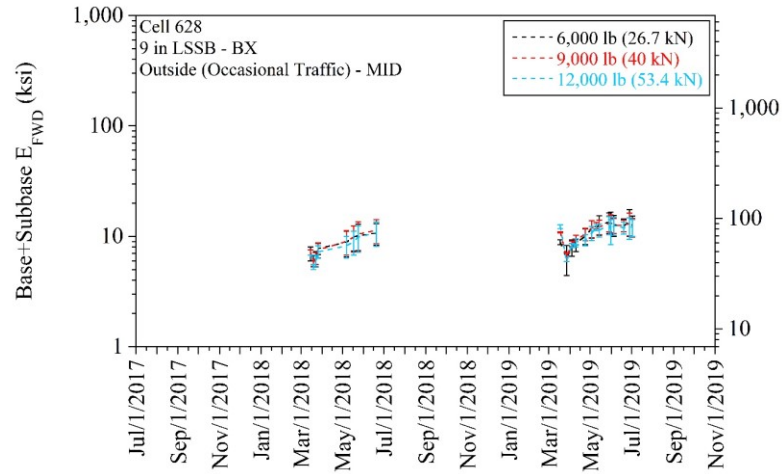
Cell 428 (9-in LSSB - TX+GT) - base+subbase E_{FWD} (error bars represent one standard deviation of the data):



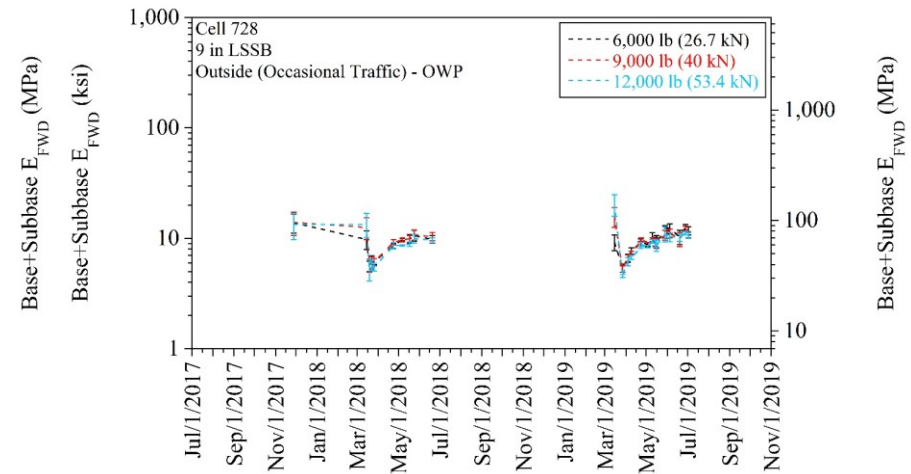
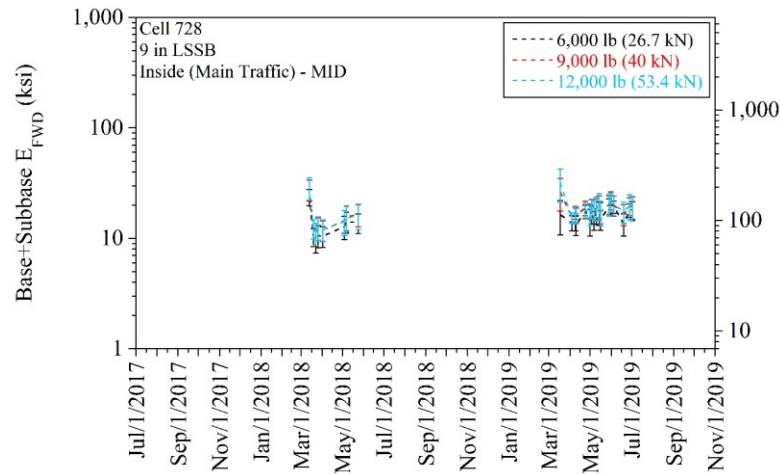
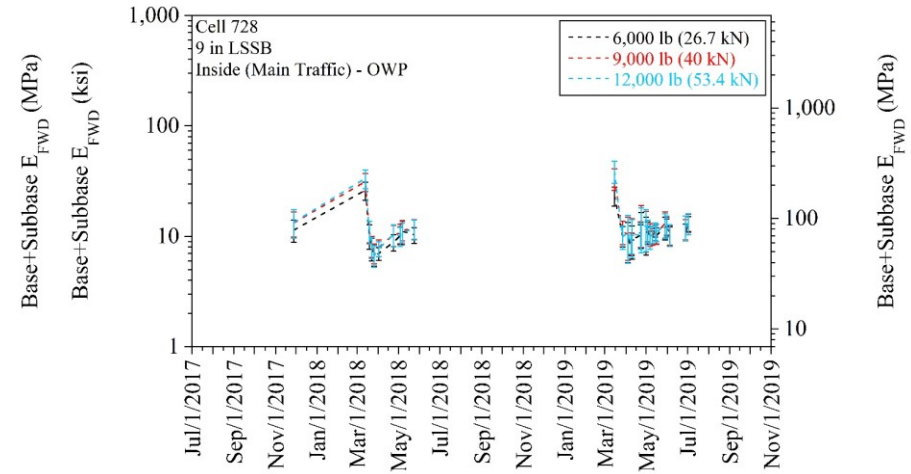
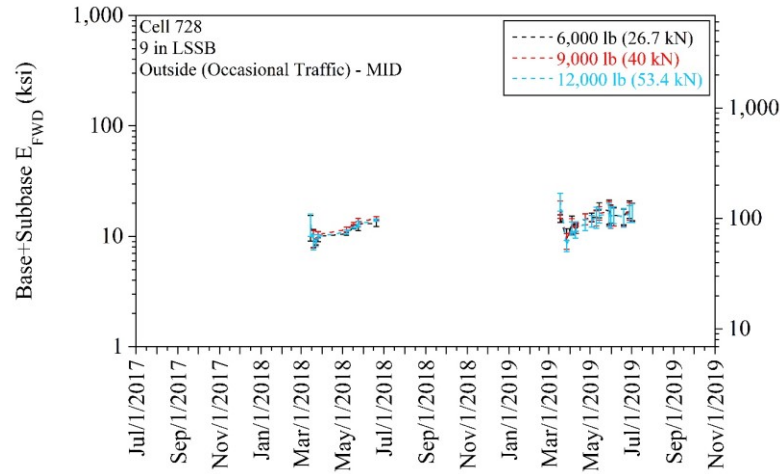
Cell 528 (9-in LSSB - BX+GT) - base+subbase E_{FWD} (error bars represent one standard deviation of the data):



Cell 628 (9-in LSSB - BX) - base+subbase E_{FWD} (error bars represent one standard deviation of the data):



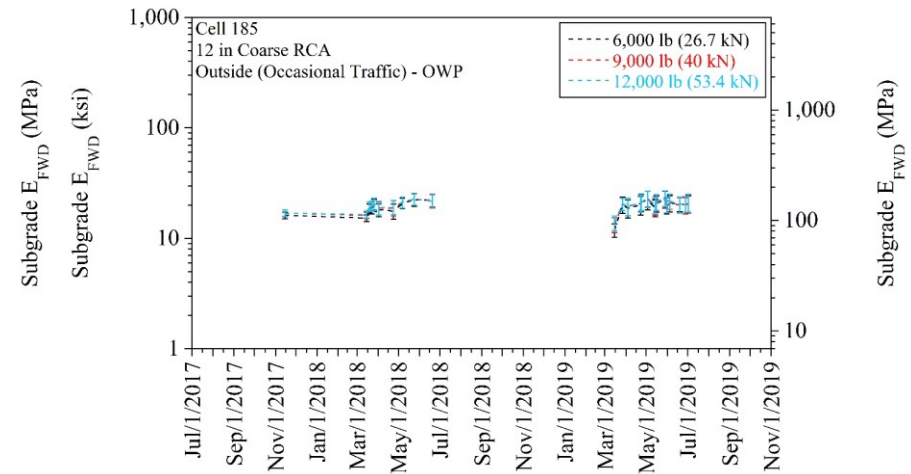
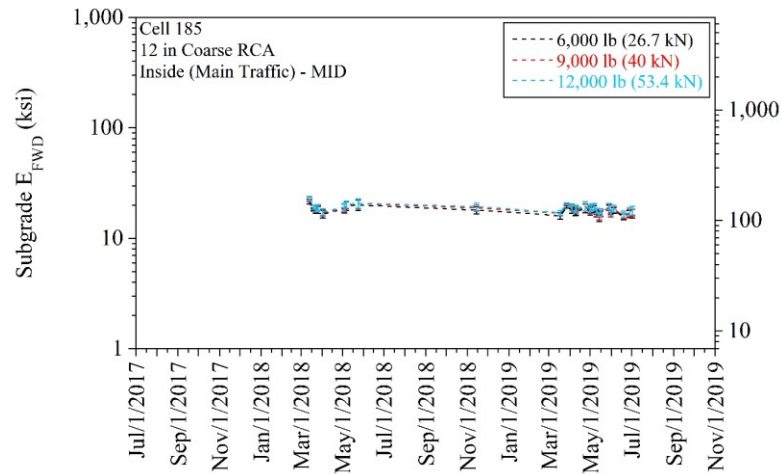
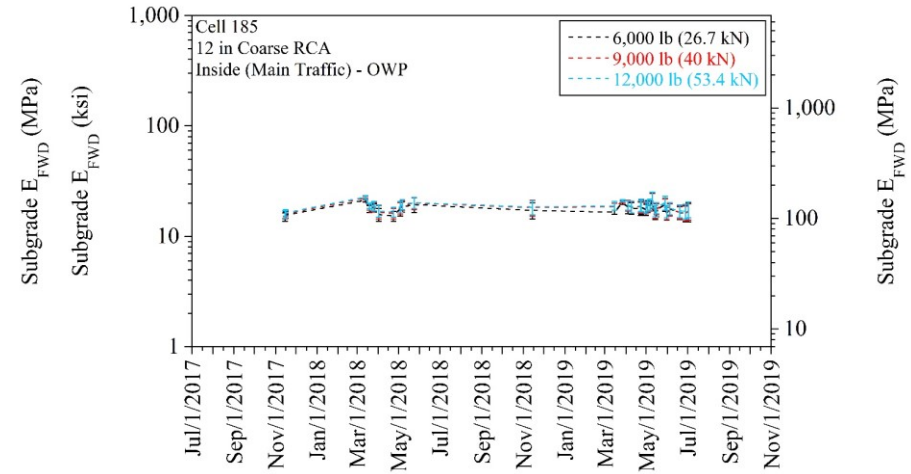
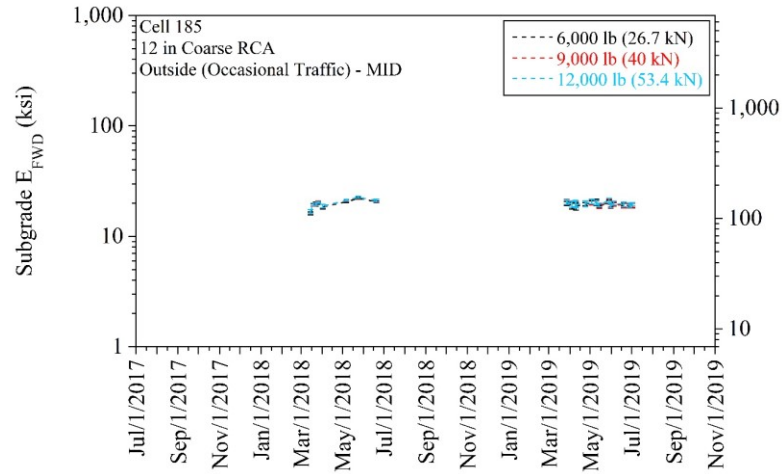
Cell 728 (9-in LSSB) - base+subbase E_{FWD} (error bars represent one standard deviation of the data):



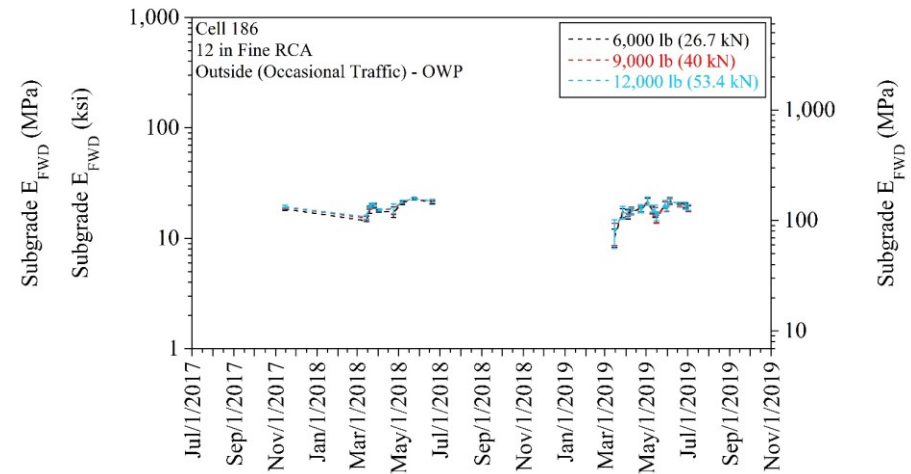
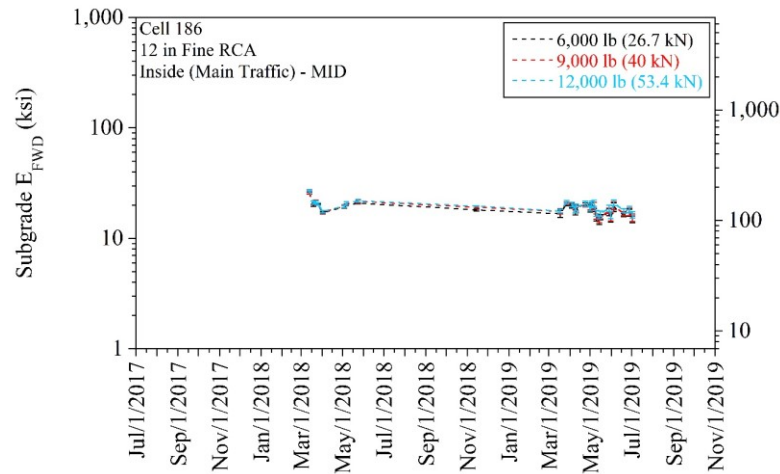
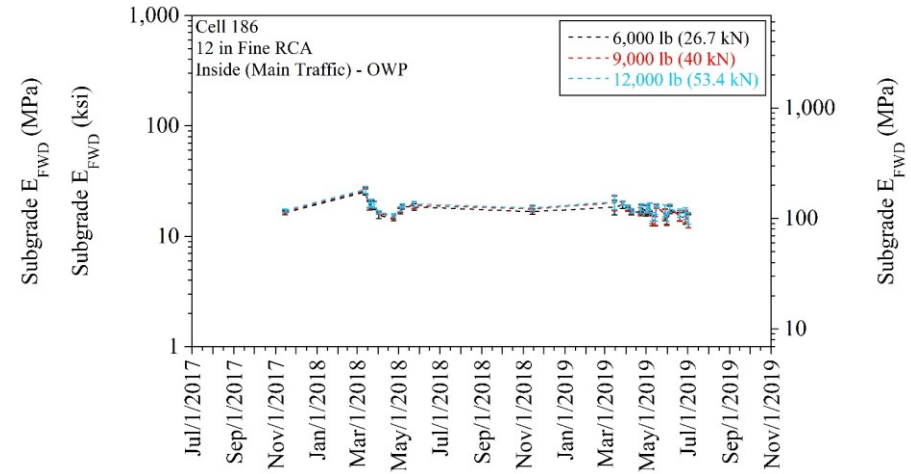
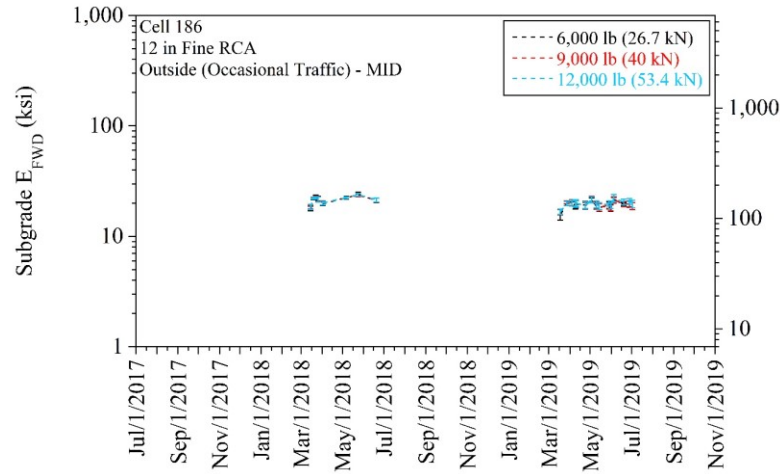
APPENDIX Y

**SUBGRADE FALLING WEIGHT DEFLECTOMETER (FWD) ELASTIC
MODULUS (E_{FWD}) AT 6,000 LB (26.7 KN), 9,000 LB (40 KN), AND
12,000 LB (53.4 KN) FOR EACH CELL**

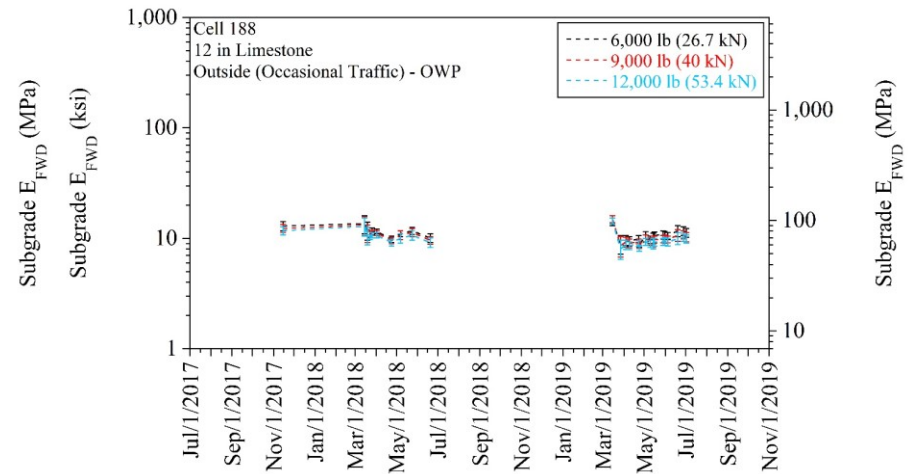
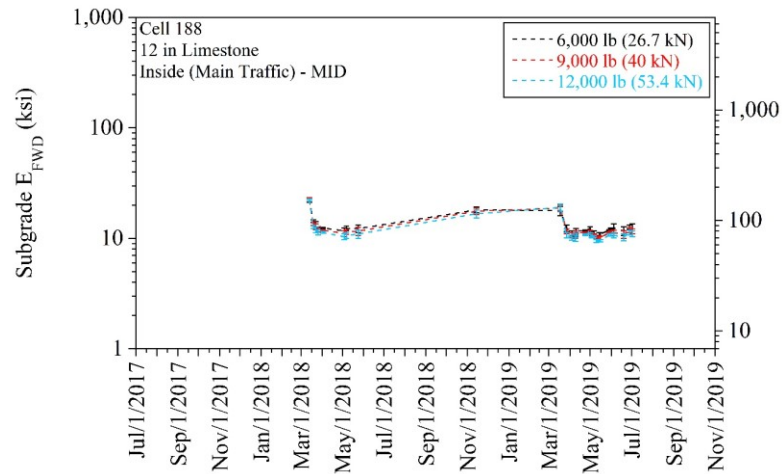
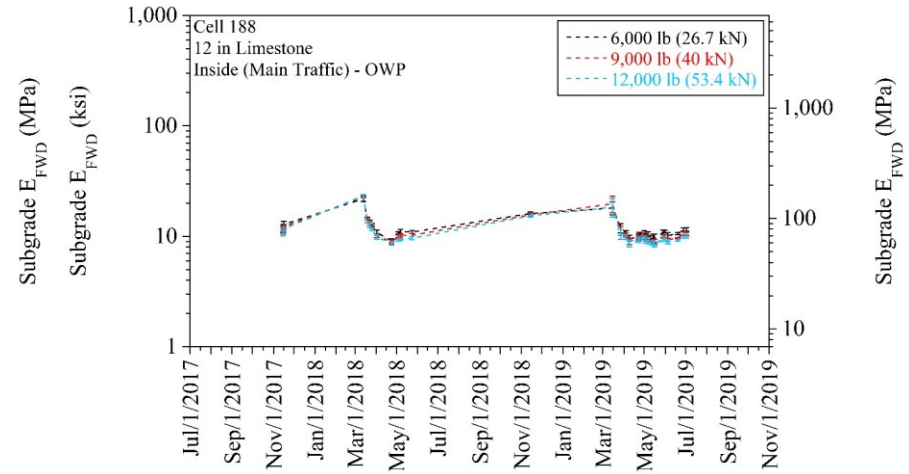
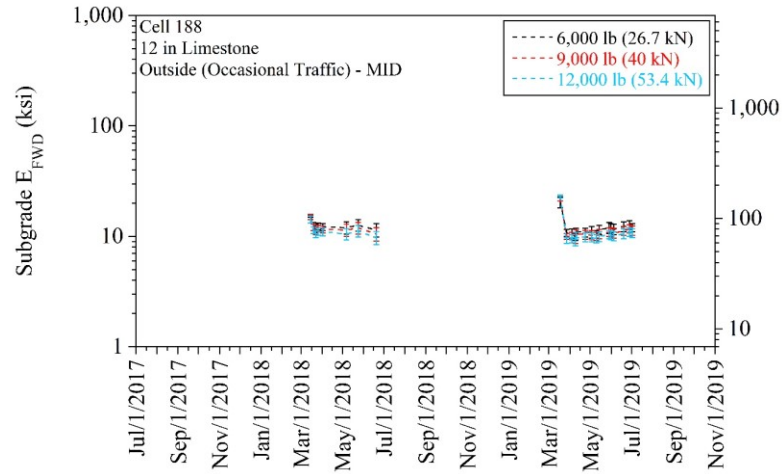
Cell 185 (12-in Coarse RCA) - subgrade E_{FWD} (error bars represent one standard deviation of the data):



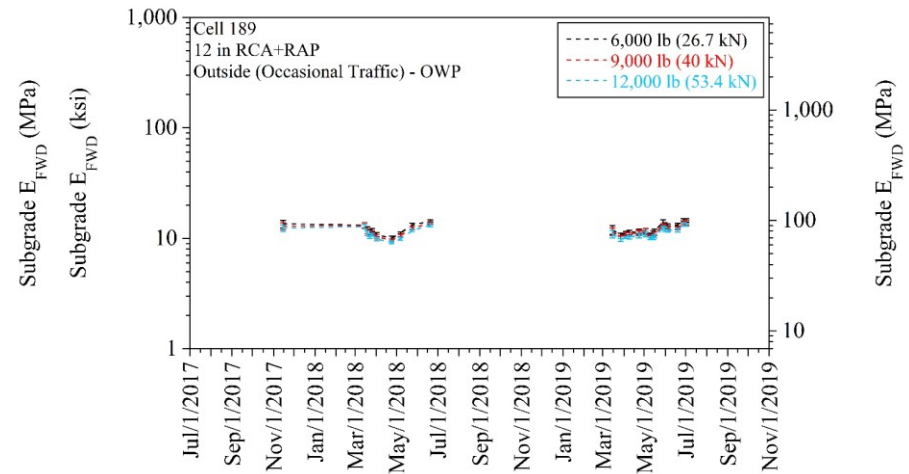
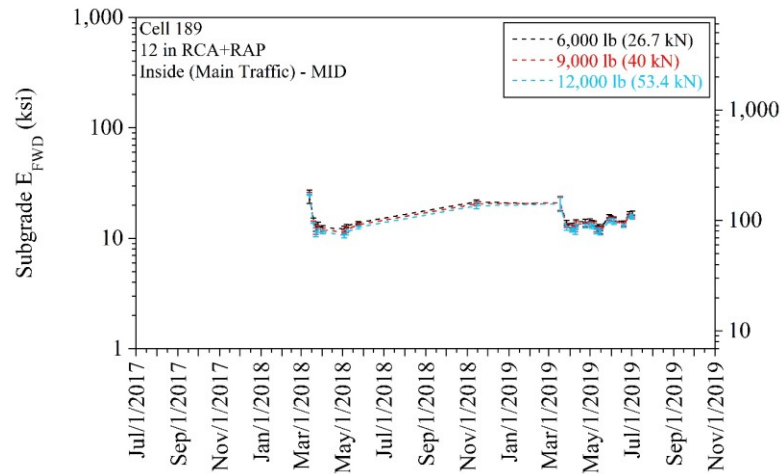
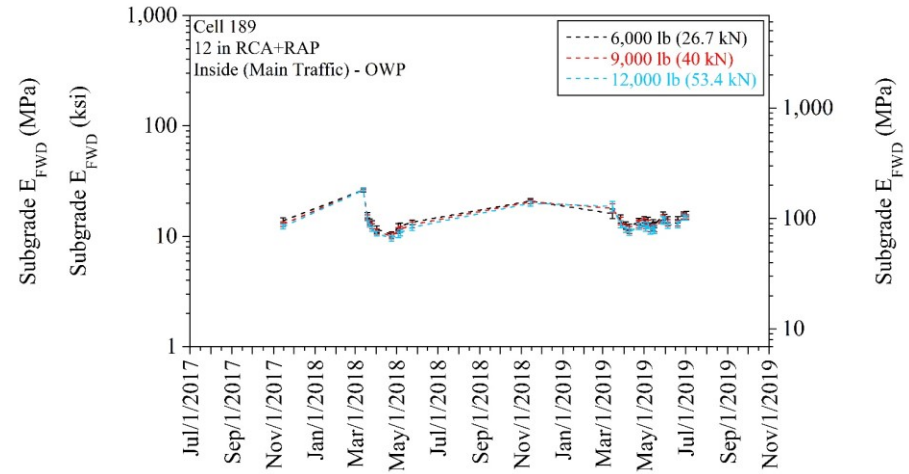
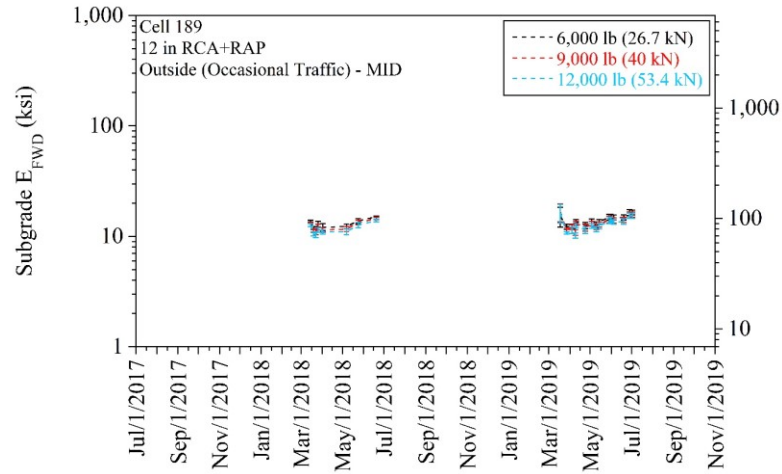
Cell 186 (12-in Fine RCA) - subgrade E_{FWD} (error bars represent one standard deviation of the data):



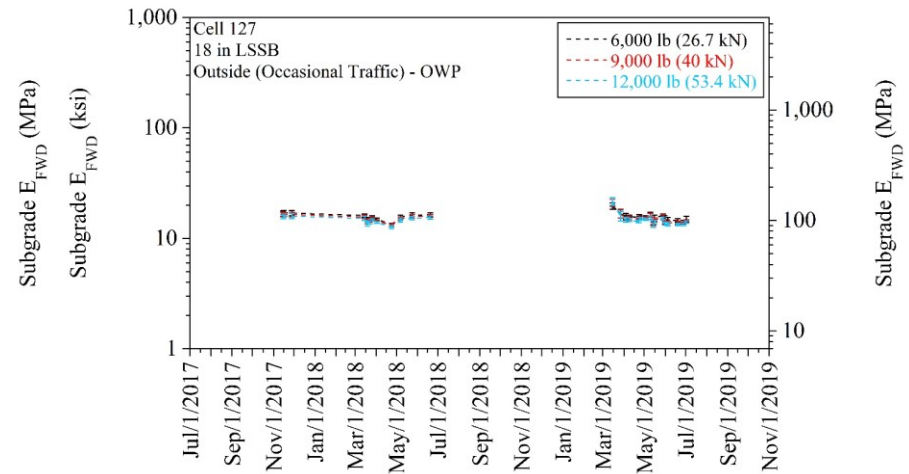
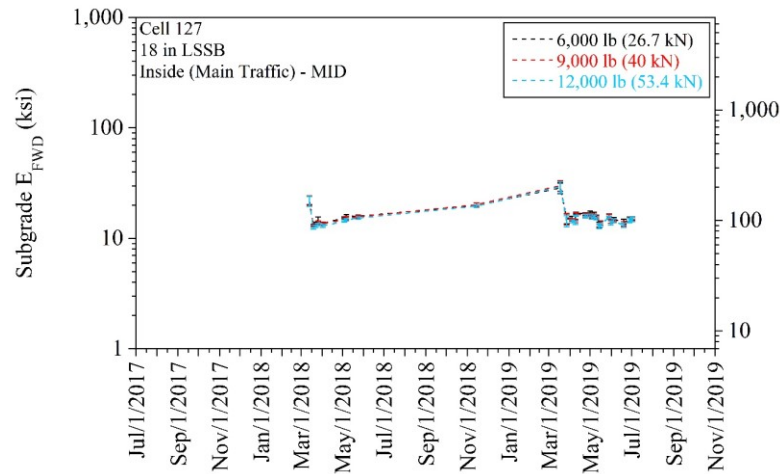
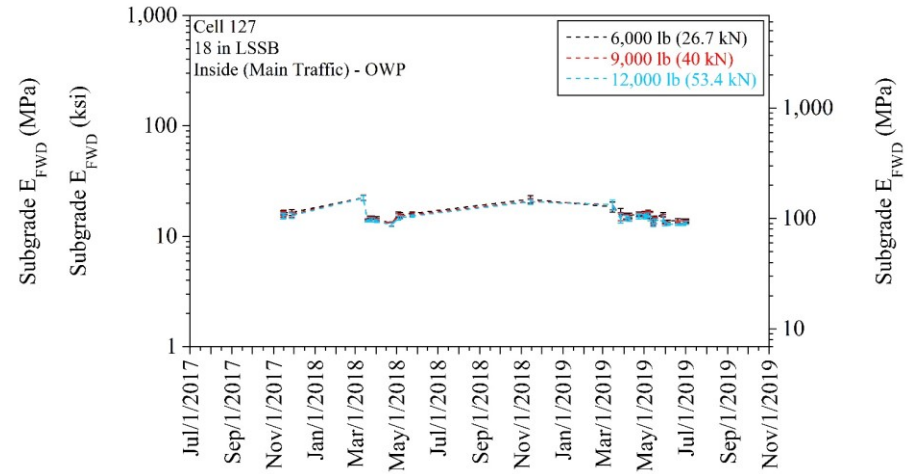
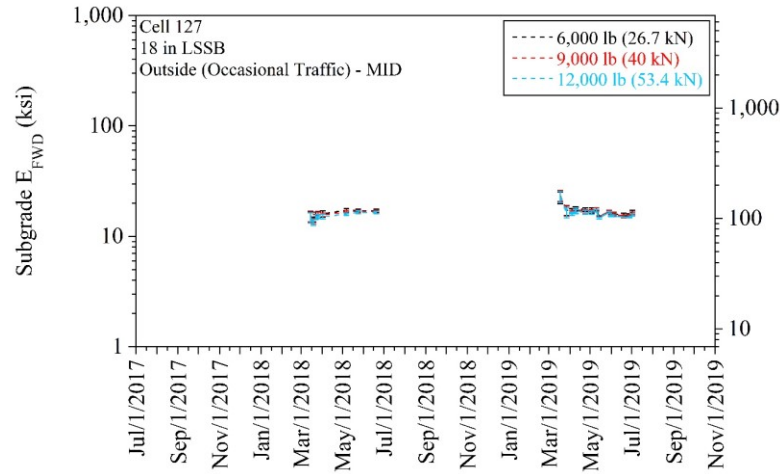
Cell 188 (12-in Limestone) - subgrade E_{FWD} (error bars represent one standard deviation of the data):



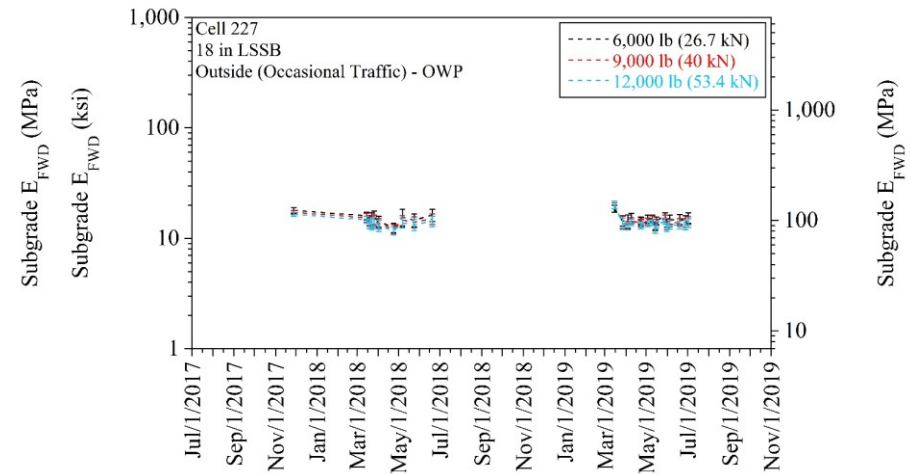
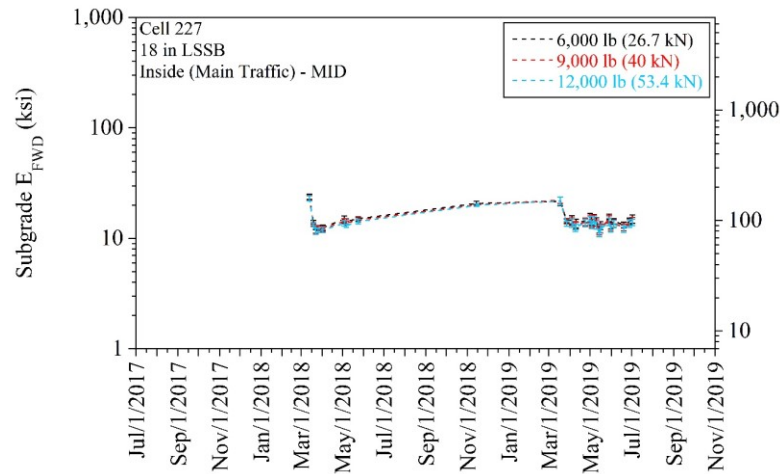
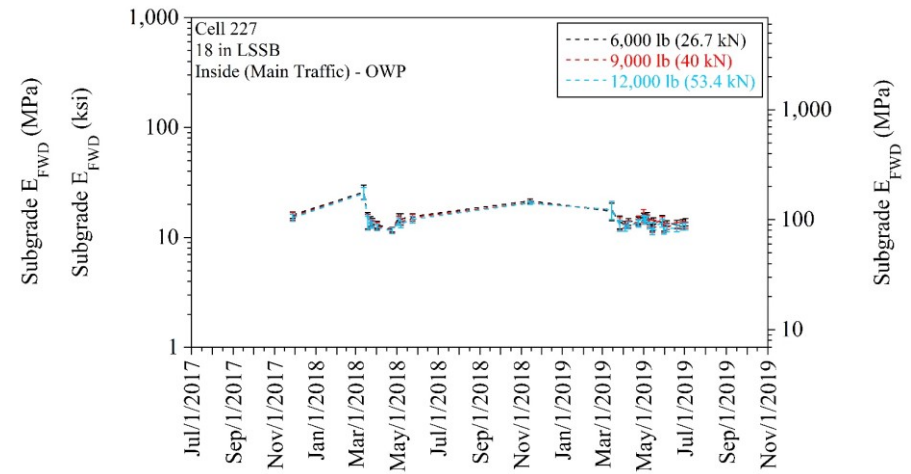
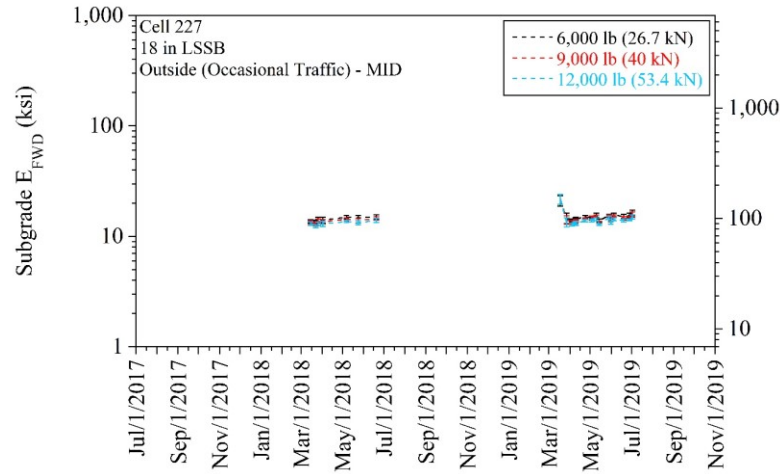
Cell 189 (12-in RCA+RAP) - subgrade E_{FWD} (error bars represent one standard deviation of the data):



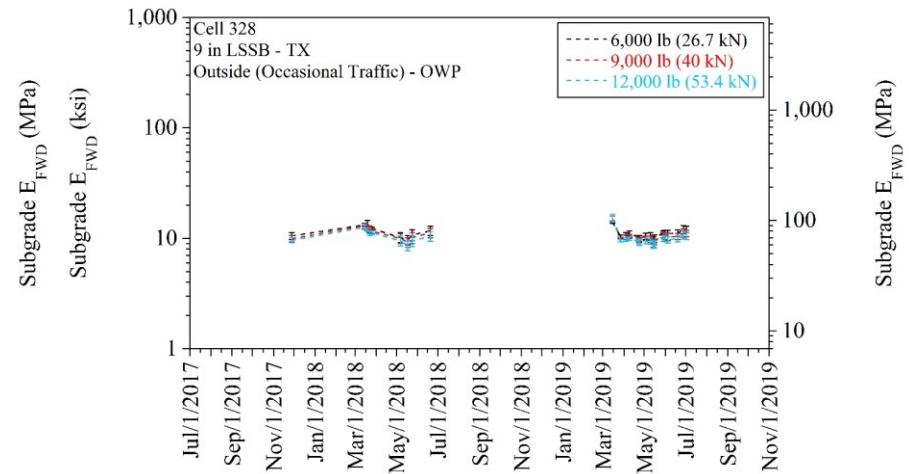
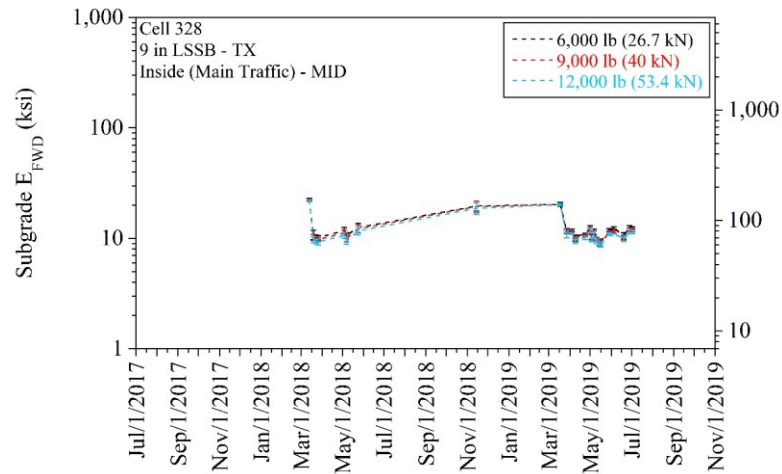
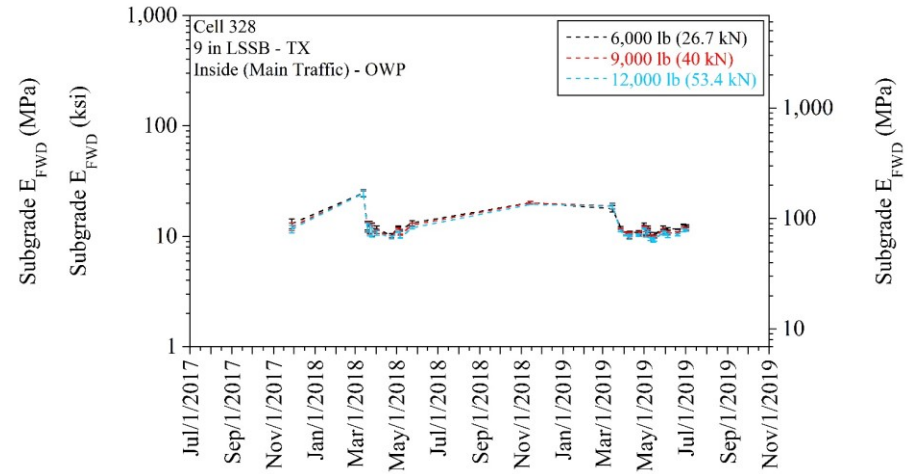
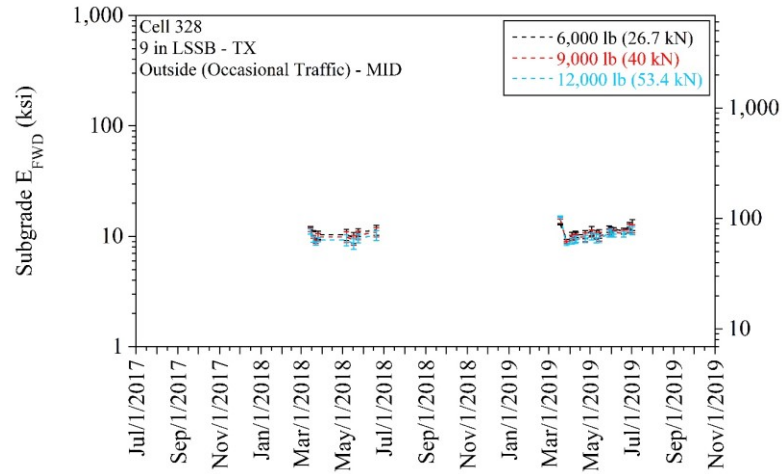
Cell 127 (18-in LSSB) - subgrade E_{FWD} (error bars represent one standard deviation of the data):



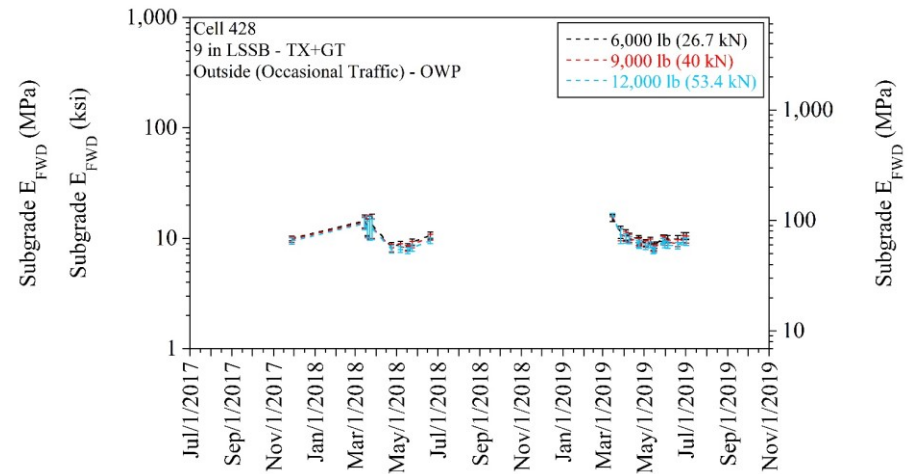
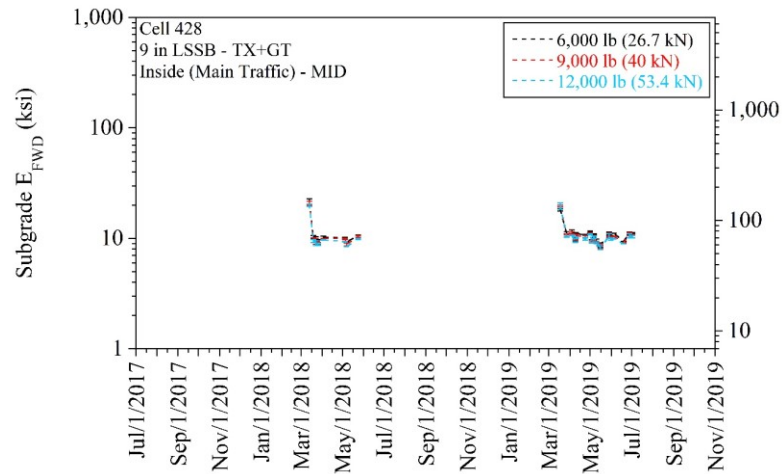
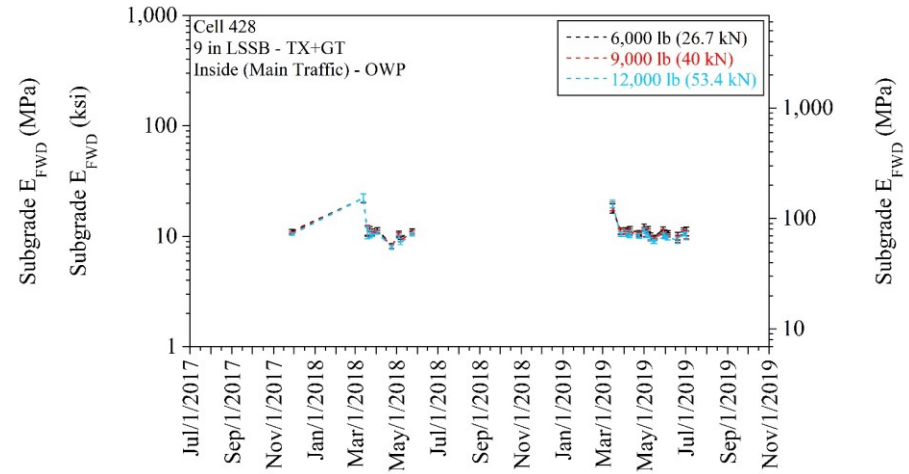
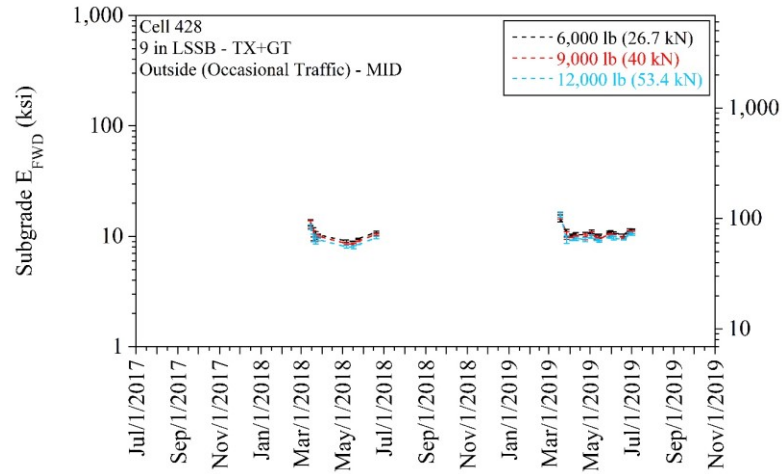
Cell 227 (18-in LSSB) - subgrade E_{FWD} (error bars represent one standard deviation of the data):



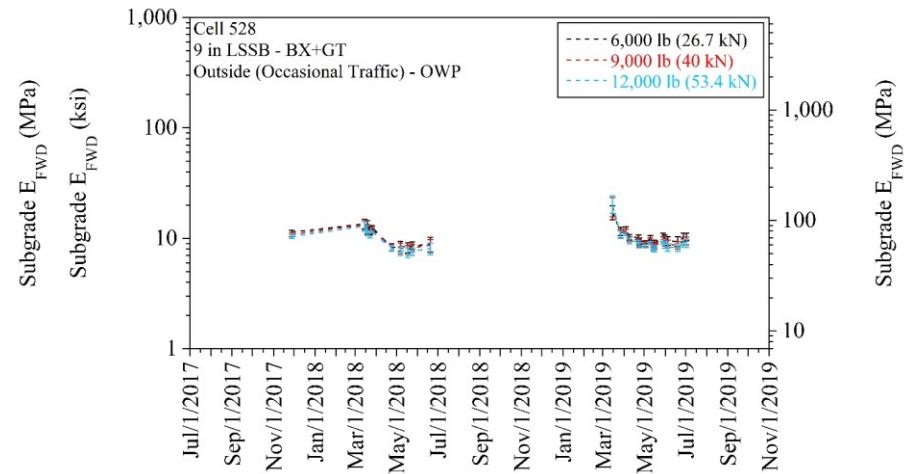
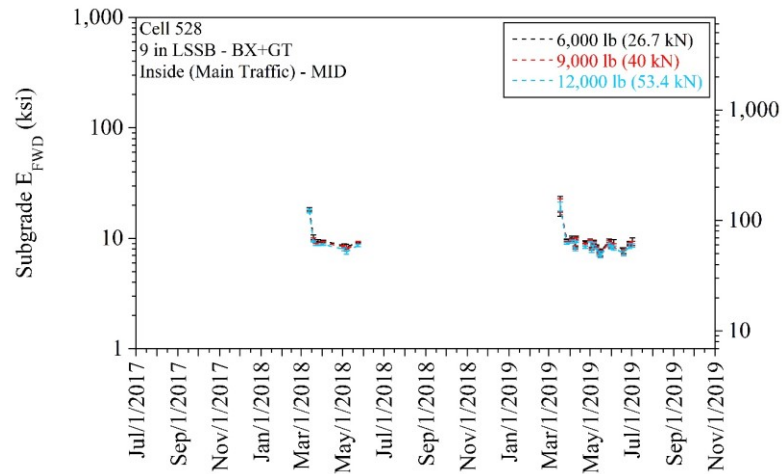
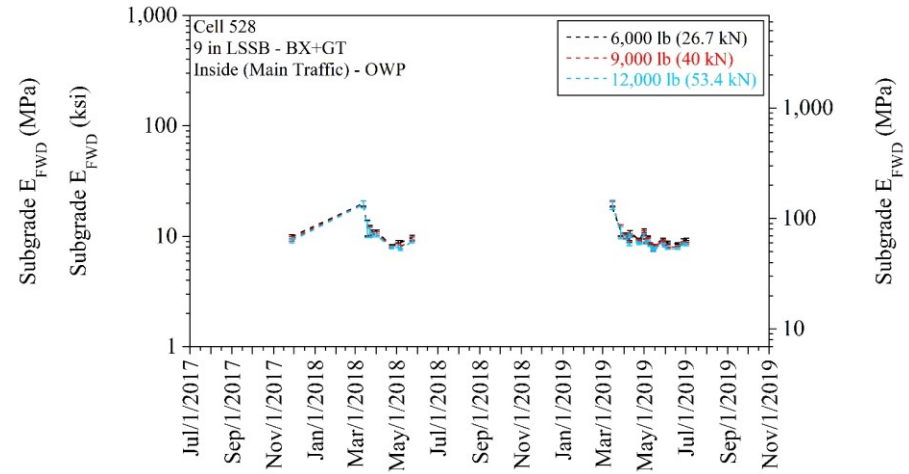
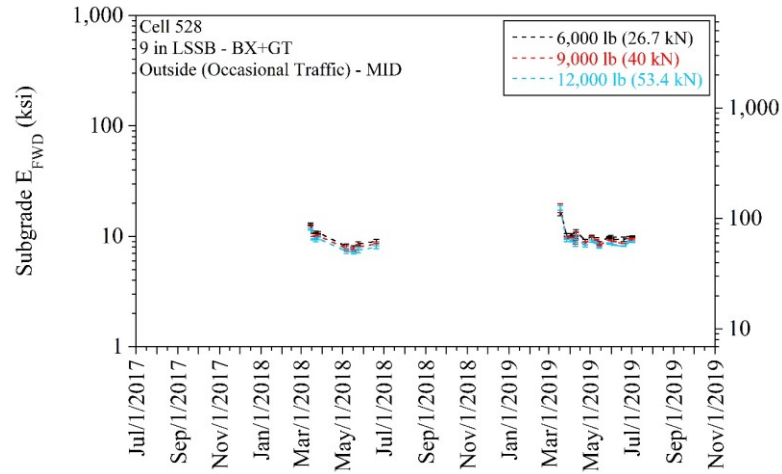
Cell 328 (9-in LSSB - TX) - subgrade E_{FWD} (error bars represent one standard deviation of the data):



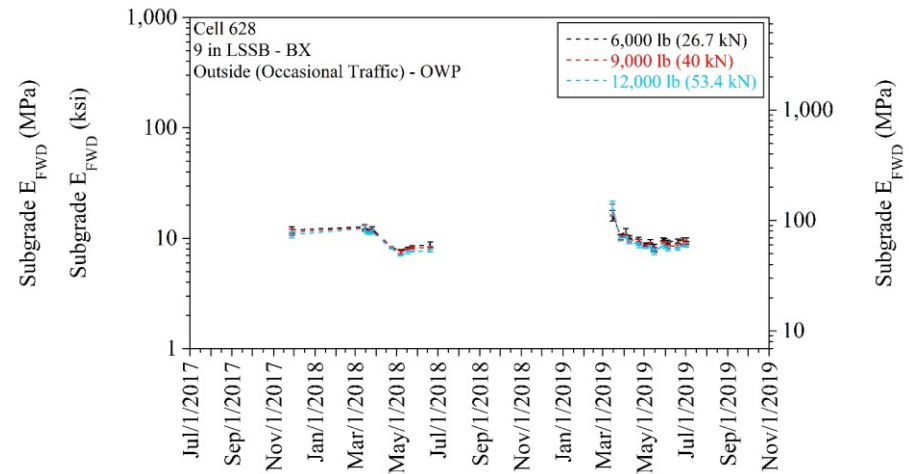
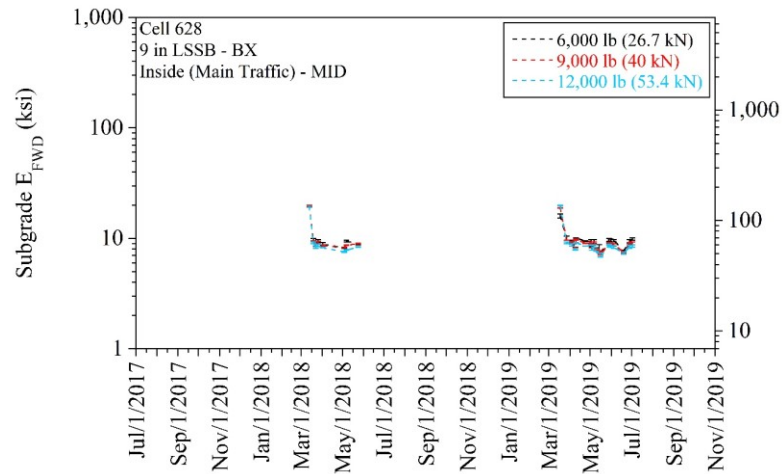
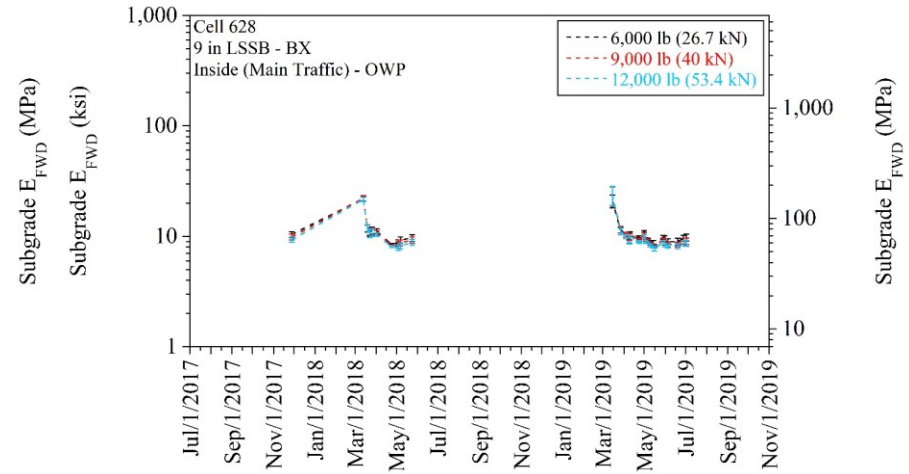
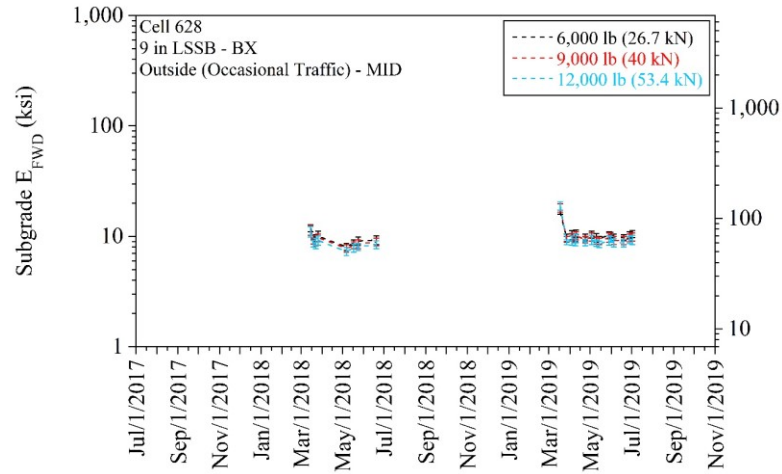
Cell 428 (9-in LSSB - TX+GT) - subgrade E_{FWD} (error bars represent one standard deviation of the data):



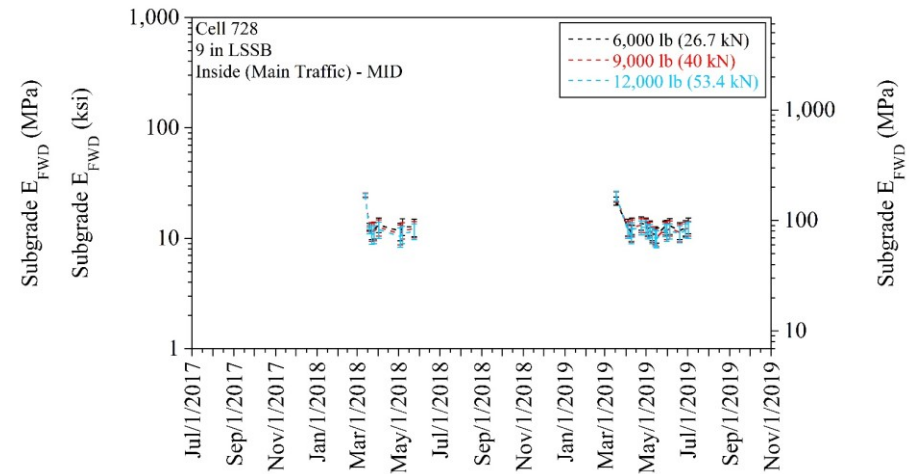
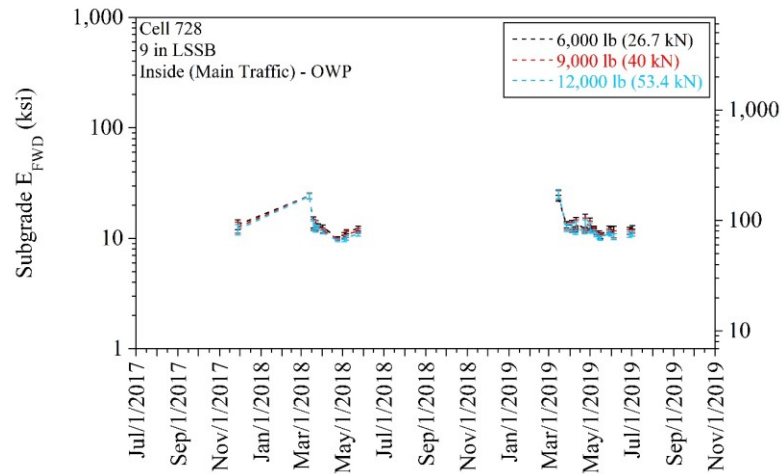
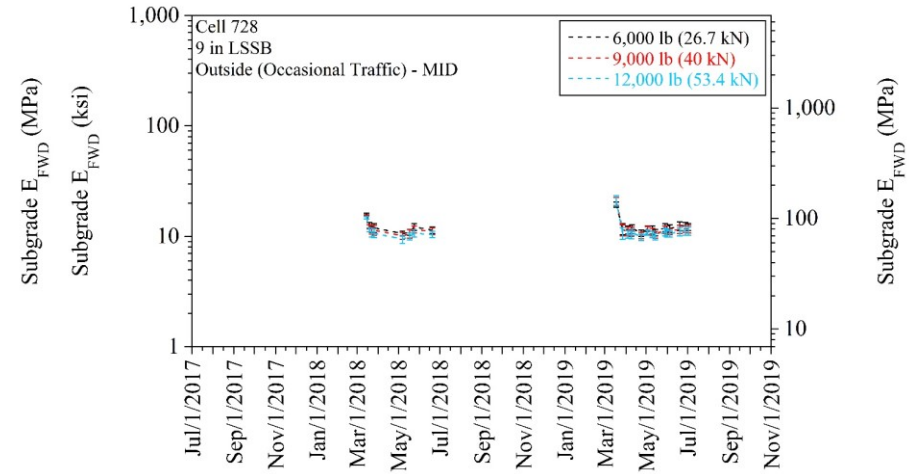
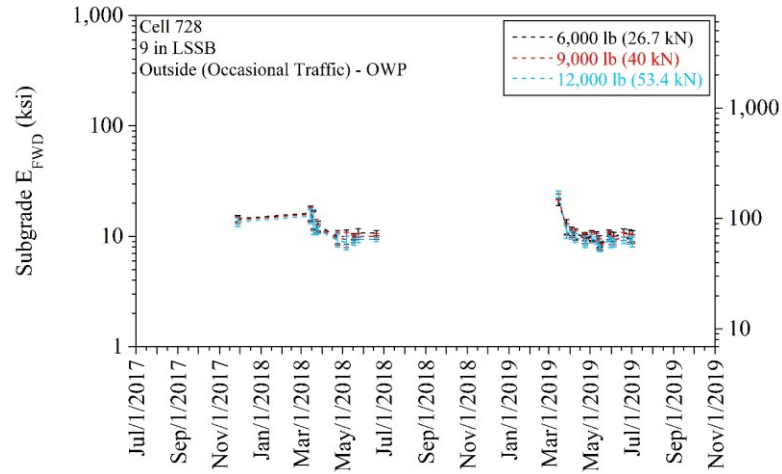
Cell 528 (9-in LSSB - BX+GT) - subgrade E_{FWD} (error bars represent one standard deviation of the data):



Cell 628 (9-in LSSB - BX) - subgrade E_{FWD} (error bars represent one standard deviation of the data):



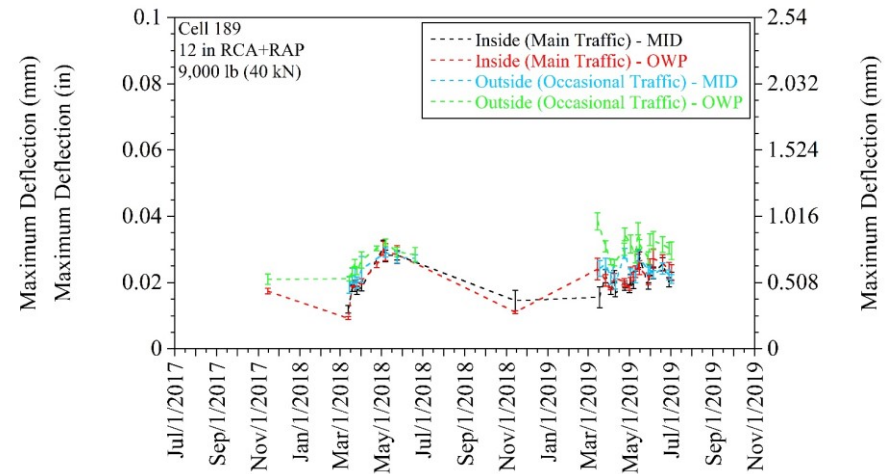
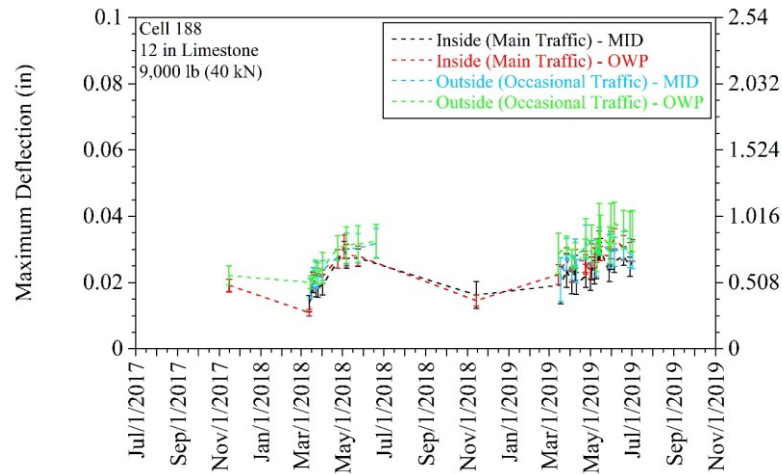
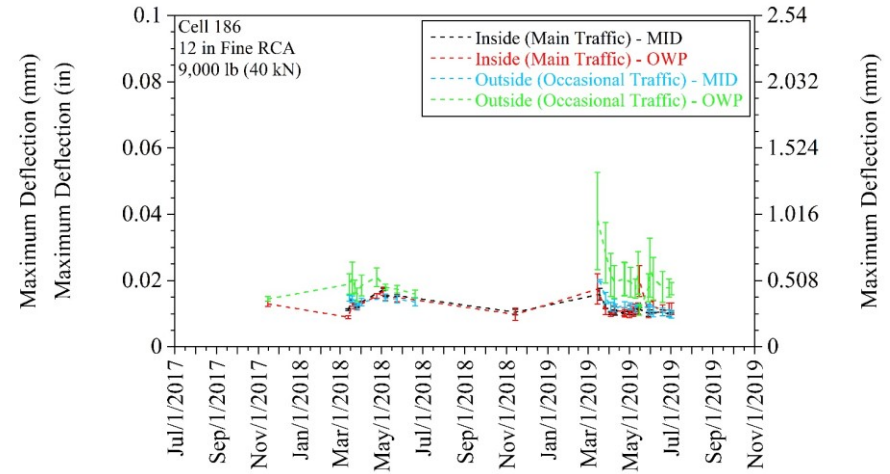
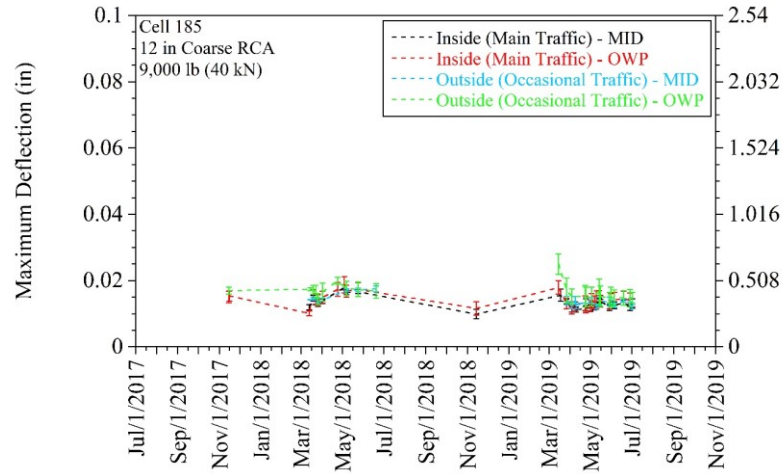
Cell 728 (9-in LSSB) - subgrade E_{FWD} (error bars represent one standard deviation of the data):

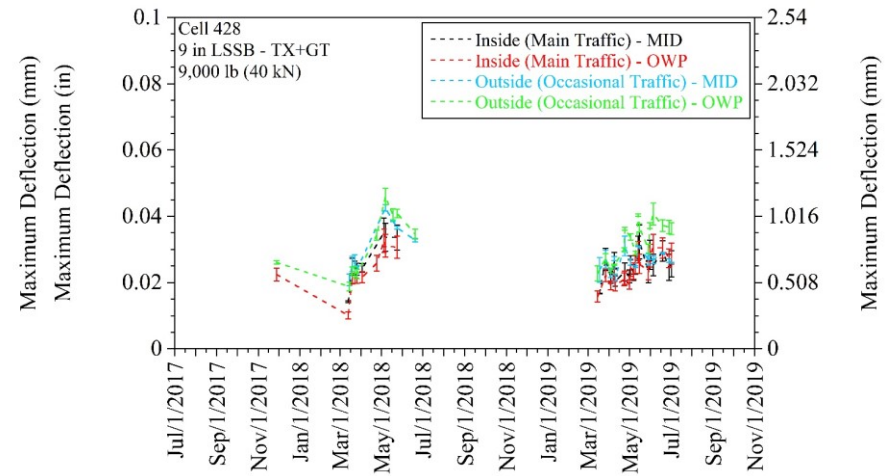
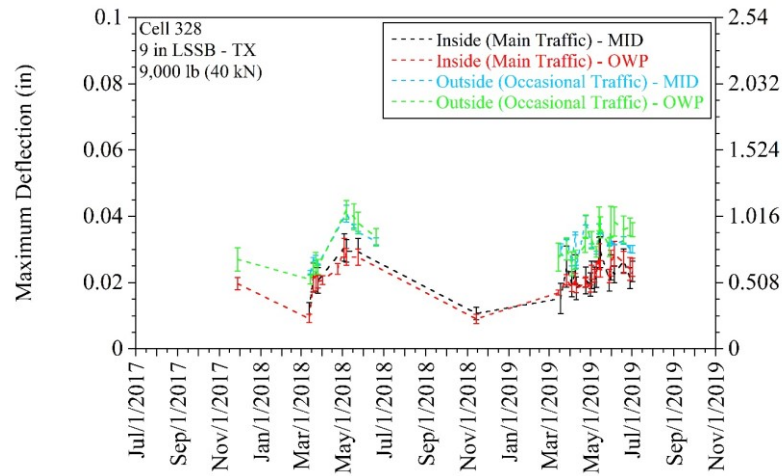
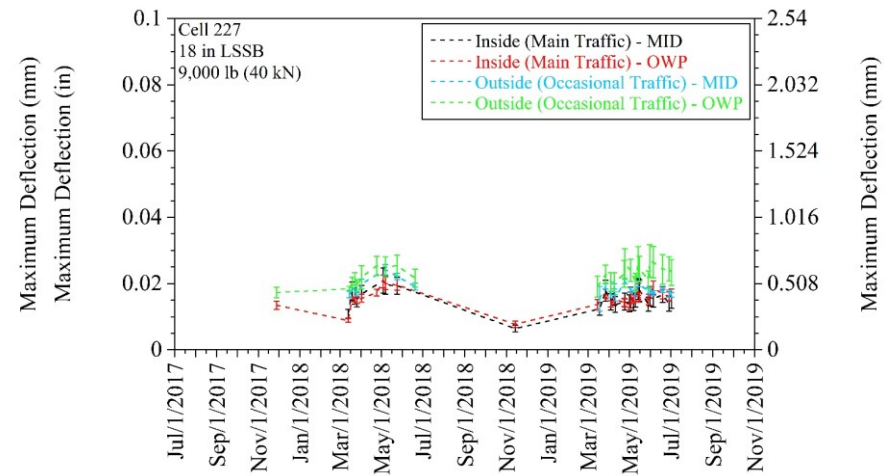
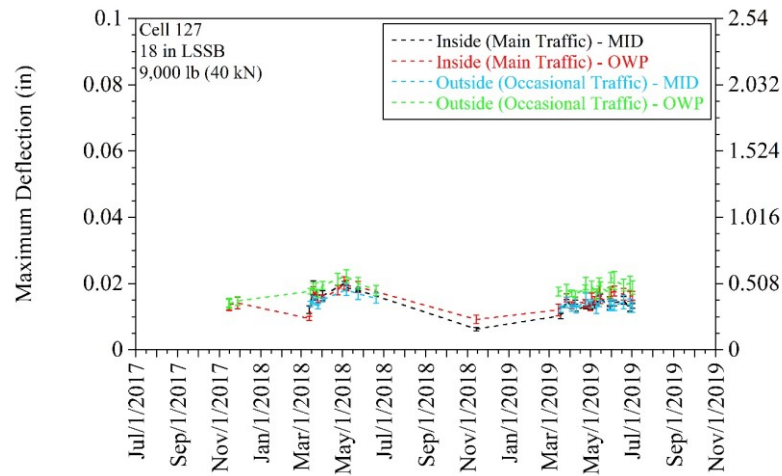


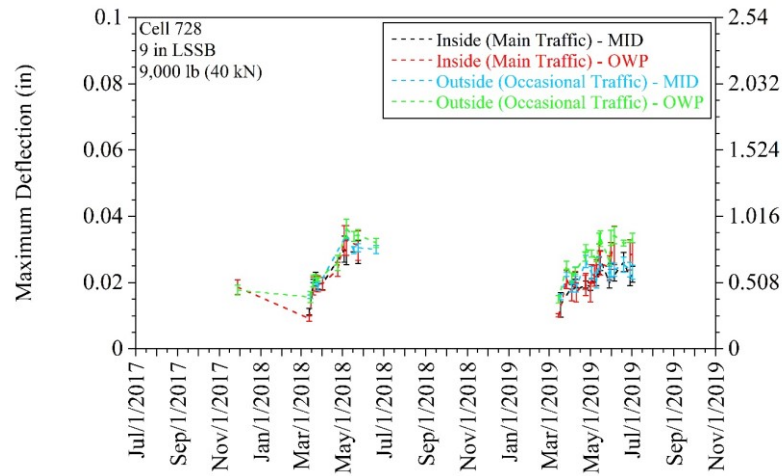
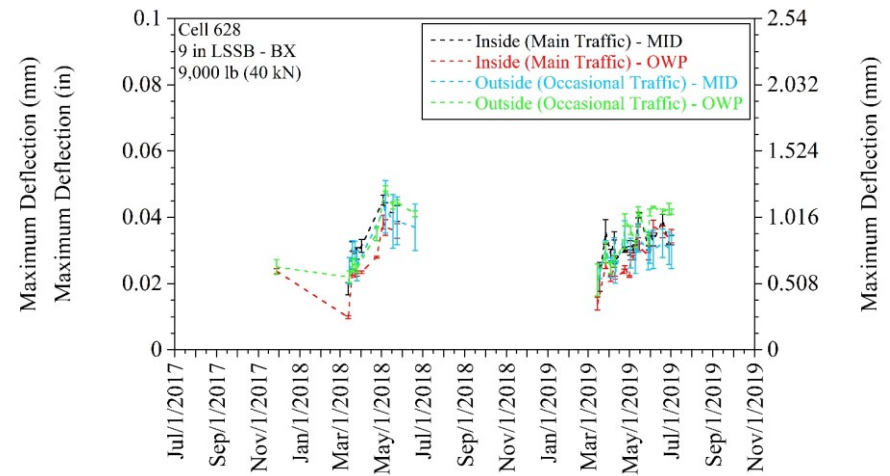
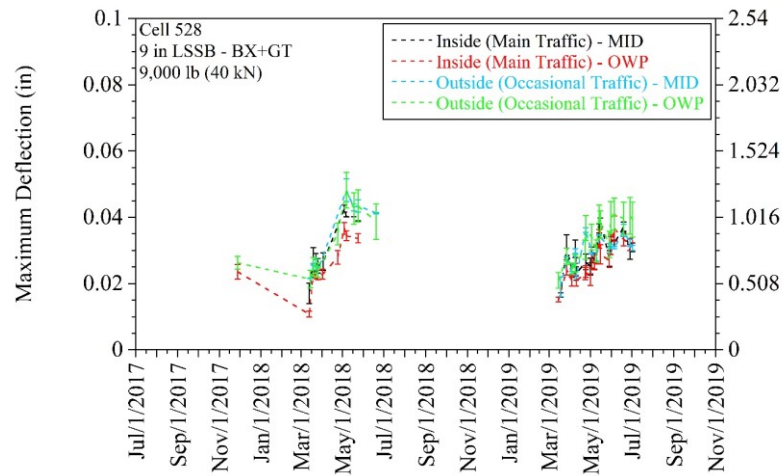
APPENDIX Z

**MAXIMUM DEFLECTIONS FOR DIFFERENT TEST LOCATIONS AT
9,000 LB (40 KN) FOR EACH CELL**

(error bars represent one standard deviation of the data)



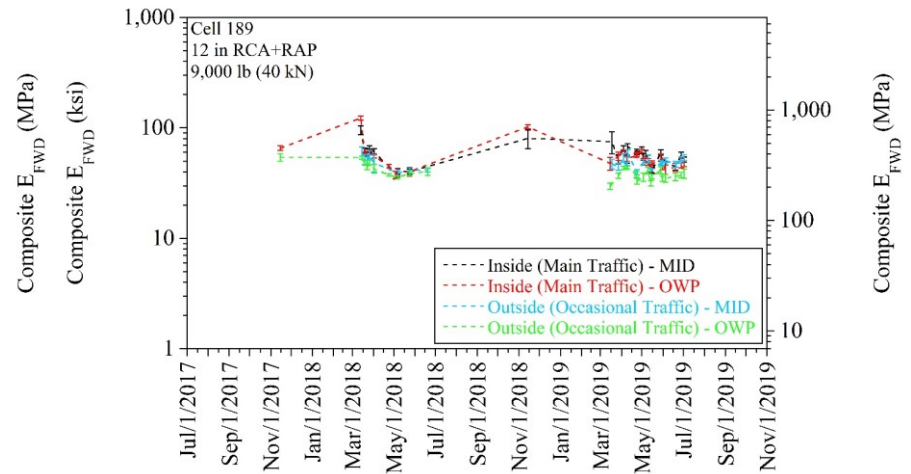
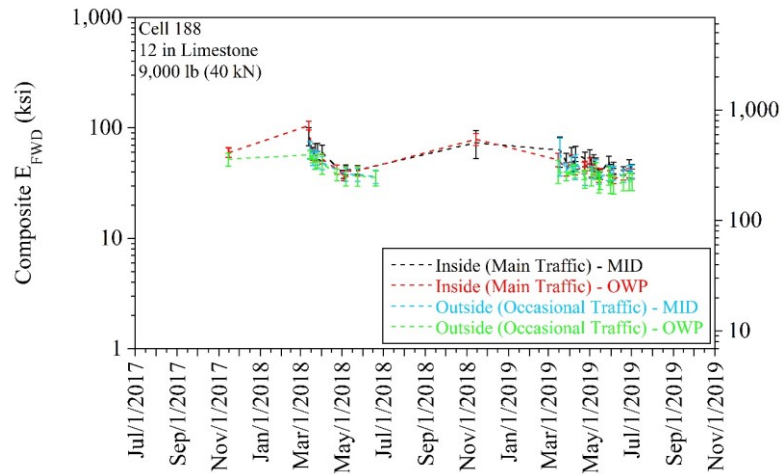
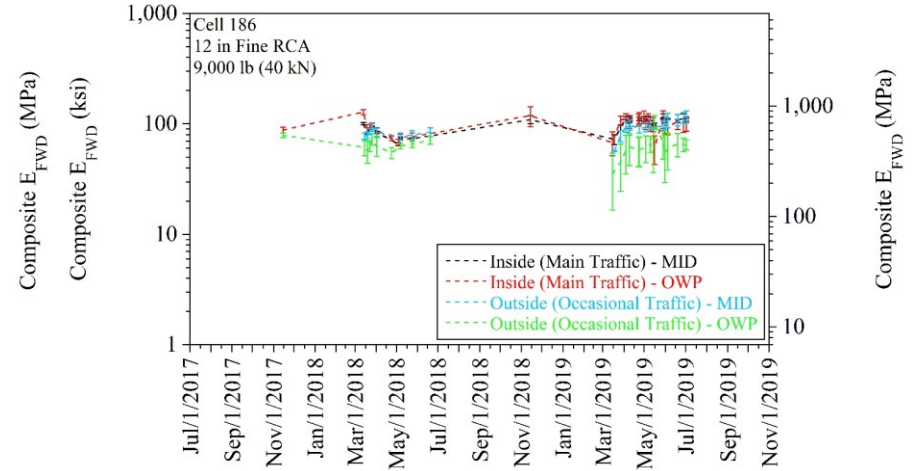
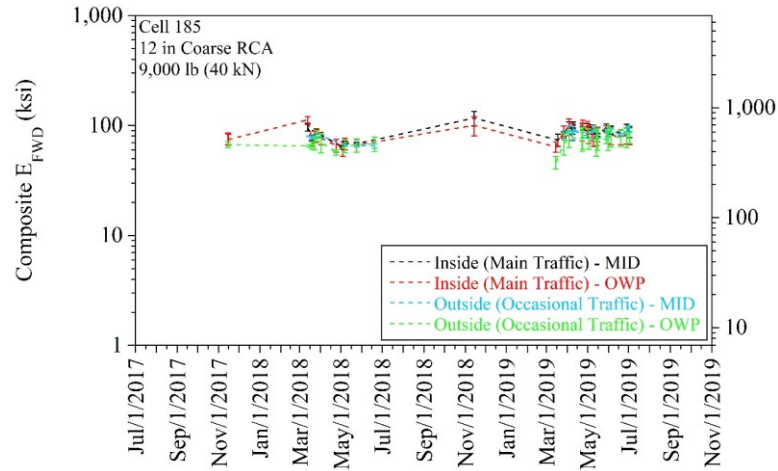


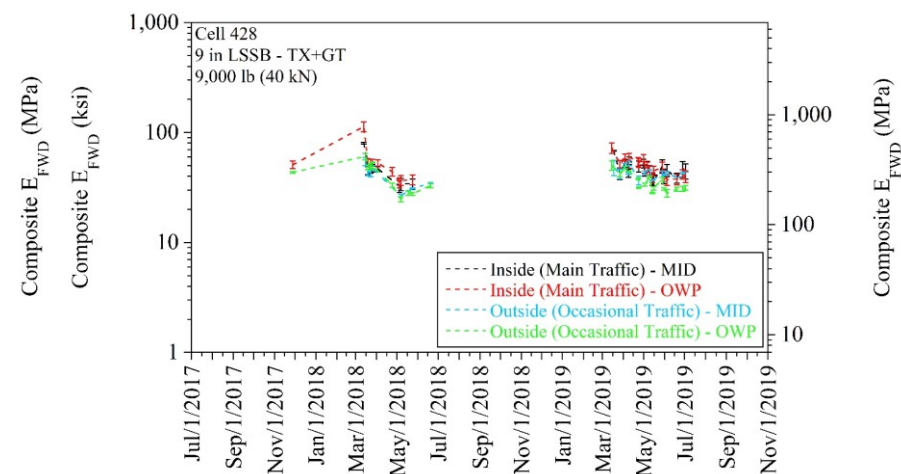
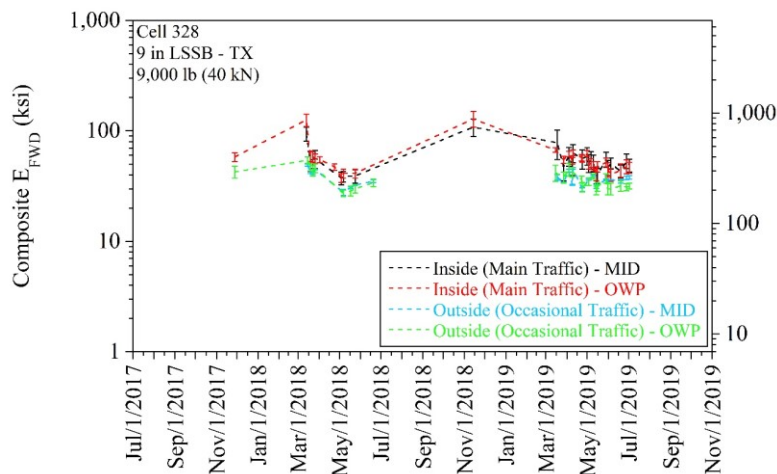
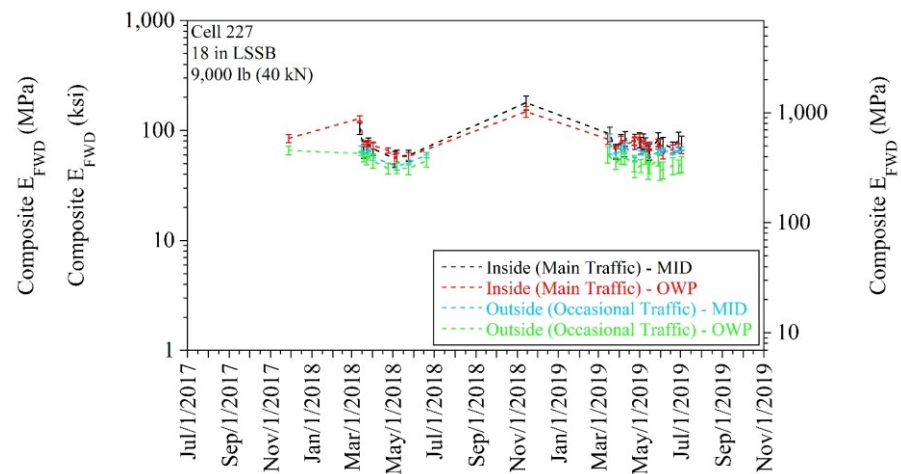
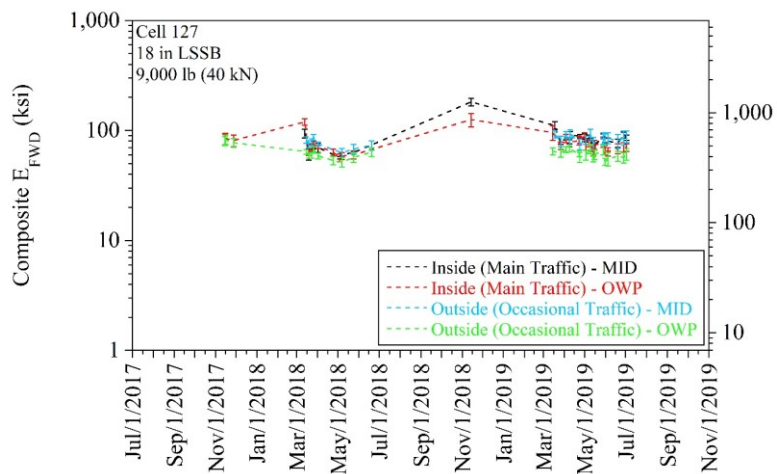


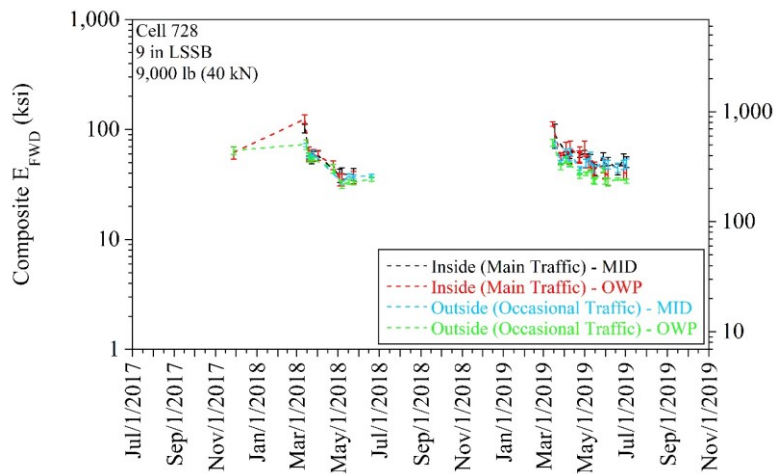
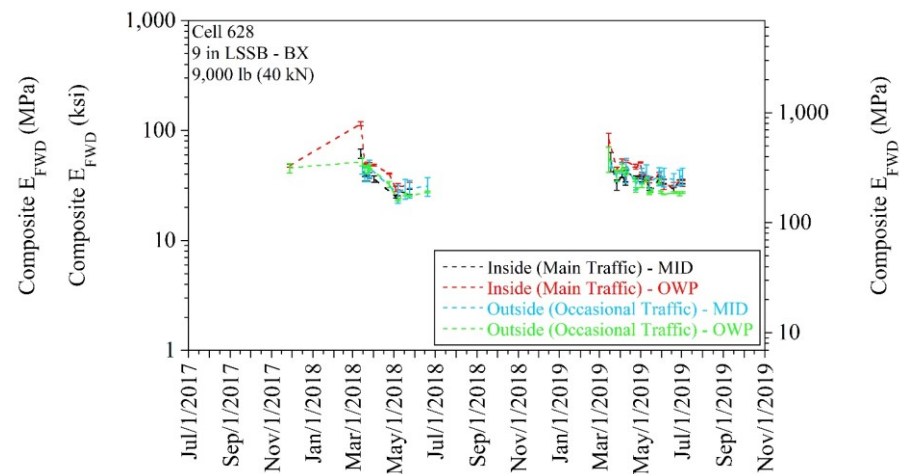
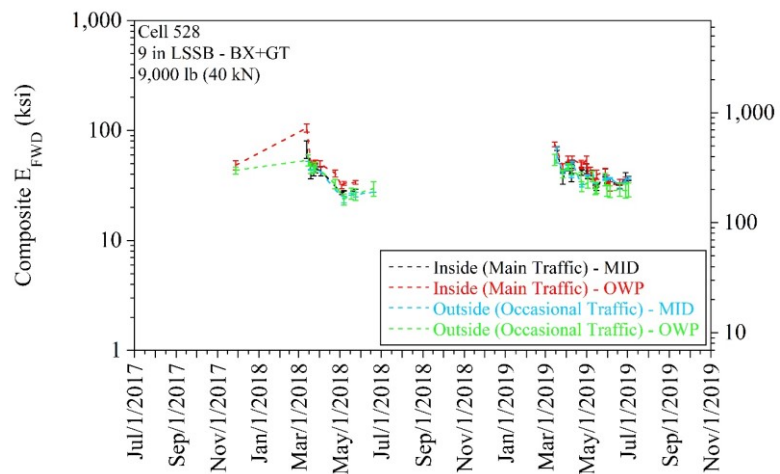
APPENDIX AA

**COMPOSITE FALLING WEIGHT DEFLECTOMETER (FWD) ELASTIC
MODULUS (E_{FWD}) FOR DIFFERENT TEST LOCATIONS AT 9,000 LB
(40 KN) FOR EACH CELL**

(error bars represent one standard deviation of the data)



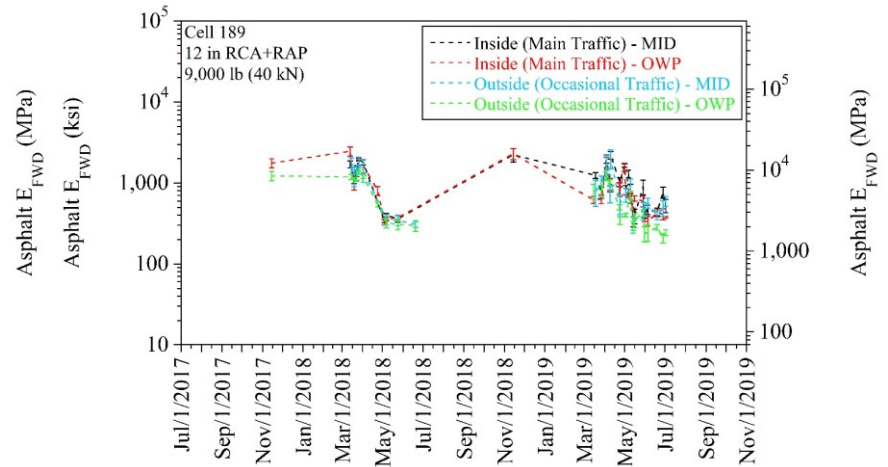
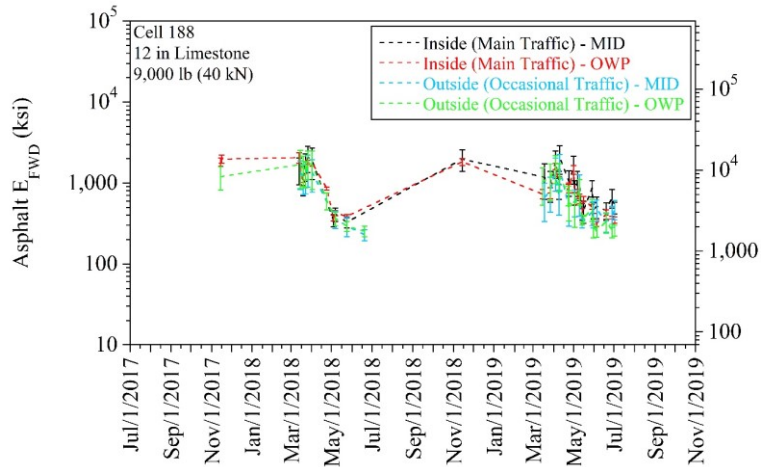
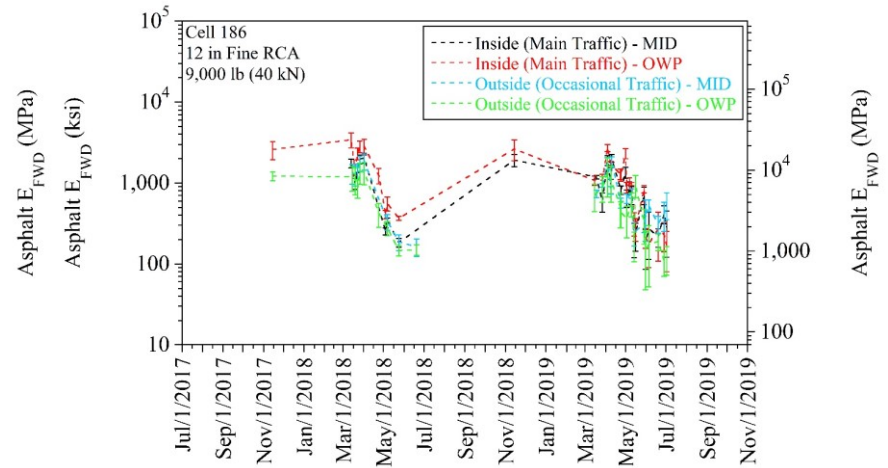
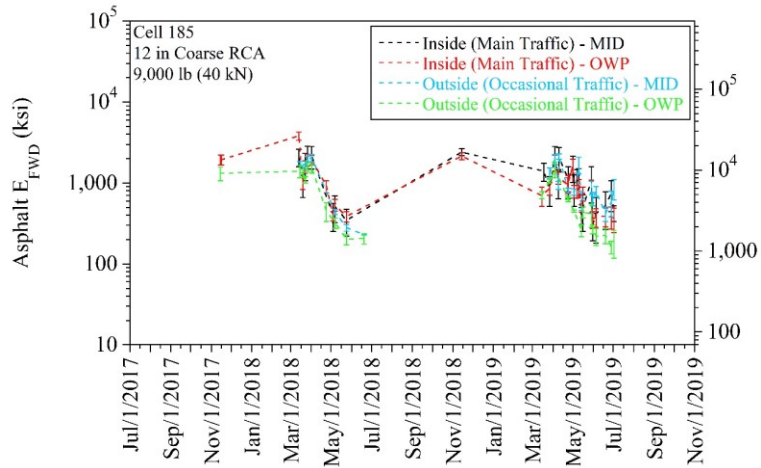


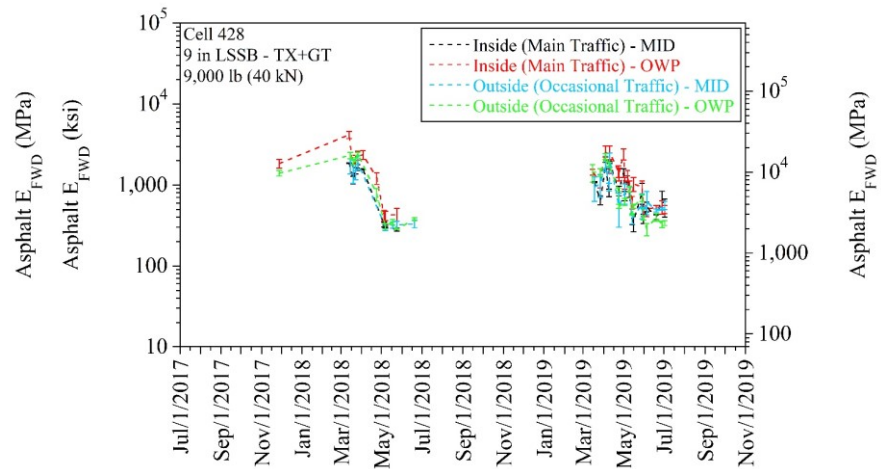
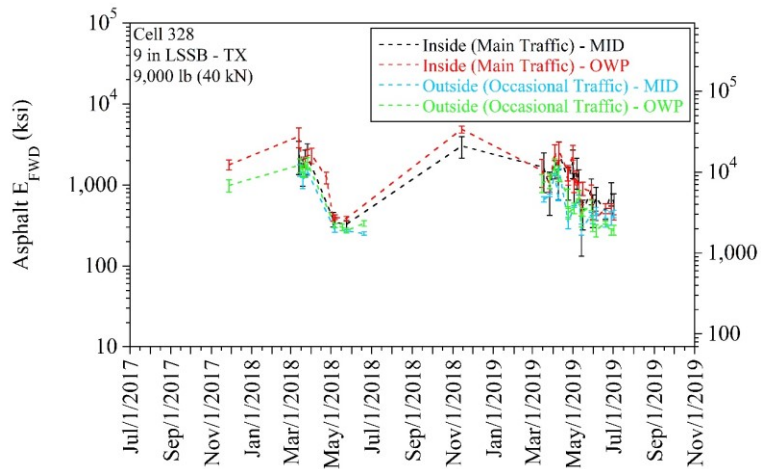
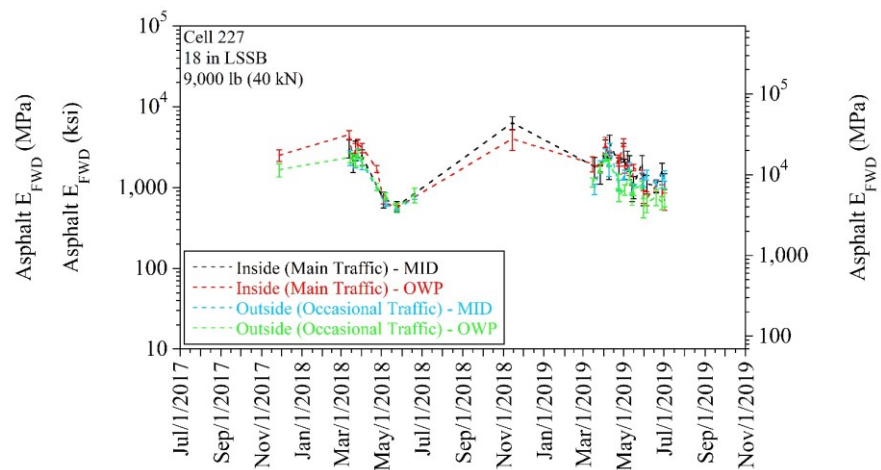
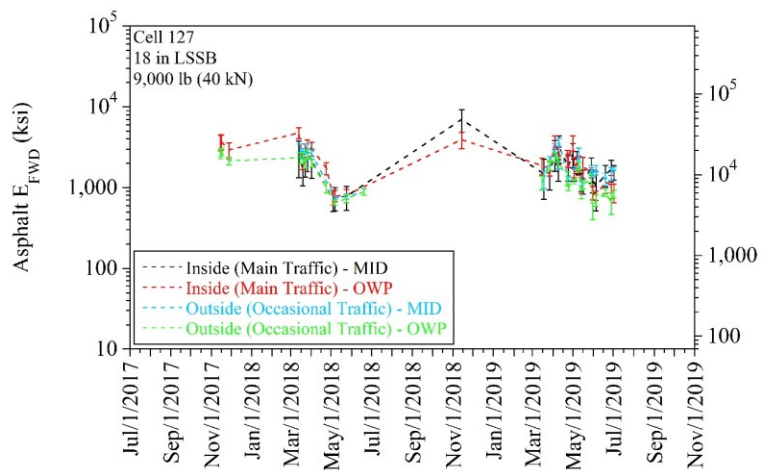


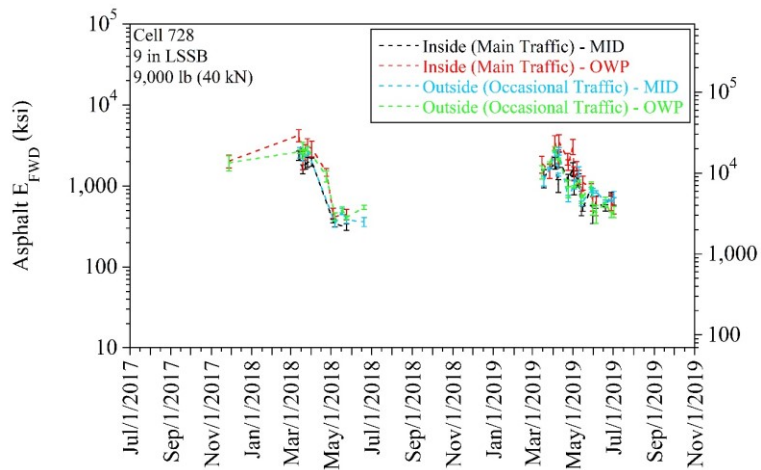
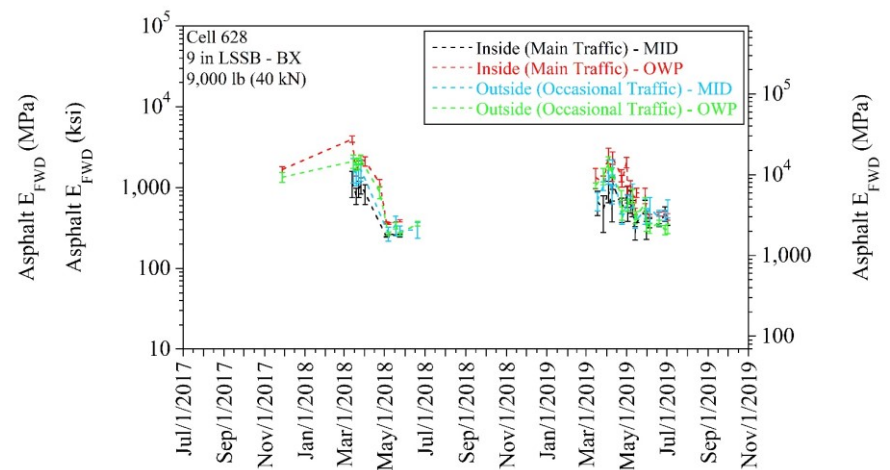
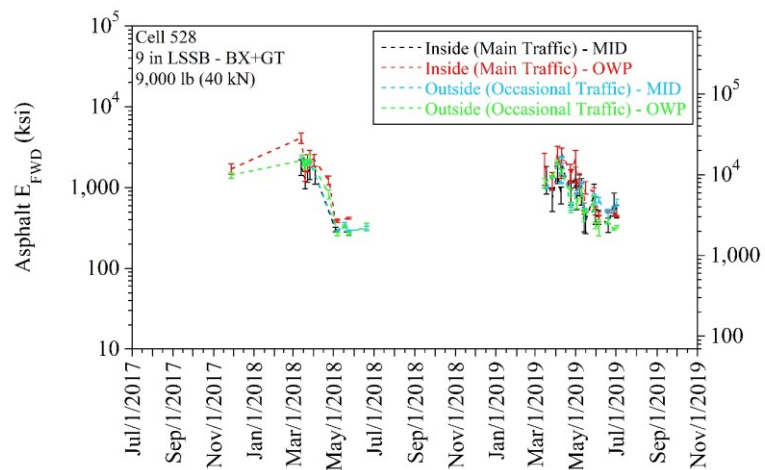
APPENDIX AB

**ASPHALT FALLING WEIGHT DEFLECTOMETER (FWD) ELASTIC
MODULUS (E_{FWD}) FOR DIFFERENT TEST LOCATIONS AT 9,000 LB
(40 KN) FOR EACH CELL**

(error bars represent one standard deviation of the data)



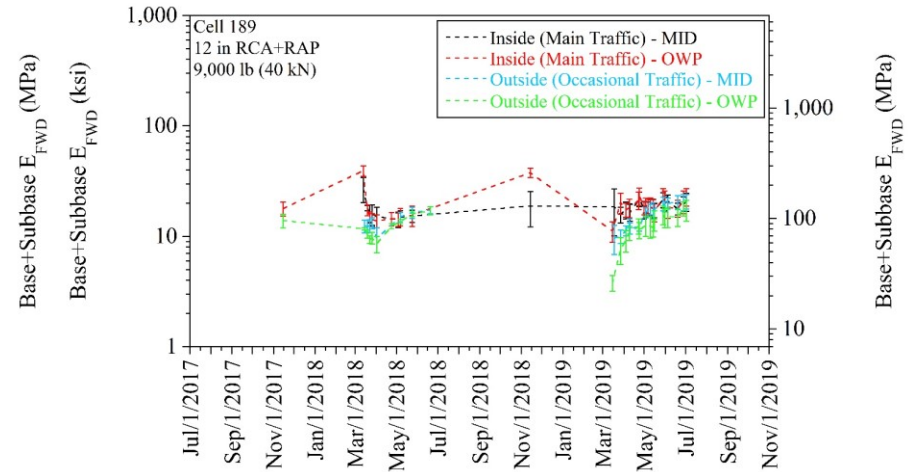
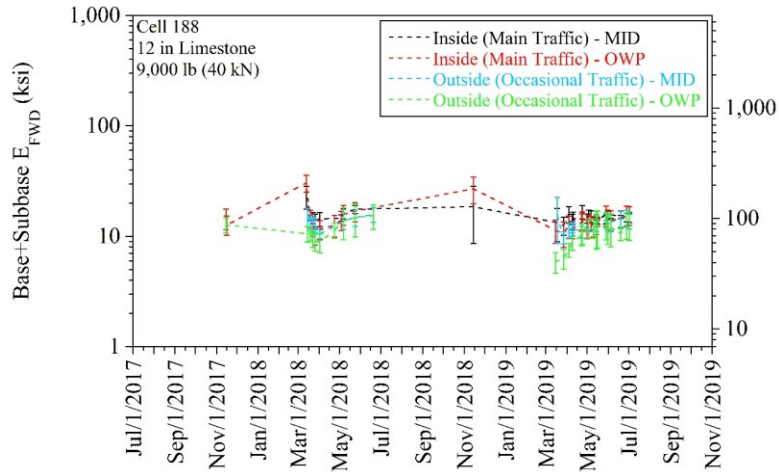
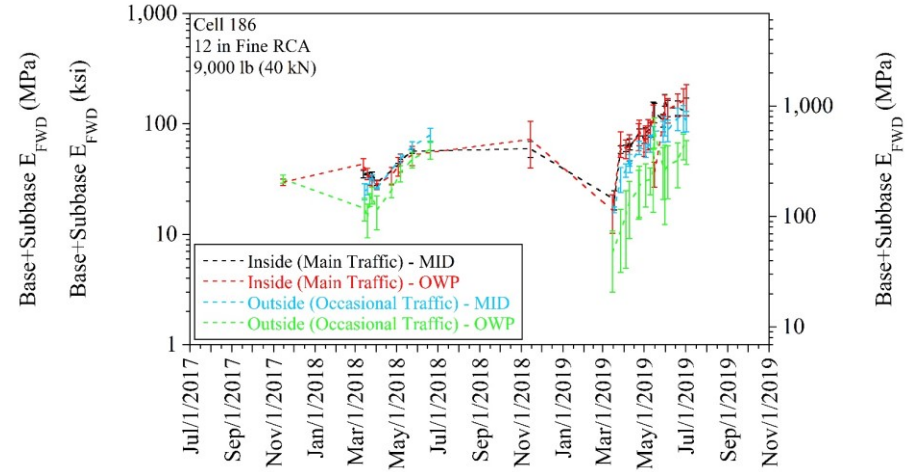
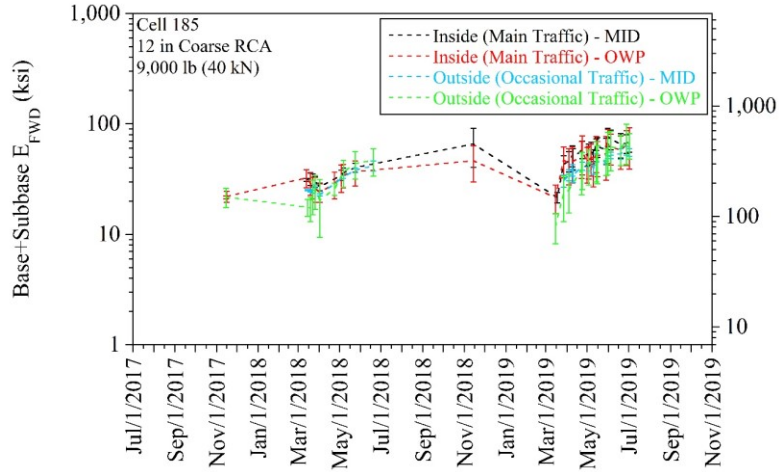


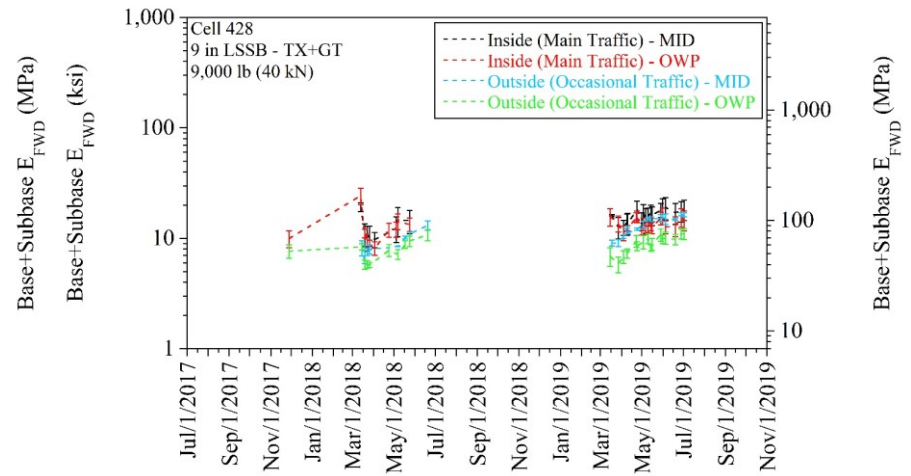
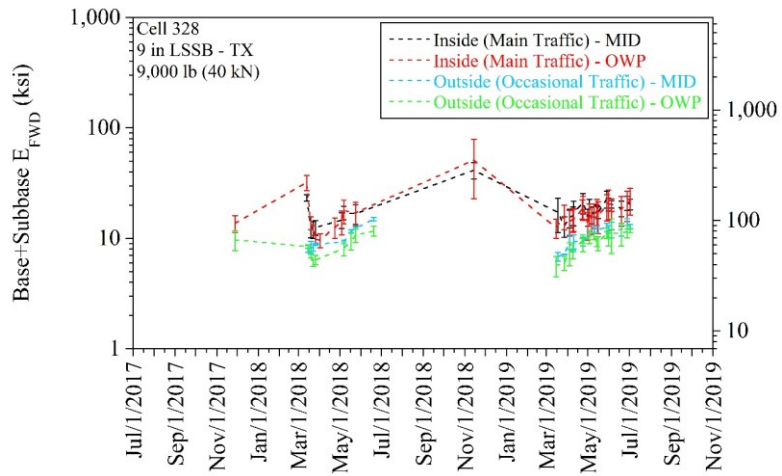
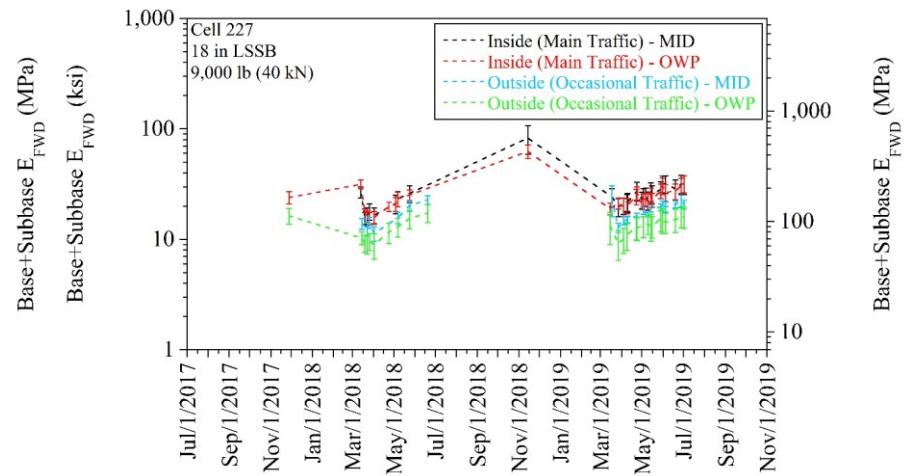
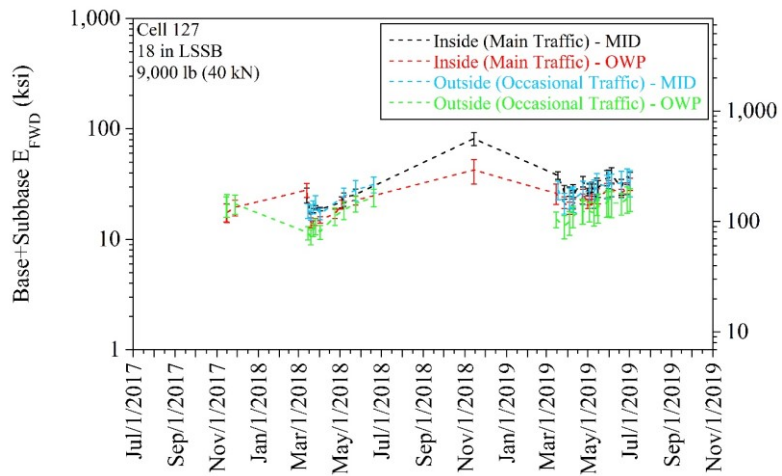


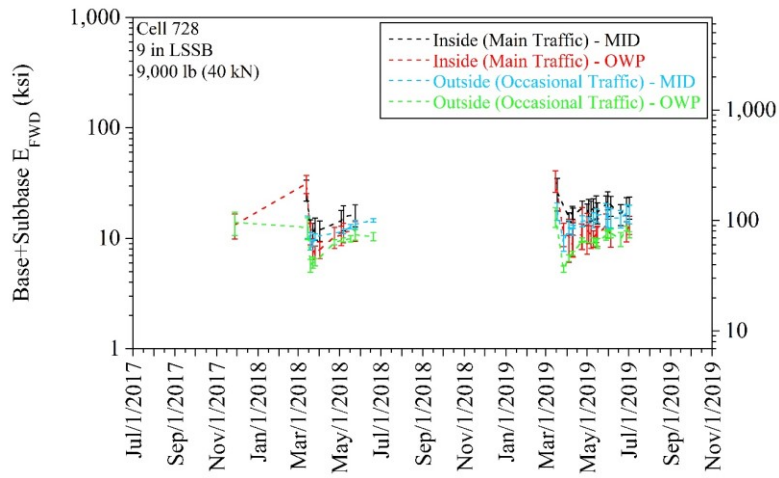
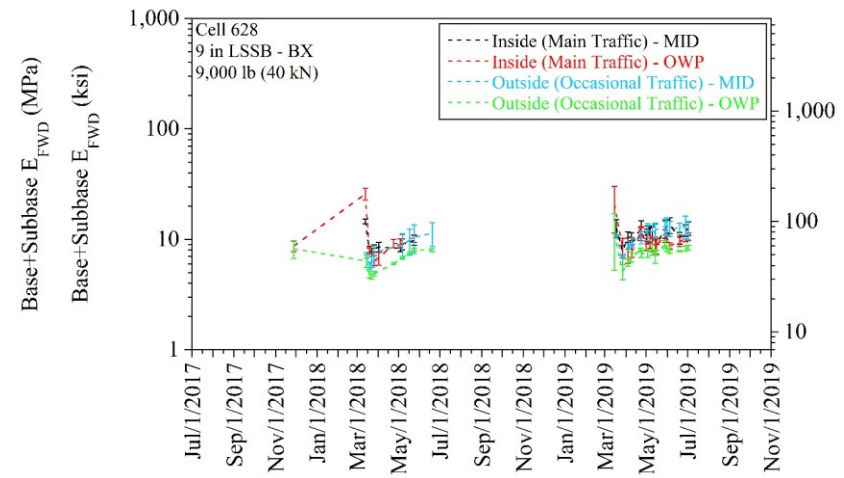
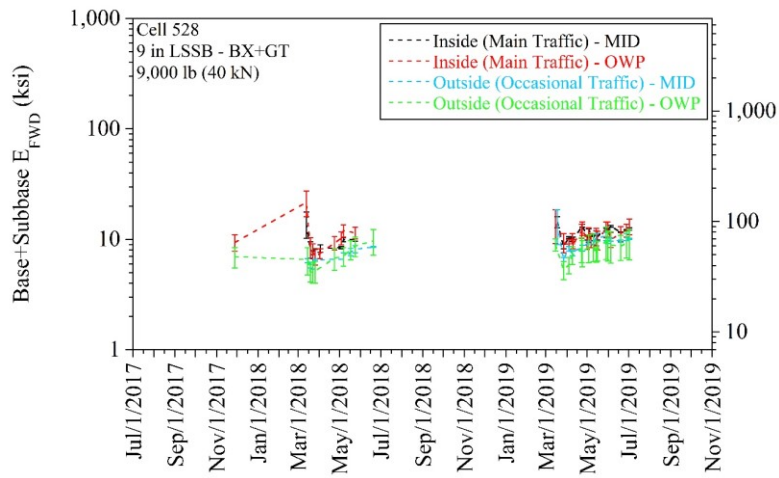
APPENDIX AC

**BASE+SUBBASE FALLING WEIGHT DEFLECTOMETER (FWD)
ELASTIC MODULUS (E_{FWD}) FOR DIFFERENT TEST LOCATIONS AT
9,000 LB (40 KN) FOR EACH CELL**

(error bars represent one standard deviation of the data)



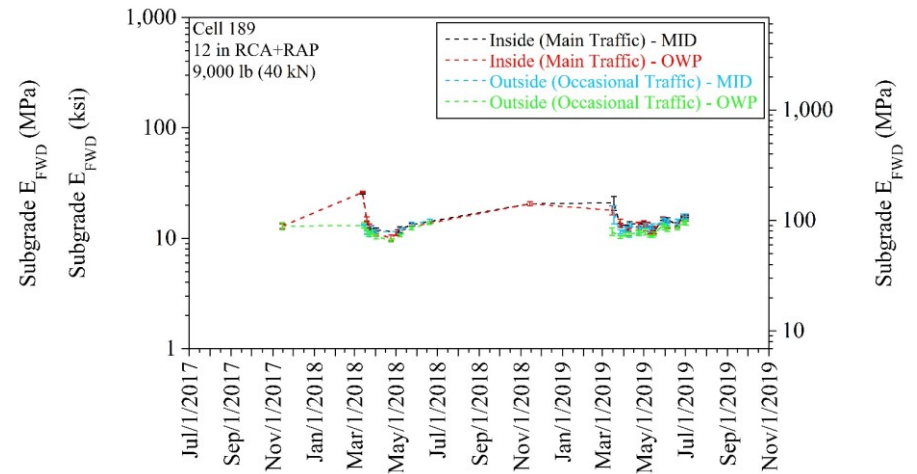
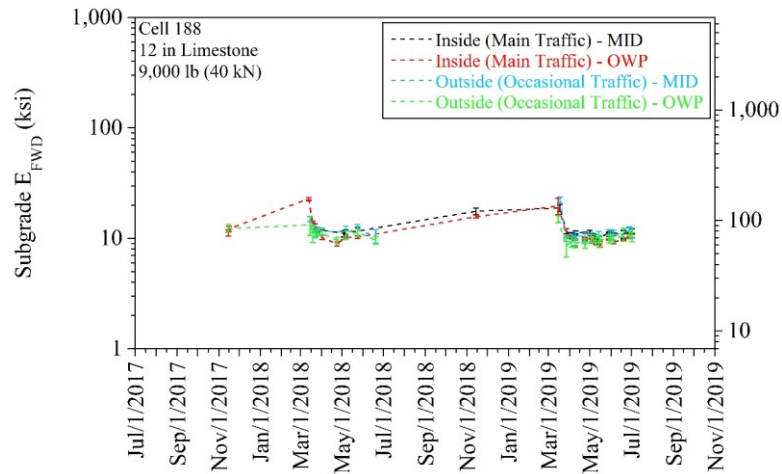
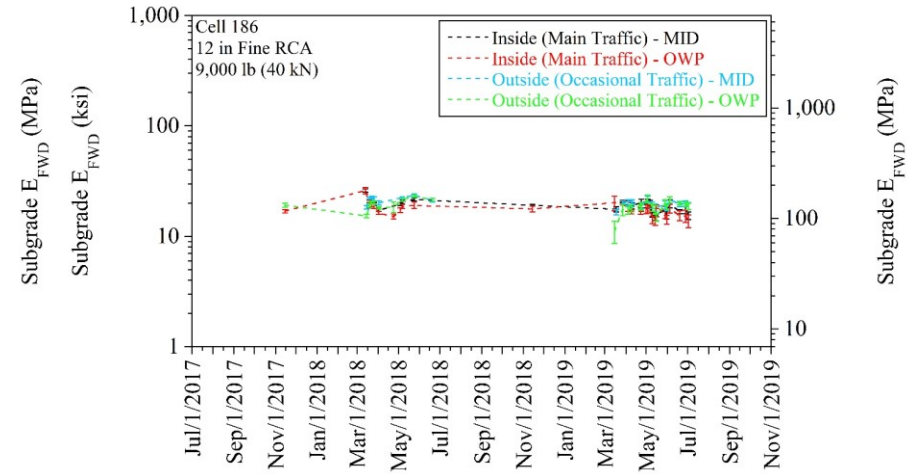
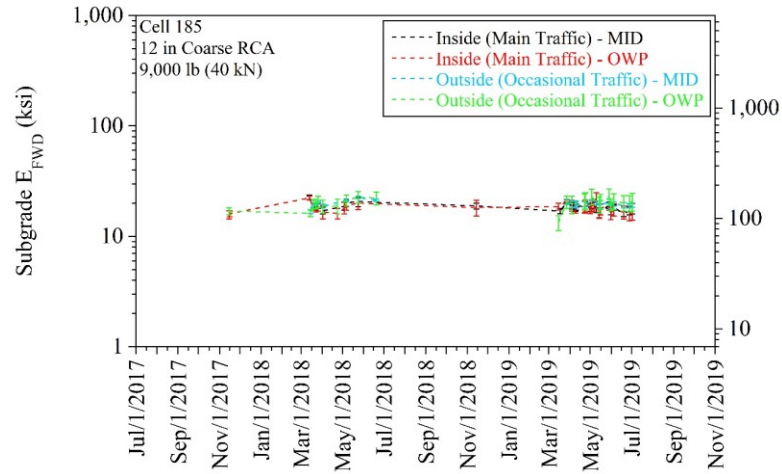


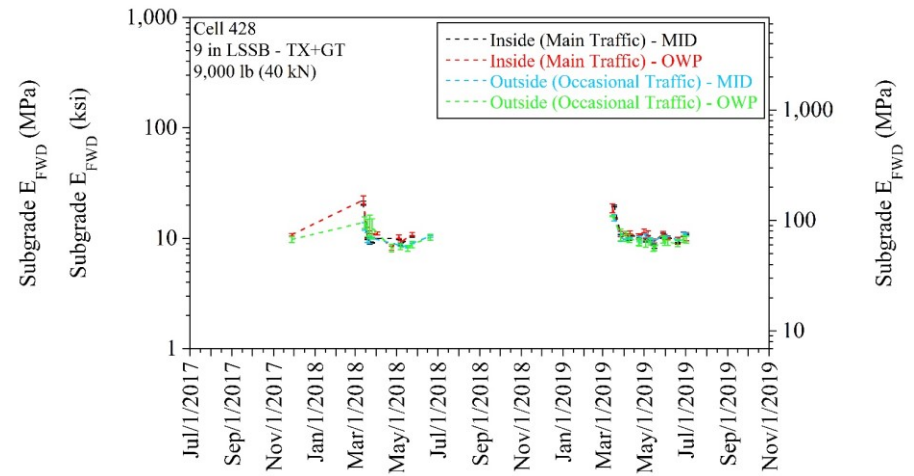
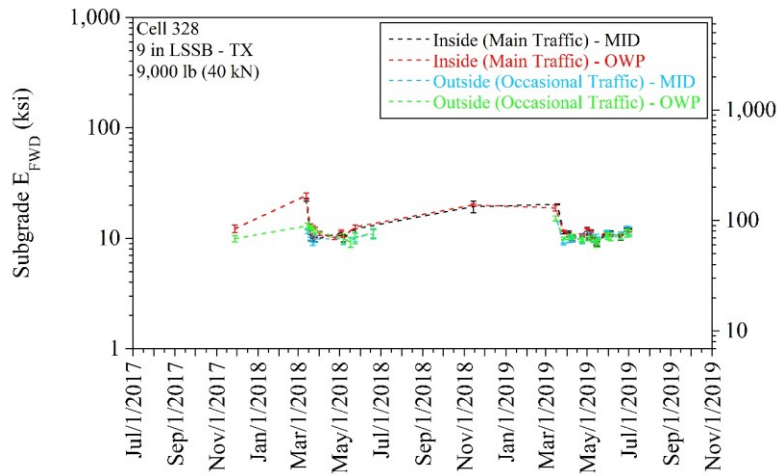
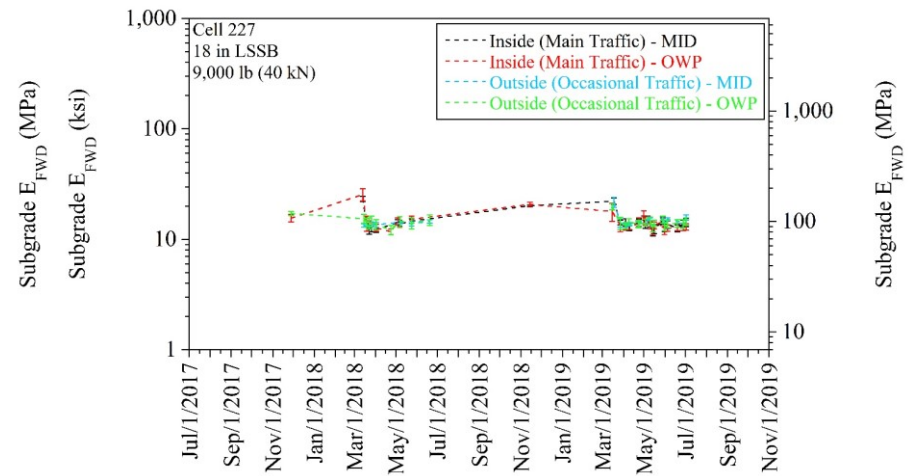
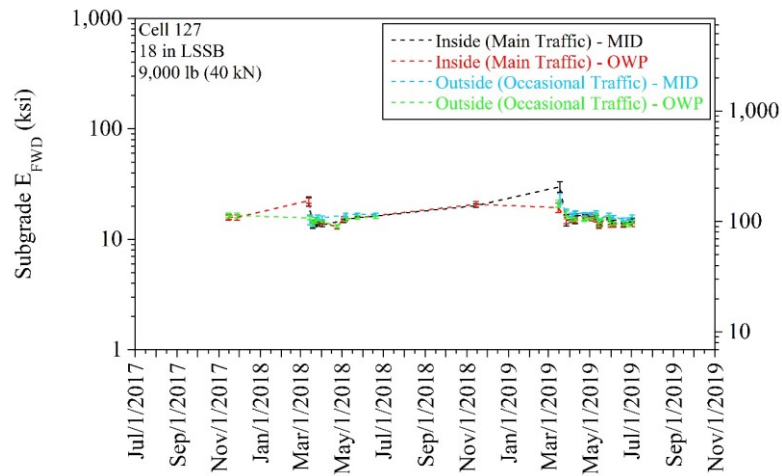


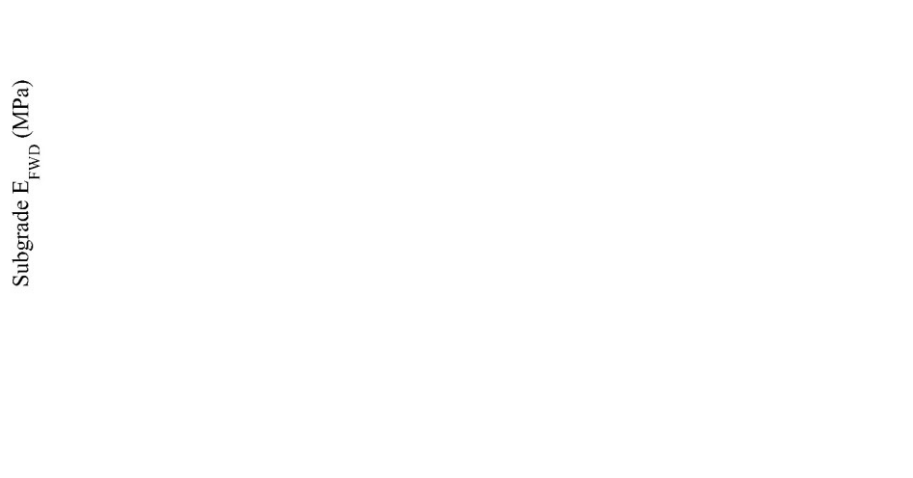
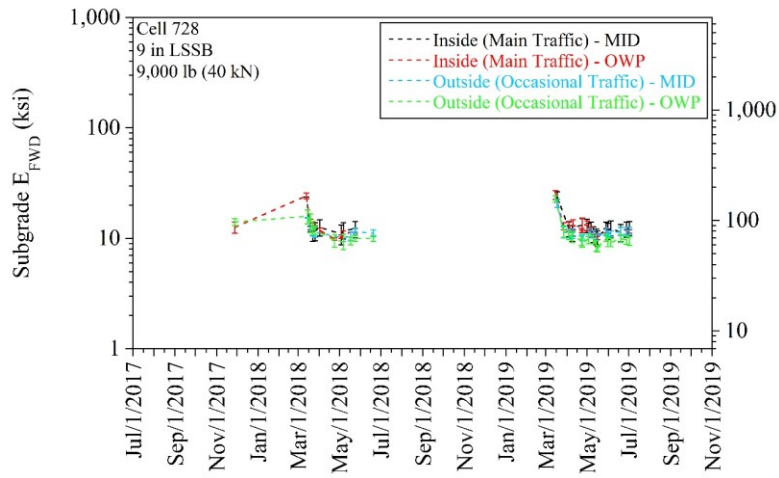
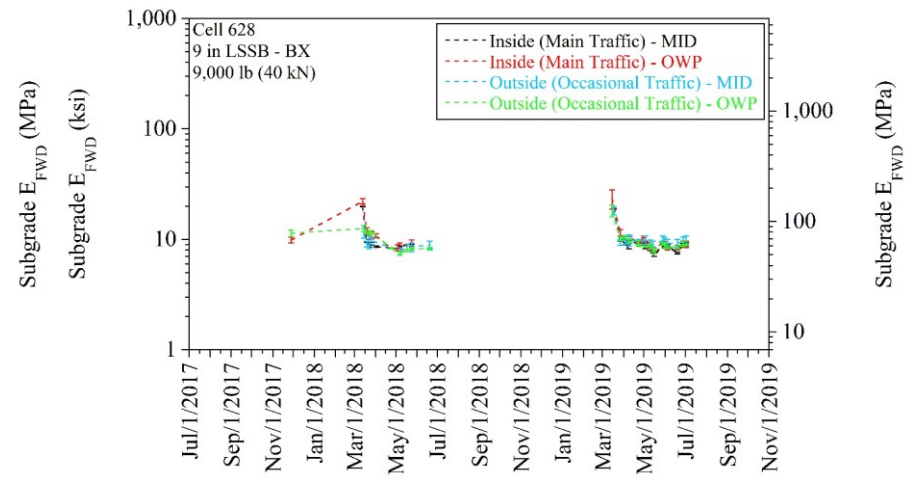
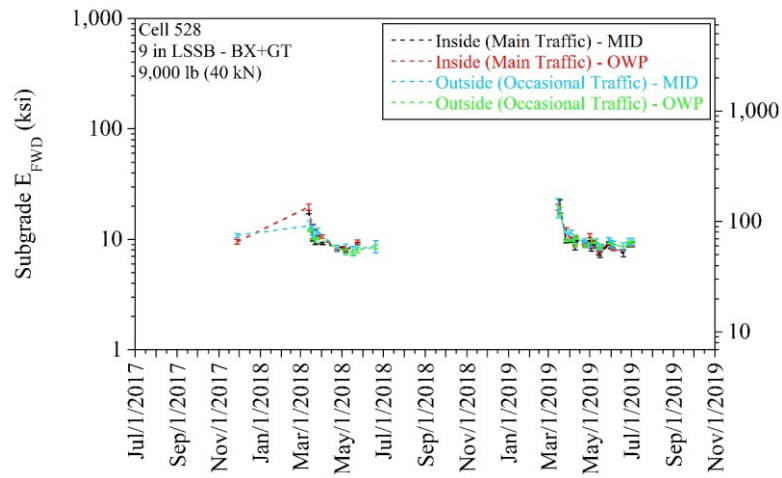
APPENDIX AD

**SUBGRADE FALLING WEIGHT DEFLECTOMETER (FWD) ELASTIC
MODULUS (E_{FWD}) FOR DIFFERENT TEST LOCATIONS AT 9,000 LB
(40 KN) FOR EACH CELL**

(error bars represent one standard deviation of the data)







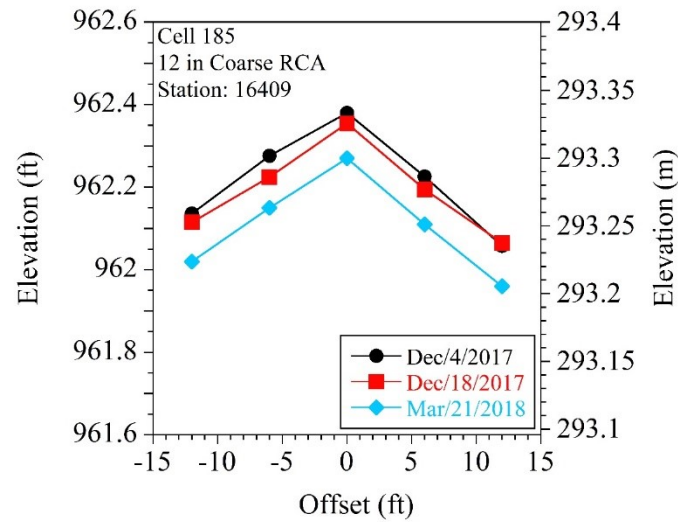
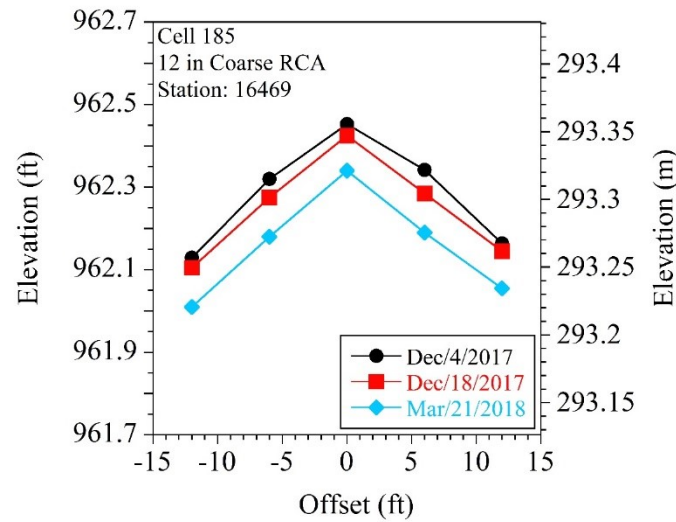
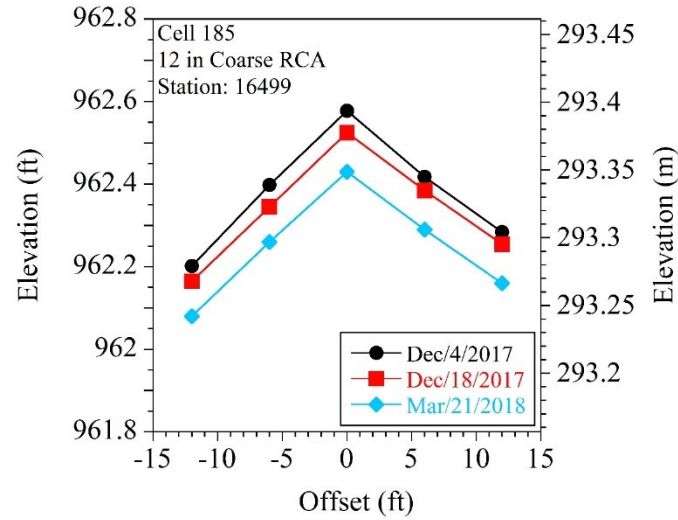
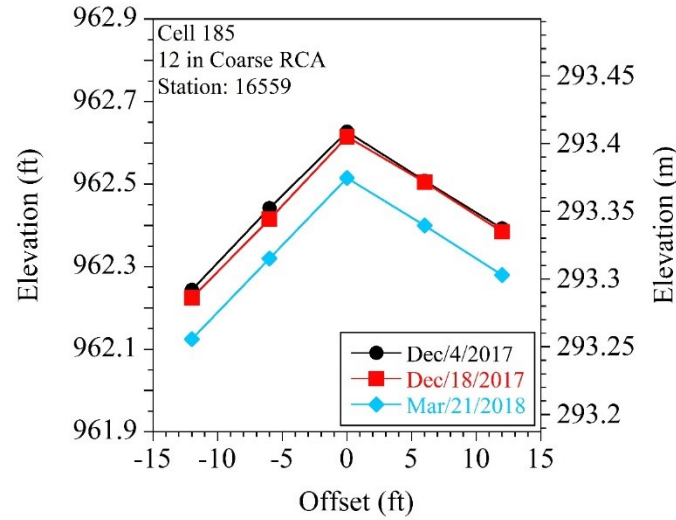
APPENDIX AE
VOLUMETRIC WATER CONTENT (VWC) VALUES DETERMINED
FOR SECOND THAWING PERIOD

The thawing period in 2019 was evaluated in three stages: (1) frozen (average VWC for one day in fully-frozen condition - right before the thawing starts), (2) during thawing (the peak VWC between fully-frozen and thawed conditions), and (3) after thawing (average VWC for one day after the peak VWC during thawing).

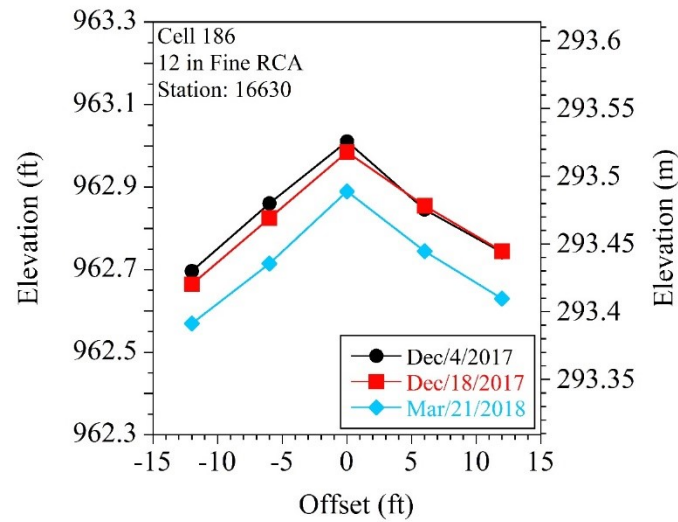
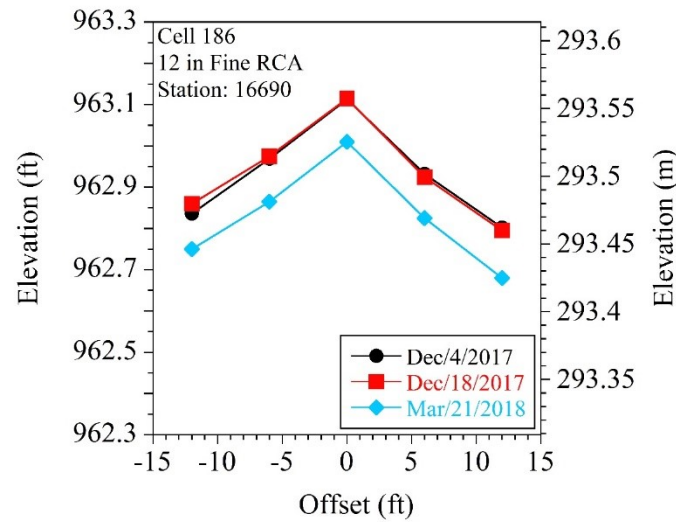
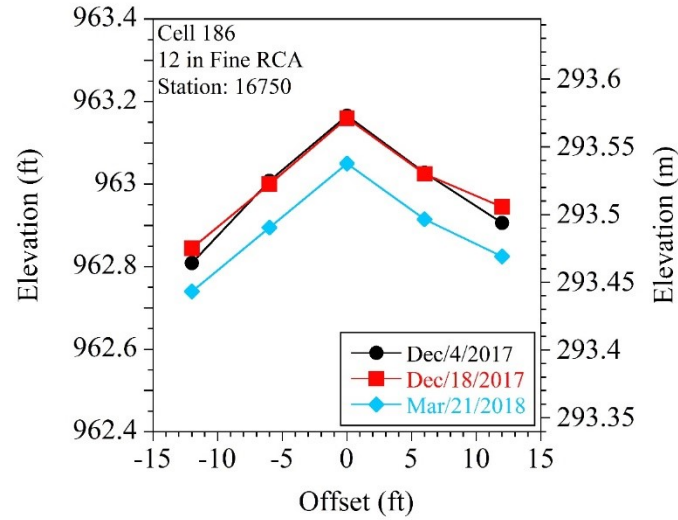
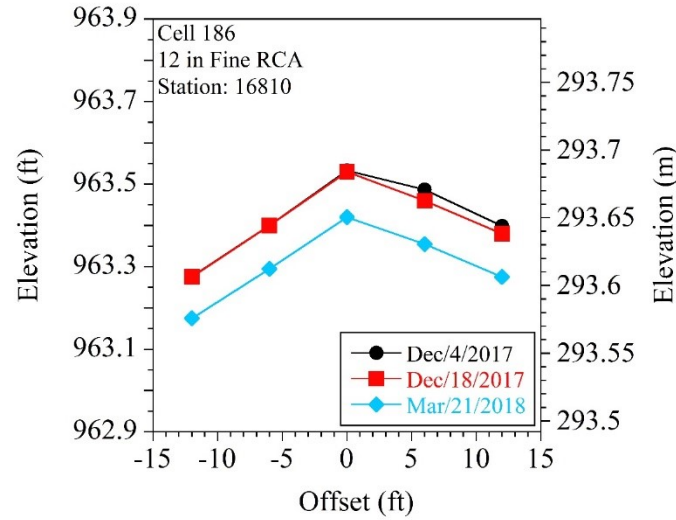
Cell	Depth (in)	Material	VWC - Thawing Period in 2019		
			Frozen	During Thawing	After Thawing
185	5	Coarse RCA	NA	NA	NA
	14	Coarse RCA	NA	NA	NA
	17	Select Granular Borrow	NA	NA	NA
	20.5	Sand Subgrade	NA	NA	NA
186	5	Fine RCA	0.0616	0.2107	0.1147
	14	Fine RCA	NA	NA	NA
	17	Select Granular Borrow	NA	NA	NA
	20.5	Sand Subgrade	NA	NA	NA
188	5	Limestone	0.0056	0.2126	0.0842
	14	Limestone	-0.011	0.416	0.0788
	17	Select Granular Borrow	0.0207	0.3042	0.2872
	20.5	Clay Loam Subgrade	0.0681	0.1719	0.1632
189	5	RCA+RAP	0.0206	0.2954	0.1196
	14	RCA+RAP	NA	0.3026	0.065
	17	Select Granular Borrow	0.0347	0.2467	0.2117
	20.5	Clay Loam Subgrade	0.1092	0.2553	0.2589
127	6.5	Class 6 Aggregate	0.017	0.3698	0.1094
	29	Clay Loam Subgrade	0.1272	0.2874	0.2778
	36	Clay Loam Subgrade	0.1398	0.2583	0.2634
728	8.5	Class 5Q Aggregate	0.0853	0.2146	0.1726
	19.5	Clay Loam Subgrade	0.1191	0.285	0.2631
	24	Clay Loam Subgrade	0.1305	0.2886	0.2865
	36	Clay Loam Subgrade	0.1425	0.3375	0.324

APPENDIX AF
ELEVATION PROFILE FOR EACH TEST CELL

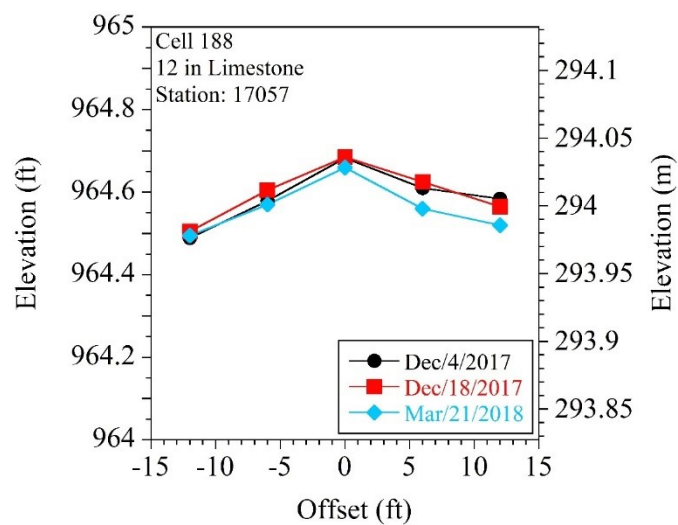
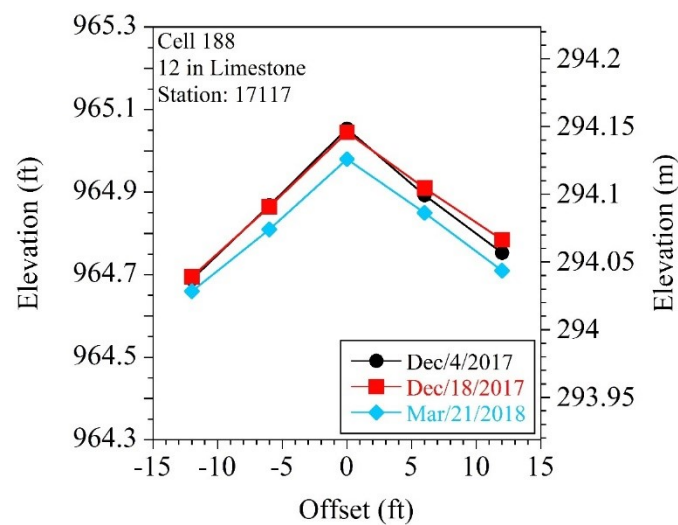
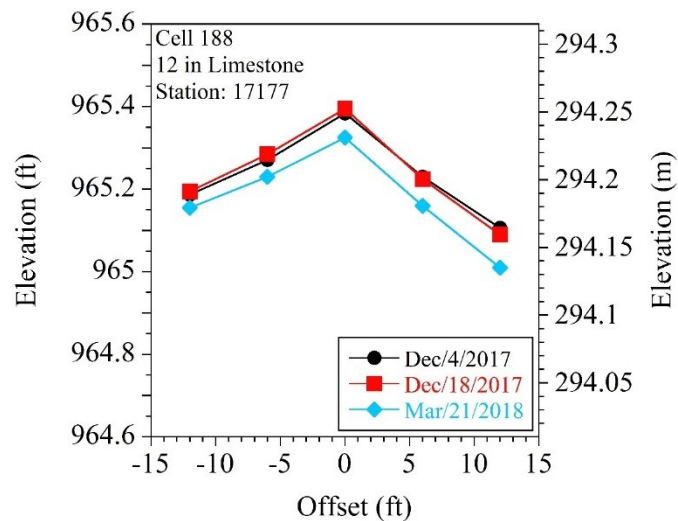
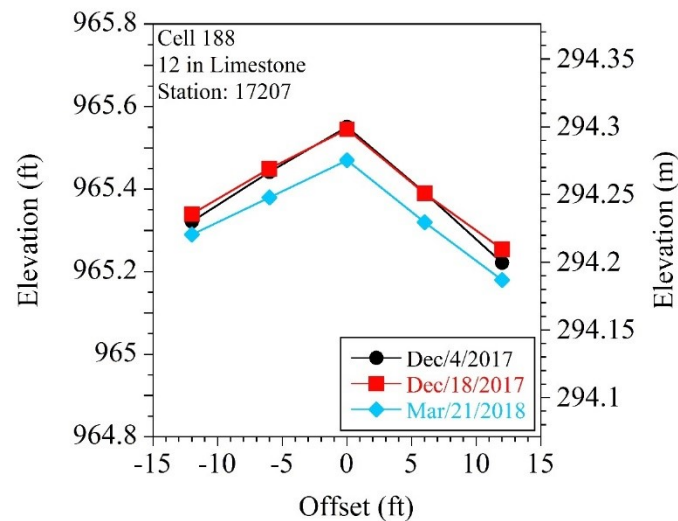
Cell 185 (12-in Coarse RCA):



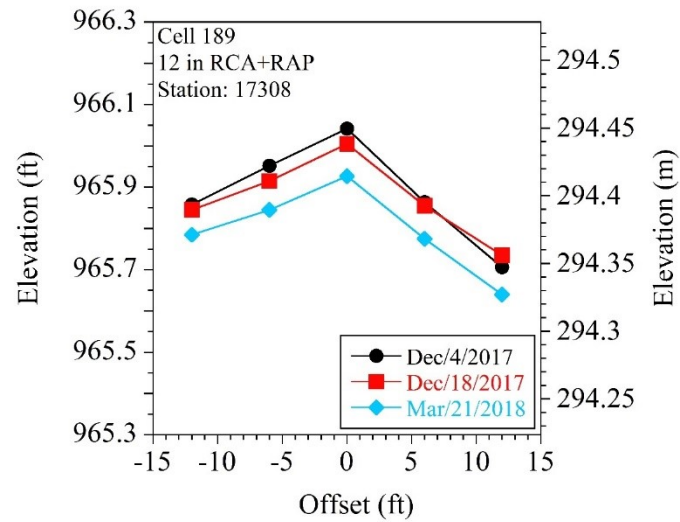
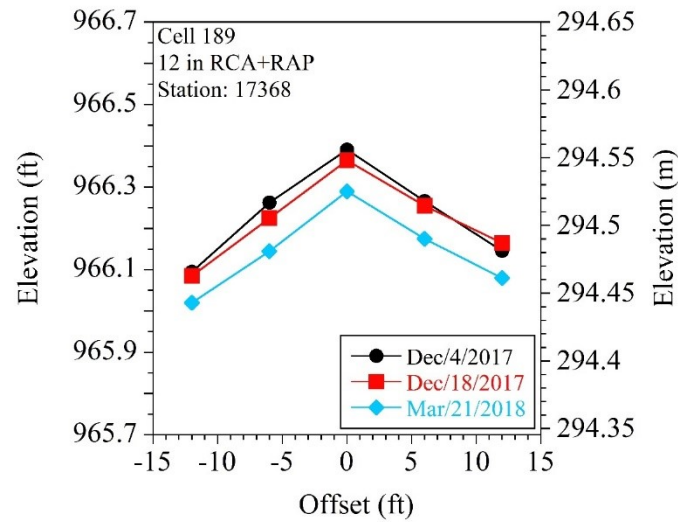
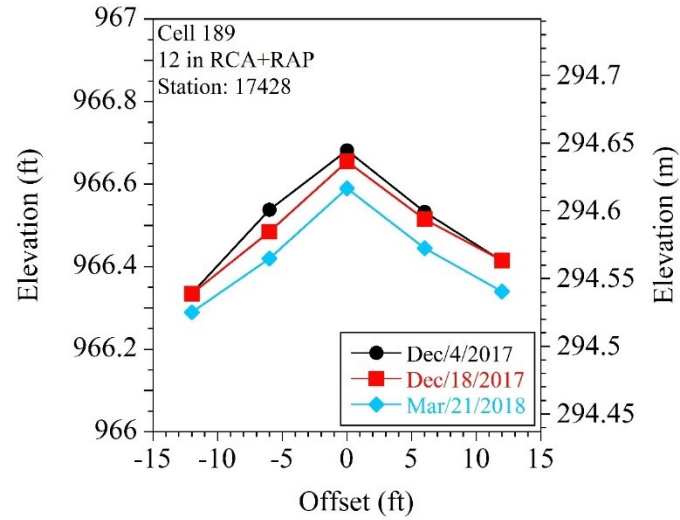
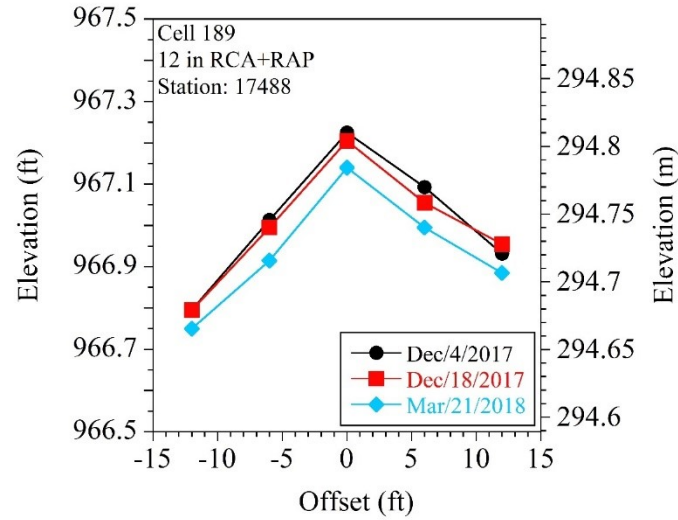
Cell 186 (12-in Fine RCA):



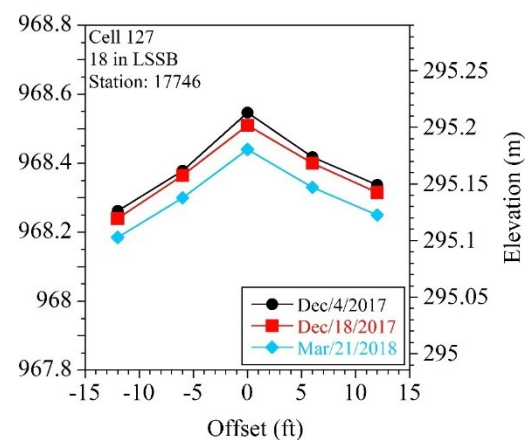
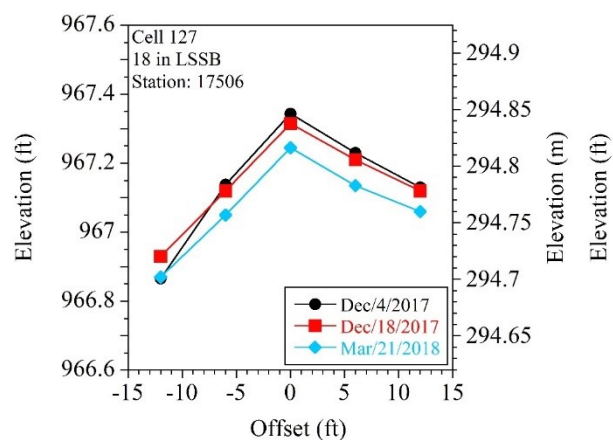
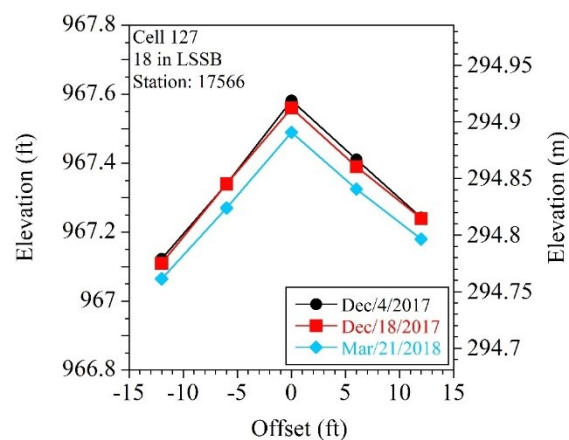
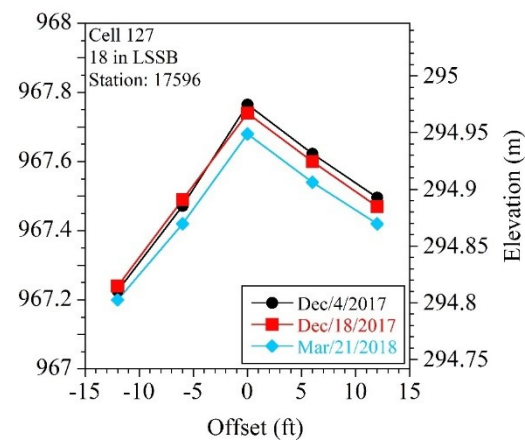
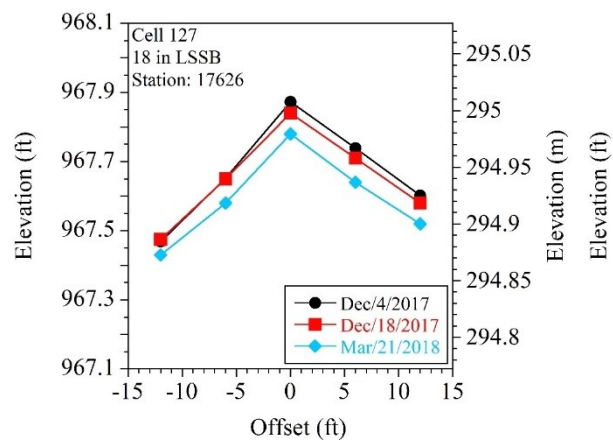
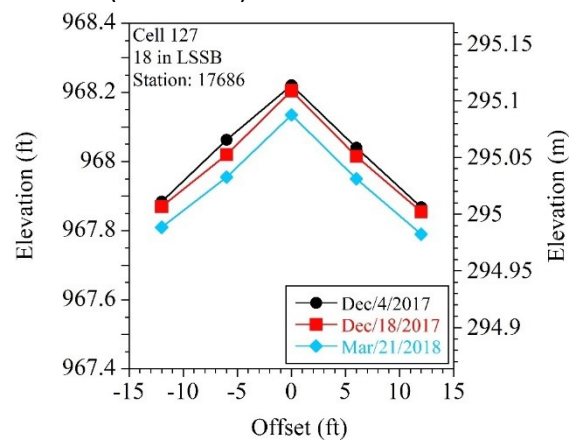
Cell 188 (12-in Limestone):



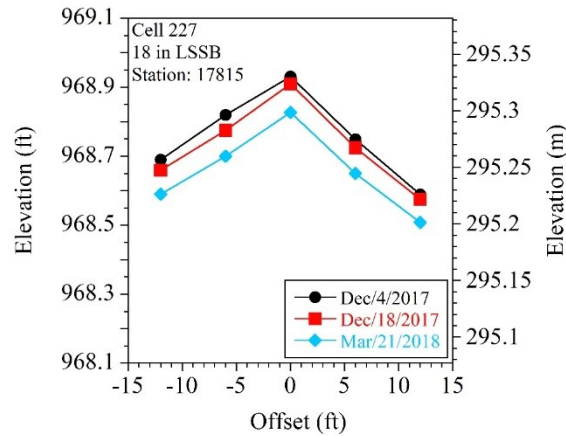
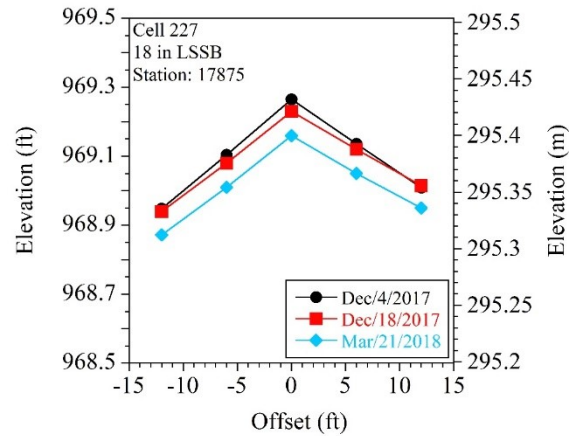
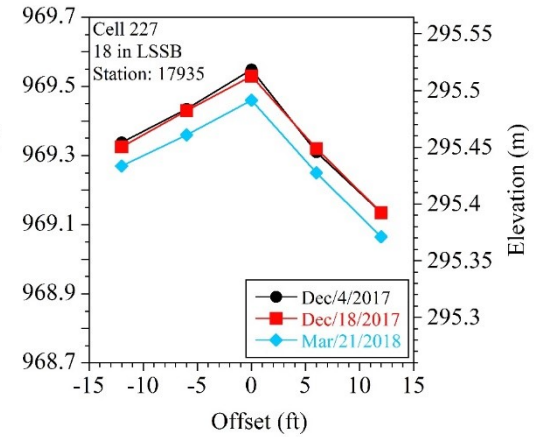
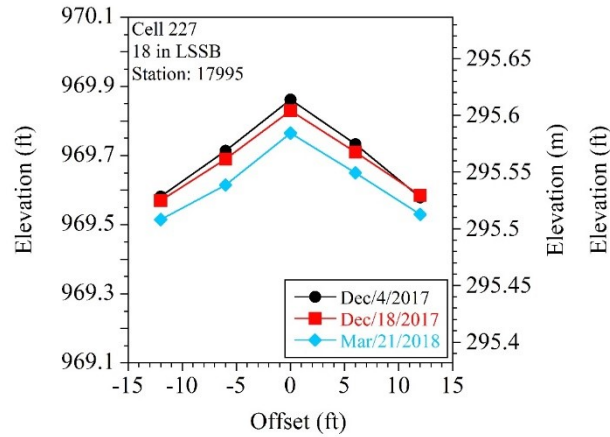
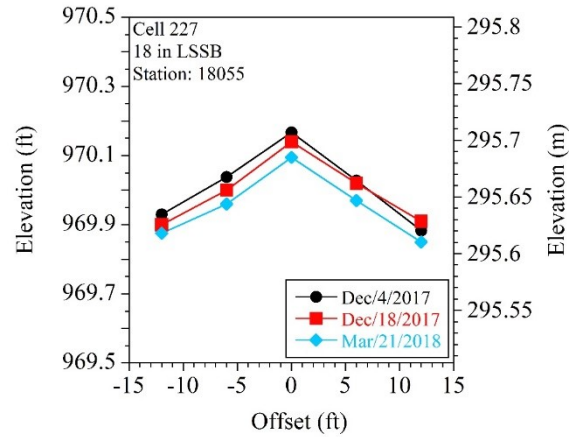
Cell 189 (12-in RCA+RAP):



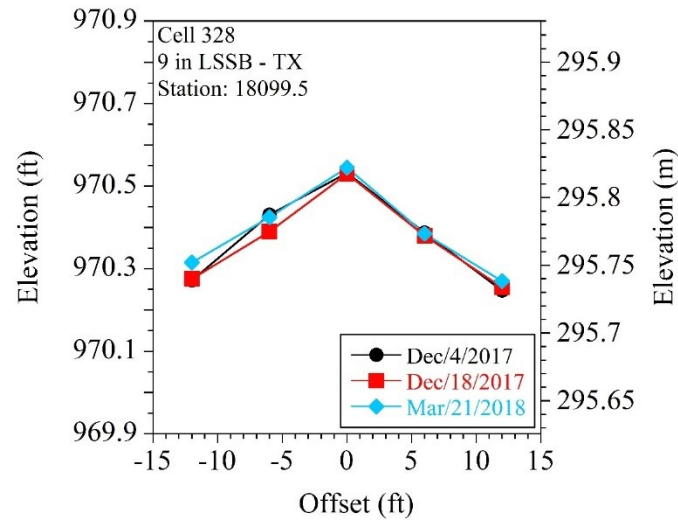
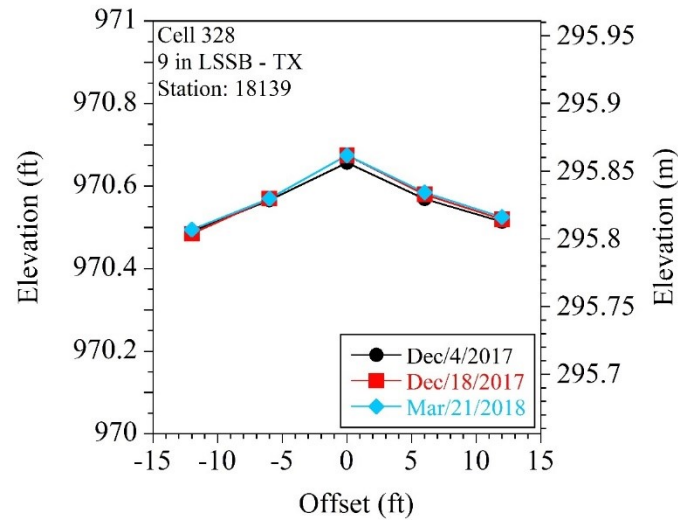
Cell 127 (18-in LSSB):



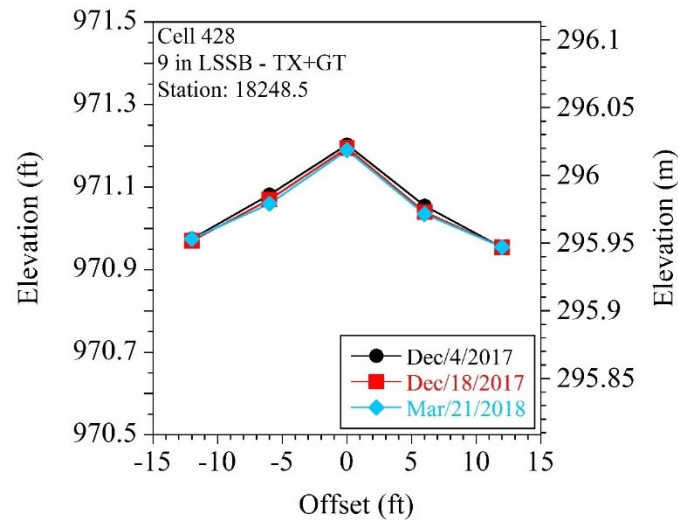
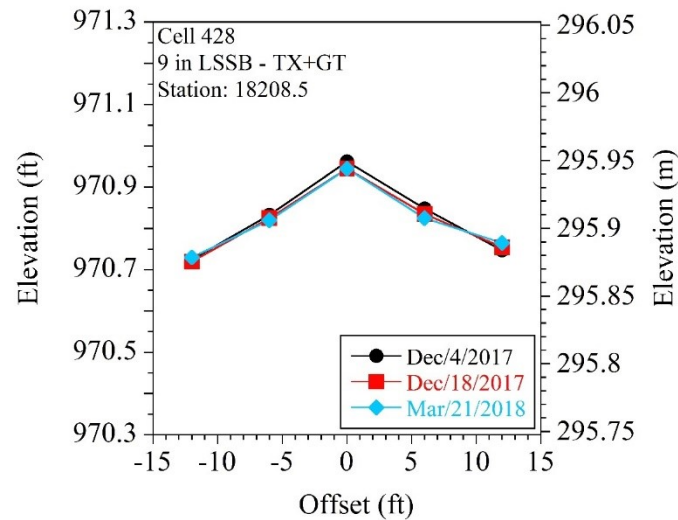
Cell 227 (18-in LSSB):



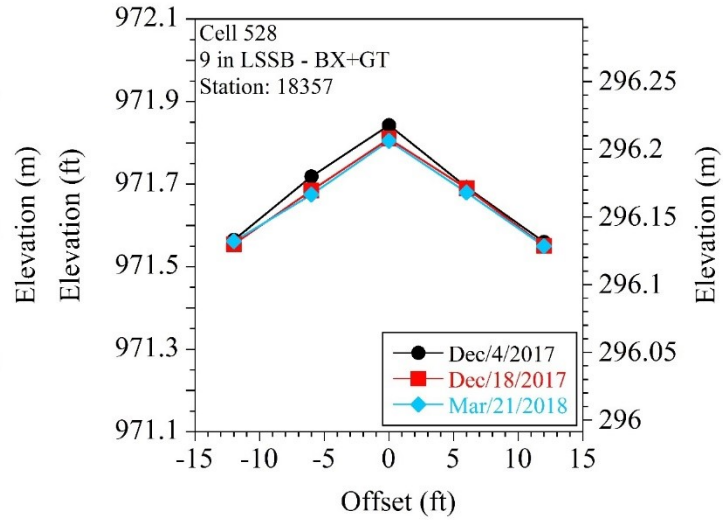
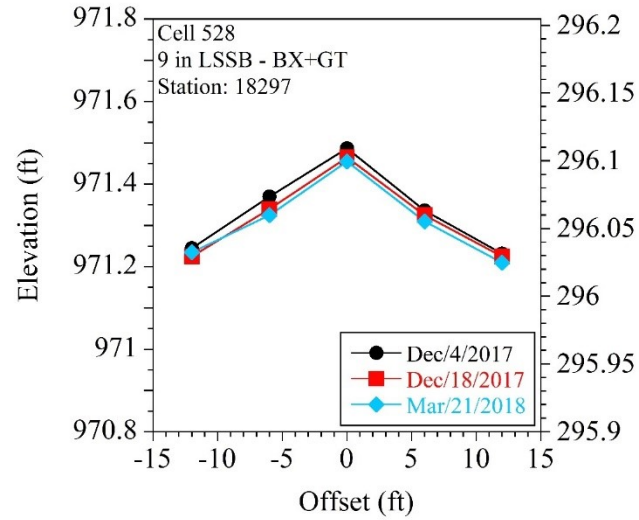
Cell 328 (9-in LSSB - TX):



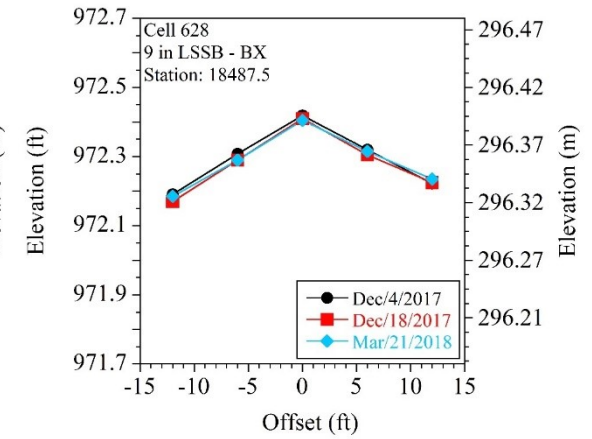
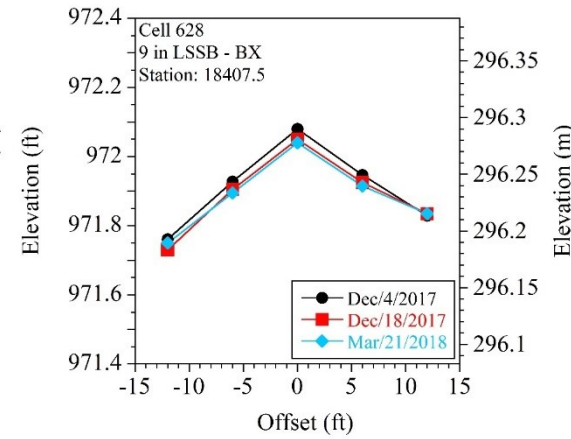
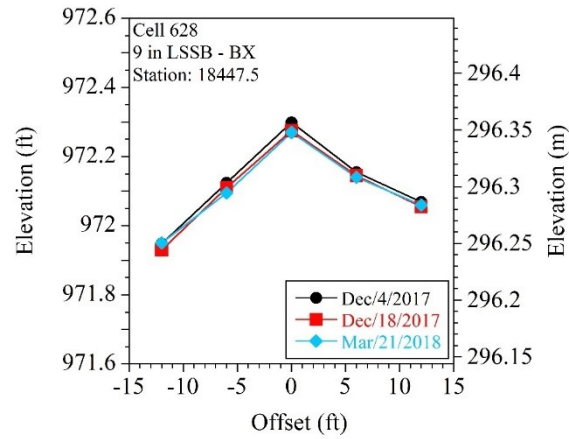
Cell 428 (9-in LSSB - TX+GT):



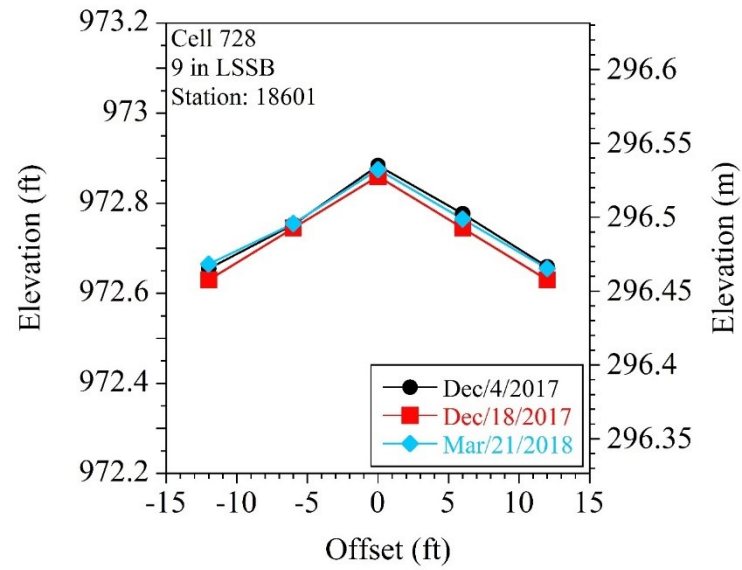
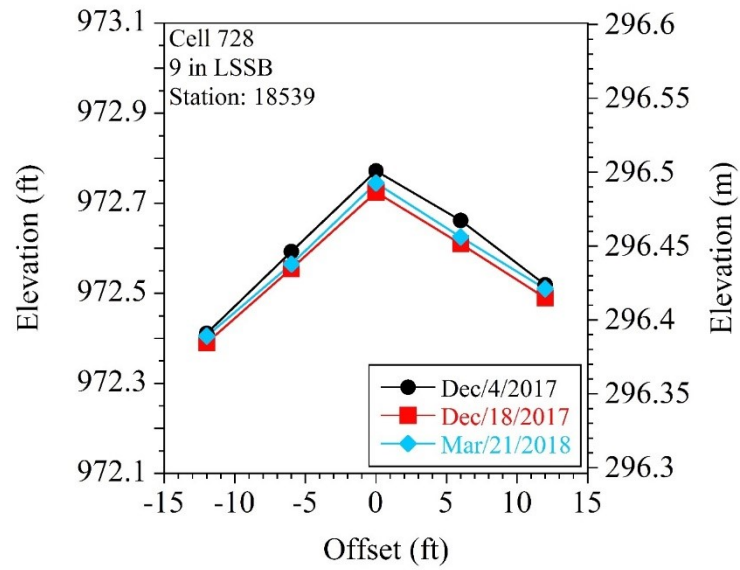
Cell 528 (9-in LSSB - BX+GT):



Cell 628 (9-in LSSB - BX):

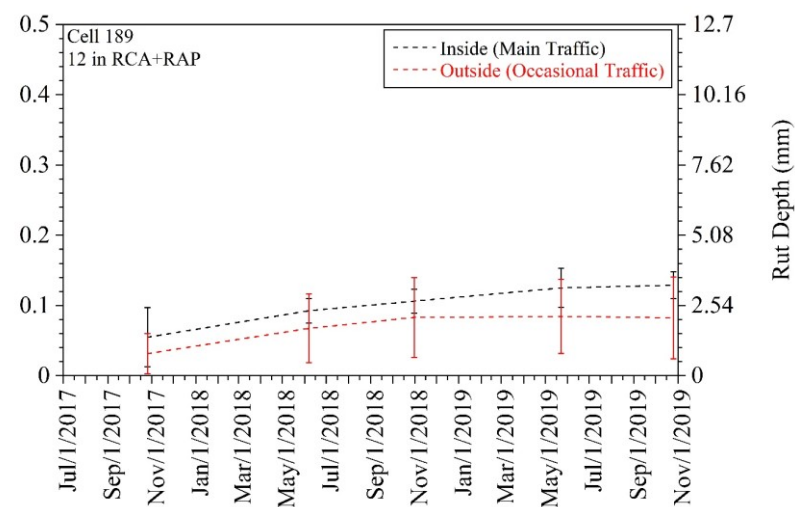
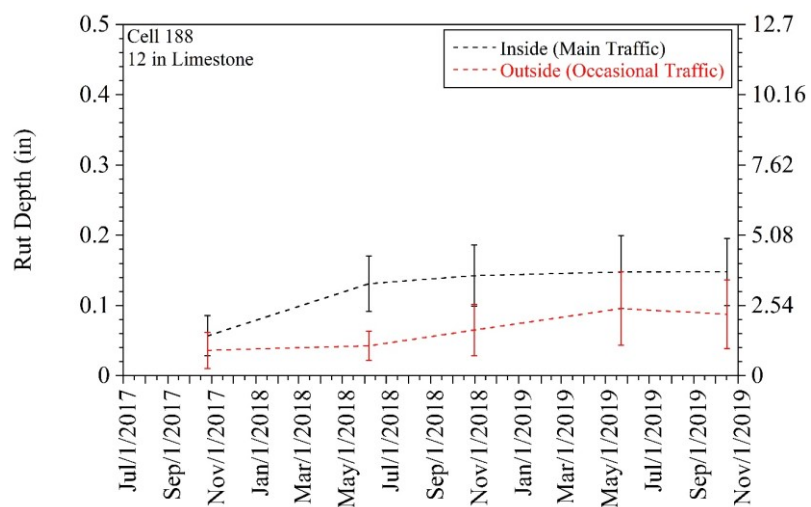
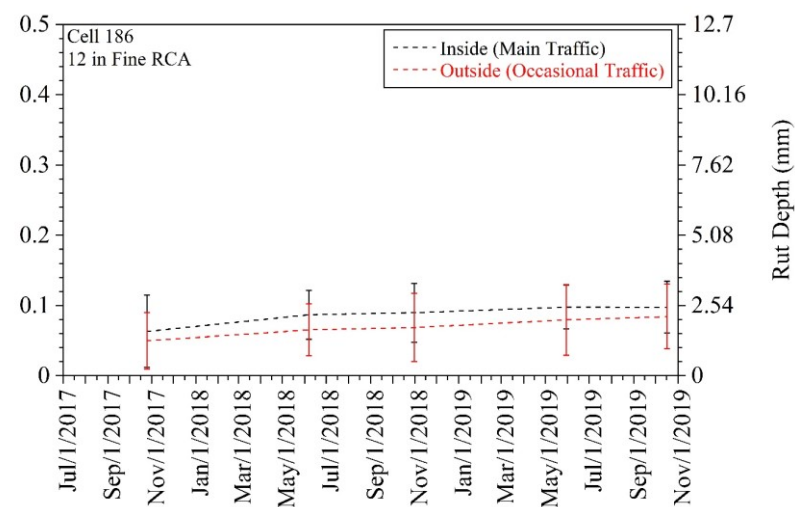
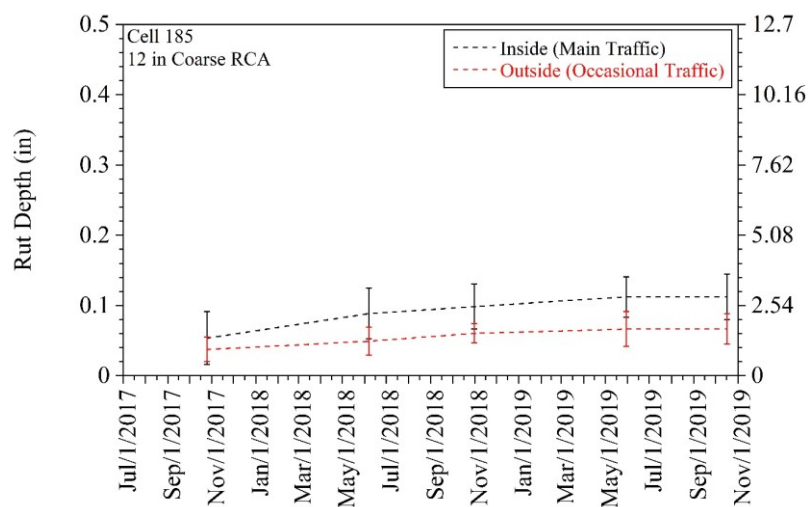


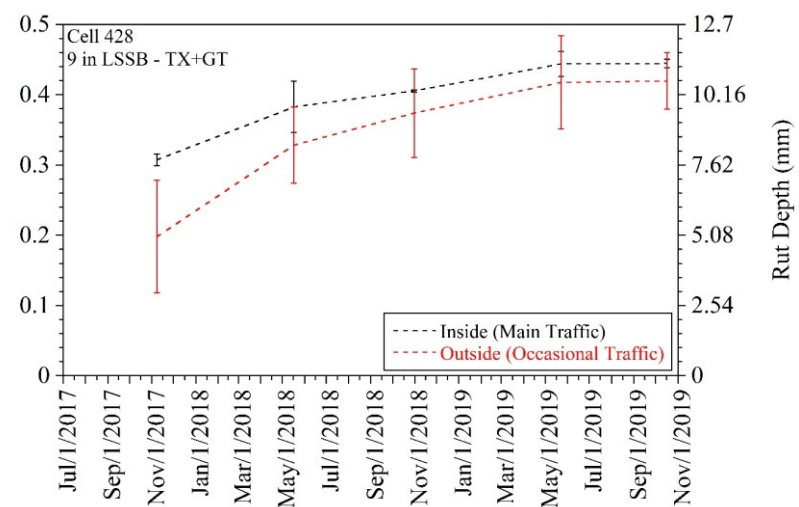
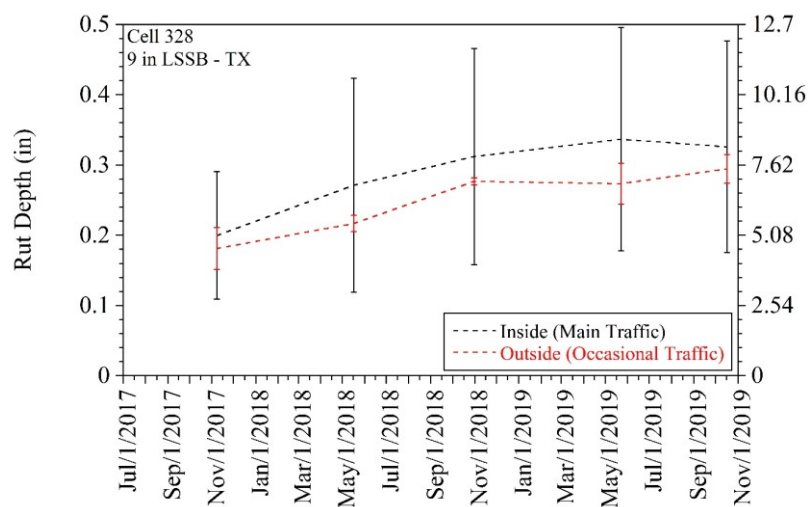
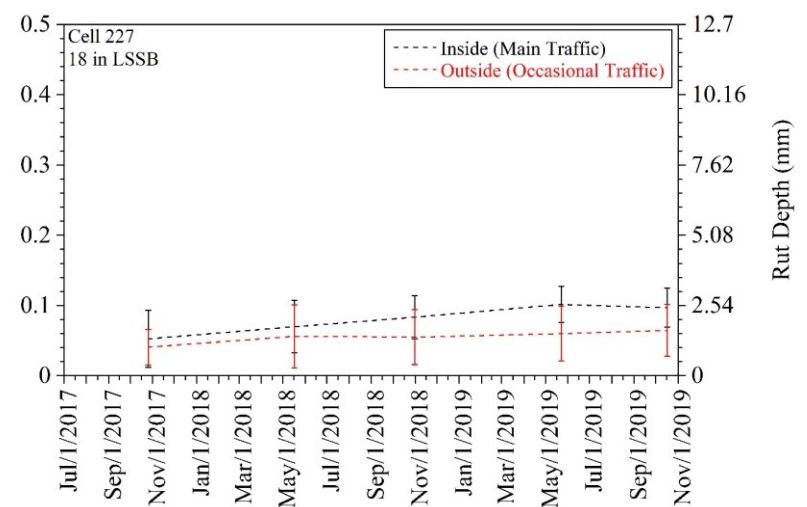
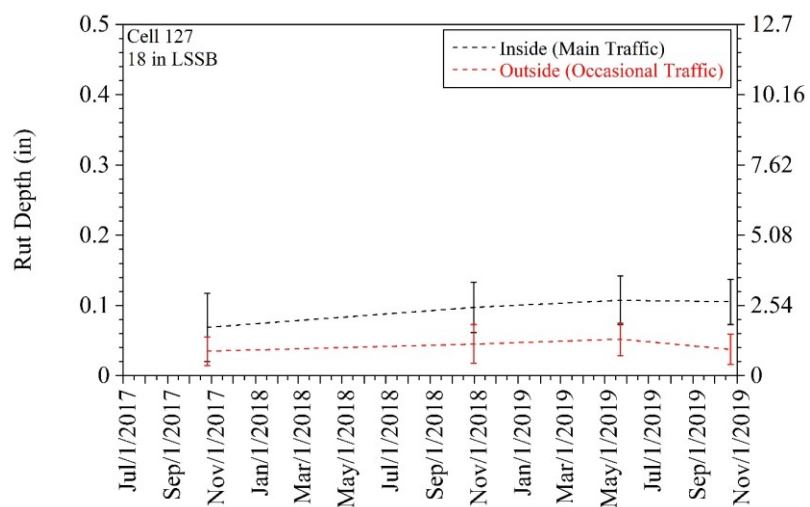
Cell 728 (9-in LSSB):

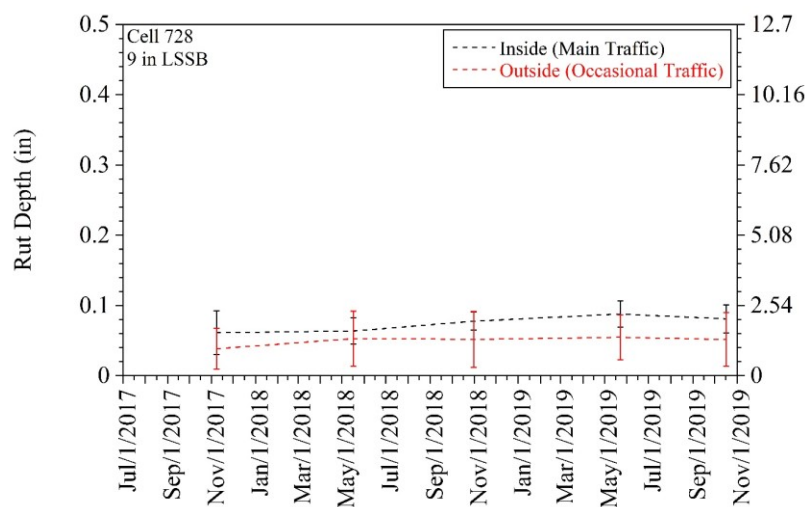
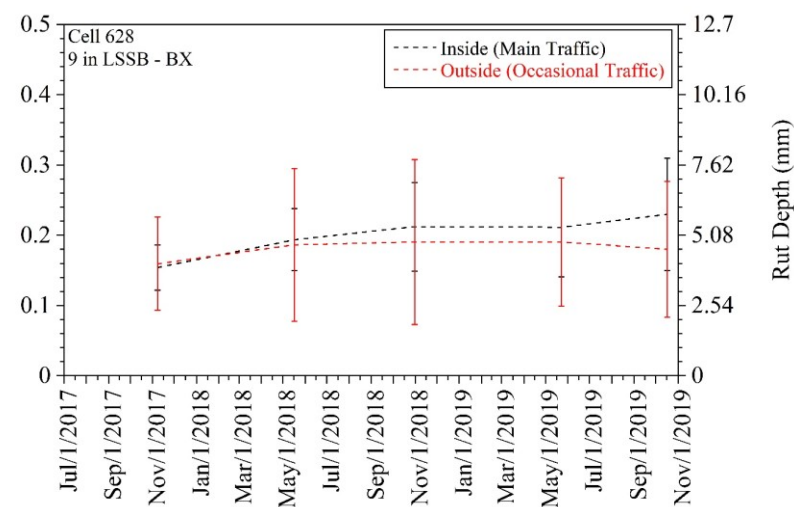
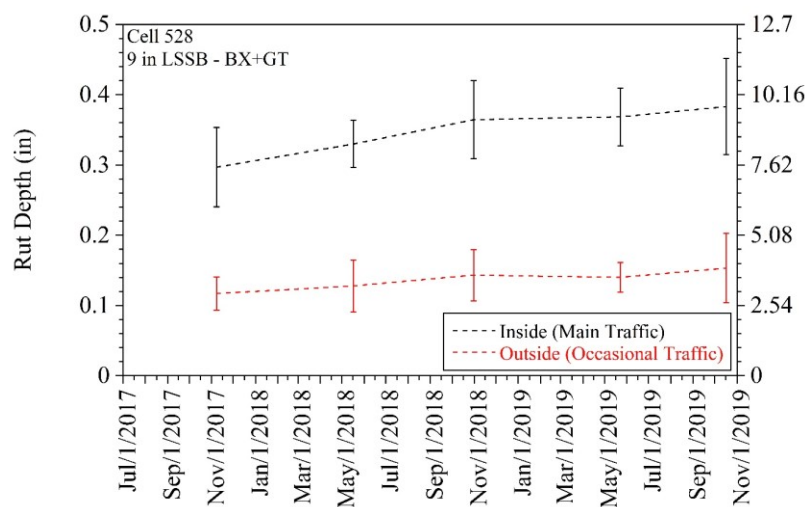


APPENDIX AG

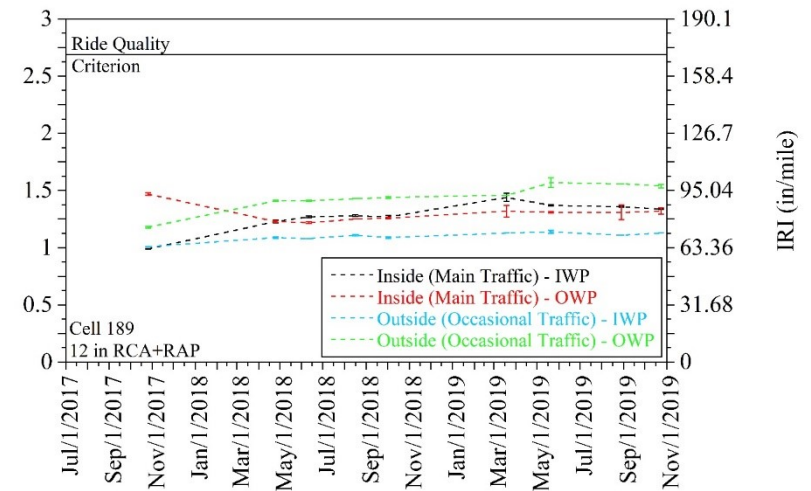
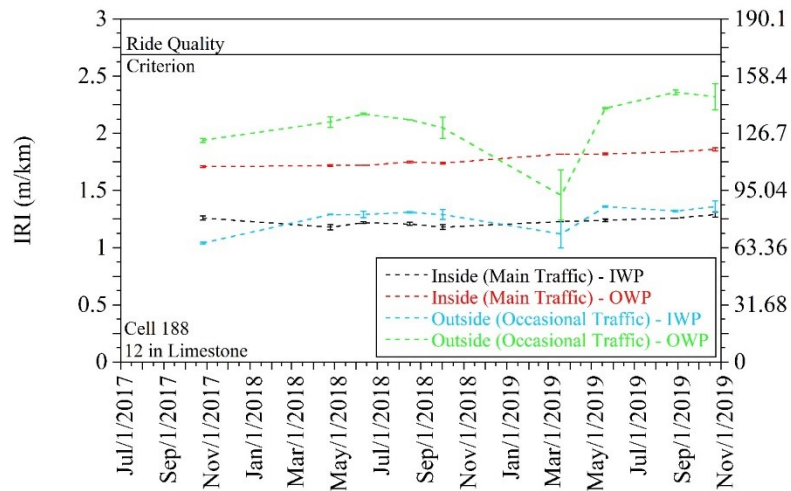
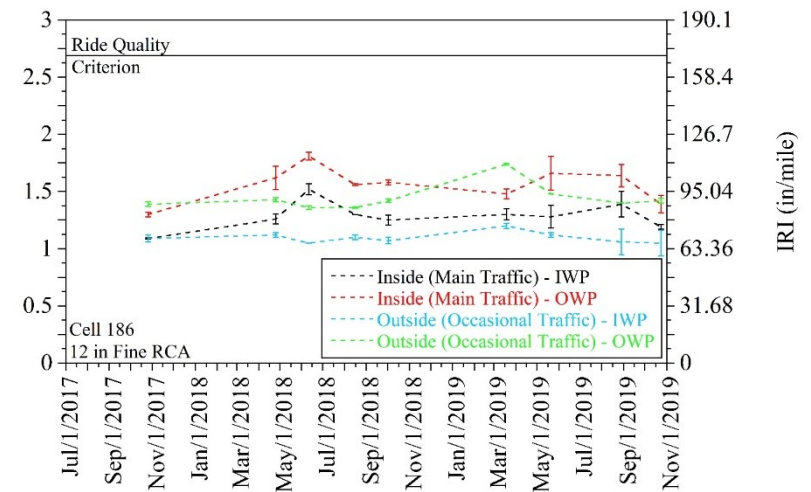
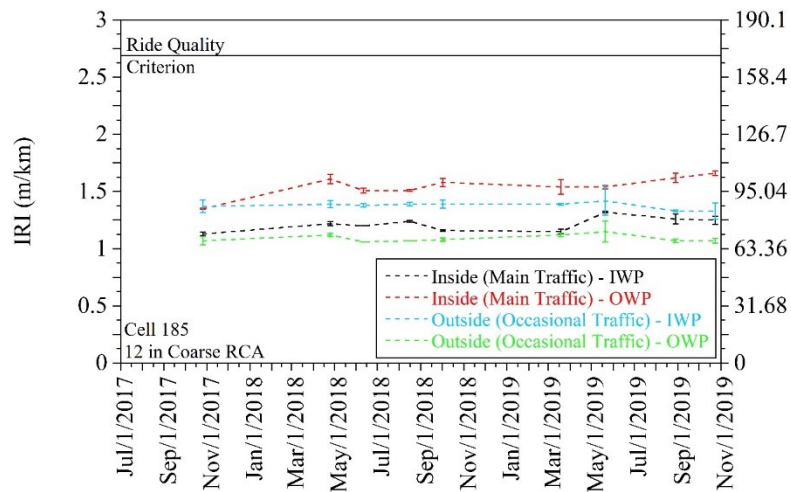
RUT DEPTH MEASUREMENTS FOR EACH CELL

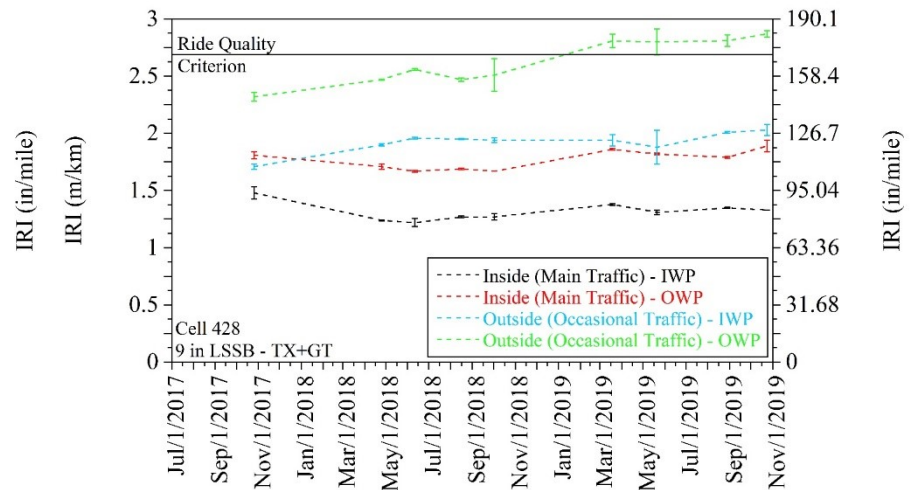
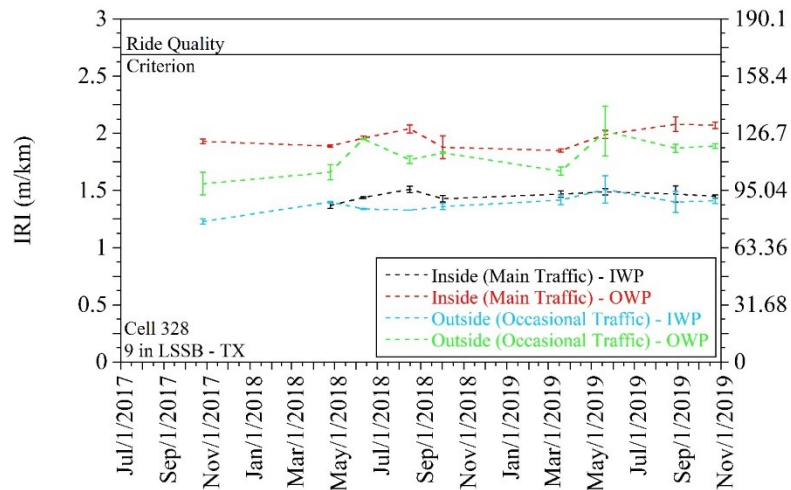
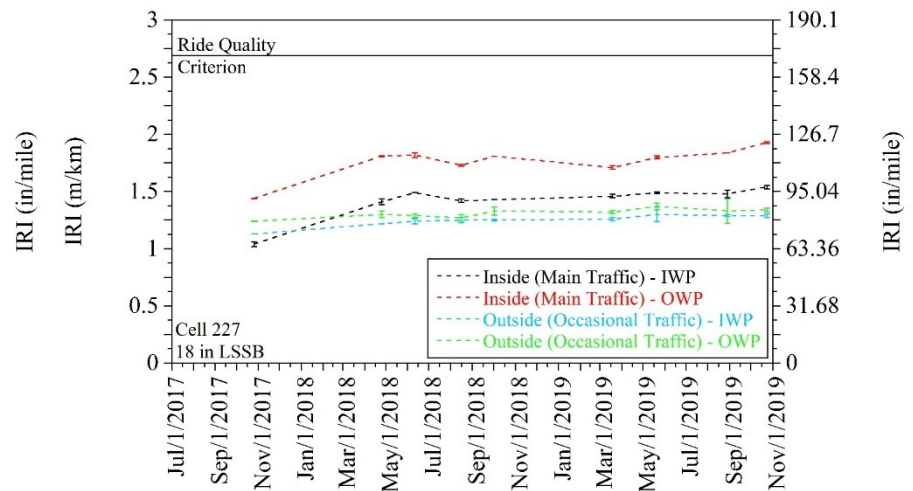
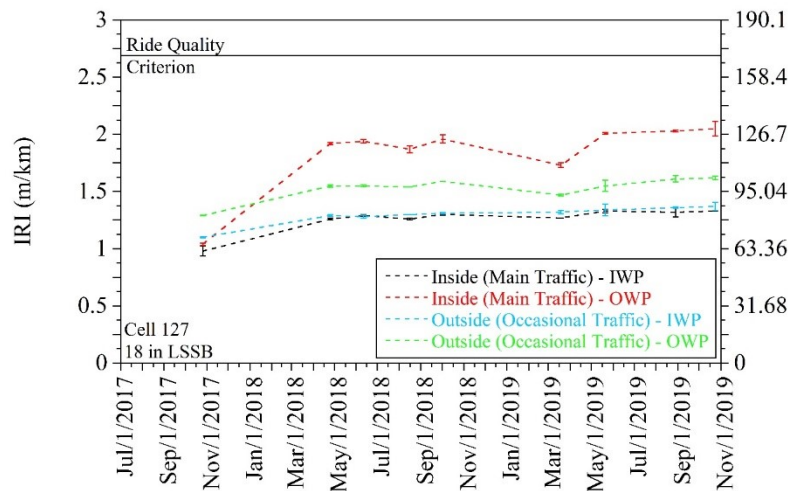


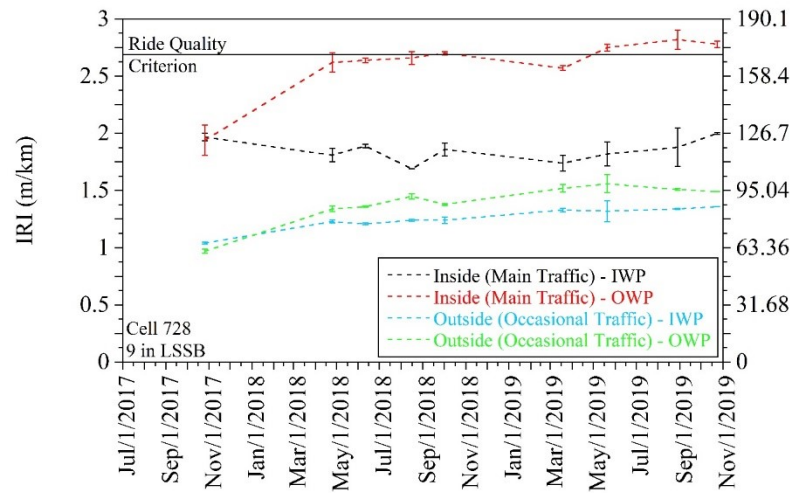
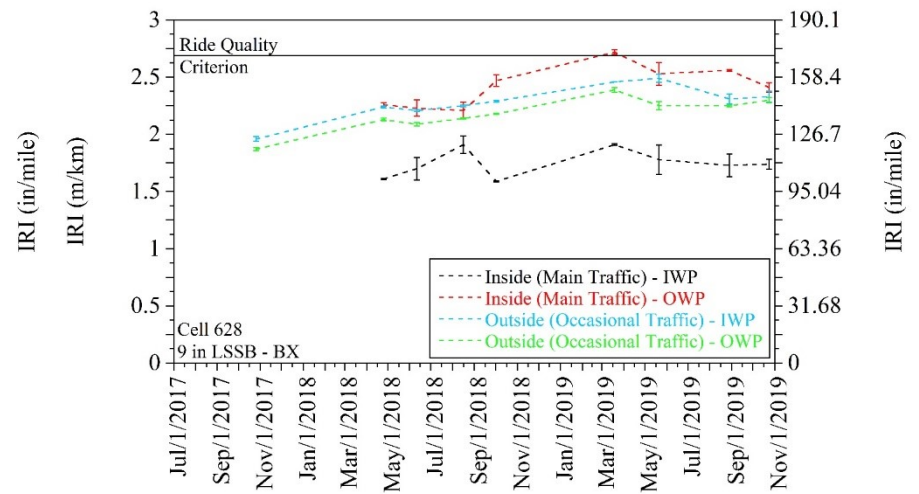
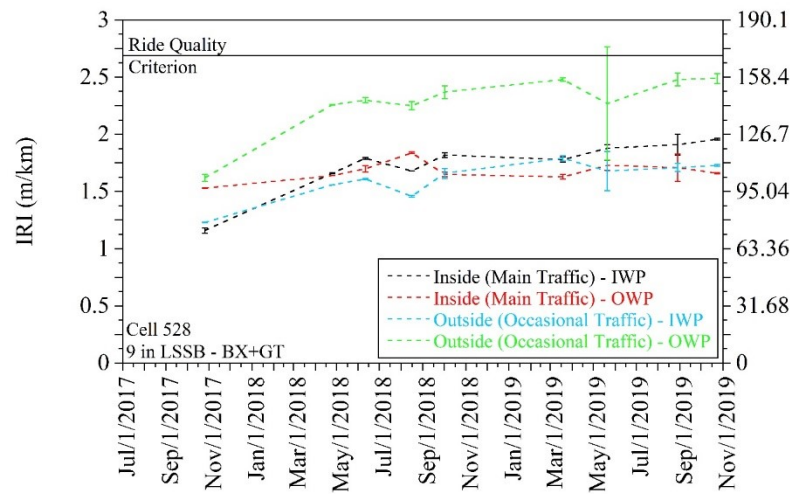




APPENDIX AH
INTERNATIONAL ROUGHNESS INDEX (IRI) TEST RESULTS FOR
EACH CELL

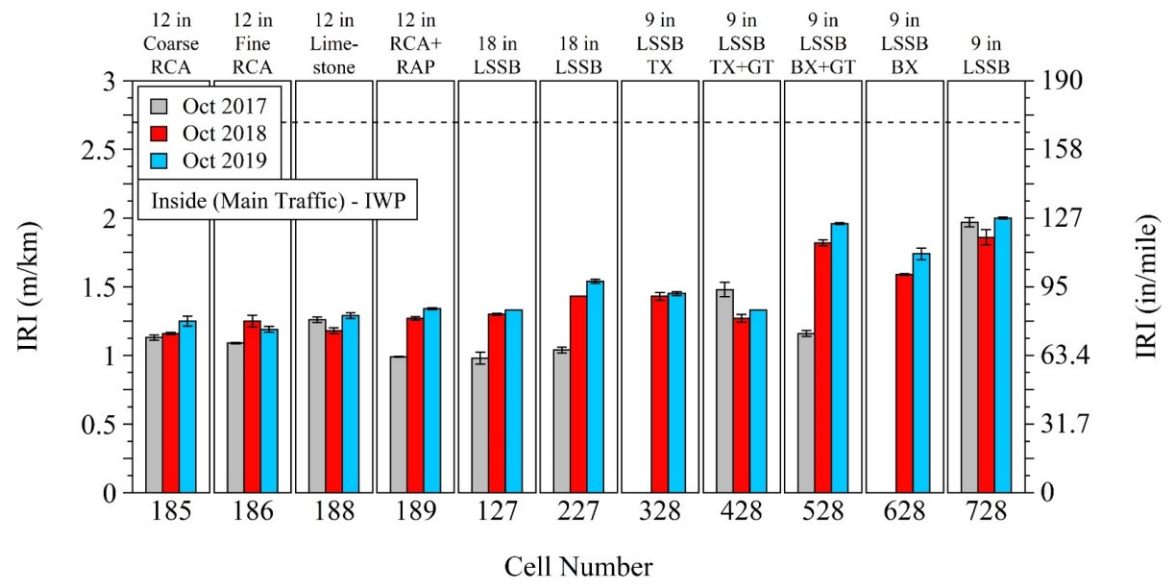






APPENDIX AI

INTERNATIONAL ROUGHNESS INDEX (IRI) IN INSIDE LANE (MAIN TRAFFIC) - IWP OF TEST CELLS



APPENDIX AJ

RAVELING IN TEST CELLS

Raveling pictures taken from the distress identification manual for the LTPP (Miller and Bellinger 2014):



Loss of fine aggregate



Loss of fine and some coarse aggregate



Loss of coarse aggregate

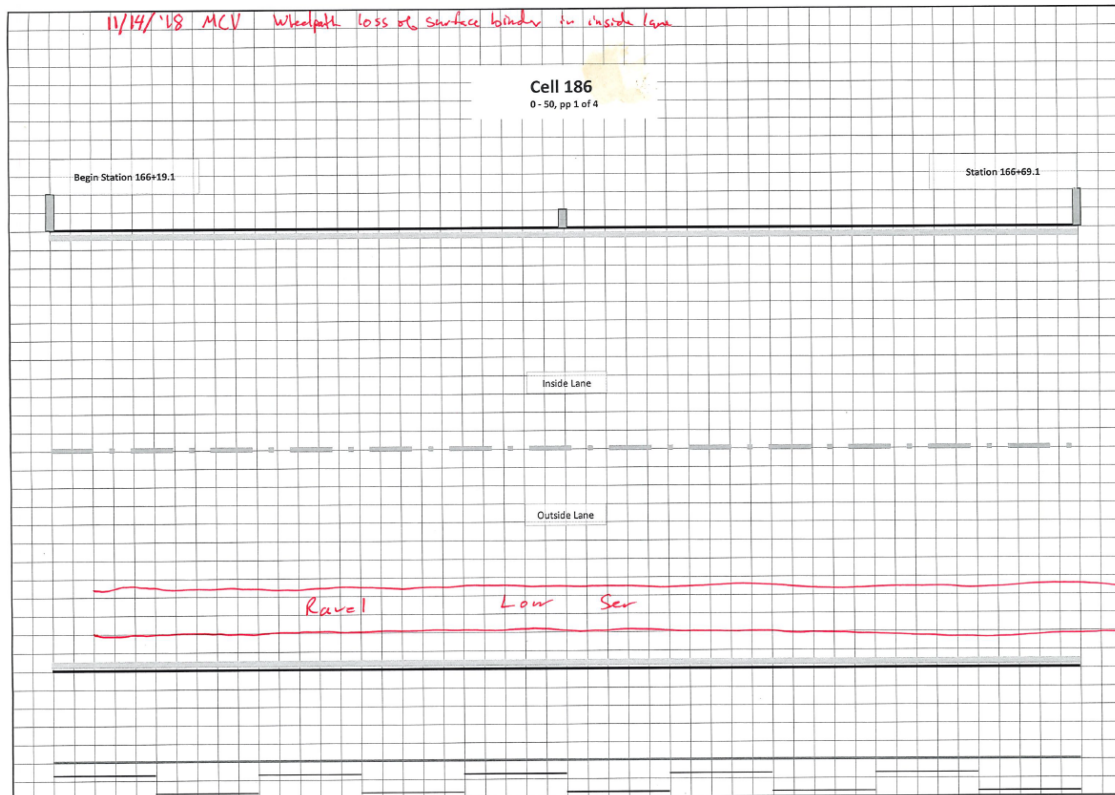


Illustration of raveling on the distress survey maps

Cell Number	Cell Description	Lane	Date	Raveling - Low Severity (Area)	Raveling - Moderate Severity (Area)
185	12-in Coarse RCA	Inside	11/14/2018	0	6
			3/26/2019	0	6
			12/4/2019	0	6
186	12-in Fine RCA	Inside	11/14/2018	0	0
			3/26/2019	0	0
			12/4/2019	0	0
188	12-in Limestone	Inside	11/14/2018	44	0
			3/26/2019	44	0
			12/4/2019	44	0
189	12-in RCA+RAP	Inside	11/14/2018	5	0
			3/26/2019	5	0
			12/4/2019	5	0
127	18-in LSSB	Inside	11/14/2018	1	0
			3/26/2019	1	0
			12/4/2019	1	0
227	18-in LSSB	Inside	11/14/2018	123	0
			3/26/2019	123	0
			12/4/2019	123	0
328	9-in LSSB - TX	Inside	12/17/2018	0	0
			4/7/2019	0	0
			12/4/2019	0	0
428	9-in LSSB - TX+GT	Inside	12/17/2018	0	0
			4/7/2019	0	0
			12/4/2019	0	0
528	9-in LSSB - BX+GT	Inside	12/17/2018	0	0
			4/7/2019	0	0
			12/4/2019	0	0
628	9-in LSSB - BX	Inside	12/17/2018	0	0
			4/7/2019	0	0
			12/4/2019	0	0
728	9-in LSSB	Inside	12/17/2018	0	0
			4/7/2019	0	0
			12/4/2019	0	0

Cell Number	Cell Description	Lane	Date	Raveling - Low Severity (Area)	Raveling - Moderate Severity (Area)
185	12-in Coarse RCA	Outside	11/14/2018	0	12
			3/26/2019	0	12
			12/4/2019	0	12
186	12-in Fine RCA	Outside	11/14/2018	0	0
			3/26/2019	0	0
			12/4/2019	0	0
188	12-in Limestone	Outside	11/14/2018	30	0
			3/26/2019	30	0
			12/4/2019	30	0
189	12-in RCA+RAP	Outside	11/14/2018	0	0
			3/26/2019	0	0
			12/4/2019	0	0
127	18-in LSSB	Outside	11/14/2018	0	0
			3/26/2019	0	0
			12/4/2019	0	0
227	18-in LSSB	Outside	11/14/2018	27	0
			3/26/2019	30	0
			12/4/2019	30	0
328	9-in LSSB - TX	Outside	12/17/2018	0	0
			4/7/2019	0	0
			12/4/2019	0	0
428	9-in LSSB - TX+GT	Outside	12/17/2018	0	0
			4/7/2019	0	0
			12/4/2019	0	0
528	9-in LSSB - BX+GT	Outside	12/17/2018	0	0
			4/7/2019	0	0
			12/4/2019	0	0
628	9-in LSSB - BX	Outside	12/17/2018	0	0
			4/7/2019	0	0
			12/4/2019	0	0
728	9-in LSSB	Outside	12/17/2018	0	0
			4/7/2019	0	0
			12/4/2019	0	0

APPENDIX AK

LABORATORY TEST RESULTS OF BASE LAYER AGGREGATES USED IN FORWARD STEPWISE REGRESSION ANALYSES

Gradation characteristics:

Material	Gravel (%)	Sand (%)	Gravel-to-Sand Ratio	Fines (%)	D ₁₀ (mm)	D ₃₀ (mm)	D ₅₀ (mm)	D ₆₀ (mm)	C _u	C _c
Coarse RCA	61.7	34.9	1.77	3.4	0.36	2.79	8.45	12.37	34.49	1.75
Fine RCA	38.3	54.6	0.7	7.1	0.13	0.82	2.98	4.49	33.93	1.12
Limestone	52.3	32.6	1.6	15.1	0.04	0.78	5.39	8.19	211.31	1.91
RCA+RAP	41	50.4	0.81	8.6	0.1	0.71	3.15	5.05	49.41	0.98
Class 6 Agg.	35.1	58.6	0.6	6.3	0.16	0.61	2.12	3.88	23.82	0.6
Class 5Q Agg.	65.9	30.9	2.13	3.2	0.4	3.75	10.05	13.49	33.69	2.6

Fines = silt and clay; D₁₀ = effective particle size; D₃₀ = particle size at which 30% of the particles are finer; D₅₀ = median particle diameter; D₆₀ = particle size at which 60% of the particles are finer; C_u = coefficient of uniformity; C_c = coefficient of curvature

Atterberg limits:

Material	LL	PL	PI
Coarse RCA	NA	NA	NP
Fine RCA	32.7	NA	NP
Limestone	17.9	NA	NP
RCA+RAP	27.4	NA	NP
Class 6 Agg.	27.4	NA	NP
Class 5Q Agg.	NA	NA	NP

LL = liquid limit; PL = plastic limit; PI = plasticity index; NA = not available; NP = non-plastic

Oven-dry (OD) specific gravity (G_s):

Material	Coarse OD G _s	Fine OD G _s	Combined OD G _s
Coarse RCA	2.4	2	2.25
Fine RCA	2.45	1.99	2.17
Limestone	2.65	2.68	2.66
RCA+RAP	2.47	2.15	2.28
Class 6 Agg.	2.45	2.3	2.35
Class 5Q Agg.	2.39	2.07	2.28

OD = oven-dry; G_s = specific gravity

Saturated-surface-dry (SSD) specific gravity (G_s):

Material	Coarse SSD G _s	Fine SSD G _s	Combined SSD G _s
Coarse RCA	2.49	2.24	2.4
Fine RCA	2.54	2.23	2.35
Limestone	2.7	2.72	2.71
RCA+RAP	2.54	2.26	2.38
Class 6 Agg.	2.52	2.4	2.44
Class 5Q Agg.	2.5	2.27	2.42

SSD = saturated-surface-dry; G_s = specific gravity

Apparent specific gravity (G_s):

Material	Coarse Apparent G_s	Fine Apparent G_s	Combined Apparent G_s
Coarse RCA	2.65	2.61	2.64
Fine RCA	2.7	2.6	2.64
Limestone	2.79	2.8	2.79
RCA+RAP	2.67	2.42	2.52
Class 6 Agg.	2.64	2.55	2.58
Class 5Q Agg.	2.68	2.59	2.65

G_s = specific gravity

Absorption:

Material	Coarse Absorption (%)	Fine Absorption (%)	Combined Absorption (%)
Coarse RCA	4.05	11.68	6.97
Fine RCA	3.7	11.73	8.65
Limestone	1.91	1.51	1.72
RCA+RAP	3.09	5.22	4.34
Class 6 Agg.	3	4.32	3.86
Class 5Q Agg.	4.62	9.62	6.32

Proctor compaction parameters, void ratio (e), and porosity (n)

Material	Uncorrected MDU (kN/m^3)	Uncorrected OMC (%)	Corrected MDU (kN/m^3)	Corrected OMC (%)	e	n
Coarse RCA	19.31	11.3	20.19	9.48	0.28	0.22
Fine RCA	19.1	11.1	19.12	11.07	0.35	0.26
Limestone	22.34	6.2	22.49	6.28	0.22	0.18
RCA+RAP	19.73	10	19.76	9.97	0.25	0.2
Class 6 Agg.	20.14	8.3	20.19	8.26	0.25	0.2
Class 5Q Agg.	19.26	11	20.11	9.63	0.29	0.23

MDU = maximum dry unit weight; OMC = optimum moisture content; e = void ratio [based on corrected MDU and apparent specific gravity (G_s)]; n = porosity [$n = e/(1+e)$]

Asphalt binder and residual mortar contents:

Material	Asphalt Binder Content by Ignition (%)	Asphalt Binder Content by Extraction (%)	Residual Mortar Content (%)
Coarse RCA	2.02	0.1	33.4
Fine RCA	2.98	0.38	29.6
Limestone	1.61	0.35	1.3
RCA+RAP	3.18	1.58	20.1
Class 6 Agg.	3.17	1.77	25.6
Class 5Q Agg.	2.15	0.28	37.1

Width-to-length ratio sphericity:

Material	Median Sphericity	PLS _{0.9} (%)	PLS _{0.7} (%)	PLS _{0.5} (%)	PLS _{0.3} (%)	PLS _{0.1} (%)
Coarse RCA	0.769729034	88	28	1	0	0
Fine RCA	0.758298649	90	32	2.5	0	0
Limestone	0.775580109	88	26	1	0	0
RCA+RAP	0.763247555	90.5	30	2	0	0
Class 6 Agg.	0.759657917	90	32	2	0	0
Class 5Q Agg.	0.756547947	90.5	33	2	0	0

PLS_{0.9} = percent less spherical than 0.9; PLS_{0.7} = percent less spherical than 0.7; PLS_{0.5} = percent less spherical than 0.5; PLS_{0.3} = percent less spherical than 0.3; PLS_{0.1} = percent less spherical than 0.1

Roundness:

Material	Median Roundness	PLR _{0.9} (%)	PLR _{0.7} (%)	PLR _{0.5} (%)	PLR _{0.3} (%)	PLR _{0.1} (%)
Coarse RCA	0.660245895	99.5	64	11	0.5	0
Fine RCA	0.657135606	99.5	66	9.5	0	0
Limestone	0.649245381	99.5	67.5	10	0	0
RCA+RAP	0.663714975	100	63.5	8.5	0	0
Class 6 Agg.	0.663310677	99	63.5	10	0	0
Class 5Q Agg.	0.641065776	100	70	12.5	0	0

PLR_{0.9} = percent less rounded than 0.9; PLR_{0.7} = percent less rounded than 0.7; PLR_{0.5} = percent less rounded than 0.5; PLR_{0.3} = percent less rounded than 0.3; PLR_{0.1} = percent less rounded than 0.1

Relative breakage (B_r):

Material	B _r After 100 Gyration	B _r After 300 Gyration	B _r After 500 Gyration
Coarse RCA	0.03407	0.03801	0.06440
Fine RCA	0.02577	0.03413	0.05325
Limestone	0.01421	0.01848	0.02582
RCA+RAP	0.02146	0.02436	0.02777
Class 6 Agg.	0.02677	0.02942	0.03870
Class 5Q Agg.	0.04644	0.06259	0.07820

B_r = relative breakage

Saturated hydraulic conductivity (K_{sat}) and soil-water characteristic curve (SWCC) parameters:

Material	K _{sat} (cm/sec)	Residual VWC	Saturated VWC	Air-Entry Pressure (kPa)
Coarse RCA	2.67E-04	0	0.2804	2.5
Fine RCA	4.85E-04	0	0.2887	6
Limestone	4.86E-05	0.0406	0.2366	2
RCA+RAP	2.06E-04	0.0048	0.2764	2
Class 6 Agg.	1.91E-04	0.0502	0.2607	3
Class 5Q Agg.	2.91E-04	0.0318	0.317	1.75

K_{sat} = saturated hydraulic conductivity; VWC = volumetric water content

Resilient modulus (M_R):

Material	SM_R (MPa)	k_1	k_2	k_3
Coarse RCA	124.99	913	0.44	-0.07
Fine RCA	122.46	882	0.45	-0.06
Limestone	96.02	762	0.32	-0.05
RCA+RAP	113.68	803	0.51	-0.12
Class 6 Agg.	NA	NA	NA	NA
Class 5Q Agg.	NA	NA	NA	NA

SM_R = summary M_R ; k_1 , k_2 , and k_3 = MEPDG M_R model fitting parameters; NA = not available

APPENDIX AL

ALTERNATIVE MODELS TO ESTIMATE UNCORRECTED OPTIMUM MOISTURE CONTENT (OMC) AND MAXIMUM DRY UNIT WEIGHT (MDU) VALUES OF AGGREGATE BASE LAYERS

For uncorrected optimum moisture content (OMC):

Equation	R ²	Adj. R ²	Std. Error
-13.7918*Combined OD G _s - 0.1033*Sand (%) - 0.1434*D ₅₀ (mm) + 47.0832	1	1	0
-13.7114*Combined OD G _s - 0.0854*Sand (%) - 0.2107*D ₃₀ (mm) + 45.6781	1	1	0.02
-13.5679*Combined OD G _s - 0.0760*Sand (%) - 1.3958*D ₁₀ (mm) + 44.8785	1	1	0.04
-13.7779*Combined OD G _s - 0.1166*Sand (%) - 0.0477*Gravel (%) + 49.2062	1	1	0.02
-13.7779*Combined OD G _s - 0.0689*Sand (%) + 0.0477*Fines (%) + 44.4357	1	1	0.05
-10.2402*Fine SSD G _s - 0.6206*Asphalt Binder Content by Extraction (%) + 0.2358*C _c + 33.8534	1	1	0.05
0.3288*Fine Absorption (%) - 9.1184*Fine Apparent G _s + 0.3155*C _c - 0.4603*Asphalt Binder Content by Extraction (%) + 30.7698	1	1	0.05
-12.6425*Combined OD G _s - 0.0632*Sand (%) + 41.8871	1	1	0
-7.6245*Fine OD G _s + 0.4420*C _c + 25.7617	1	1	0.14
-11.8099*Fine SSD G _s - 0.9615*Asphalt Binder Content by Ignition (%) + 39.8574	1	0.99	0.18
-19.6912*Combined SSD G _s - 1.7824*Asphalt Binder Content by Ignition (%) + 62.3518	0.99	0.98	0.29
-13.6173*Combined OD G _s - 1.2124*Asphalt Binder Content by Ignition (%) + 44.4507	0.99	0.97	0.32
-10.9676*Combined OD G _s + 0.1602*D ₆₀ (mm) + 33.9536	0.98	0.97	0.35
-10.8351*Combined OD G _s + 0.2065*D ₅₀ (mm) + 33.8059	0.98	0.97	0.35
-11.7264*Combined OD G _s + 0.9328*C _c + 35.5972	0.98	0.97	0.35
-17.0353*Combined SSD G _s - 0.0793*Sand (%) + 54.8267	0.98	0.97	0.36
-15.6546*Combined SSD G _s + 1.2149*C _c + 46.1668	0.97	0.95	0.45
-14.0096*Combined SSD G _s + 0.2540*D ₅₀ (mm) + 42.5928	0.97	0.94	0.49
-10.9123*Combined OD G _s + 35.0921	0.96	0.92	0.56
0.7431*Combined Absorption (%) + 5.7034	0.87	0.84	0.81
-13.6175*Combined SSD G _s + 42.9932	0.83	0.79	0.93

G_s = specific gravity; SSD = saturated-surface-dry; OD = oven-dry; C_c = coefficient of curvature

For uncorrected maximum dry unit weight (MDU):

Equation	R ²	Adj. R ²	Std. Error
6.3812*Combined SSD G _s - 0.4756*Coarse Absorption (%) + 5.9683	1	1	0.07
5.4082*Combined OD G _s - 0.3449*Coarse Absorption (%) + 8.5401	1	0.99	0.09
6.5823*Combined OD G _s - 0.1496*D ₃₀ (mm) + 4.8677	1	0.99	0.1
4.9439*Combined OD G _s - 0.0304*Residual Mortar Content (%) + 9.1974	1	0.99	0.11
4.5928*Fine SSD G _s - 0.0280*Residual Mortar Content (%) + 9.8594	1	0.99	0.11
5.4125*Combined OD G _s + 0.0730*Fines (%) + 6.8279	0.99	0.99	0.12
5.6446*Combined SSD G _s - 0.0401*Residual Mortar Content (%) + 7.1398	0.99	0.98	0.16
9.5737*Combined SSD G _s - 0.3991*C _c - 2.8669	0.99	0.98	0.17
9.0361*Combined SSD G _s - 0.0852*D ₅₀ (mm) - 1.6901	0.99	0.98	0.17
7.9065*Combined SSD G _s - 2.0737*D ₁₀ (mm) + 1.0323	0.99	0.98	0.18
9.0976*Combined SSD G _s - 0.0648*D ₆₀ (mm) - 1.7844	0.99	0.98	0.19
-0.2085*Fine Absorption (%) + 6.9277*Combined Apparent G _s + 3.2383	0.97	0.96	0.25
-1.3568*Coarse Absorption (%) + 0.8841*Gravel-to-Sand Ratio + 23.4612	0.97	0.95	0.26
-1.3618*Coarse Absorption (%) + 0.7804*C _c + 23.4353	0.97	0.95	0.27
6.9110*Combined OD G _s + 3.8658	0.97	0.96	0.23
-1.5319*Coarse Absorption (%) + 0.1977*D ₅₀ (mm) + 24.1188	0.97	0.94	0.29
-0.3613*Combined Absorption (%) + 4.5591*Fine Apparent G _s + 10.0660	0.96	0.93	0.33
-1.0944*Coarse Absorption (%) - 0.7557*Asphalt Binder Content by Ignition (%) + 25.5955	0.96	0.93	0.33
-1.4842*Coarse Absorption (%) + 0.1448*D ₆₀ (mm) + 23.8709	0.96	0.93	0.33
-0.3588*Combined Absorption (%) + 6.1792*Combined Apparent G _s + 5.5866	0.96	0.92	0.33
-0.3175*Combined Absorption (%) + 11.6006*Coarse Apparent G _s - 9.5334	0.96	0.93	0.33
-1.4232*Coarse Absorption (%) + 0.0446*Gravel (%) + 22.6210	0.96	0.93	0.33
8.9049*Combined SSD G _s - 1.8244	0.94	0.92	0.34
-0.4286*Combined Absorption (%) + 22.2548	0.77	0.71	0.65

G_s = specific gravity; SSD = saturated-surface-dry; OD = oven-dry; C_c = coefficient of curvature

APPENDIX AM

ALTERNATIVE MODELS TO ESTIMATE CORRECTED OPTIMUM MOISTURE CONTENT (OMC) AND MAXIMUM DRY UNIT WEIGHT (MDU) VALUES OF AGGREGATE BASE LAYERS

For corrected optimum moisture content (OMC):

Equation	R ²	Adj. R ²	Std. Error
$0.9066 \cdot \text{Uncorrected OMC (\%)} - 0.3036 \cdot D_{60} \text{ (mm)} + 0.8947 \cdot C_c + 1.4338$	1	1	0.11
$0.8501 \cdot \text{Uncorrected OMC (\%)} - 0.1533 \cdot D_{60} \text{ (mm)} + 2.1258$	0.97	0.96	0.34
$1.0244 \cdot \text{Uncorrected OMC (\%)} - 5.5904 \cdot D_{10} \text{ (mm)} + 0.3445$	0.97	0.95	0.37
$0.8580 \cdot \text{Uncorrected OMC (\%)} - 0.1930 \cdot D_{50} \text{ (mm)} + 1.8711$	0.97	0.94	0.4
$0.8252 \cdot \text{Uncorrected OMC (\%)} - 0.0470 \cdot \text{Gravel (\%)} + 3.4571$	0.97	0.94	0.4
$0.9422 \cdot \text{Uncorrected OMC (\%)} - 0.5206 \cdot D_{30} \text{ (mm)} + 0.8448$	0.96	0.94	0.41
$-11.7635 \cdot \text{Combined SSD } G_s + 37.9200$	0.88	0.85	0.64
$0.7499 \cdot \text{Uncorrected OMC (\%)} + 1.8796$	0.84	0.8	0.74

OMC = optimum moisture content; C_c = coefficient of curvature; SSD = saturated-surface-dry; G_s = specific gravity

For corrected maximum dry unit weight (MDU):

Equation	R ²	Adj. R ²	Std. Error
1.3991*Uncorrected MDU (kN/m ³) + 0.8096*D ₅₀ - 3.4342*Gravel-to-Sand Ratio - 7.6185	1	1	0.04
-0.4399*Uncorrected OMC (%) - 1.2115*Asphalt Binder Content by Ignition (%) - 2.1556*Fine Apparent G _s + 33.1997	1	1	0.05
0.9264*Uncorrected MDU (kN/m ³) + 0.0938*D ₆₀ (mm) + 1.0596	1	0.99	0.1
1.1356*Uncorrected MDU (kN/m ³) + 3.3492*D ₁₀ (mm) - 3.0446	0.99	0.99	0.13
0.9375*Uncorrected MDU (kN/m ³) + 0.1195*D ₅₀ (mm) + 0.9394	0.99	0.99	0.14
0.8999*Uncorrected MDU (kN/m ³) + 0.0297*Gravel (%) + 0.8753	0.99	0.99	0.14
1.0342*Uncorrected MDU (kN/m ³) + 0.3132*D ₃₀ (mm) - 0.8455	0.99	0.98	0.14
0.8580*Uncorrected MDU (kN/m ³) + 0.5861*Gravel-to-Sand Ratio + 2.4342	0.99	0.98	0.16
-0.3939*Uncorrected OMC (%) - 0.9332*Asphalt Binder Content by Ignition (%) + 26.4608	0.99	0.98	0.17
-0.4655*Uncorrected OMC (%) - 0.0494*Sand (%) + 26.9591	0.99	0.98	0.18
0.8015*Uncorrected MDU (kN/m ³) - 0.0310*Sand (%) + 5.6495	0.98	0.97	0.2
0.7185*Uncorrected MDU (kN/m ³) - 0.6171*Asphalt Binder Content by Ignition (%) + 7.5096	0.98	0.97	0.2
3.6328*Fine OD G _s - 0.0368*Sand (%) + 13.9284	0.98	0.96	0.22
5.0802*Fine SSD G _s - 0.0290*Sand (%) + 9.6254	0.98	0.96	0.23
4.2779*Fine OD G _s + 0.1074*D ₆₀ (mm) + 10.0510	0.98	0.96	0.23
5.7675*Fine SSD G _s + 0.0815*D ₆₀ (mm) + 6.0954	0.98	0.96	0.23
1.4339*Uncorrected MDU (kN/m ³) + 0.7989*Coarse Absorption (%) - 11.0475	0.98	0.96	0.23
-0.5524*Uncorrected OMC (%) + 0.0475*Gravel (%) + 23.3136	0.97	0.96	0.24
3.9122*Fine OD G _s + 0.6678*Gravel-to-Sand Ratio + 10.8568	0.97	0.95	0.26
4.3220*Fine OD G _s + 0.1350*D ₅₀ (mm) + 10.0800	0.97	0.95	0.26
-0.5099*Uncorrected OMC (%) + 0.9094*Gravel-to-Sand Ratio + 24.0760	0.97	0.94	0.27
-0.5817*Uncorrected OMC (%) + 0.1881*D ₅₀ (mm) + 24.9159	0.96	0.93	0.31
0.8848*Uncorrected MDU (kN/m ³) + 2.6339	0.88	0.85	0.44
-0.4764*Uncorrected OMC (%) + 24.9076	0.71	0.63	0.69

MDU = maximum dry unit weight; OMC = optimum moisture content; G_s = specific gravity; SSD = saturated-surface-dry

APPENDIX AN
ALTERNATIVE MODELS TO ESTIMATE SATURATED HYDRAULIC
CONDUCTIVITY (K_{SAT}) VALUES OF AGGREGATE BASE LAYERS

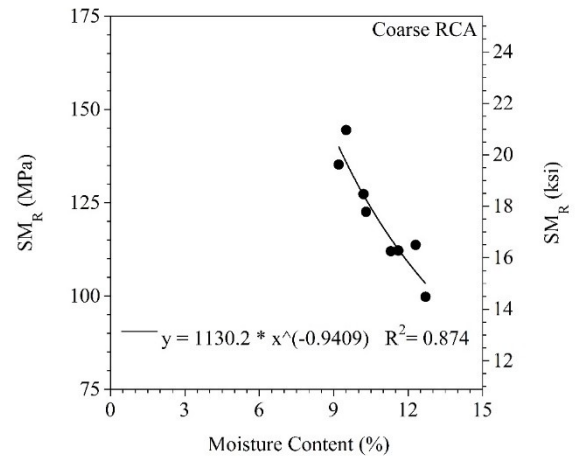
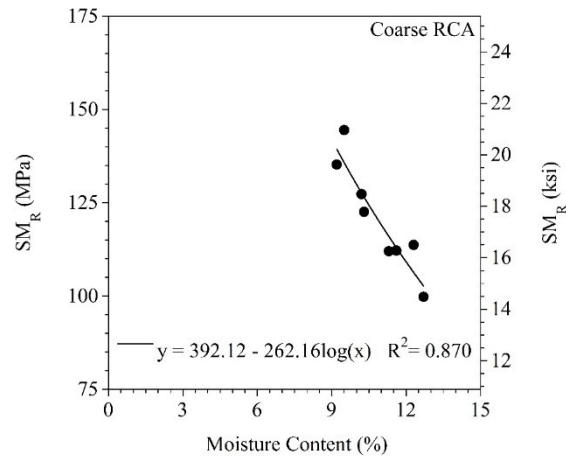
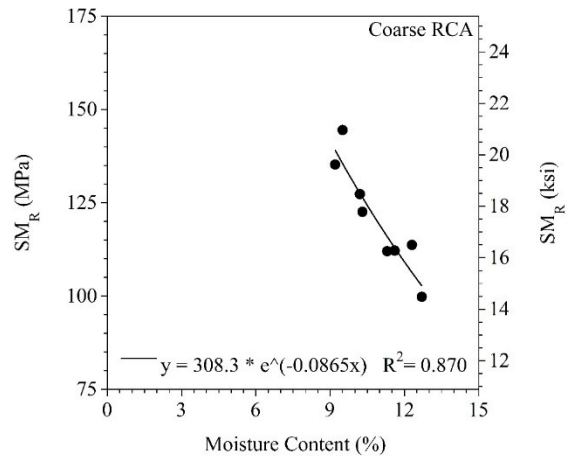
Equation	R ²	Adj. R ²	Std. Error
0.001581*Corrected MDU (kN/m ³) - 0.012708*Combined Apparent G _s + 0.046235*n - 0.008281	1	1	4.23E-06
0.002988*e - 0.000185*Combined Apparent G _s - 8.53E-05	1	1	7.14E-06
0.002735*e - 0.000165*Combined SSD G _s - 9.97E-05	1	1	9.99E-06

MDU = maximum dry unit weight; G_s = specific gravity; e = void ratio [based on corrected MDU and apparent specific gravity (G_s)]; n = porosity [n = e/(1+e)]; SSD = saturated-surface-dry

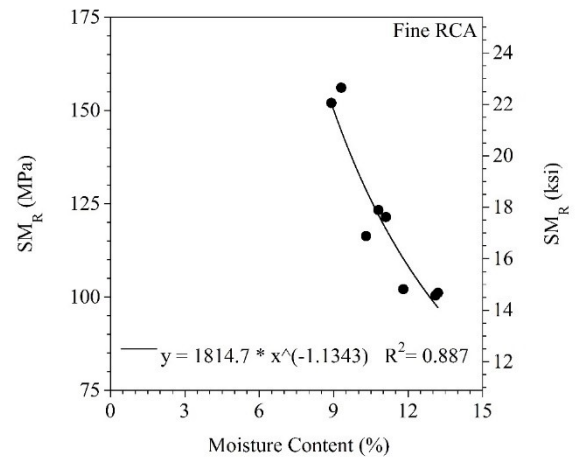
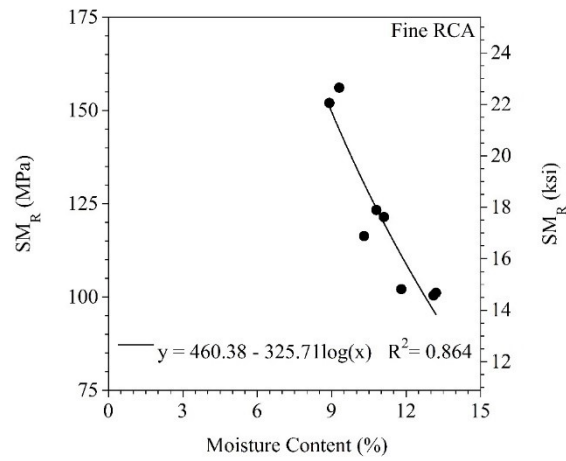
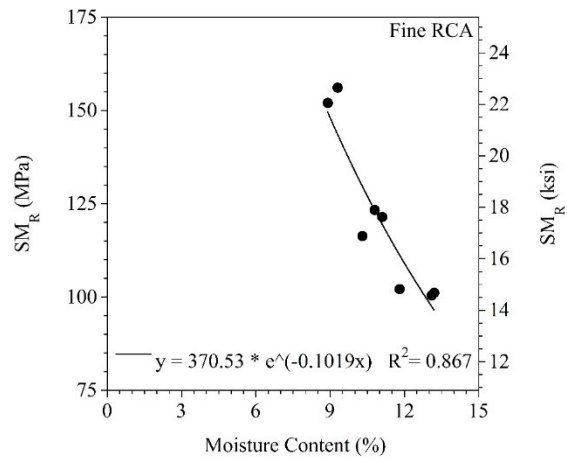
APPENDIX AO

SUMMARY RESILIENT MODULUS (SM_R) VS. MOISTURE CONTENT

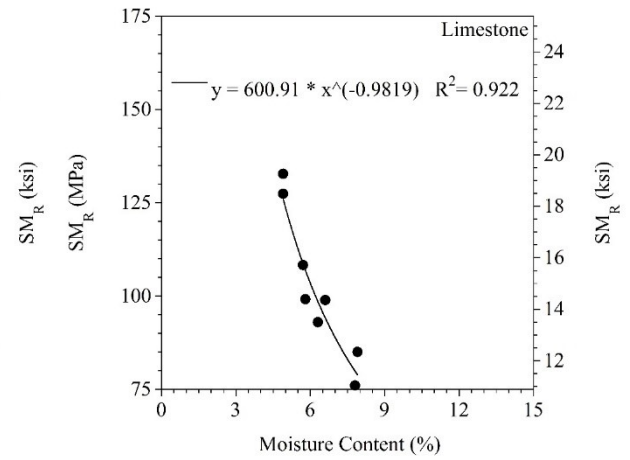
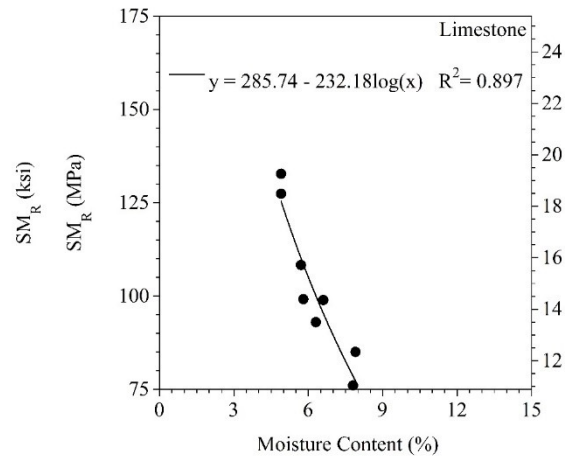
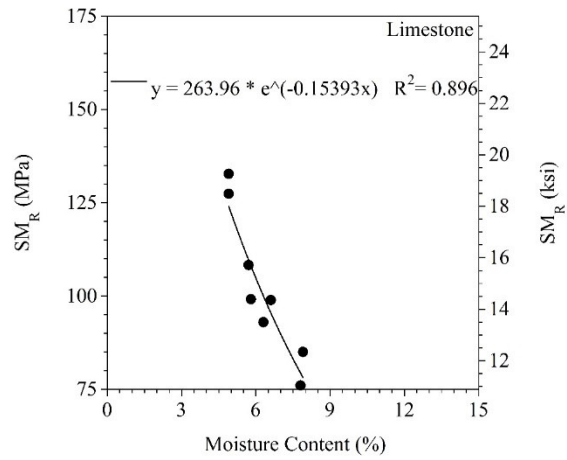
For Coarse RCA:



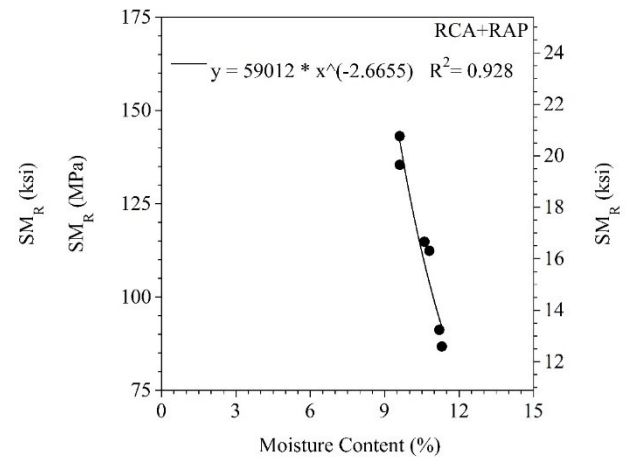
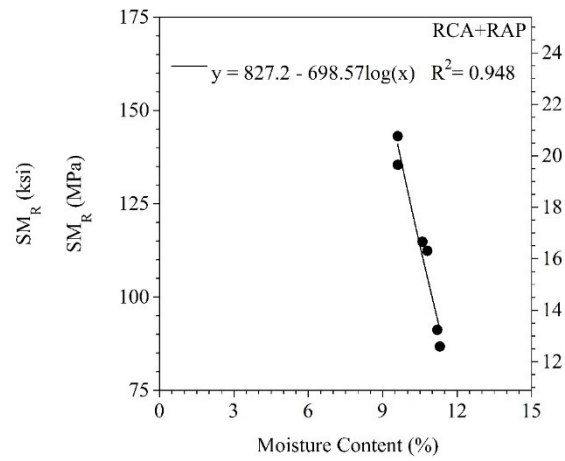
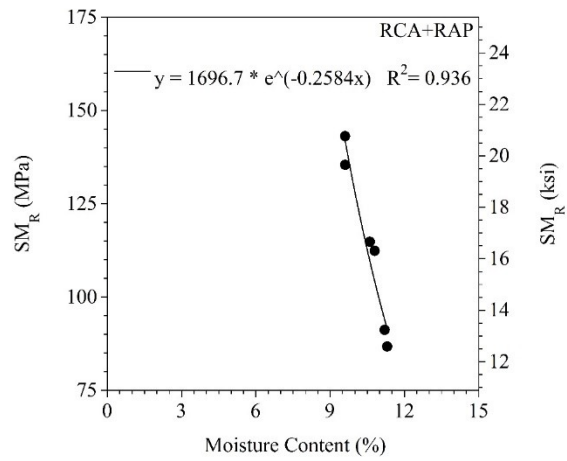
For Fine RCA:



For Limestone:



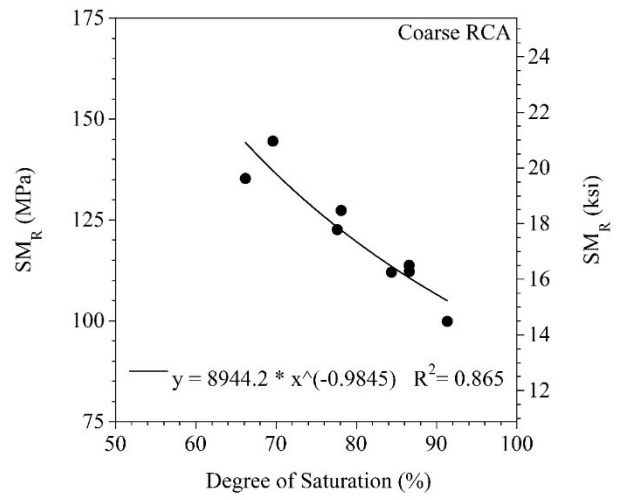
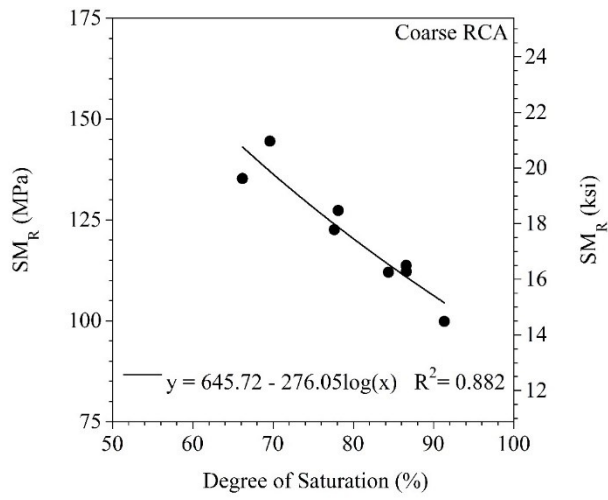
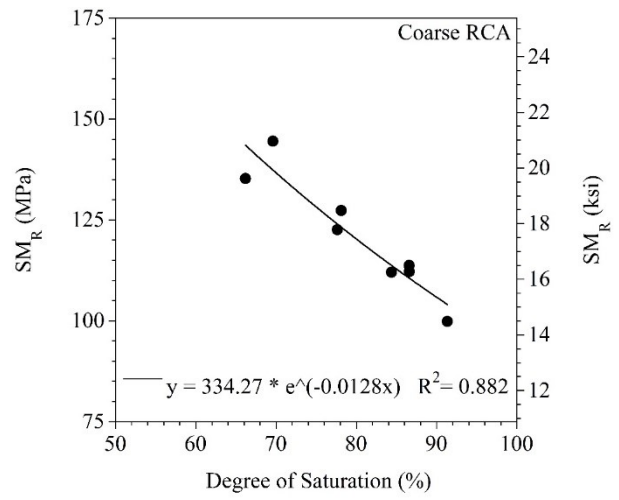
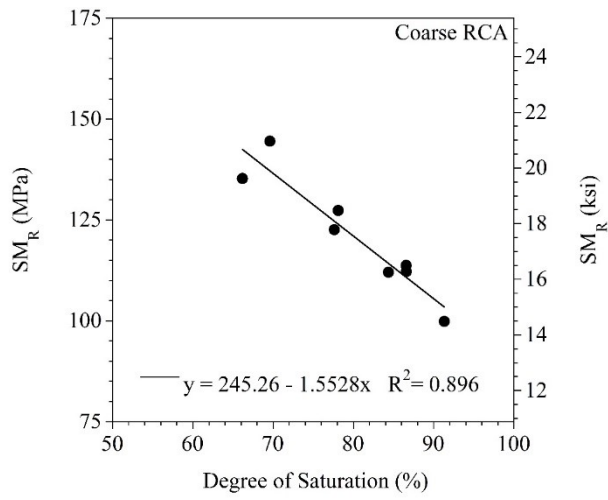
For RCA+RAP:



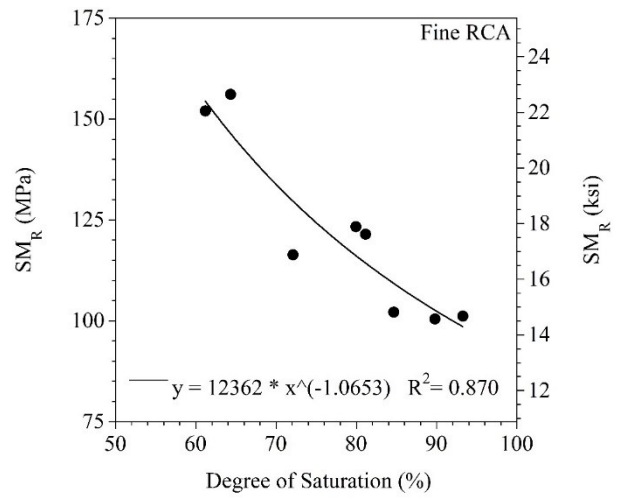
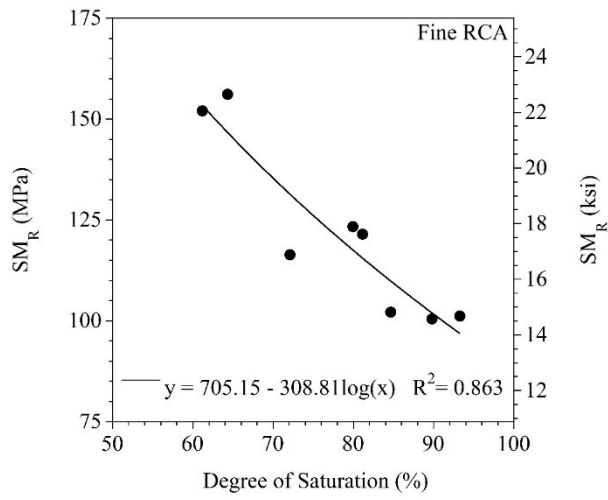
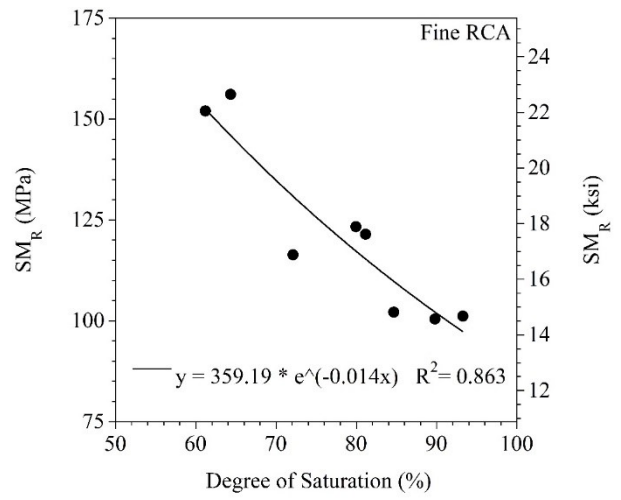
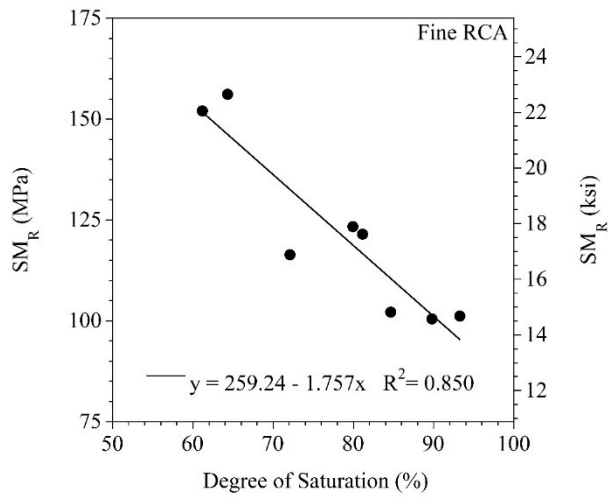
APPENDIX AP

SUMMARY RESILIENT MODULUS (SM_R) VS. DEGREE OF SATURATION (DOS)

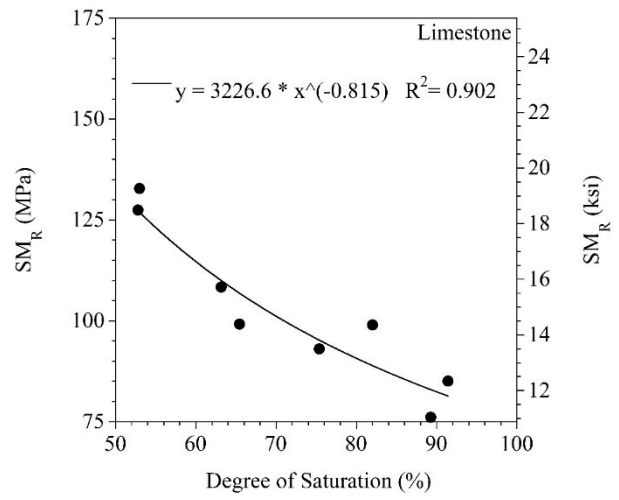
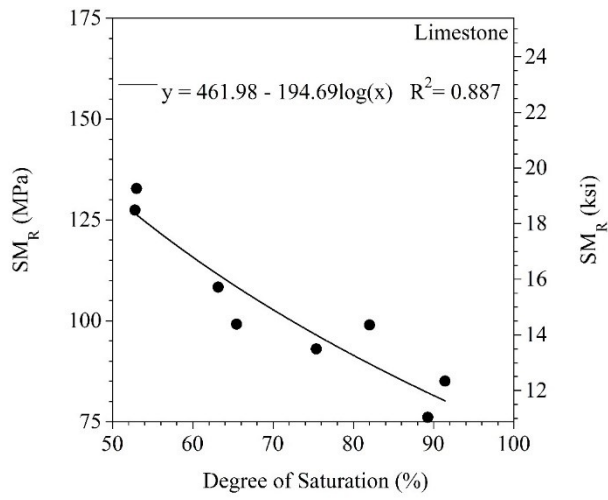
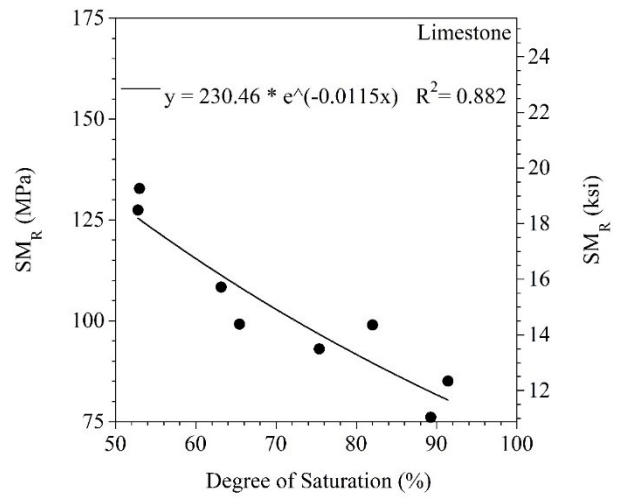
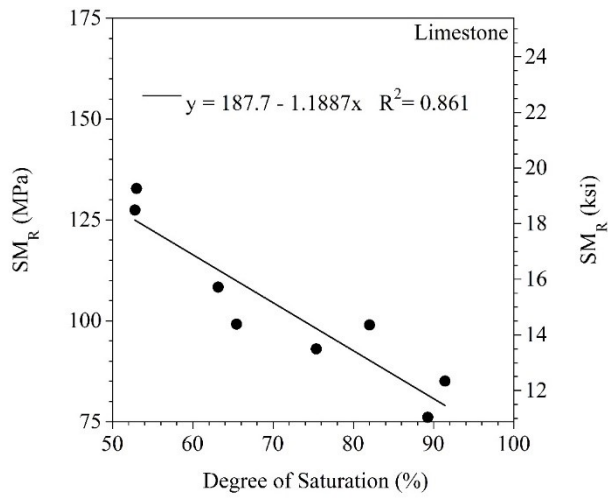
For Coarse RCA:



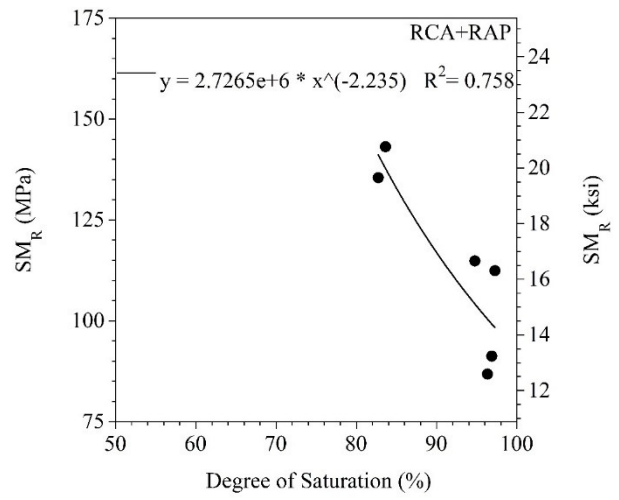
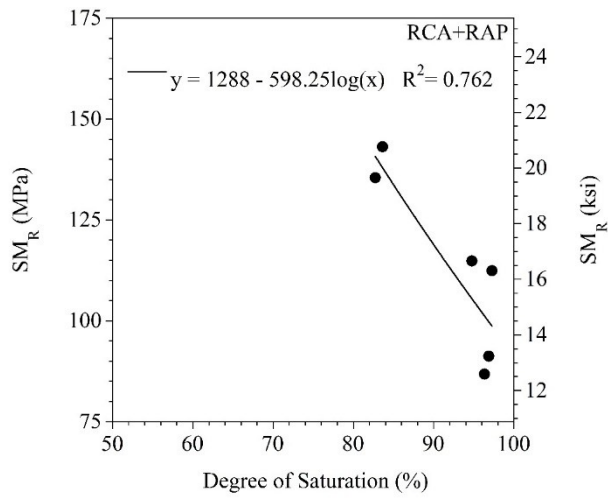
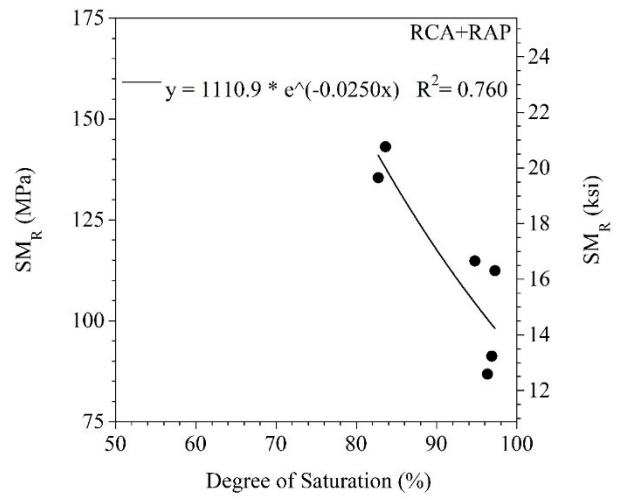
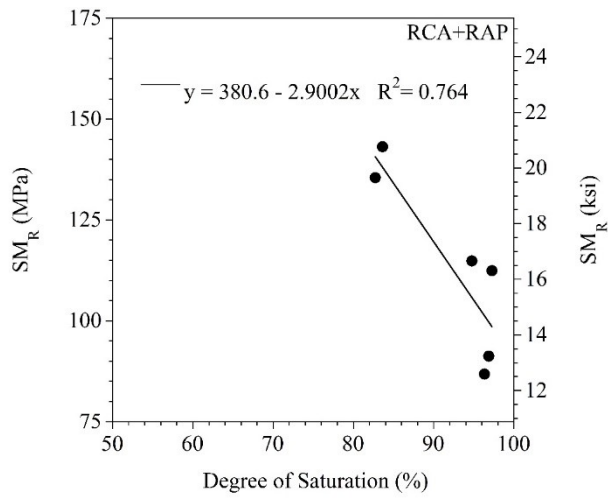
For Fine RCA:



For Limestone:



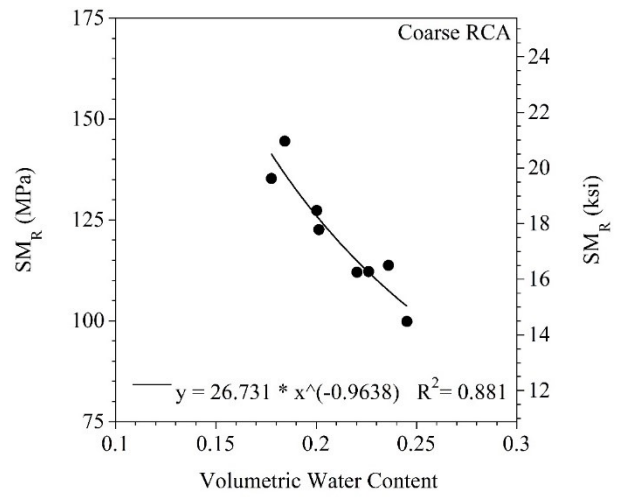
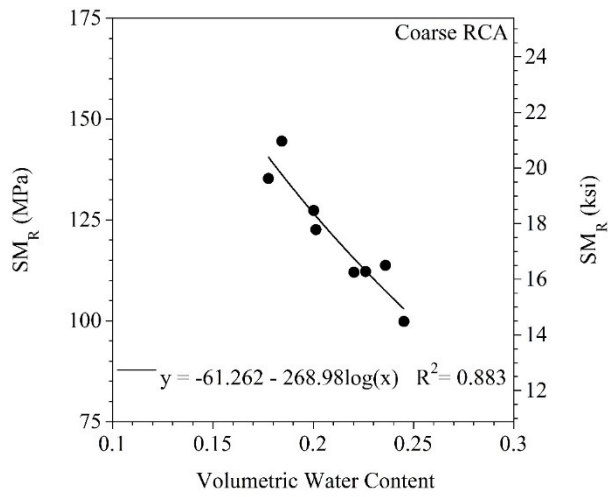
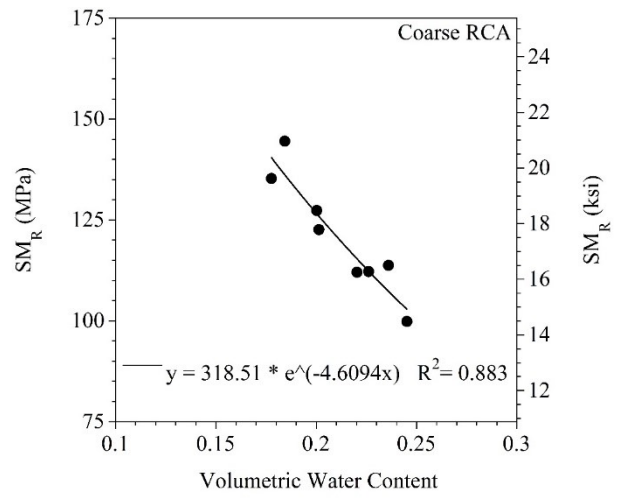
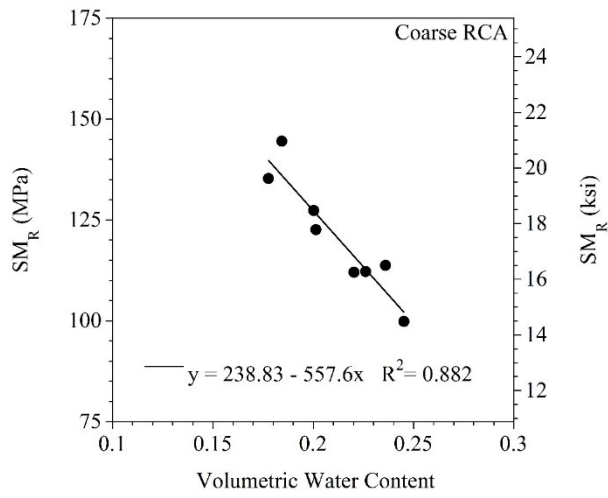
For RCA+RAP:



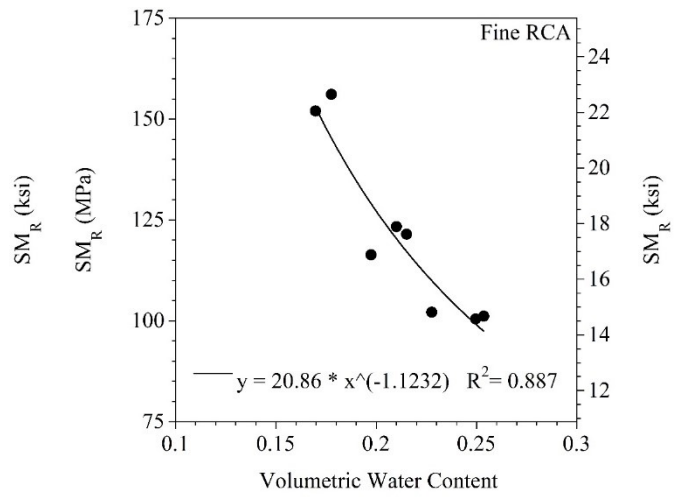
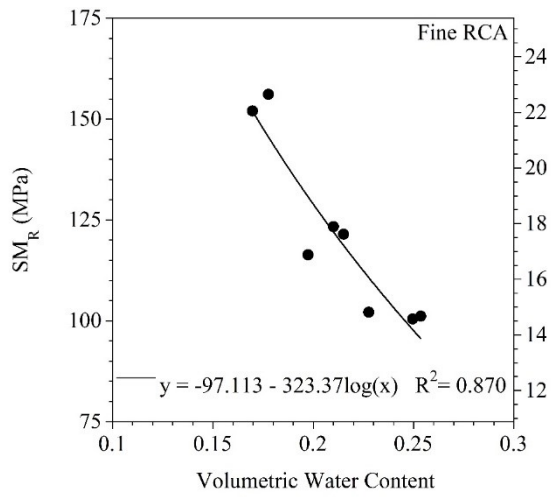
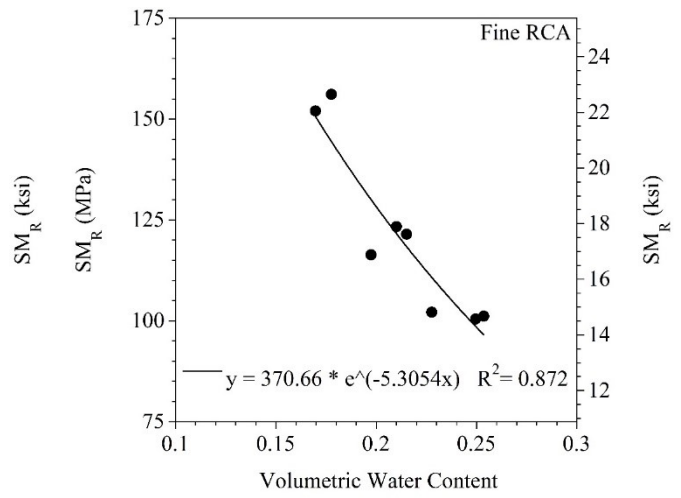
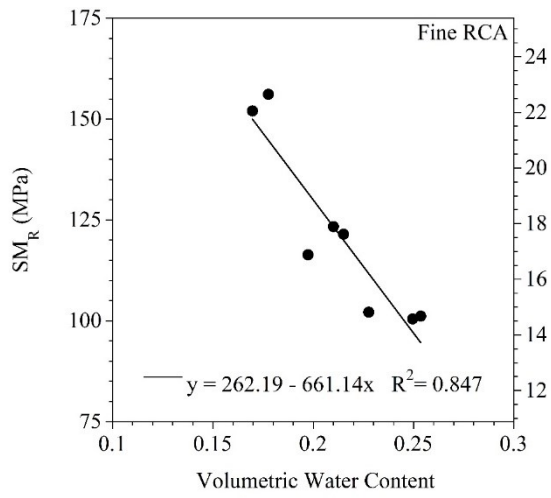
APPENDIX AQ

SUMMARY RESILIENT MODULUS (SM_R) VS. VOLUMETRIC WATER CONTENT (VWC)

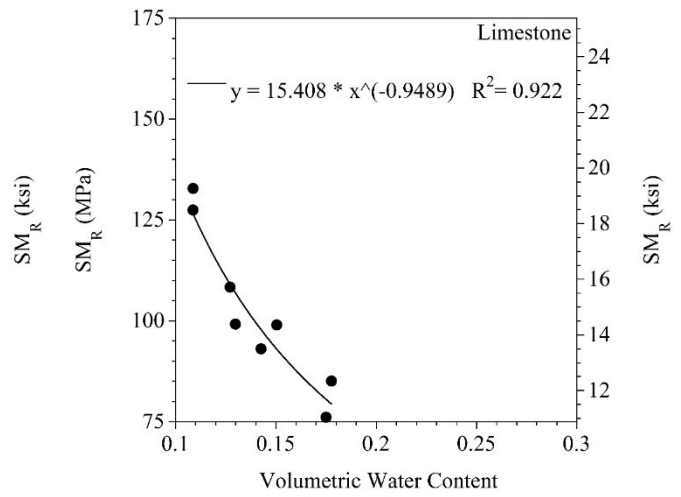
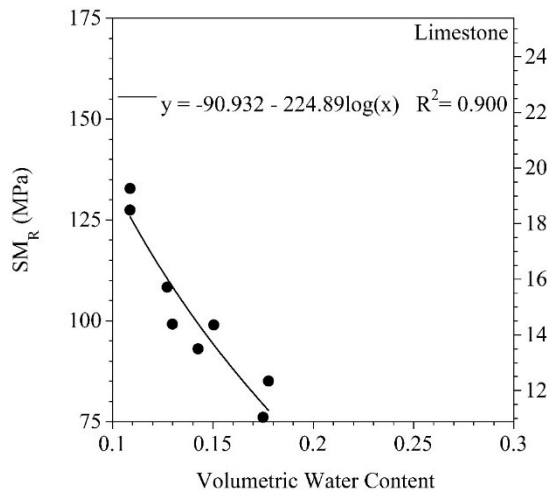
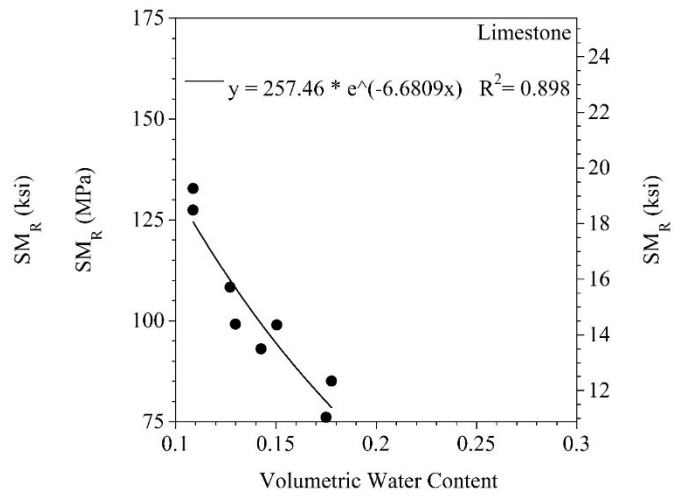
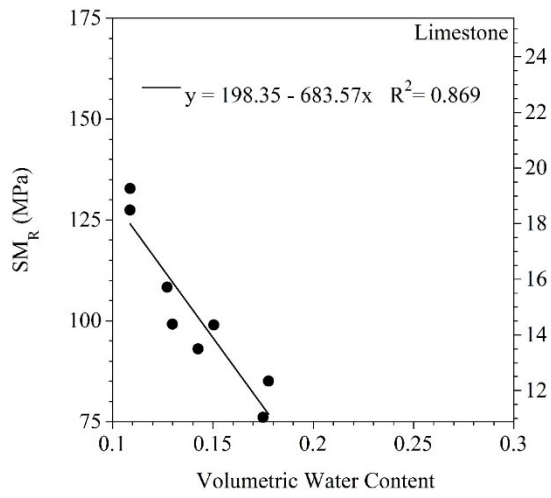
For Coarse RCA:



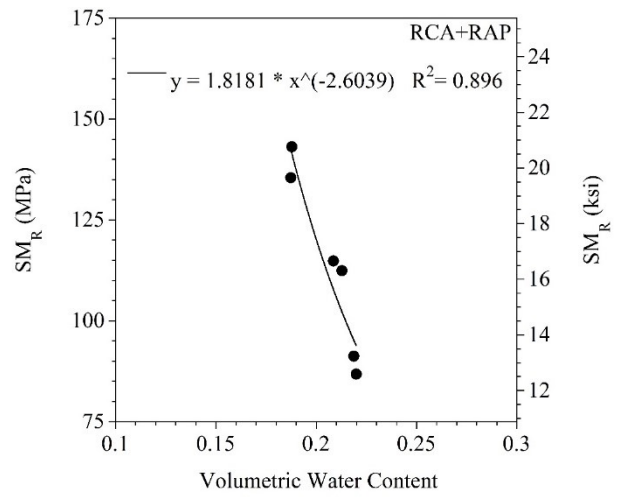
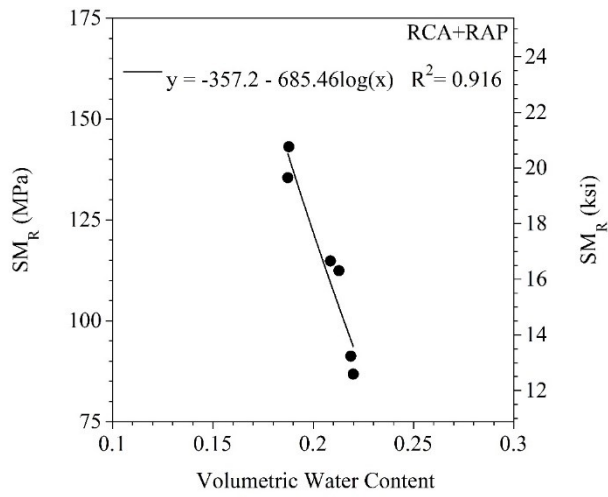
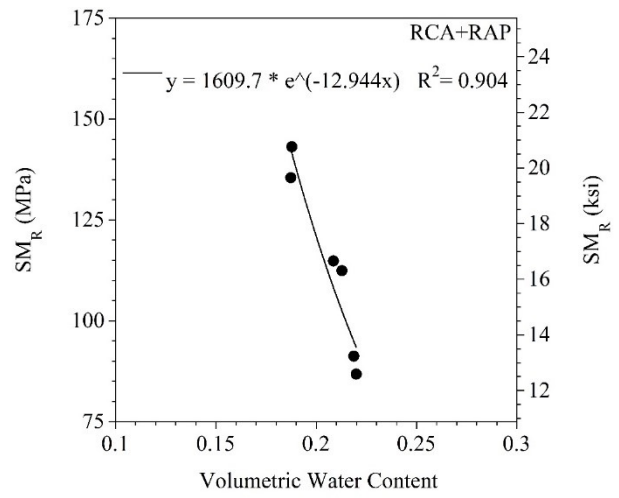
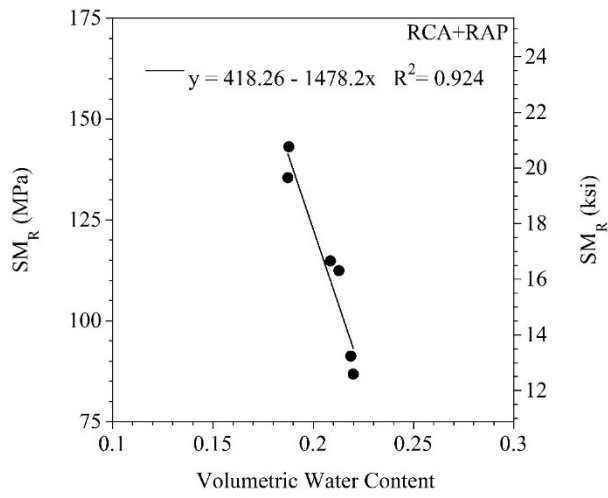
Fine RCA:



For Limestone:



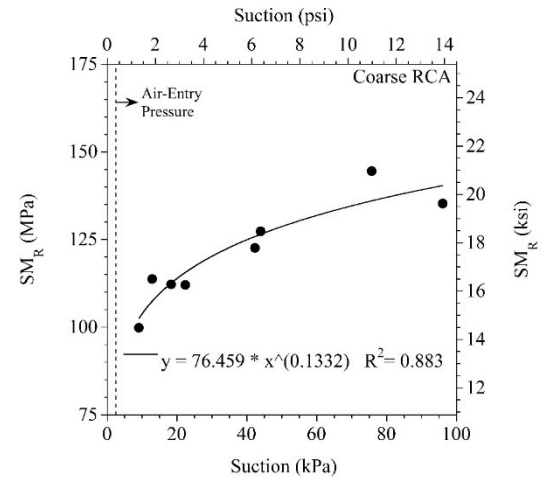
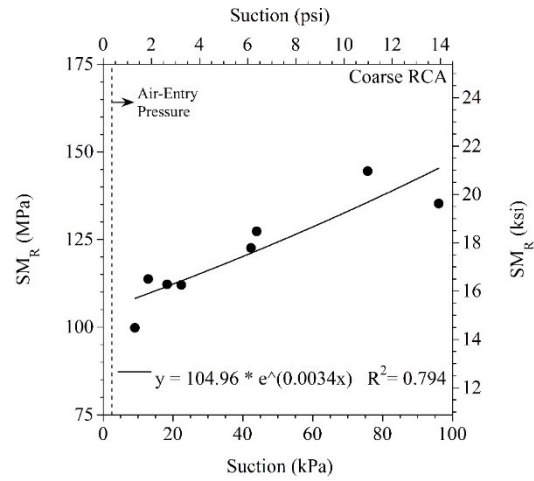
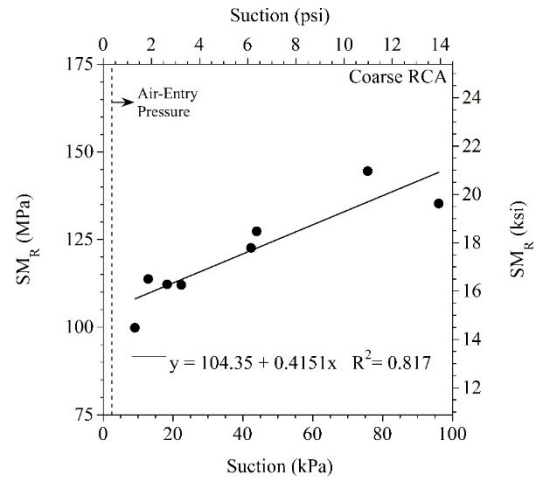
For RCA+RAP:



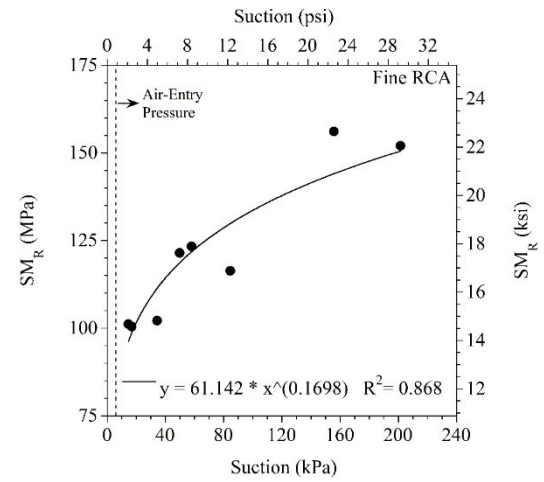
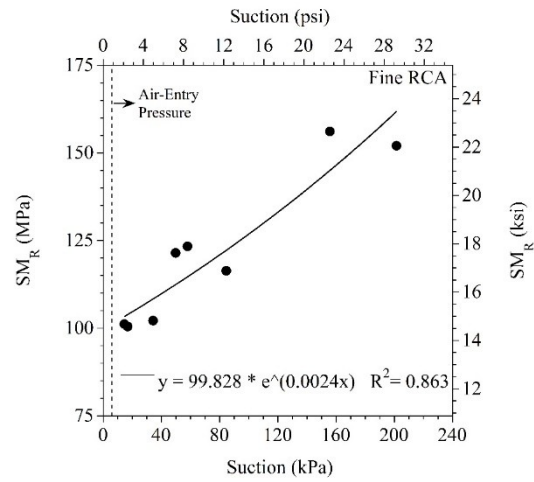
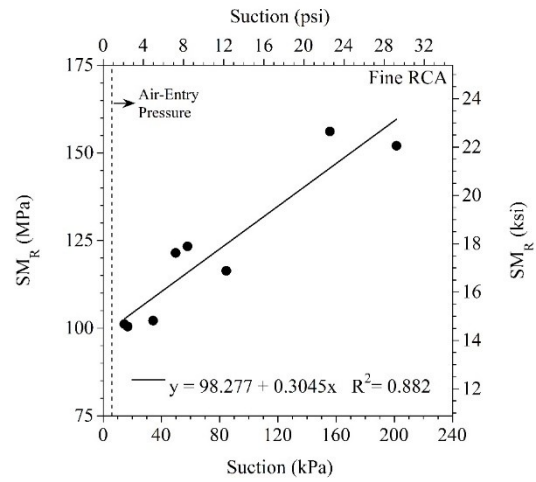
APPENDIX AR

SUMMARY RESILIENT MODULUS (SM_R) VS. MATRIC SUCTION

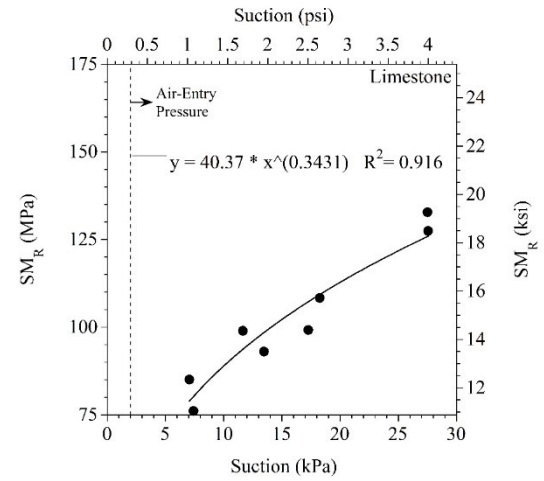
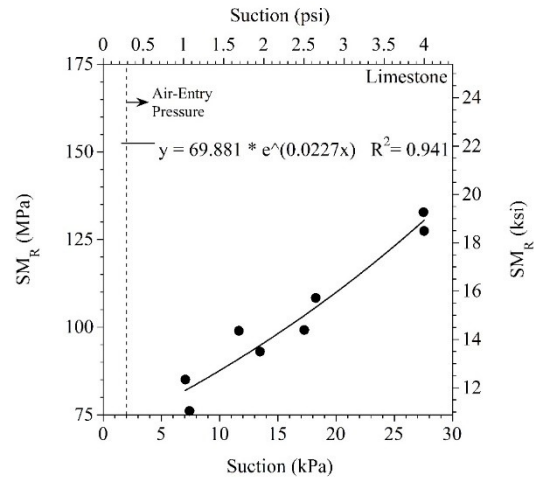
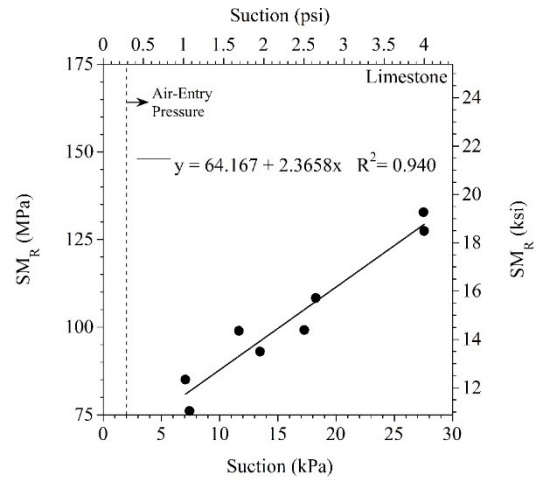
For Coarse RCA:



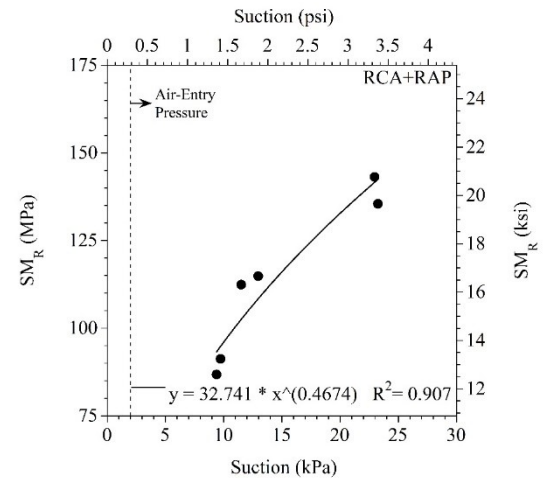
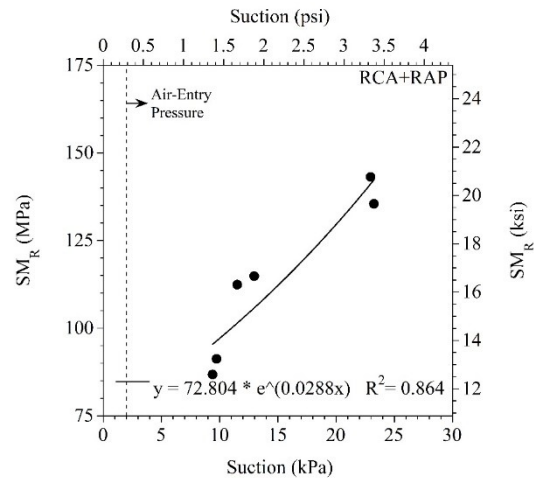
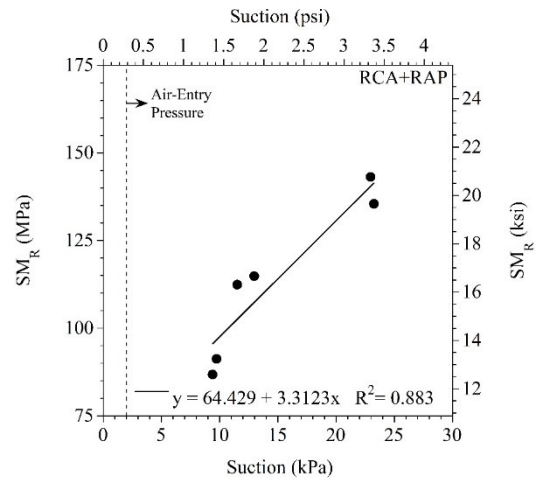
For Fine RCA:



For Limestone:



For RCA+RAP:



APPENDIX AS
ALTERNATIVE MODELS TO ESTIMATE SUMMARY RESILIENT
MODULUS (SM_R) AT OPTIMUM MOISTURE CONTENT (OMC)

Equation	R ²	Adj. R ²	Std. Error
-8.5917*Uncorrected MDU (kN/m ³) + 3.0558*PLR _{0.5} (%) + 257.3496	1	1	0.25
-209.7556*Coarse SSD G _s + 3.7592*PLR _{0.7} (%) + 407.9011	1	1	0.48
-68.7070*Combined OD G _s - 3.6657* PLS _{0.9} (%) + 601.7242	1	1	0.45
-56.4223*Combined OD G _s + 246.2814	0.91	0.86	4.89

MDU = maximum dry unit weight; SSD = saturated-surface-dry; OD = oven-dry; G_s = specific gravity; PLR_{0.5} = percent less rounded than 0.5; PLR_{0.7} = percent less rounded than 0.7; PLS_{0.9} = percent less spherical than 0.9

APPENDIX AT
REASSESSMENT OF MODELS PROVIDED IN EDIL ET AL. (2012)

Index properties, compaction characteristics, and summary resilient modulus (SRM) values based on power function [Equation (AT1)] for the materials used in Edil et al. (2012) are shown in Table AT1, Table AT2, and Table AT3, respectively. The empirical correlations reported by Edil (2012) were reevaluated.

Table AT1. Index properties of the materials (Edil et al. 2012)

Material	States	D ₁₀ (mm)	D ₃₀ (mm)	D ₅₀ (mm)	D ₆₀ (mm)	C _u	C _c	G _s	Absorption (%)	Asphalt Content /Mortar Content (%)	Impurities (%)	Gravel (%)	Sand (%)	Fines (%)	USCS	AASHTO
Class 5 Aggregate	MN	0.1	0.4	1.0	1.7	21	1.4	2.57	—	—	0.25	22.9	67.6	9.5	GW-GM	A-1-b
Blend	MN	0.2	0.6	1.5	2.8	13	0.5	—	—	—	0.36	32.7	63.8	3.4	SP	A-1-b
RCA	MN	0.1	0.4	1.0	1.7	21	1.4	2.39	5.0	55	0.87	31.8	64.9	3.3	SW	A-1-a
	MI	0.4	4.1	9.7	12.3	35	3.9	2.37	5.4	—	0.35	68.5	28.3	3.2	GP	A-1-a
	CO	0.1	0.6	2.8	4.9	66	1.1	2.28	5.8	47	0.26	40.9	46.3	12.8	SC	A-1-b
	CA	0.3	1.7	4.8	6.8	22	1.4	2.32	5.0	37	0.26	50.6	47.1	2.3	GW	A-1-a
	TX	0.4	6.5	13.3	16.3	38	6.0	2.27	5.5	45	0.86	76.3	21.6	2.1	GW	A-1-a
	OH	0.2	1.2	3.4	5.3	34	1.7	2.24	6.5	65	0.16	43.2	49.5	7.3	SW-SM	A-1-a
	NJ	0.2	0.5	2.0	5.1	28	0.3	2.31	5.4	—	1.67	41.2	54.6	4.3	SP	A-1-b
RAP	MN	0.3	0.7	1.6	2.3	7	0.7	2.41	1.8	7.1	0.06	26.3	71.2	2.5	SP	A-1-a
	CO	0.4	0.9	2.2	3.3	9	0.7	2.23	3.0	5.9	0.09	31.7	67.7	0.7	SP	A-1-a
	CA	0.3	1.3	3.0	4.2	13	1.2	2.56	2.0	5.7	0.33	36.8	61.4	1.8	SW	A-1-a
	TX	0.7	2.5	5.4	7.9	11	1.1	2.34	1.3	4.7	0.05	41.0	44.9	1.0	SW	A-1-a
	OH	0.5	1.6	2.9	3.8	7	1.3	2.43	0.6	6.2	0.06	32.1	66.2	1.7	SW	A-1-a
	NJ	1.0	2.8	4.9	5.9	6	1.3	2.37	2.1	5.2	0.48	50.9	48.4	0.7	GW	A-1-a
	WI	0.6	1.4	2.7	3.6	6	0.9	2.37	1.5	6.2	0.08	30.9	68.5	0.5	SP	A-1-b
RPM	NJ	0.5	2.1	5.8	8.7	18	1.0	2.35	2.6	4.3	0.04	55.7	43.6	0.6	GW	A-1-b
	MI	0.4	1.7	4.6	6.5	17	1.1	2.39	1.7	5.3	0.13	49.3	50.4	0.4	SW	A-1-b

D₁₀ = effective size; D₃₀ = particle size for 30% finer; D₅₀ = median particle size; D₆₀ = particle size for 60% finer; C_u = coefficient of uniformity; C_c = coefficient of curvature; G_s = specific gravity; USCS = unified soil classification system; AASHTO: the American Association of State Highway and Transportation Officials

Note 1: Asphalt content determined for RAP/RPM and mortar content determined for available RCA. RPM was a recycled pavement material that included HMA and base layer aggregate and possibly some subgrade soil like in full-depth reclamation.

Note 2: Particle size analysis conducted following ASTM D 422, G_s determined by ASTM D 854, Absorption of coarse aggregate were determined by ASTM C127-07, USCS classification determined by ASTM D 2487, AASHTO classification determined by ASTM D 3282, asphalt content determined by ASTM D 6307

Note 3: Blend consists of 50% RCA (MN) and 50% Class 5 aggregate obtained at MNROAD field site

Table AT2. Maximum dry unit weight and optimum water content of the materials (Edil et al. (2012))

Specimens	States	Optimum Water Content W_{opt} (%)	Maximum Dry Unit Weight γ_{dmax} (kN/m ³)
Class 5 Aggregate	MN	8.9	20.1
Blend*	MN	8	21.3
RCA	MN	11.2	19.5
	MI	8.7	20.8
	CO	11.9	18.9
	CA	10.4	19.9
	TX	9.2	19.7
	OH	11.8	19.4
	NJ	9.5	19.8
RAP	MN	6.7	20.8
	CO	5.7	20.7
	CA	6.1	20.7
	TX	8	20.3
	OH	8.8	19.8
	NJ	6.5	20.4
	WI	7.3	20
RPM	MI	5.2	21.5
	NJ	6.3	20.6

Note: Blend consists of 50% RCA (MN) and 50% Class 5 aggregate obtained at MNROAD field site

Table AT3. Summary resilient modulus (SRM), power function model fitting parameters k_1 and k_2 , and plastic strain [based on Equation (AT1)] (Edil et al. 2012)

Material	States	External			Internal			Plastic Strain (%)	SRM _{INT} /SRM _{EXT}
		k_1	k_2	SRM (MPa)	k_1	k_2	SRM(MPa)		
Class 5 Aggregate	MN	14.9	0.43	152	43.2	0.47	525	1.60	3.5
Blend*	MN	18.2	0.43	182	50.2	0.49	675	1.05	3.7
RCA	MN	18.5	0.44	189	38.3	0.54	680	0.63	3.6
	MI	14.3	0.46	171	40.7	0.54	715	0.80	4.2
	CO	17.4	0.43	175	41.5	0.49	580	0.73	3.3
	CA	15.2	0.46	178	33.0	0.54	627	0.70	3.5
	TX	9.1	0.54	164	17.6	0.64	549	0.83	3.3
	OH	12.6	0.48	163	27.7	0.56	554	0.57	3.4
	NJ	22.0	0.42	208	49.6	0.50	735	0.55	3.5
RAP	MN	23.0	0.39	180	26.3	0.61	674	1.35	3.7
	CO	25.6	0.37	184	75.0	0.41	673	1.47	3.7
	CA	12.3	0.49	173	36.4	0.53	627	1.16	3.6
	TX	21.6	0.42	198	52.4	0.52	776	1.38	3.9
	OH	15.6	0.48	197	42.7	0.52	699	1.32	3.6
	NJ	23.5	0.41	209	54.6	0.48	715	2.13	3.4
	WI	29.5	0.41	266	65.0	0.51	968	0.89	3.6
RPM	MI	14.7	0.46	168	43.5	0.50	631	1.49	3.8
	NJ	26.3	0.43	264	61.6	0.52	989	1.26	3.8

Note: Plastic strains were determined for base materials from M_R testing by using the measured permanent deformations from the internal LVDTs with the power function model. Plastic strains were calculated as the sum of the plastic strains for each loading sequence during resilient modulus test by excluding the plastic strains in the conditioning phase (Sequence 1).

The power function model proposed by Moossazedh and Witczak (1981):

$$M_R = k_1 \theta^{k_2} \quad (\text{AT1})$$

where M_R is the resilient modulus, θ is the bulk stress, and k_1 and k_2 are empirical fitting parameters.

In Edil et al. (2012), based on the index properties (Table AT1) and compaction characteristics (Table AT2) of the materials, the forward stepwise regression technique was performed by using multiple linear regressions to develop correlations (models) to predict the compaction characteristics of RCA and RAP based on their gradation characteristics (Table AT4). A significance level of 0.05 [or alpha (α) = 0.05], which gives 95% confidence, was used to determine whether the model is statistically significant. In Edil et al. (2012), it was stated that all the independent variables used in the models shown in Table AT4 had p-values smaller than 0.05, which showed the statistical significance of those variables. As can be seen in Table AT4, for both RCA and RAP materials, W_{opt} was a function of C_u and absorption. In addition, γ_{dmax} was a function of W_{opt} .

Table AT4. Equations to estimate optimum moisture content (W_{opt}) and maximum dry unit weight (γ_{dmax}) of the materials (Edil et al. 2012)

Materials	Compaction Characteristics	Correlation Equations	R^2
RCA	W_{opt} (%)	$-0.064 * C_u + 0.763 * Absorption(\%) + 7.75$	0.65
	γ_{dmax} (kN/m ³)	$-0.374 * W_{opt}(\%) + 23.6$	0.83
RAP	W_{opt} (%)	$-0.0626 * C_u - 1.349 * Absorption(\%) + 9.84$	0.92
	γ_{dmax} (kN/m ³)	$-0.289 * W_{opt}(\%) + 22.42$	0.83

W_{opt} = optimum moisture content; γ_{dmax} = maximum dry unit weight; C_u = coefficient of uniformity

An effort was made to reassess the equations given in Table AT4 using the data generated in Edil et al. (2012). First, the actual (based on the laboratory test results) and estimated (based on the equations given in Table AT4) W_{opt} and γ_{dmax} values were compared. Figure AT1 shows the actual W_{opt} vs. predicted W_{opt} for RCA and RAP. Figure AT2 shows the actual γ_{dmax} vs. predicted γ_{dmax} for RCA and RAP. Based on Figure AT1 and Figure AT2, it was observed that while the models for W_{opt} of RAP and γ_{dmax} of RCA and RAP were somewhat successful, the W_{opt} model of RCA was not satisfactory.

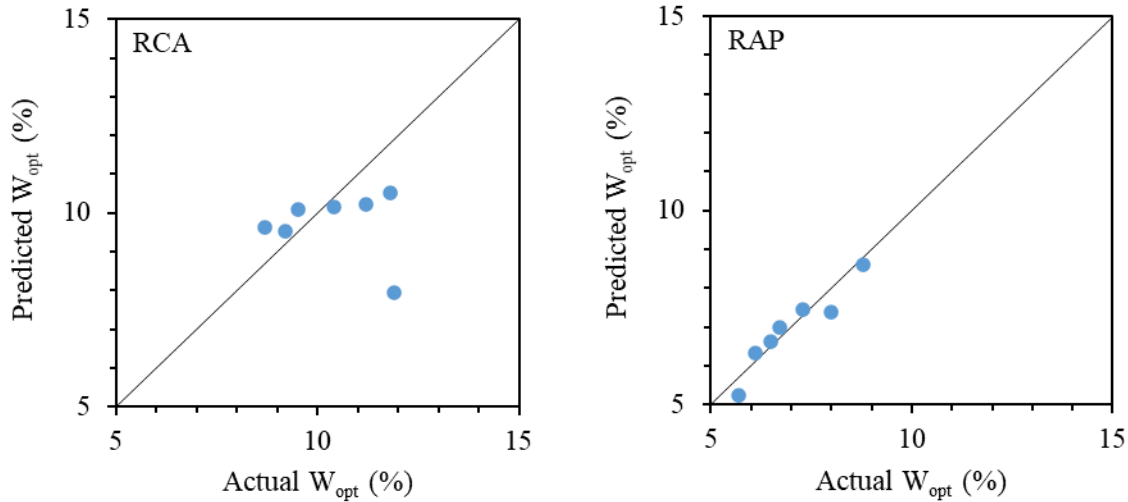


Figure AT1. Actual W_{opt} vs. predicted W_{opt} for RCA (left) and RAP (right)

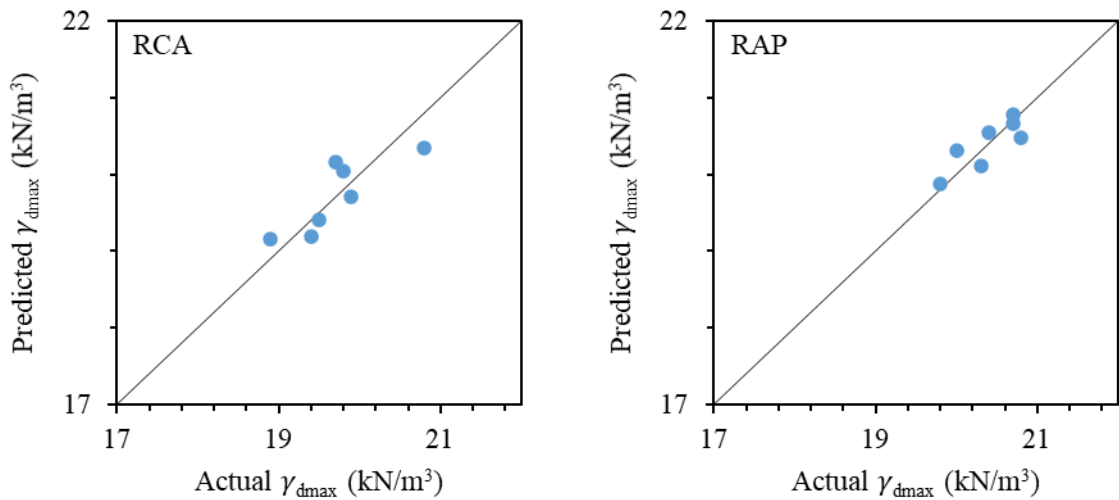


Figure AT2. Actual γ_{dmax} vs. predicted γ_{dmax} for RCA (left) and RAP (right)

The data generated by Edil et al (2012) were used to develop models that were the most convenient with statistical significance. To do so, forward stepwise regression technique, described previously, was used by considering all the parameters shown in Table AT1 and Table AT2, and new models were established.

Table AT5 summarizes the new equations to estimate W_{opt} . According to Table AT4, W_{opt} was a function of C_u and absorption for both RCA and RAP materials. However, as can be seen from Table AT5, there was no equation that contained both C_u and absorption parameters. For RCA, neither C_u nor absorption was statistically significant (Table AT5). For RAP, while absorption was statistically significant, C_u was insignificant. The combination of G_s and absorption was found to be statistically significant for RAP materials. In addition to separate regression analyses for RCA and RAP materials, these materials were combined with each other and with class 5 aggregate to establish more models (Table AT5).

Table AT6 summarizes the new equations to estimate γ_{dmax} . According to Table AT4, γ_{dmax} was a function of W_{opt} for both RCA and RAP. As can be seen from Table AT6, both equations shown in Table AT4 were statistically significant. In Table AT4, the R^2 values of both models were reported as 0.83. However, after reassessing the reported equations, it was found that multiple R values, which were 0.83, were reported instead of R^2 values. According to Table AT6, the correct R^2 values were 0.690 and 0.694 for RCA and RAP, respectively. In addition to separate regression analyses for RCA and RAP materials, these materials were combined with each other and with class 5 aggregate to establish more models (Table AT6).

Table AT5. New equations to estimate optimum moisture content (W_{opt}) (%) of the materials

Material	Equation	R^2	Adj. R^2	Std. Error
RCA	$-8.2941 \cdot D_{10} \text{ (mm)} + 12.4000$	0.67	0.6	0.81
RAP	$-1.3891 \cdot \text{Absorption (\%)} + 9.4552$	0.9	0.88	0.38
	$-1.5831 \cdot \text{Absorption (\%)} - 3.5587 \cdot G_s + 18.2910$	0.99	0.98	0.16
RCA and RAP	$0.7619 \cdot \text{Absorption (\%)} + 5.9300$	0.55	0.52	1.45
	$0.0889 \cdot C_u + 6.7750$	0.54	0.5	1.48
	$0.4642 \cdot \text{Fines (\%)} + 7.2345$	0.54	0.5	1.48
	$\#0.0769 \cdot \text{Mortar Content (\%)} + 7.0368$	0.81	0.79	1.04
RCA, RAP, and Class 5	$\#0.0725 \cdot \text{Mortar Content (\%)} + 7.2647$	0.76	0.73	1.12
	$\#0.0598 \cdot \text{Mortar Content (\%)} + 0.1864 \cdot \text{Fines (\%)} + 6.8460$	0.84	0.81	0.94
RCA and Class 5	$\#0.0482 \cdot \text{Mortar Content (\%)} - 0.3237 \cdot D_{30} \text{ (mm)} + 9.1488$	0.92	0.86	0.49
	$\#0.0472 \cdot \text{Mortar Content (\%)} - 0.4115 \cdot C_c + 9.5007$	0.93	0.88	0.44

#RCA-MI and RCA-NJ materials were removed because their mortar contents were not reported

Table AT6. New equations to estimate maximum dry unit weight (γ_{dmax}) (kN/m³) of the materials

Material	Equation	R^2	Adj. R^2	Std. Error
RCA	$-0.3743 \cdot W_{opt} \text{ (\%)} + 23.6015$	0.69	0.63	0.35
	$3.4559 \cdot D_{10} \text{ (mm)} + 18.8750$	0.57	0.49	0.42
RAP	$-0.2900 \cdot W_{opt} \text{ (\%)} + 22.4195$	0.69	0.63	0.23
	$0.4714 \cdot \text{Absorption (\%)} + 0.2977 \cdot \text{Fines (\%)} + 19.1788$	0.90	0.85	0.15
RCA and RAP	$-0.2413 \cdot W_{opt} \text{ (\%)} + 22.1494$	0.74	0.72	0.31
	$\#-0.0179 \cdot \text{Mortar Content (\%)} + 20.3795$	0.64	0.61	0.37
RCA, RAP, and Class 5	$-0.2410 \cdot W_{opt} \text{ (\%)} + 22.1531$	0.74	0.72	0.30
	$\#-0.0172 \cdot \text{Mortar Content (\%)} + 20.3453$	0.62	0.59	0.36
RCA and Class 5	$-0.3557 \cdot W_{opt} \text{ (\%)} + 23.3907$	0.70	0.65	0.33

#RCA-MI and RCA-NJ materials were removed because their mortar contents were not reported

In Edil et al. (2012), based on the index properties (Table AT1), compaction characteristics (Table AT2), and SRM values (based on power function) of the materials, the forward stepwise regression technique was performed by using multiple linear regressions to develop correlations (models) to predict the SRM values (based on power function) (Table AT3). A significance level of 0.05 [or alpha (α) = 0.05], which

gives 95% confidence, was used to determine whether the model is statistically significant. In Edil et al. (2012), it was stated that all the independent variables used in the models shown in Table AT7 had p-values smaller than 0.05, which showed the statistical significance of those variables.

Table AT7. Equations to estimate the summary resilient modulus (SRM) of the materials determined by the power function model (Edil et al. 2012)

Materials	Summary Resilient Modulus (SRM) (Mpa)	Correlation Equations	R ²
RCA	SMR _{EXT}	$171.646 - (3.482 * D_{30}) + (22.378 * \text{Impurities } \%)$	0.89
	SMR _{INT}	$14683.478 - (36.764 * D_{30}) - (72.719 * W_{opt})$	0.89
RAP	SMR _{EXT}	$(117.493 * D_{30}) + (19.472 * \gamma_{dmax} + (27.128 * \text{Asphalt Content}(\%)) - (18.510 * \text{Absorption}(\%)) - 427.329$	0.99
	SMR _{INT}	$(-2268.783) - (285.884 * \text{Fines } \%) + (628.742 * \text{Asphalt content } (\%)) + (201.107 * D_{60}) - (483.158 * G_s) - (58.243 * \text{Absorption } (\%))$	0.99

D₃₀ = particle size for 30% finer; W_{opt} = optimum moisture content; γ_{dmax} = maximum dry unit weight; G_s = specific gravity

An effort was made to reassess the equations given in Table AT7. First, the actual (based on the laboratory test results) and estimated (based on the equations given in Table AT7) SM_R values were compared. Figure AT3 shows the actual SRM based on external linear variable differential transformer (LVDT) (SRM_{EXT}) vs. predicted SRM_{EXT} for RCA and RAP. Figure AT4 shows the actual SRM based on internal linear LVDT (SRM_{INT}) vs. predicted SRM_{INT} for RCA and RAP. Based on Figure AT3 and Figure AT4, it was observed that while the models for RCA were somewhat successful, the models for RAP was not satisfactory.

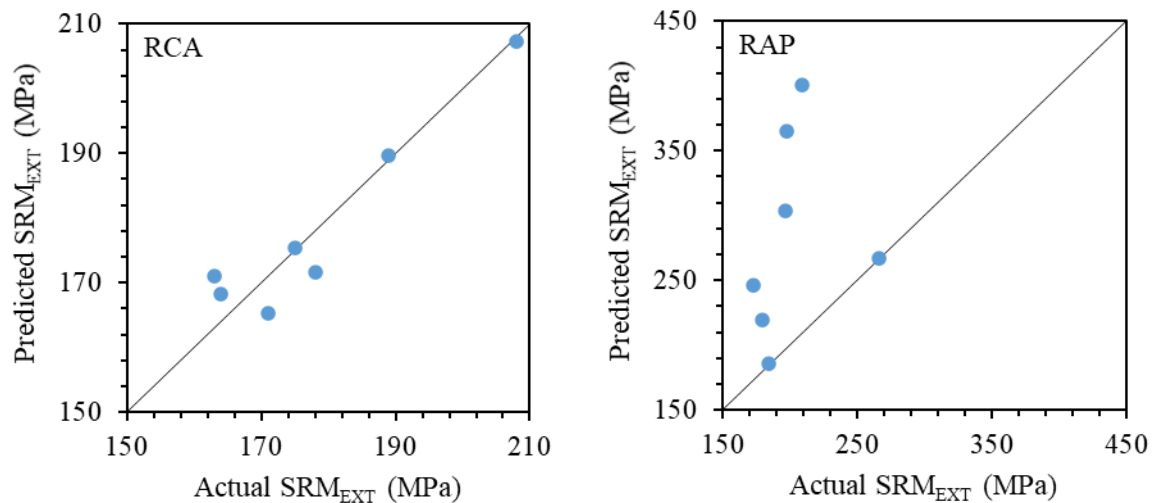


Figure AT3. Actual SRM_{EXT} vs. predicted SRM_{EXT} for RCA (left) and RAP (right)

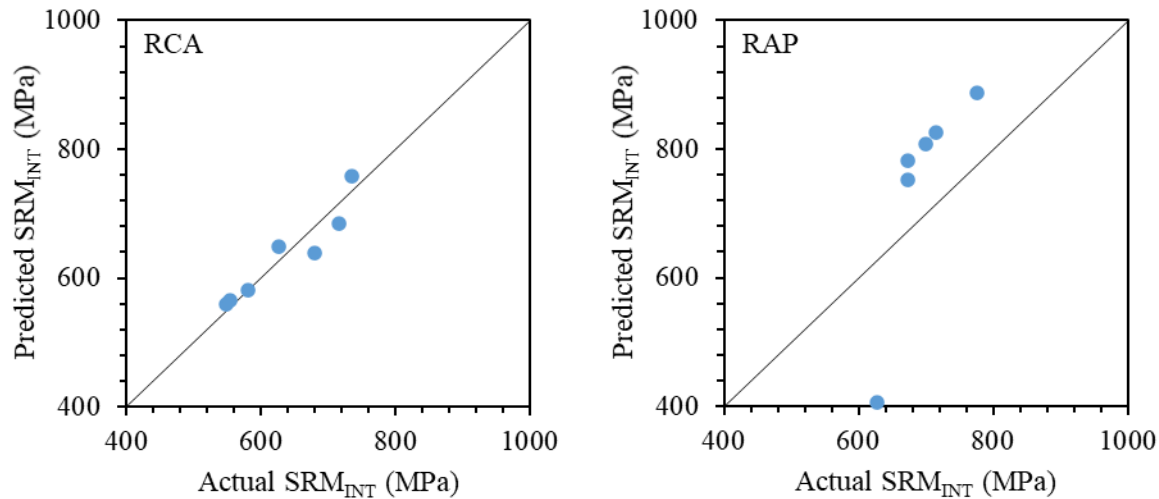


Figure AT4. Actual SRM_{INT} vs. predicted SRM_{INT} for RCA (left) and RAP (right)

The data generated by Edil et al (2012) were used to develop models that are the most convenient with statistical significance. The forward stepwise regression method was performed by using multiple linear regressions to develop correlations (models) to predict the SRM values (based on power function) (Table AT3).

Table AT8 summarizes the new equations to estimate SRM_{EXT}. According to Table AT7, the SRM_{EXT} of RCA materials was a function of D_{30} and impurities. As can be seen from Table AT8, both D_{30} and impurities were statistically significant for SRM_{EXT} of RCA. In addition, Table AT8 shows that not only D_{30} but also C_c can be used in combination with impurities to estimate SRM_{EXT} of RCA. While Table AT7 shows a complex equation to estimate SRM_{EXT} of RAP, reassessment of the laboratory data revealed that none of those parameters was statistically significant. Therefore, no statistically significant equation could be found for SRM_{EXT} of RAP. In addition to the separate regression analyses for RCA and RAP materials, these materials were combined with each other and with class 5 aggregate to establish more models. Among the combinations, only the combination of RCA and class 5 aggregate provided an equation (Table AT8).

Table AT9 summarizes the new equations to estimate SRM_{INT}. According to Table AT7, the SRM_{INT} of RCA materials was a function of D_{30} and W_{opt} . As can be seen from Table AT9, both D_{30} and W_{opt} were statistically significant for SRM_{INT} of RCA. In addition, Table AT9 shows that G_s can also be used to estimate SRM_{INT} of RCA. While Table AT7 shows a complex equation to estimate SRM_{INT} of RAP, reassessment of the laboratory data revealed that none of those parameters had a statistical significance. Thus, any equation, which are statistically significant, could not be found for SRM_{INT} of RAP. In addition to the separate regression analyses for RCA and RAP materials, these materials were combined with each other and with class 5 aggregate to establish more models. However, no statistically significant equations could be found for the combinations (Table AT9).

Table AT8. New equations to estimate SRM_{EXT} (MPa) of the materials

Material	Equation	R^2	Adj. R^2	Std. Error
RCA	$23.0770 * \text{Impurities (\%)} + 163.6812$	0.63	0.55	10.58
	$21.0281 * \text{Impurities (\%)} - 4.3410 * C_c + 174.7761$	0.92	0.88	5.5
	$22.0836 * \text{Impurities (\%)} - 3.5436 * D_{30} \text{ (mm)} + 171.9035$	0.89	0.84	6.31
RAP	No Equation			
RCA and RAP	No Equation			
RCA, RAP, and Class 5	No Equation			
RCA and Class 5	$28.1646 * \text{Impurities (\%)} + 159.6937$	0.62	0.55	11.6

C_c = coefficient of curvature

Table AT9. New equations to estimate SRM_{INT} (MPa) of the materials

Material	Equation	R^2	Adj. R^2	Std. Error
RCA	$1091.5850 * G_s - 1888.8350$	0.59	0.5	54.10
	$-36.8275 * D_{30} \text{ (mm)} - 72.9428 * W_{opt} \text{ (\%)} + 1470.7646$	0.89	0.83	31.37
RAP	No Equation			
RCA and RAP	No Equation			
RCA, RAP, and Class 5	No Equation			
RCA and Class 5	No Equation			

G_s = specific gravity; W_{opt} = optimum moisture content

APPENDIX AU
FIELD TEST RESULTS (DURING CONSTRUCTION) USED IN
FORWARD STEPWISE REGRESSION ANALYSES

Cell Number	Median NDG Moisture Content (%)	Median NDG Dry Unit Weight (kN/m ³)	Median Relative OMC (%)	Median Relative MDU (%)	Median DCPI (mm/blow)	Median CBR (%)	Median E _{LWD} (MPa)	Median E _{FWD} (MPa)	Median IC M _R at 69 kPa (MPa)	Median IC M _R at 207 kPa (MPa)
185	6.86	18.65	72.33	92.34	7.58	30.24	98.06	165.47	265.04	305.98
186	7.5	18.27	67.71	95.59	7.49	30.62	99.52	222.01	278.43	311.51
188	4.43	21.28	70.53	94.62	8.46	27.01	84.85	102.04	171.48	166.4
189	6.57	18.53	65.91	93.79	9.87	22.57	71.88	77.91	144.05	134.81
127	5.49	18.99	66.46	94.07	9	24.92	79.52	102.04	216.39	208.48
227	5.62	19.2	68.1	95.08	7	33.03	82.79	108.25	153.74	146.92
328	7.7	17.86	79.99	88.79	9.5	23.54	64.03	43.44	120.51	97.87
428	7.89	17.82	81.94	88.6	9	24.92	46.7	31.37	105.7	81.65
528	6.2	17.01	64.38	84.58	10.5	21.03	25.68	23.79	85.02	66.87
628	8.03	18.15	83.4	90.25	10.5	21.03	47.49	35.85	106.88	89.65
728	8.5	17.36	88.28	86.31	11	19.91	59.88	60.67	115.96	109.82

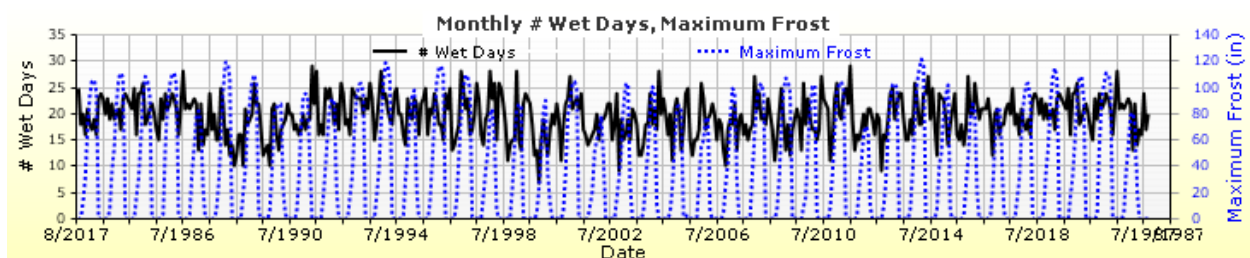
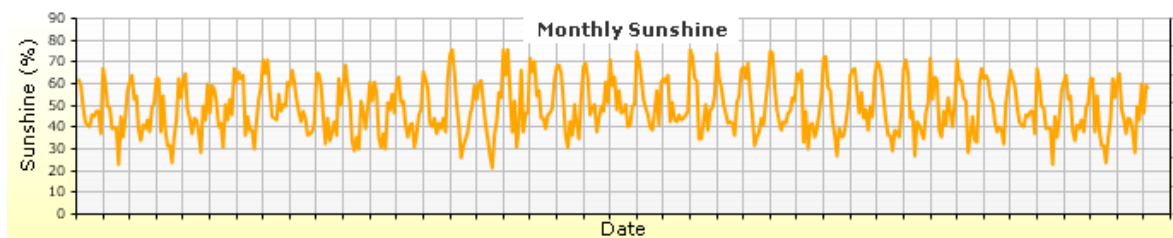
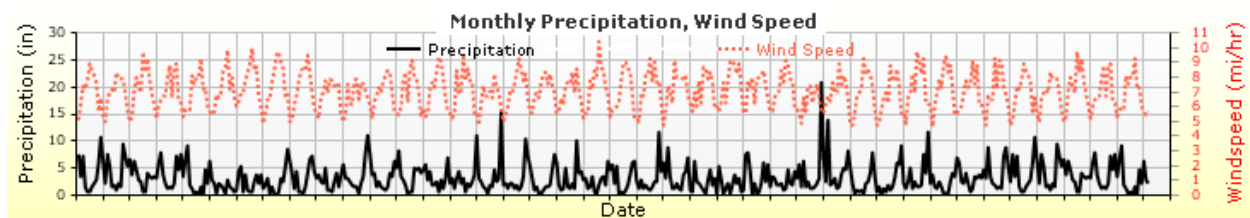
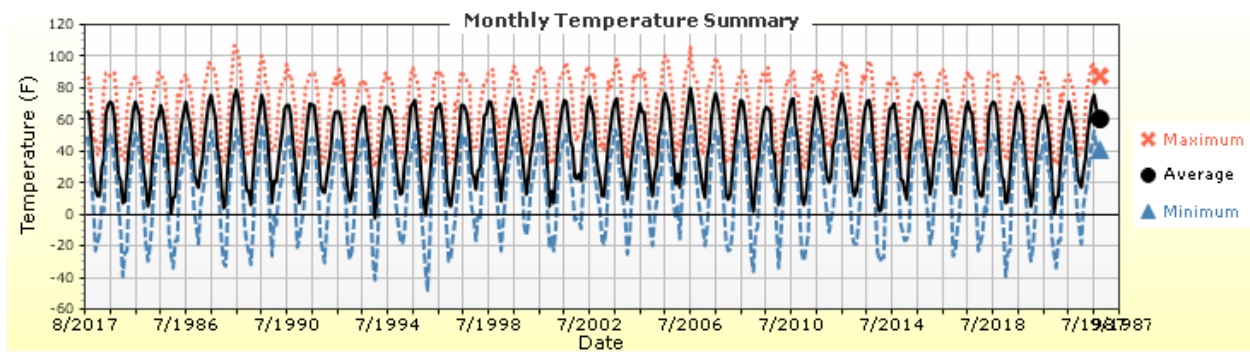
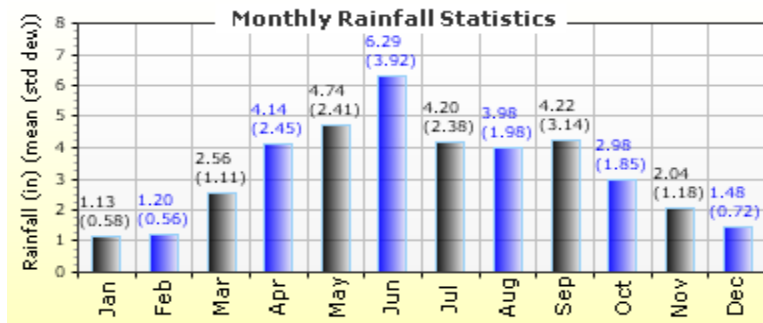
NDG = nuclear density gauge; OMC = optimum moisture content; MDU = maximum dry unit weight; DCPI = dynamic cone penetration (DCP) index; CBR = field California bearing ratio; E_{LWD} = light weight deflectometer (LWD) elastic modulus; E_{FWD} = falling weight deflectometer (FWD) elastic modulus; IC M_R = intelligent compaction resilient modulus

APPENDIX AV
ALTERNATIVE MODELS TO ESTIMATE INTELLIGENT
COMPACTION (IC) RESILIENT MODULUS (M_R) AT 207 KPA (30
PSI)

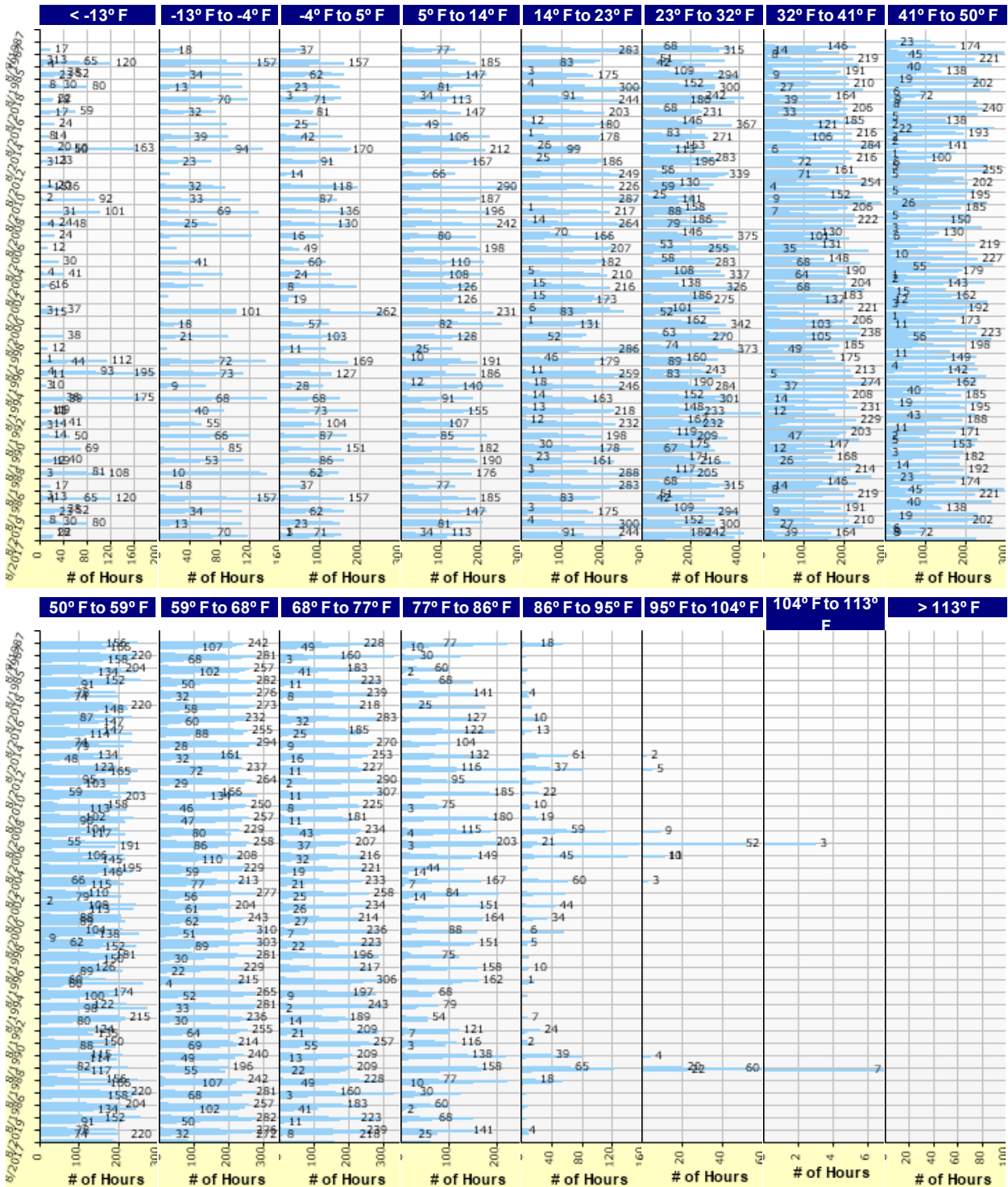
Equation	R ²	Adj. R ²	Std. Error
3.0066*Median E _{LWD} (MPa) + 30.0589*Combined Absorption (%) - 31.5527*Median NDG Moisture Content (%) - 3.6529	0.94	0.91	25.65
3.1960*Median E _{LWD} (MPa) + 16.8517*Fine Absorption (%) - 31.3564*Median NDG Moisture Content (%) + 15.5679	0.94	0.91	26.01
1.8399*Median E _{LWD} (MPa) + 26.0419*Fine Absorption (%) - 86.9710*Coarse Absorption (%) + 154.2450	0.93	0.9	27.54
3.2263*Median E _{LWD} (MPa) + 10.2064*Fine Absorption (%) - 2.8517*Median Relative OMC (%) + 62.4653	0.93	0.9	27.68
3.4006*Median E _{LWD} (MPa) + 14.0113*Combined Absorption (%) - 156.4348	0.87	0.83	34.92
3.4875*Median E _{LWD} (MPa) + 7.8616*Fine Absorption (%) - 146.8084	0.87	0.83	35.04

E_{LWD} = light weight deflectometer (LWD) elastic modulus; OMC = optimum moisture content; NDG = nuclear density gauge

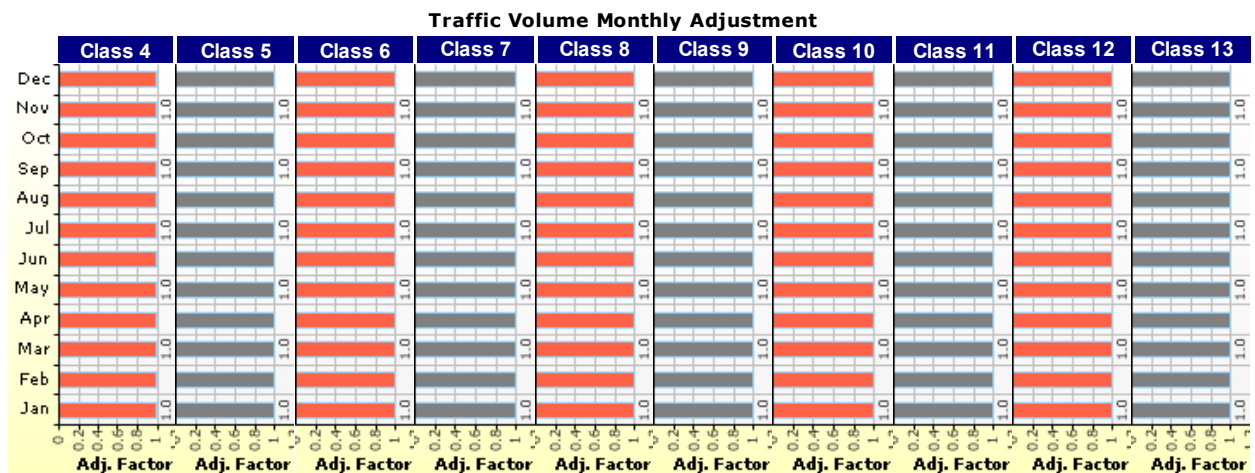
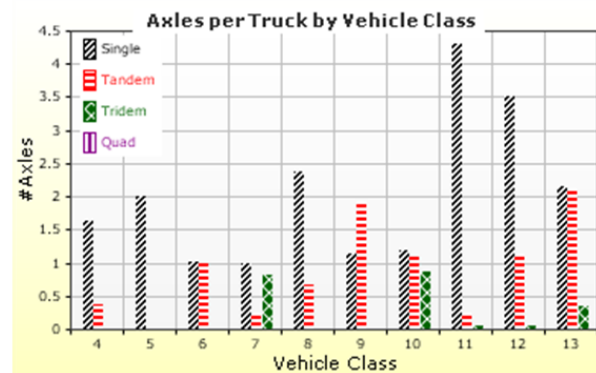
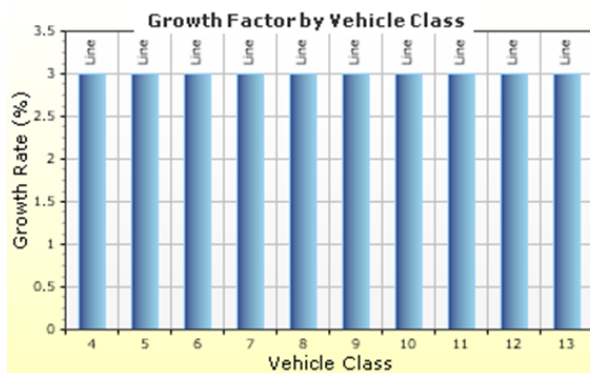
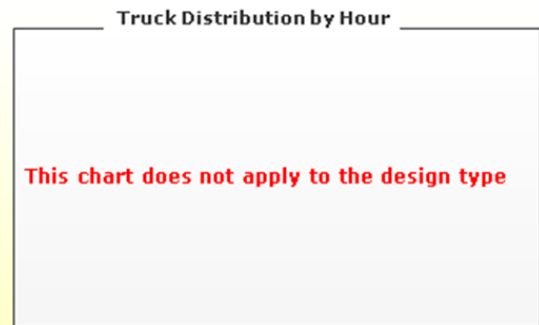
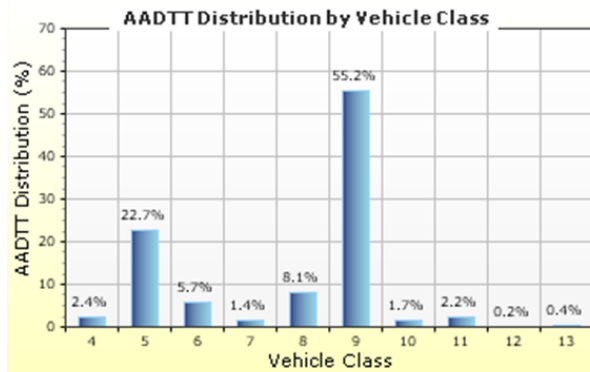
APPENDIX AW
MONTHLY RAINFALL STATISTICS, MONTHLY CLIMATE
SUMMARY, AND HOURLY AIR TEMPERATURE DISTRIBUTION BY
MONTH FOR MINNESOTA ROAD RESEARCH PROJECT (MNROAD)
LOW VOLUME ROAD (LVR) TEST FACILITY



Hourly Air Temperature Distribution by Month:



APPENDIX AX
GRAPHICAL AND TABULAR REPRESENTATIONS OF TRAFFIC
INPUTS AND AXLE CONFIGURATION



Volume Monthly Adjustment Factors

Level 3: Default MAF

Month	Vehicle Class									
	4	5	6	7	8	9	10	11	12	13
January	1.0	1.0	1.0	1.0	1.0	1.0	1.0	1.0	1.0	1.0
February	1.0	1.0	1.0	1.0	1.0	1.0	1.0	1.0	1.0	1.0
March	1.0	1.0	1.0	1.0	1.0	1.0	1.0	1.0	1.0	1.0
April	1.0	1.0	1.0	1.0	1.0	1.0	1.0	1.0	1.0	1.0
May	1.0	1.0	1.0	1.0	1.0	1.0	1.0	1.0	1.0	1.0
June	1.0	1.0	1.0	1.0	1.0	1.0	1.0	1.0	1.0	1.0
July	1.0	1.0	1.0	1.0	1.0	1.0	1.0	1.0	1.0	1.0
August	1.0	1.0	1.0	1.0	1.0	1.0	1.0	1.0	1.0	1.0
September	1.0	1.0	1.0	1.0	1.0	1.0	1.0	1.0	1.0	1.0
October	1.0	1.0	1.0	1.0	1.0	1.0	1.0	1.0	1.0	1.0
November	1.0	1.0	1.0	1.0	1.0	1.0	1.0	1.0	1.0	1.0
December	1.0	1.0	1.0	1.0	1.0	1.0	1.0	1.0	1.0	1.0

Distributions by Vehicle Class

Vehicle Class	AADTT Distribution (%) (Level 3)	Growth Factor	
		Rate (%)	Function
Class 4	2.4%	3%	Linear
Class 5	22.7%	3%	Linear
Class 6	5.7%	3%	Linear
Class 7	1.4%	3%	Linear
Class 8	8.1%	3%	Linear
Class 9	55.2%	3%	Linear
Class 10	1.7%	3%	Linear
Class 11	2.2%	3%	Linear
Class 12	0.2%	3%	Linear
Class 13	0.4%	3%	Linear

Axle Configuration

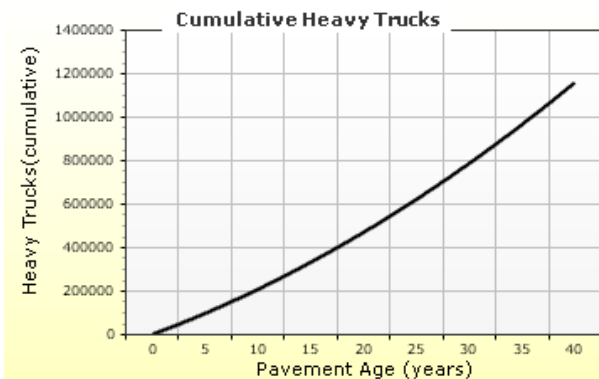
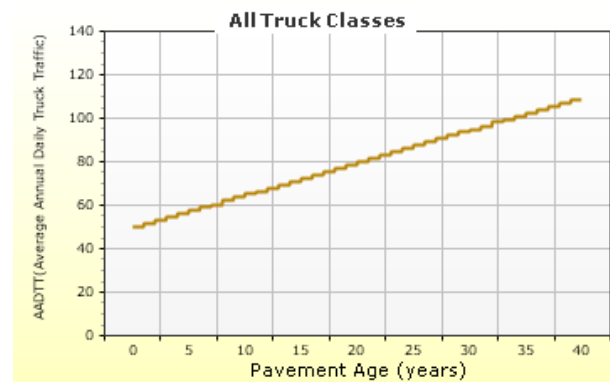
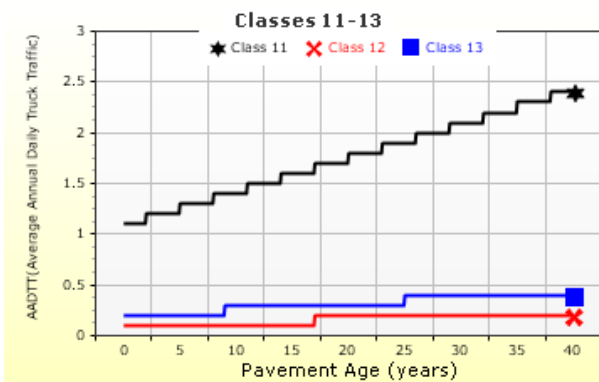
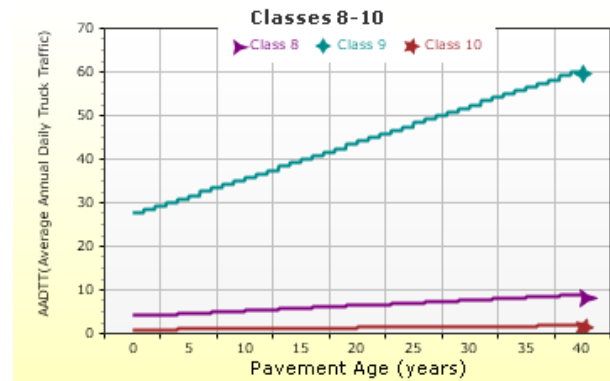
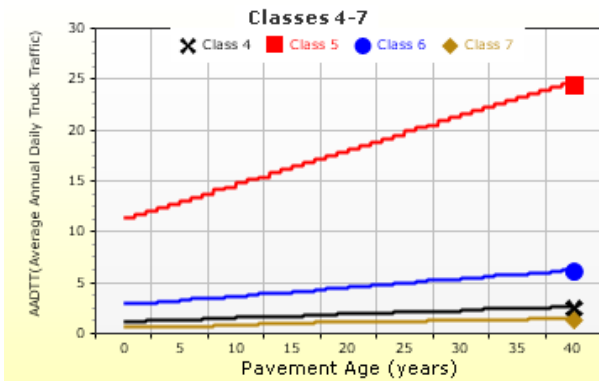
Traffic Wander		Axle Configuration	
Mean wheel location (in)	18.0	Average axle width (ft)	8.5
Traffic wander standard deviation (in)	10.0	Dual tire spacing (in)	12.0
Design lane width (ft)	12.0	Tire pressure (psi)	120.0
Average Axle Spacing		Wheelbase does not apply	
Tandem axle spacing (in)	51.6		
Tridem axle spacing (in)	49.2		
Quad axle spacing (in)	49.2		

Number of Axles per Truck

Vehicle Class	Single Axle	Tandem Axle	Tridem Axle	Quad Axle
Class 4	1.62	0.39	0	0
Class 5	2	0	0	0
Class 6	1.02	0.99	0	0
Class 7	1	0.26	0.83	0
Class 8	2.38	0.67	0	0
Class 9	1.13	1.93	0	0
Class 10	1.19	1.09	0.89	0
Class 11	4.29	0.26	0.06	0
Class 12	3.52	1.14	0.06	0
Class 13	2.15	2.13	0.35	0

AADTT (Average Annual Daily Truck Traffic) Growth

* Traffic cap is not enforced



APPENDIX AY

ASPHALT LAYER PARAMETERS (LEVEL 3) IN PAVEMENT ME

HMA Design Properties

Use Multilayer Rutting Model	False	Layer Name	Layer Type	Interface Friction
Using G* based model (not nationally calibrated)	False	Layer 1 Flexible : Default asphalt concrete	Flexible (1)	1.00
Is NCHRP 1-37A HMA Rutting Model Coefficients	True	Layer 2 Non-stabilized Base : A-1-a	Non-stabilized Base (4)	1.00
Endurance Limit	-	Layer 3 Non-stabilized Base : A-1-b	Non-stabilized Base (4)	1.00
Use Reflective Cracking	True	Layer 4 Subgrade : A-1-b	Subgrade (5)	-
Structure - ICM Properties				
AC surface shortwave absorptivity	0.85			

Master Curve Plot

Delta	2.8417502
Alpha	3.870018
Beta	-0.6501216
Gamma	0.313351
c	1.255882
SSE	0
Se/Sy	0

log(Reducer)	E* (psi)	14 oF	40 oF	70 oF	100 oF	130 oF
-6.0271108	2682441.7	2682441.7				
-5.6291708	2477445	2477445				
-4.6291708	1949019.2	1949019.2				
-4.3281408	1790705.9	1790705.9				
-3.597245	1419160.5		1419160.5			
-3.1993049	1229267.8		1229267.8			
-2.1993049	809542.6		809542.6			
-1.8982749	702304.56		702304.56			
-1.39794	545336.95			545336.95		
-1	439474.08			439474.08		
0	242381.01			242381.01		
0.30103	200015.76			200015.76		
0.3203962	197523.86				197523.86	
0.7183362	152018.74				152018.74	
1.7183362	76682.67				76682.67	
2.0193662	62165.031				62165.031	
1.6808806	78707.012					78707.012
2.0788206	59637.836					59637.836
3.0788206	29842.823					29842.823
3.3798506	24350.865					24350.865

Shift Factor Plot

c	1.255882
---	----------

Temp (F)	Shift	14 oF	40 oF	70 oF	100 oF	130 oF
14	4.6291708	4.6291708				
40	2.1993049		2.1993049			
70	0			0		
100	-1.7183362				-1.7183362	
130	-3.0788206					-3.0788206

Temperature Viscosity

Ao	10.035
VTSO	-3.35

Log Temp	Log(Viscosity (cp))
2.6987093	9.87014833
2.72403	8.118944837
2.7479553	6.750714198
2.7706311	5.667424222

Thermal Cracking

Thermal Contraction

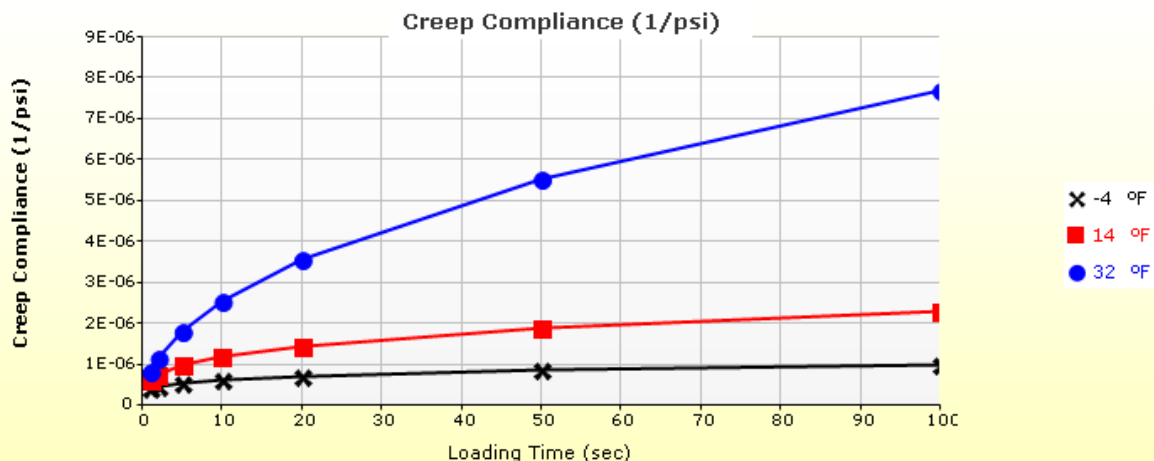
Is thermal contraction calculated?	True
Mix coefficient of thermal contraction (in/in/°F)	-
Aggregate coefficient of thermal contraction (in/in/°F)	5.0e-006
Voids in Mineral Aggregate (%)	18.6

Indirect Tensile Strength (Input Level: 3)

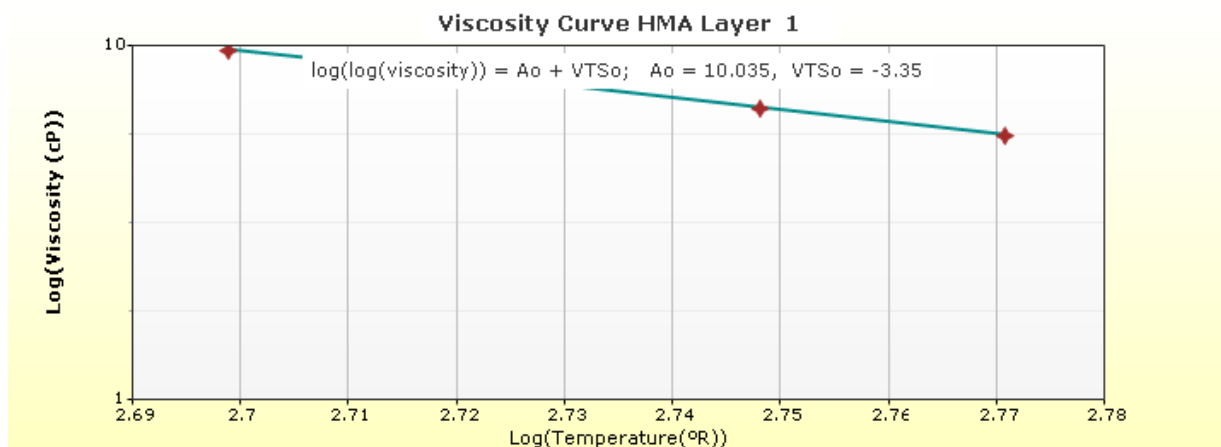
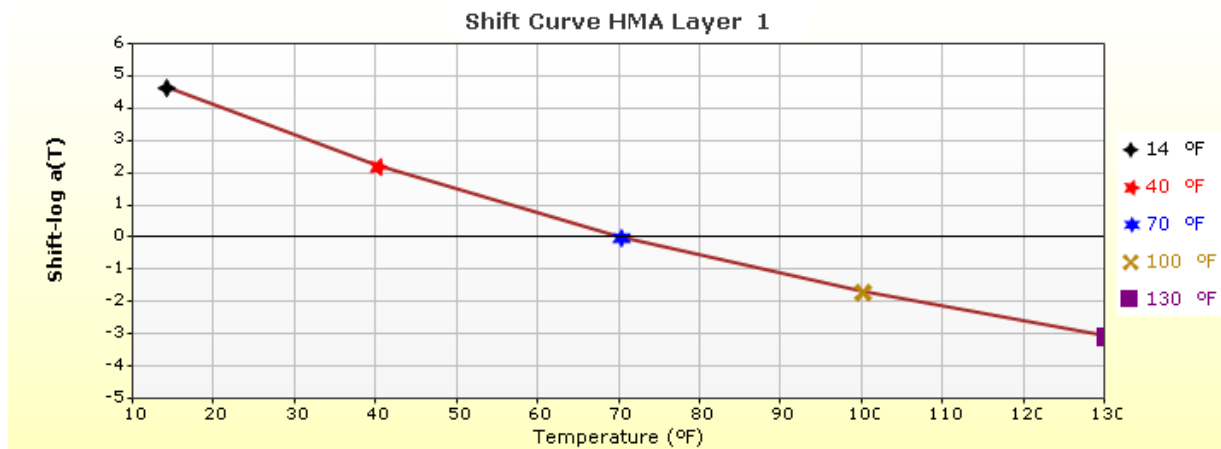
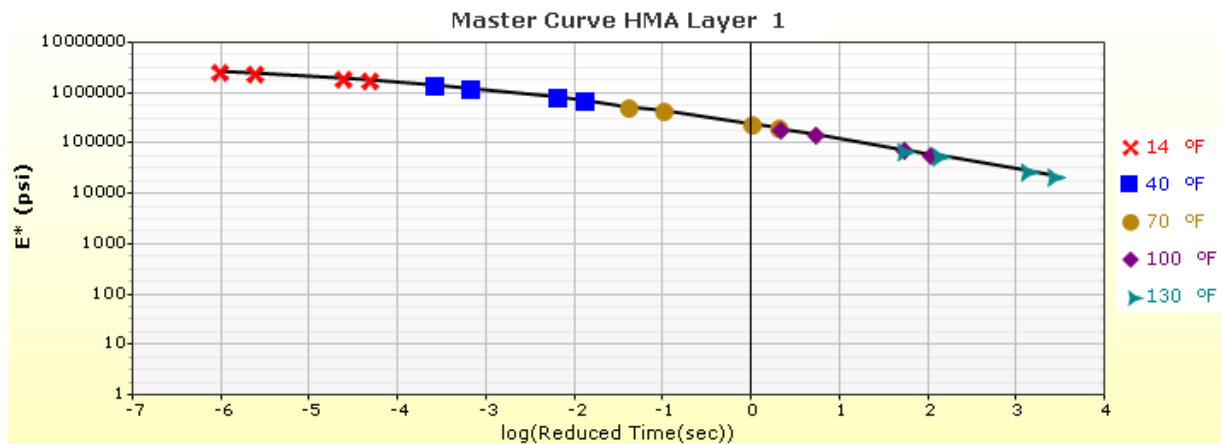
Test Temperature (°F)	Indirect Tensile Strength (psi)
14.0	473.35

Creep Compliance (1/psi) (Input Level: 3)

Loading time (sec)	-4 °F	14 °F	32 °F
1	4.14e-007	6.27e-007	8.50e-007
2	4.72e-007	7.63e-007	1.19e-006
5	5.62e-007	9.89e-007	1.84e-006
10	6.42e-007	1.20e-006	2.56e-006
20	7.32e-007	1.46e-006	3.57e-006
50	8.71e-007	1.90e-006	5.55e-006
100	9.94e-007	2.31e-006	7.73e-006



HMA Layer 1: Layer 1 Flexible : Default asphalt concrete



Layer 1 Flexible : Default asphalt concrete

Asphalt		
Thickness (in)	3.5	
Unit weight (pcf)	150.0	
Poisson's ratio	Is Calculated?	False
	Ratio	0.30
	Parameter A	-
	Parameter B	-

Asphalt Dynamic Modulus (Input Level: 3)

Gradation	Percent Passing
3/4-inch sieve	100
3/8-inch sieve	77
No.4 sieve	60
No.200 sieve	6

Asphalt Binder

Parameter	Value
Grade	Superpave Performance Grade
Binder Type	58-34
A	10.035
VTS	-3.35

General Info

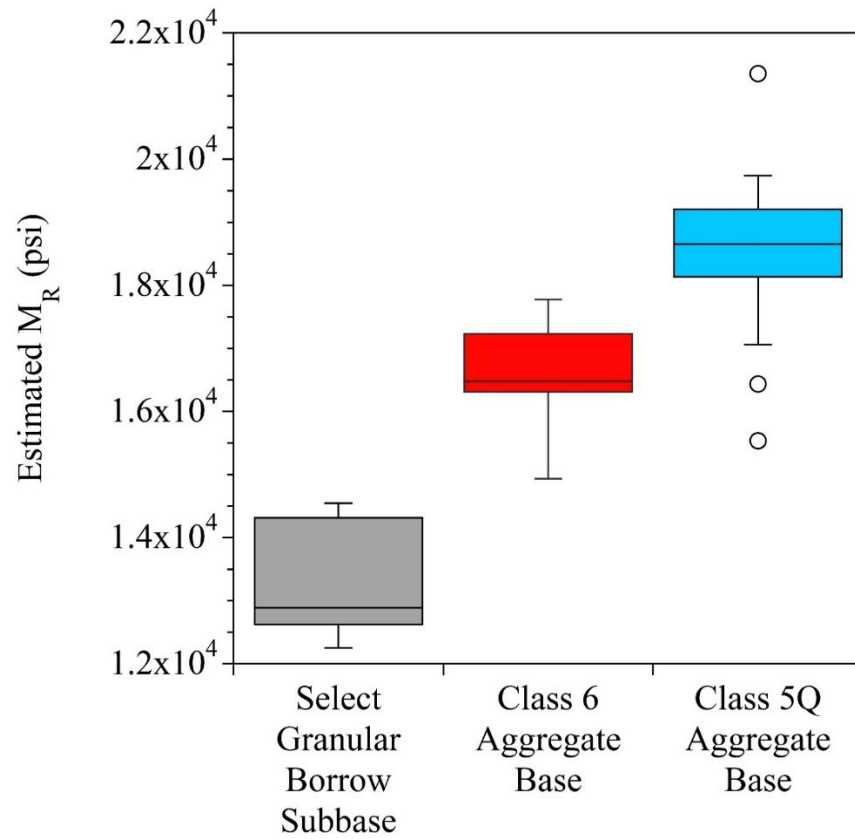
Name	Value
Reference temperature (°F)	70
Effective binder content (%)	11.6
Air voids (%)	7
Thermal conductivity (BTU/hr-ft-°F)	0.67
Heat capacity (BTU/lb-°F)	0.23

Identifiers

Field	Value
Display name/identifier	Default asphalt concrete
Description of object	
Author	
Date Created	10/30/2010 12:00:00 AM
Approver	
Date approved	10/30/2010 12:00:00 AM
State	
District	
County	
Highway	
Direction of Travel	
From station (miles)	
To station (miles)	
Province	
User defined field 1	
User defined field 2	
User defined field 3	
Revision Number	0

APPENDIX AZ

ESTIMATION OF SUMMARY RESILIENT MODULUS (SM_R) FOR SELECT GRANULAR BORROW, CLASS 6 AGGREGATE, AND CLASS 5Q AGGREGATE



Median SM_R values:

Select Granular Borrow subbase = 12,888 psi

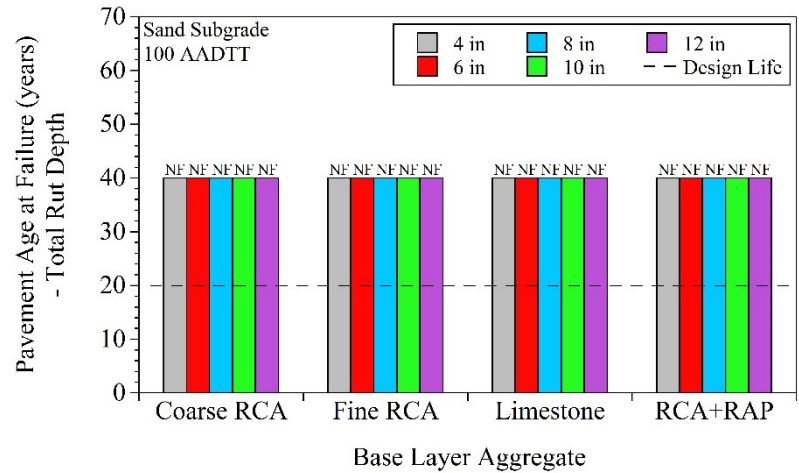
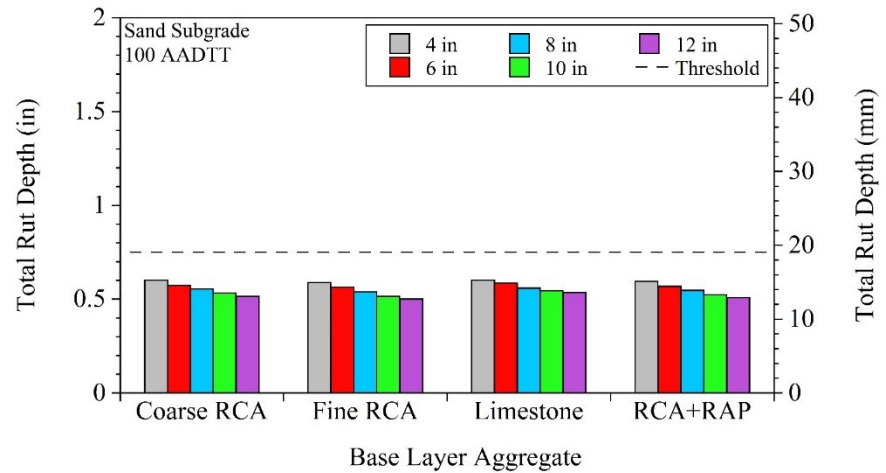
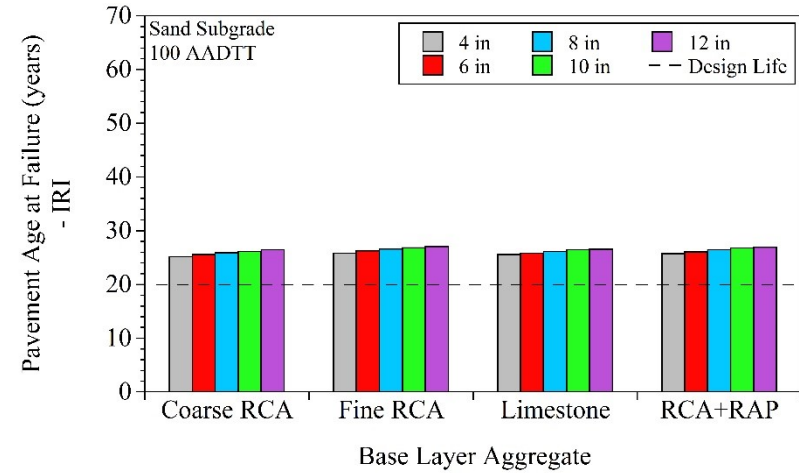
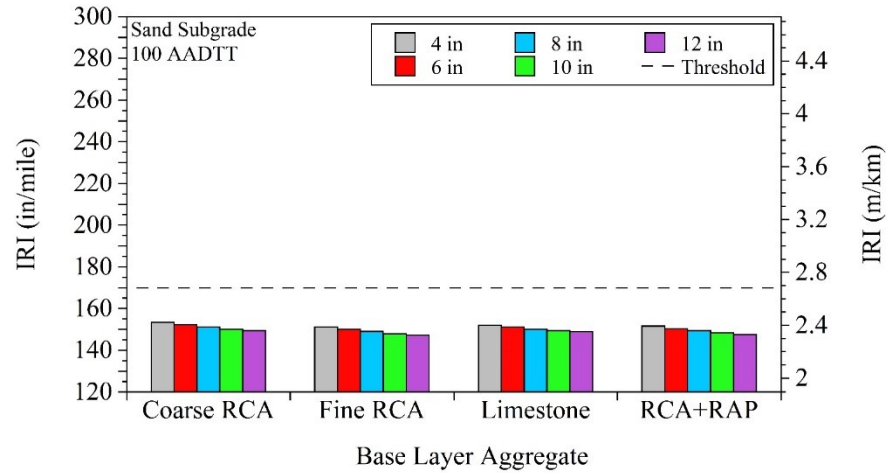
Class 6 Aggregate base = 16,478.9 psi

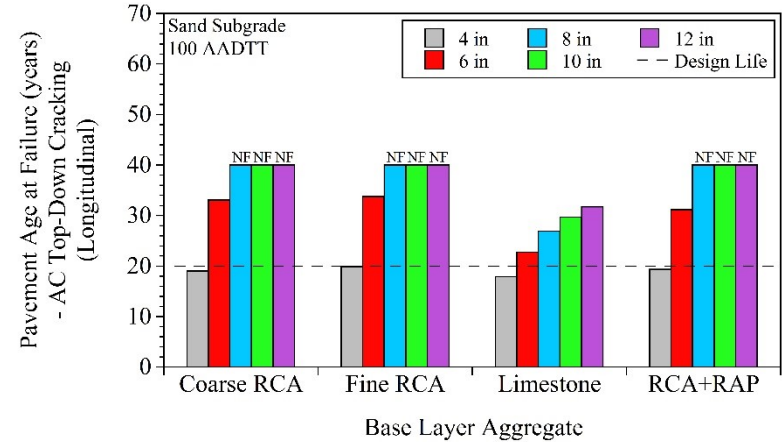
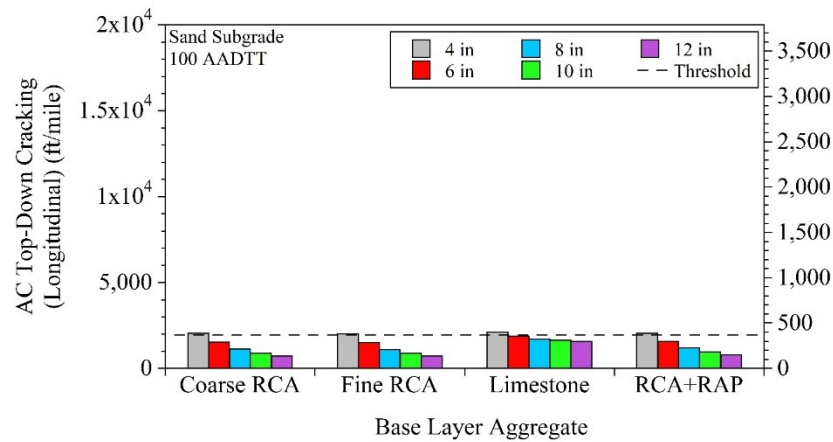
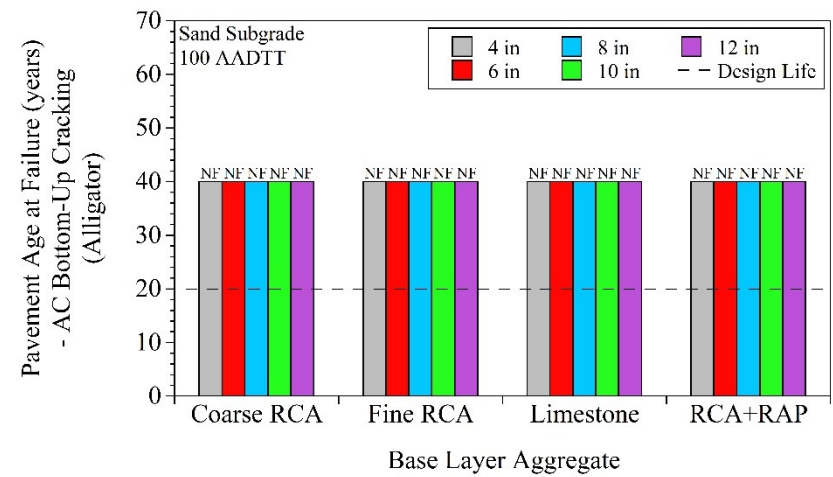
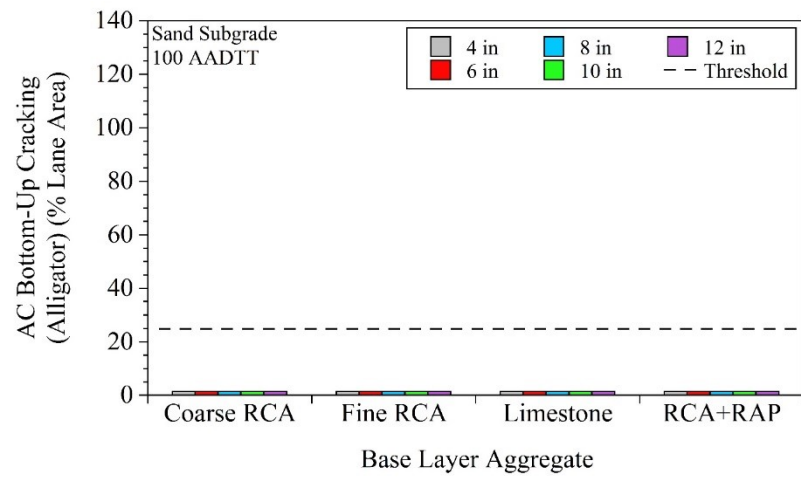
Class 5Q Aggregate base = 18,651.1 psi

APPENDIX BA

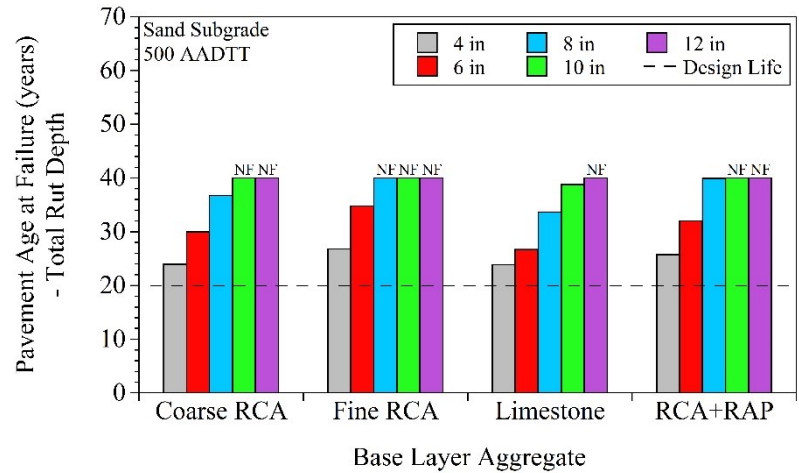
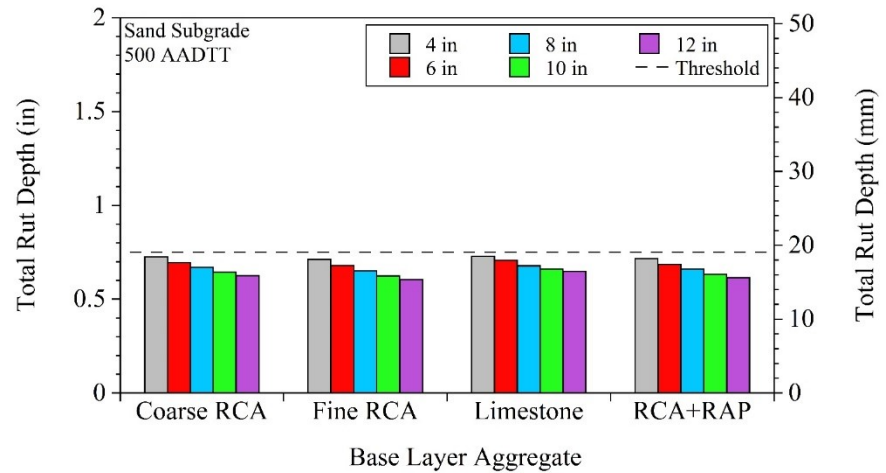
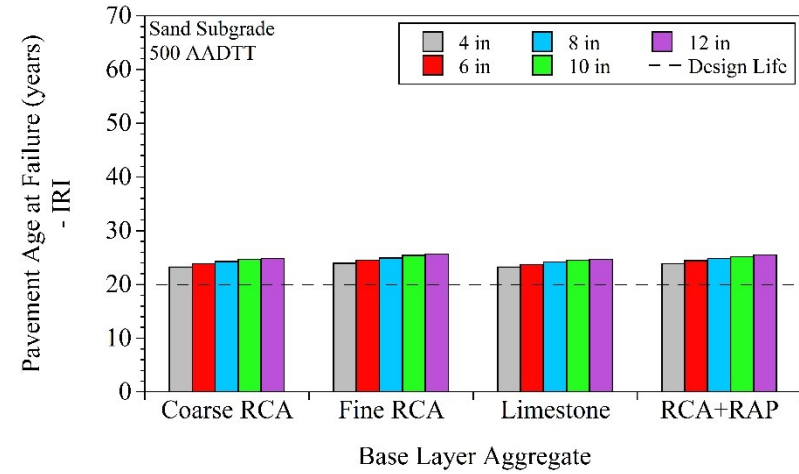
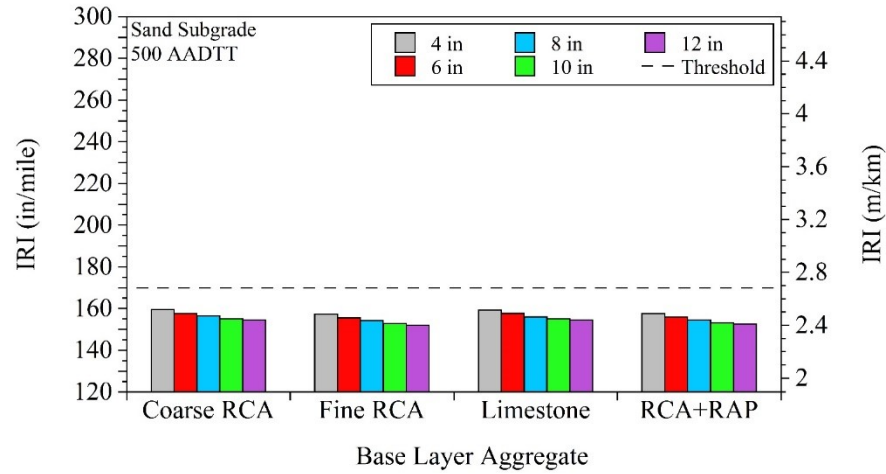
EFFECT OF AGGREGATE BASE LAYER THICKNESS ON PAVEMENT PERFORMANCE PREDICTIONS

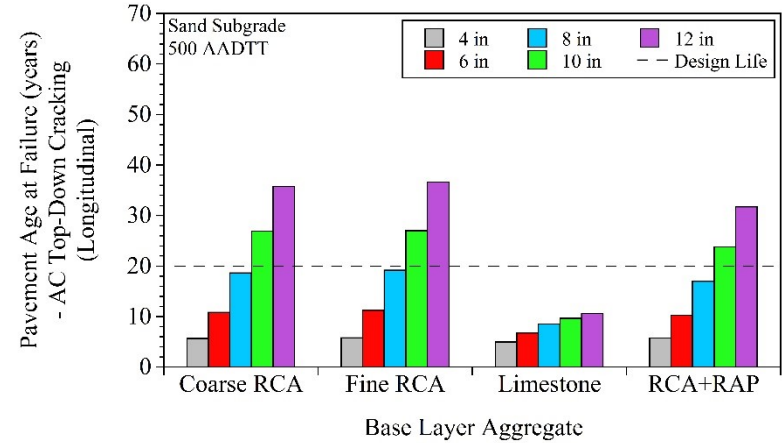
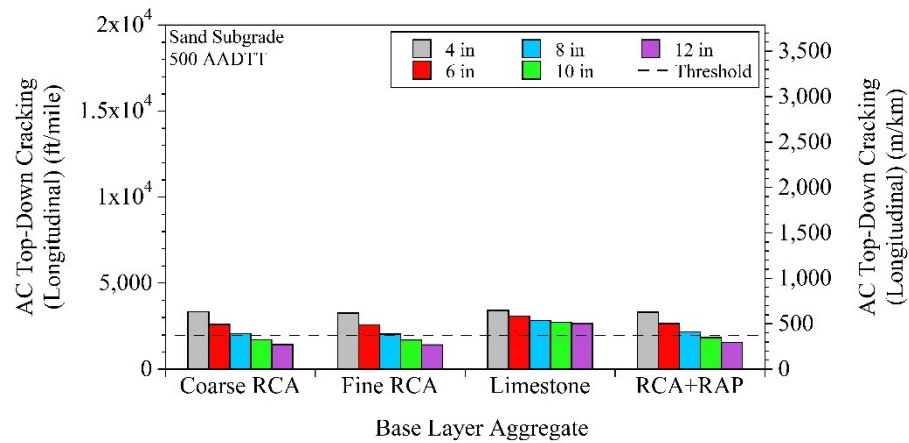
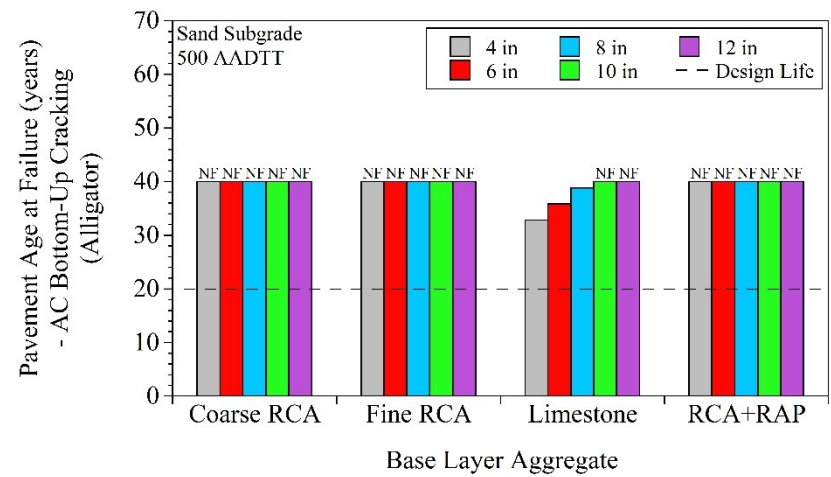
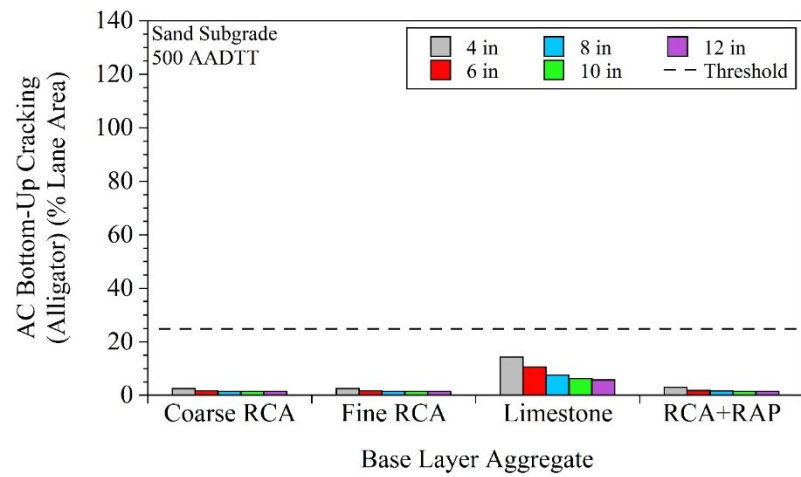
For pavement models that contained Sand Subgrade - 100 AADTT:



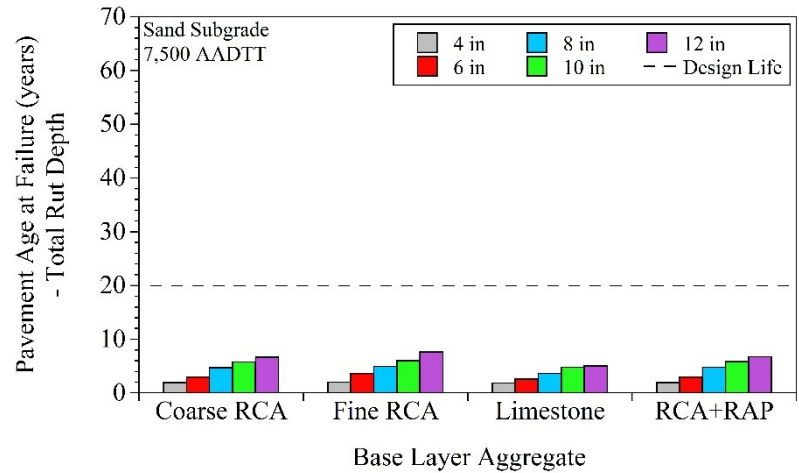
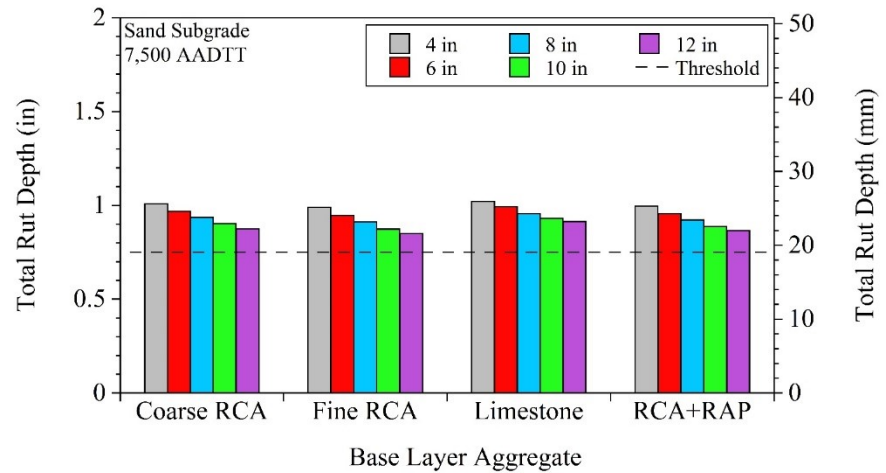
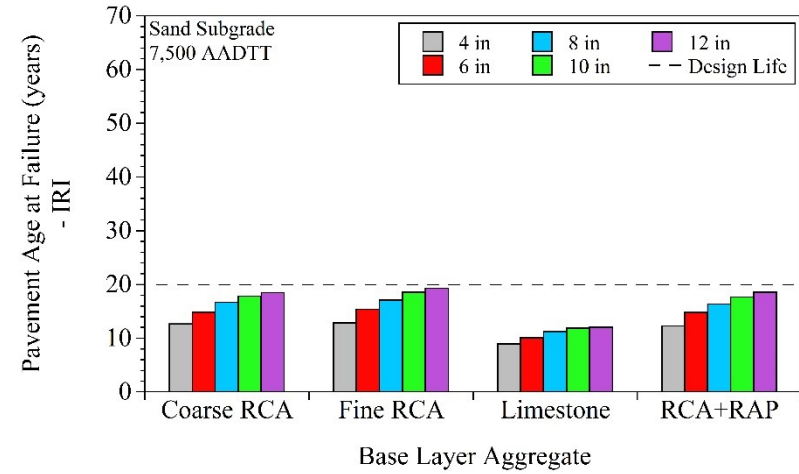
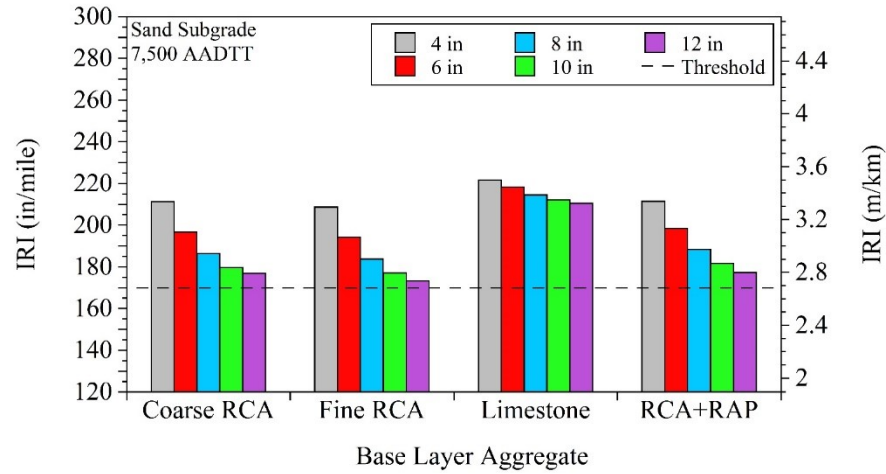


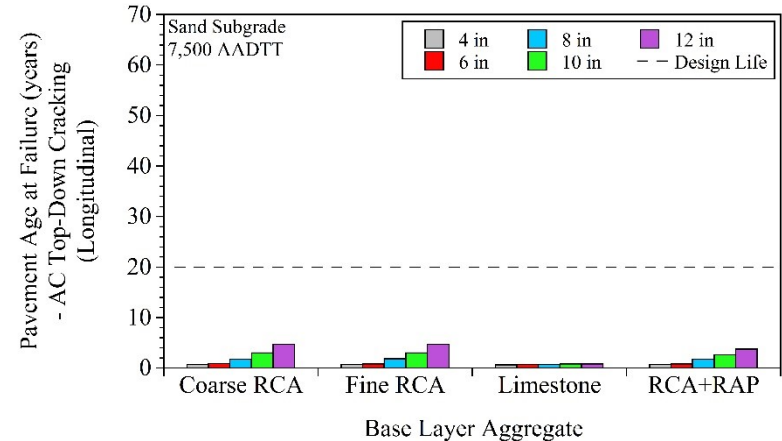
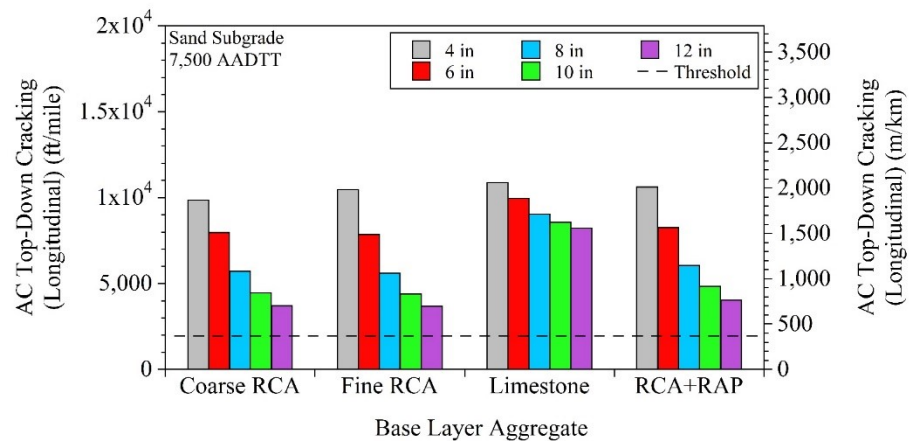
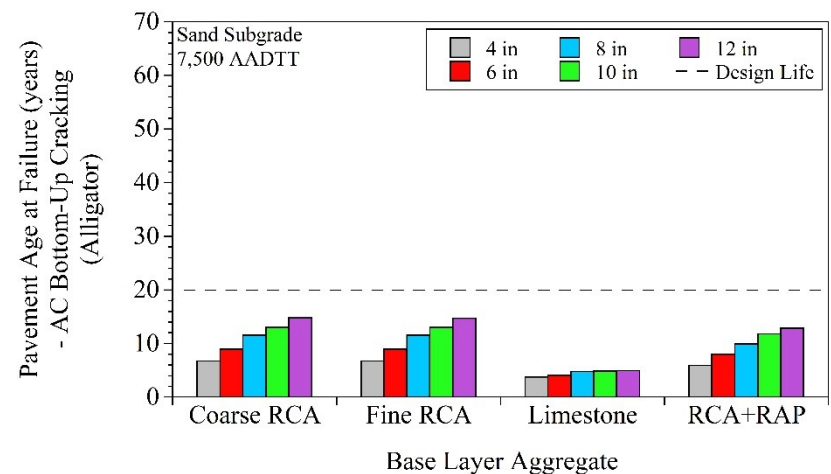
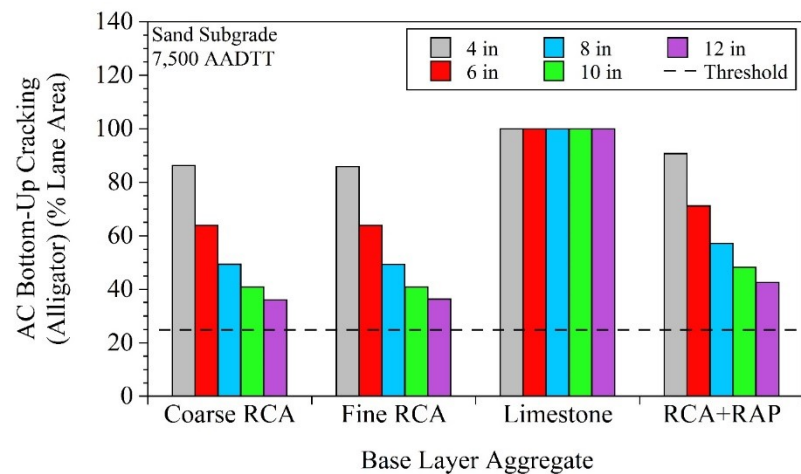
For pavements that contained Sand Subgrade - 500 AADTT:



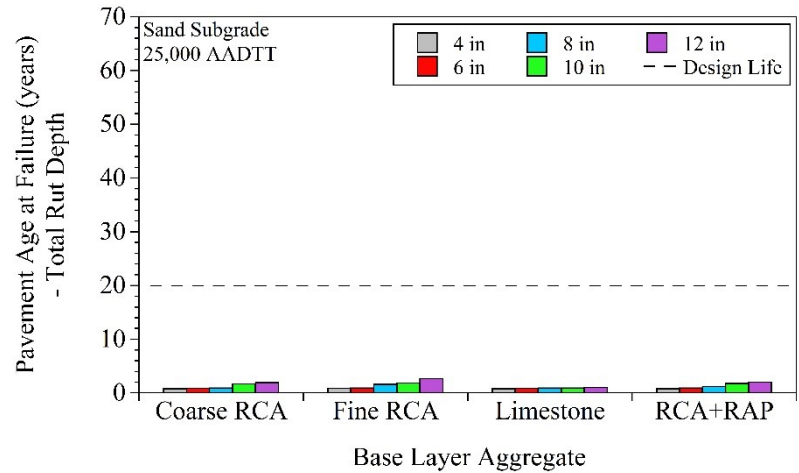
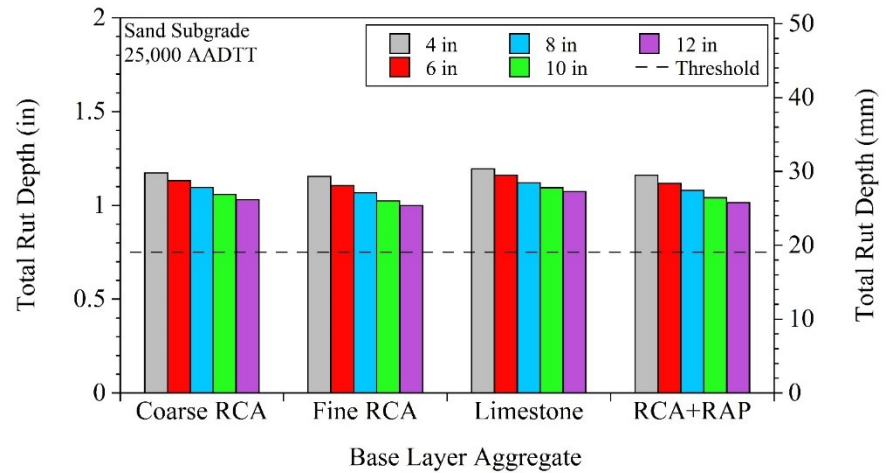
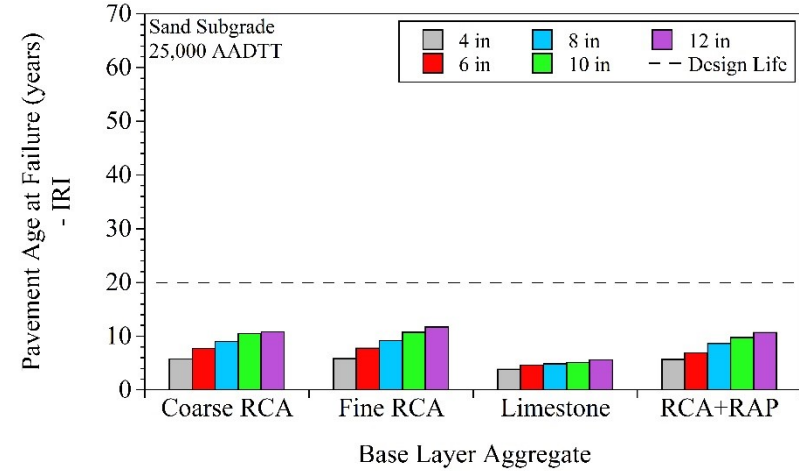
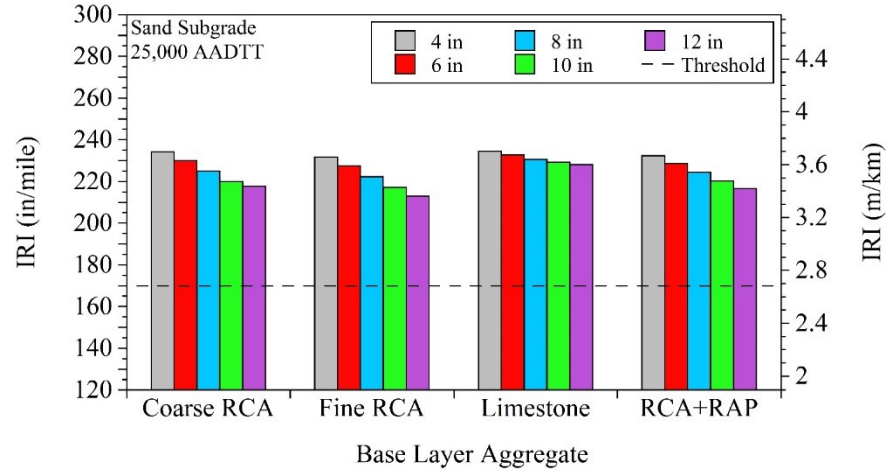


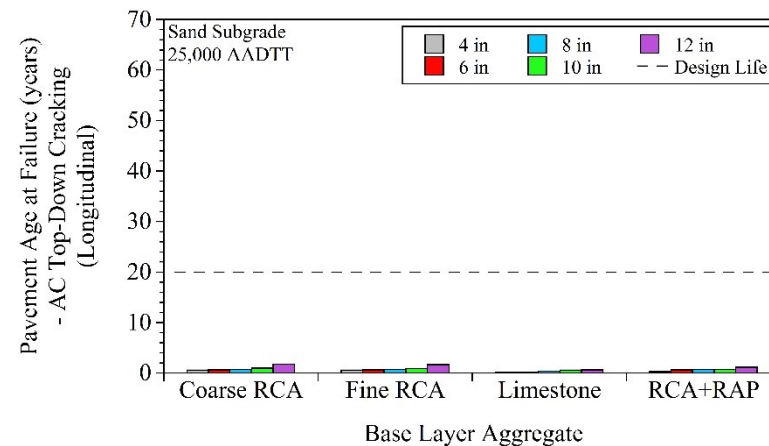
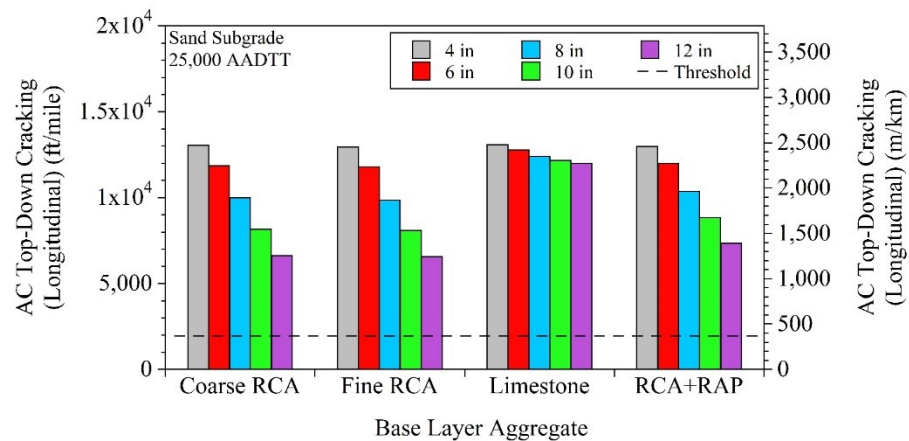
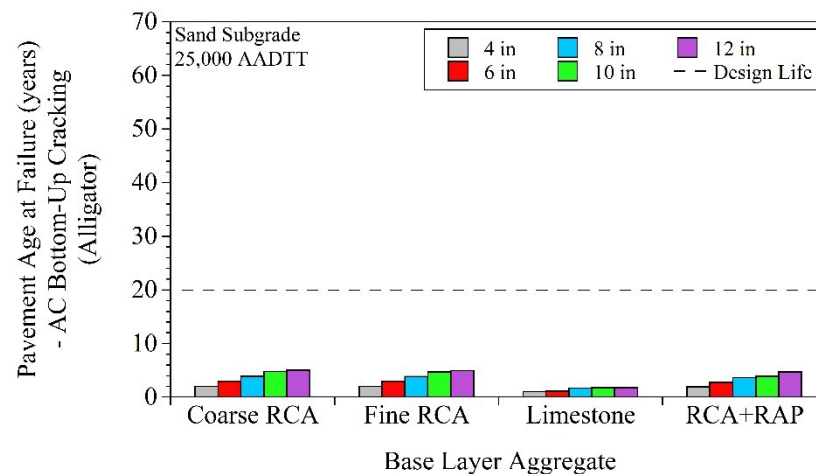
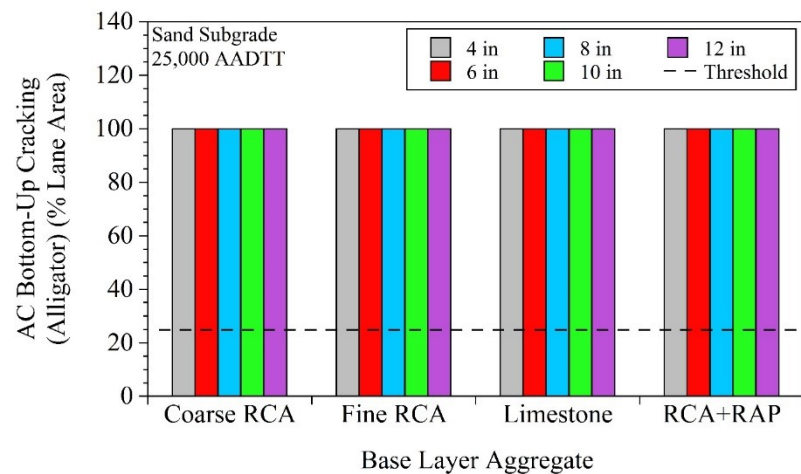
For pavements that contained Sand Subgrade - 7,500 AADTT:



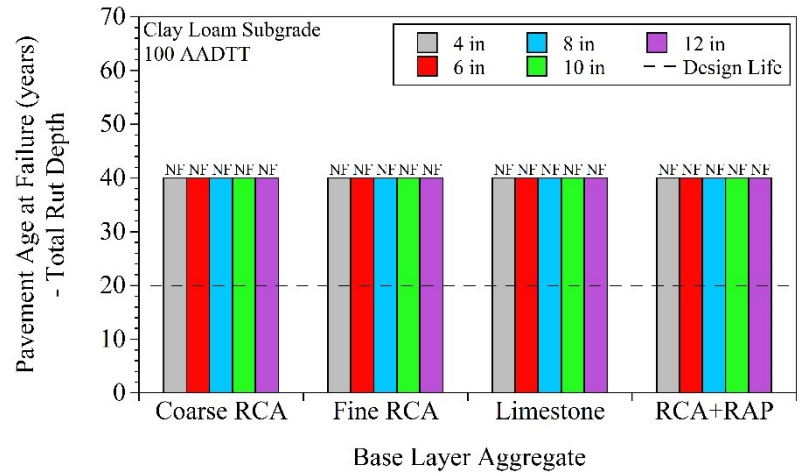
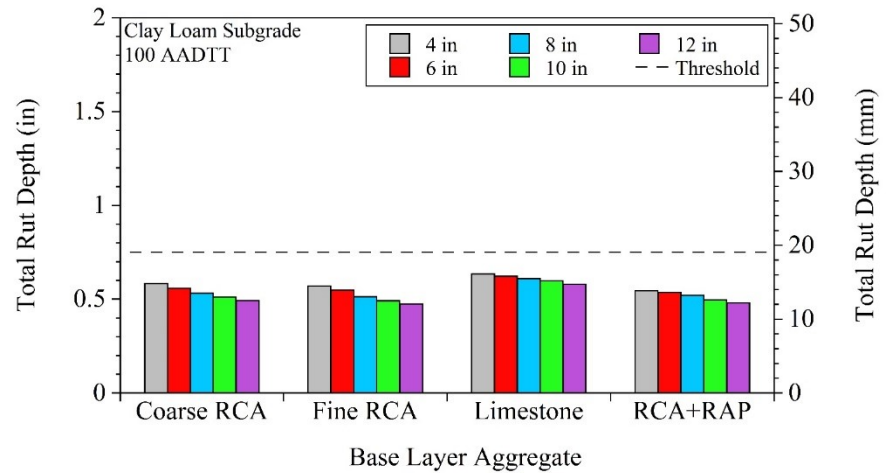
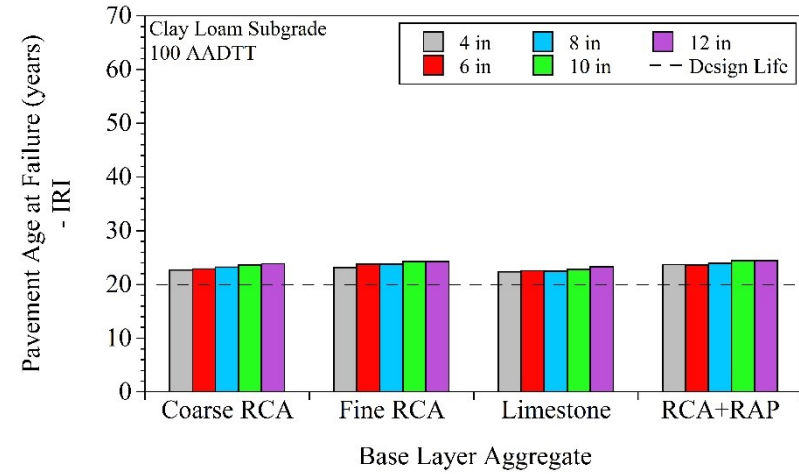
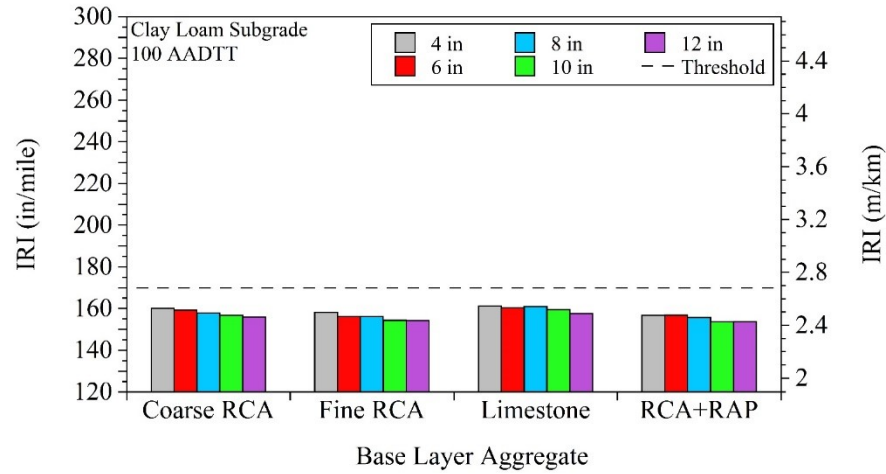


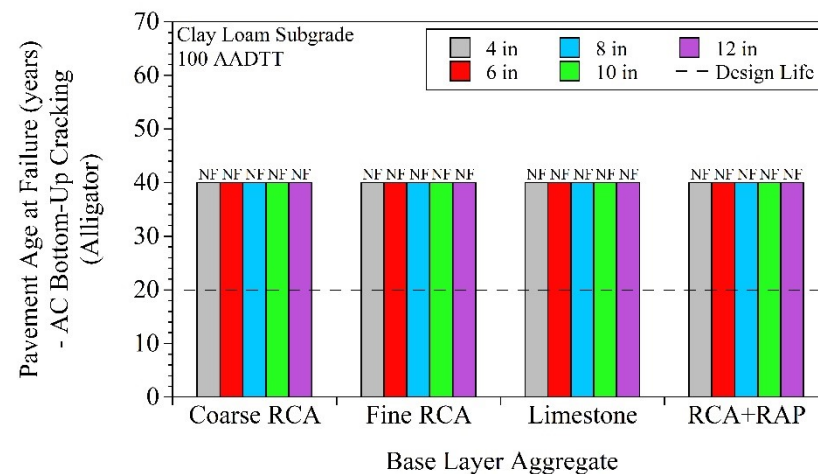
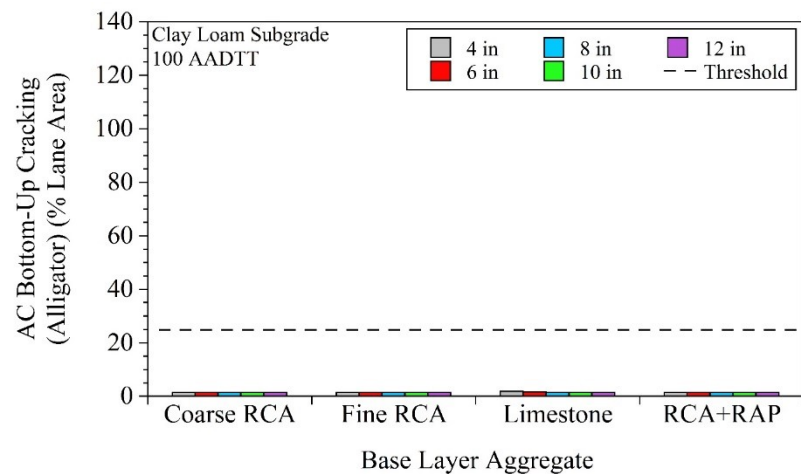
For pavements that contained Sand Subgrade - 25,000 AADTT:



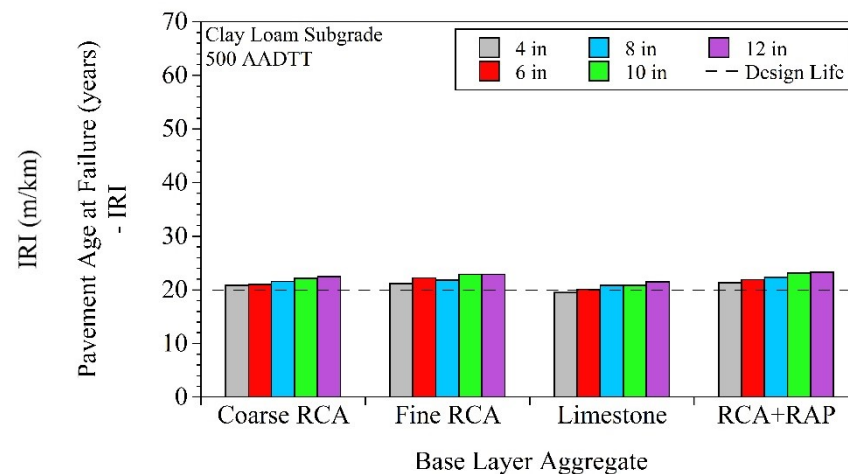
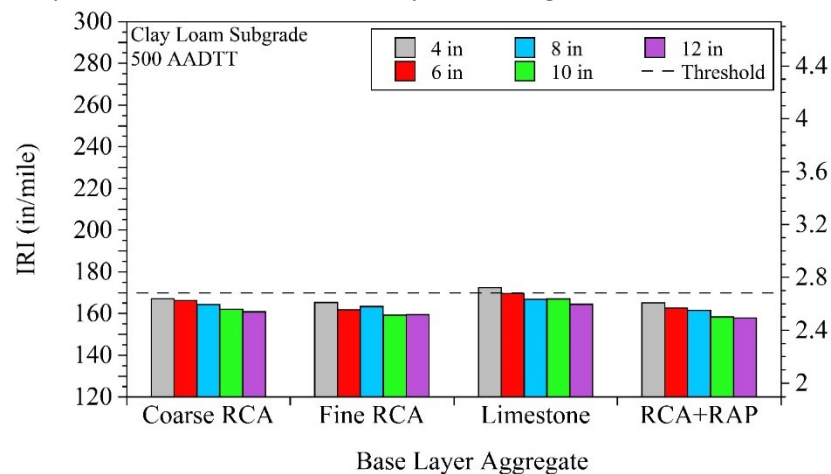


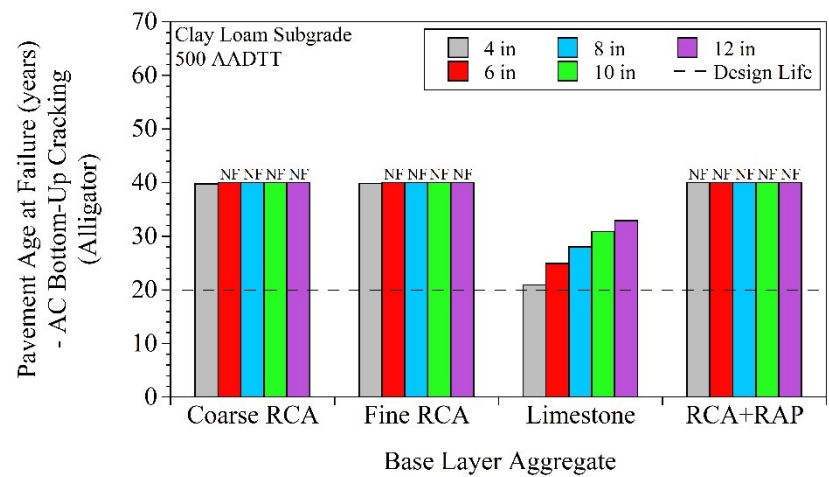
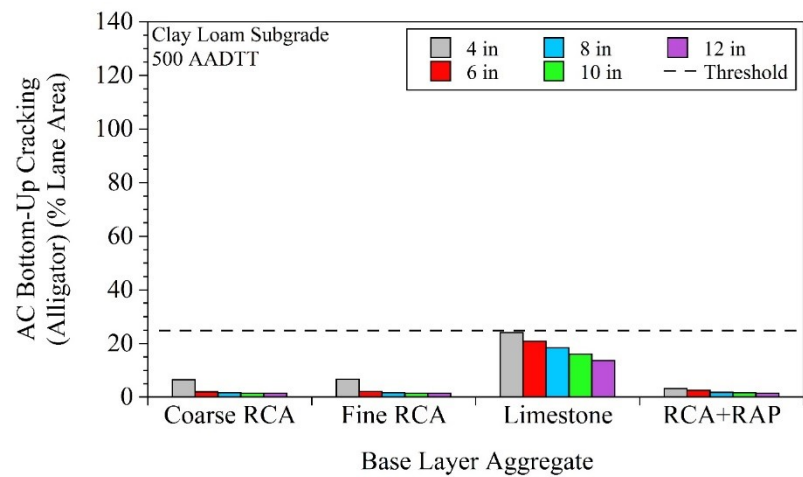
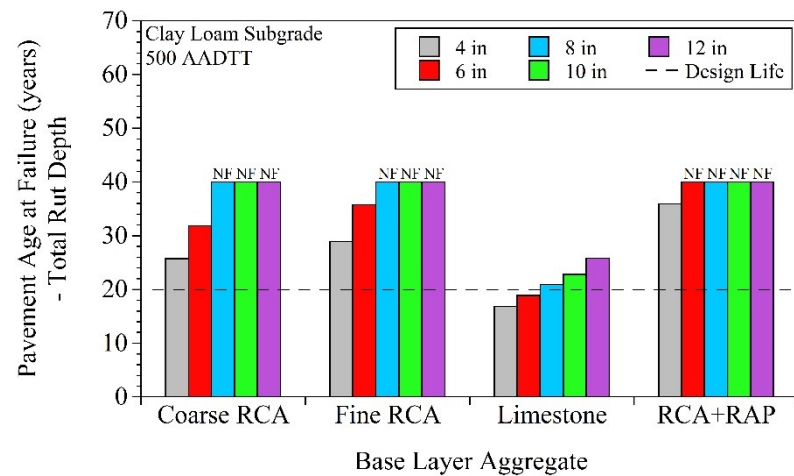
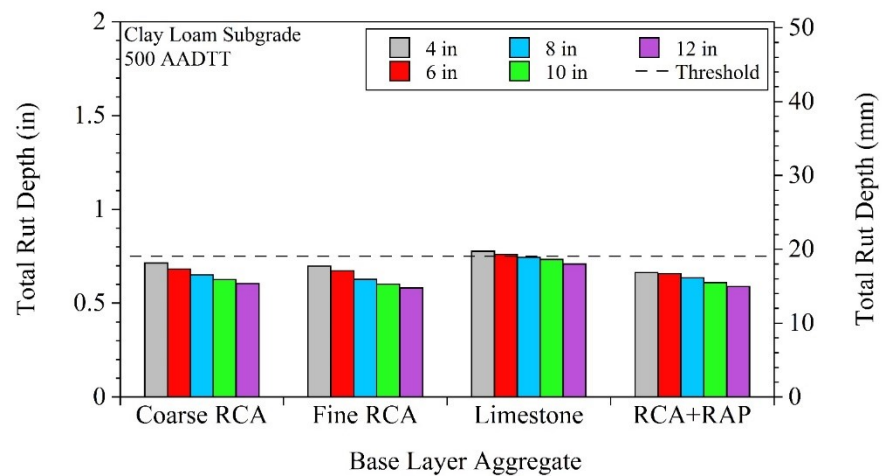
For pavements that contained Clay Loam subgrade - 100 AADTT:



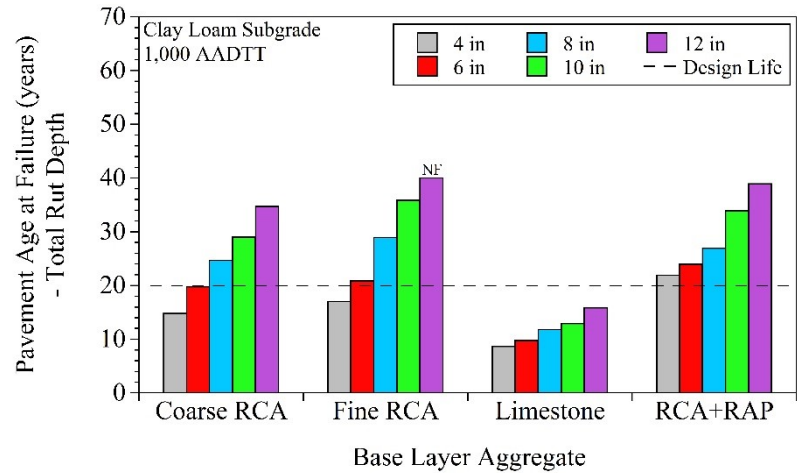
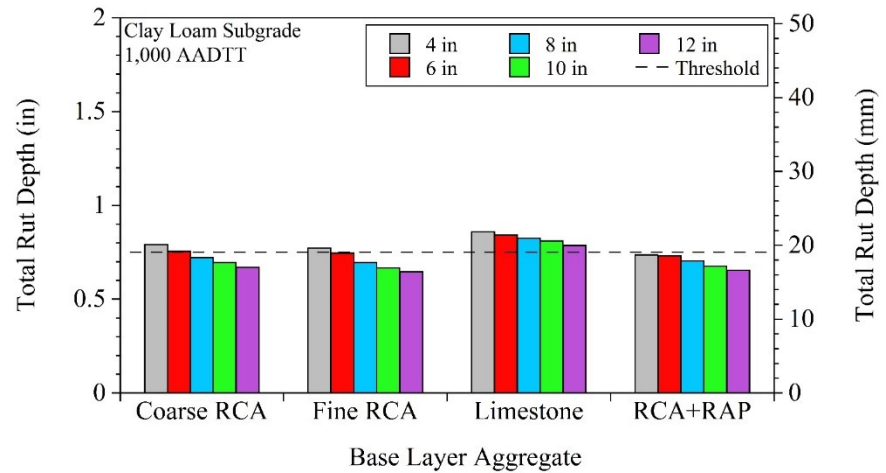
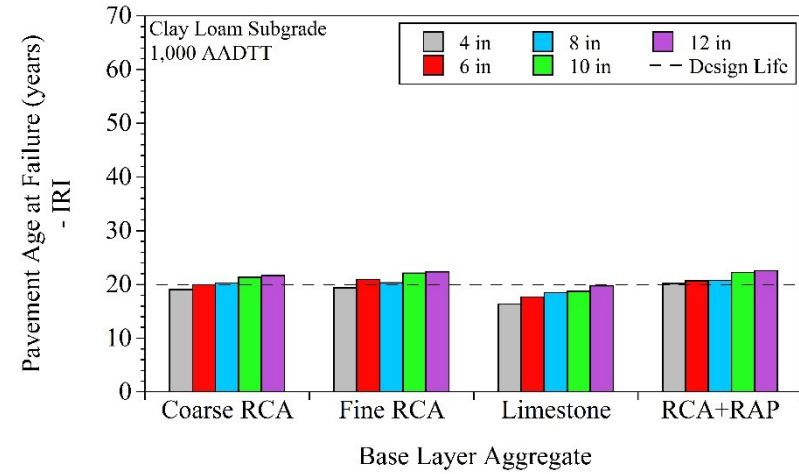
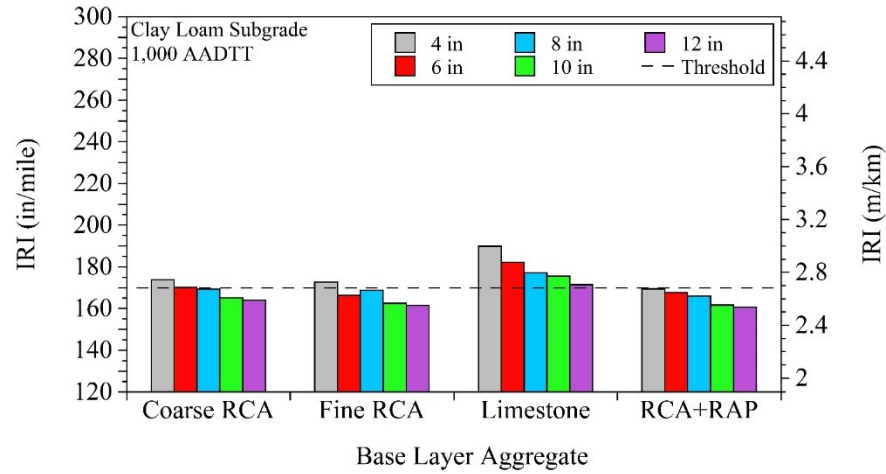


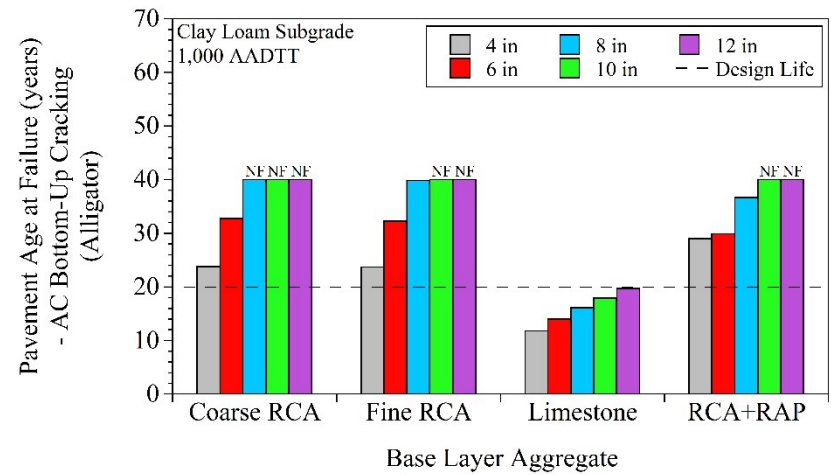
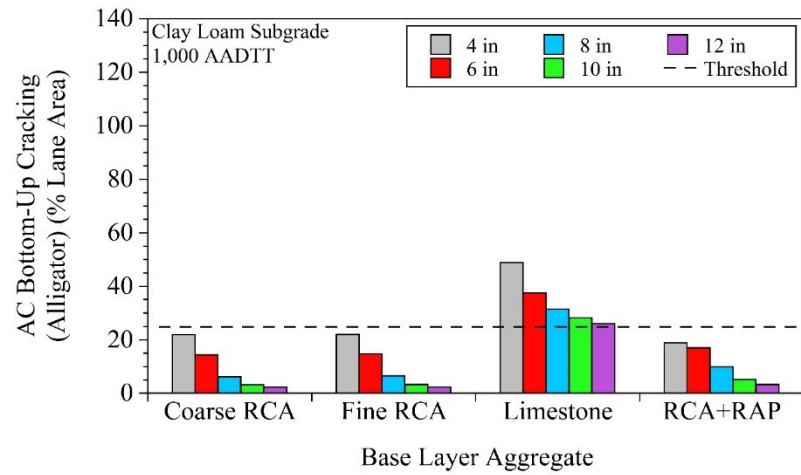
For pavements that contained Clay Loam subgrade - 500 AADTT:



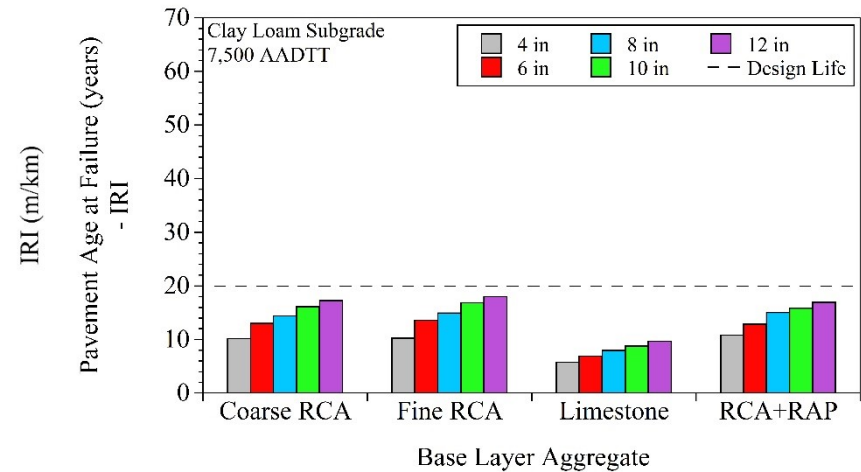
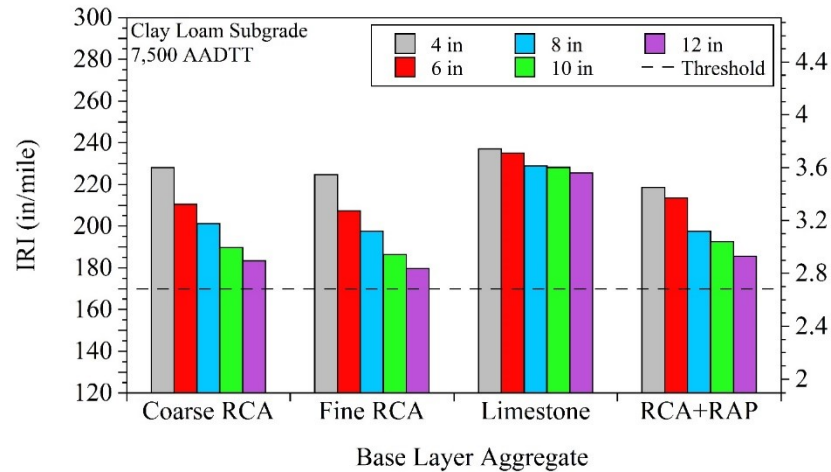


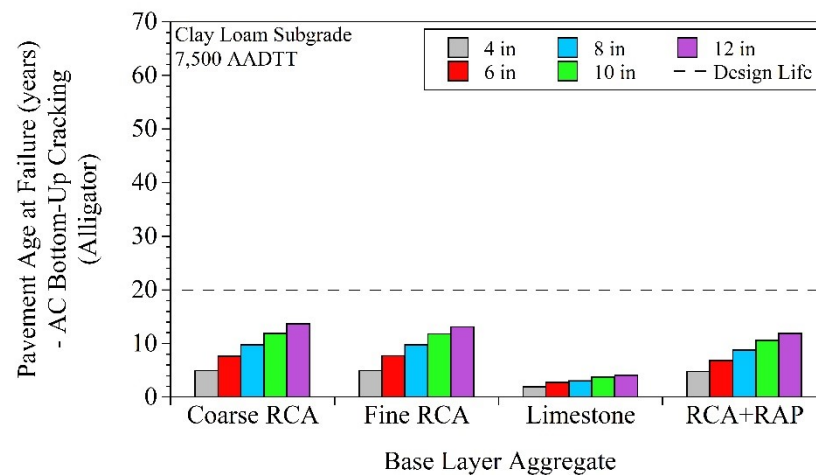
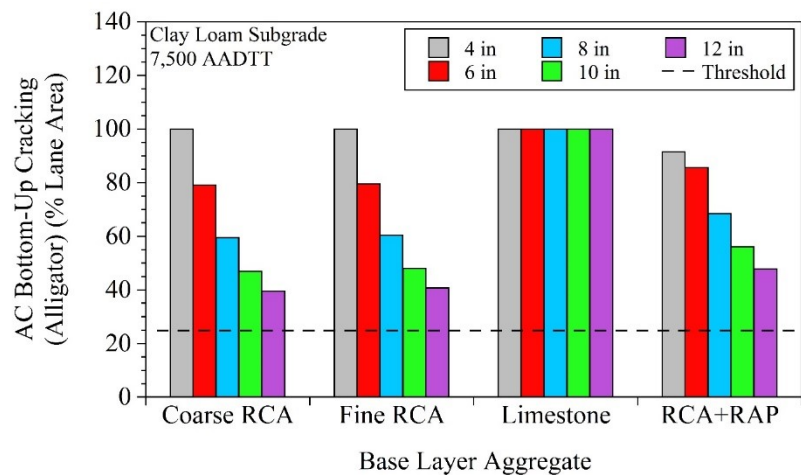
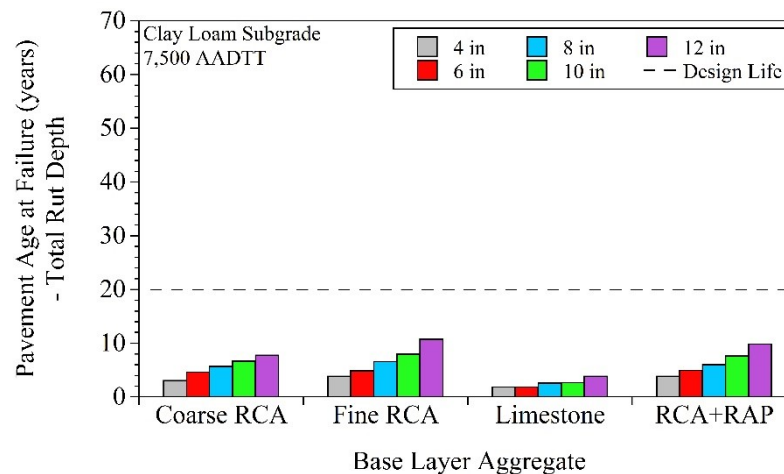
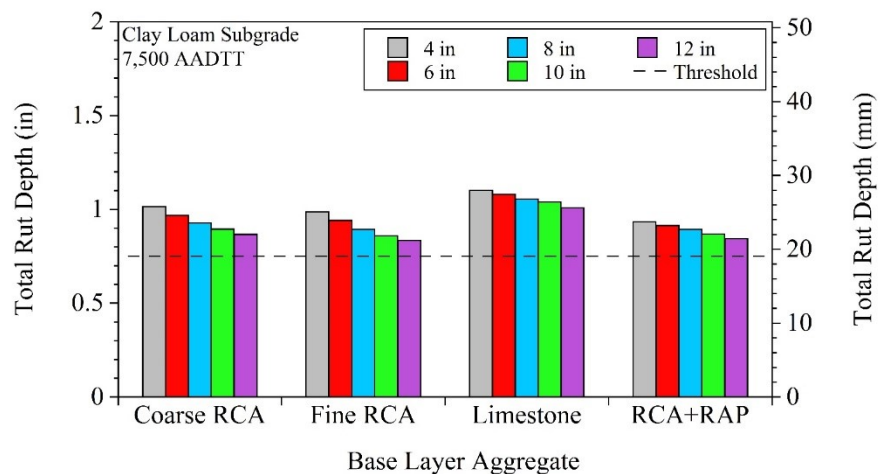
For pavements that contained Clay Loam subgrade - 1,000 AADTT:



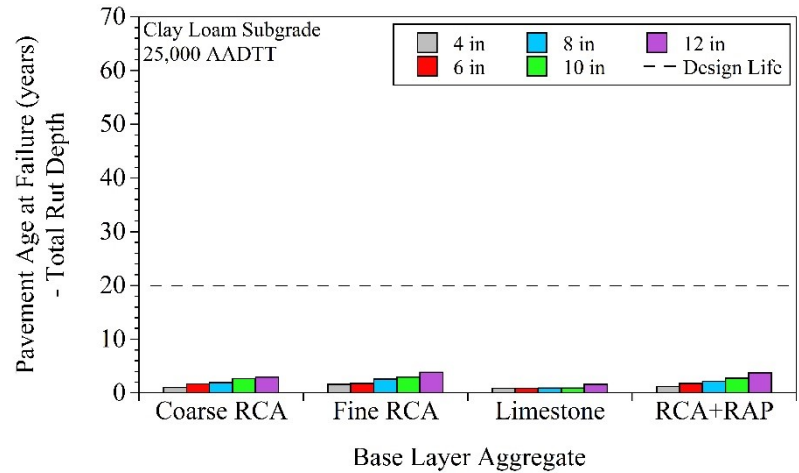
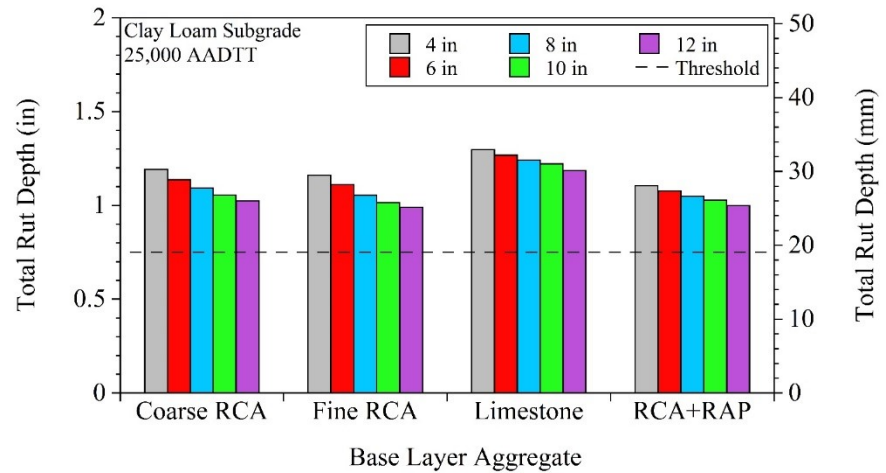
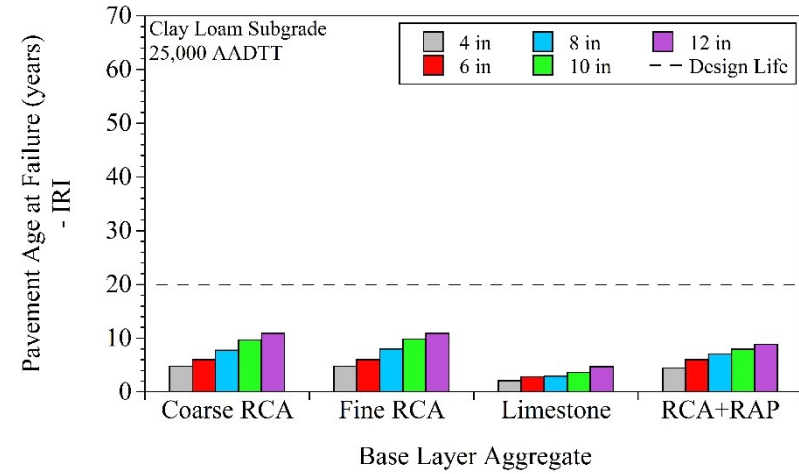
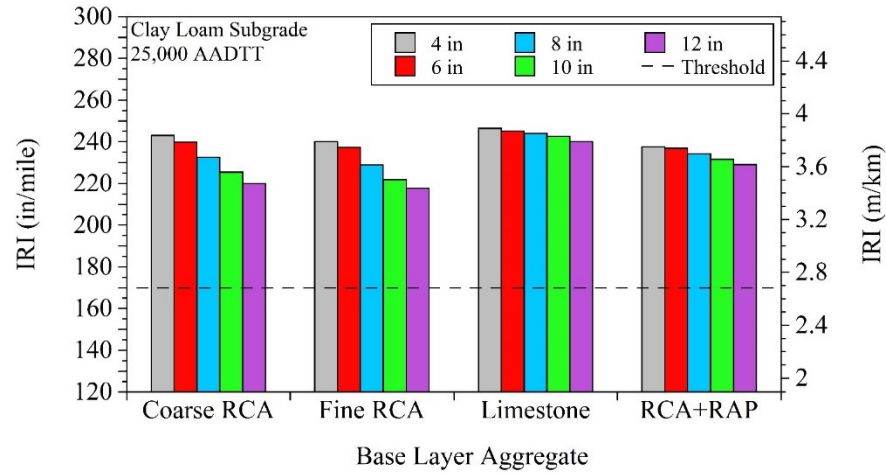


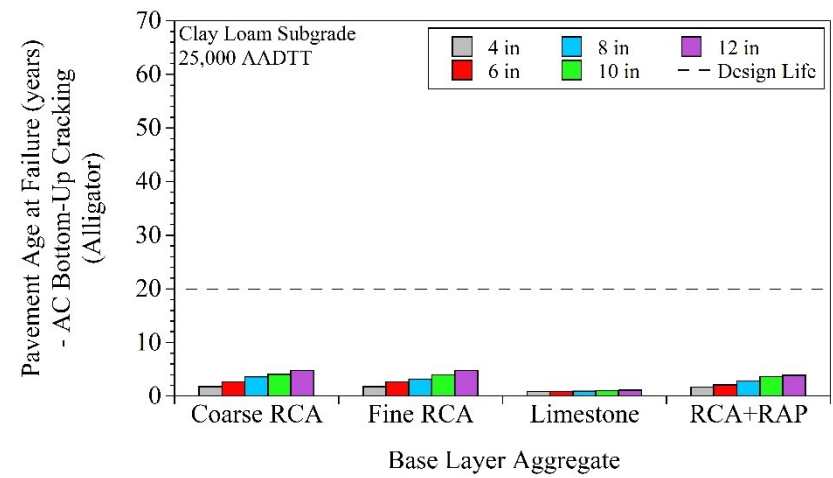
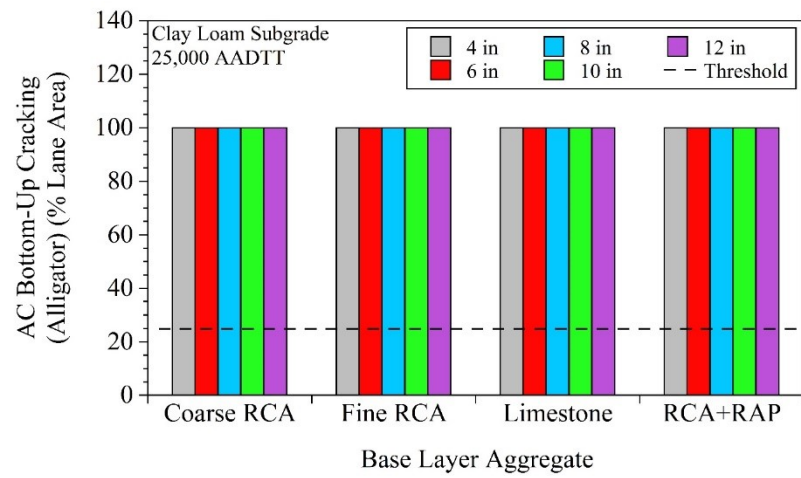
For pavements that contained Clay Loam subgrade - 7,500 AADTT:





For pavements that contained Clay Loam subgrade - 25,000 AADTT:

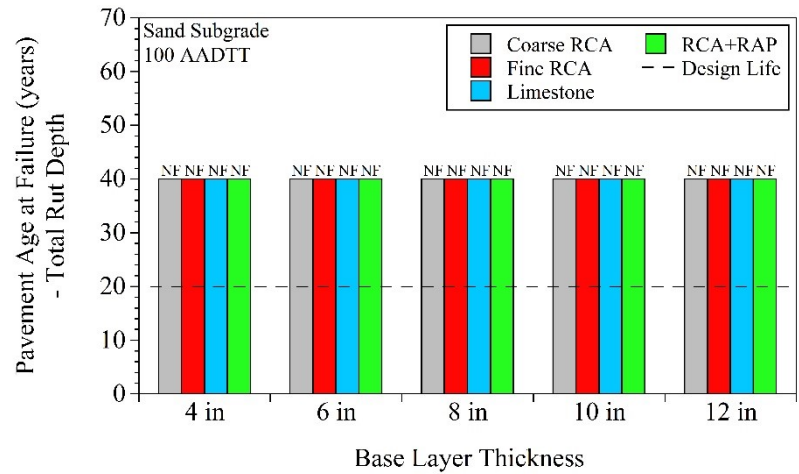
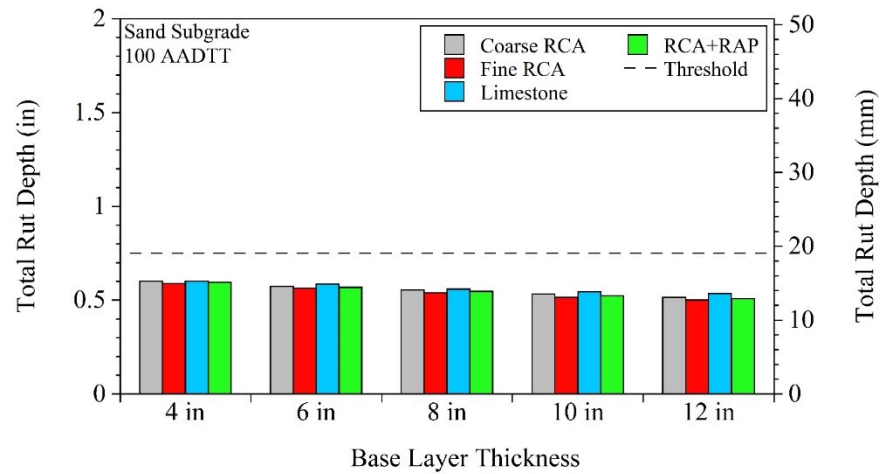
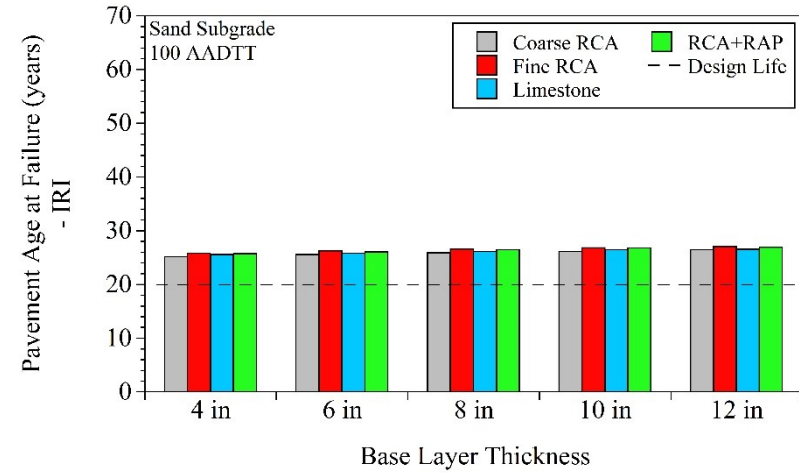
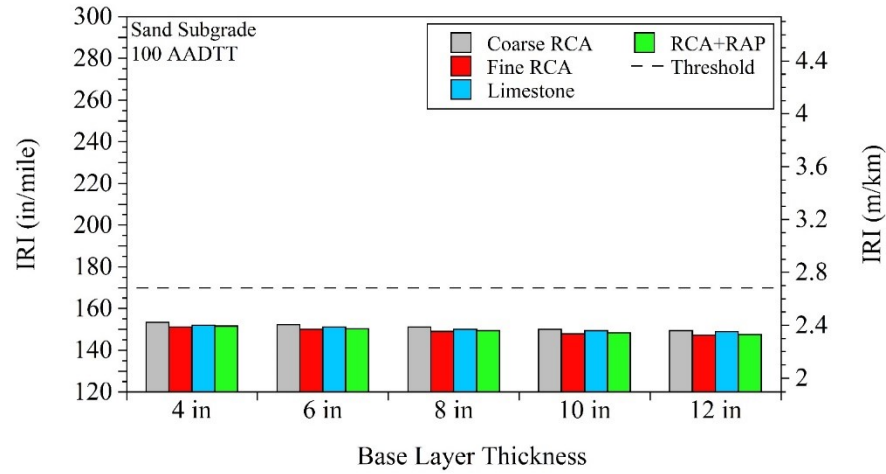


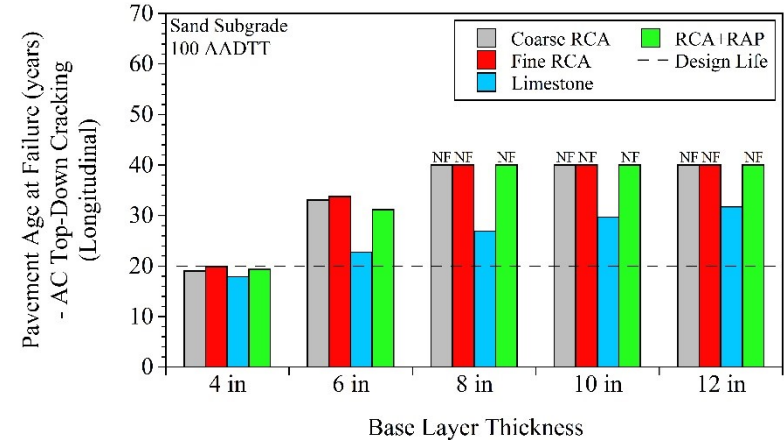
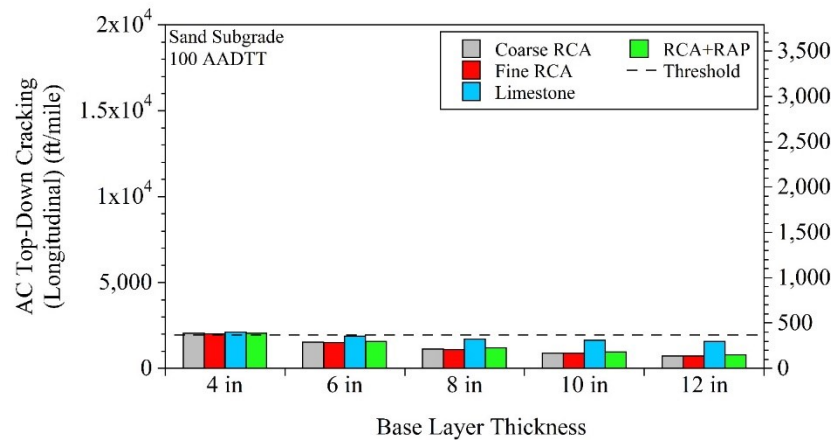
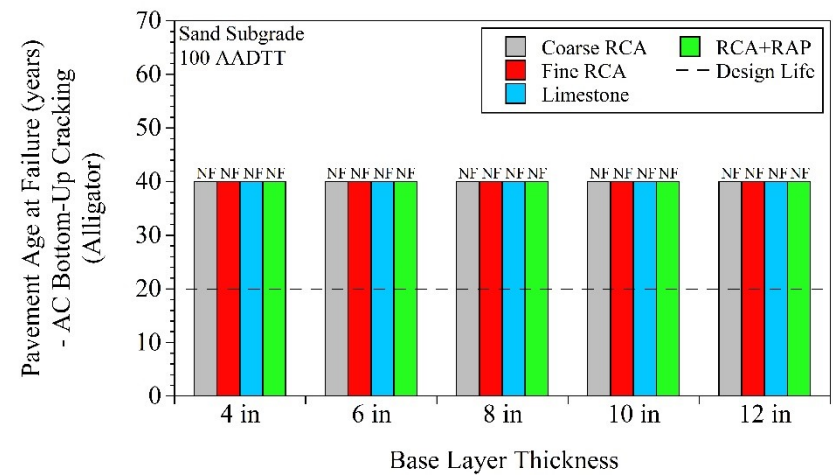
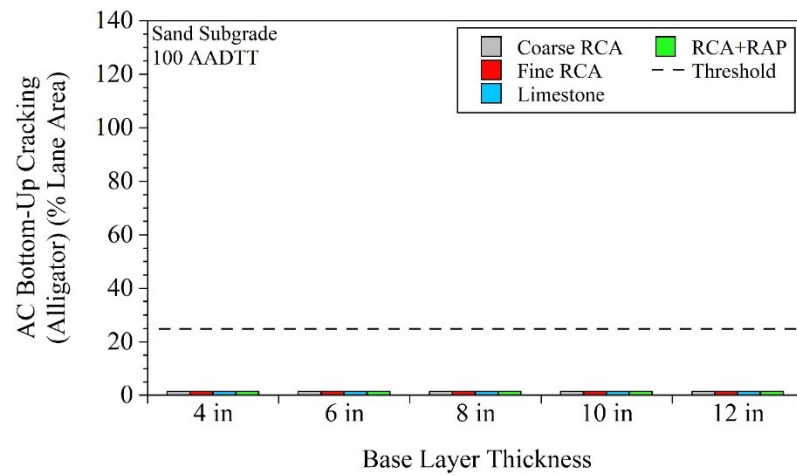


APPENDIX BB

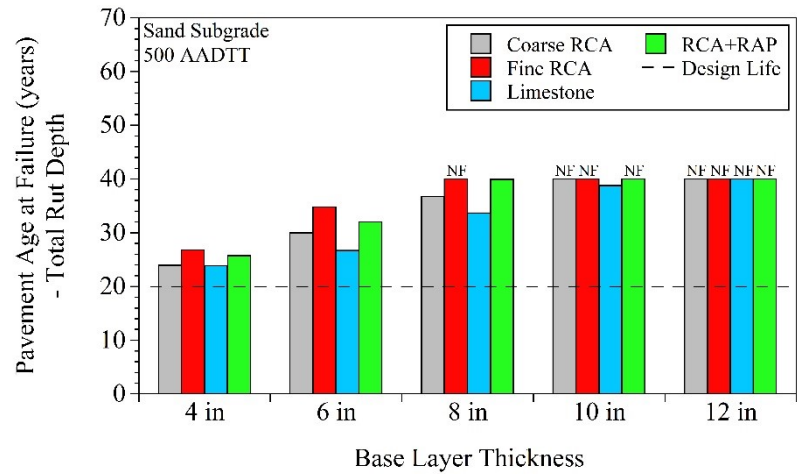
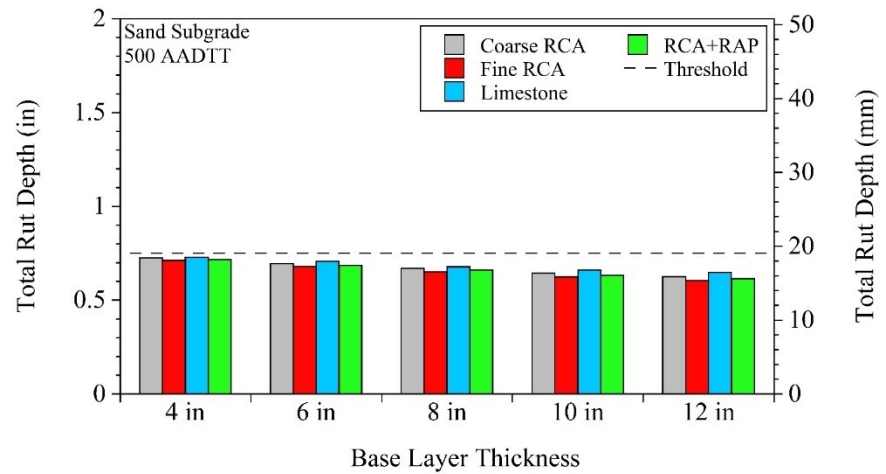
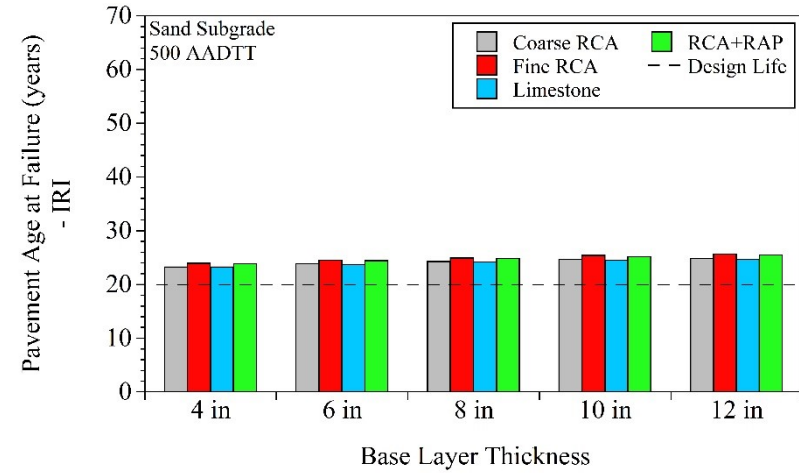
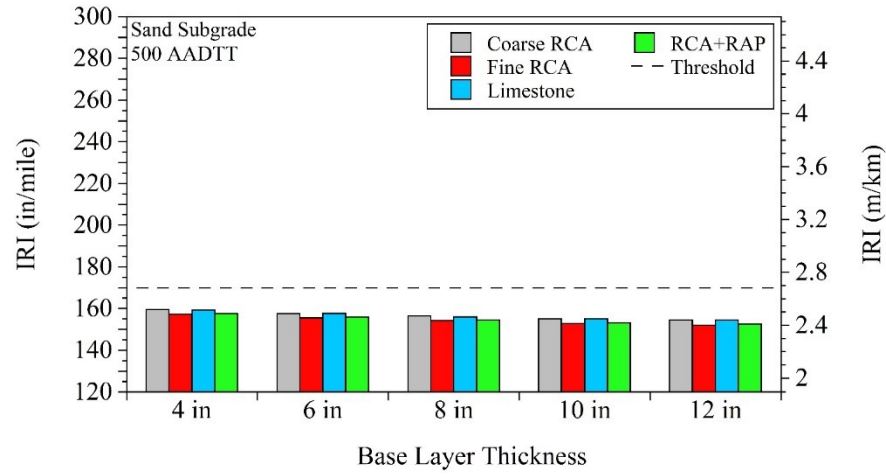
EFFECT OF BASE LAYER AGGREGATE TYPE ON PAVEMENT PERFORMANCE PREDICTIONS

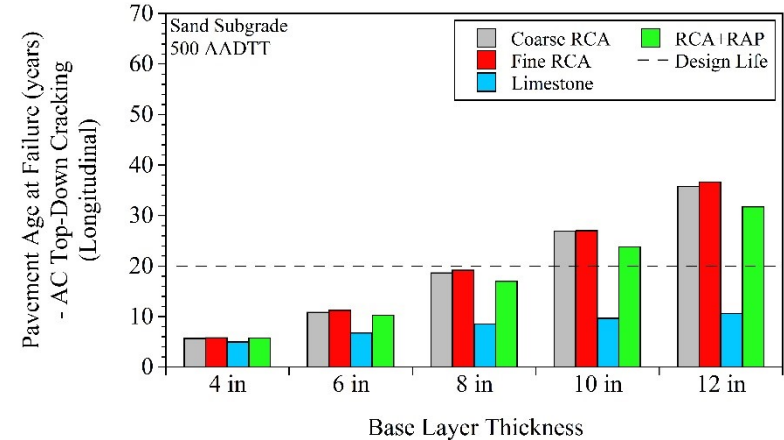
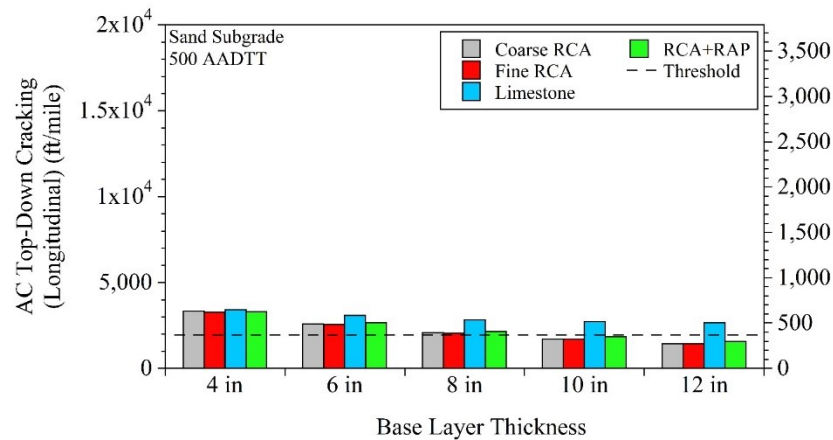
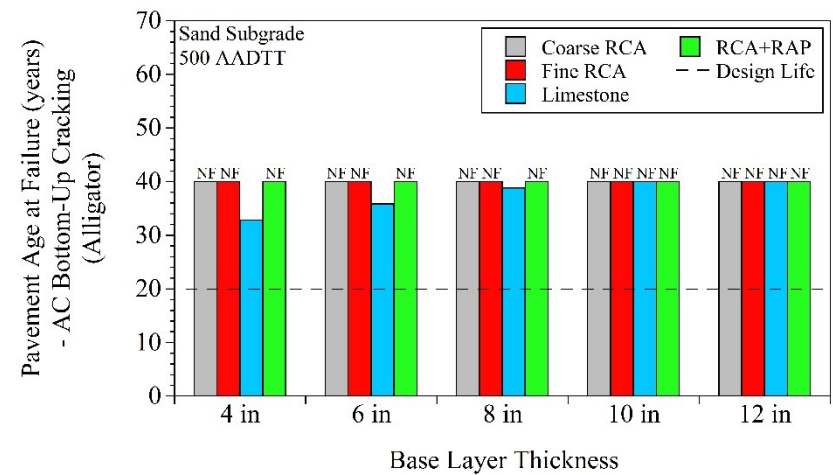
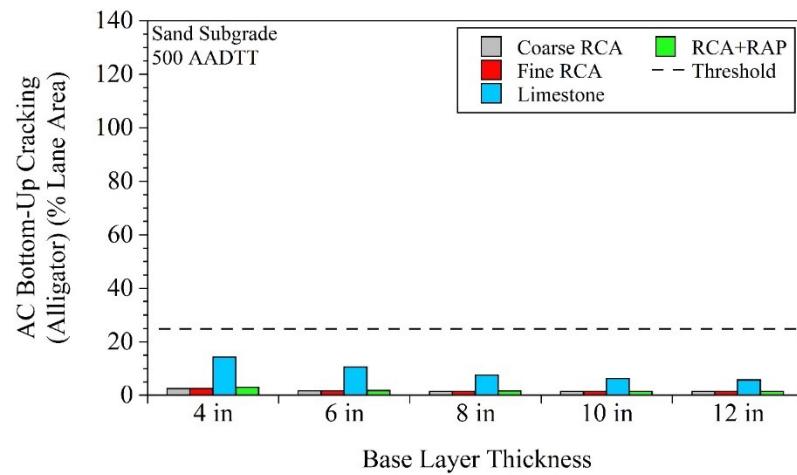
For pavements that contained Sand Subgrade - 100 AADTT:



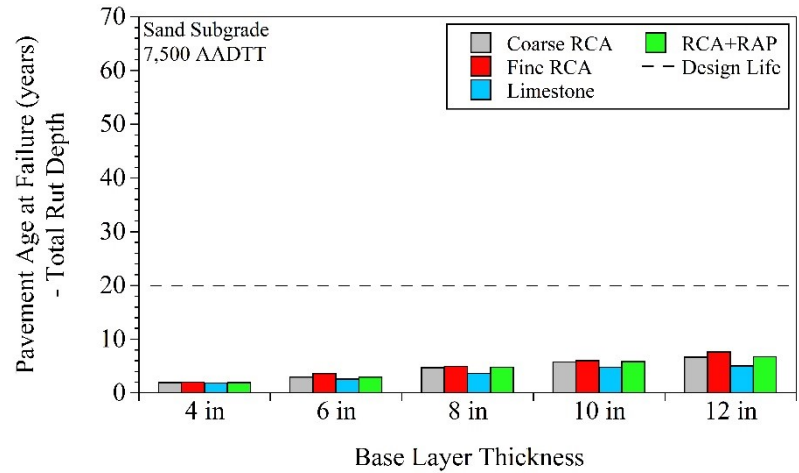
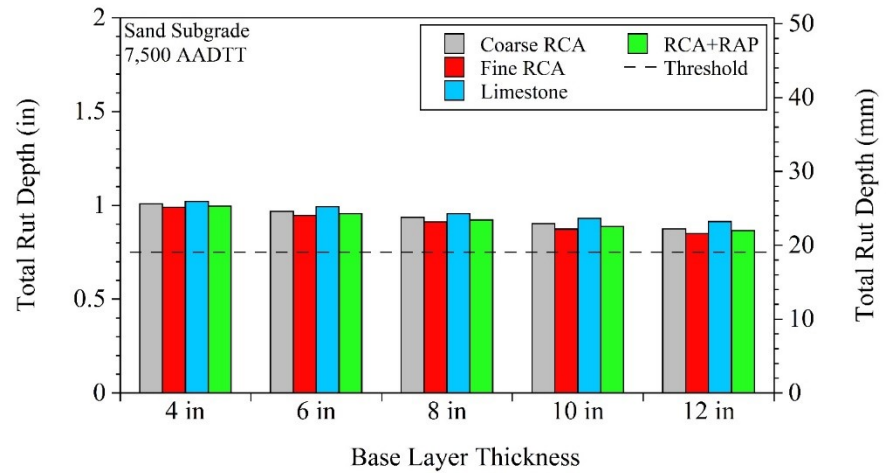
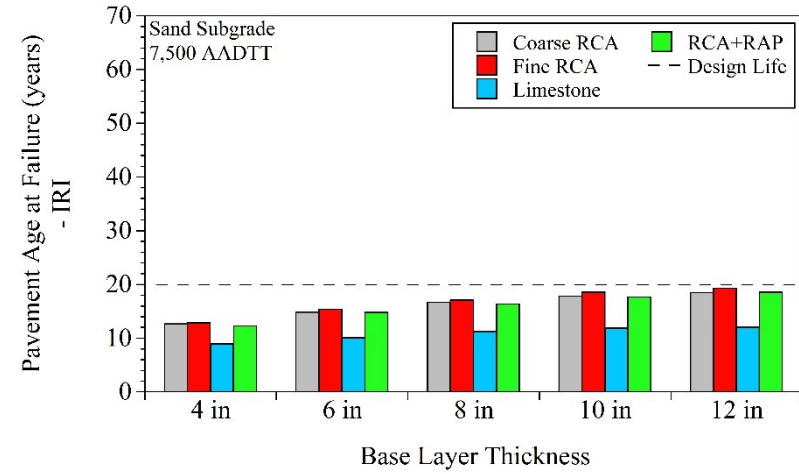
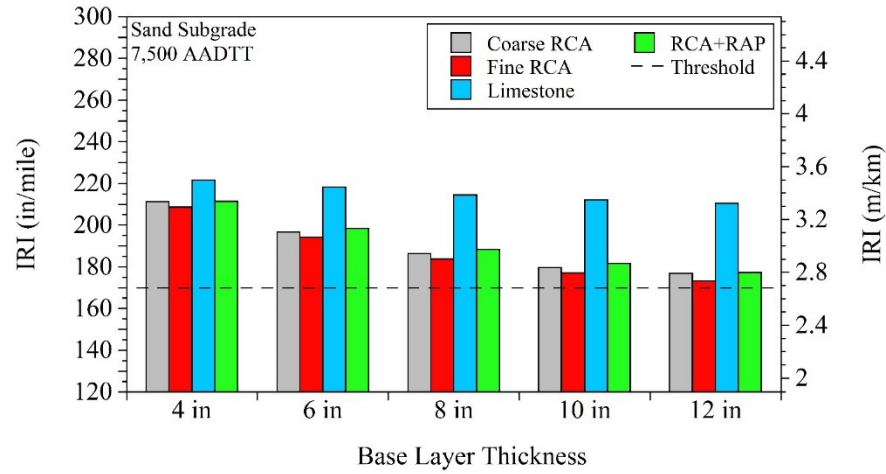


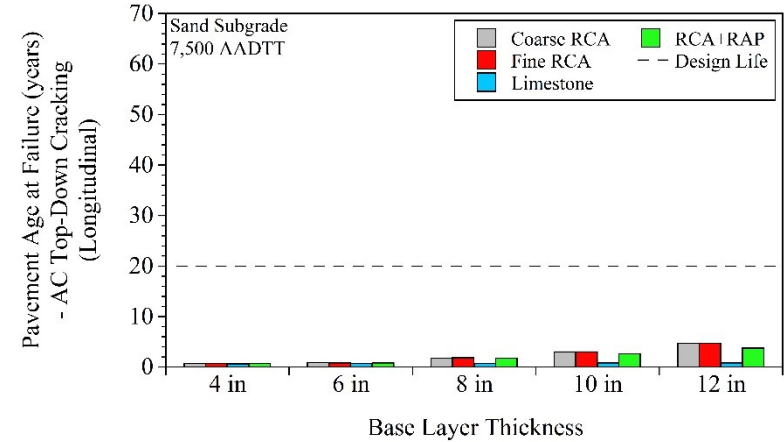
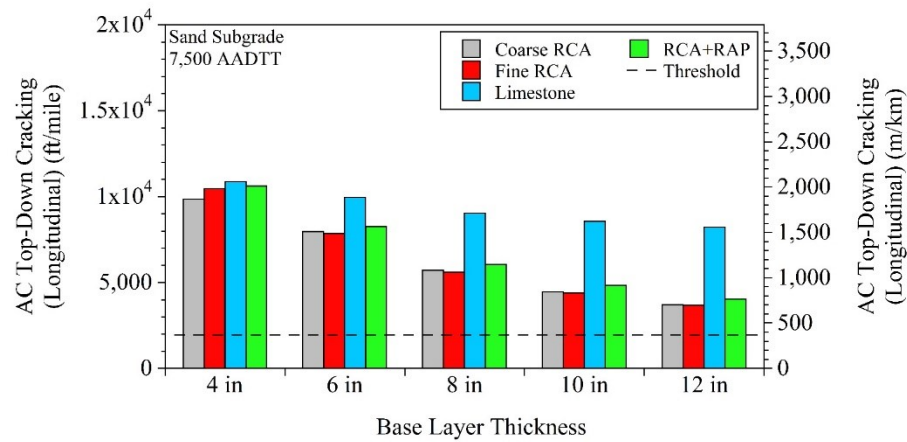
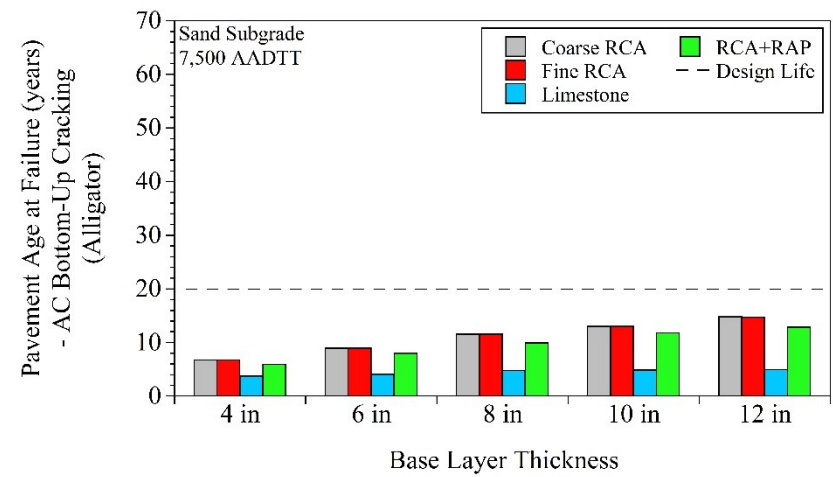
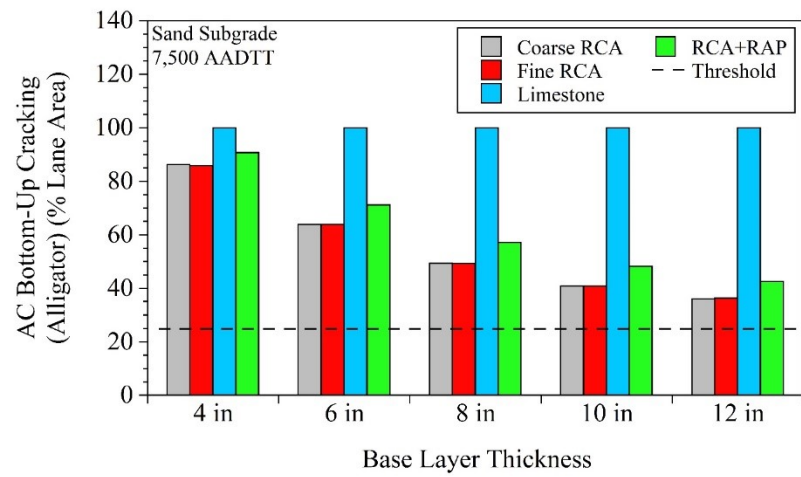
For pavements that contained Sand Subgrade - 500 AADTT:



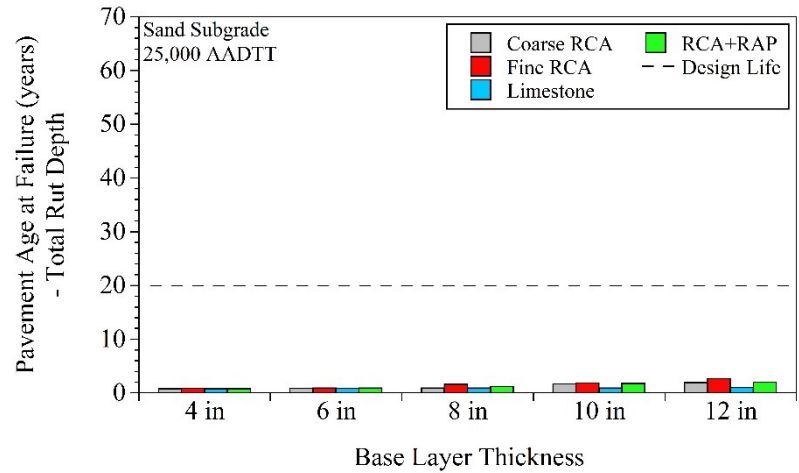
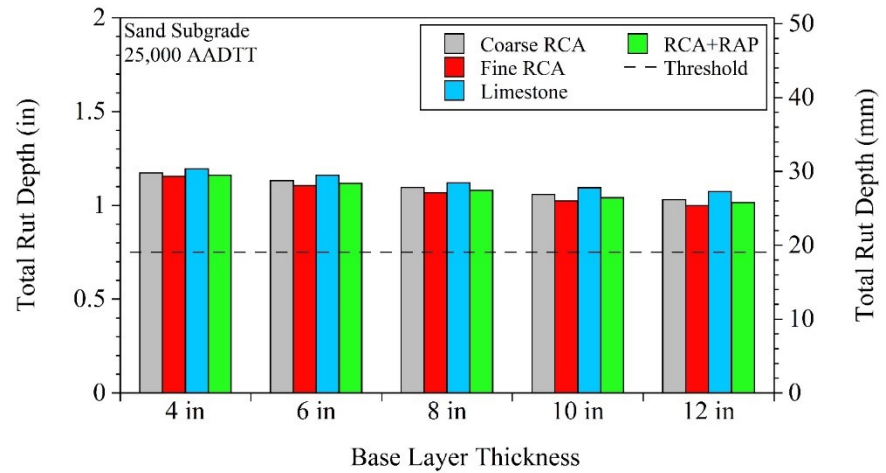
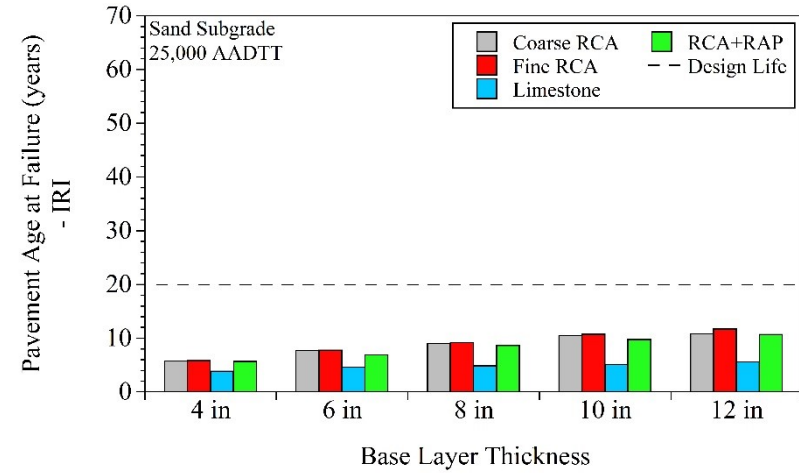
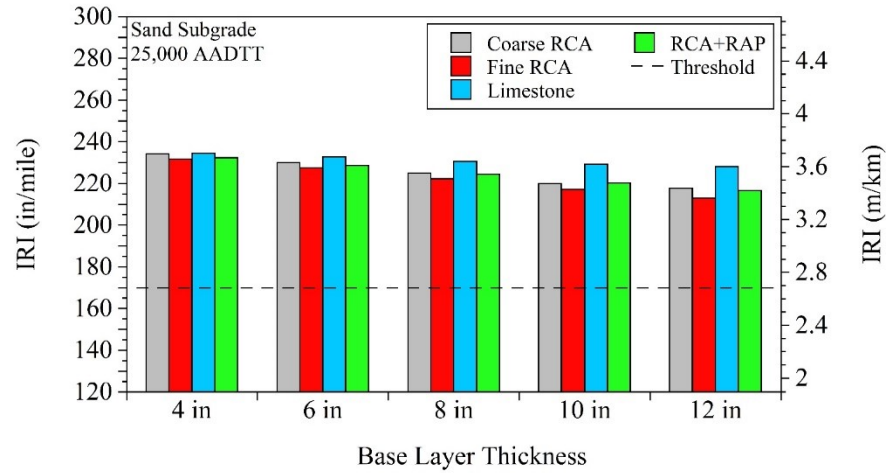


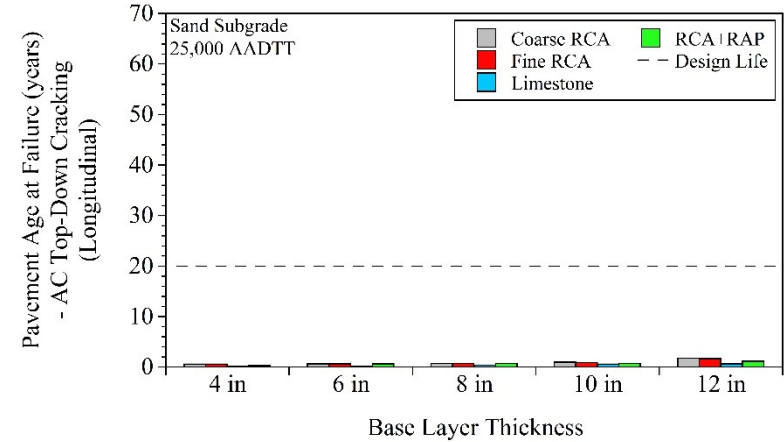
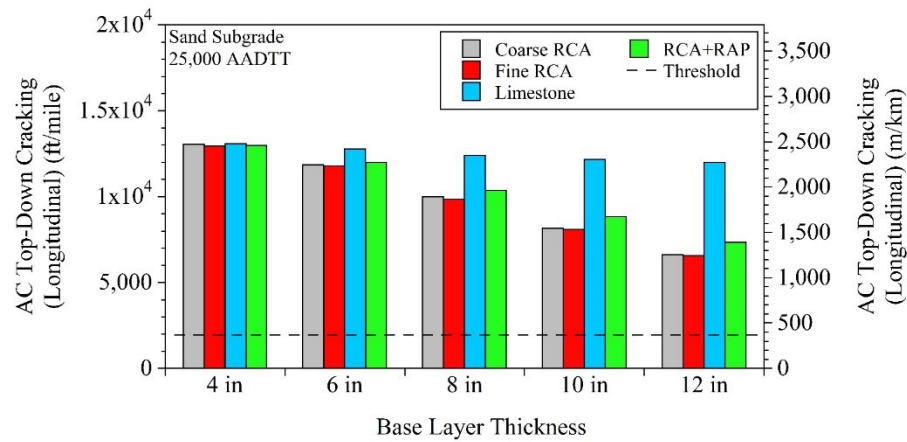
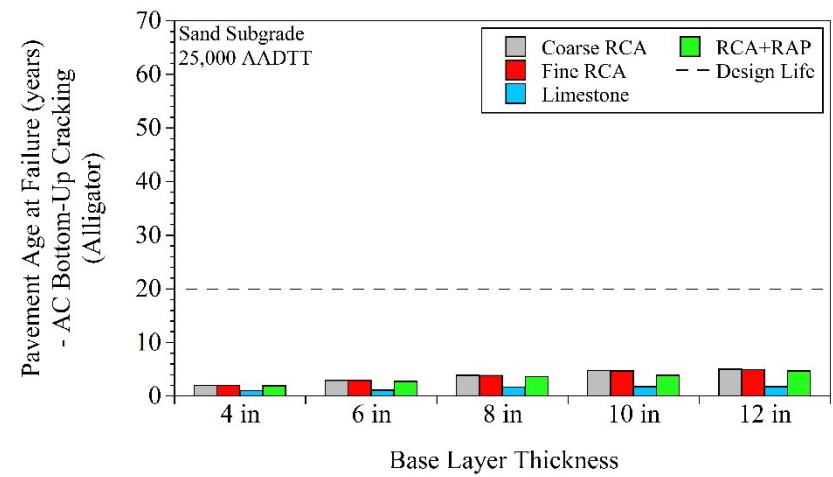
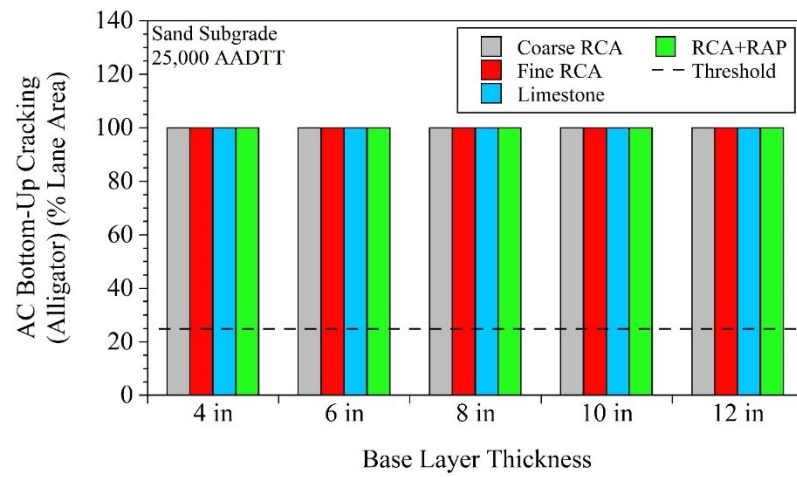
For pavements that contained Sand Subgrade - 7,500 AADTT:



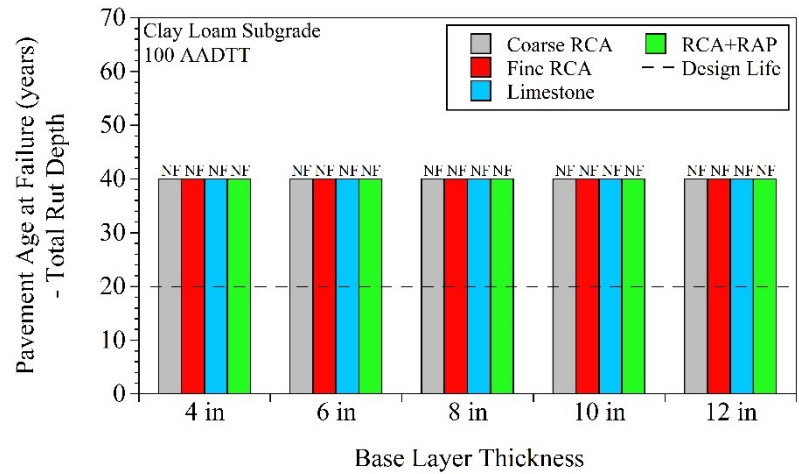
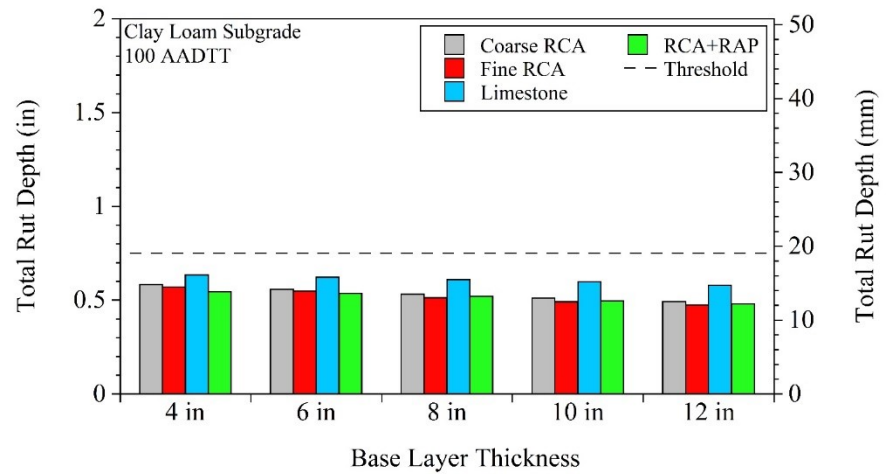
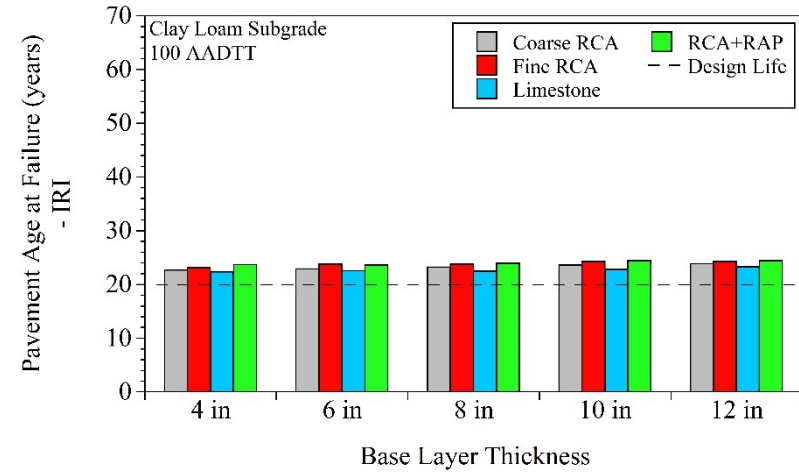
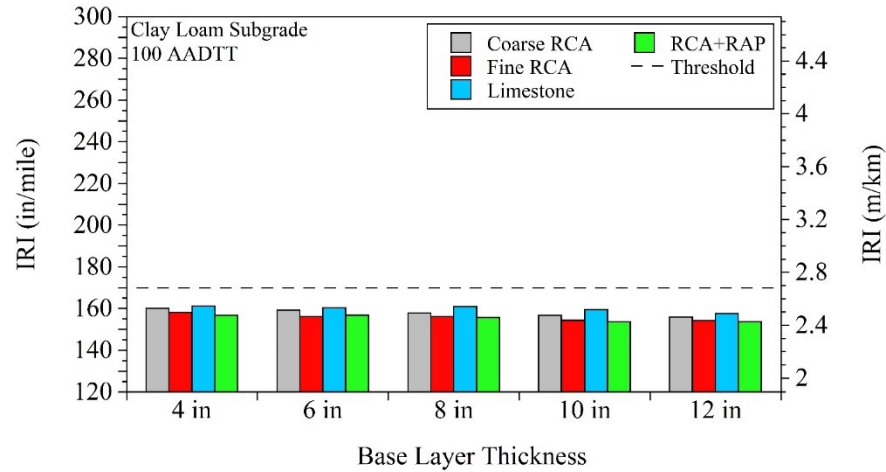


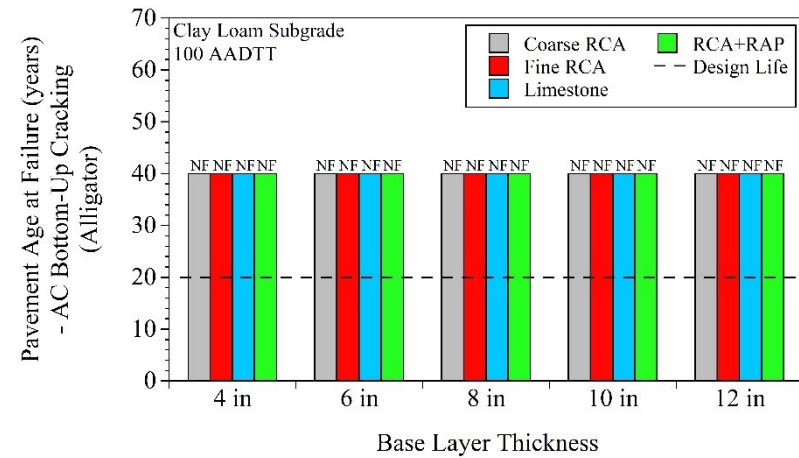
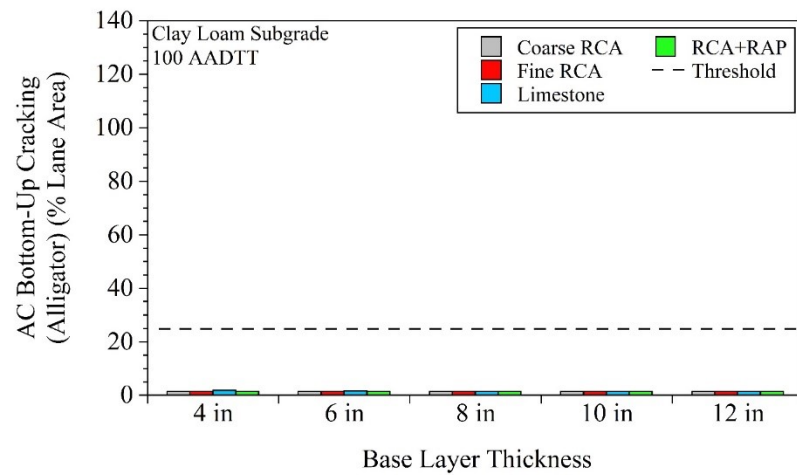
For pavements that contained Sand Subgrade - 25,000 AADTT:



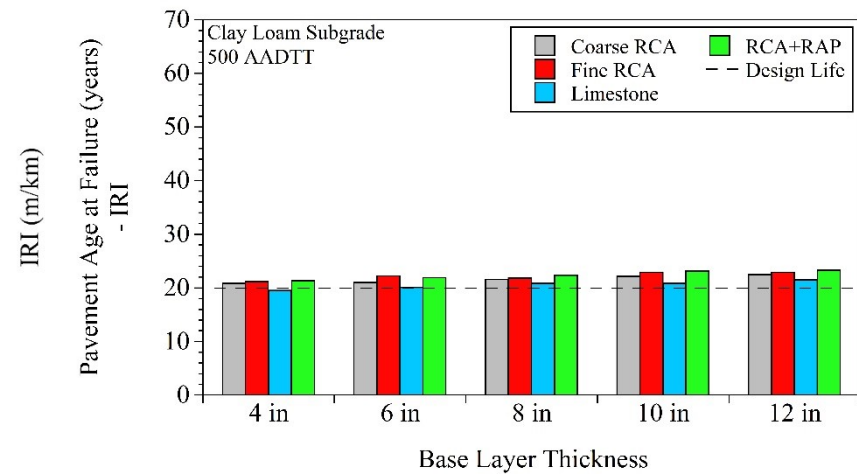
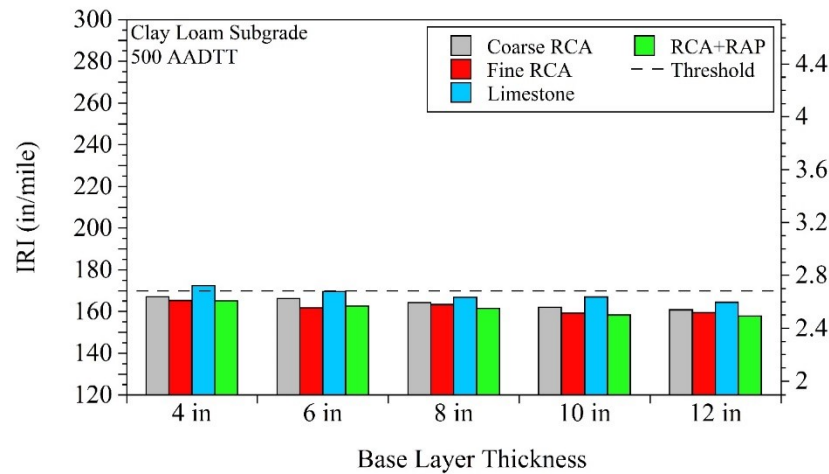


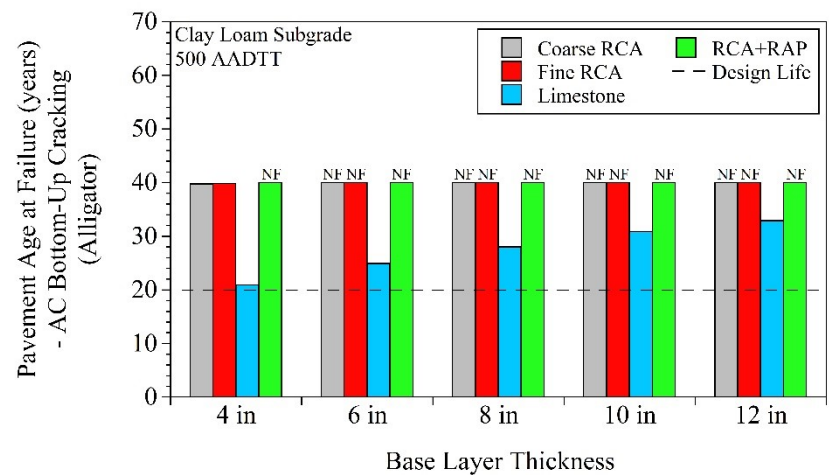
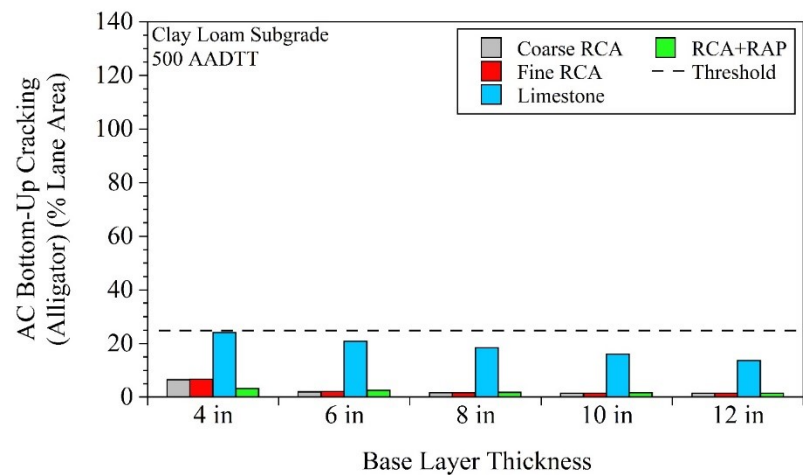
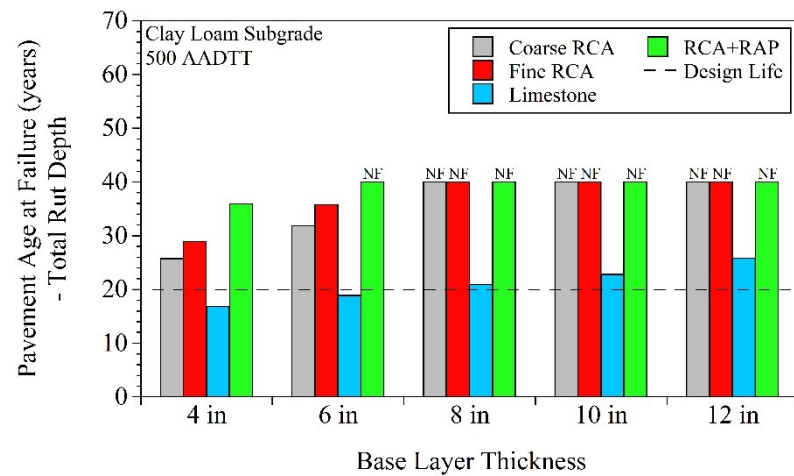
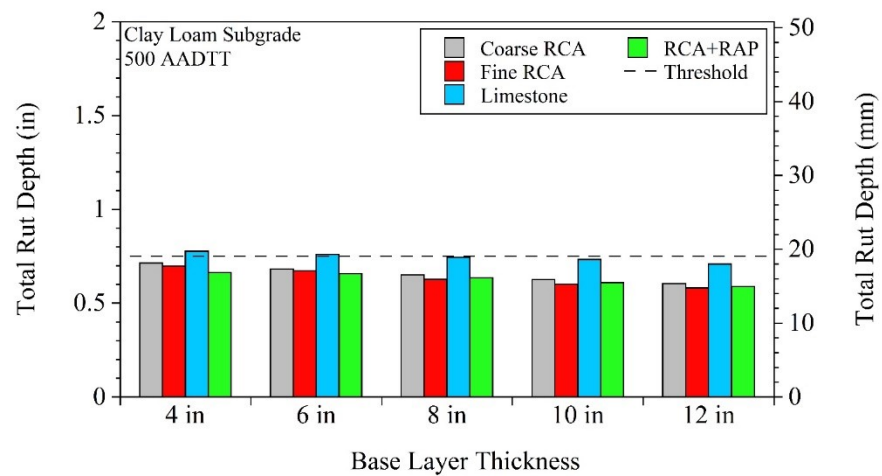
For pavements that contained Clay Loam subgrade - 100 AADTT:



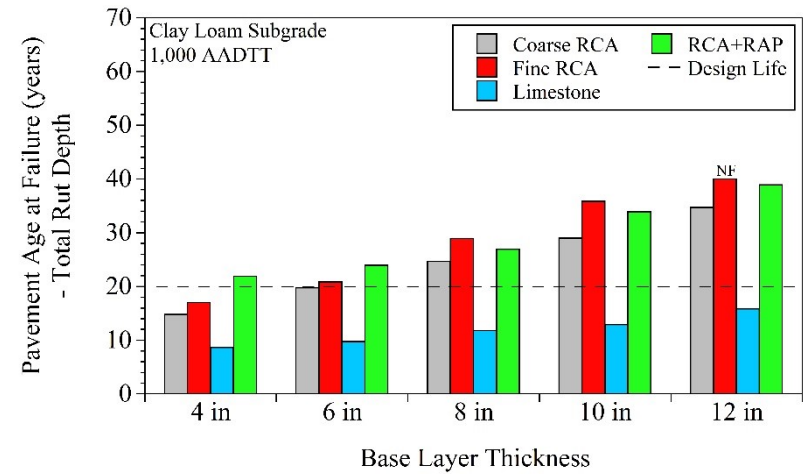
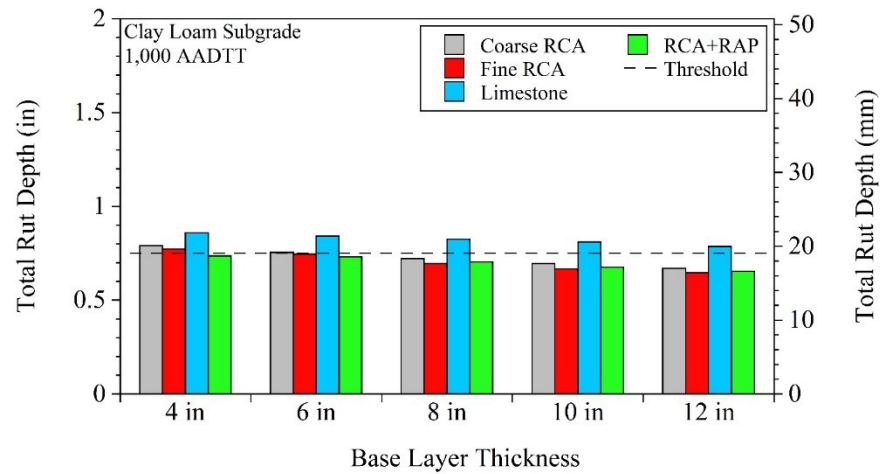
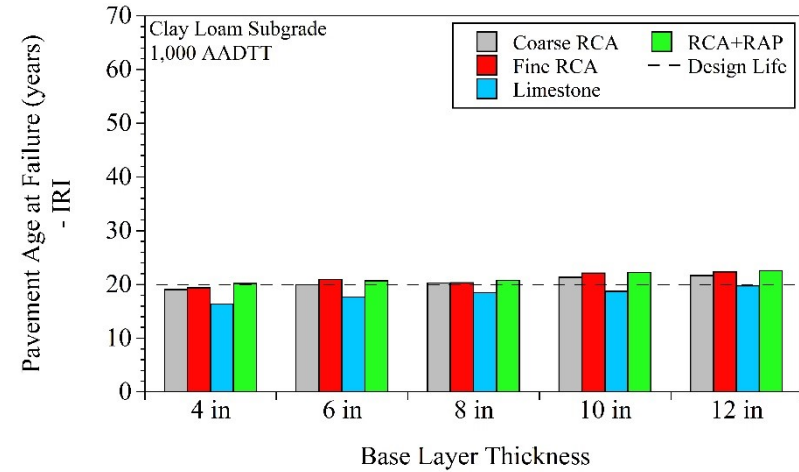
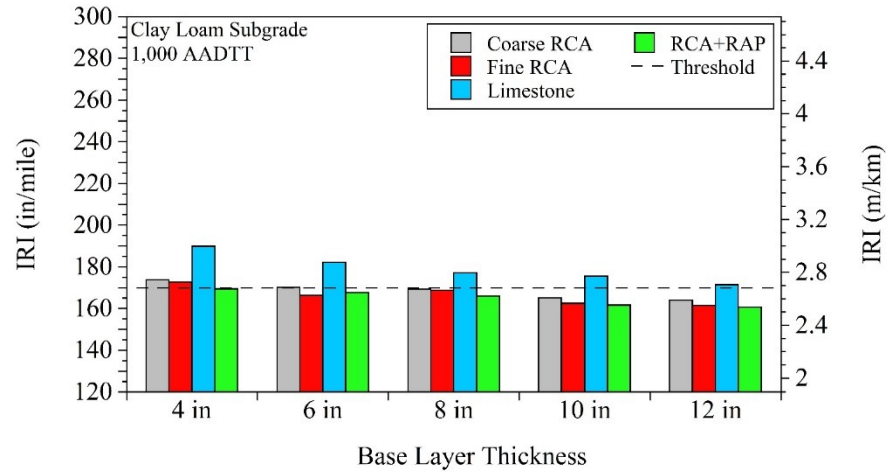


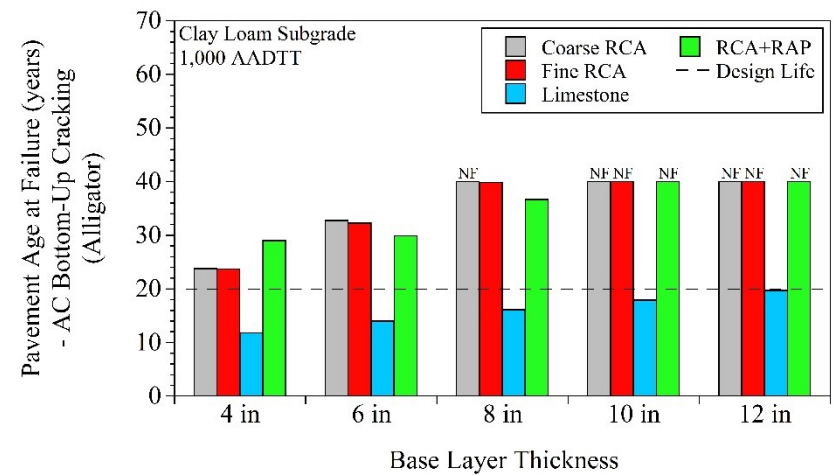
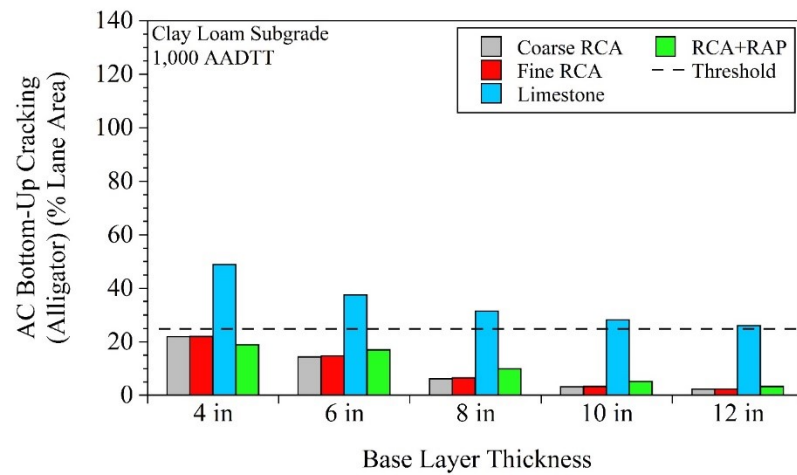
For pavements that contained Clay Loam subgrade - 500 AADTT:



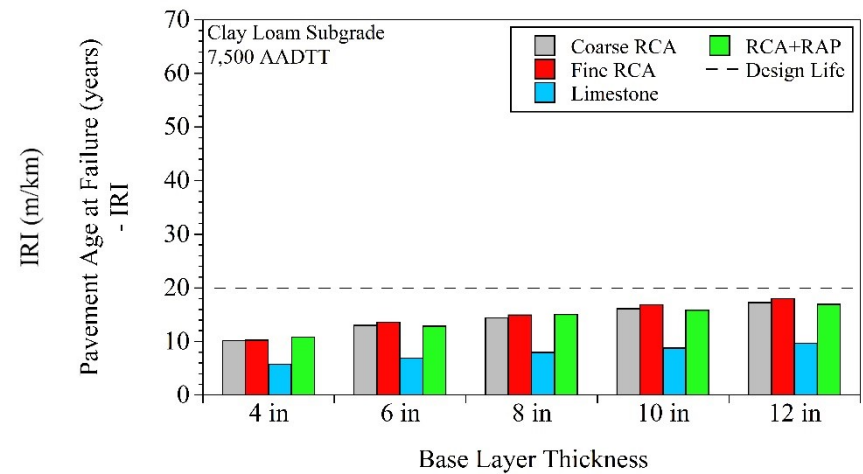
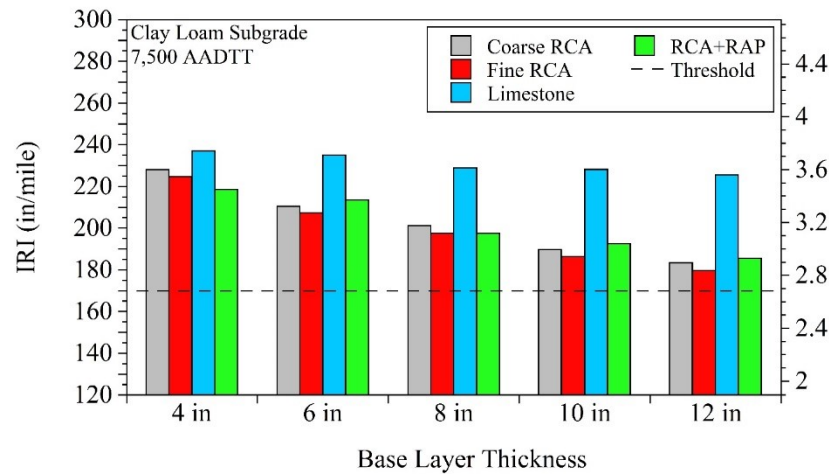


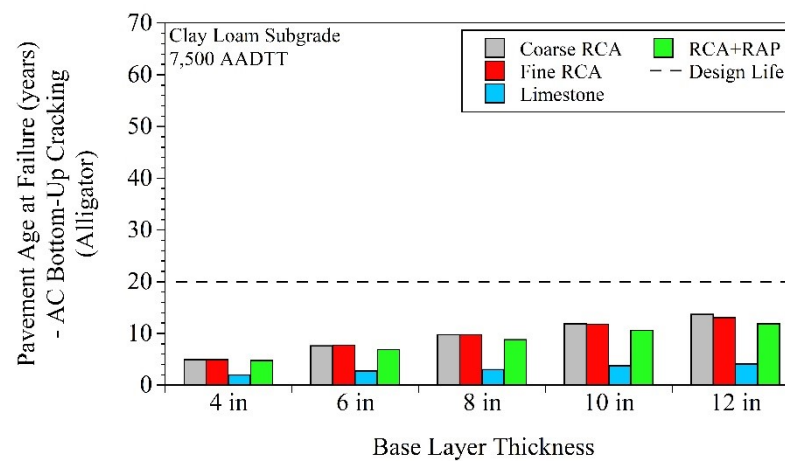
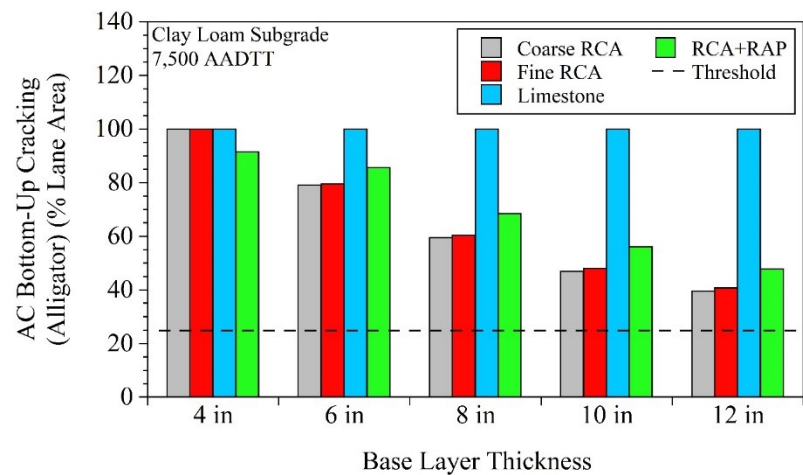
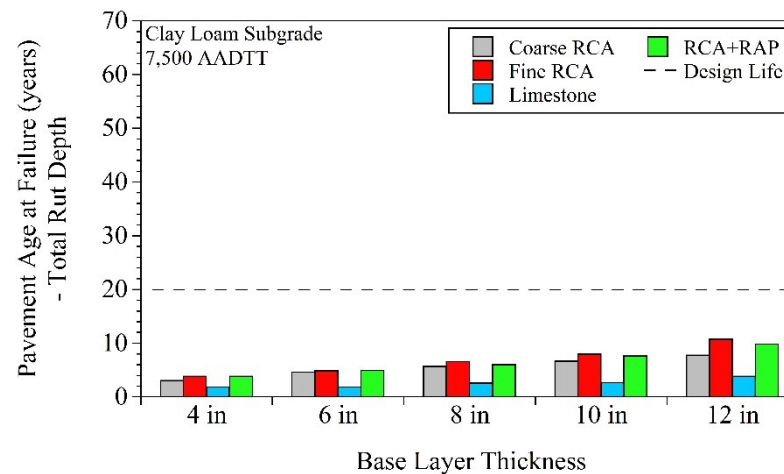
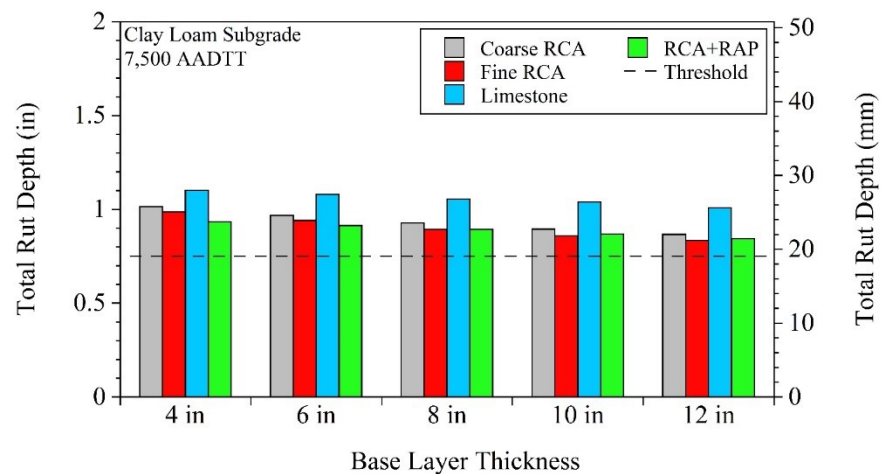
For pavements that contained Clay Loam subgrade - 1,000 AADTT:



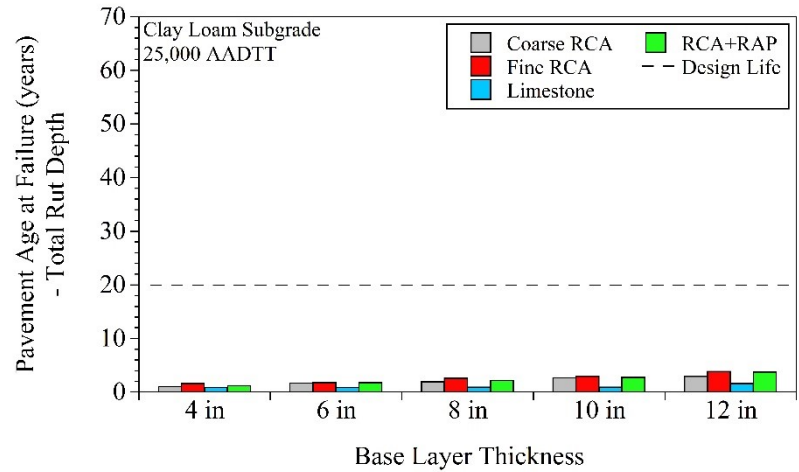
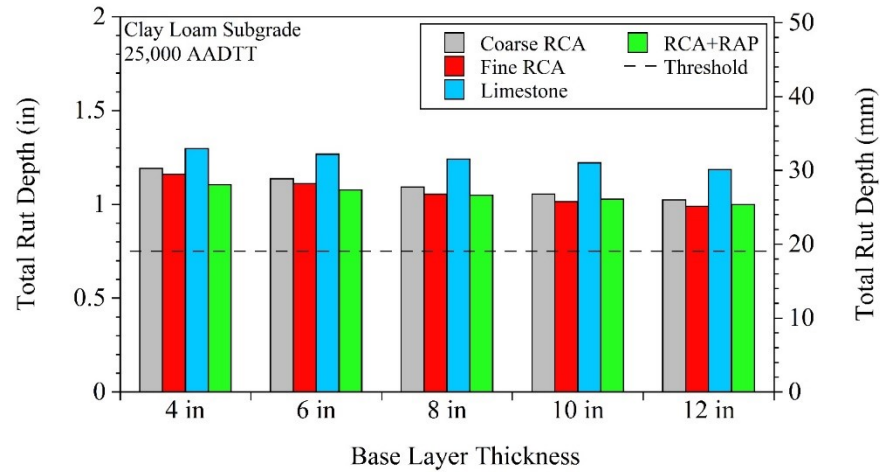
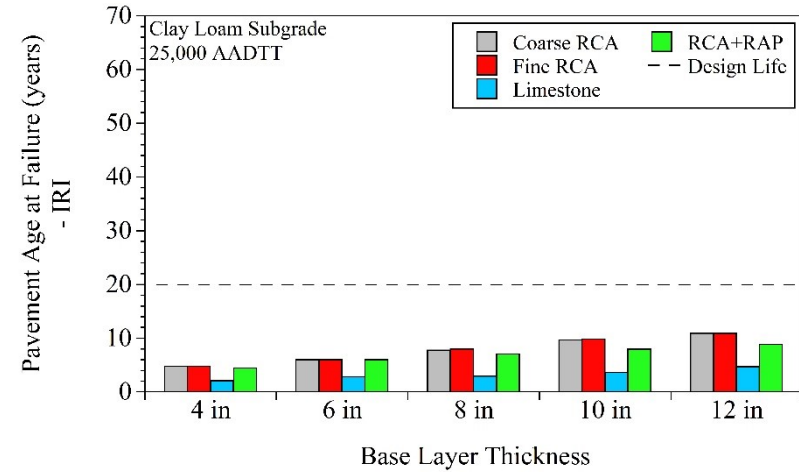
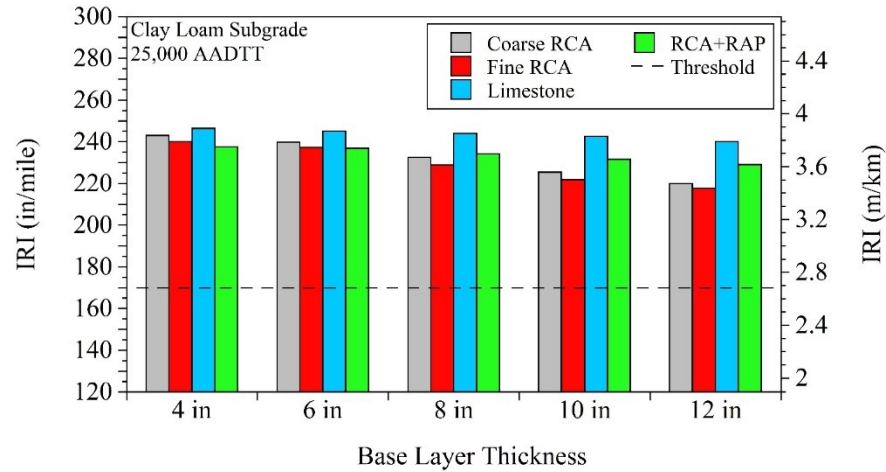


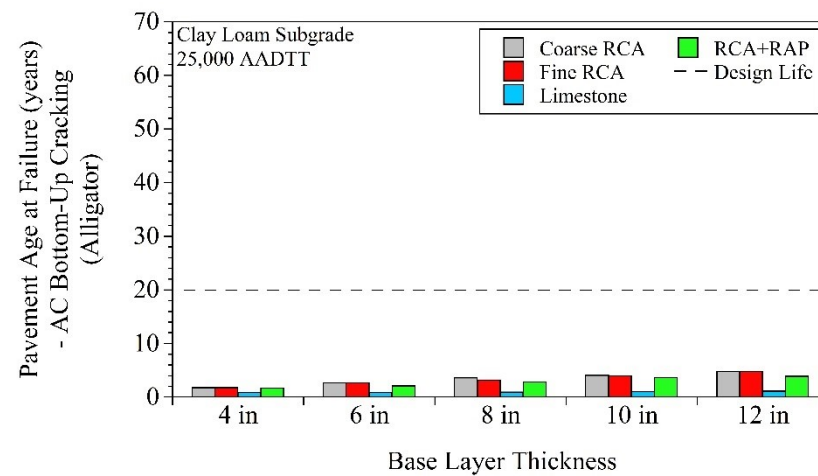
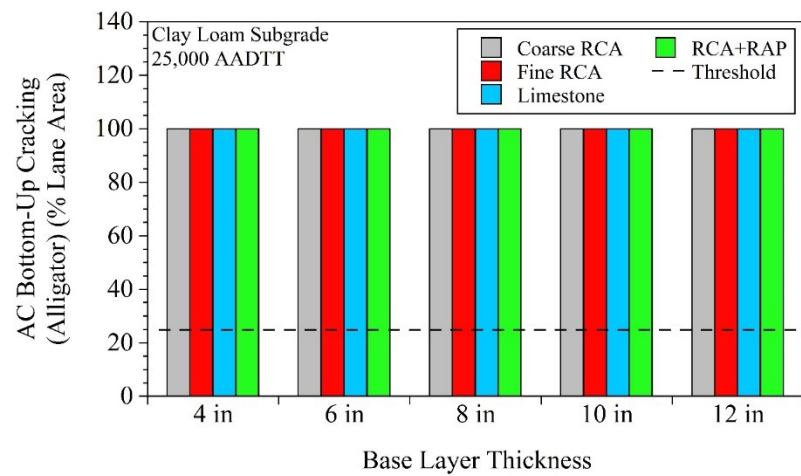
For pavements that contained Clay Loam subgrade - 7,500 AADTT:





For pavements that contained Clay Loam subgrade - 25,000 AADTT:

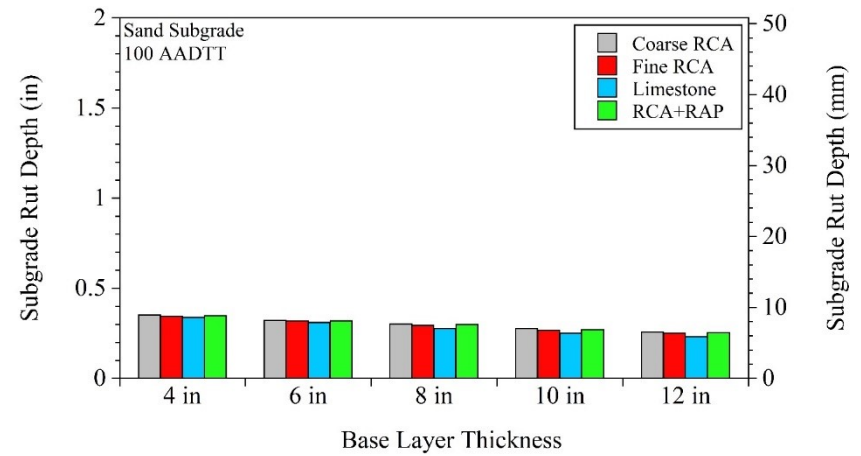
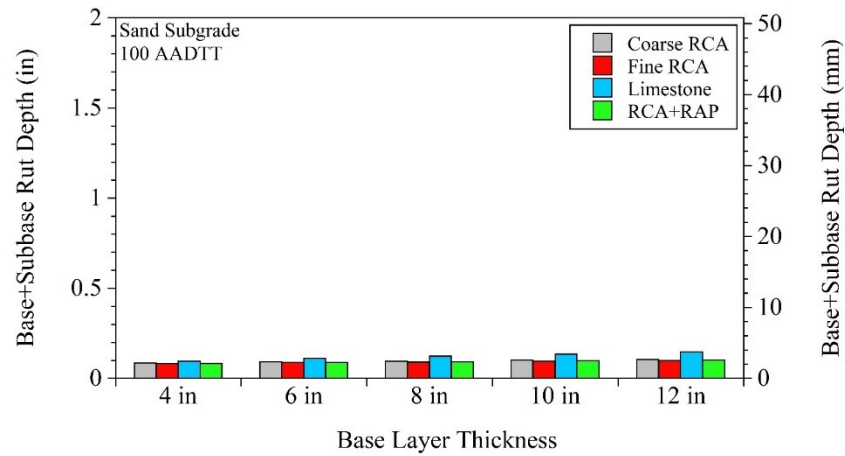
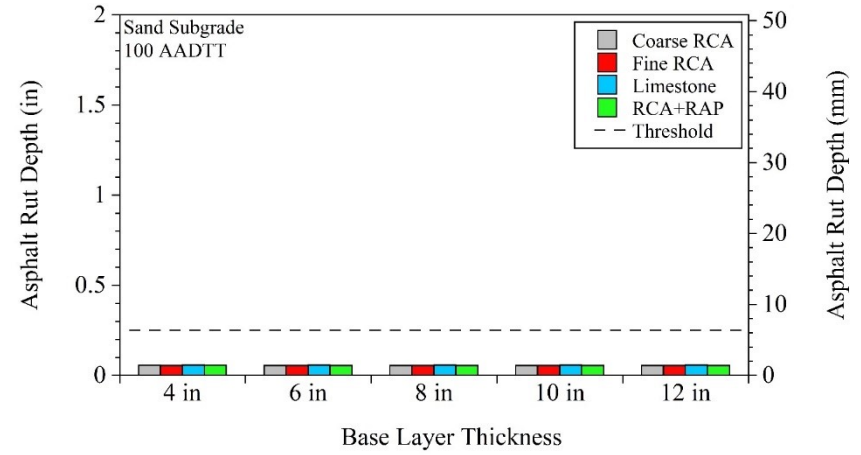
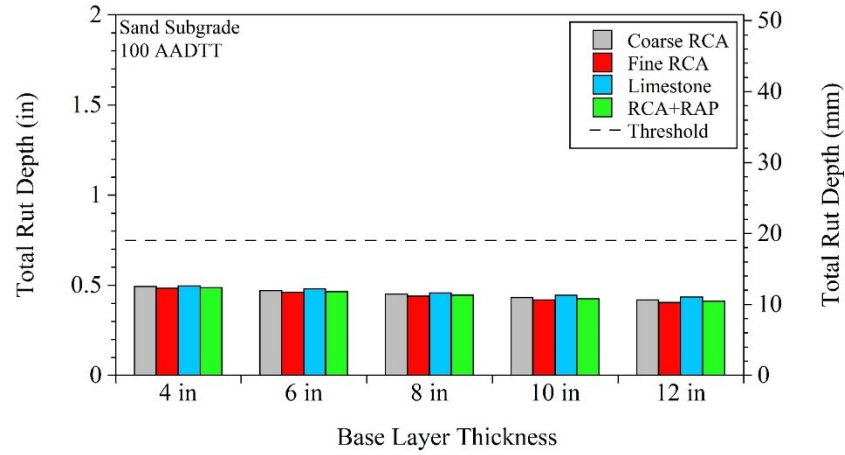




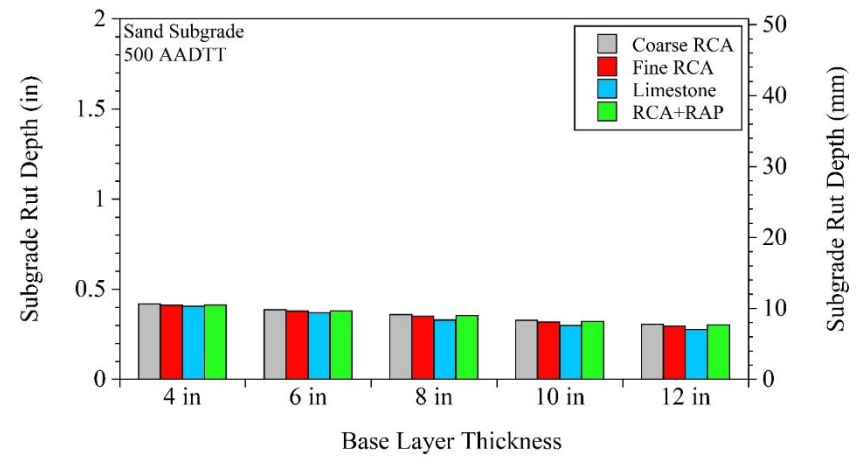
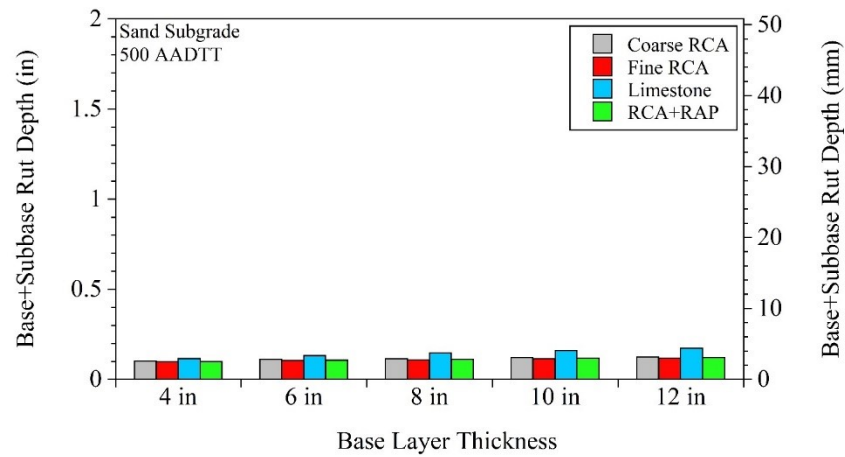
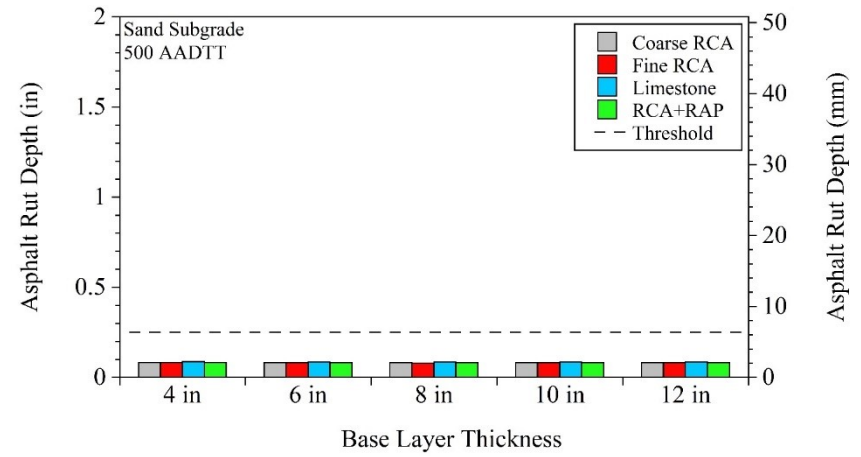
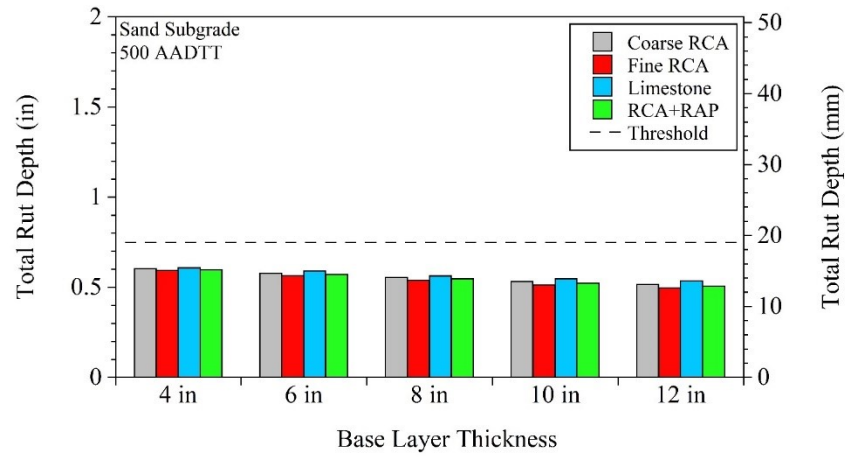
APPENDIX BC

TOTAL, ASPHALT, BASE+SUBBASE, AND SUBGRADE LAYER RUTTING AT 50% RELIABILITY FOR RECYCLED AGGREGATE BASE (RAB) GROUP

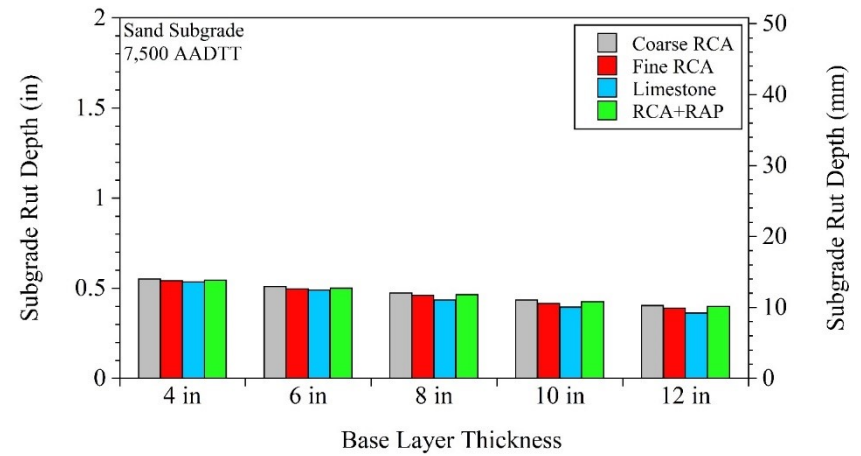
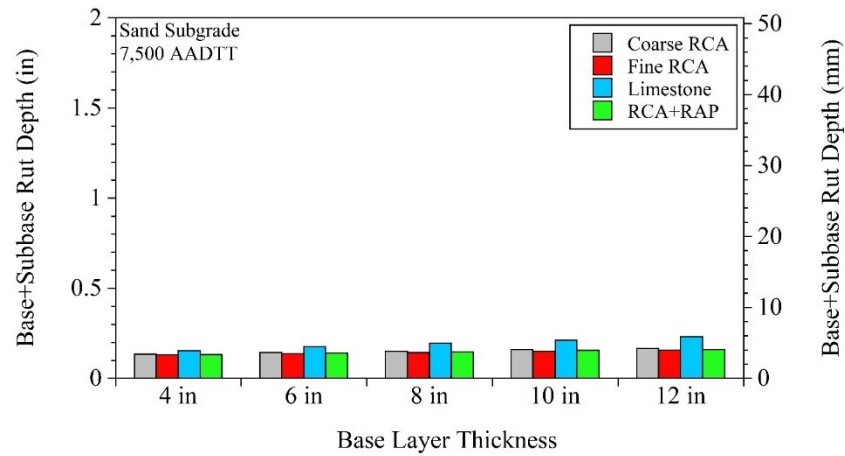
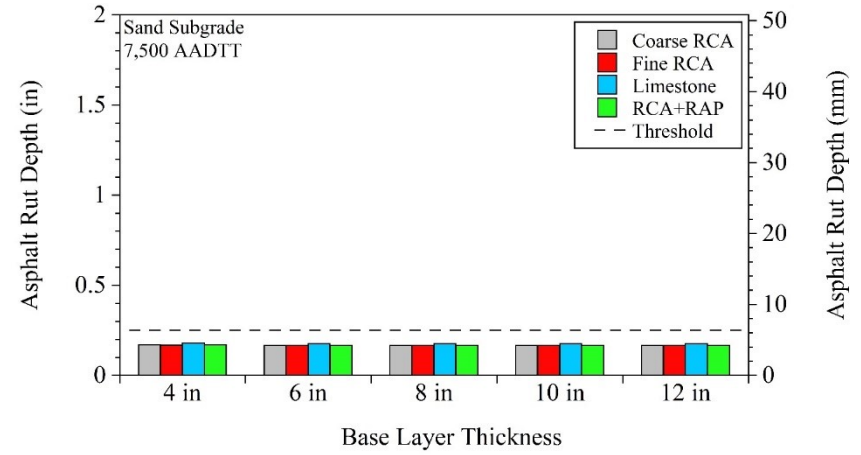
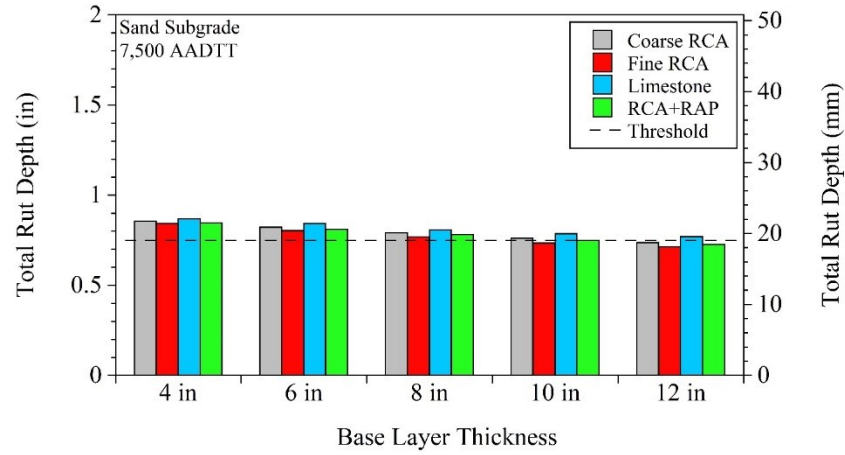
For pavements that contained Sand Subgrade - 100 AADTT:



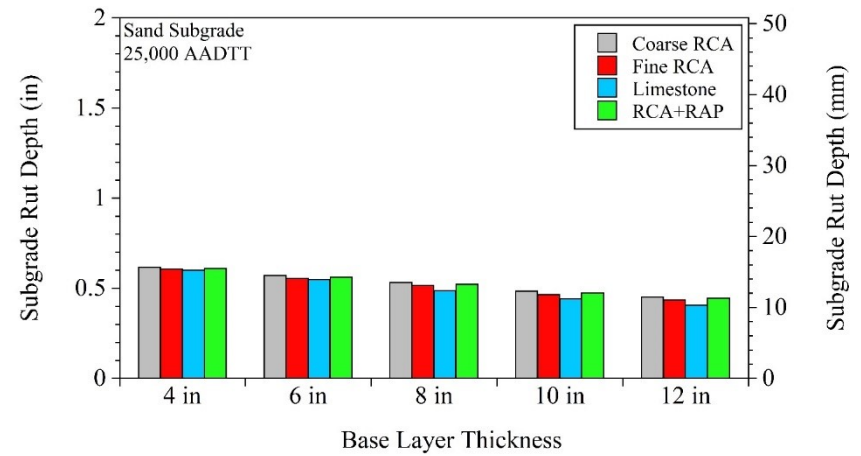
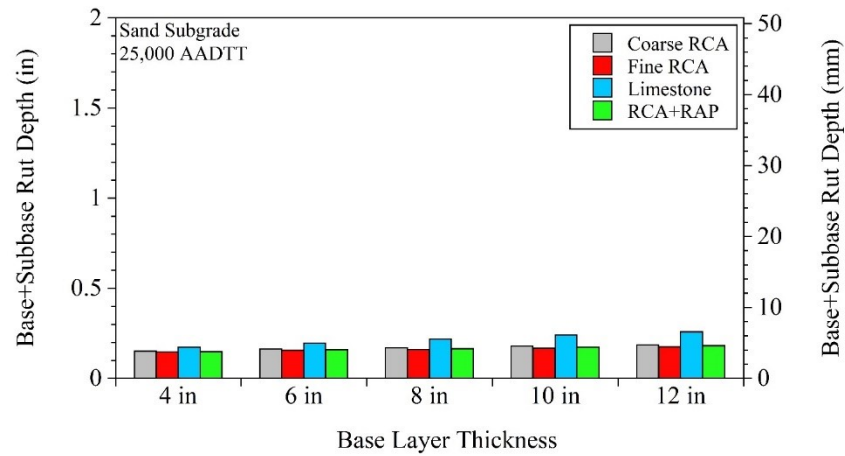
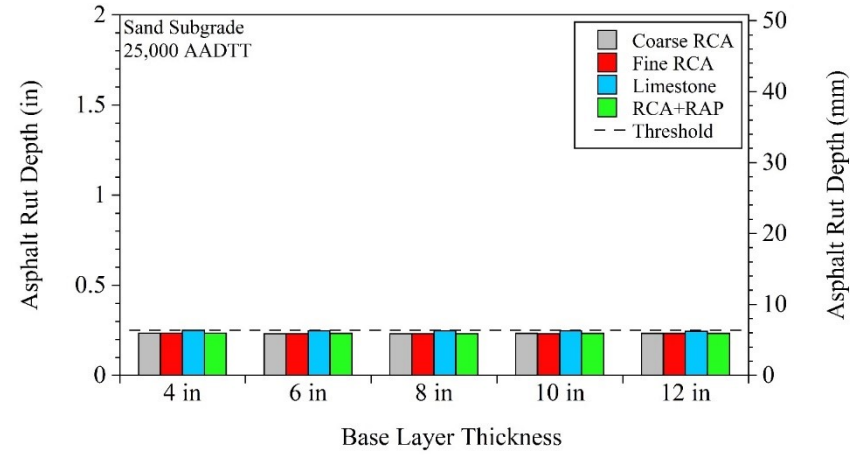
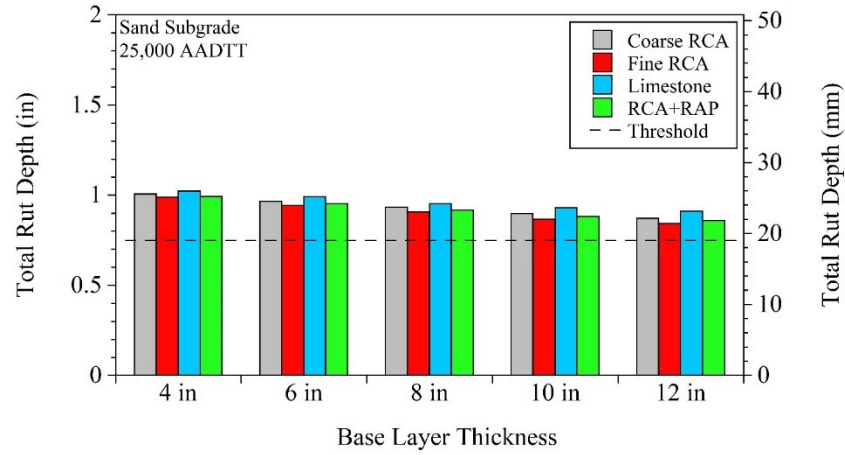
For pavements that contained Sand Subgrade - 500 AADTT:



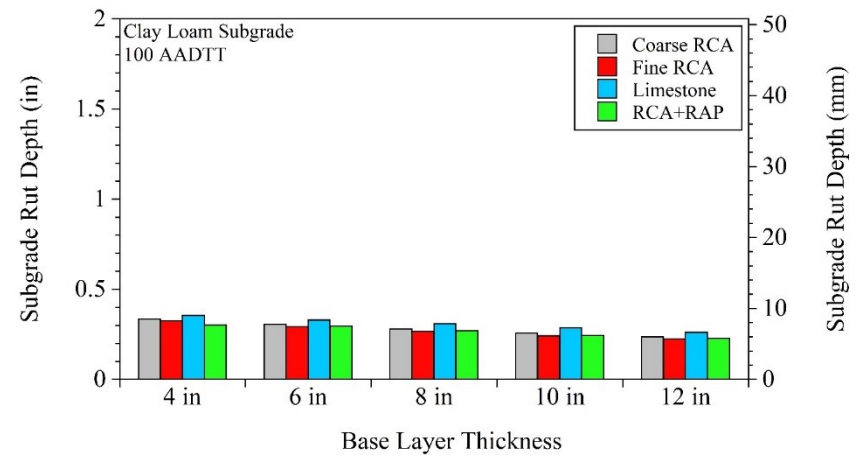
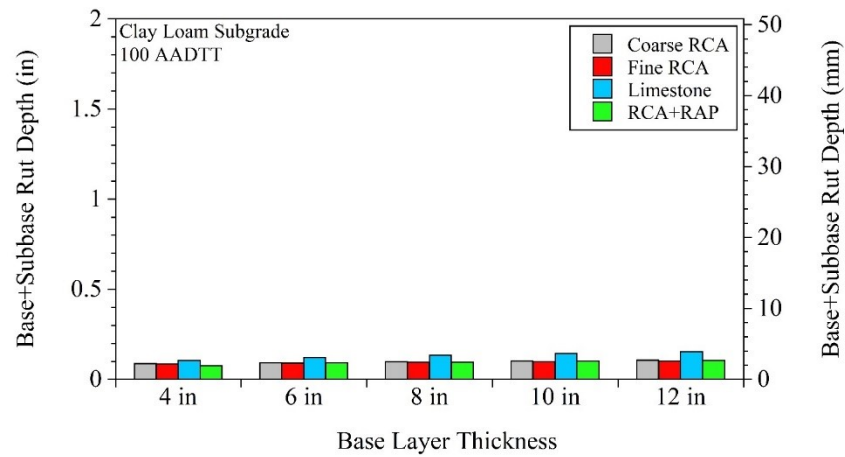
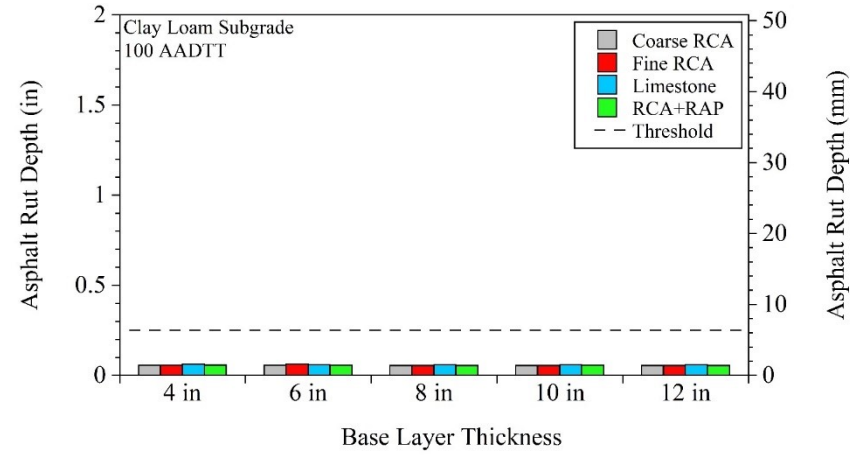
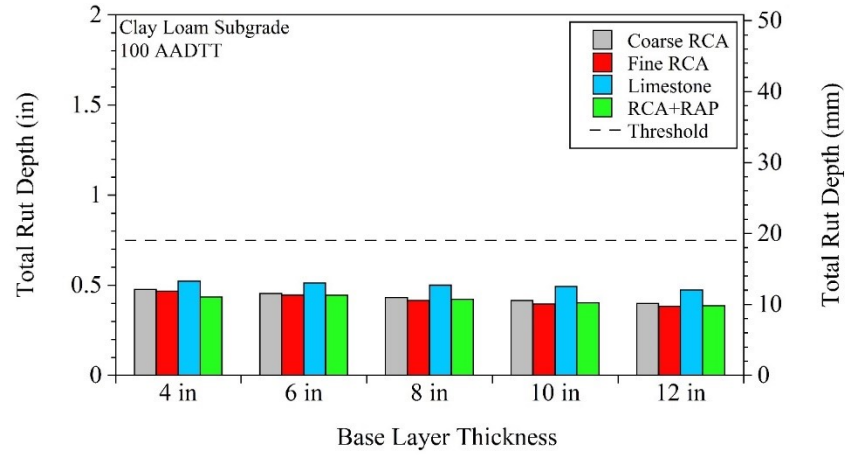
For pavements that contained Sand Subgrade - 7,500 AADTT:



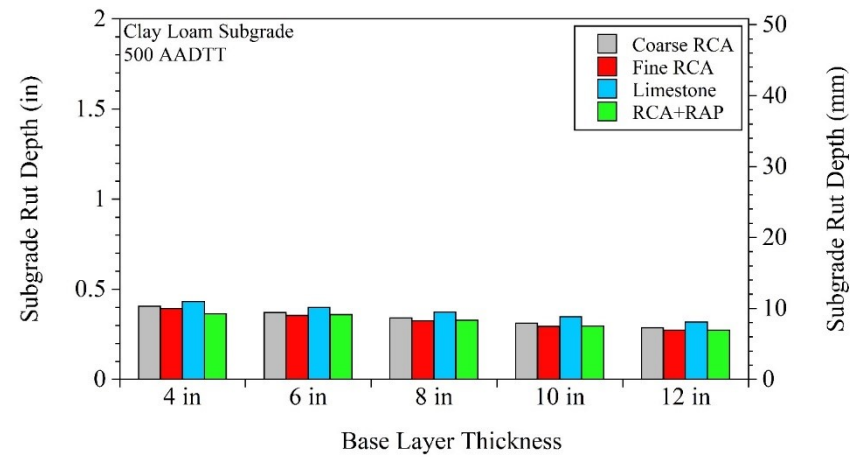
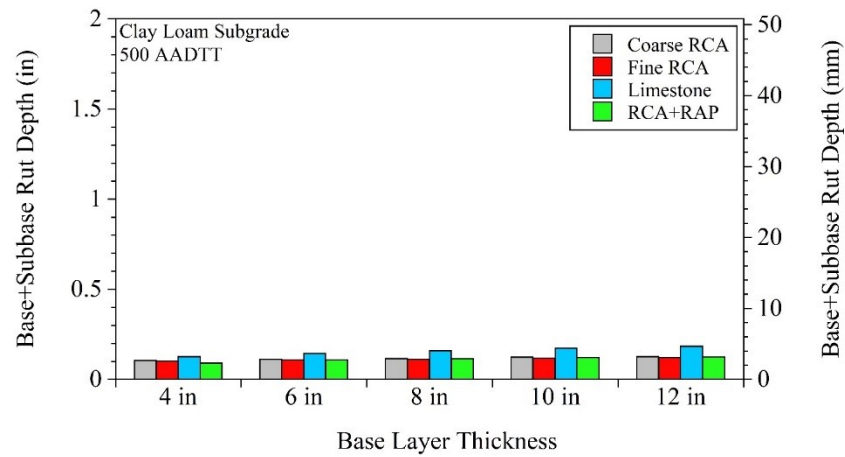
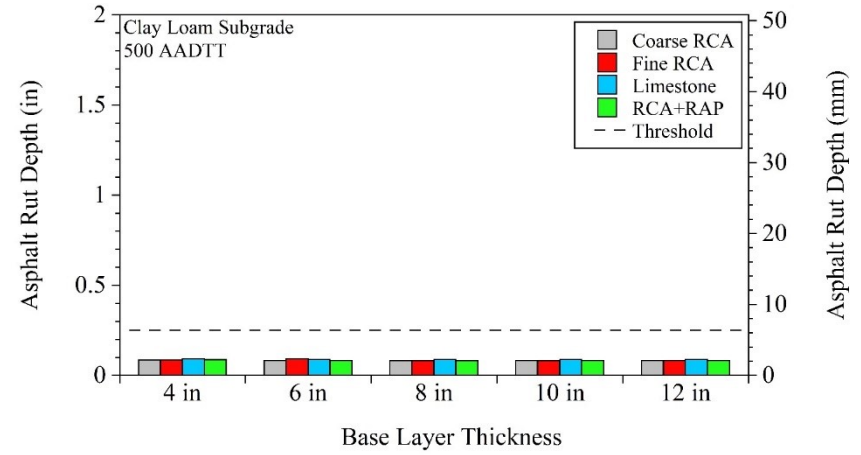
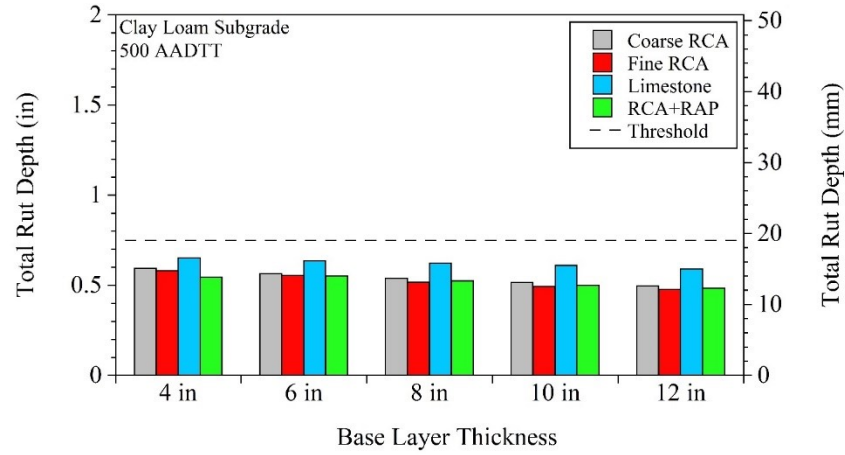
For pavements that contained Sand Subgrade - 25,000 AADTT:



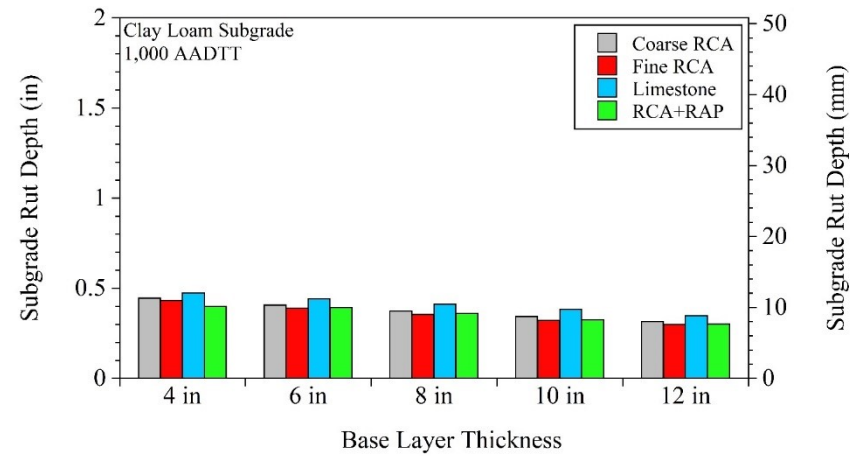
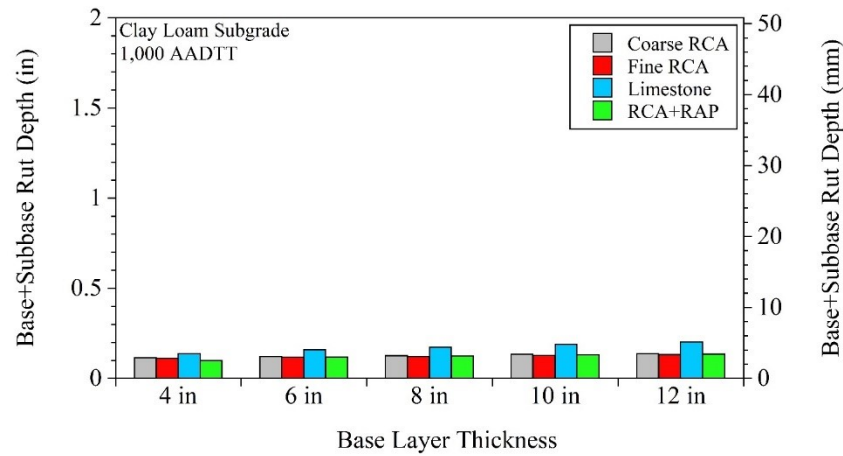
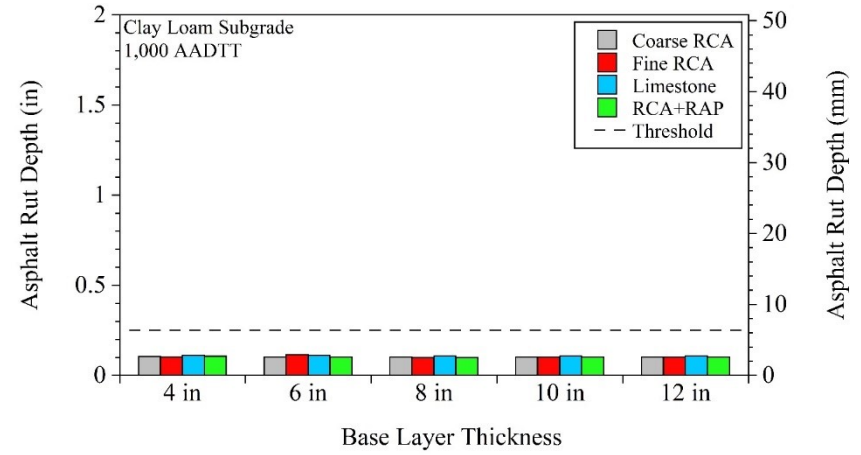
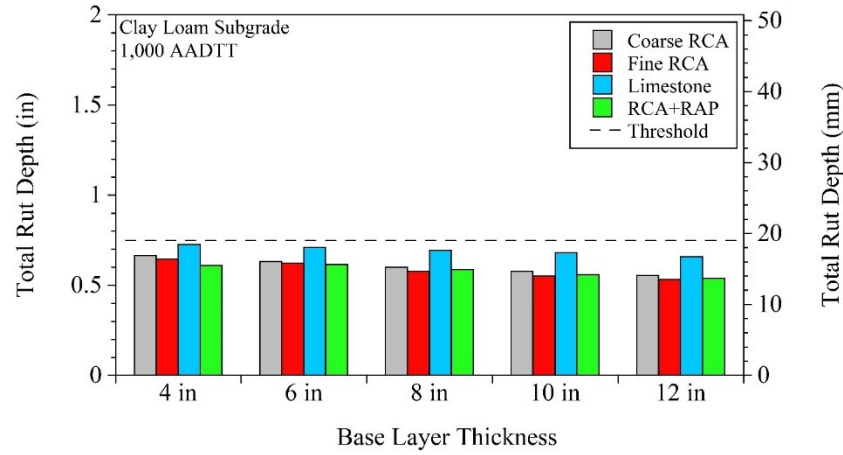
For pavements that contained Clay Loam subgrade - 100 AADTT:



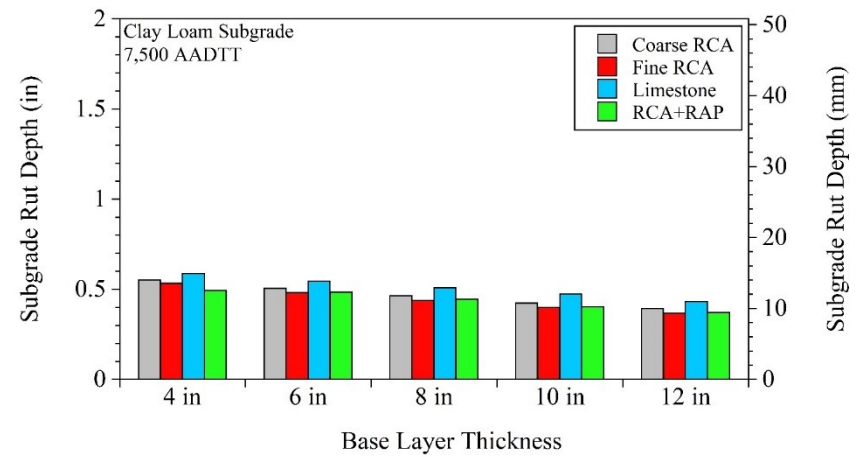
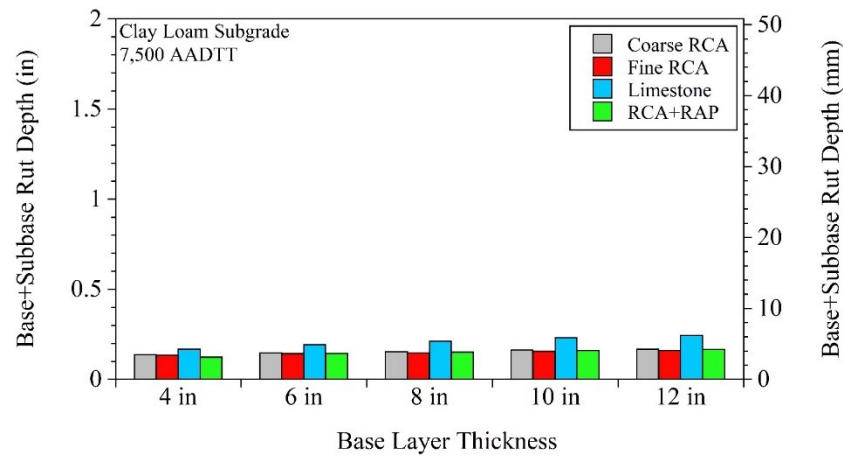
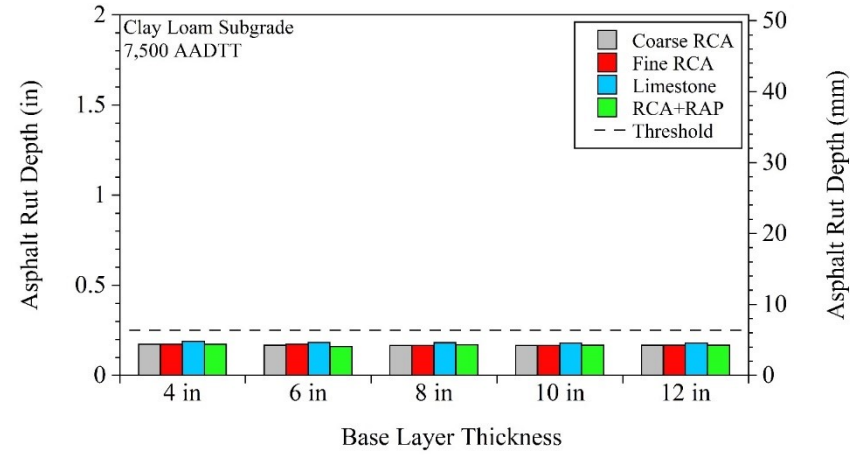
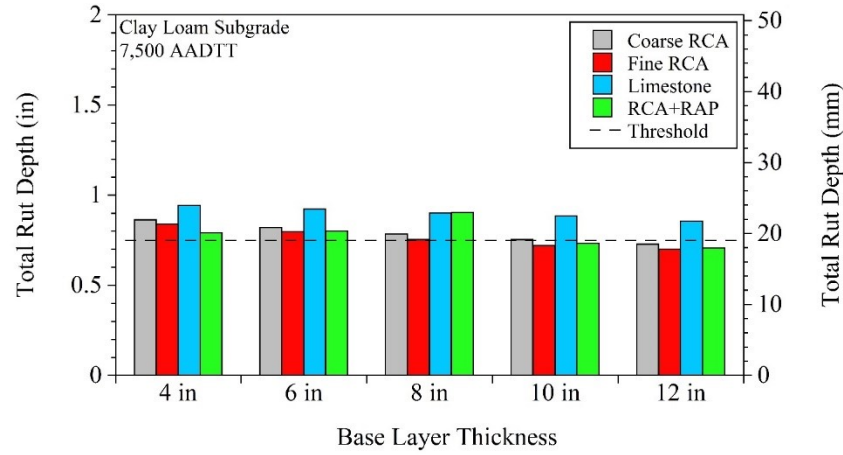
For pavements that contained Clay Loam subgrade - 500 AADTT:



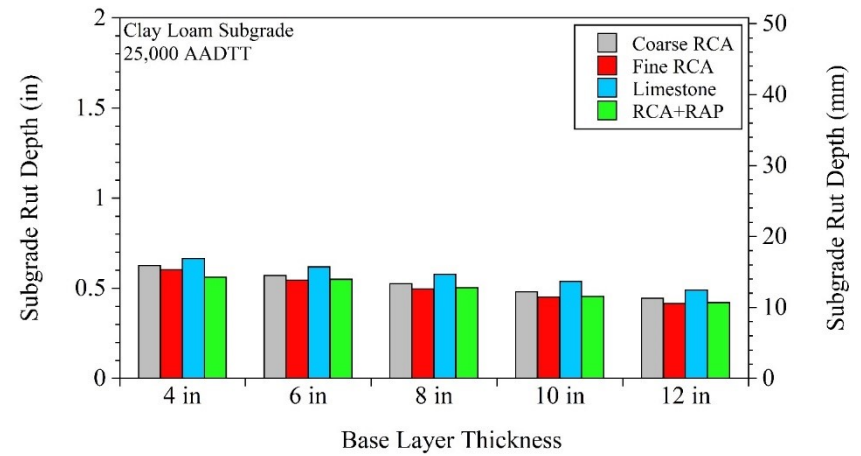
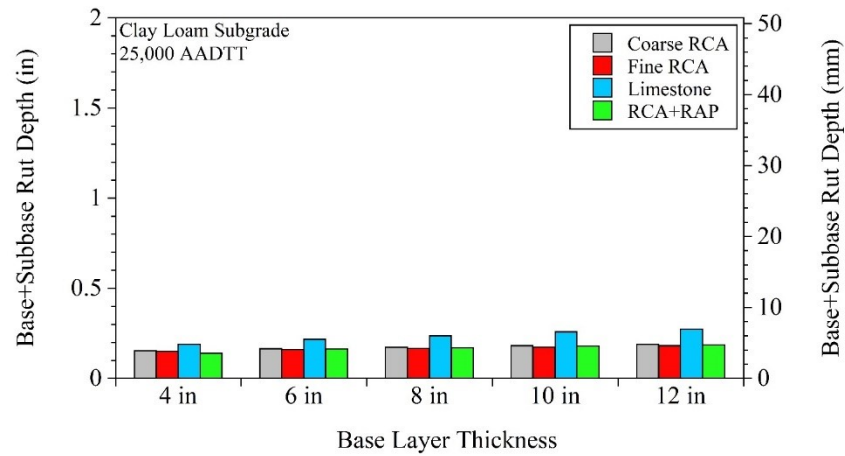
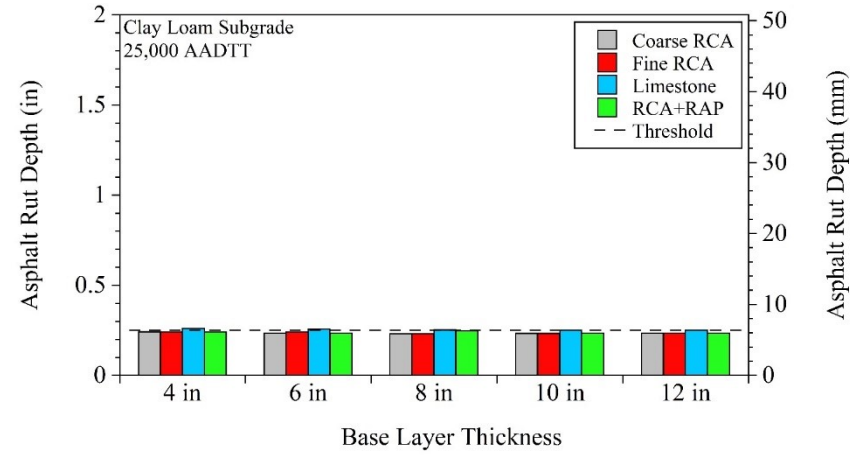
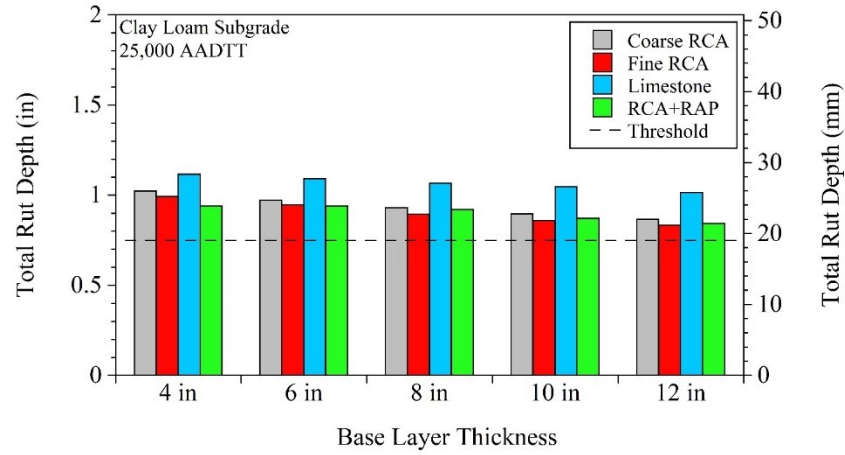
For pavements that contained Clay Loam subgrade - 1,000 AADTT:



For pavements that contained Clay Loam subgrade - 7,500 AADTT:



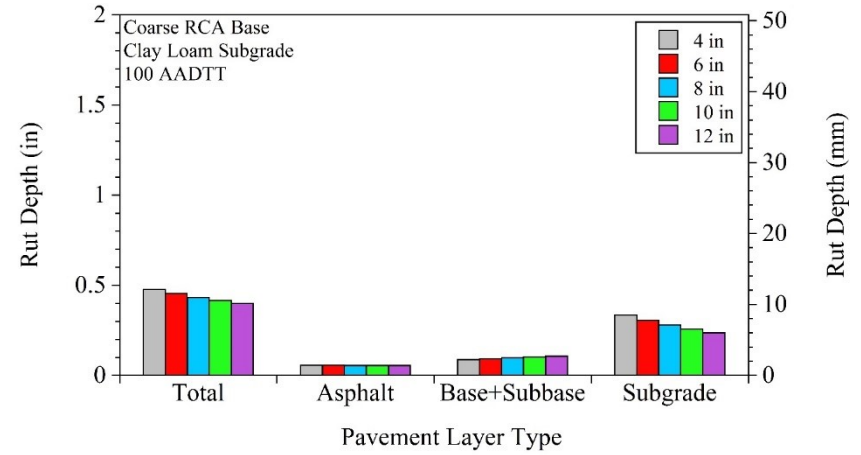
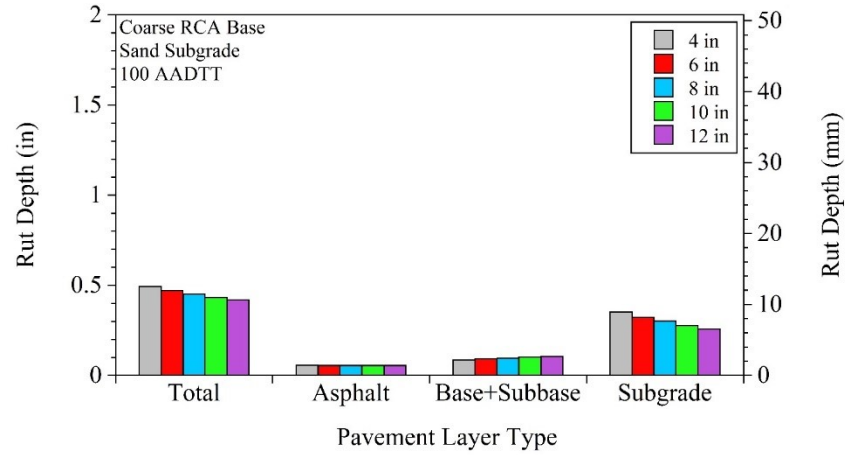
For pavements that contained Clay Loam subgrade - 25,000 AADTT:



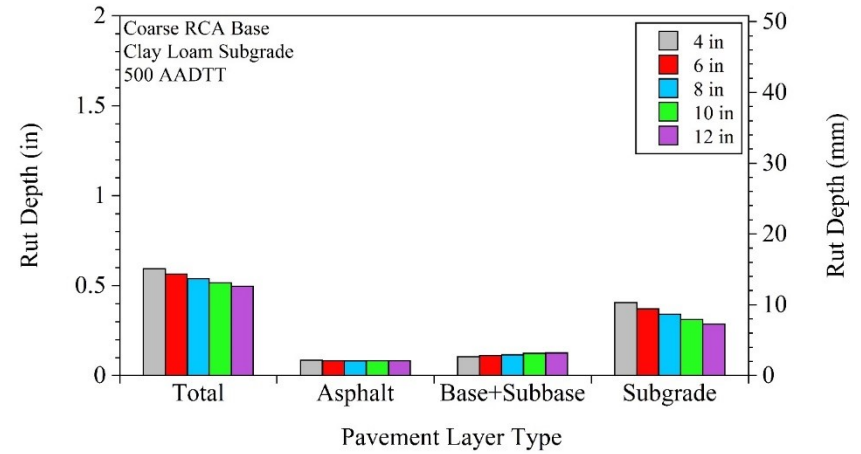
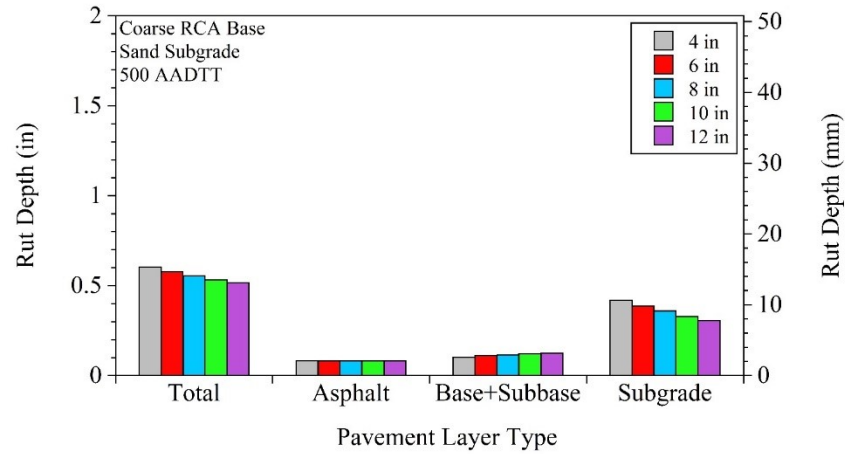
APPENDIX BD

TOTAL AND LAYER RUTTING AT 50% RELIABILITY FOR RECYCLED AGGREGATE BASE (RAB) GROUP

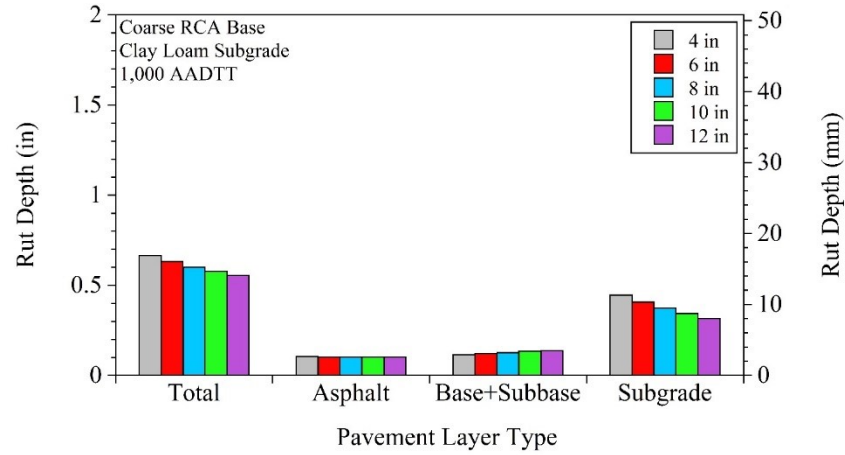
For pavements that contained Coarse RCA base - 100 AADTT:



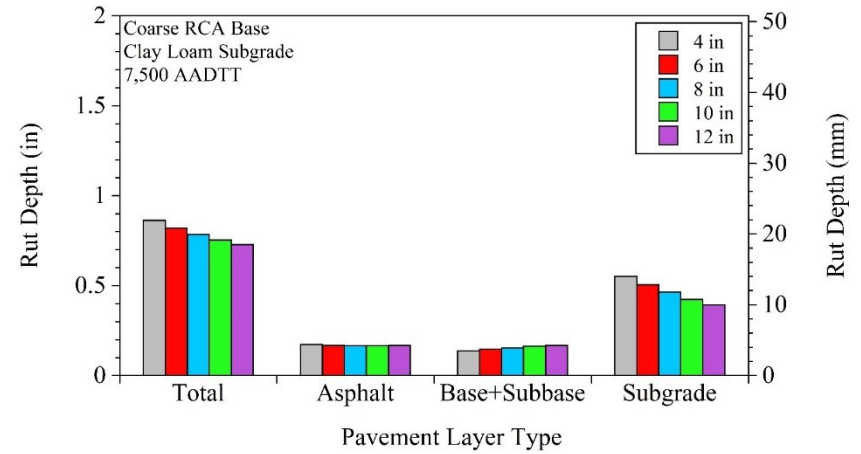
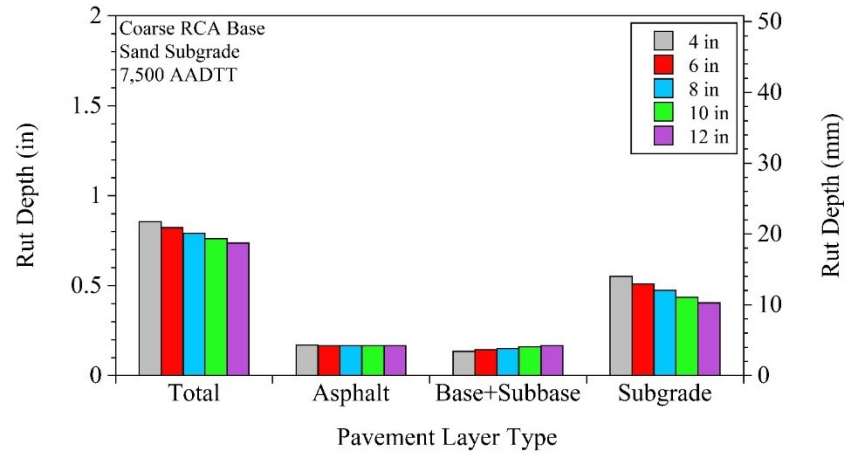
For pavements that contained Coarse RCA base - 500 AADTT:



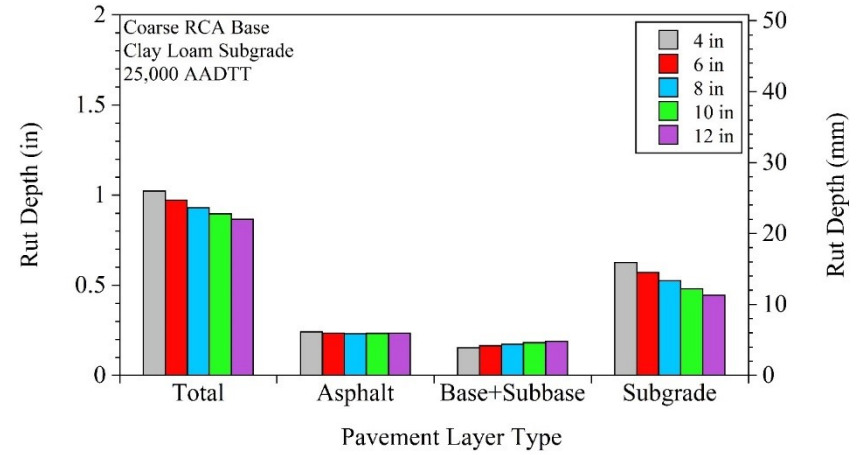
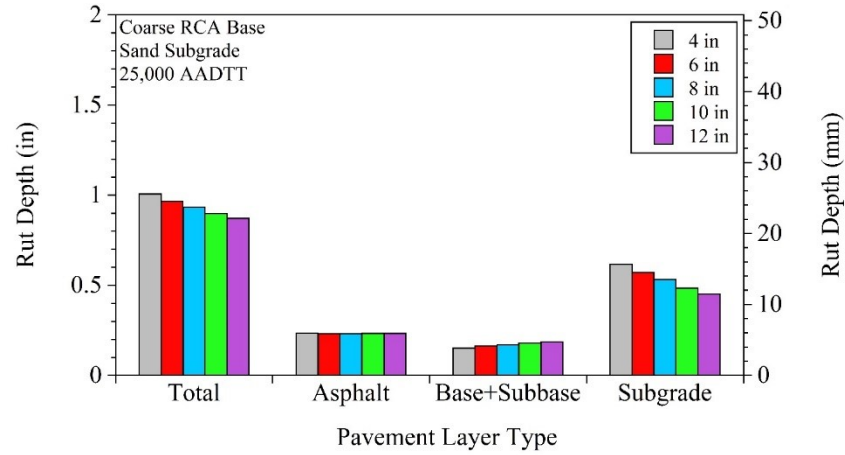
For pavements that contained Coarse RCA base - 1,000 AADTT:



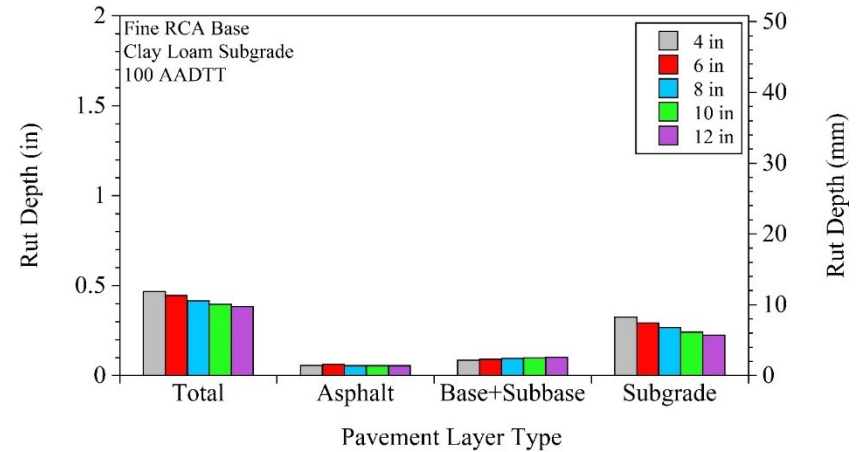
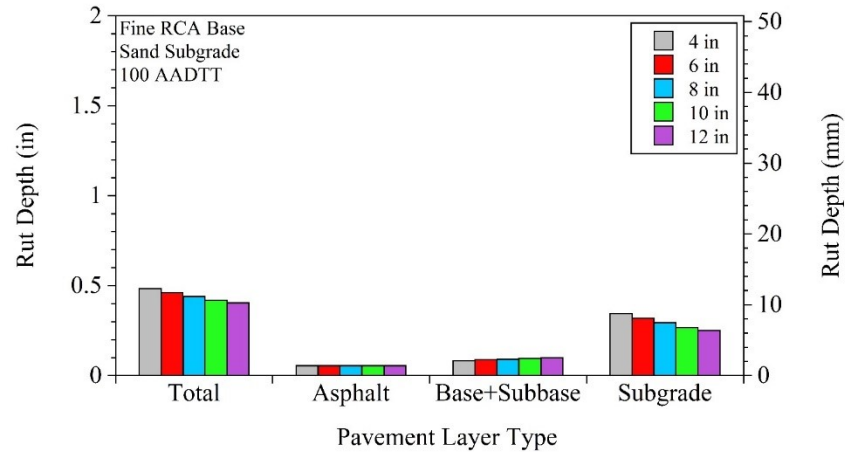
For pavements that contained Coarse RCA base - 7,500 AADTT:



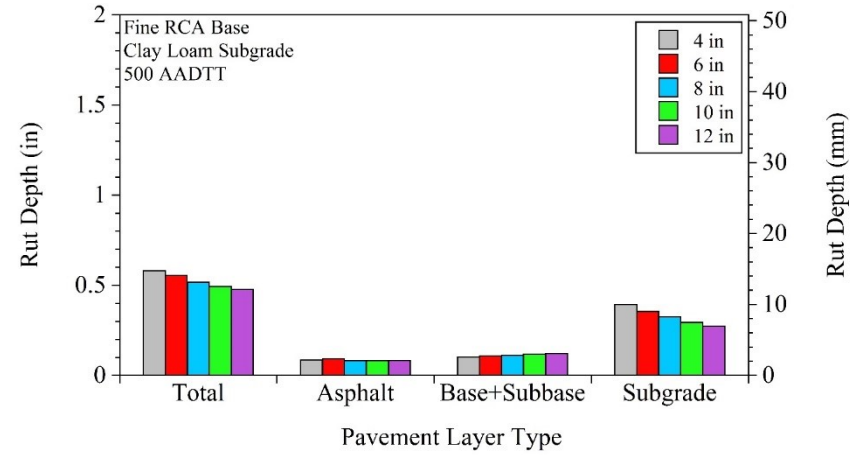
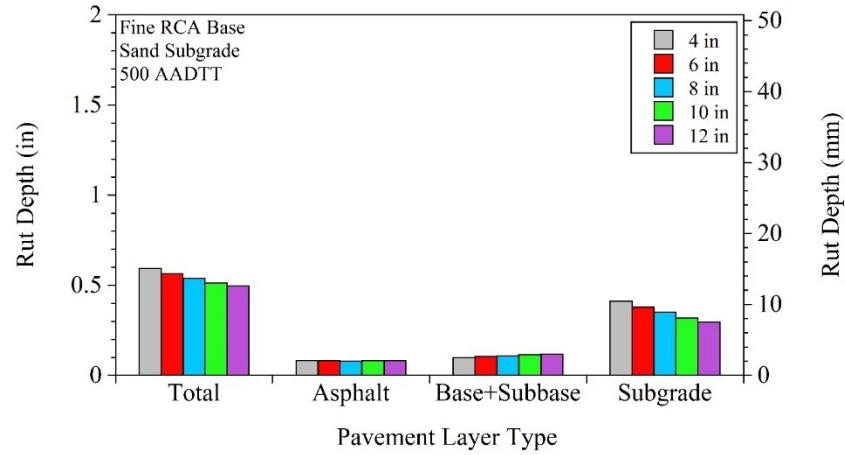
For pavements that contained Coarse RCA base - 25,000 AADTT:



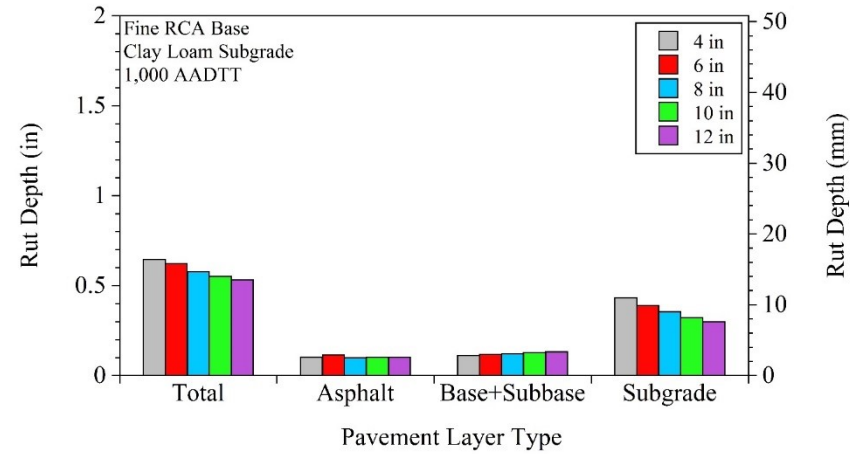
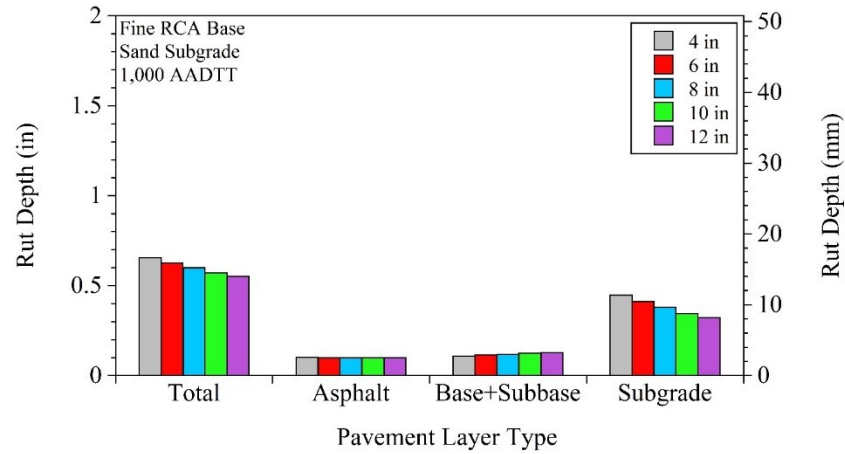
For pavements that contained Fine RCA base - 100 AADTT:



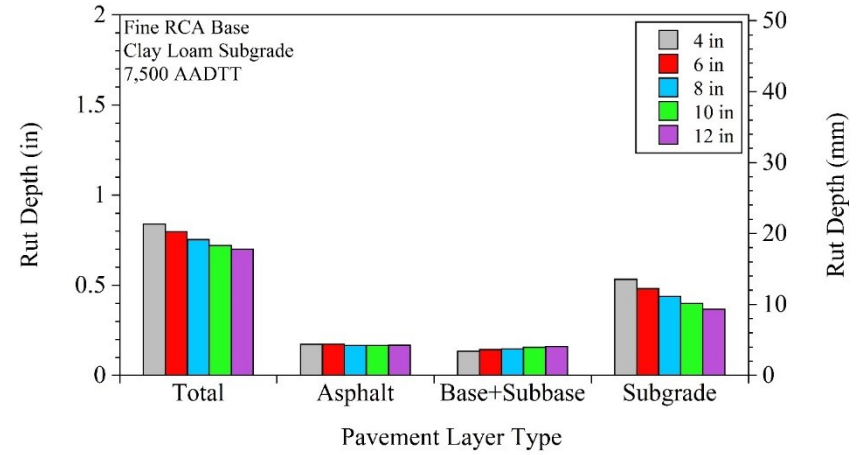
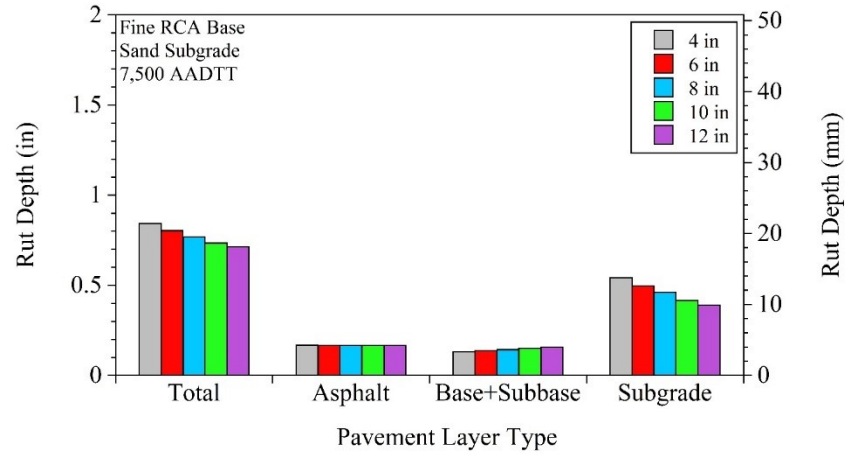
For pavements that contained Fine RCA base - 500 AADTT:



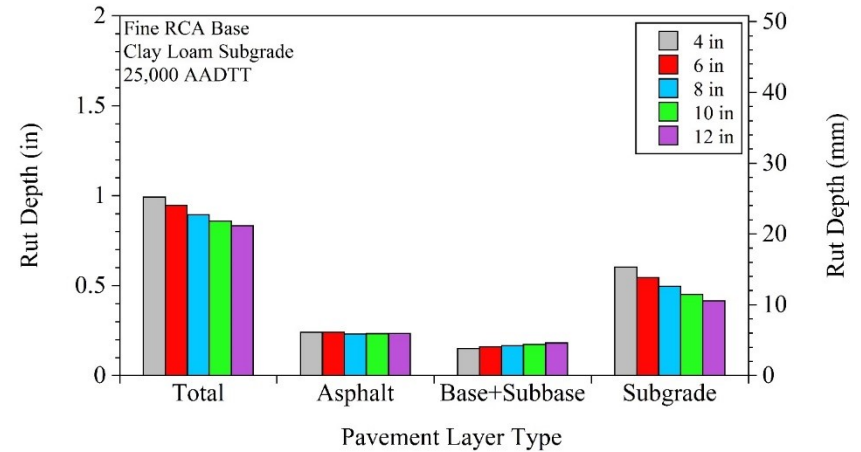
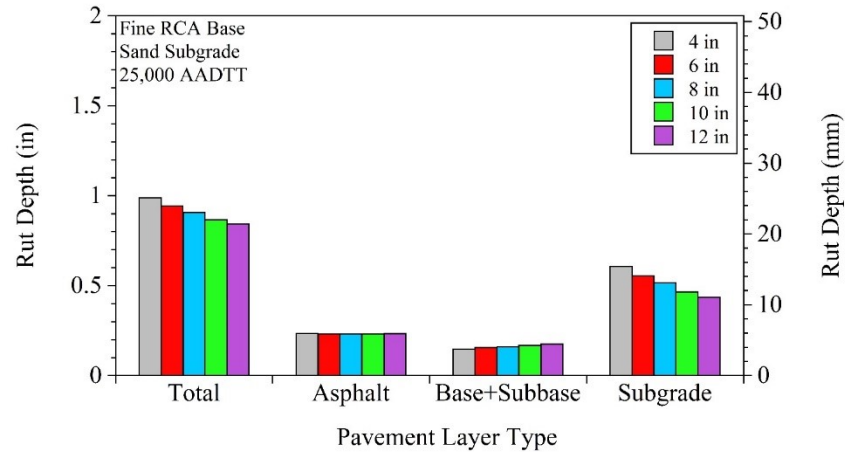
For pavements that contained Fine RCA base - 1,000 AADTT:



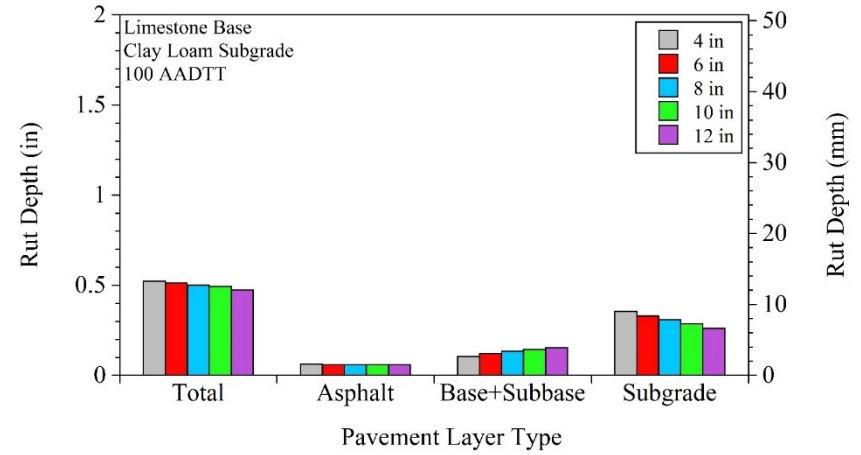
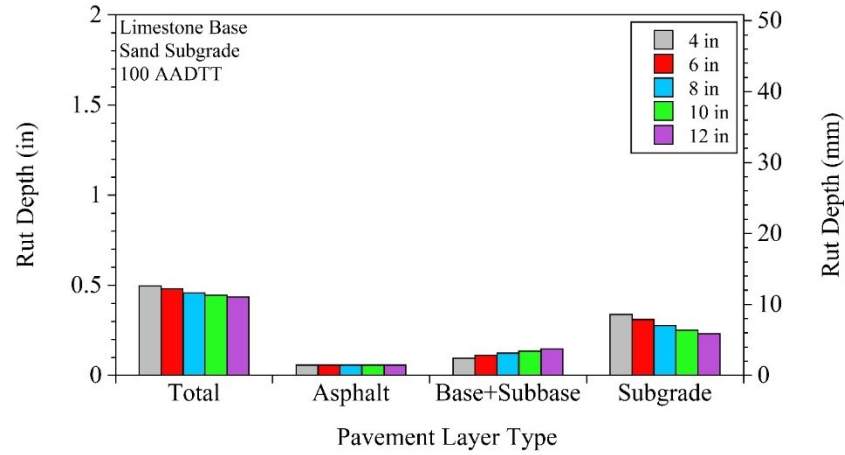
For pavements that contained Fine RCA base - 7,500 AADTT:



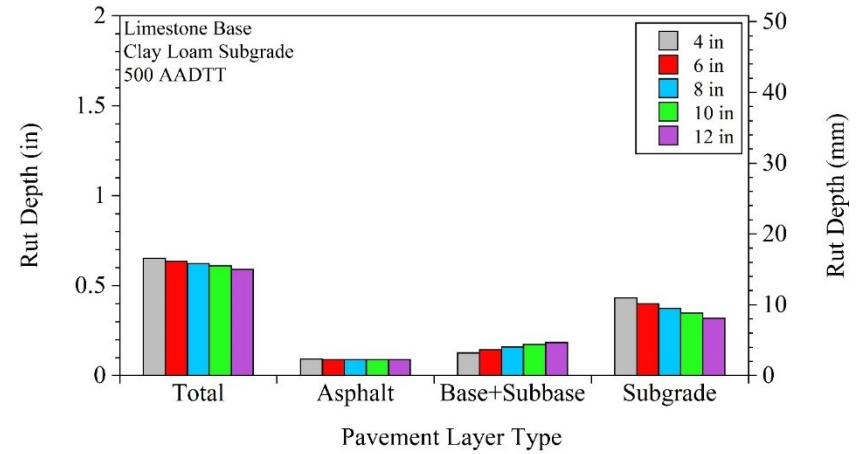
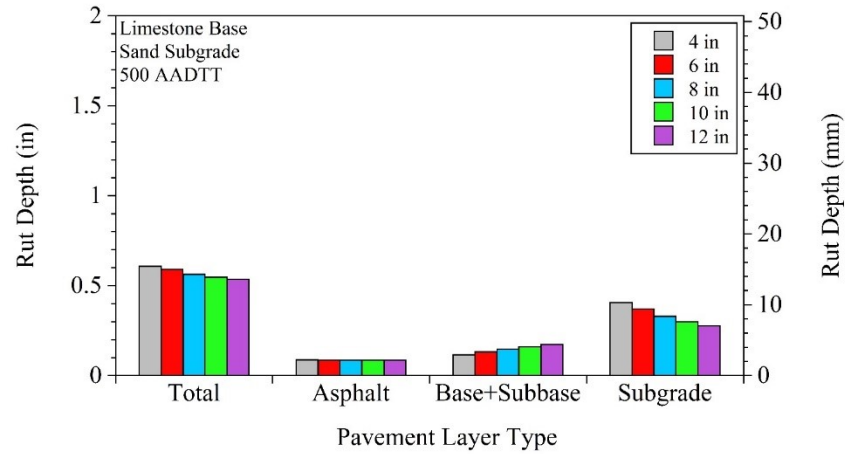
For pavements that contained Fine RCA base - 25,000 AADTT:



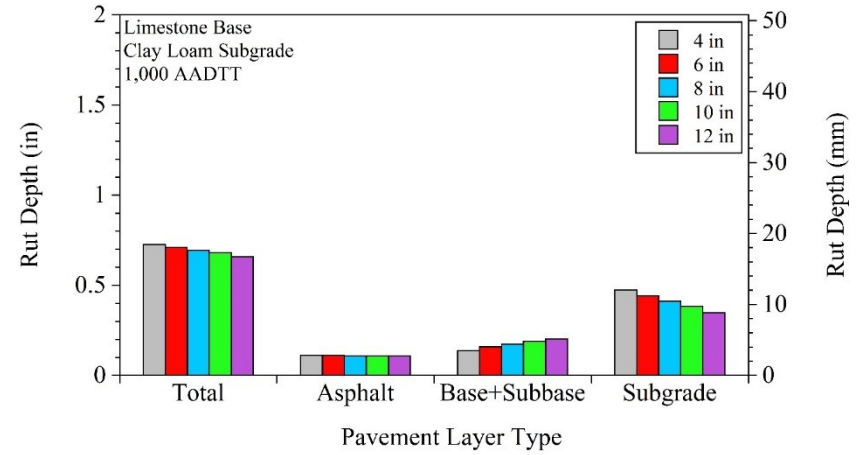
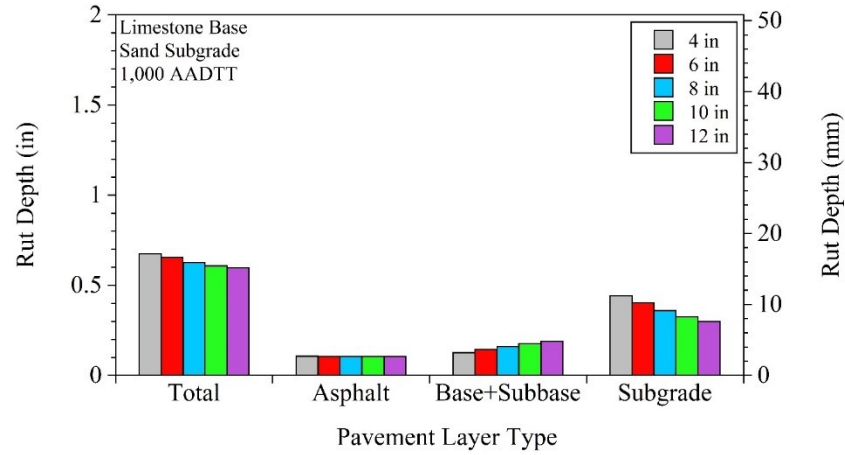
For pavements that contained Limestone base - 100 AADTT:



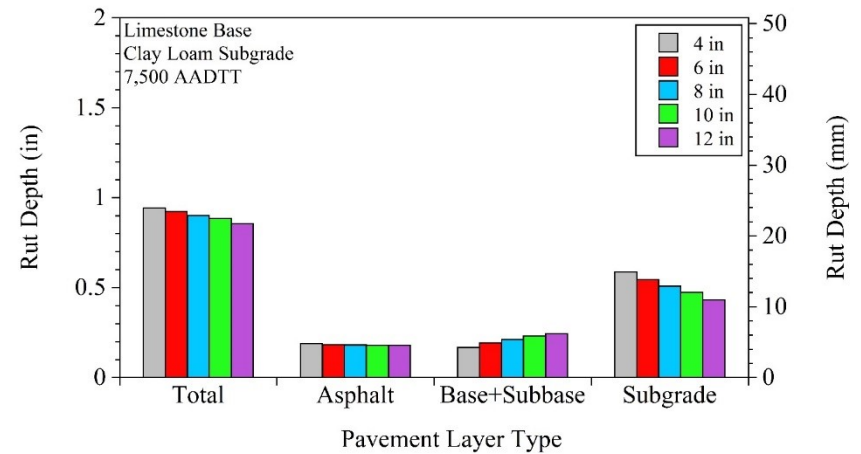
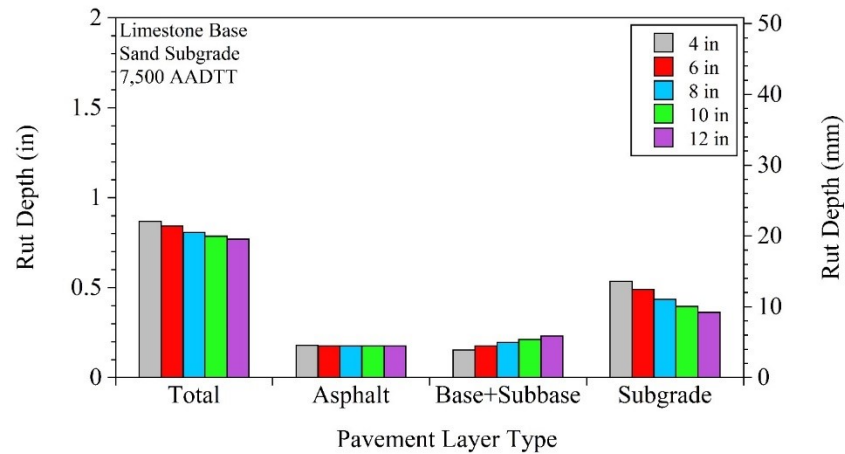
For pavements that contained Limestone base - 500 AADTT:



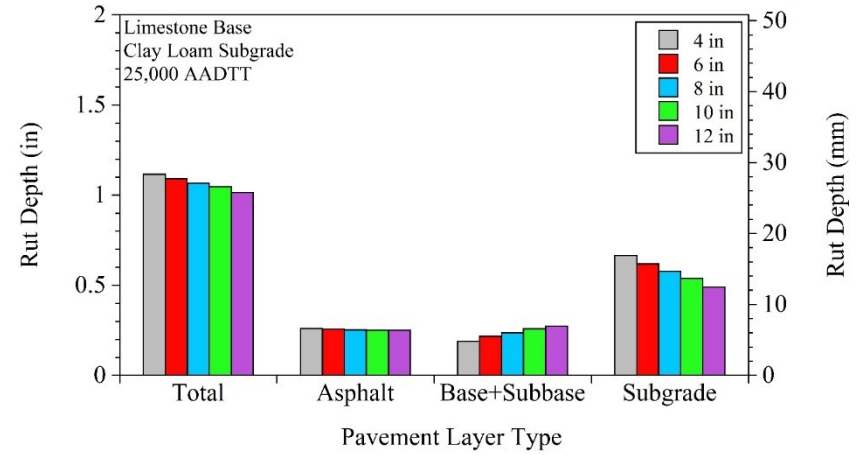
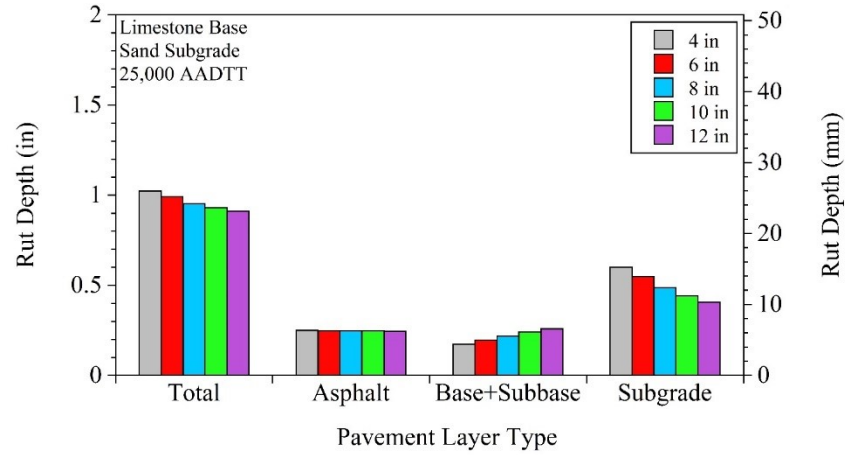
For pavements that contained Limestone base - 1,000 AADTT:



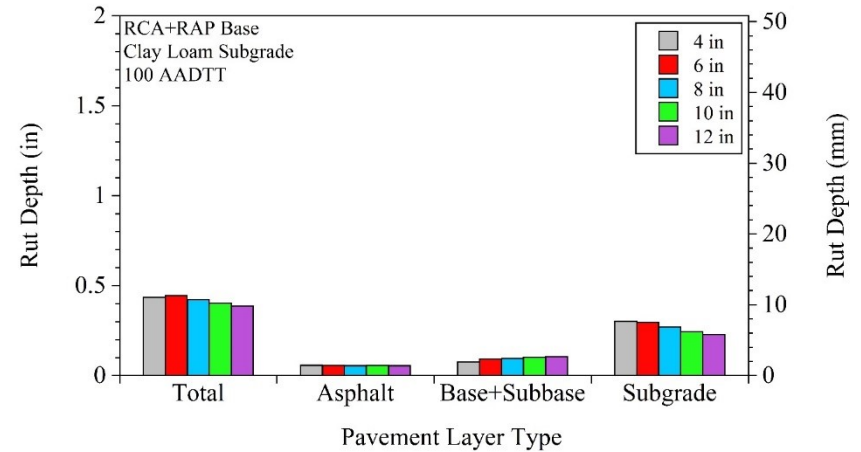
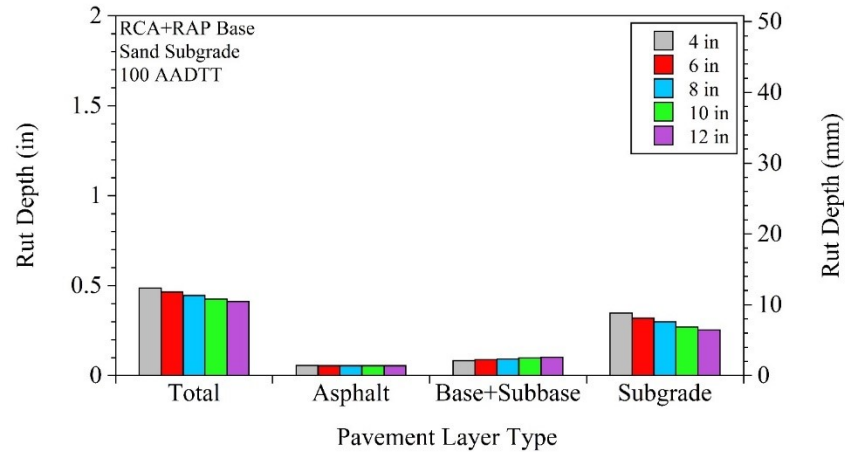
For pavements that contained Limestone base - 7,500 AADTT:



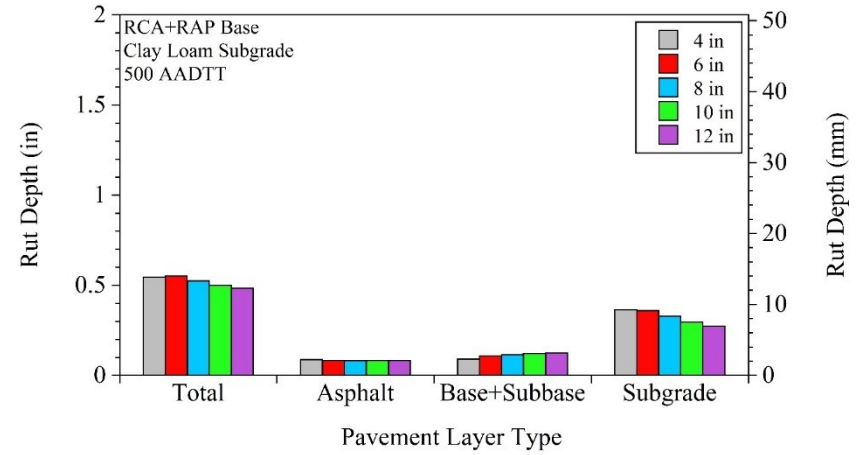
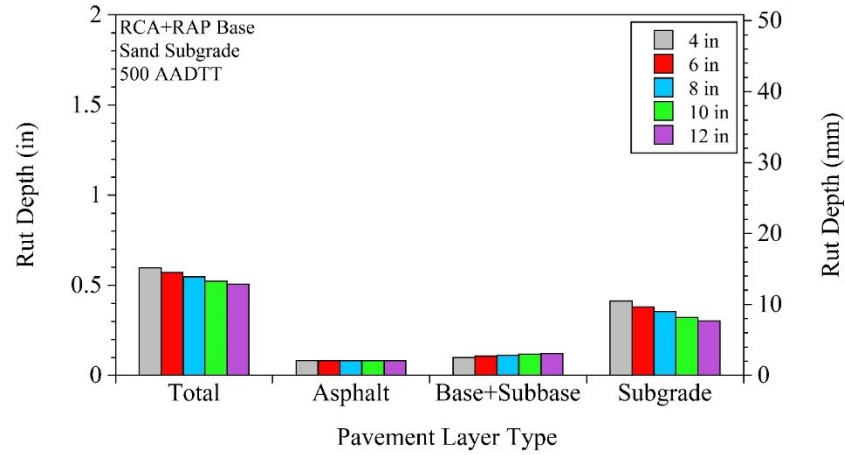
For pavements that contained Limestone base - 25,000 AADTT:



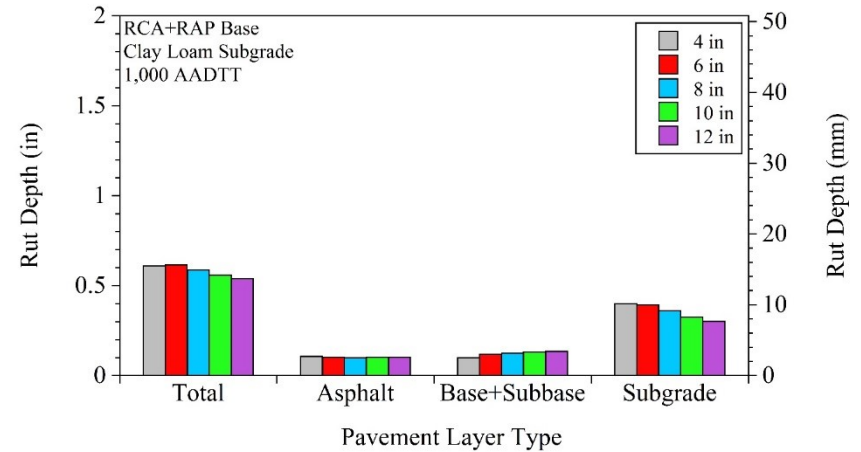
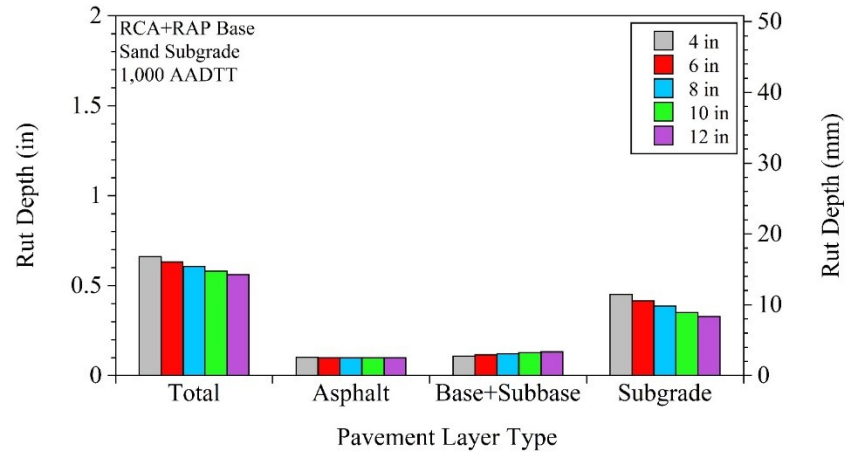
For pavements that contained RCA+RAP base - 100 AADTT:



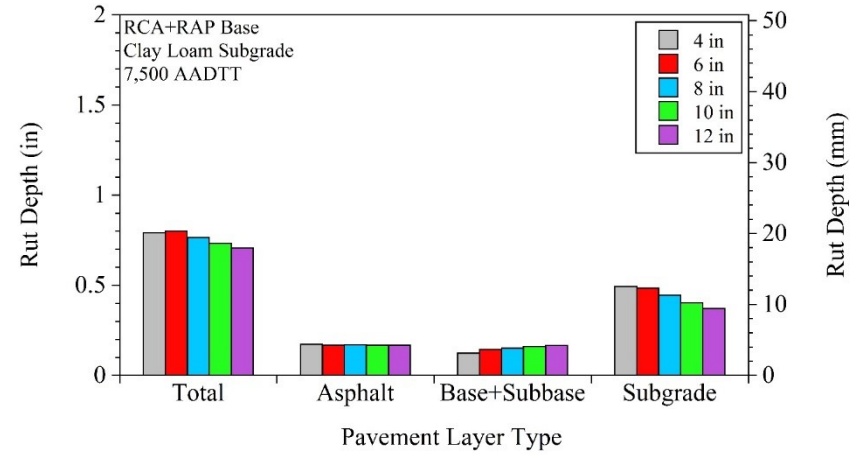
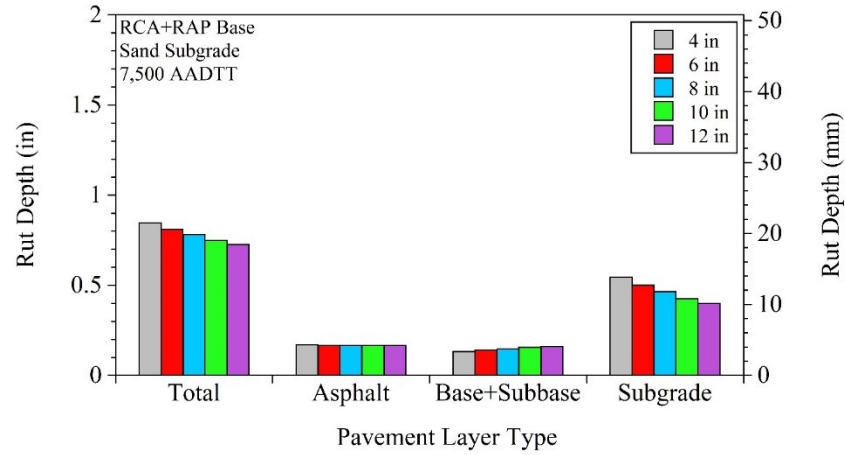
For pavements that contained RCA+RAP base - 500 AADTT:



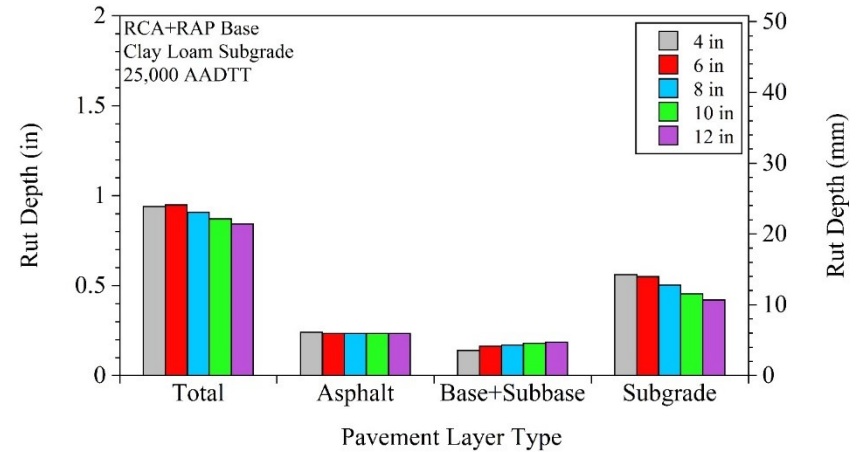
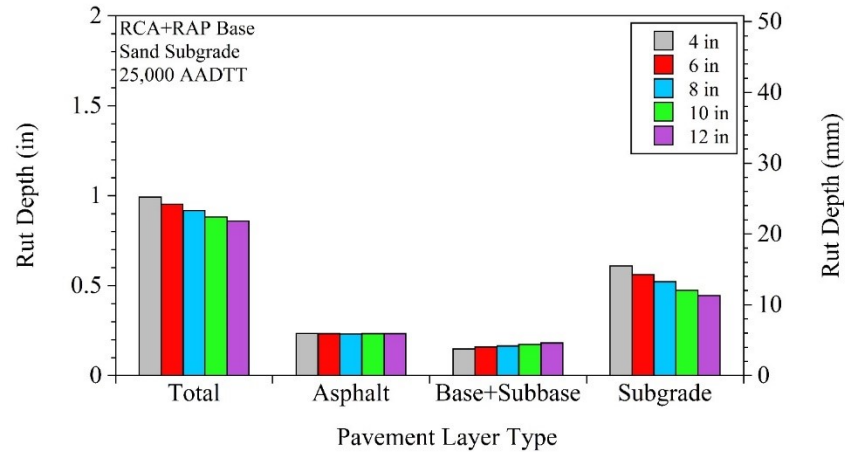
For pavements that contained RCA+RAP base - 1,000 AADTT:



For pavements that contained RCA+RAP base - 7,500 AADTT:

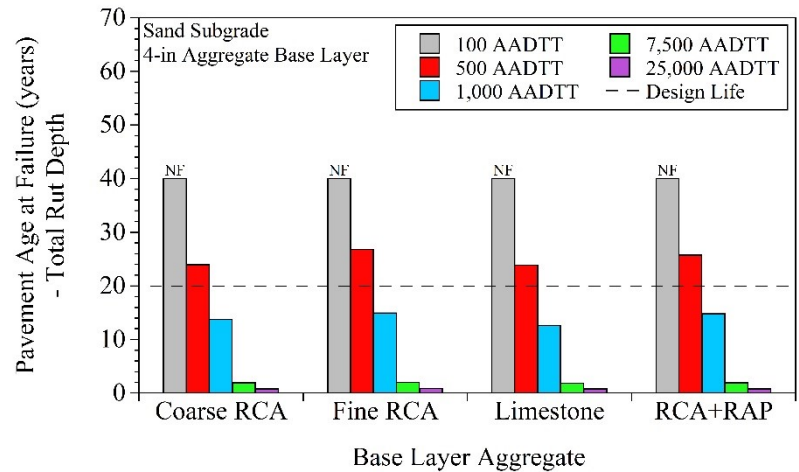
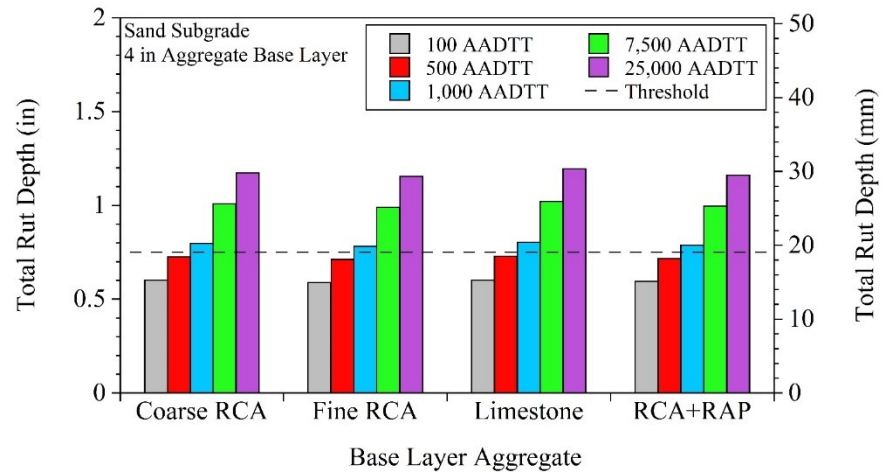
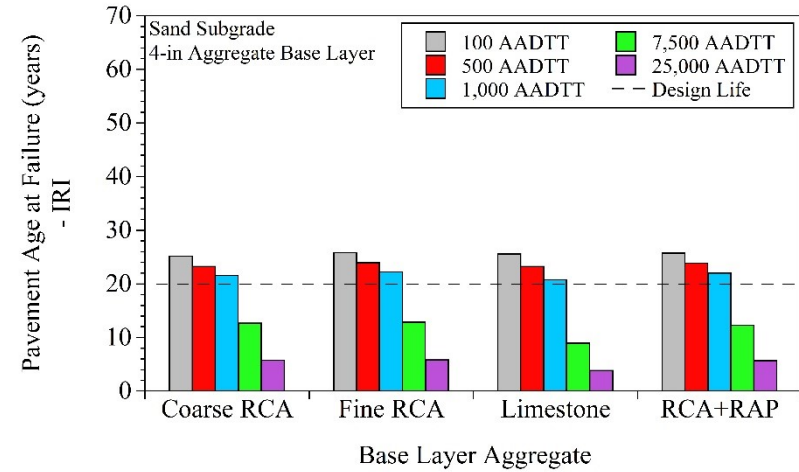
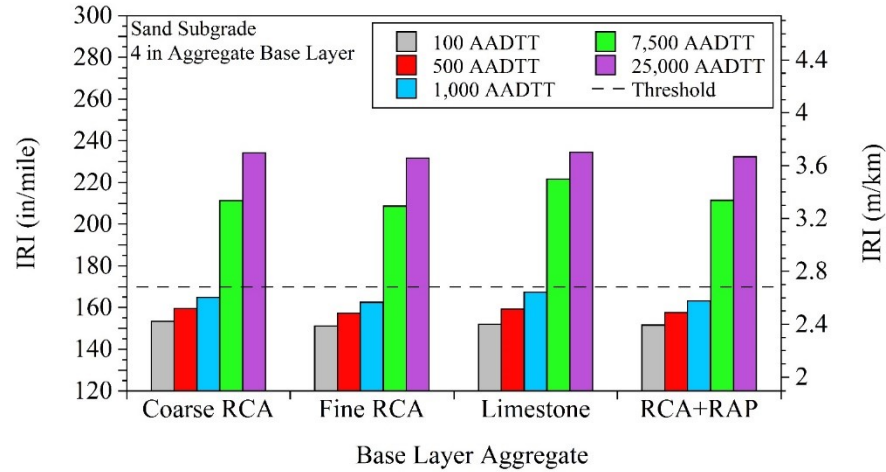


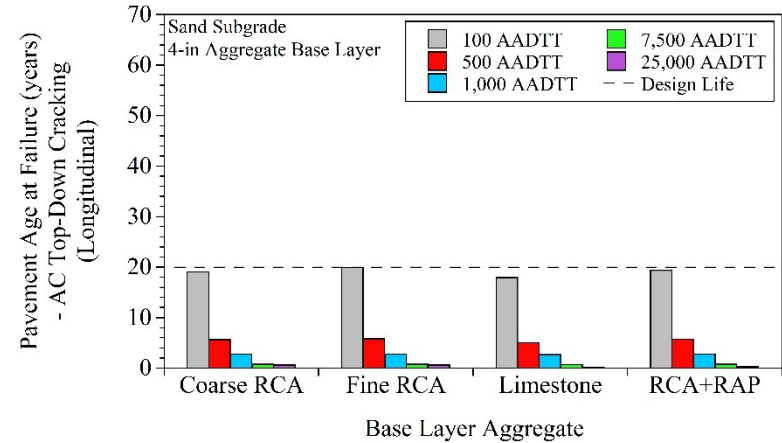
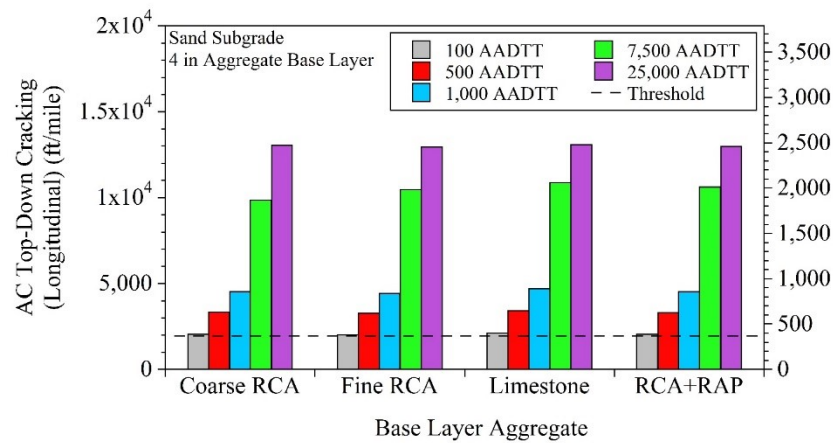
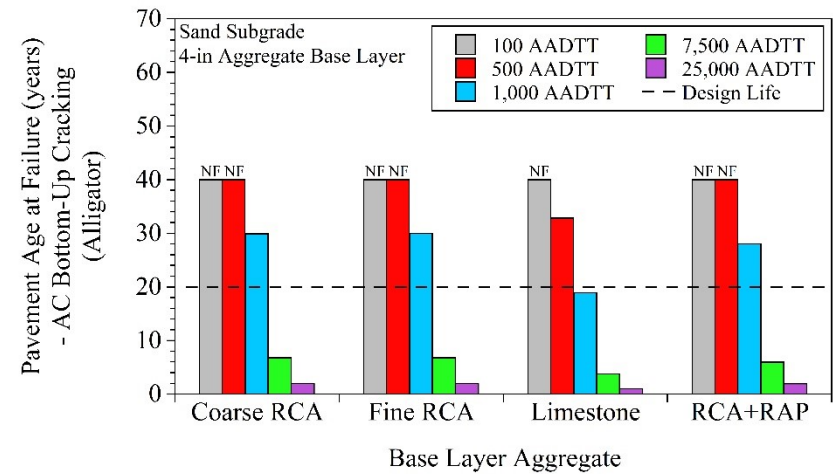
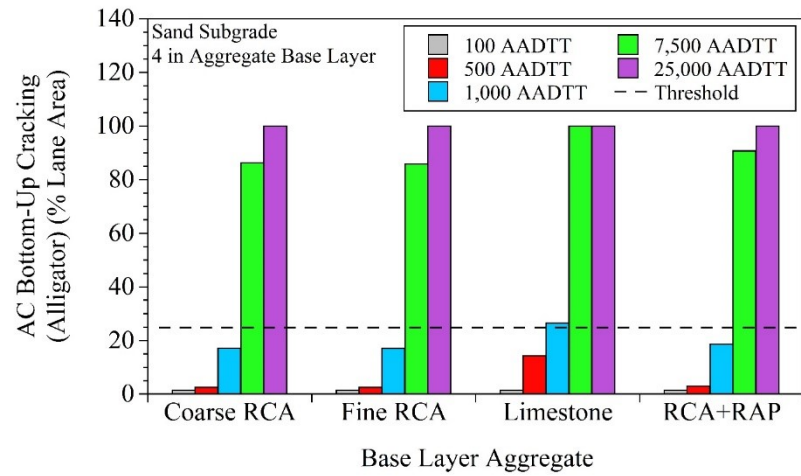
For pavements that contained RCA+RAP base - 25,000 AADTT:



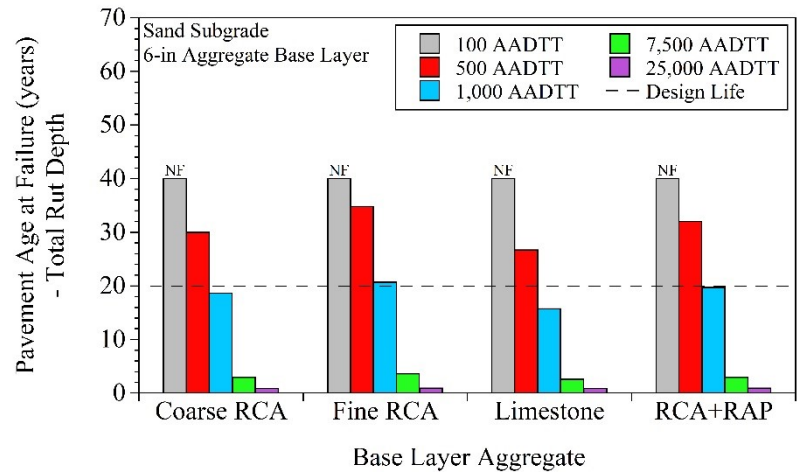
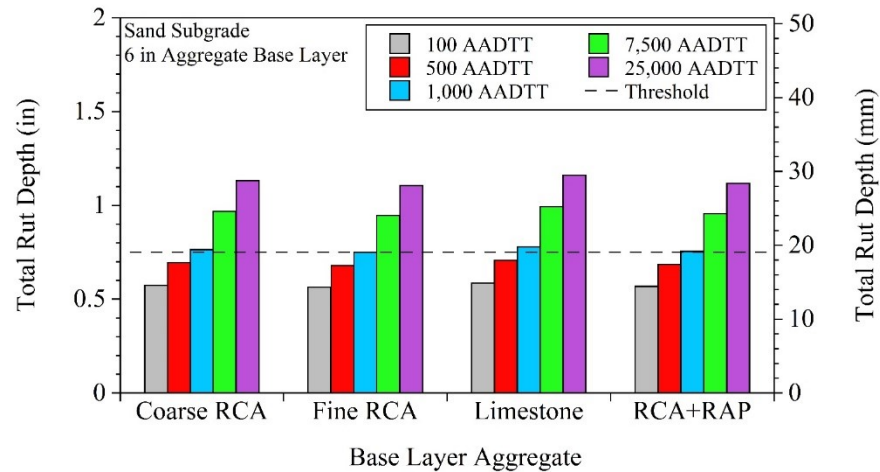
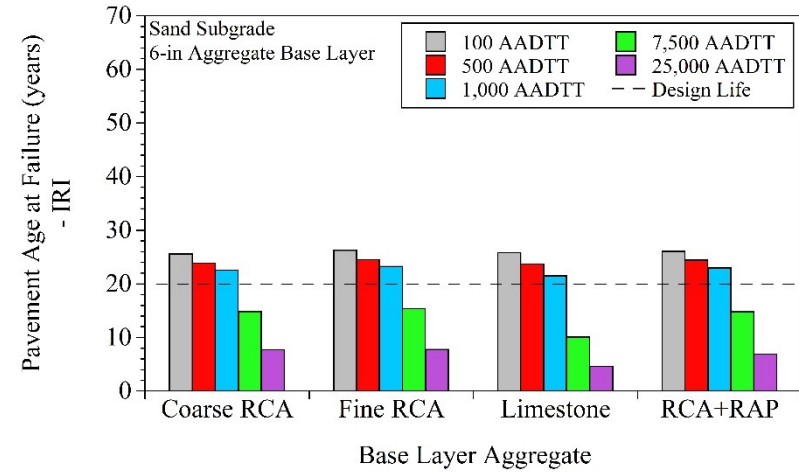
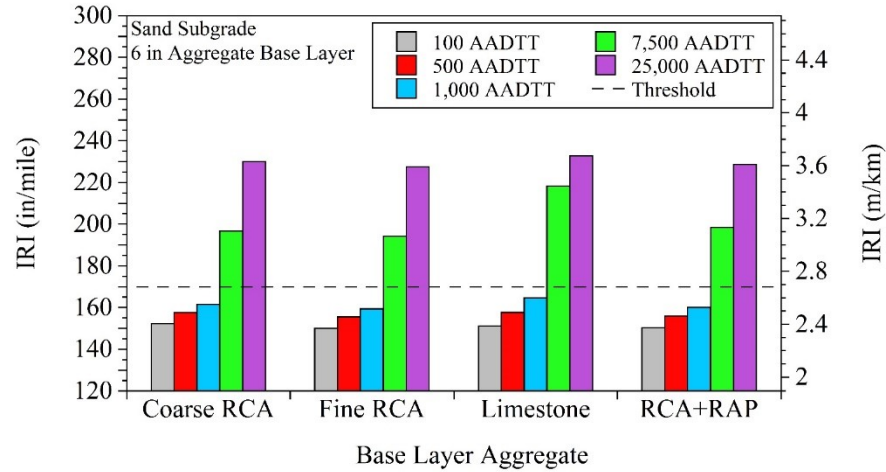
APPENDIX BE
EFFECT OF TRAFFIC LEVEL ON PAVEMENT PERFORMANCE
PREDICTIONS

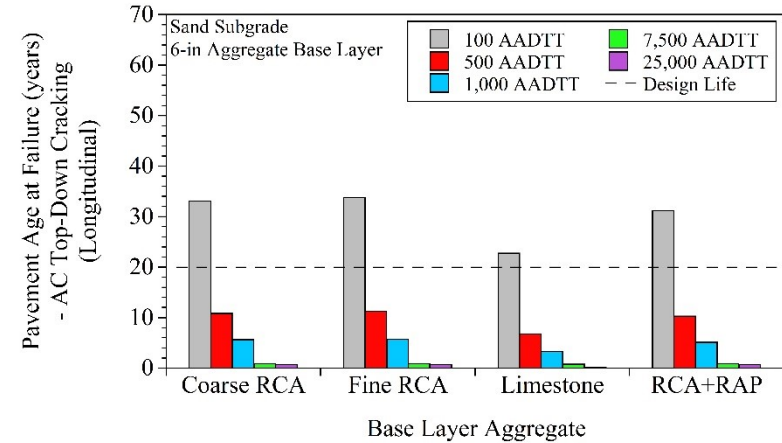
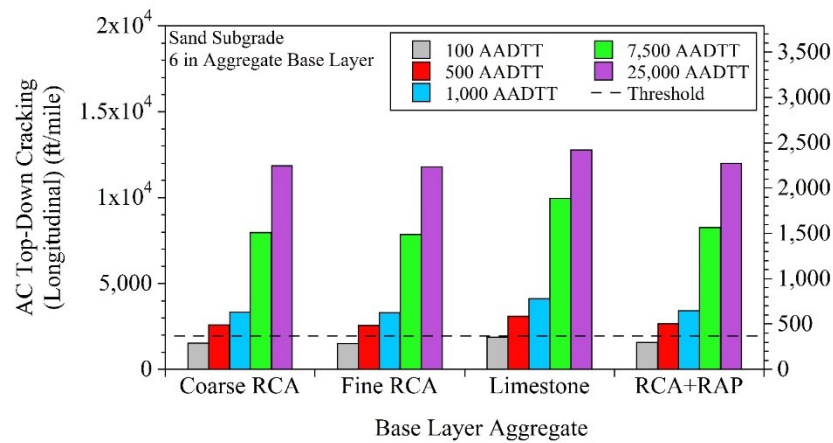
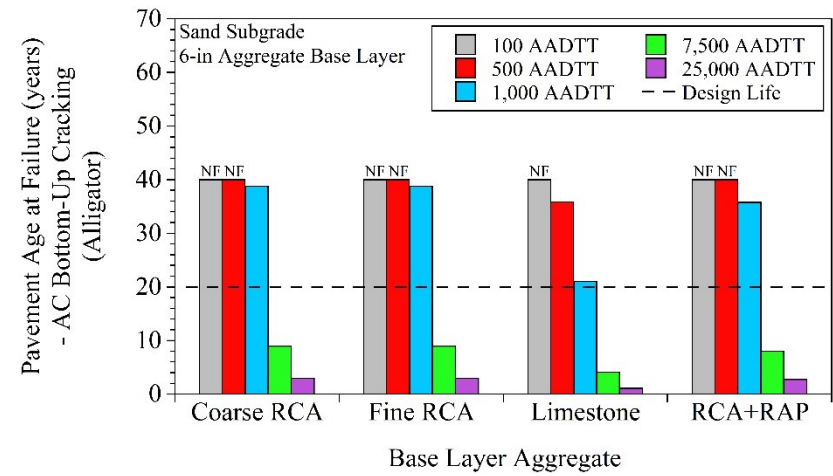
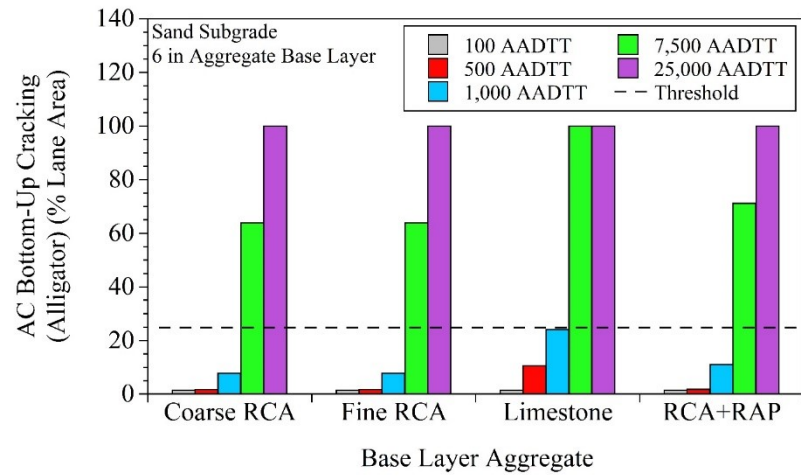
For pavements that contained Sand Subgrade and 4-in aggregate base:



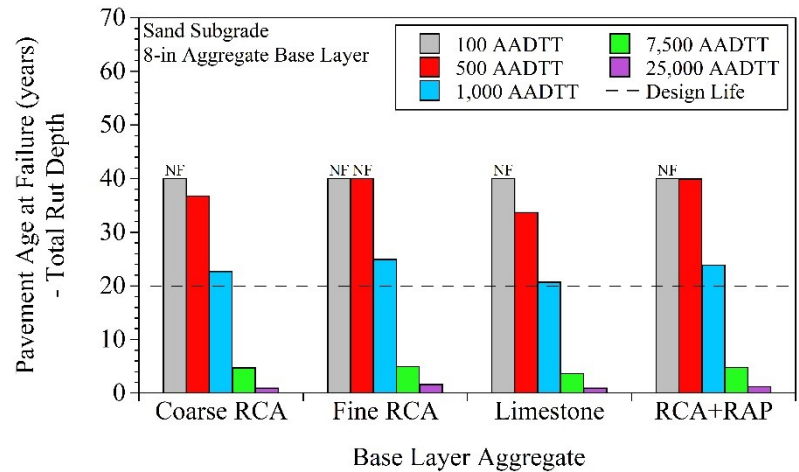
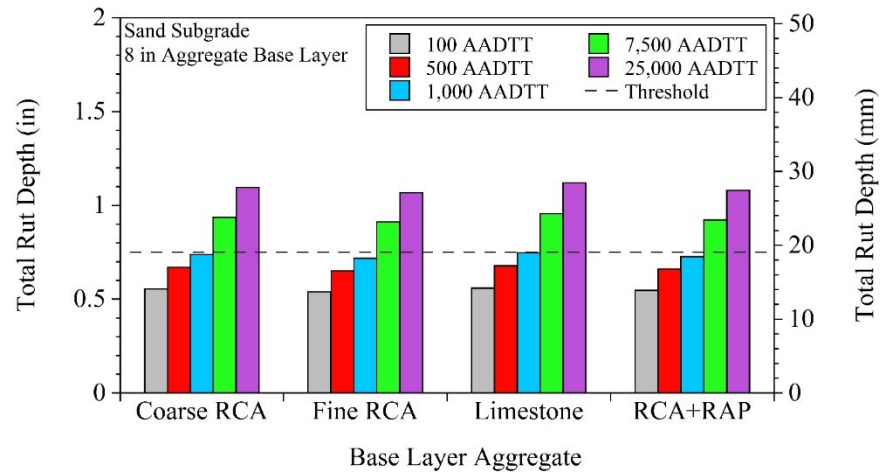
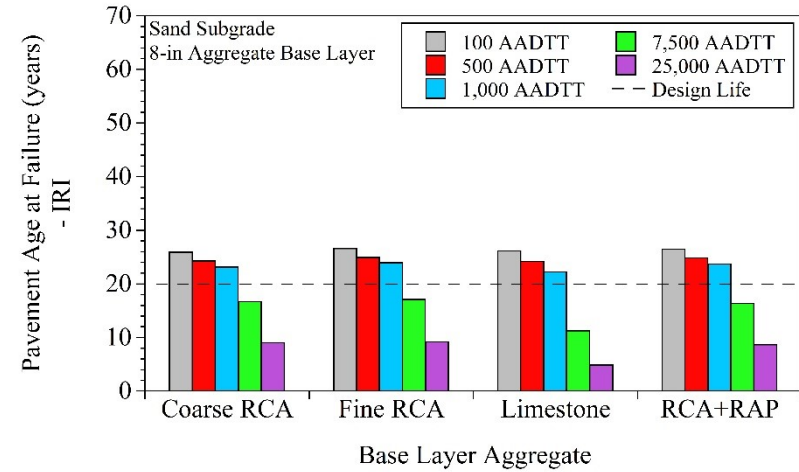
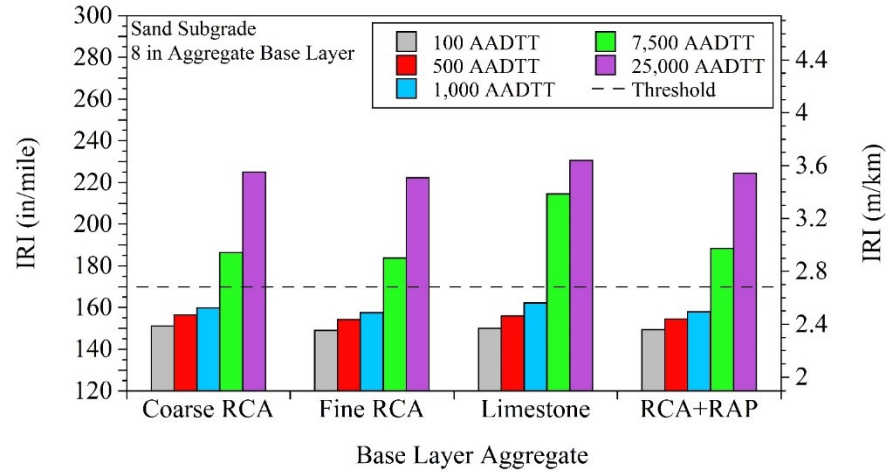


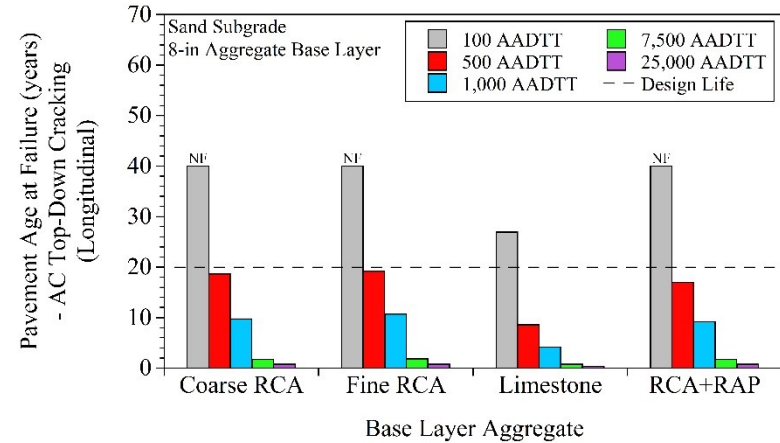
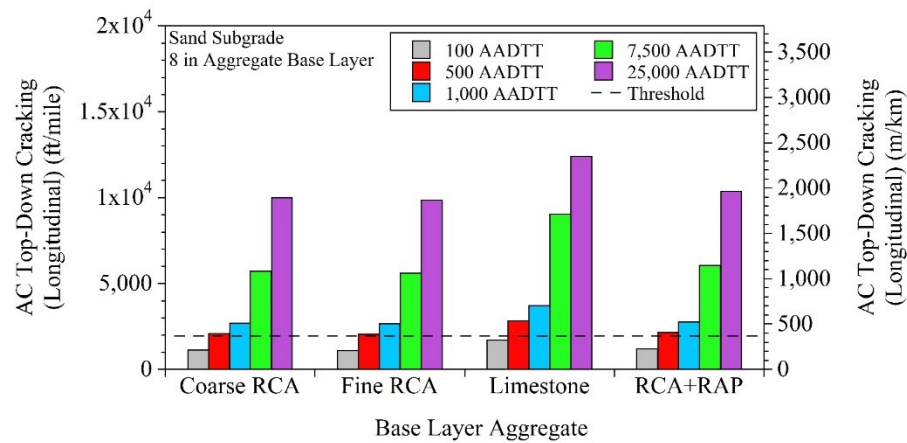
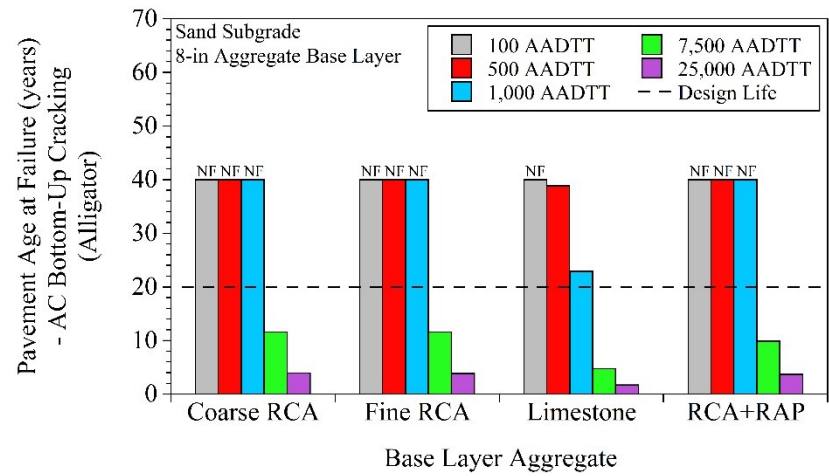
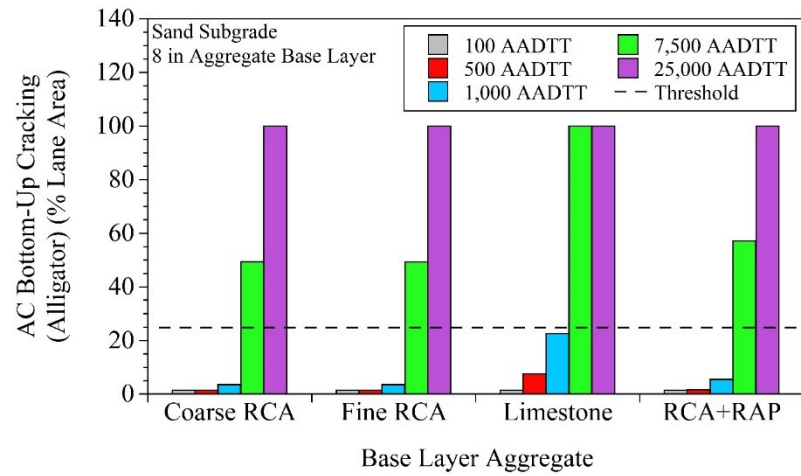
For pavements that contained Sand Subgrade and 6-in aggregate base:



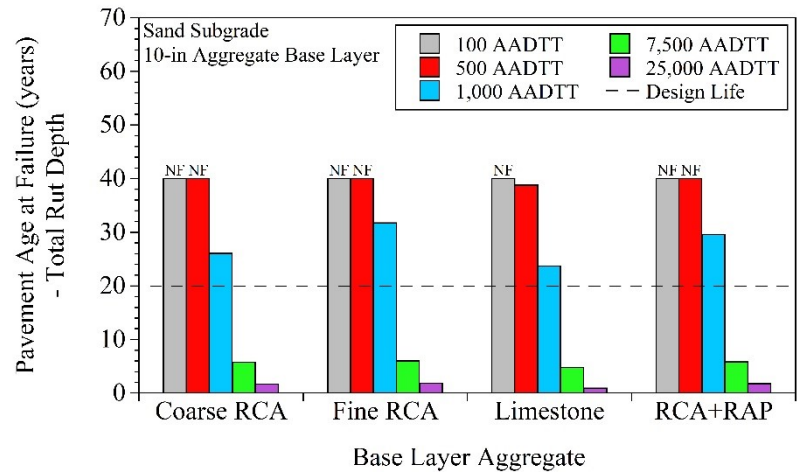
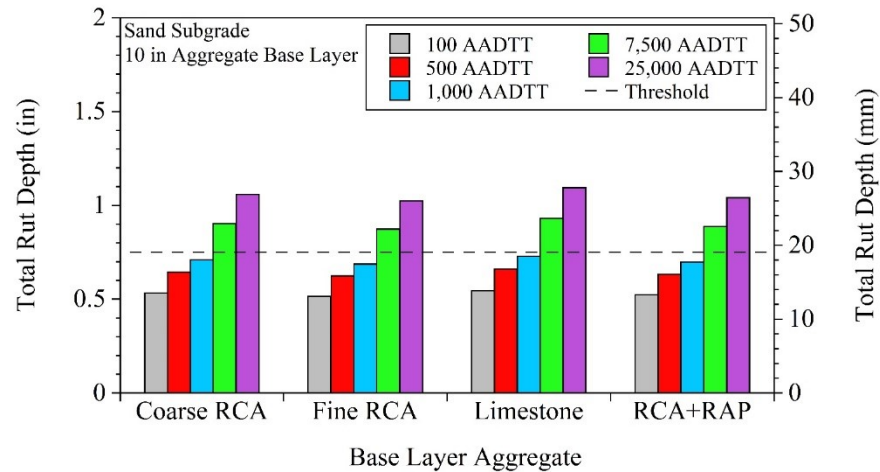
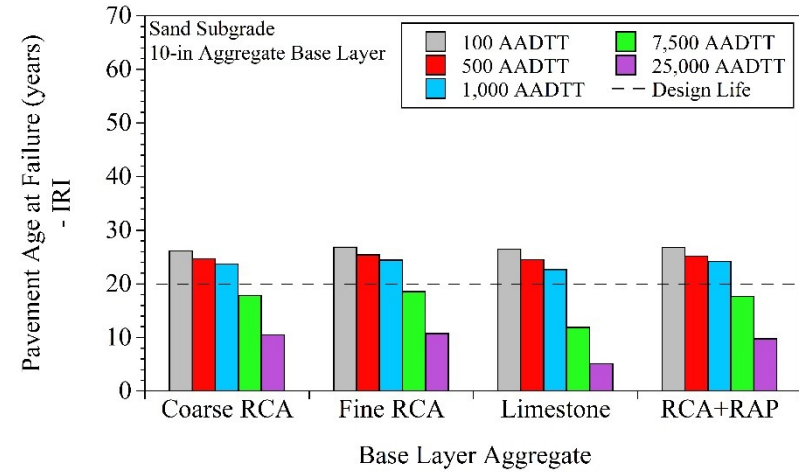
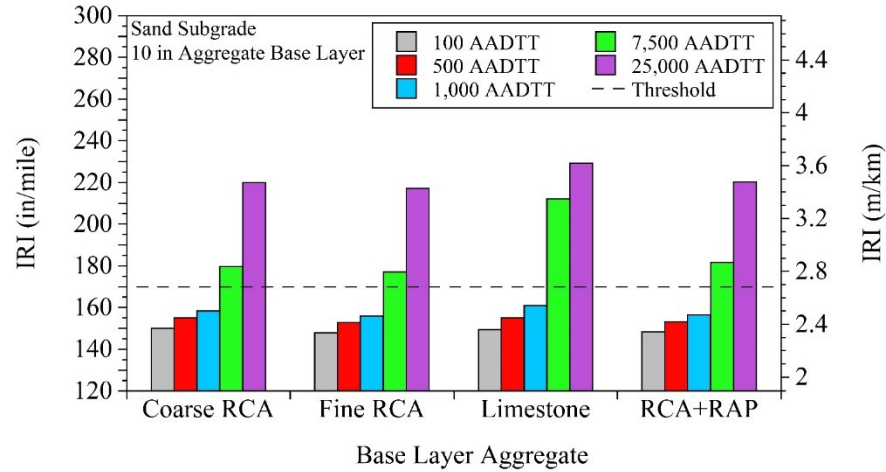


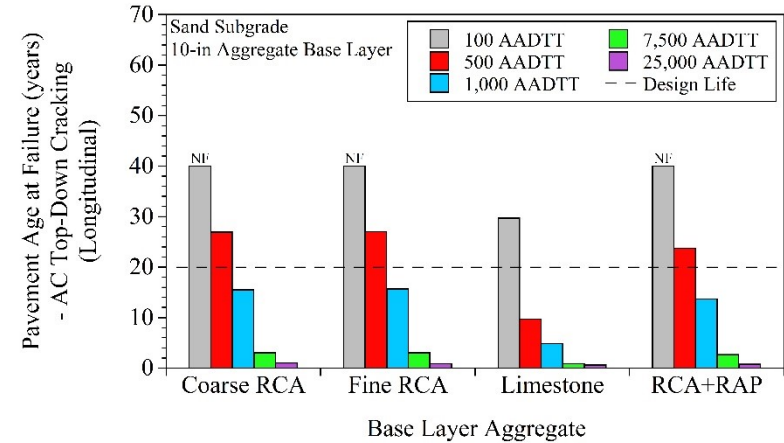
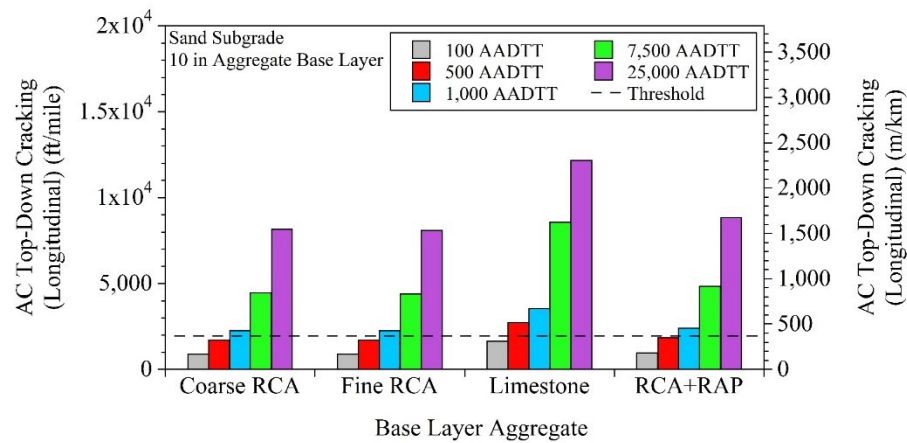
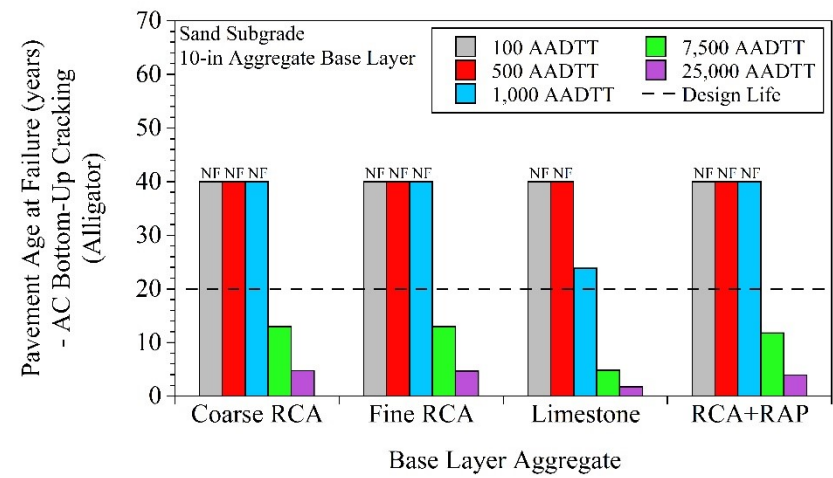
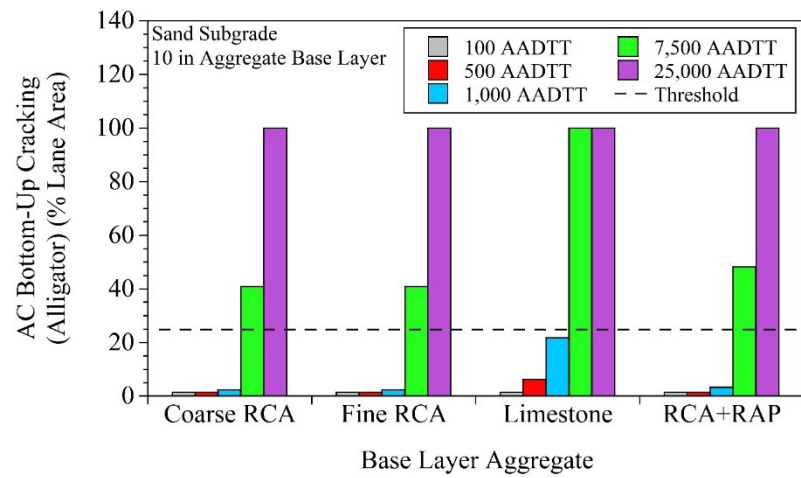
For pavements that contained Sand Subgrade and 8-in aggregate base:



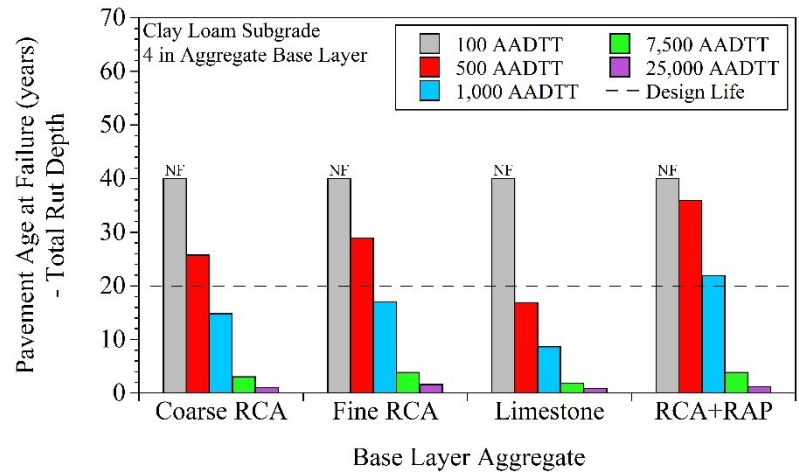
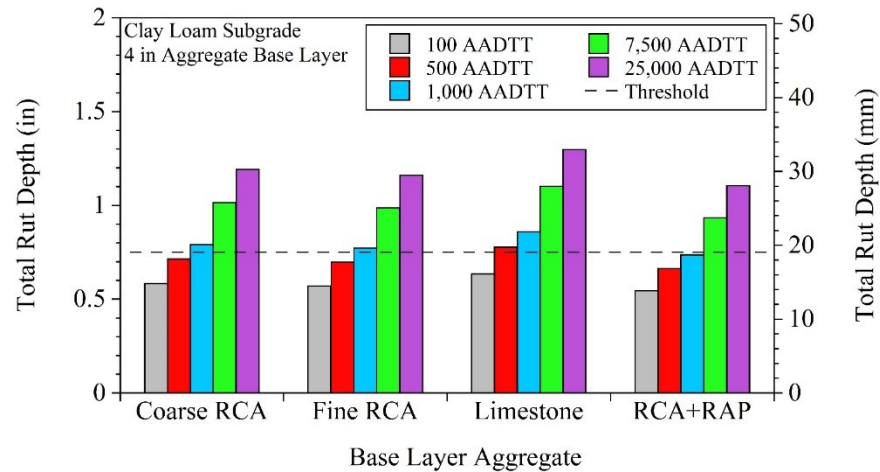
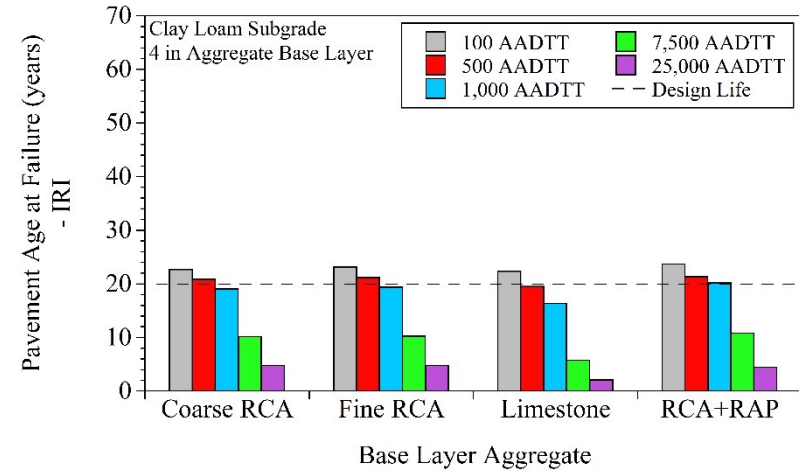
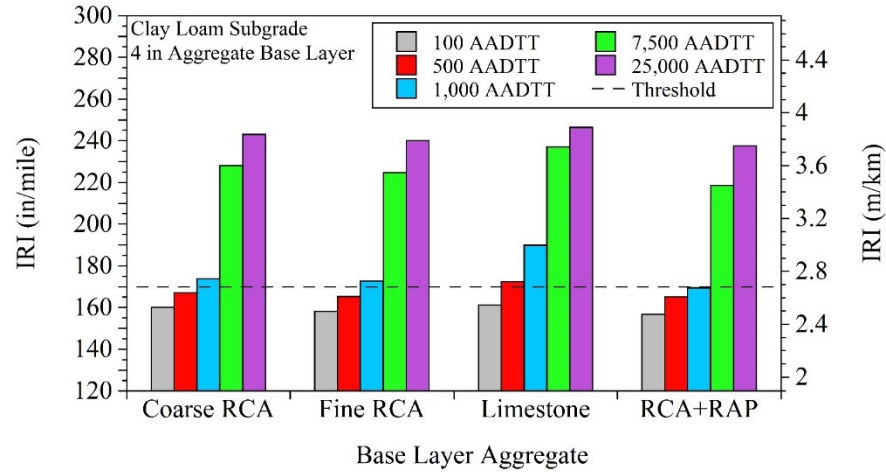


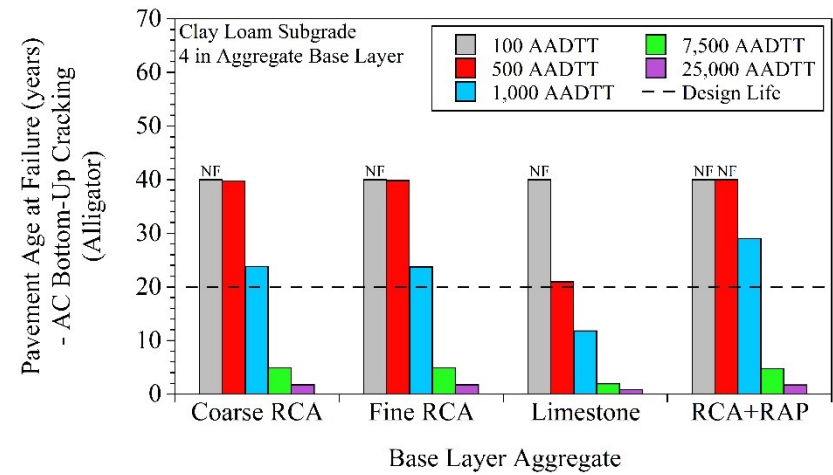
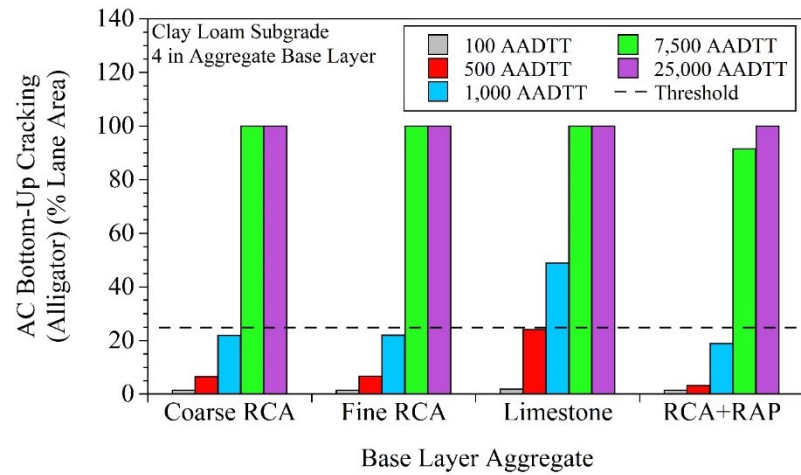
For pavements that contained Sand Subgrade and 10-in aggregate base:



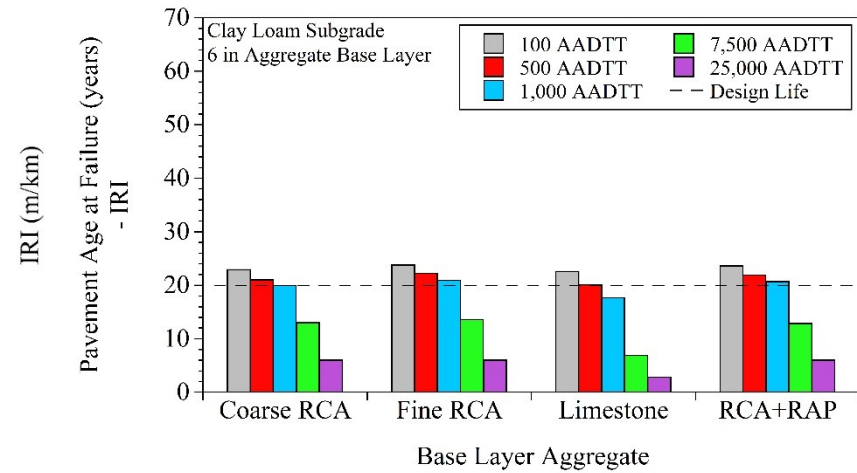
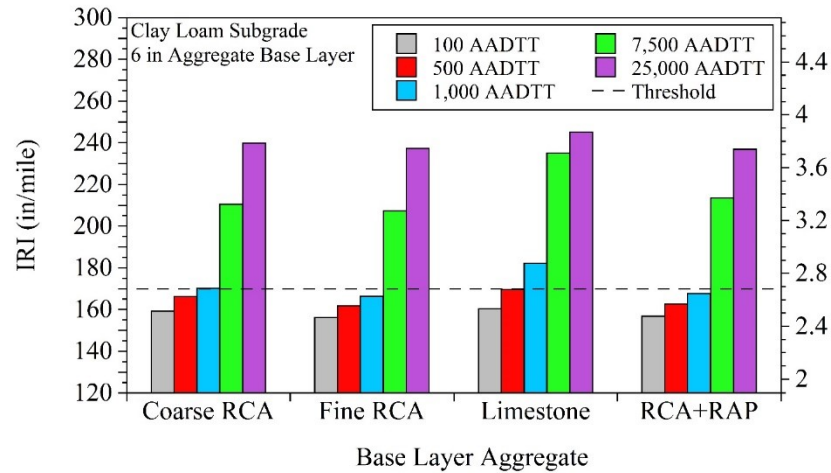


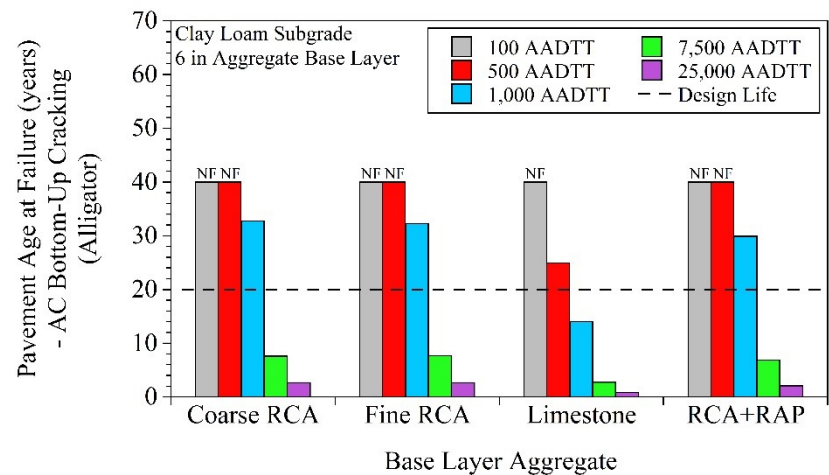
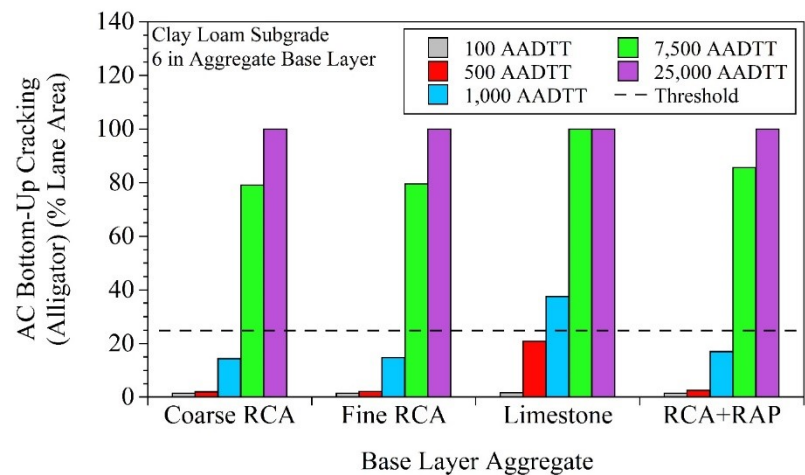
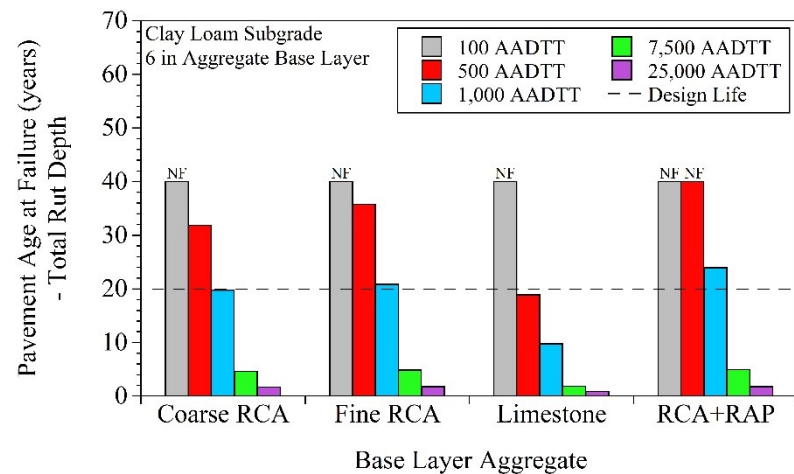
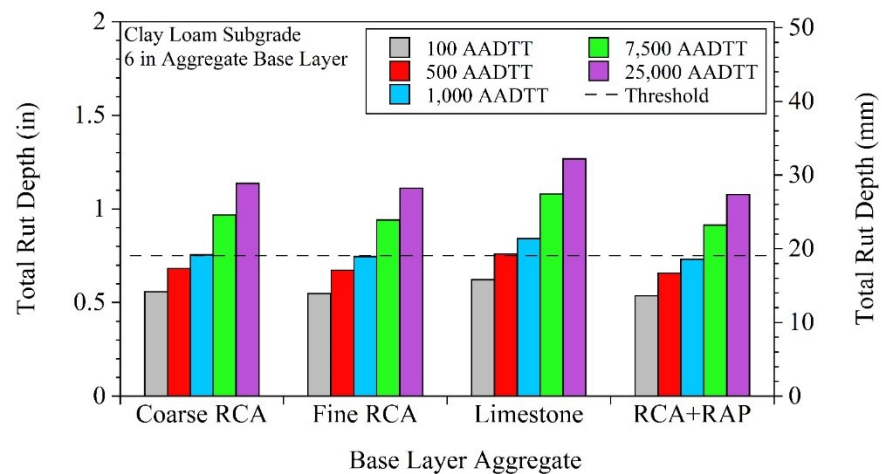
For pavements that contained Clay Loam subgrade and 4-in aggregate base:



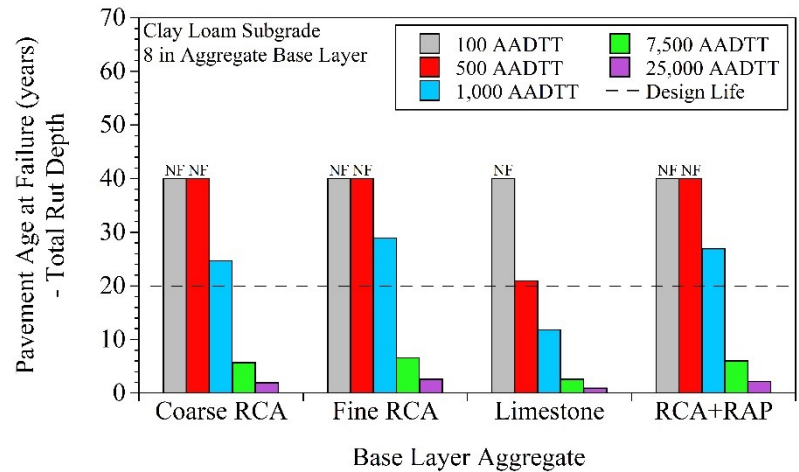
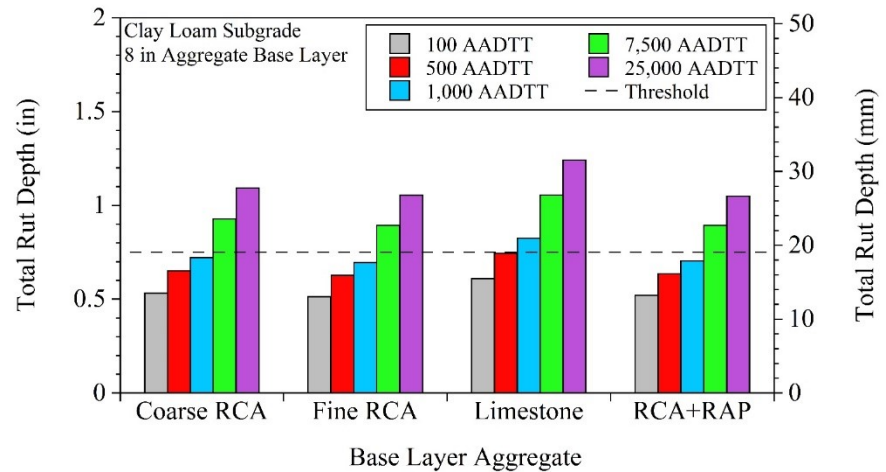
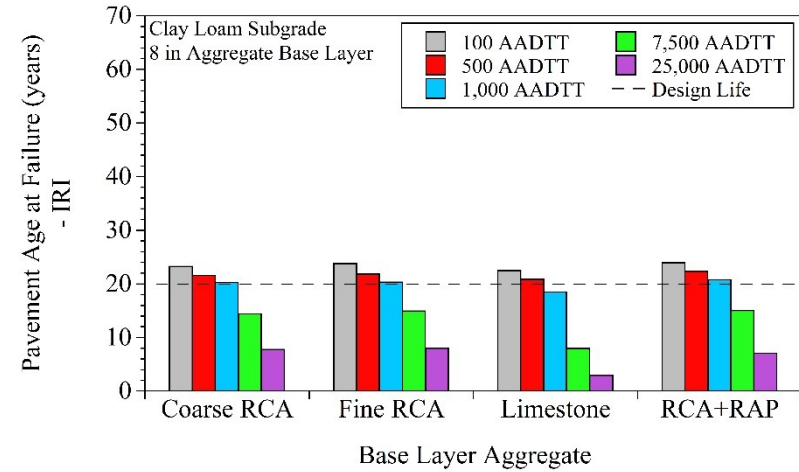
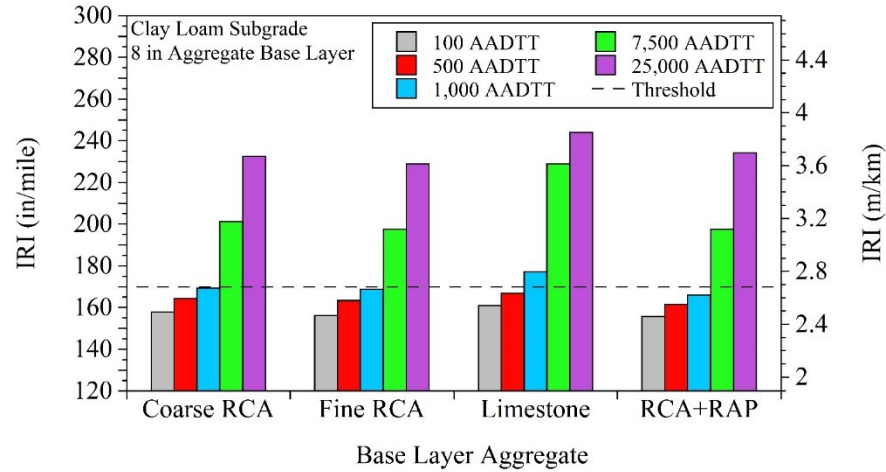


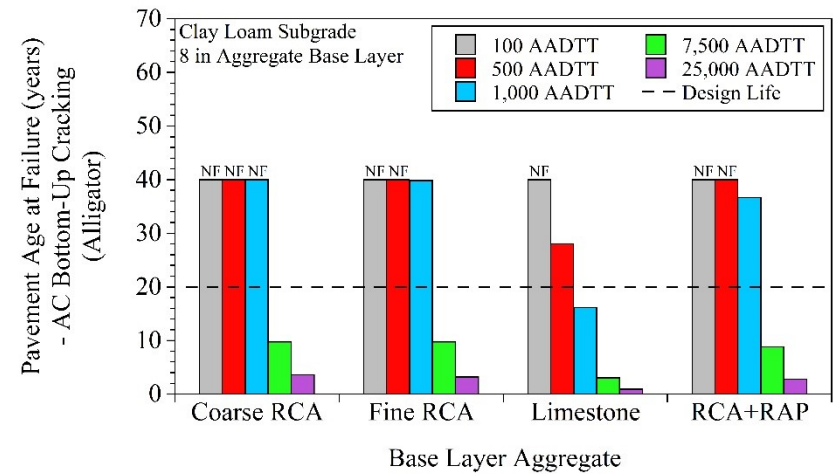
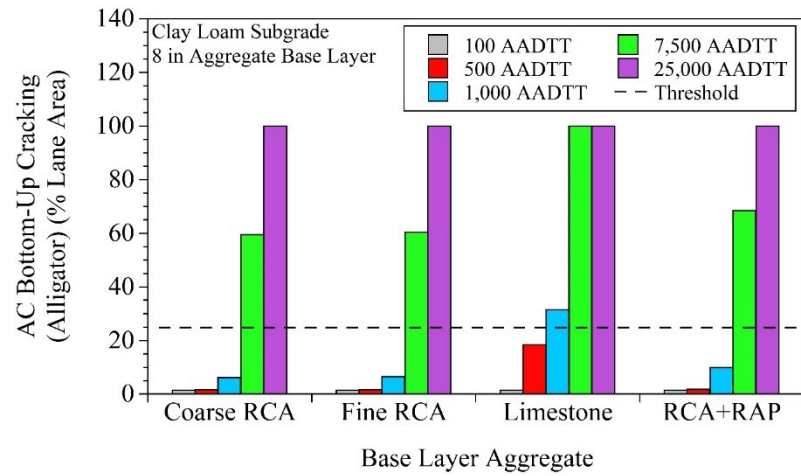
For pavements that contained Clay Loam subgrade and 6-in aggregate base:



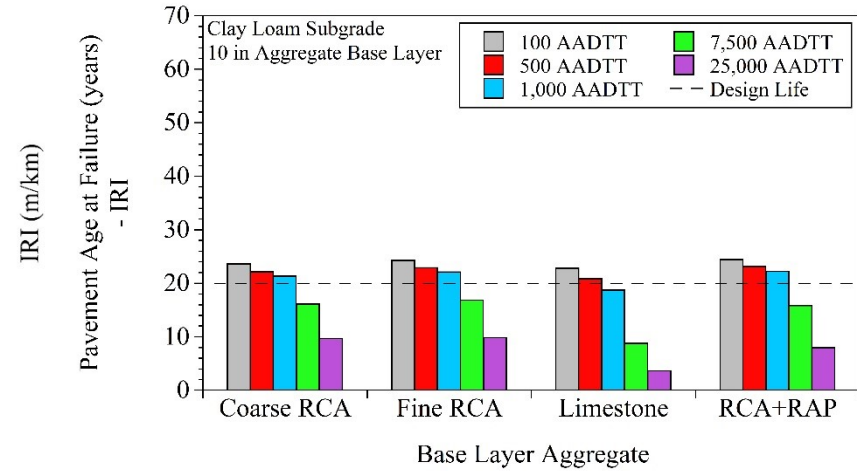
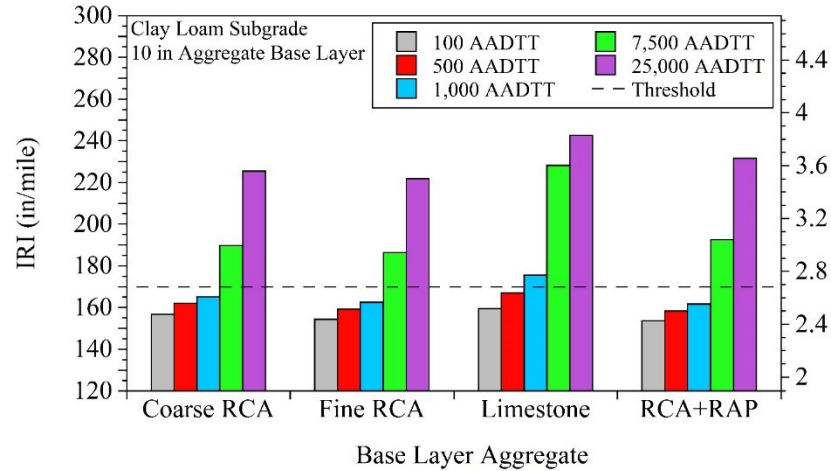


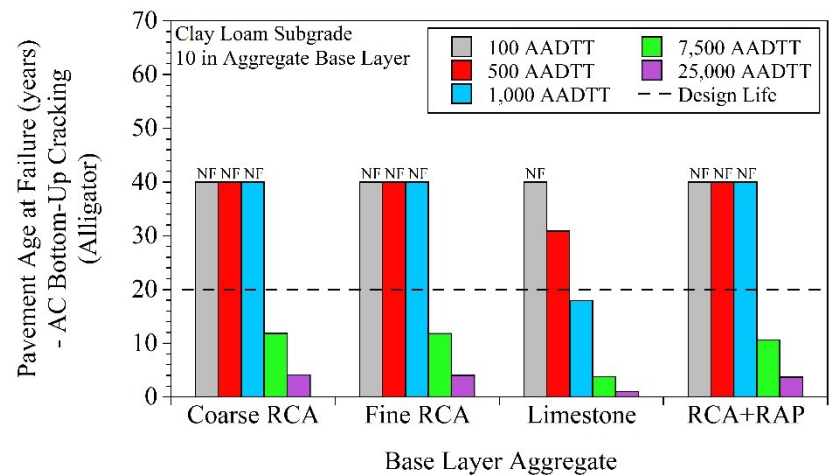
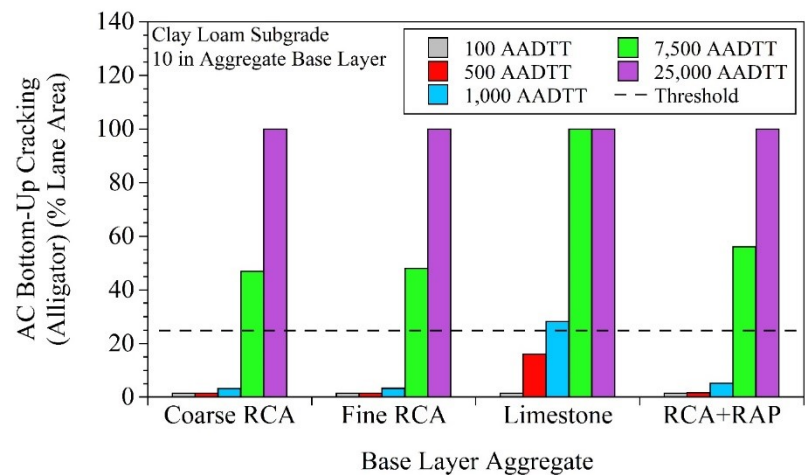
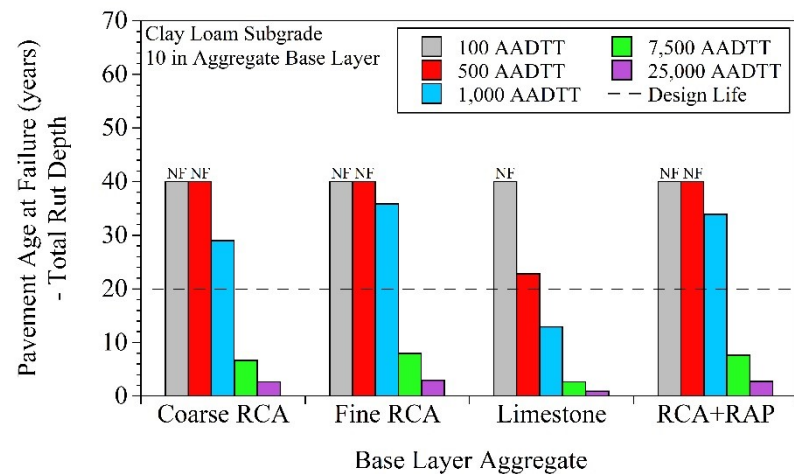
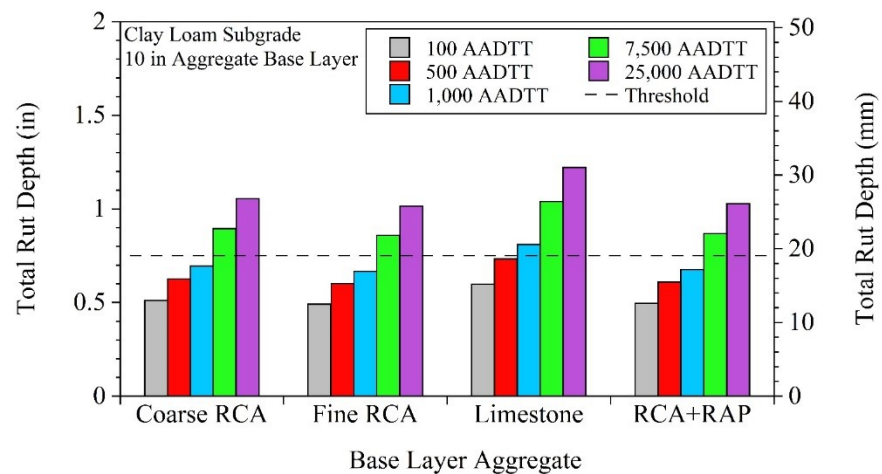
For pavements that contained Clay Loam subgrade and 8-in aggregate base:



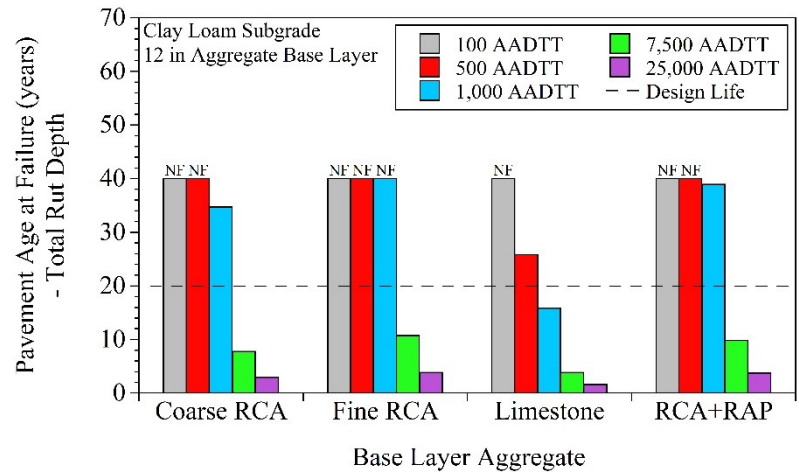
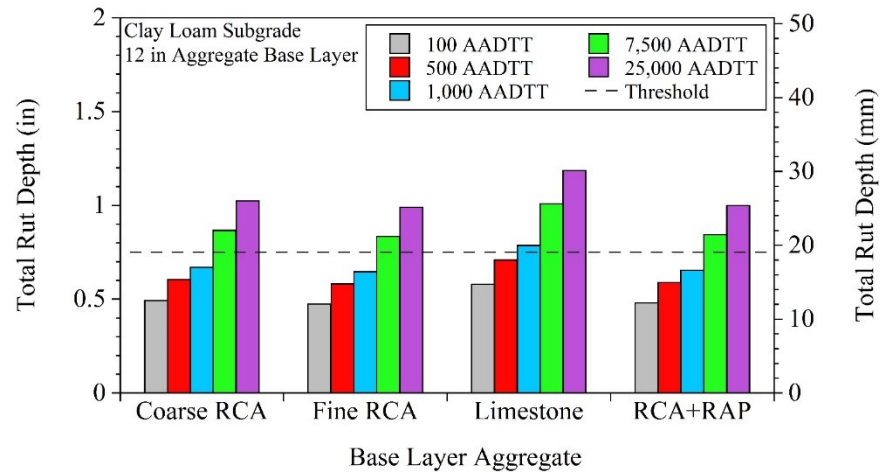
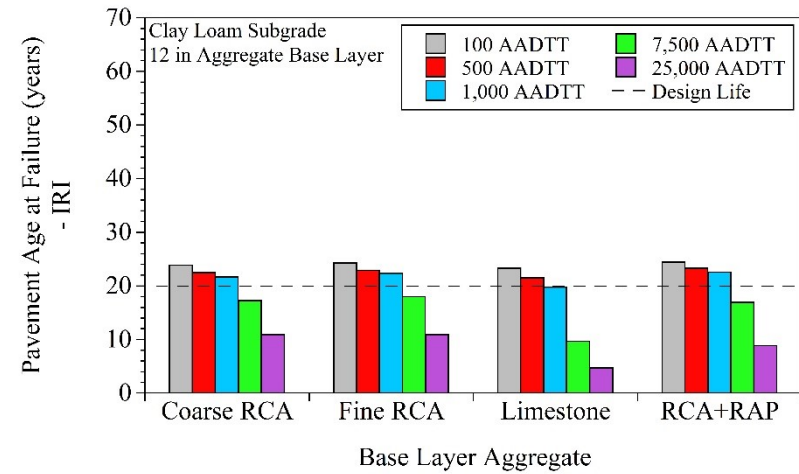
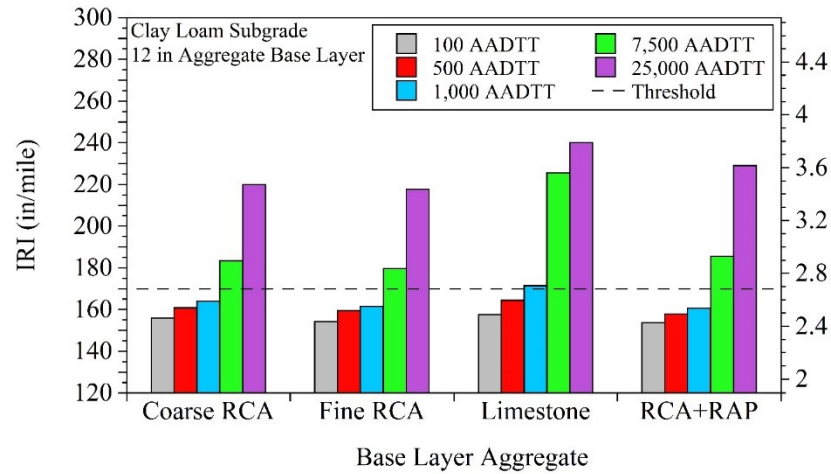


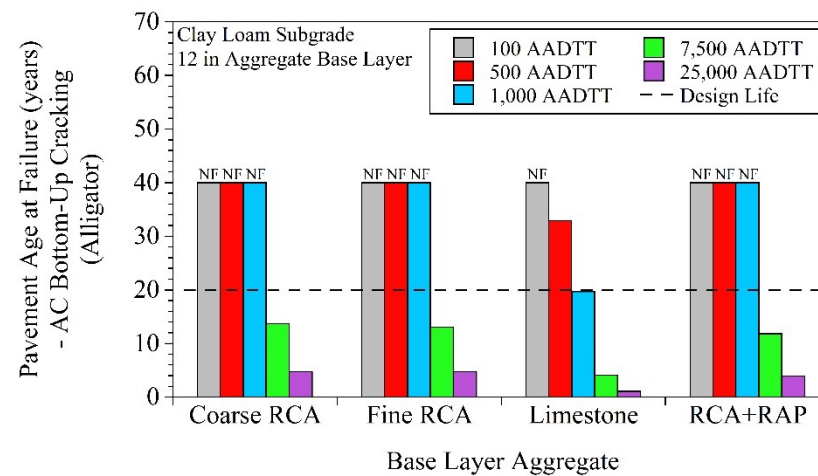
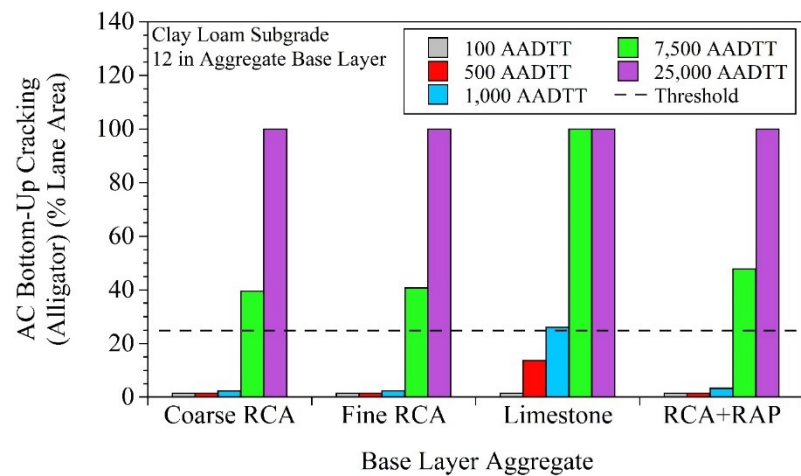
For pavements that contained Clay Loam subgrade and 10-in aggregate base:





For pavements that contained Clay Loam subgrade and 12-in aggregate base:

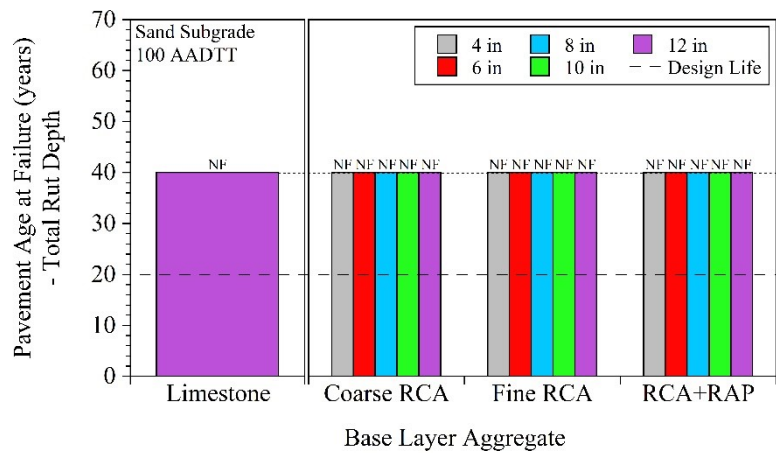
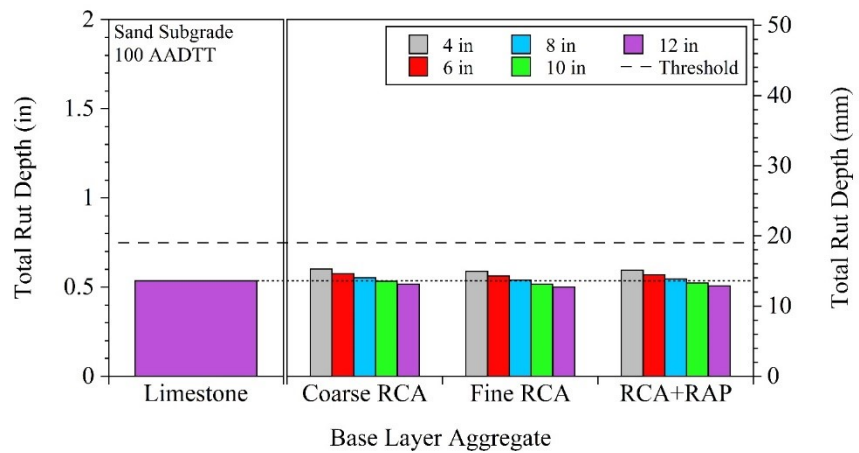
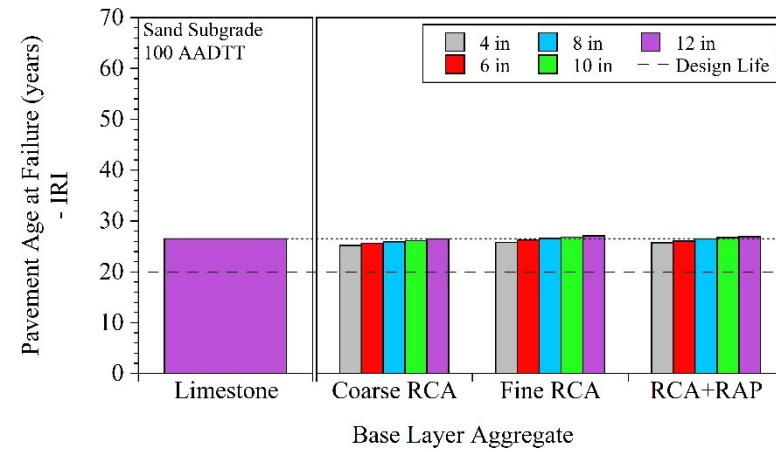
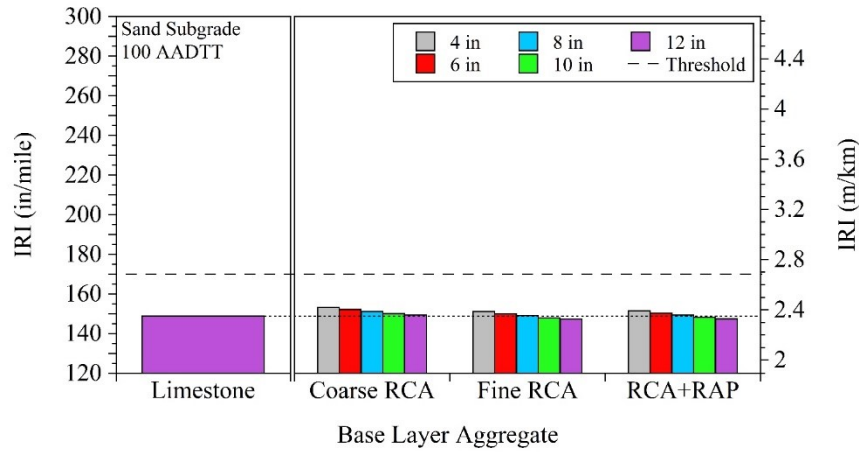


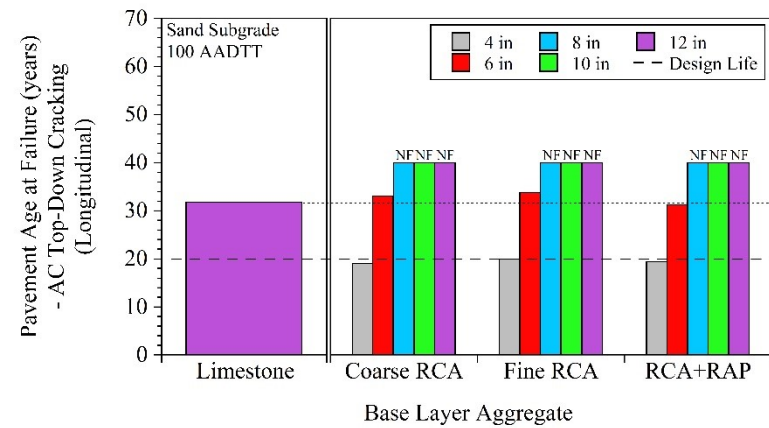
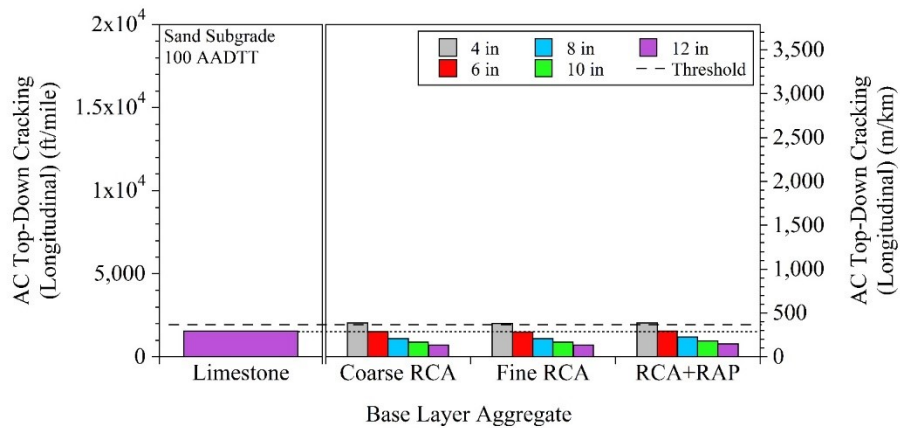
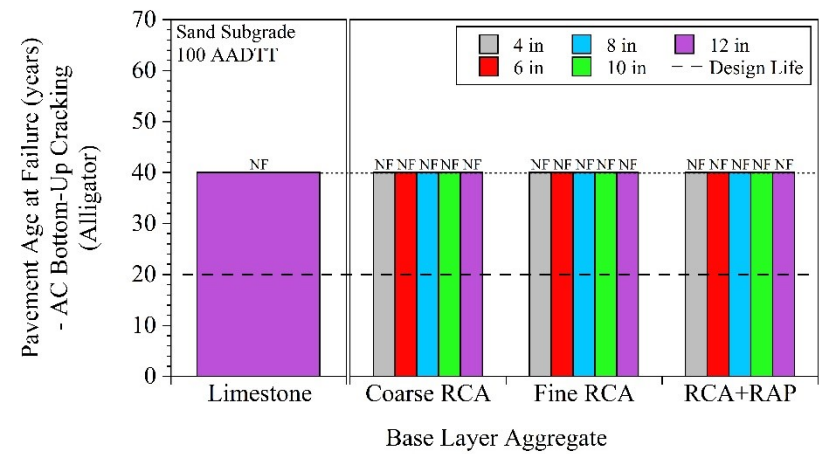
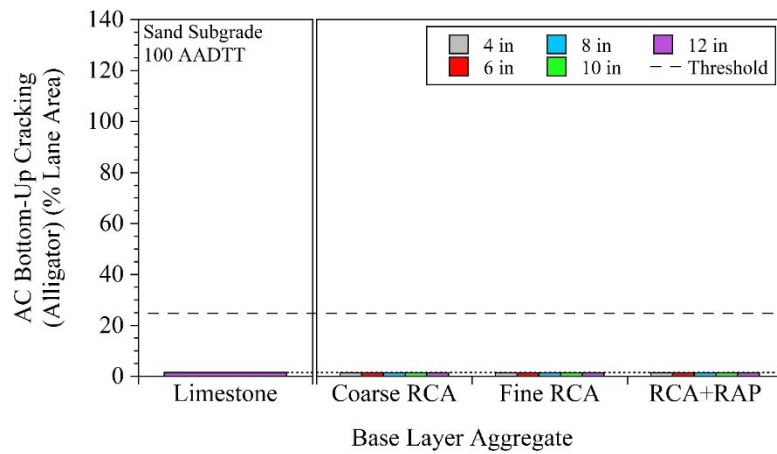


APPENDIX BF

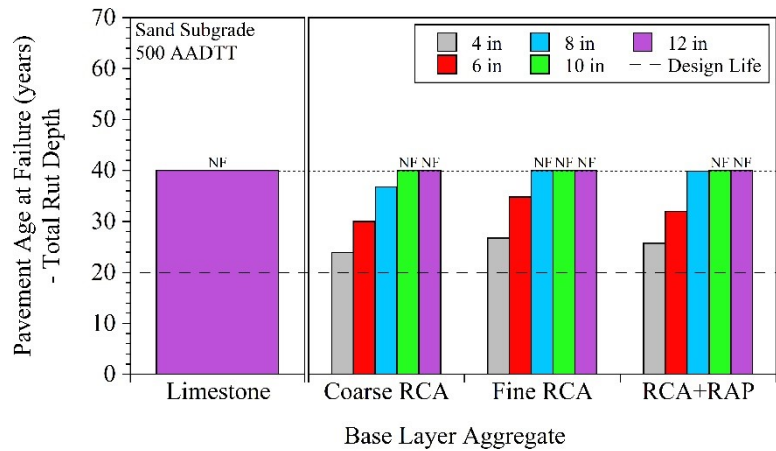
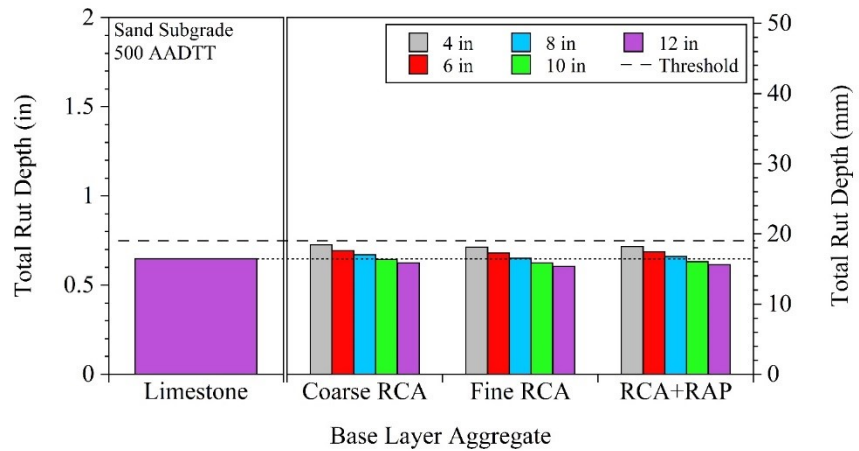
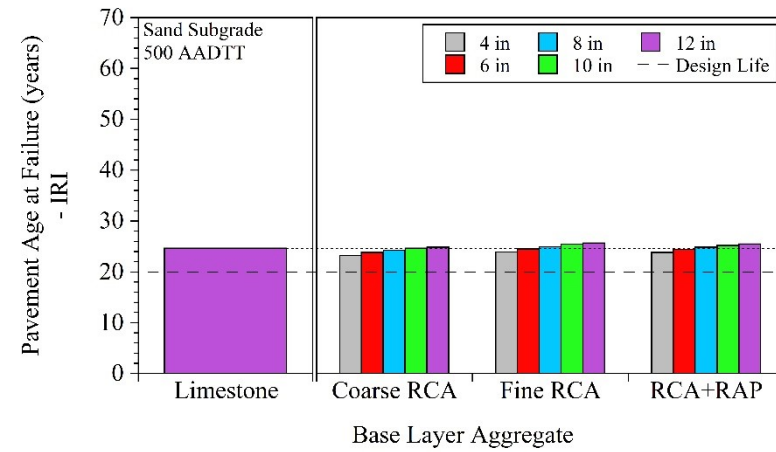
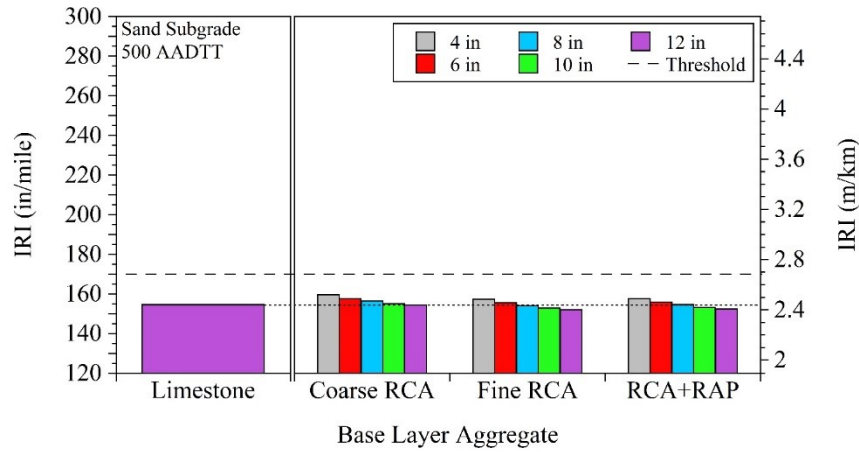
RELATIVE RECYCLED AGGREGATE BASE (RAB) LAYER THICKNESS

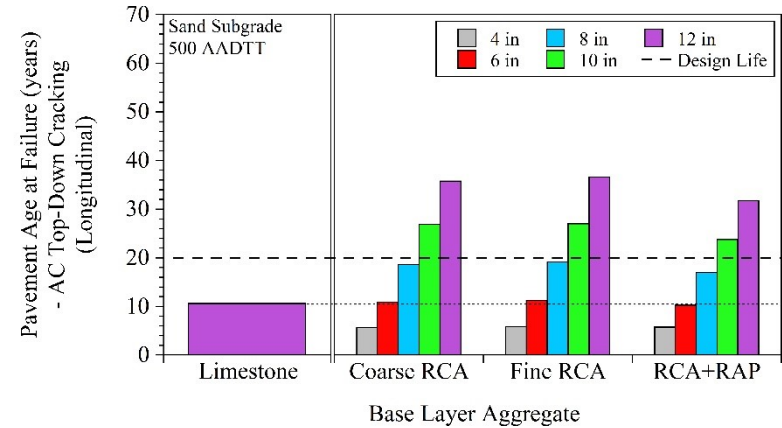
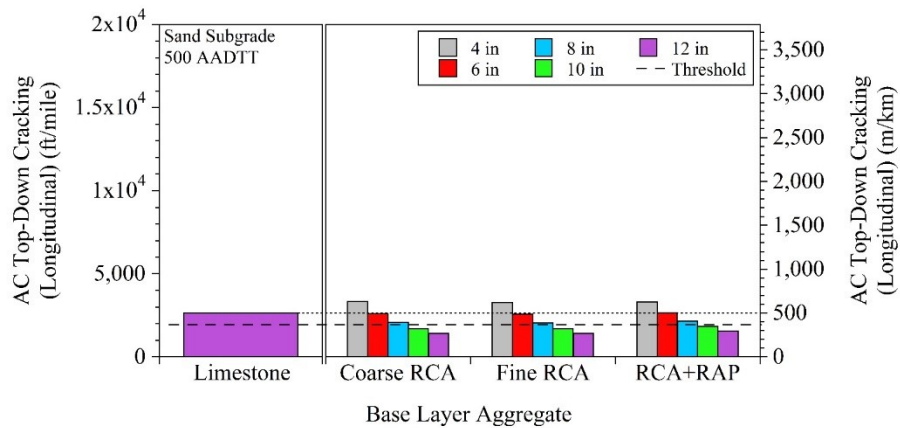
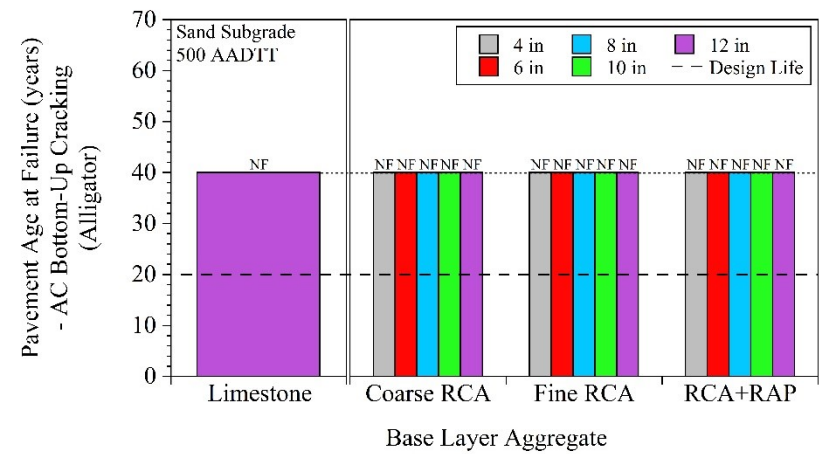
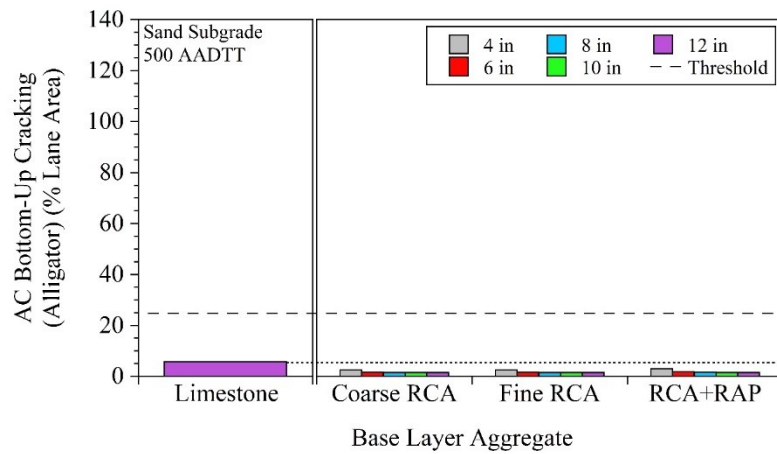
For pavements that contained Sand Subgrade - 100 AADTT:



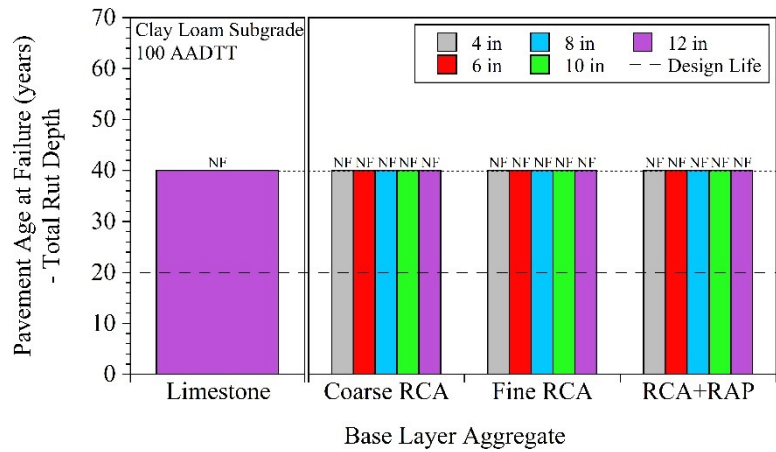
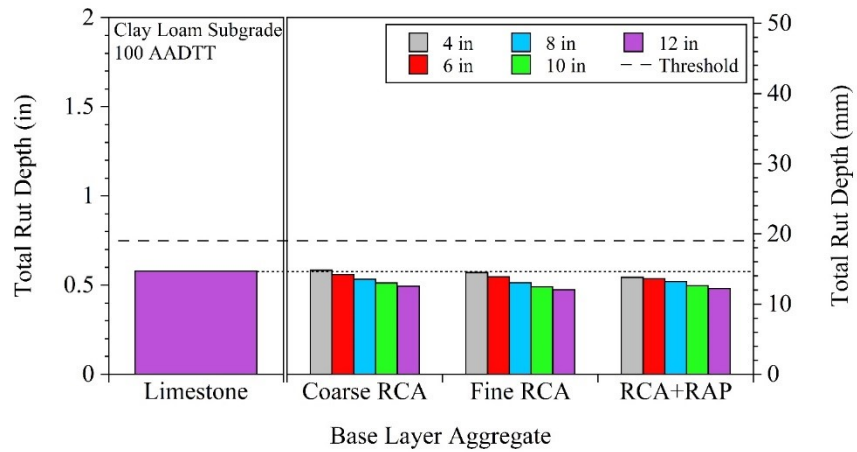
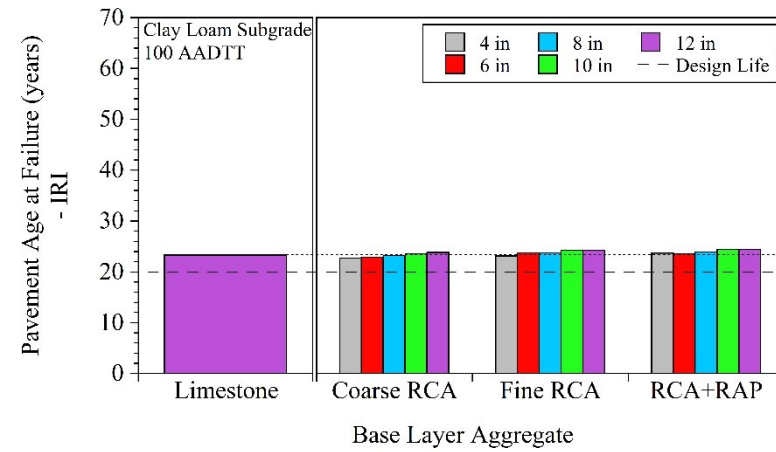
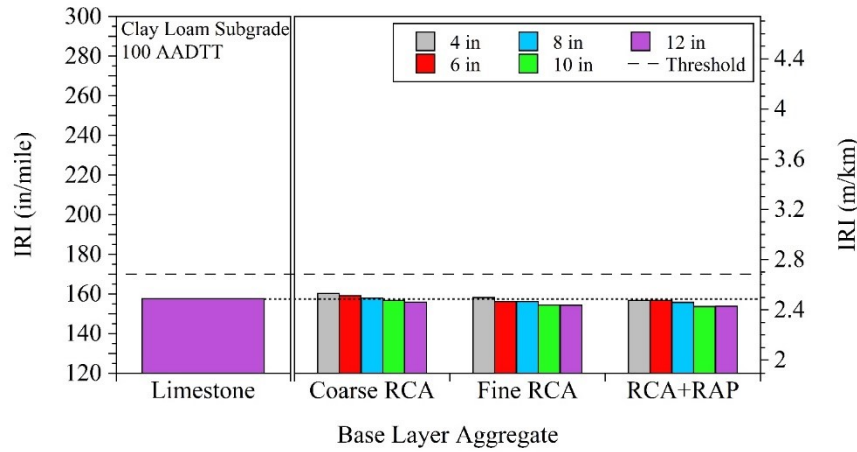


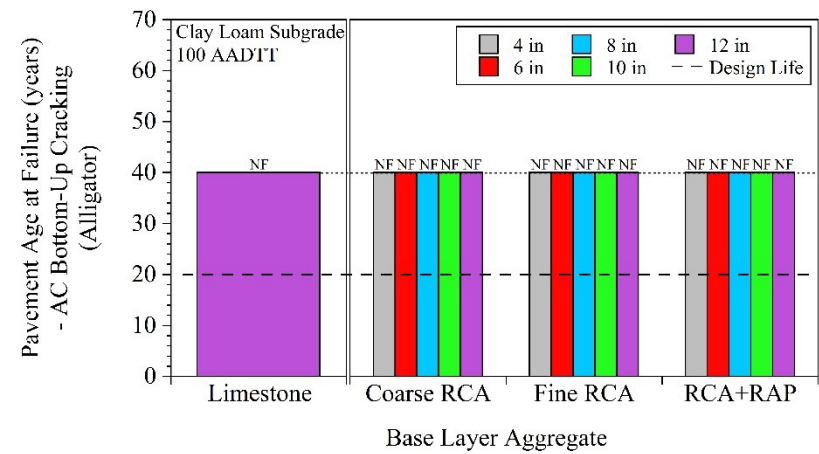
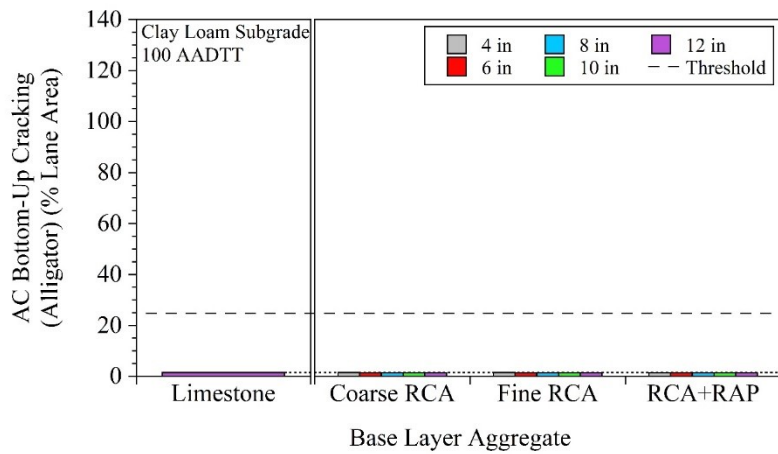
For pavements that contained Sand Subgrade - 500 AADTT:



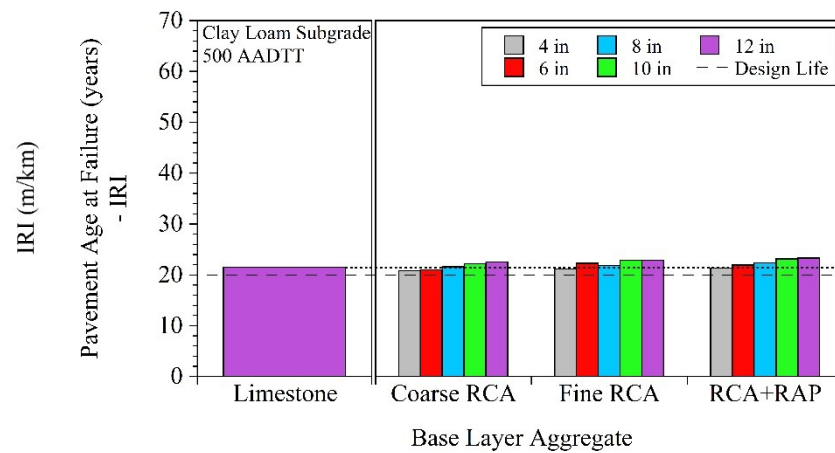
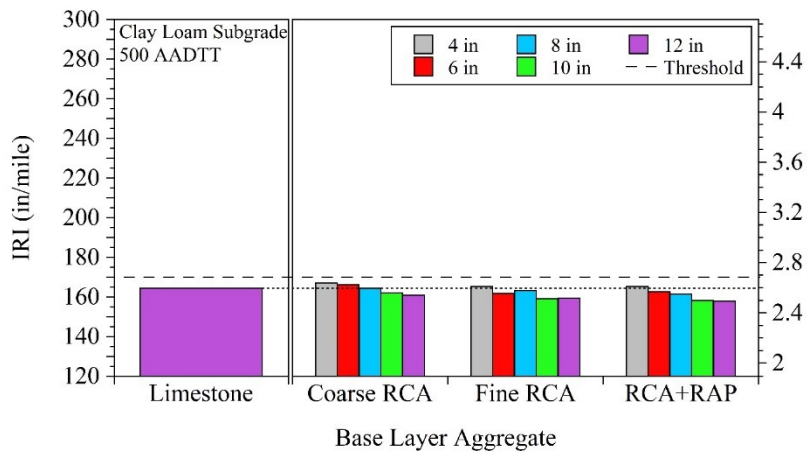


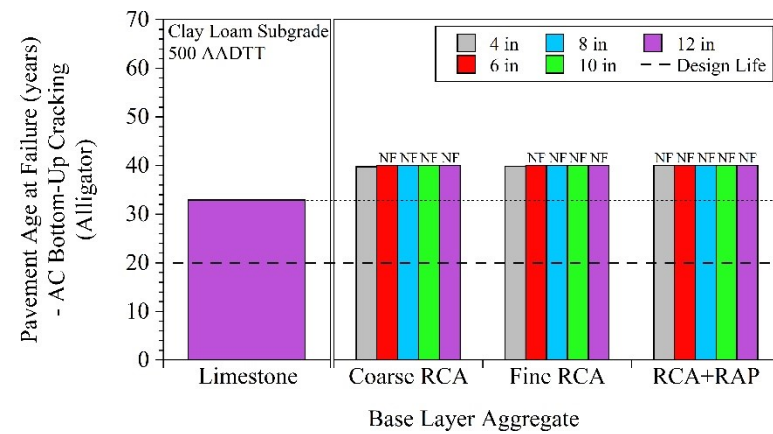
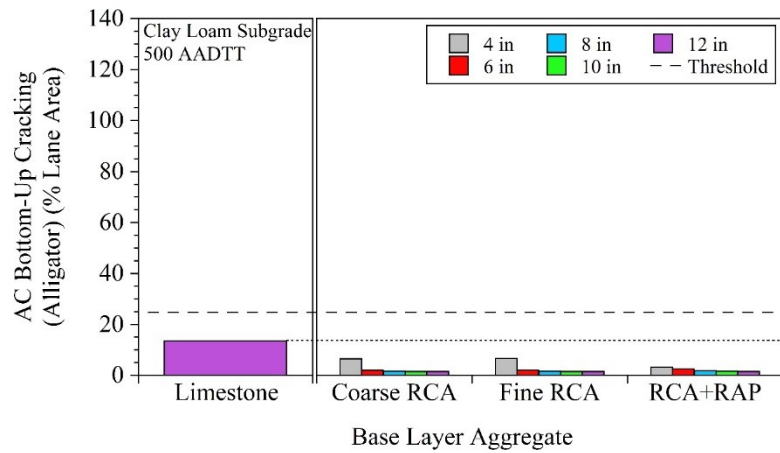
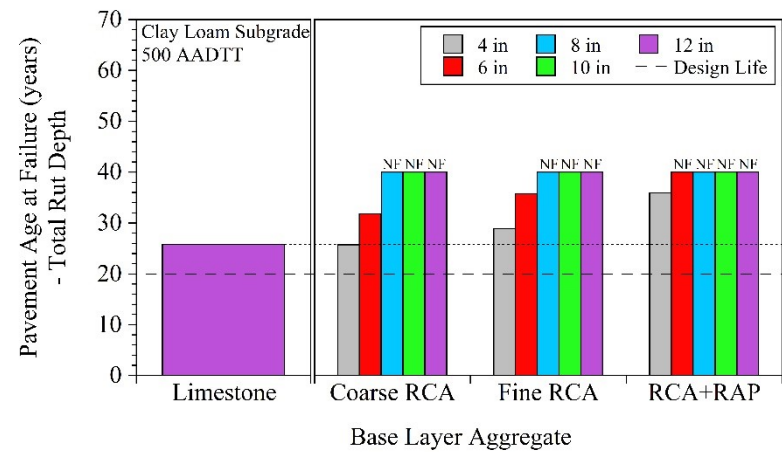
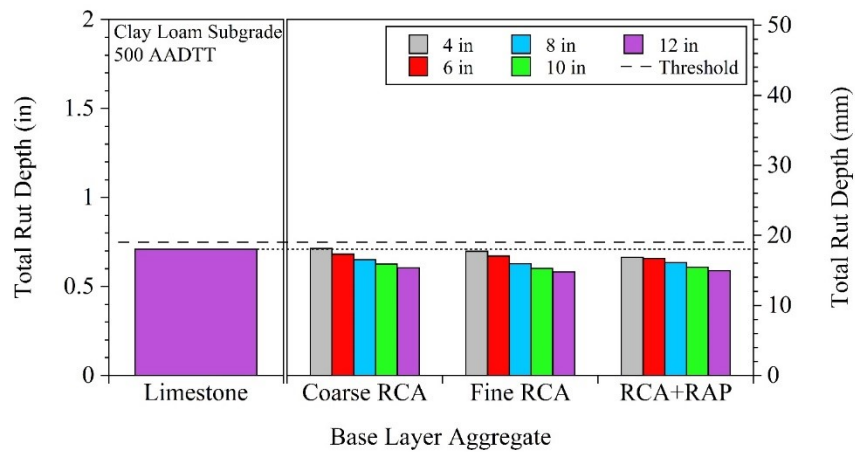
For pavements that contained Clay Loam subgrade - 100 AADTT:



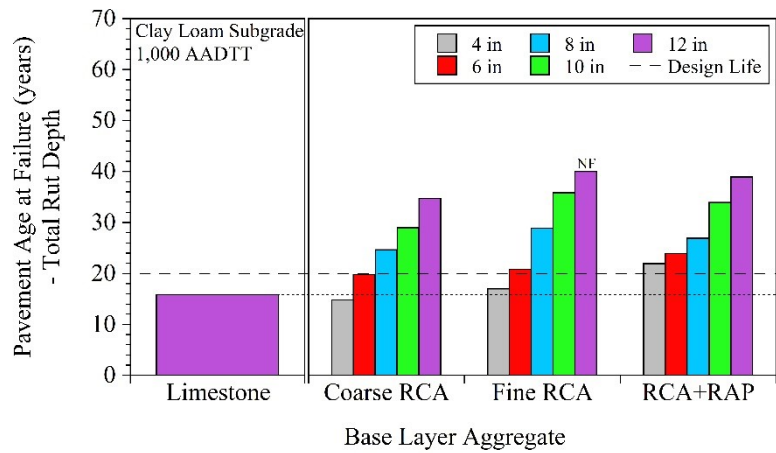
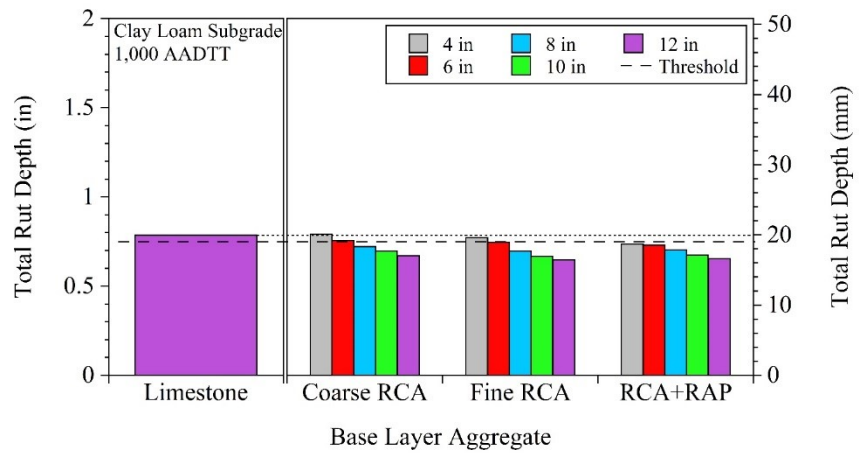
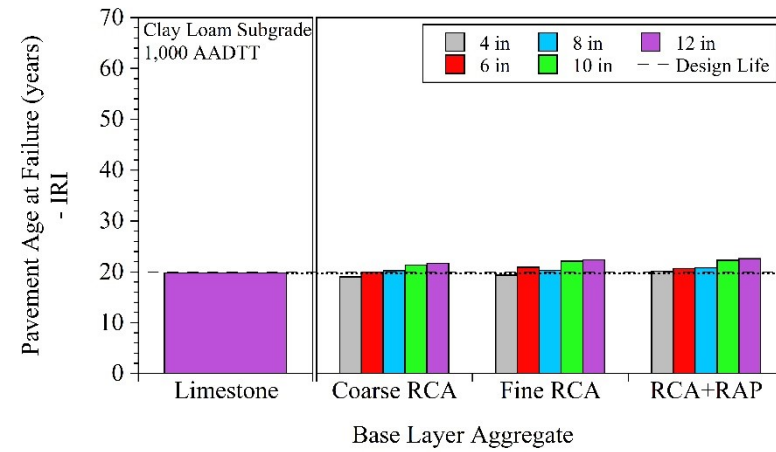
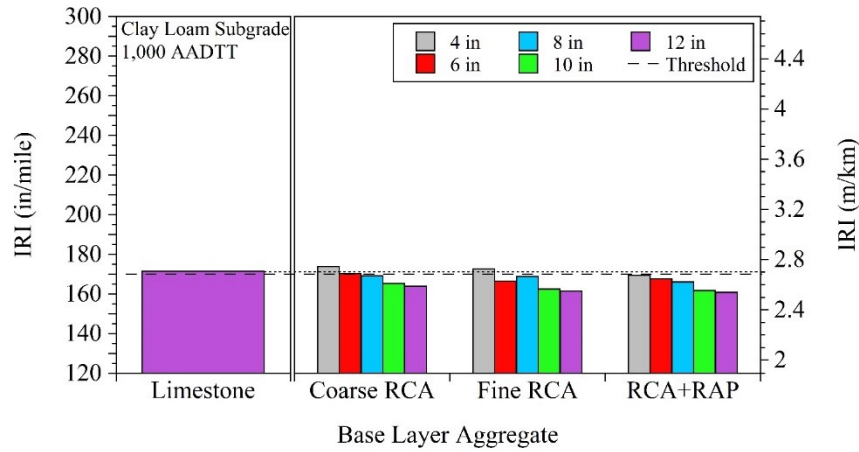


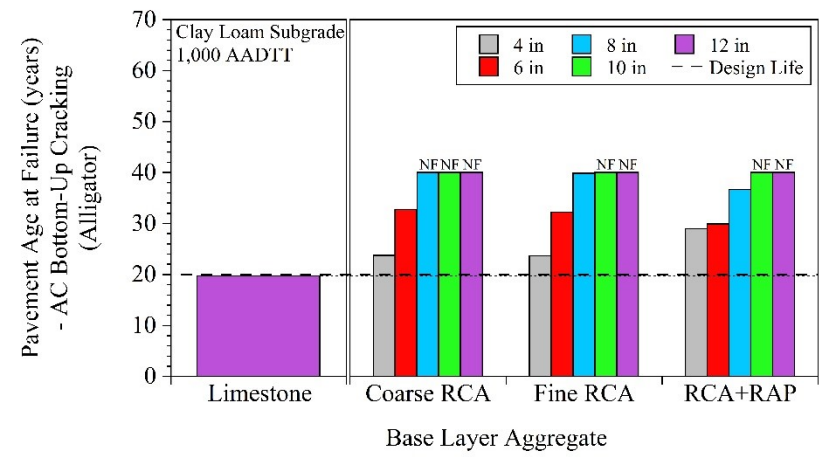
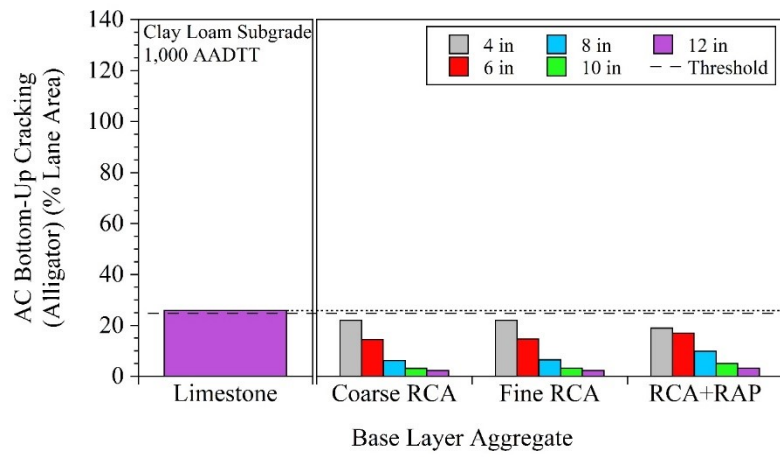
For pavements that contained Clay Loam subgrade - 500 AADTT:





For pavements that contained Clay Loam subgrade - 1,000 AADTT:

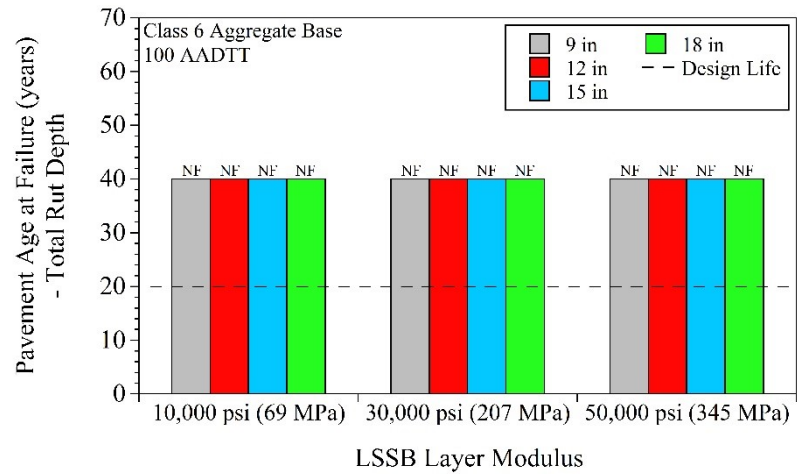
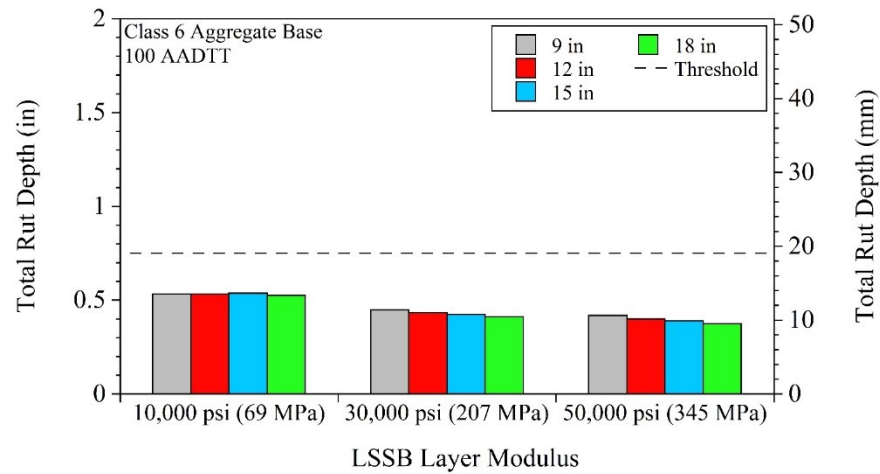
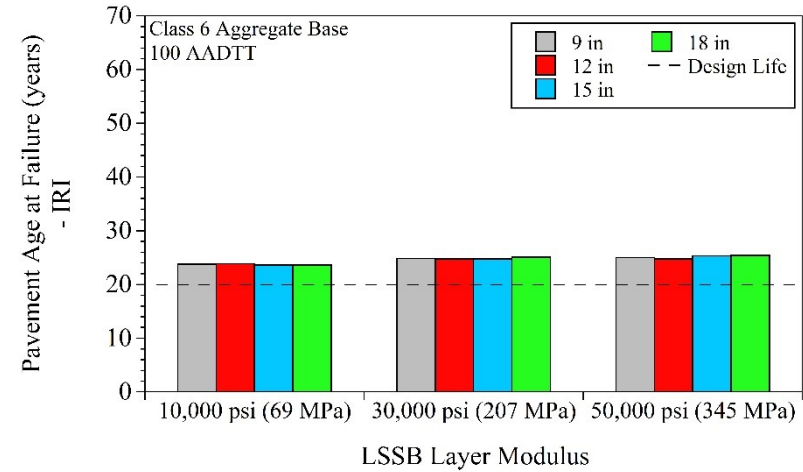
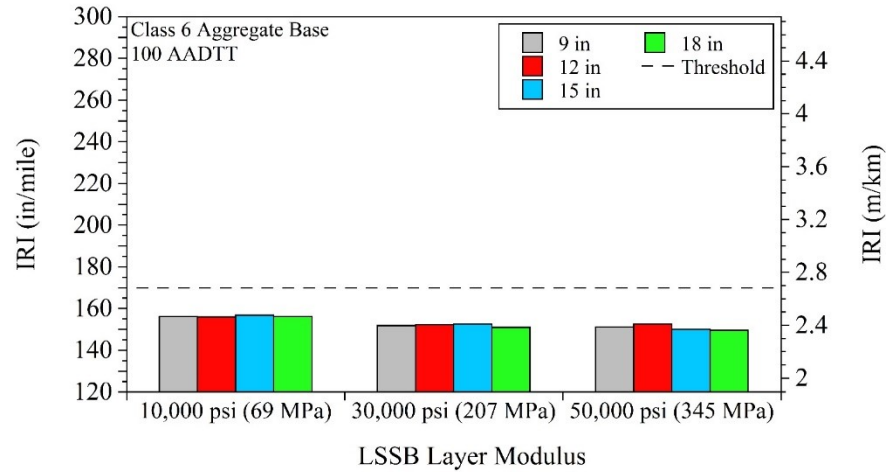


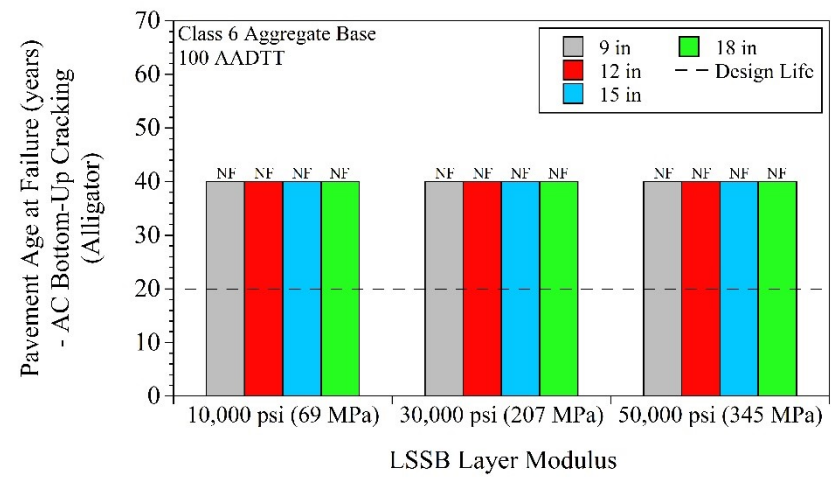
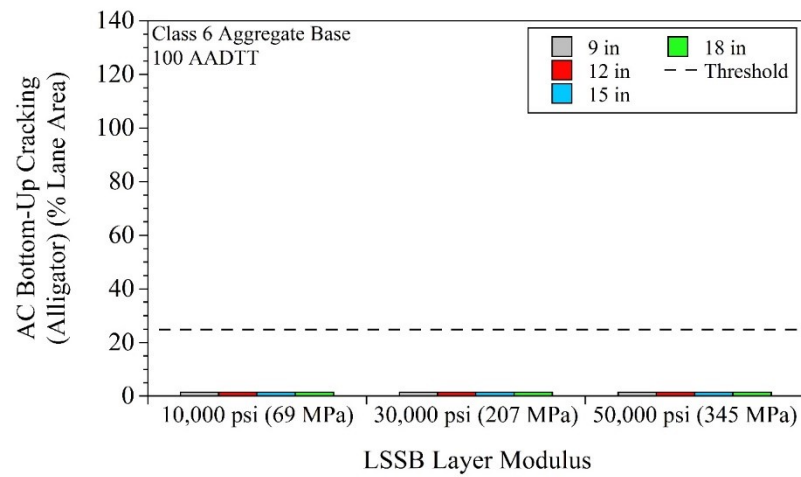


APPENDIX BG

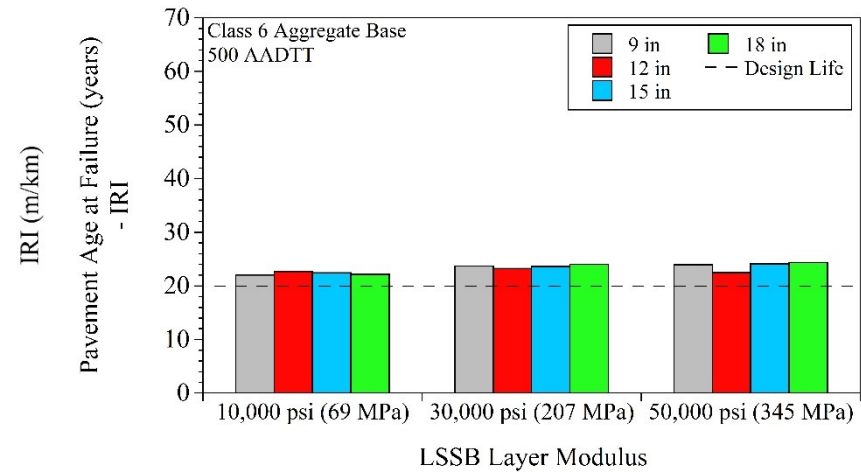
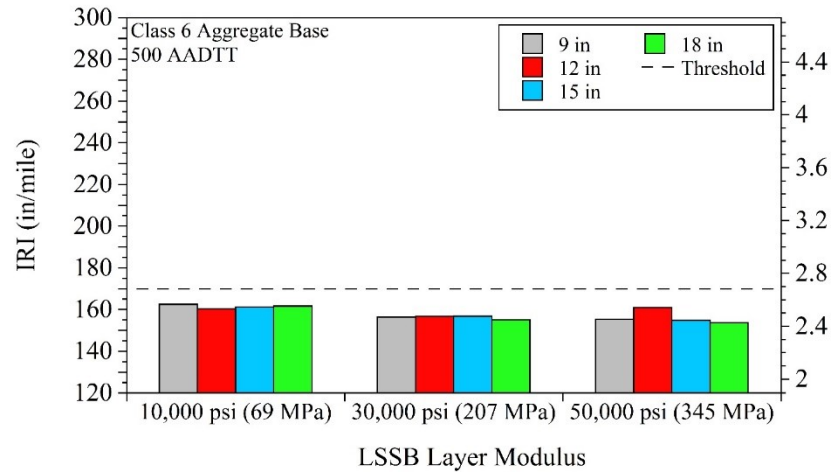
EFFECT OF LARGE STONE SUBBASE (LSSB) THICKNESS ON PAVEMENT PERFORMANCE PREDICTIONS

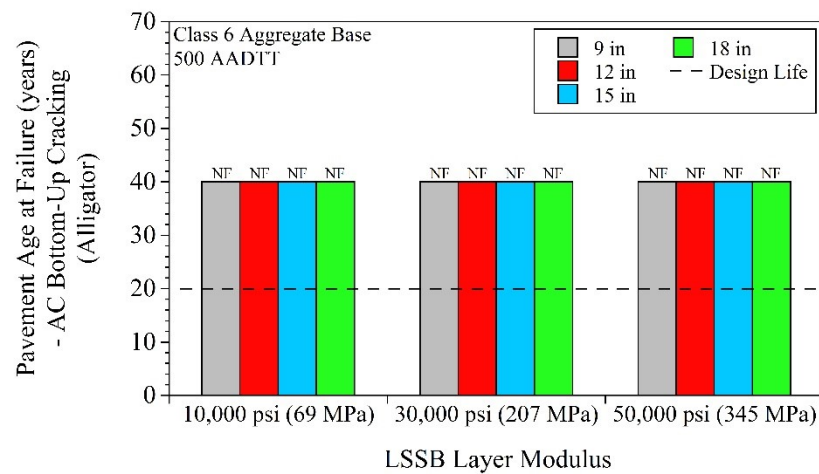
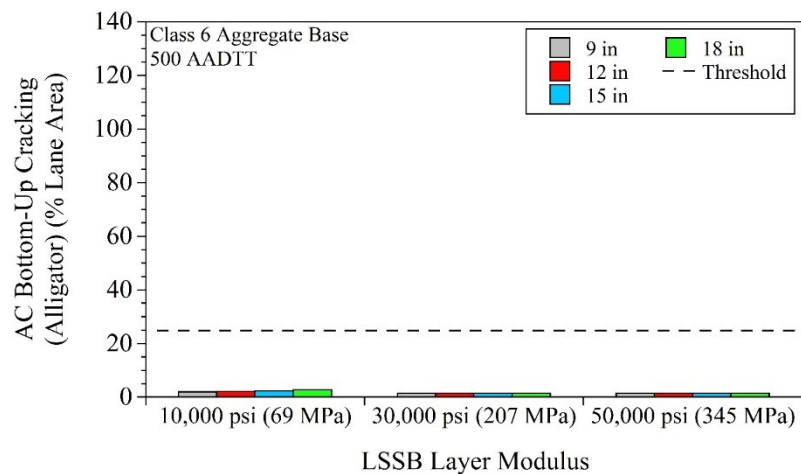
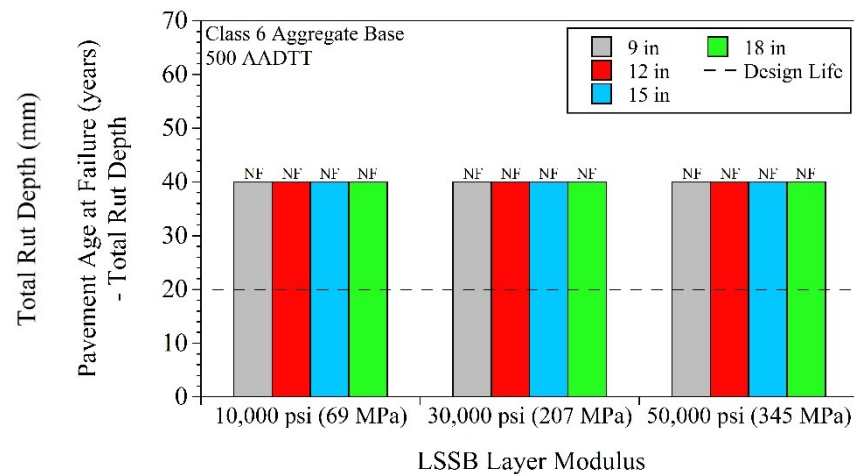
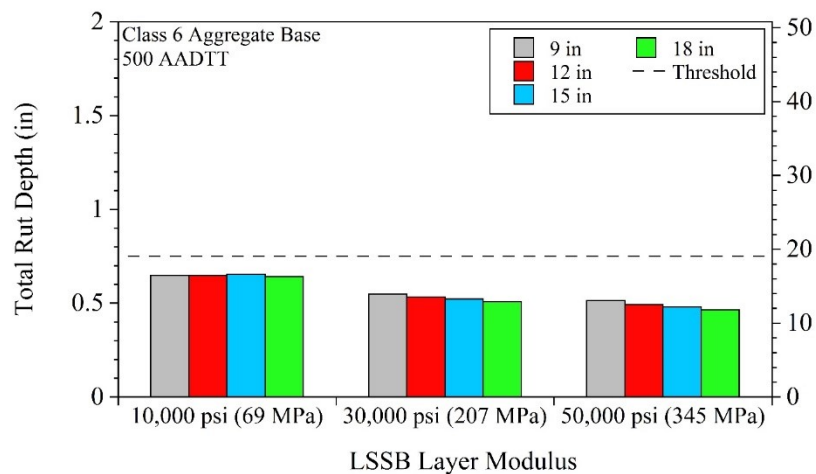
For pavement models that contained Class 6 Aggregate base - 100 AADTT:



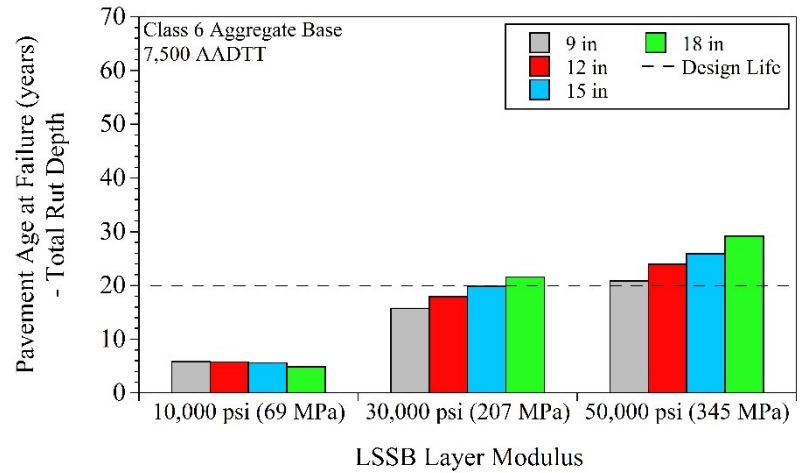
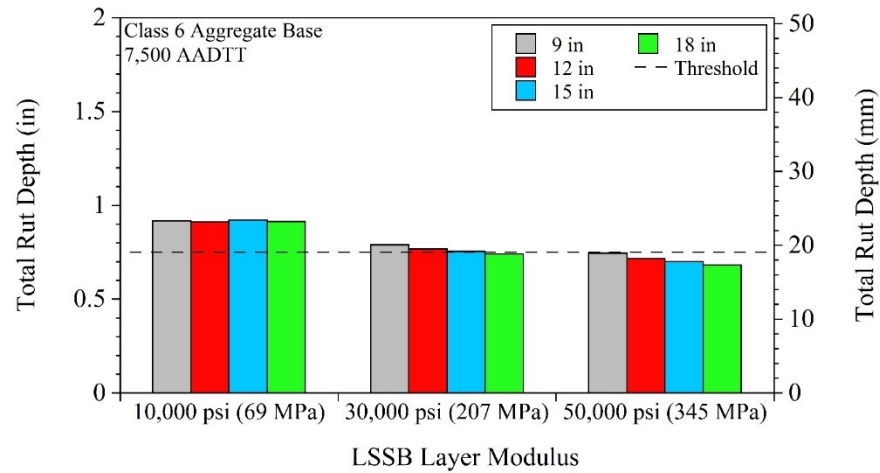
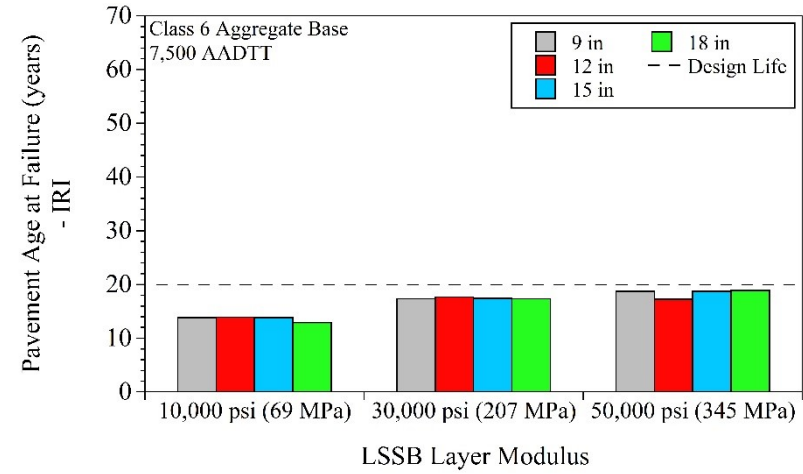
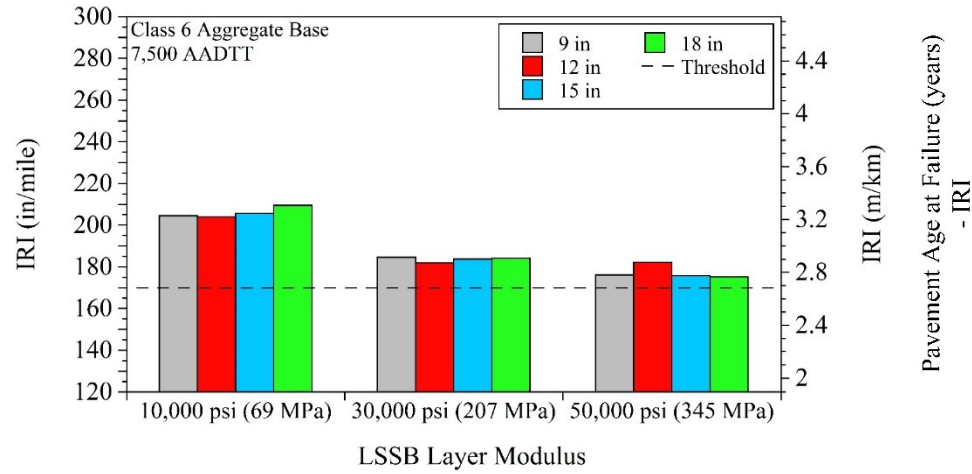


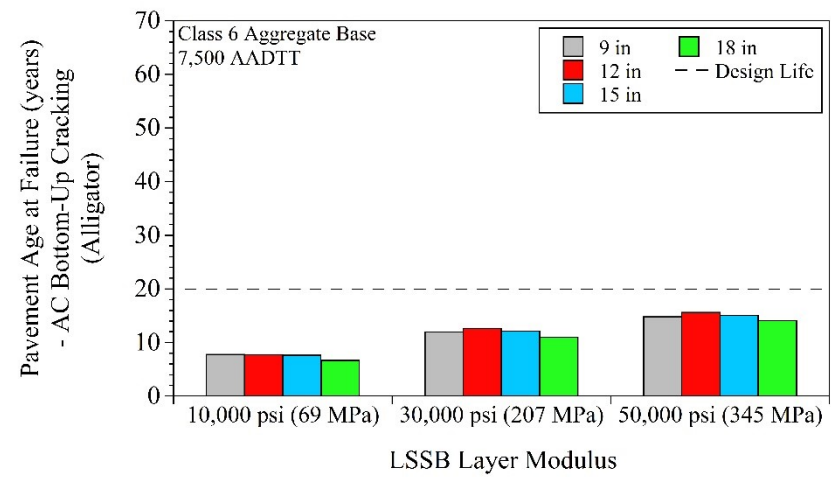
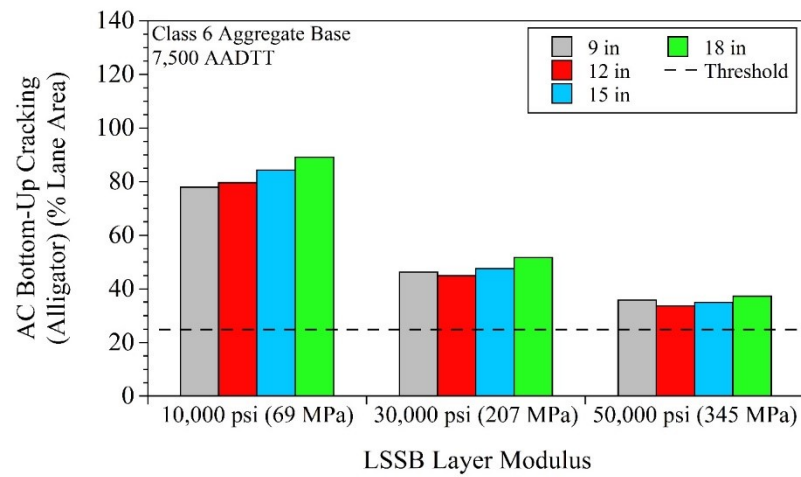
For pavement models that contained Class 6 Aggregate base - 500 AADTT:



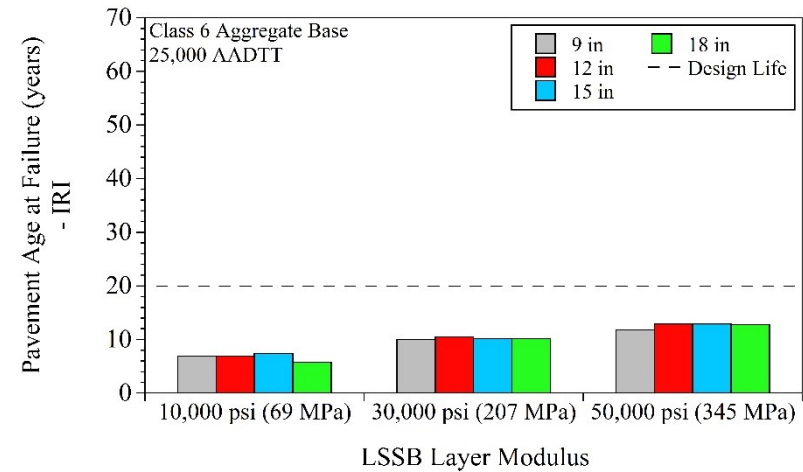
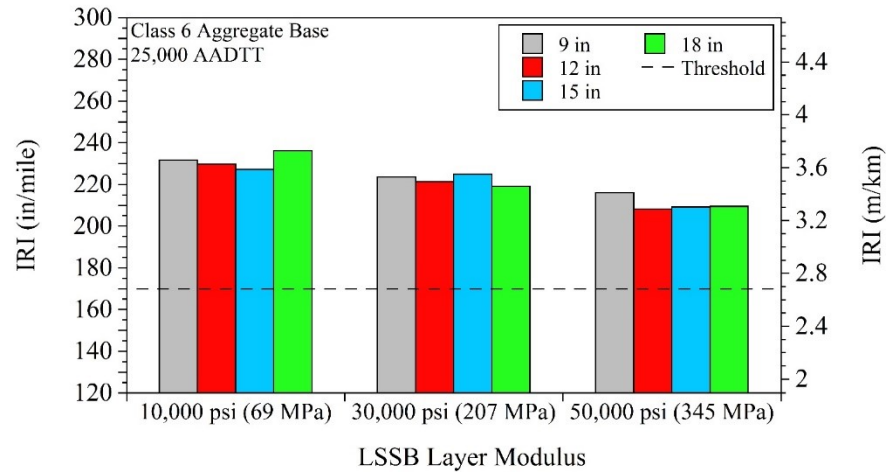


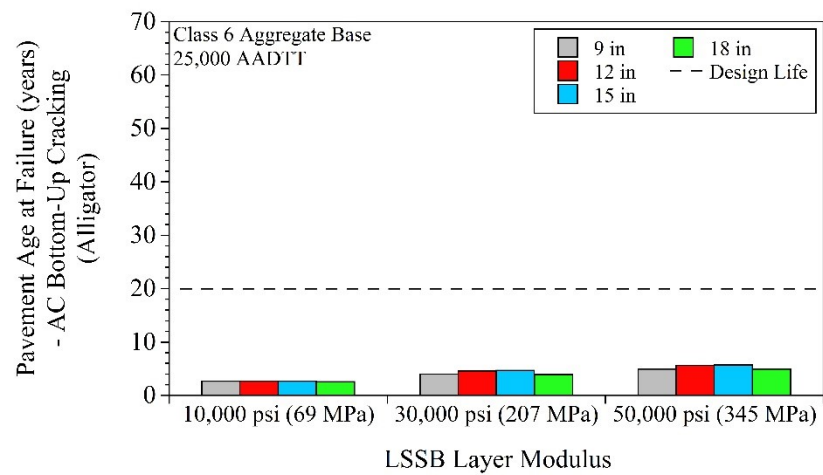
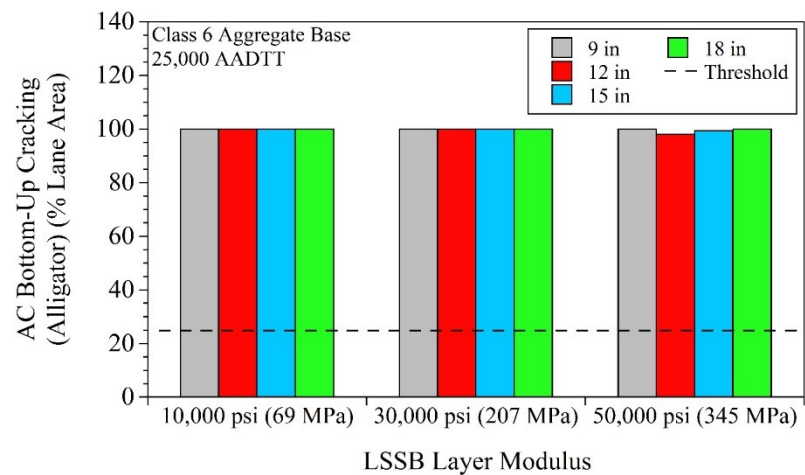
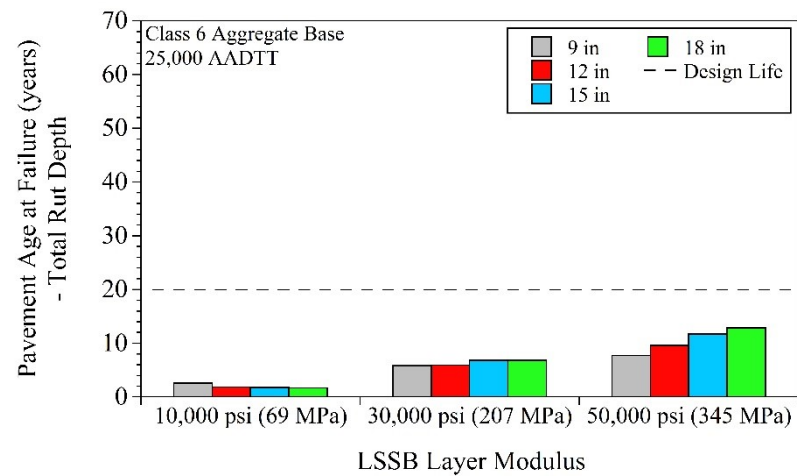
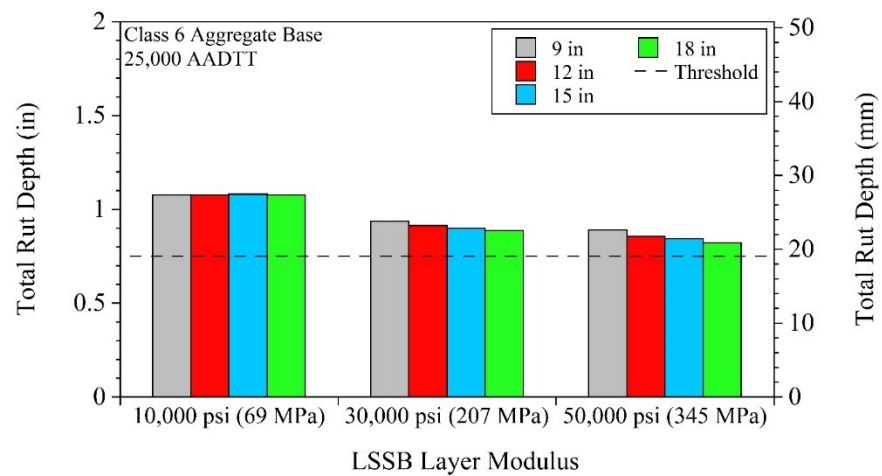
For pavement models that contained Class 6 Aggregate base - 7,500 AADTT:



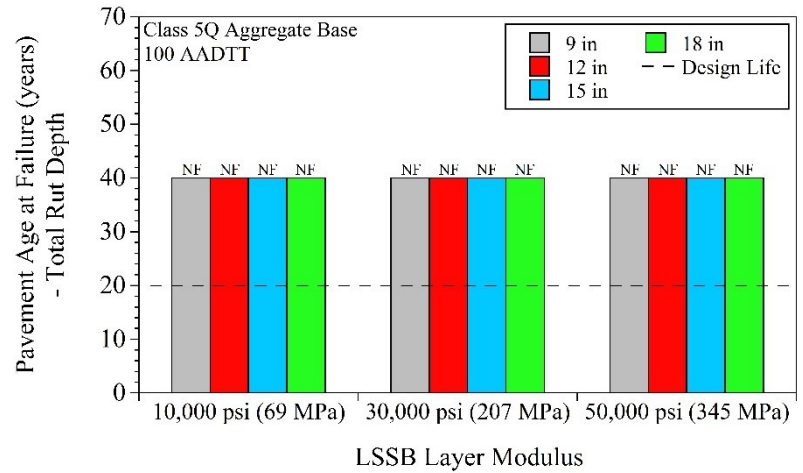
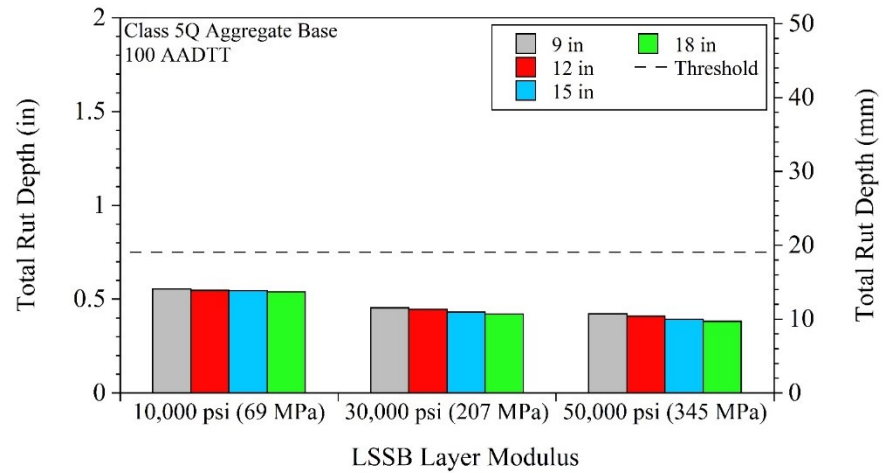
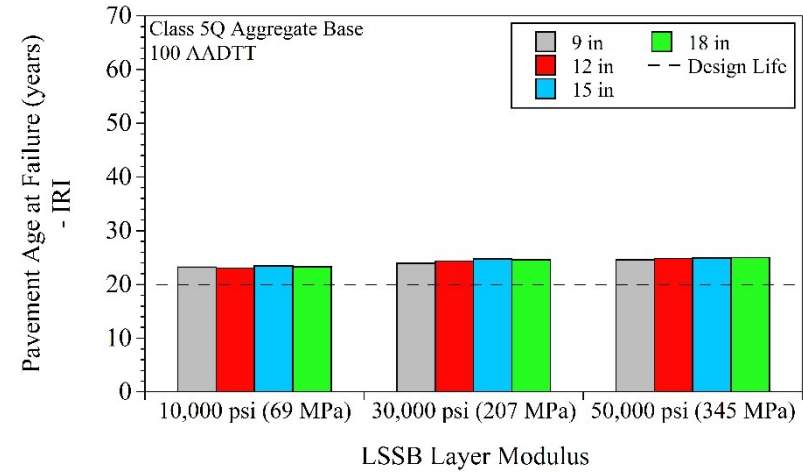
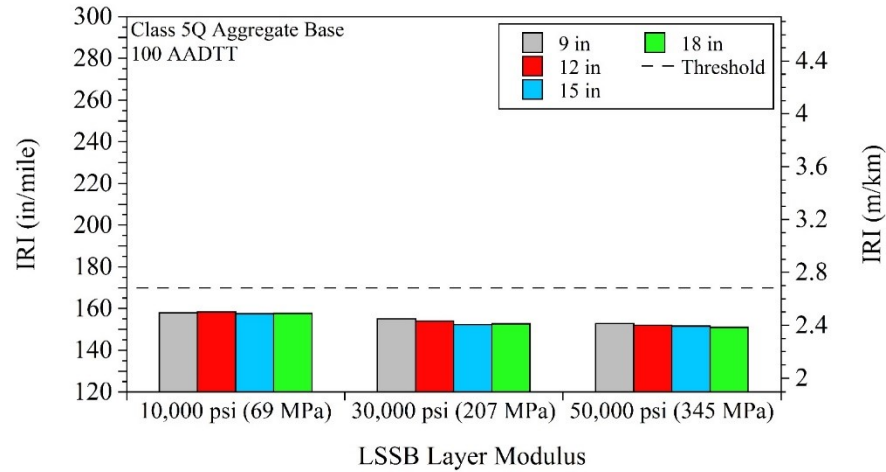


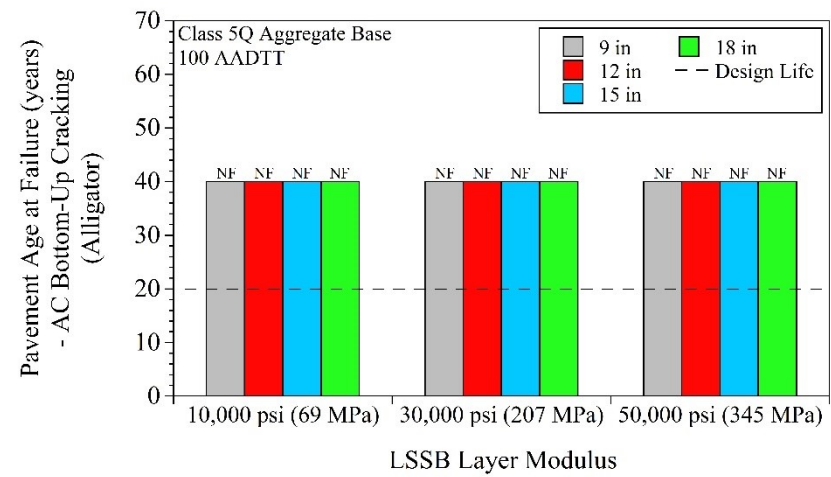
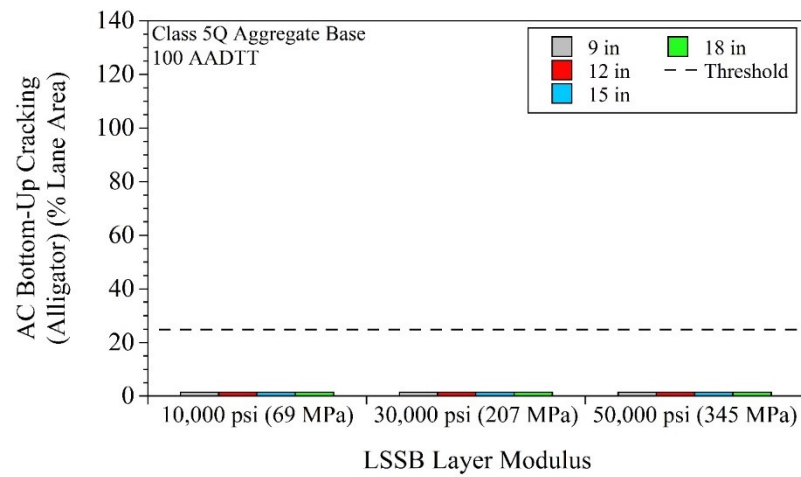
For pavement models that contained Class 6 Aggregate base - 25,000 AADTT:



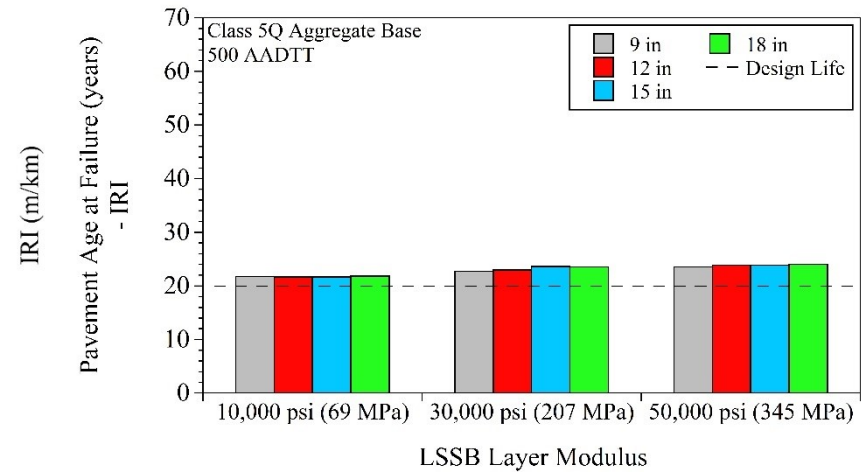
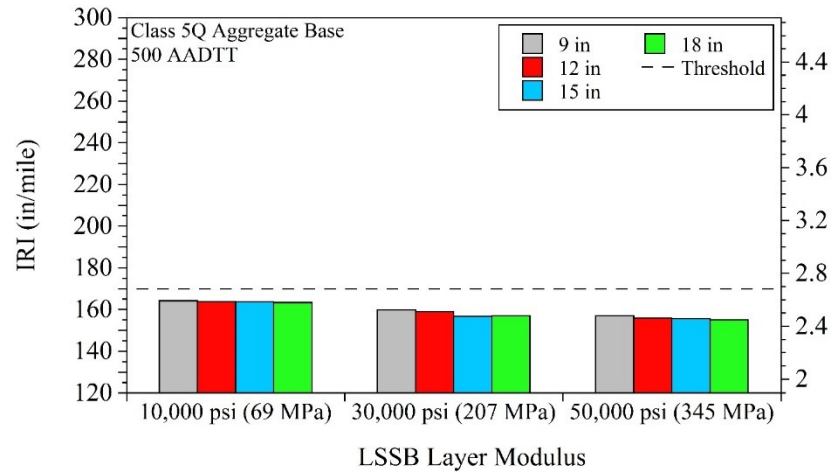


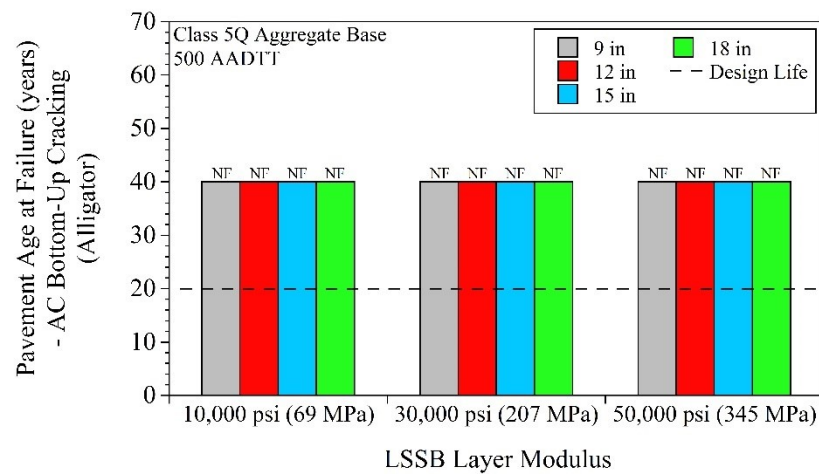
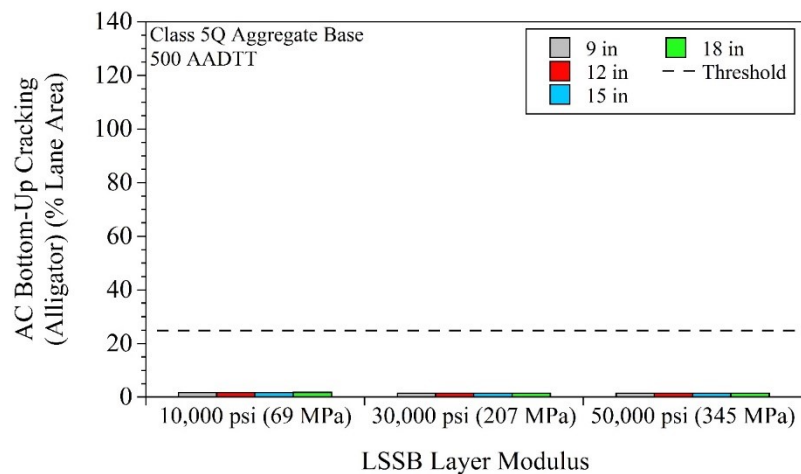
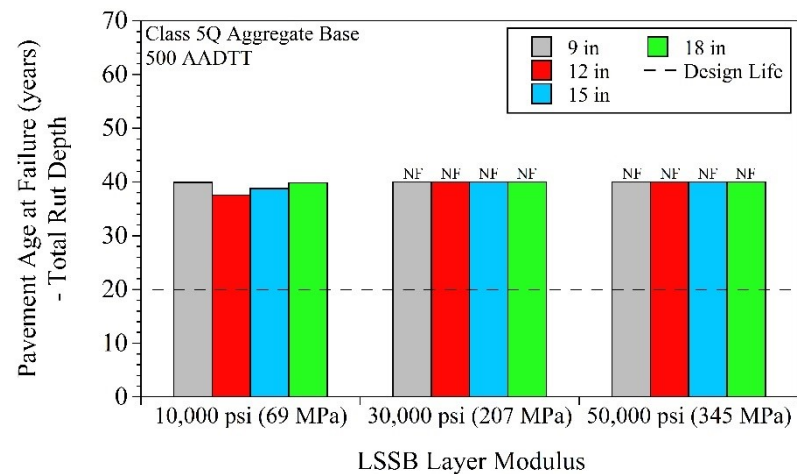
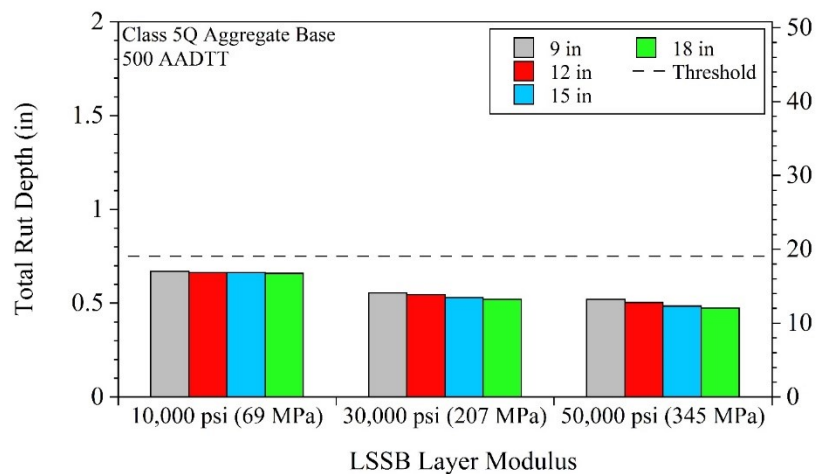
For pavement models that contained Class 5Q Aggregate base - 100 AADTT:



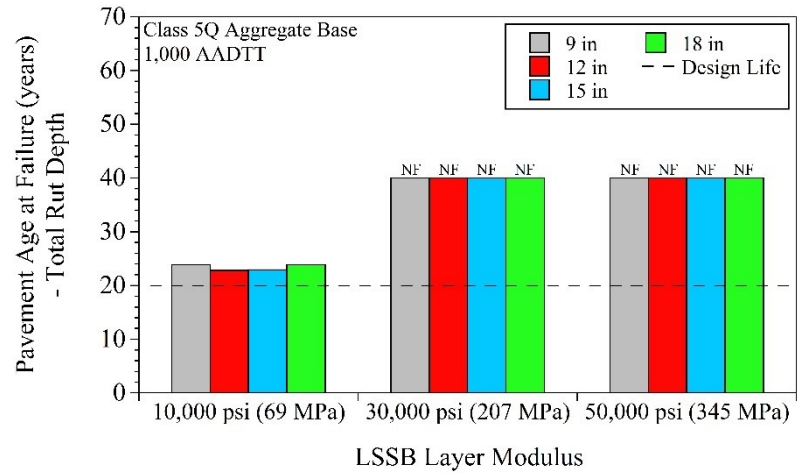
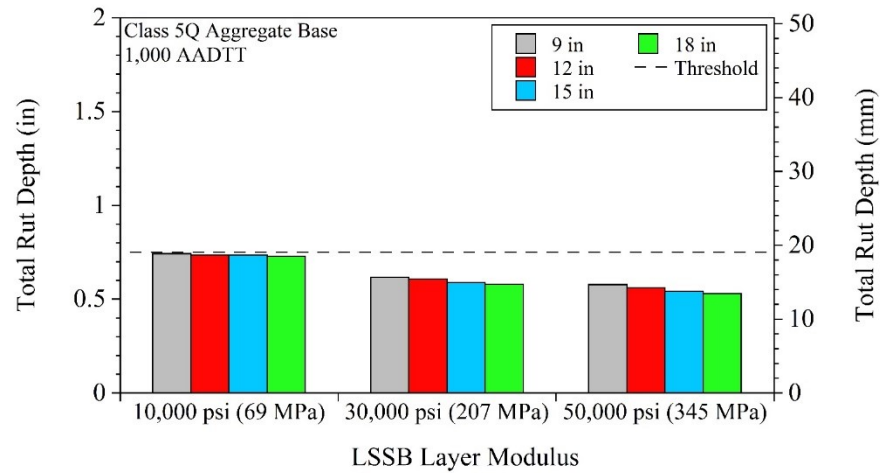
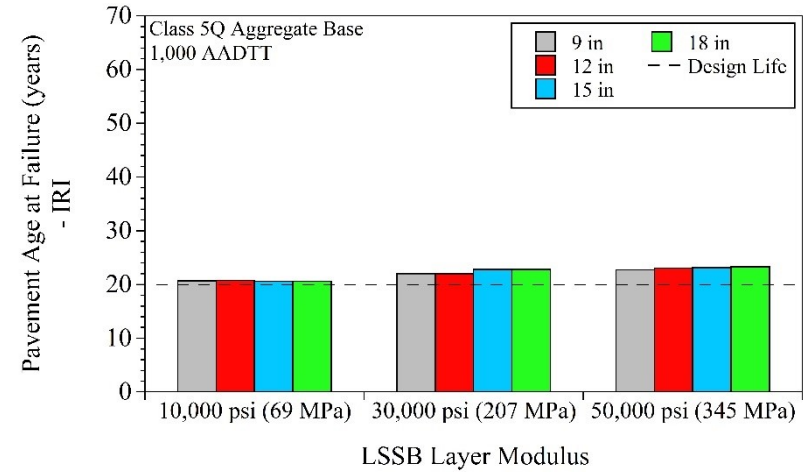
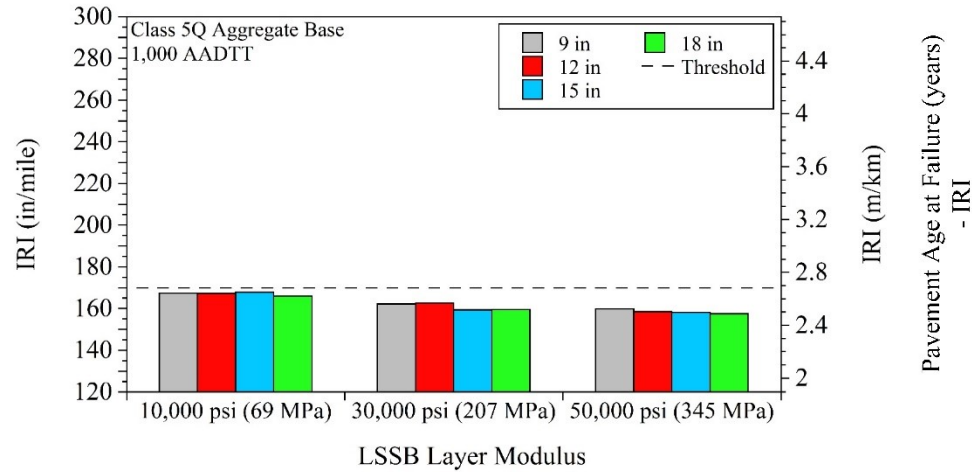


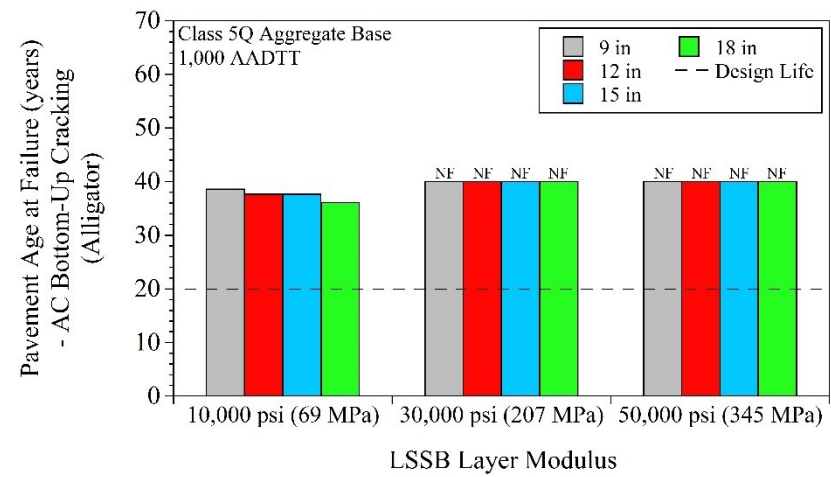
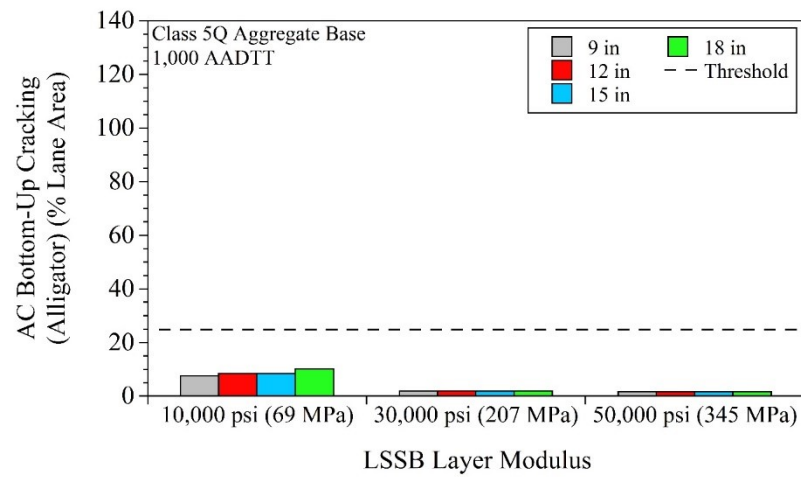
For pavement models that contained Class 5Q Aggregate base - 500 AADTT:



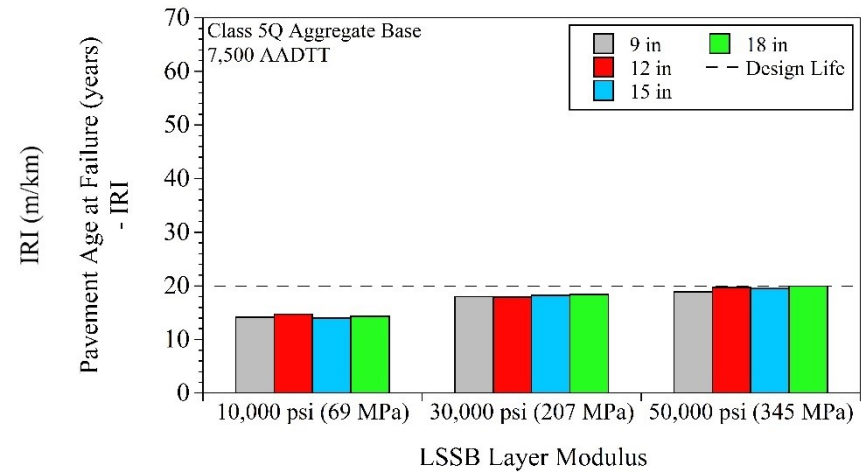
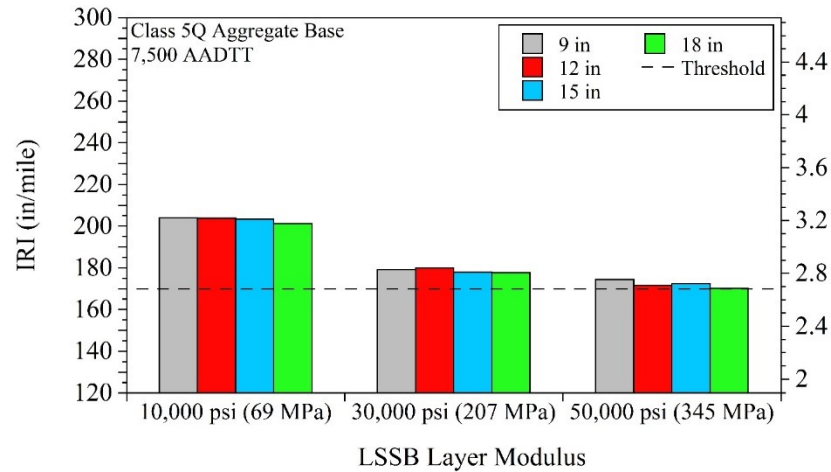


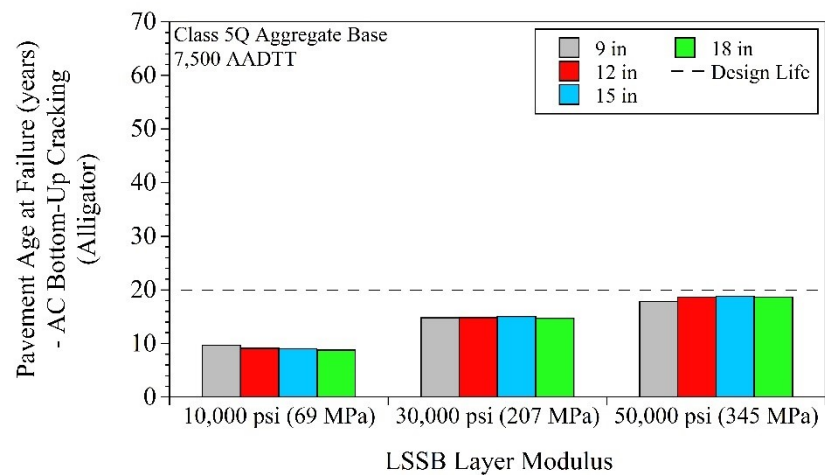
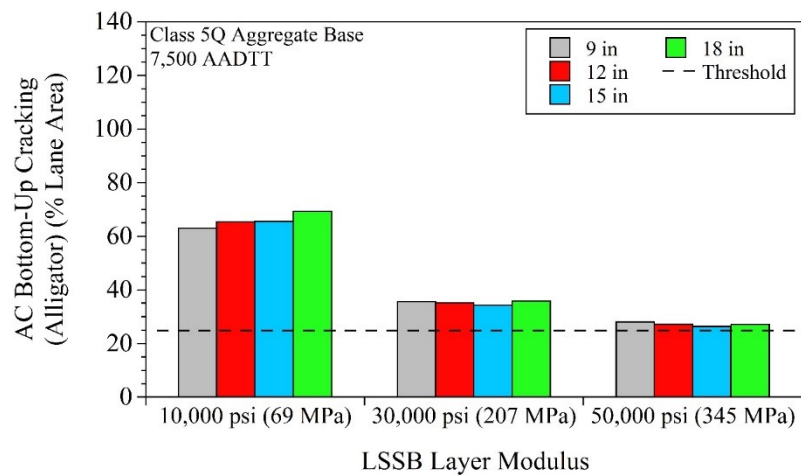
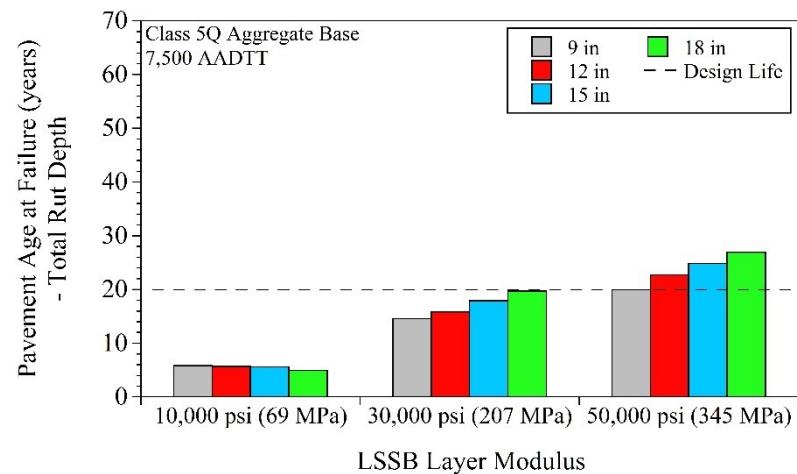
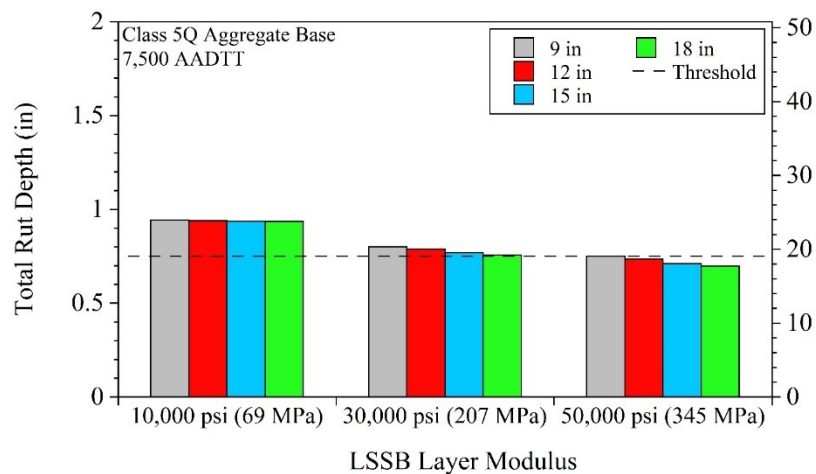
For pavement models that contained Class 5Q Aggregate base - 1,000 AADTT:



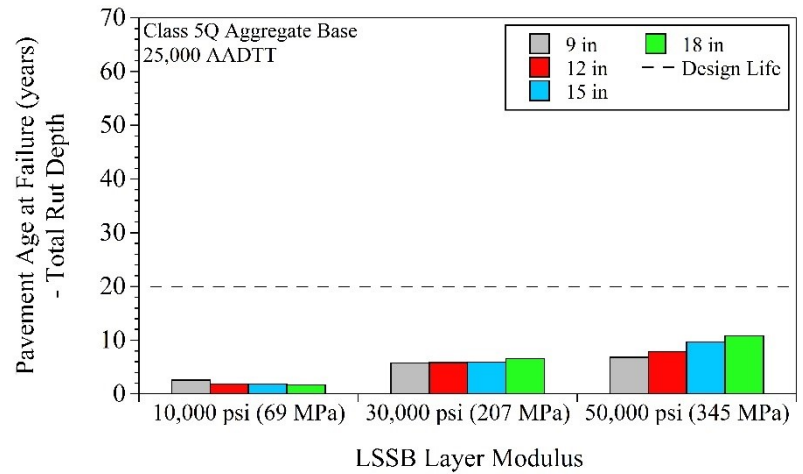
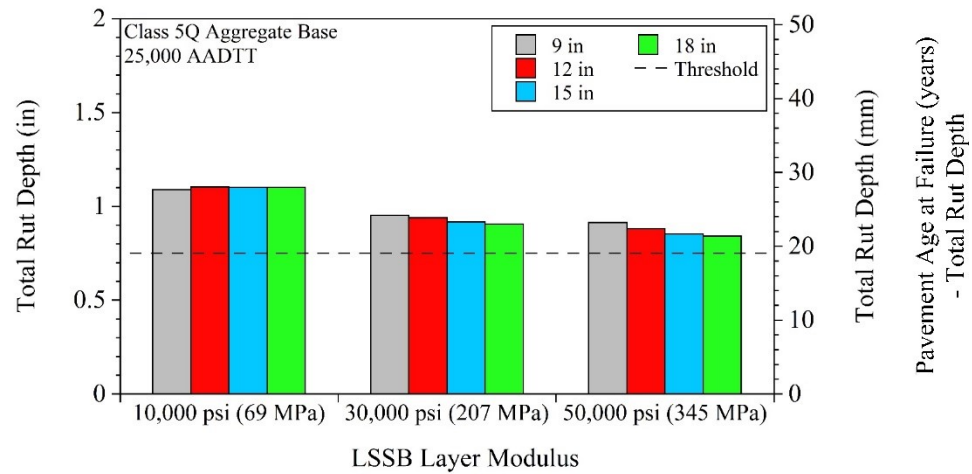
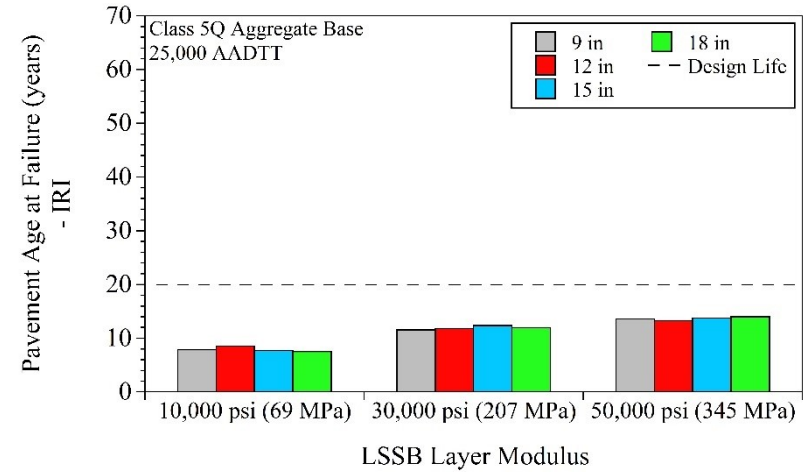
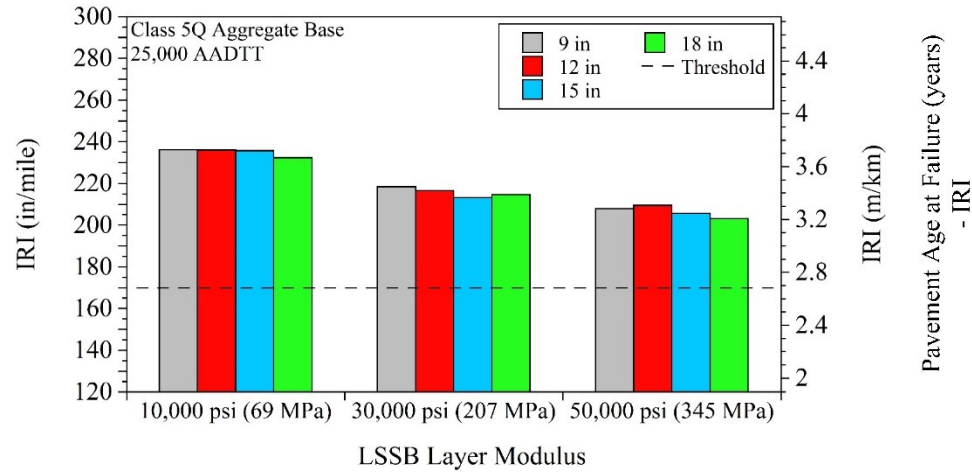


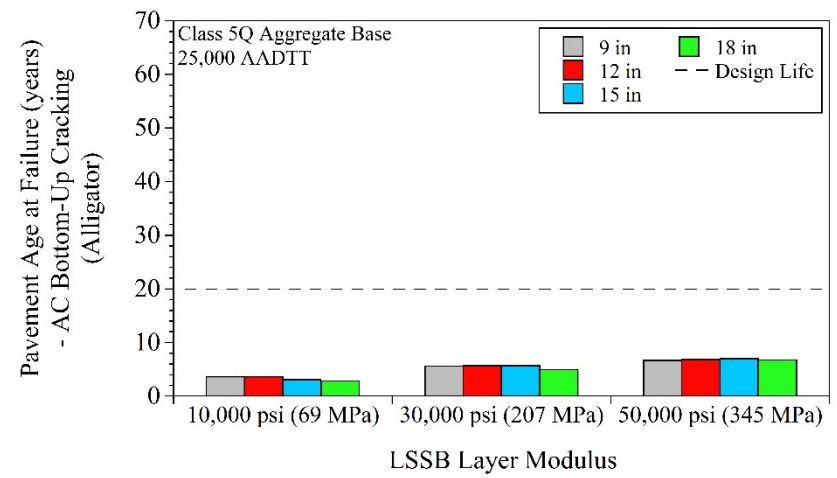
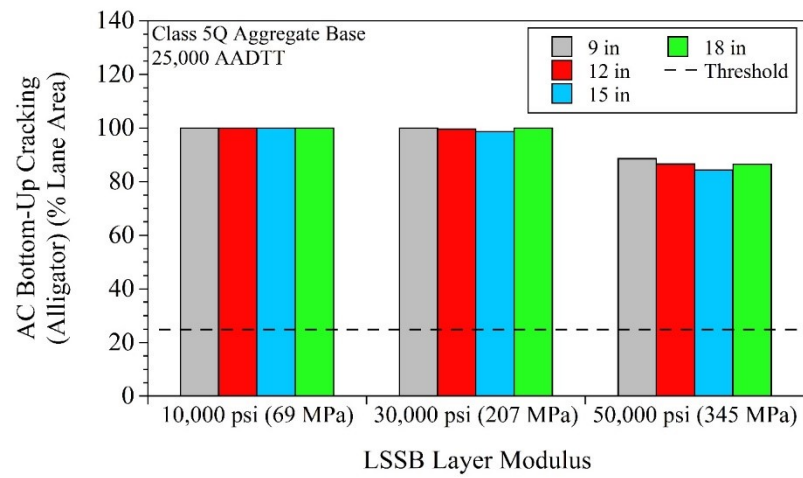
For pavement models that contained Class 5Q Aggregate base - 7,500 AADTT:





For pavement models that contained Class 5Q Aggregate base - 25,000 AADTT:

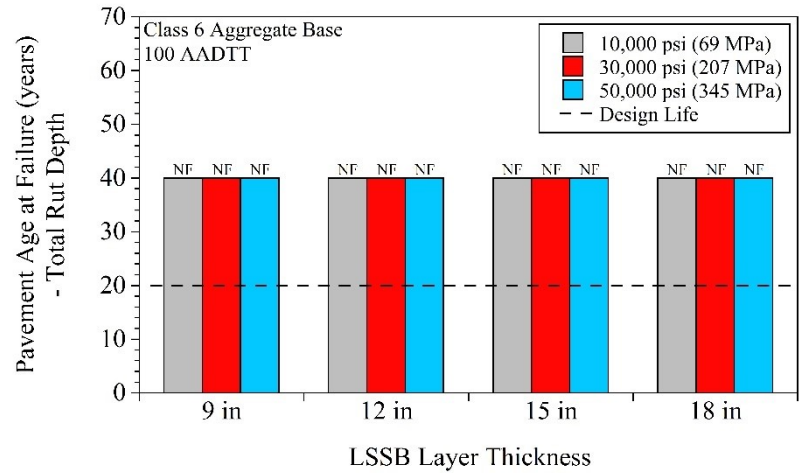
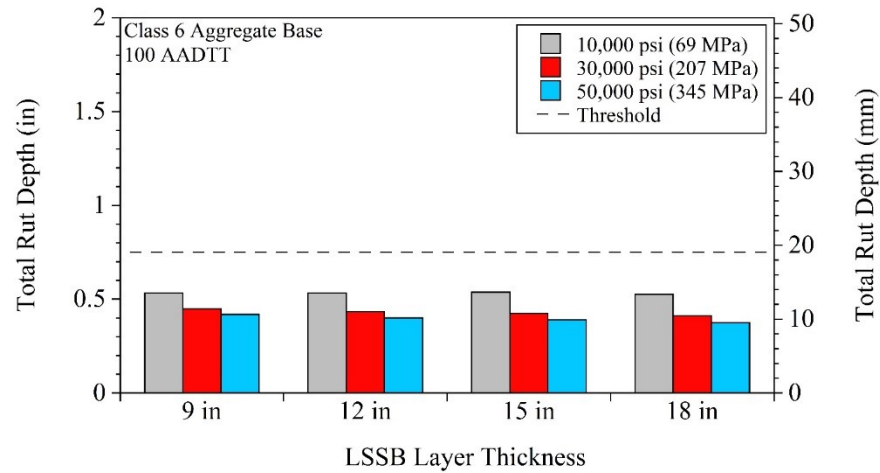
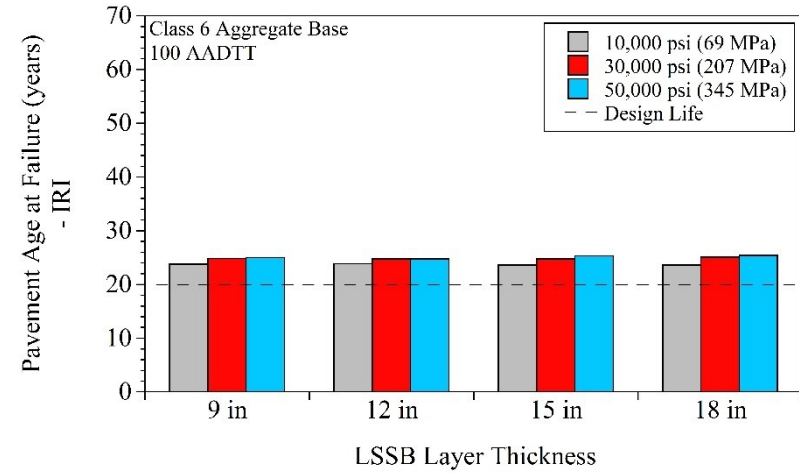
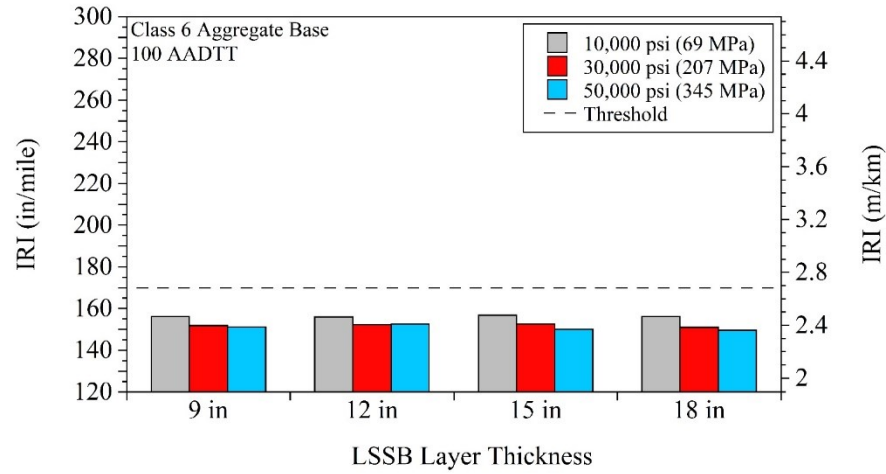


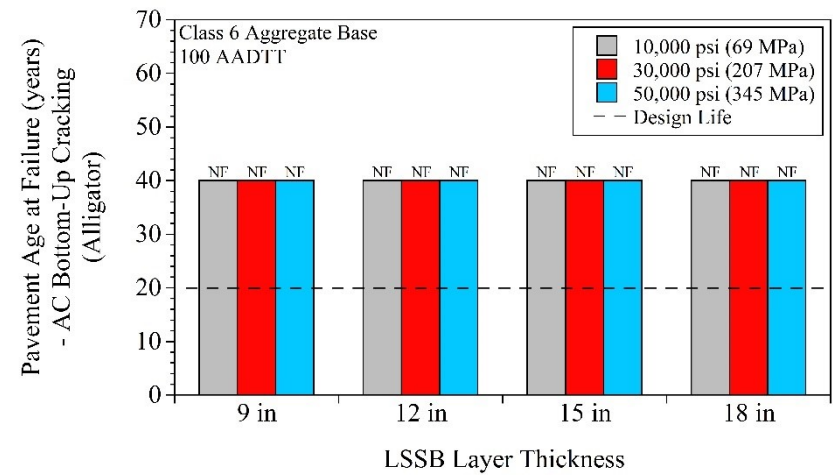
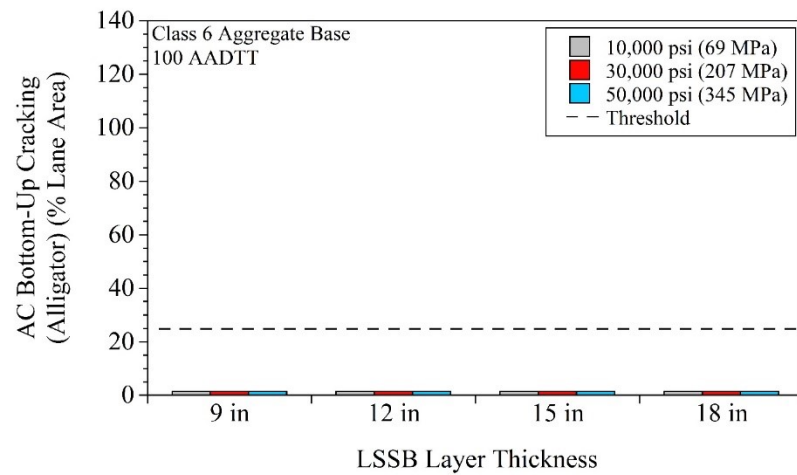


APPENDIX BH

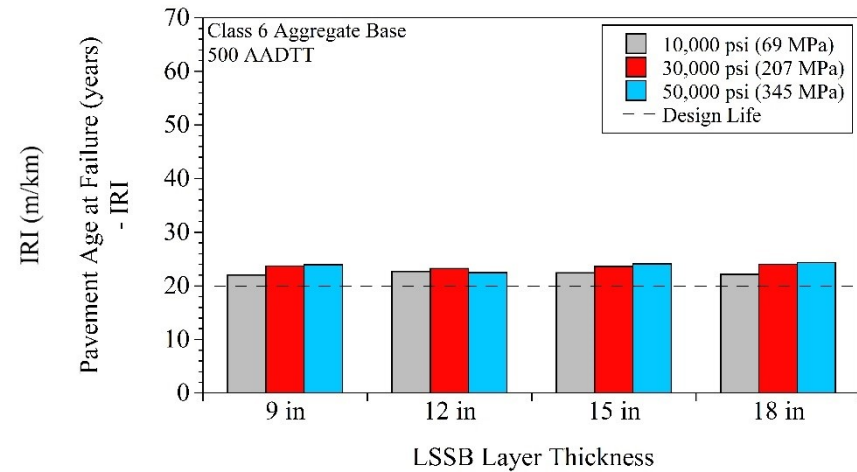
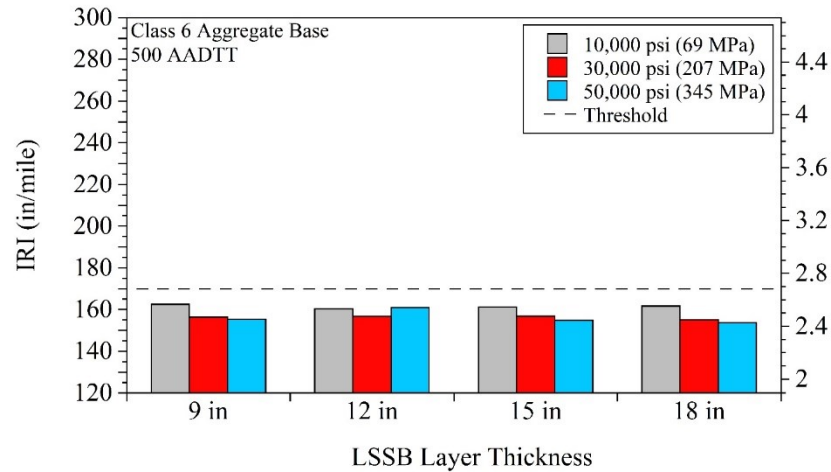
EFFECT OF LARGE STONE SUBBASE (LSSB) LAYER MODULUS ON PAVEMENT PERFORMANCE PREDICTIONS

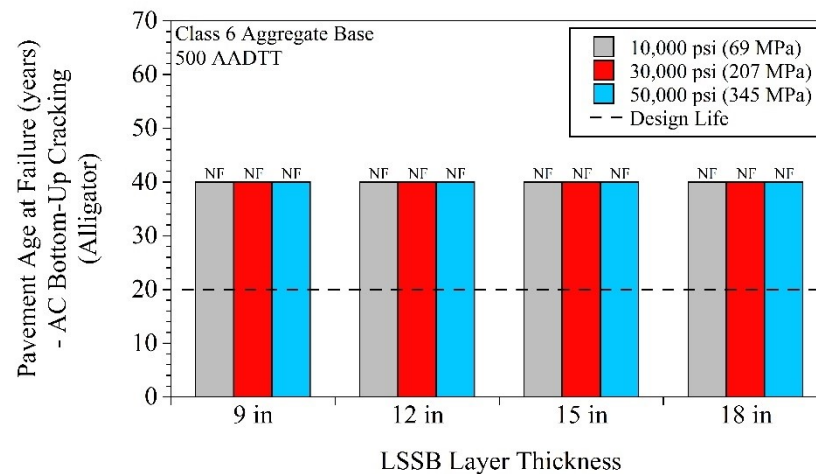
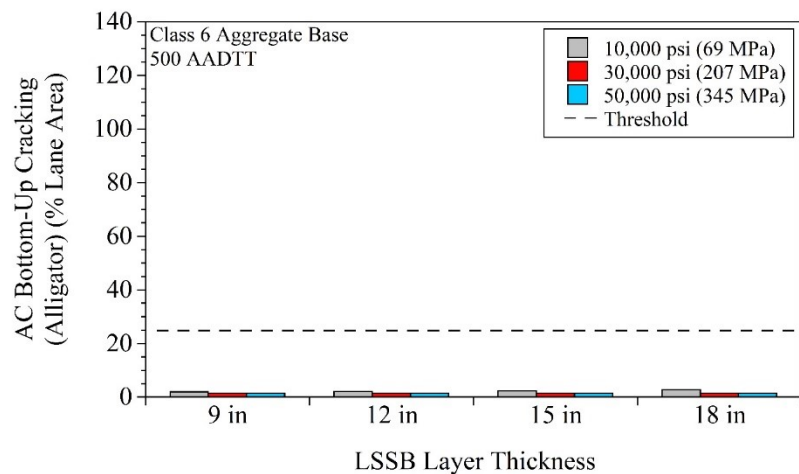
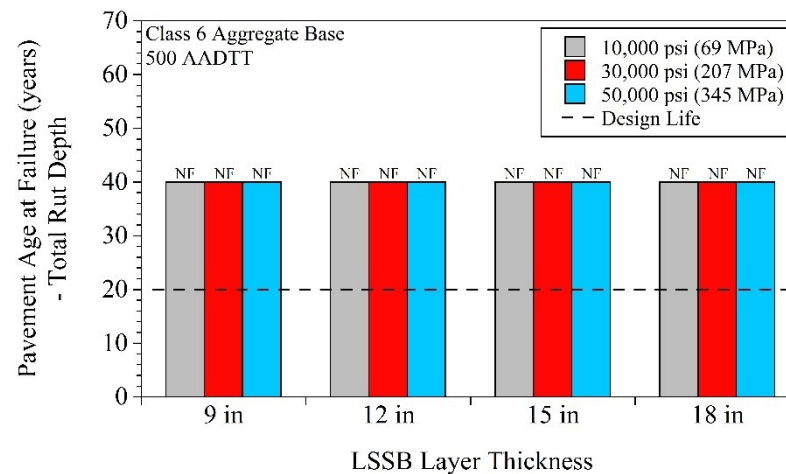
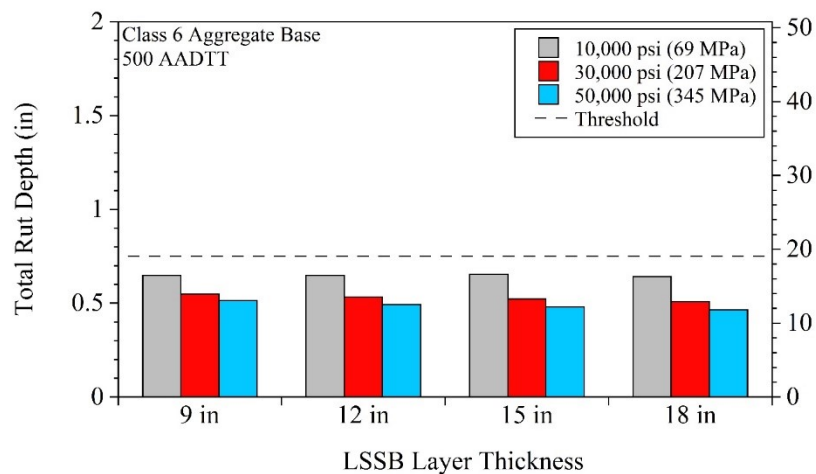
For pavement models that contained Class 6 Aggregate base - 100 AADTT:



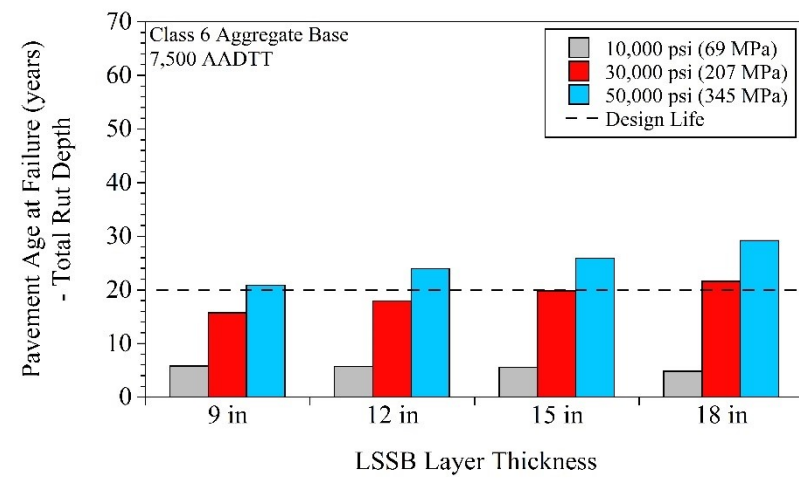
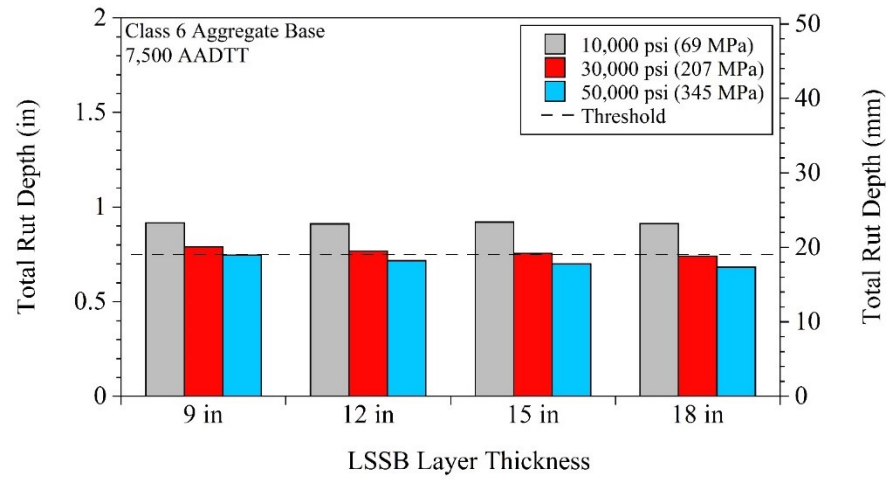
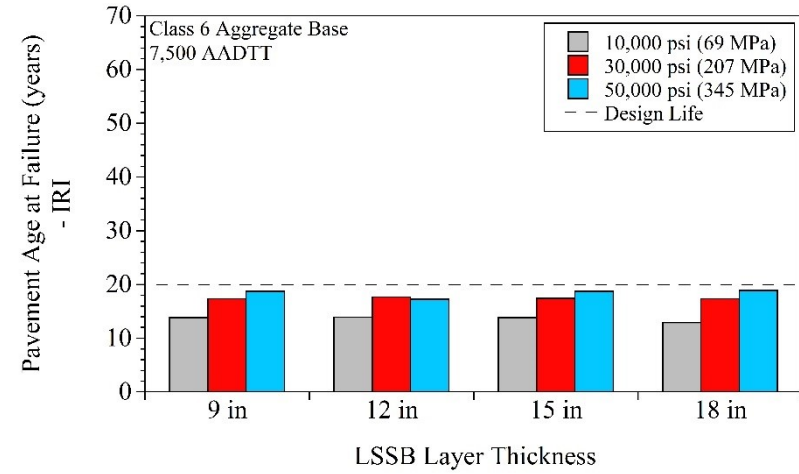
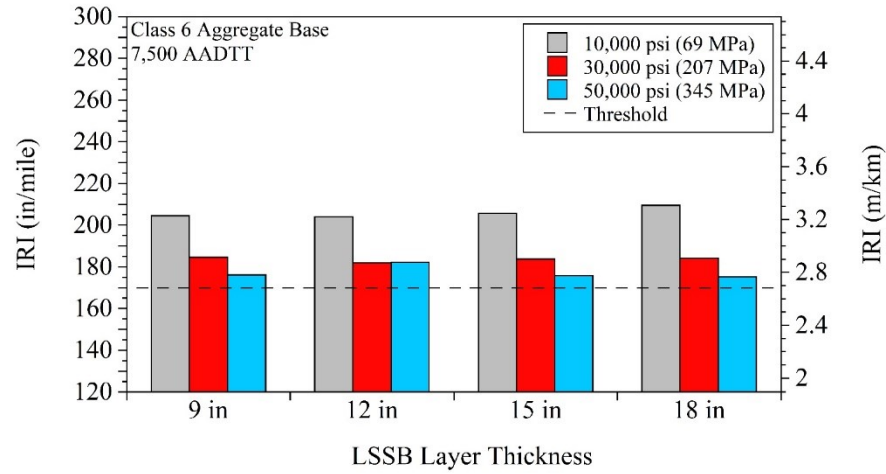


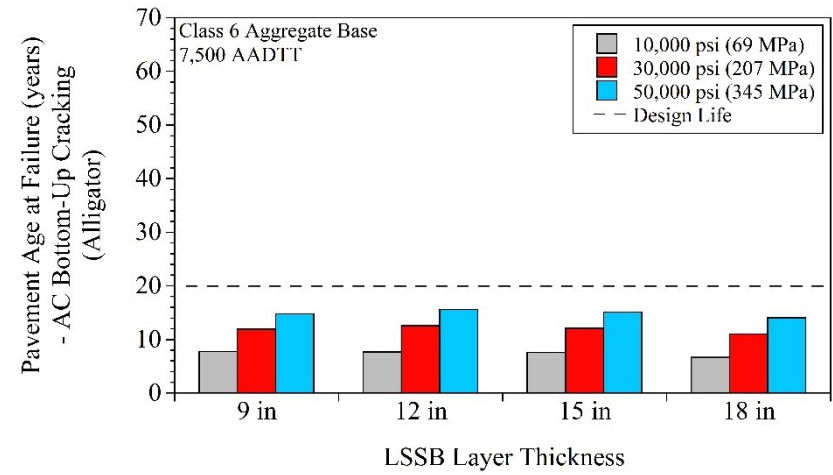
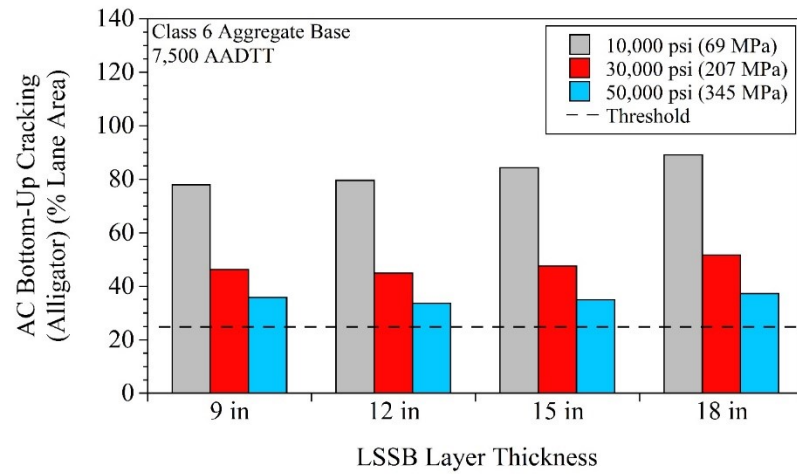
For pavement models that contained Class 6 Aggregate base - 500 AADTT:



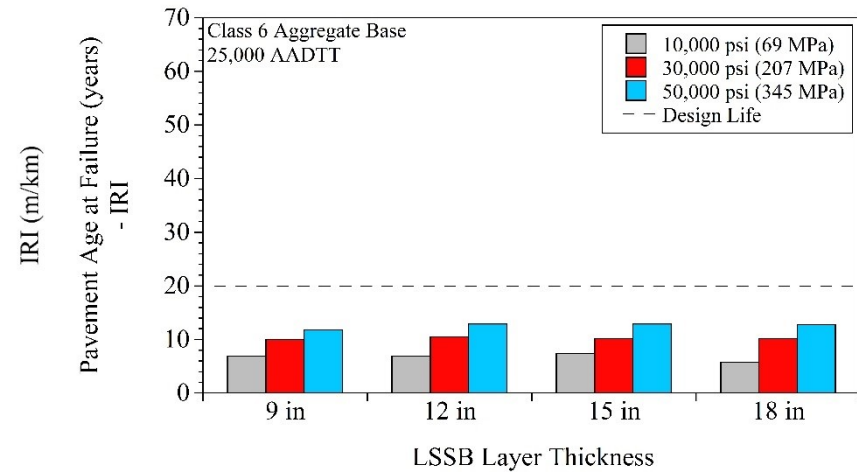
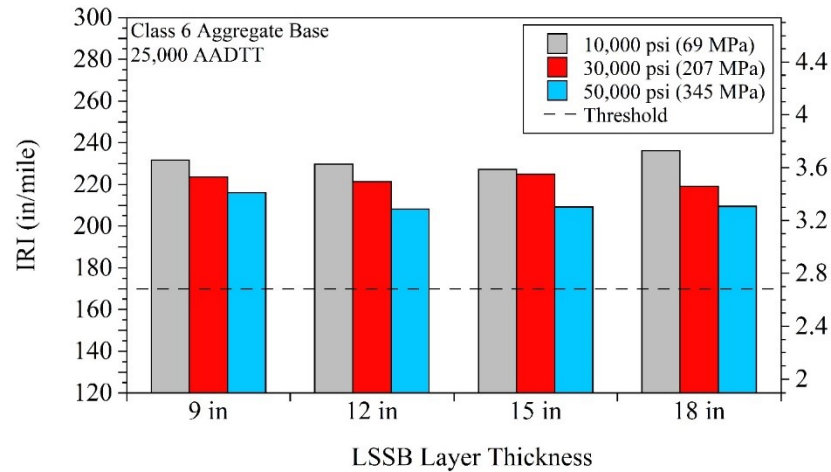


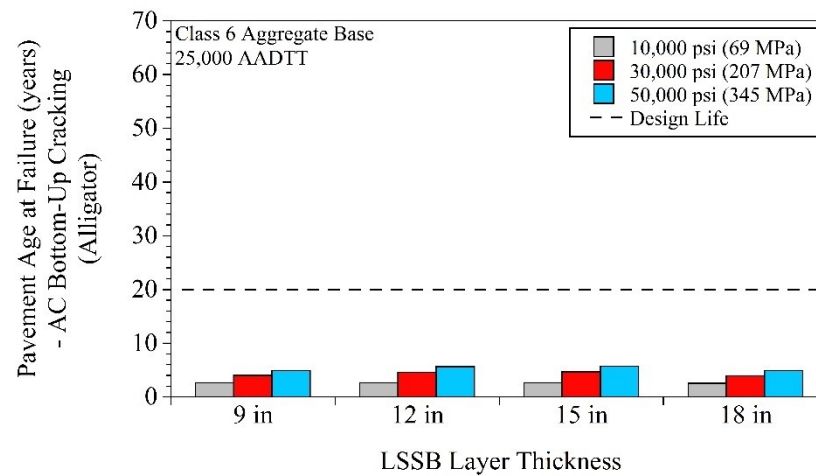
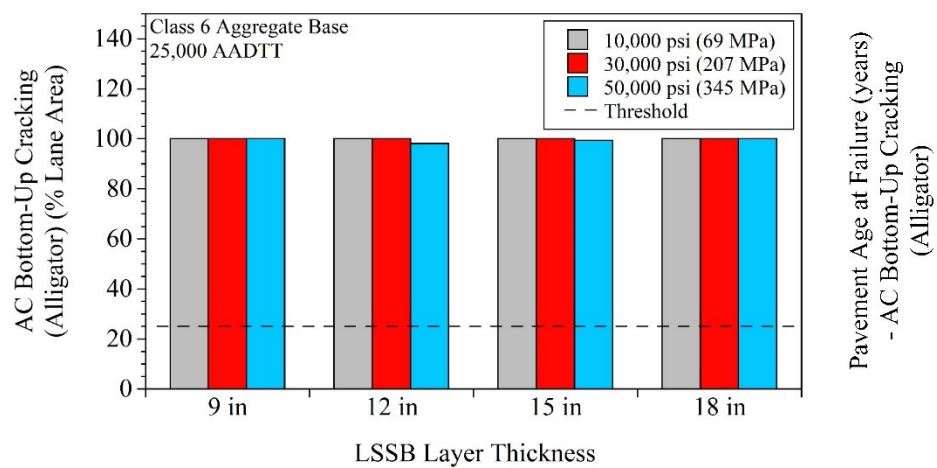
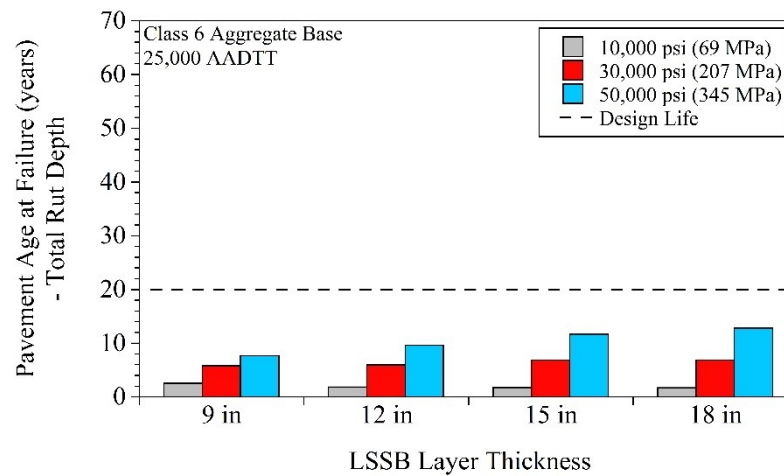
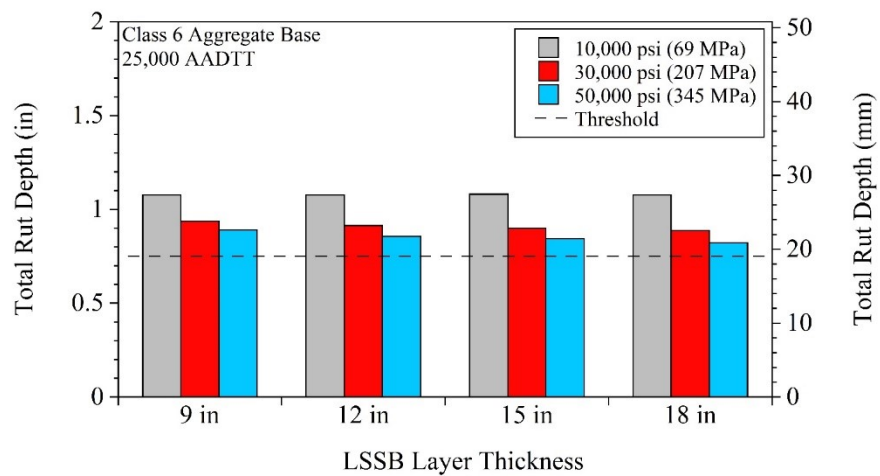
For pavement models that contained Class 6 Aggregate base - 7,500 AADTT:



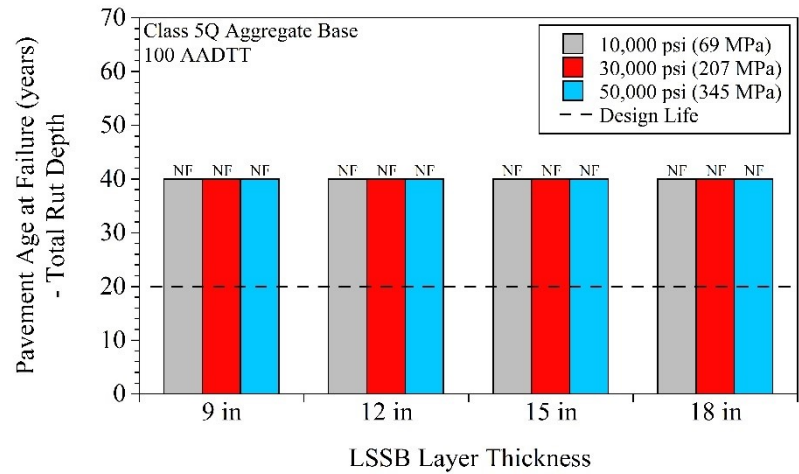
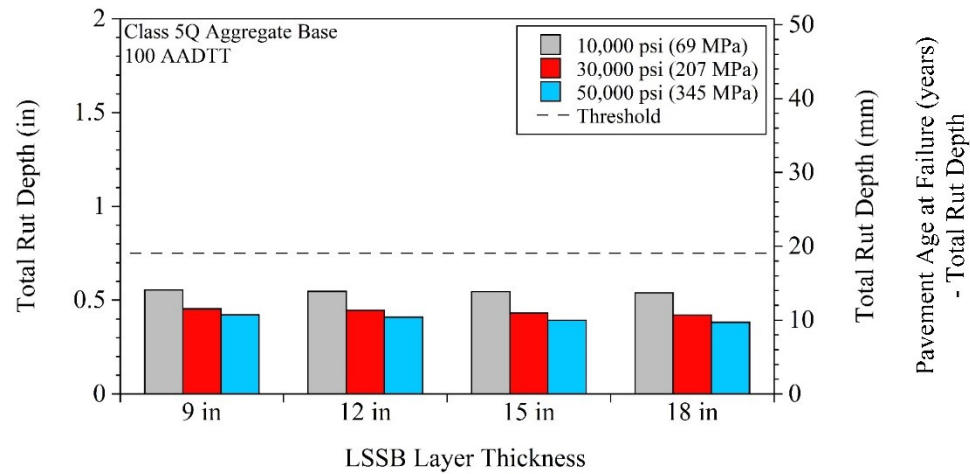
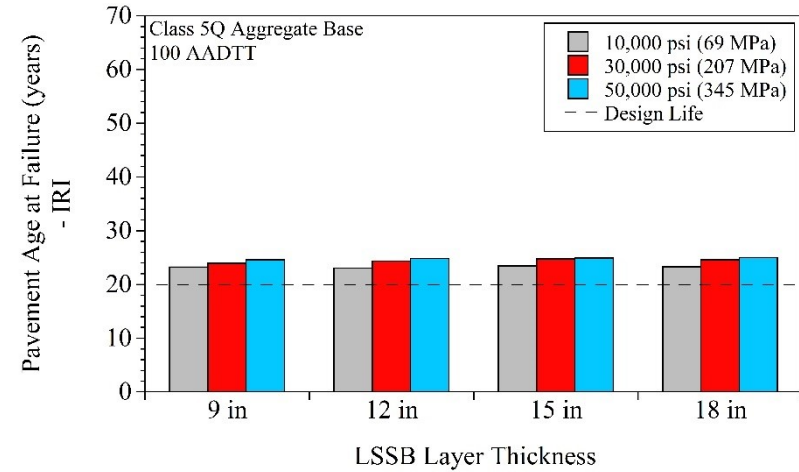
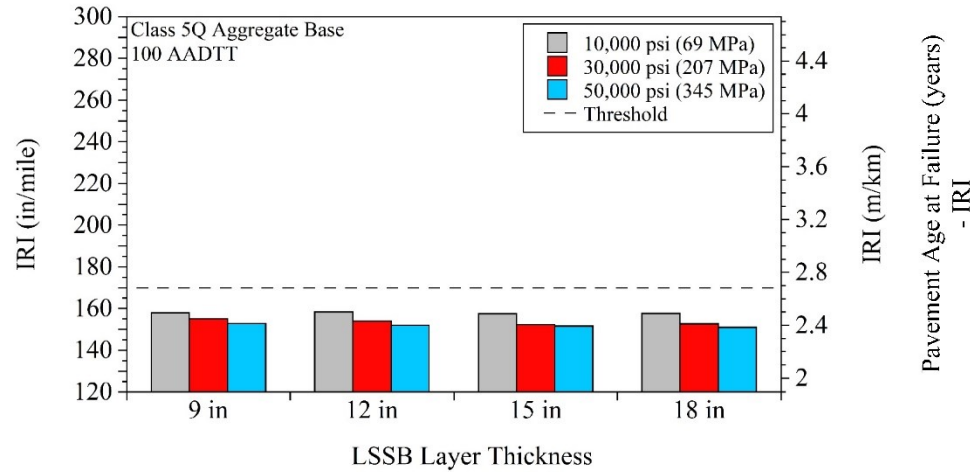


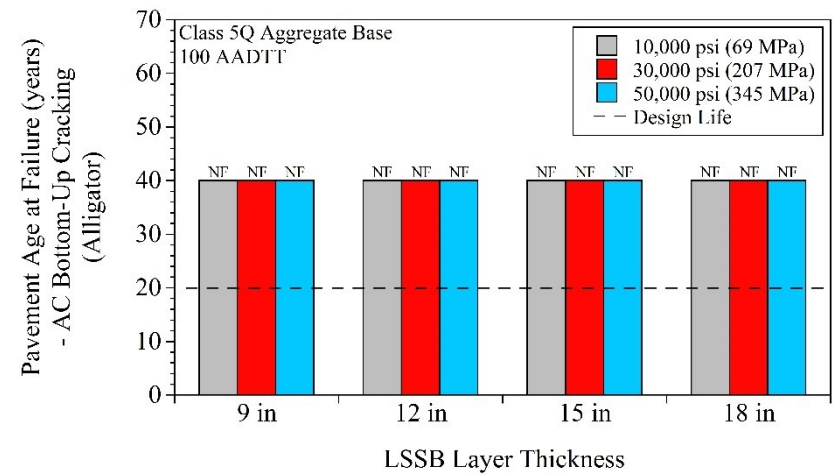
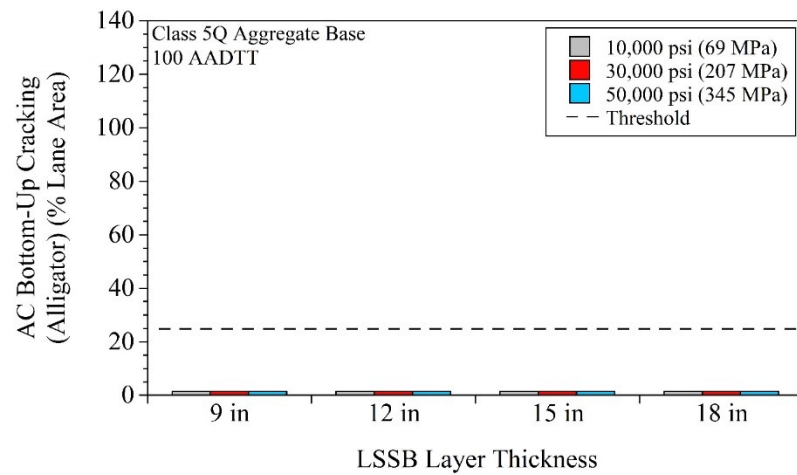
For pavement models that contained Class 6 Aggregate base - 25,000 AADTT:



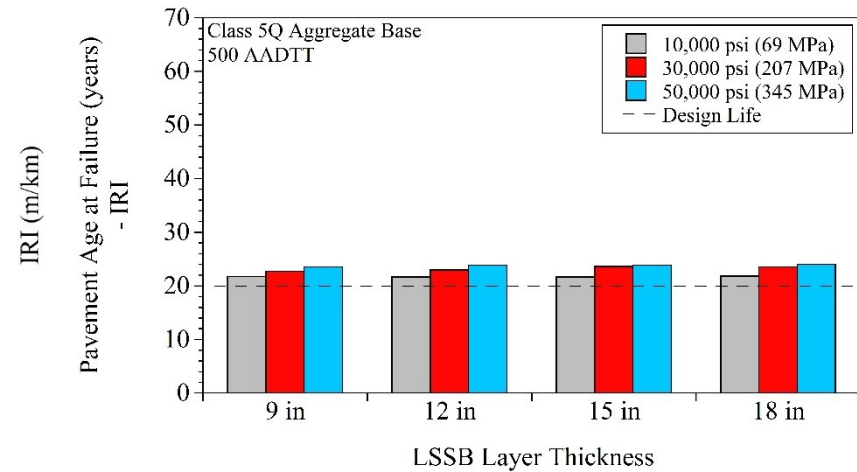
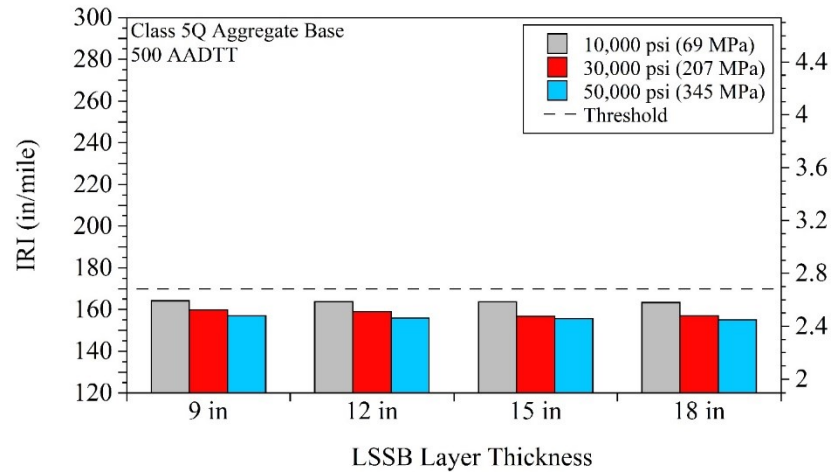


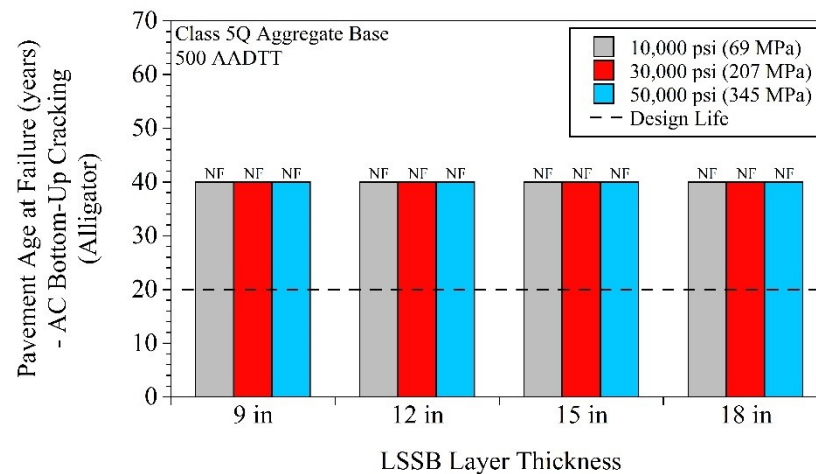
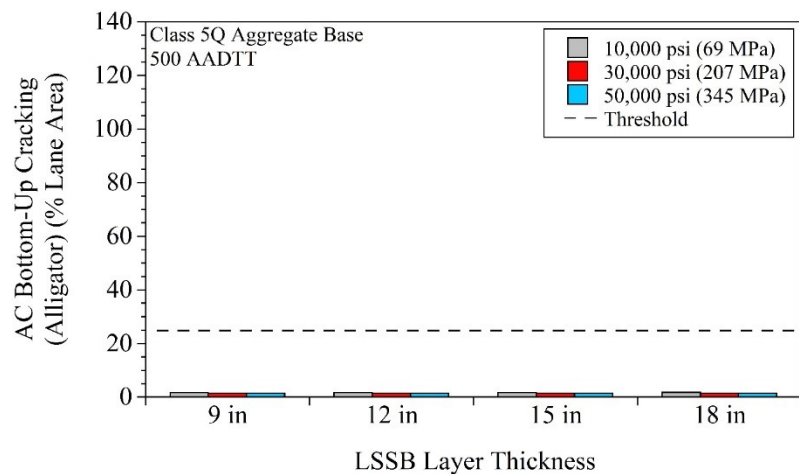
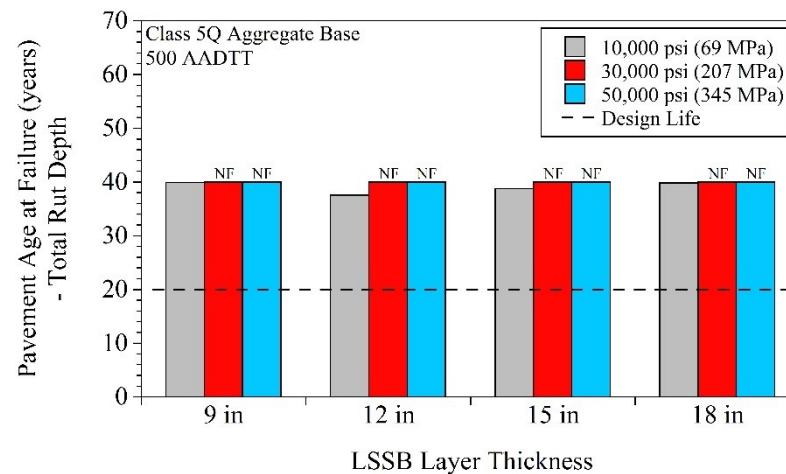
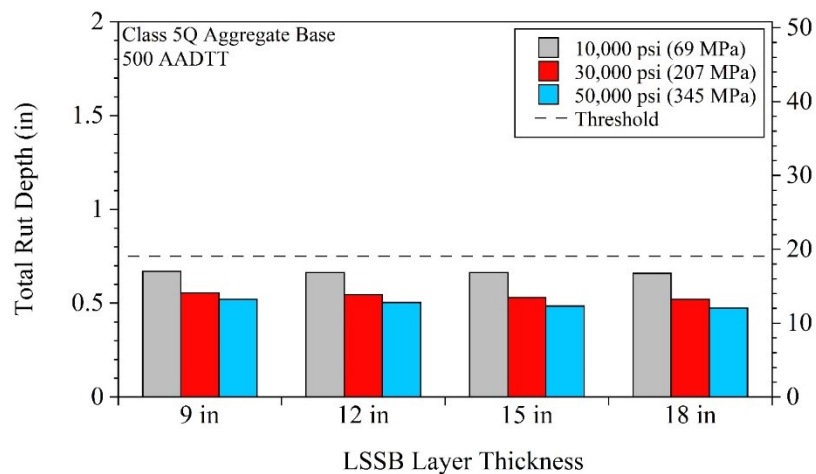
For pavement models that contained Class 5Q Aggregate base - 100 AADTT:



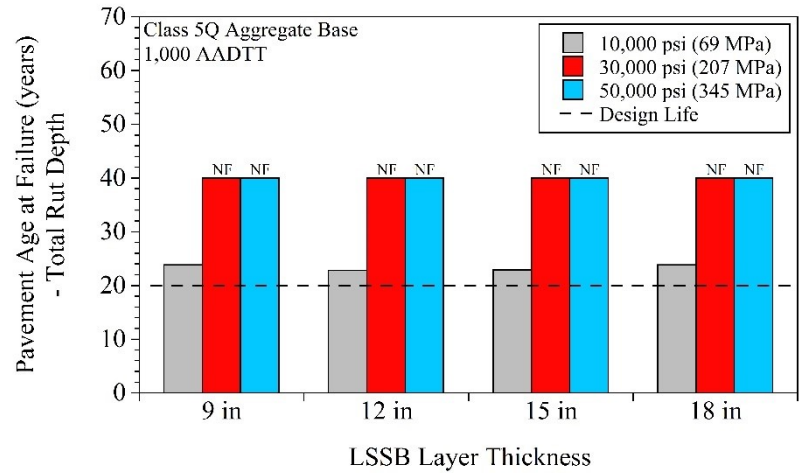
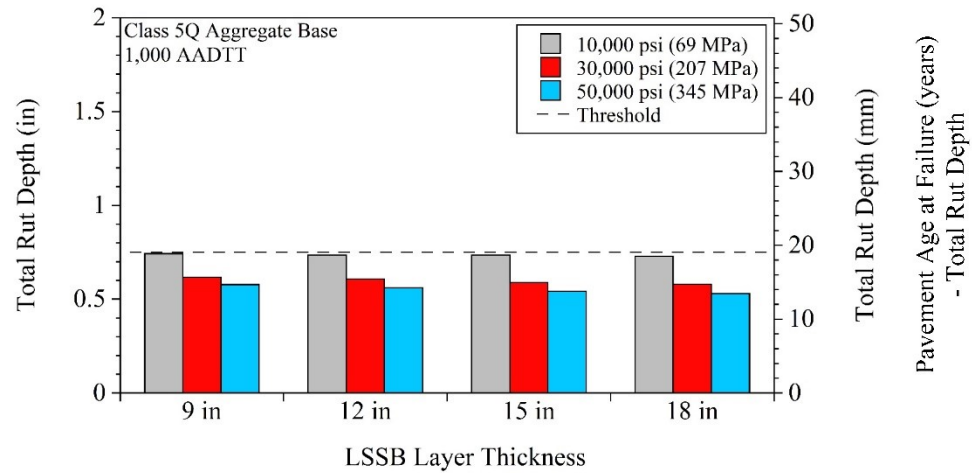
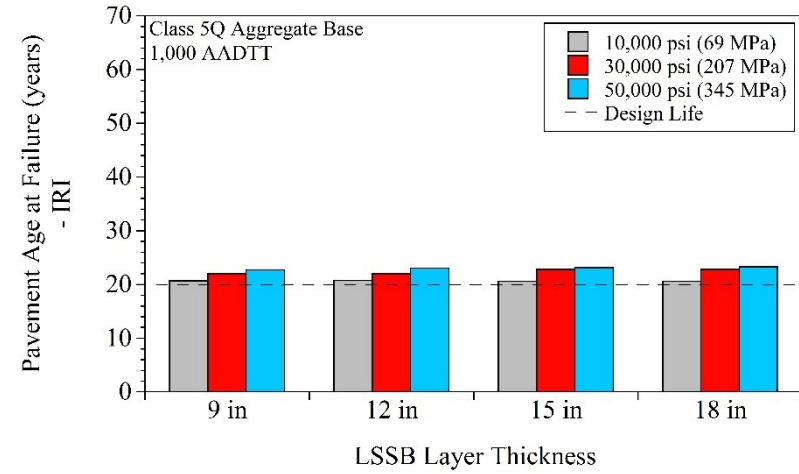
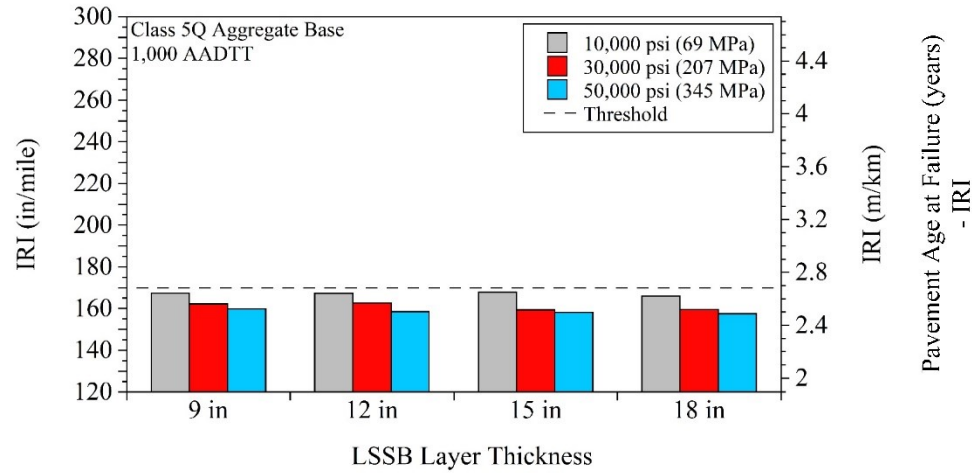


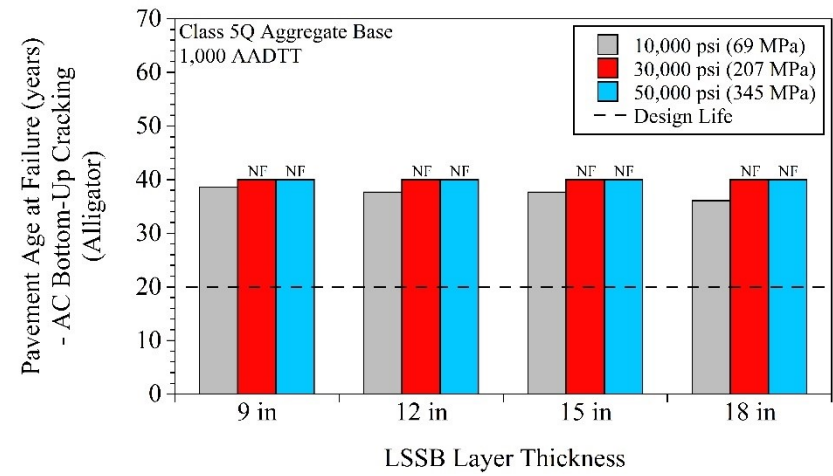
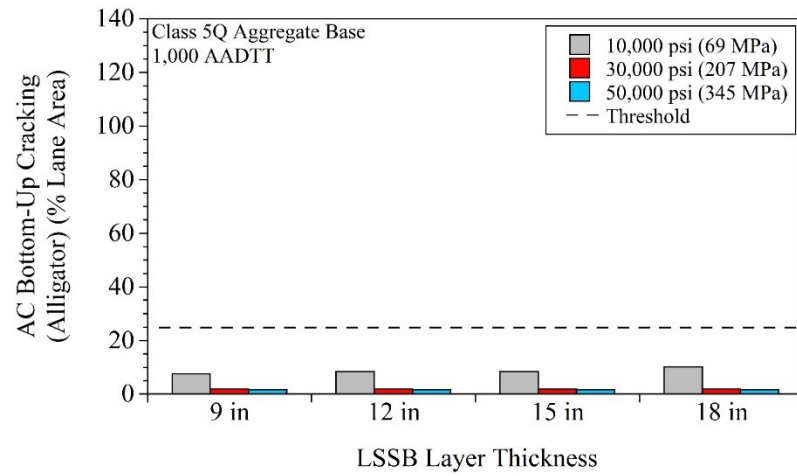
For pavement models that contained Class 5Q Aggregate base - 500 AADTT:



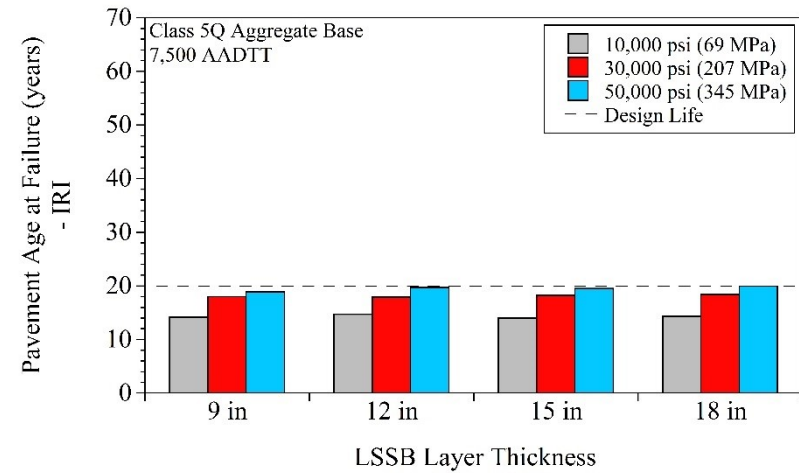
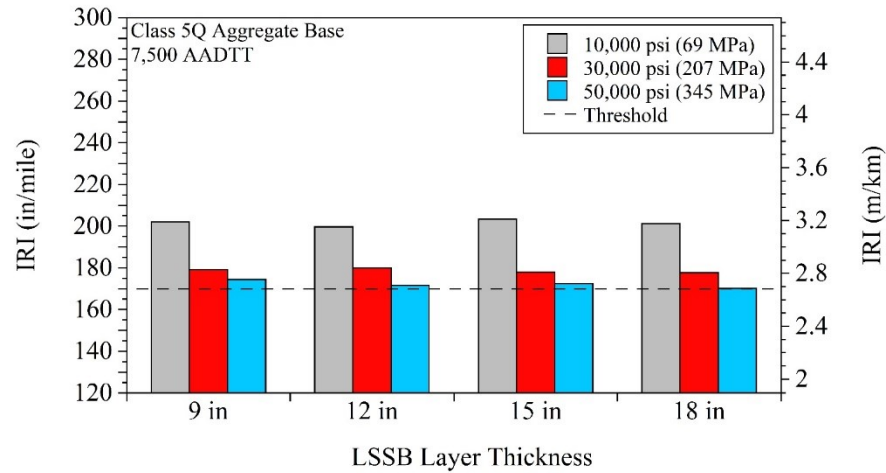


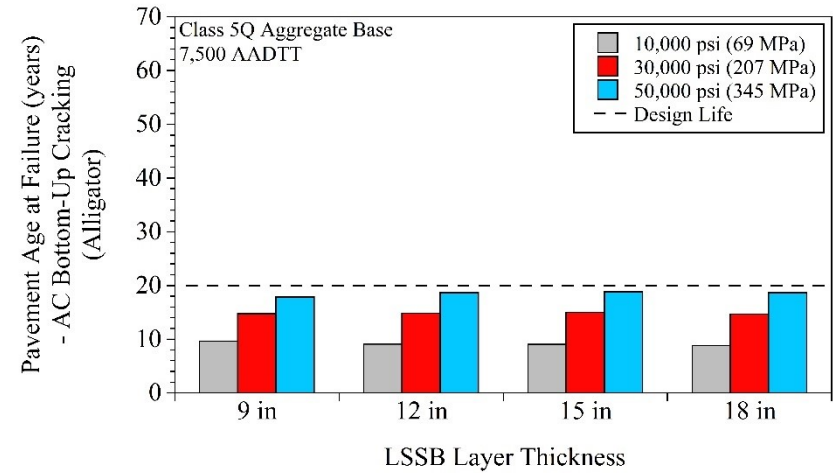
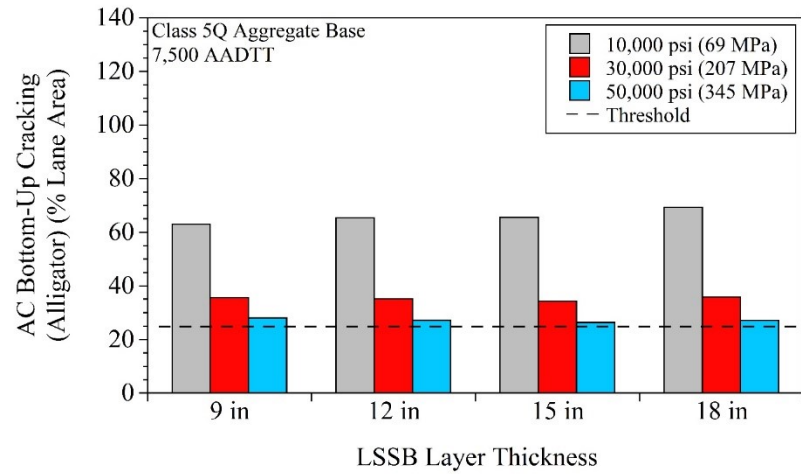
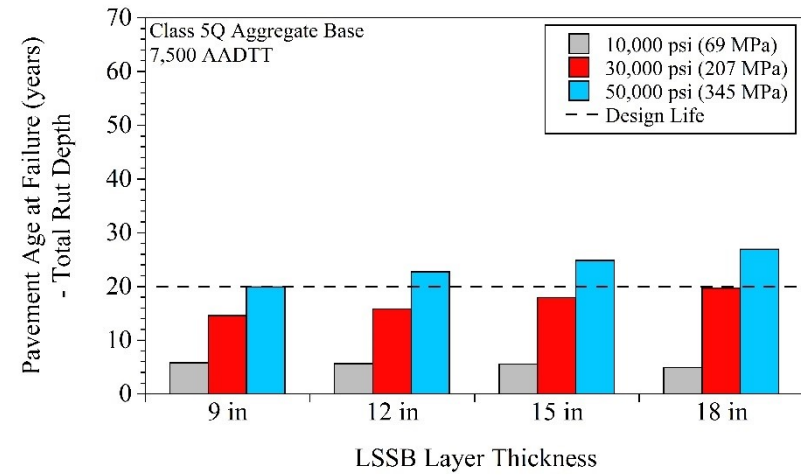
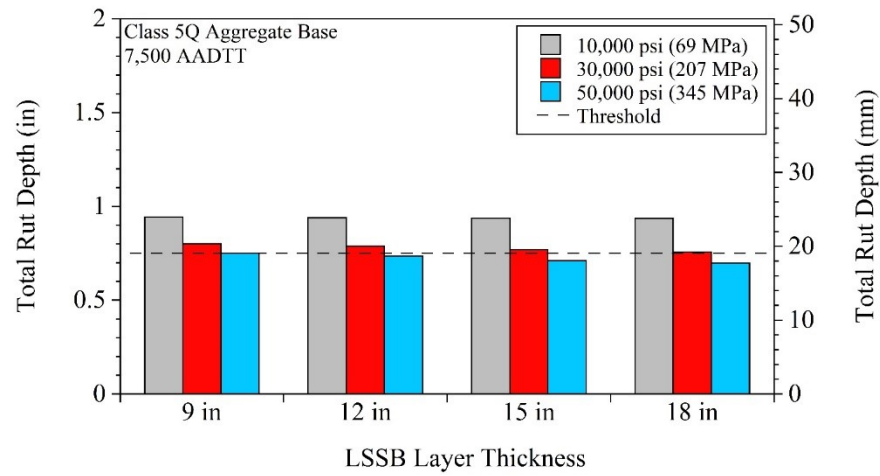
For pavement models that contained Class 5Q Aggregate base - 1,000 AADTT:



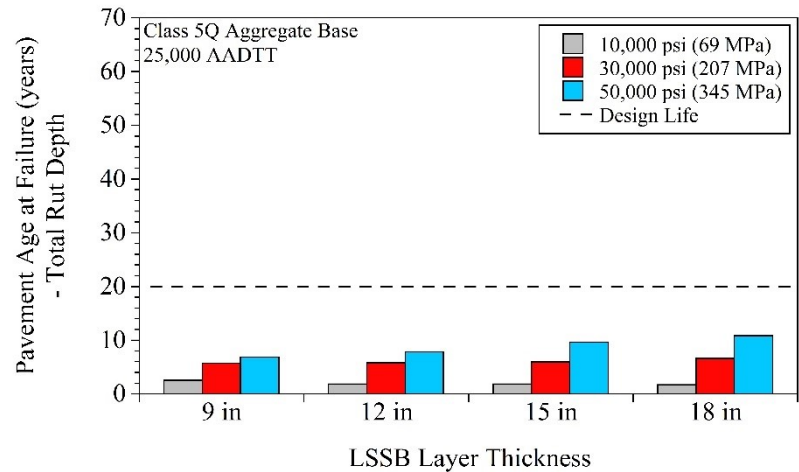
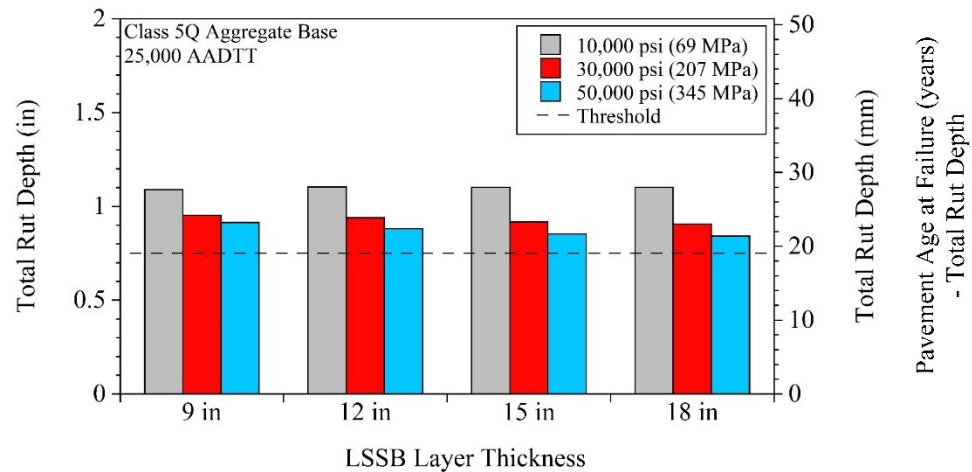
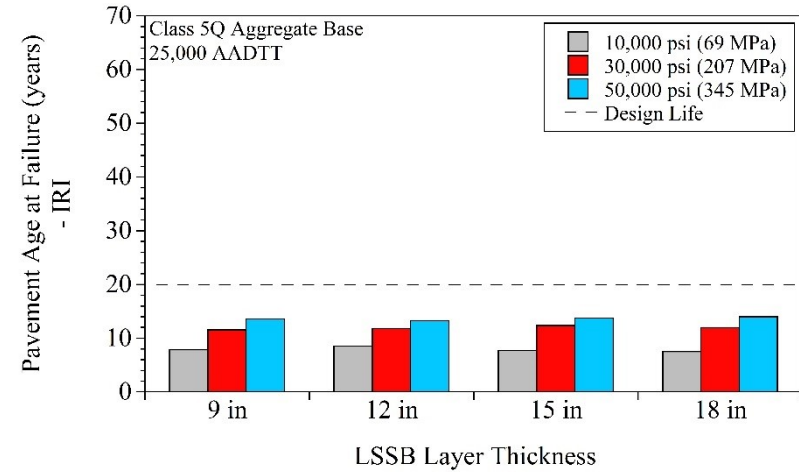
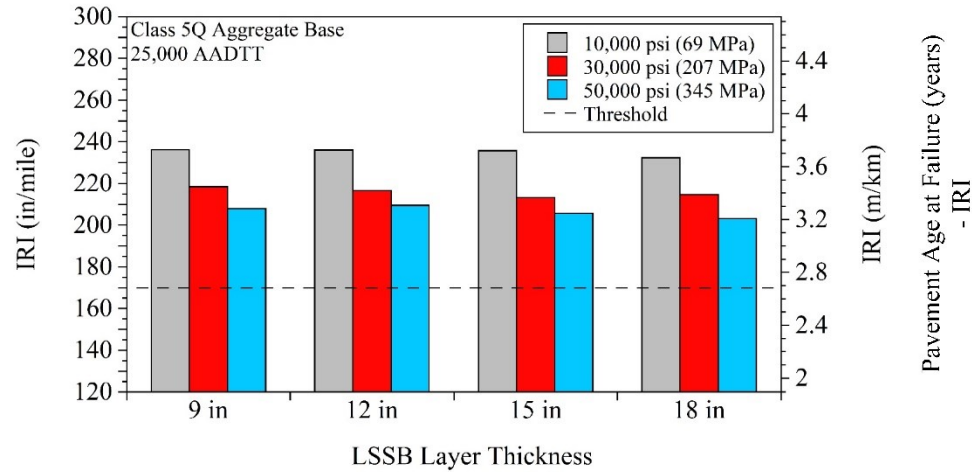


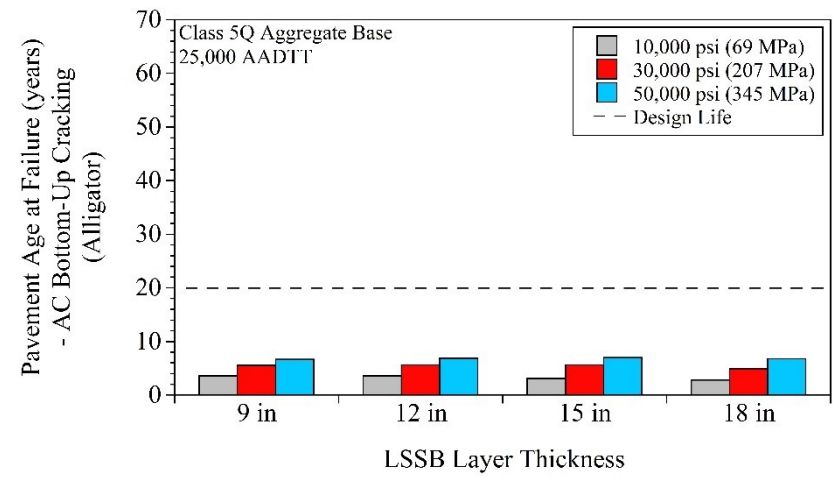
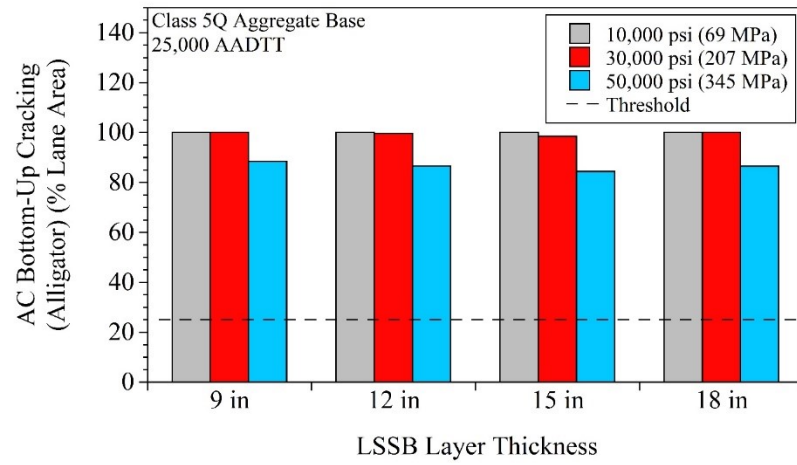
For pavement models that contained Class 5Q Aggregate base - 7,500 AADTT:





For pavement models that contained Class 5Q Aggregate base - 25,000 AADTT:

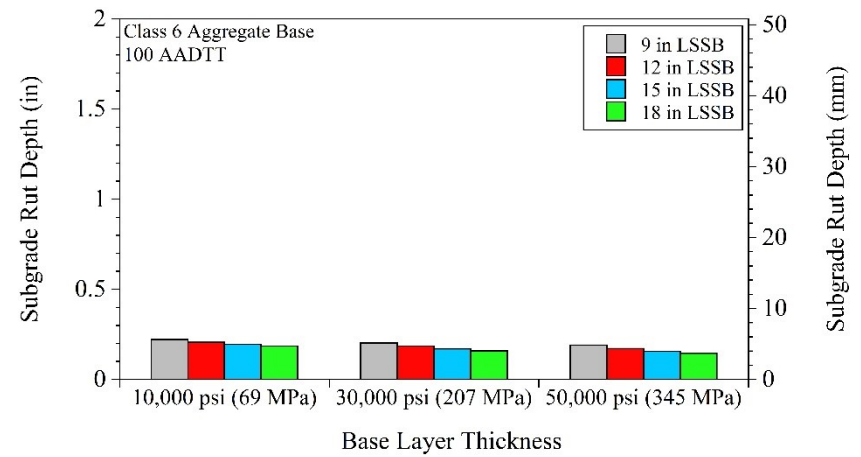
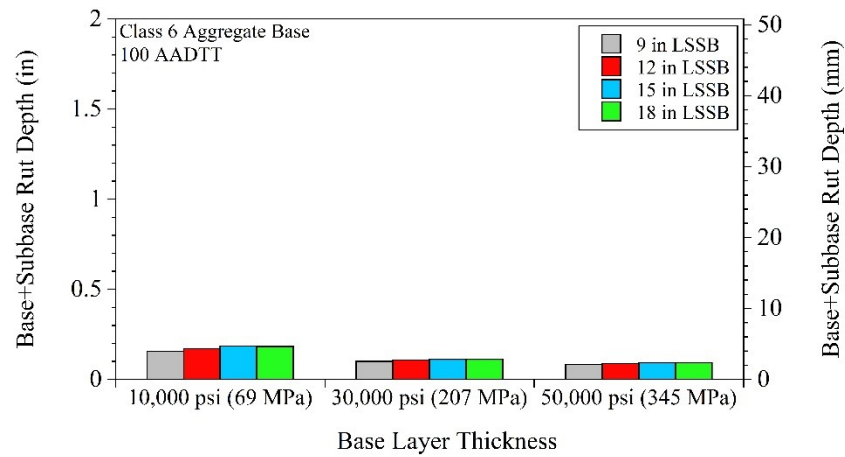
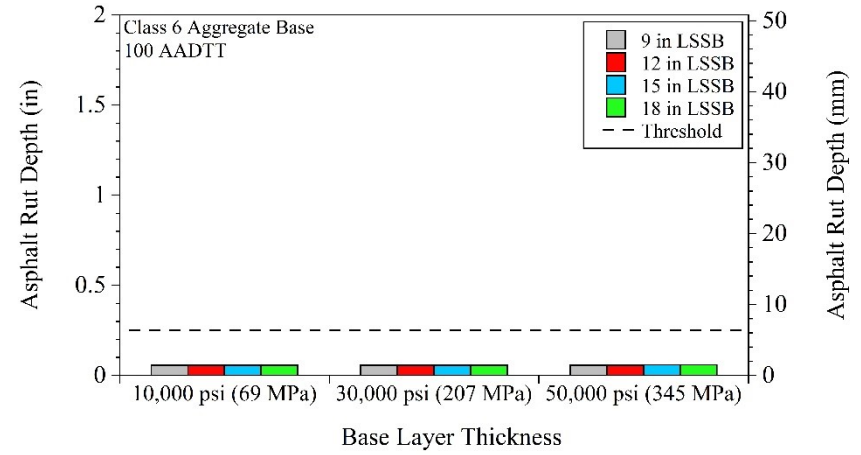
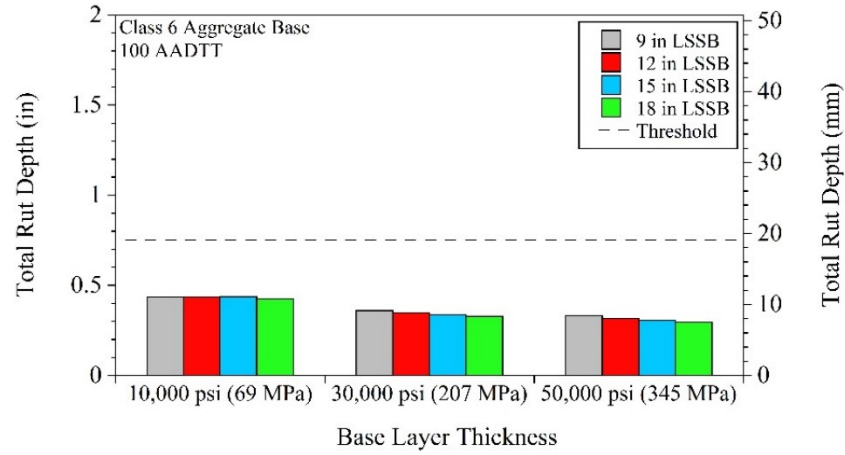




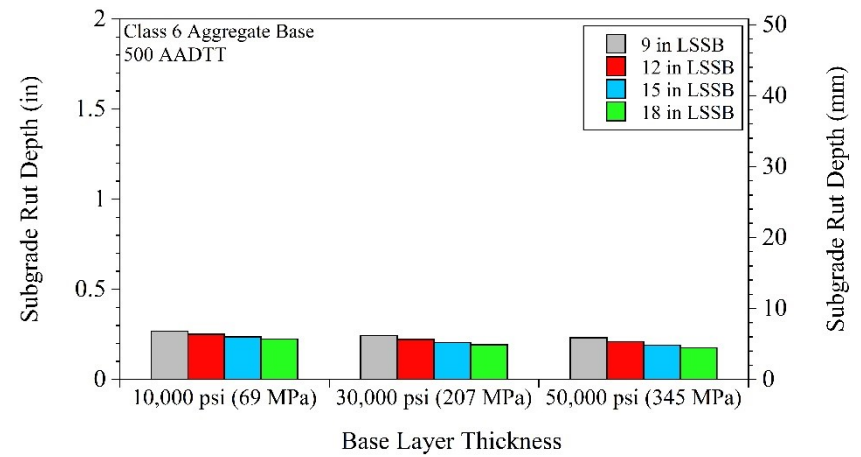
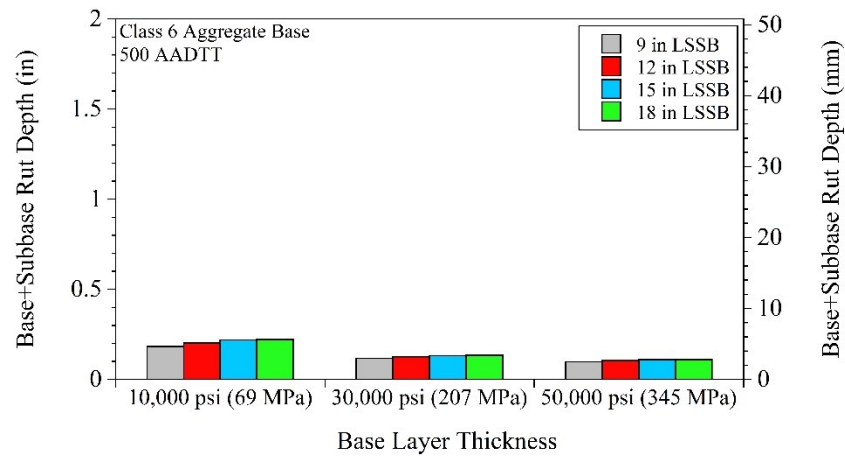
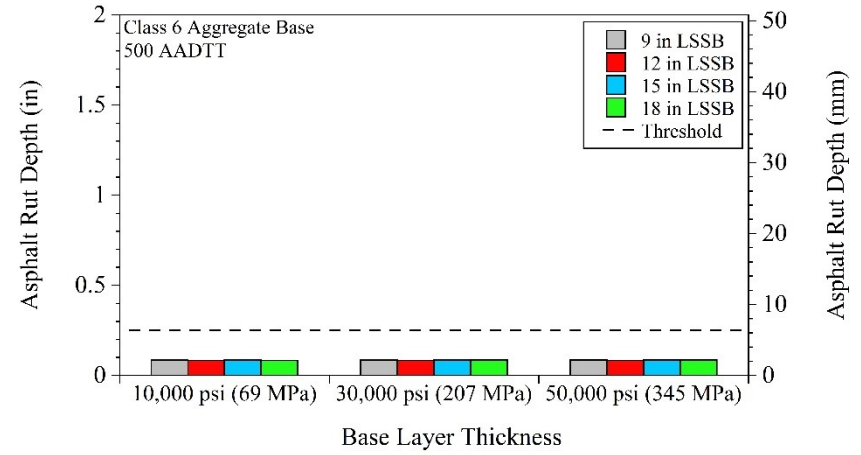
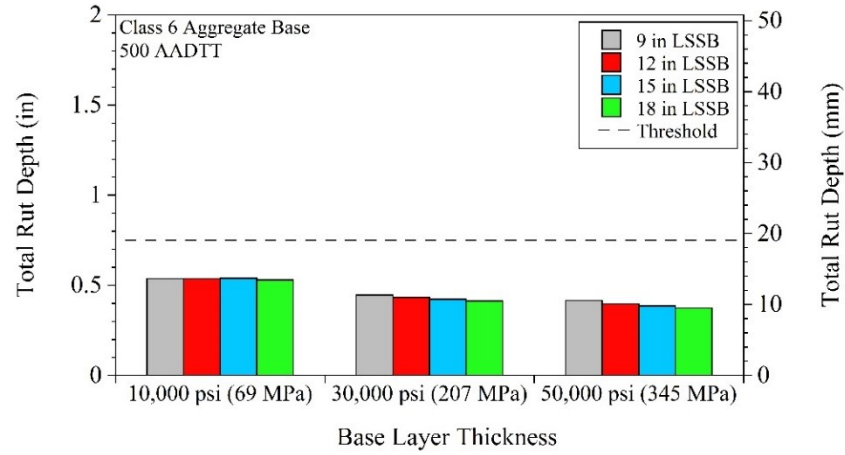
APPENDIX BI

TOTAL, ASPHALT, BASE+SUBBASE, AND SUBGRADE LAYER RUTTING AT 50% RELIABILITY FOR LARGE STONE SUBBASE (LSSB) GROUPS

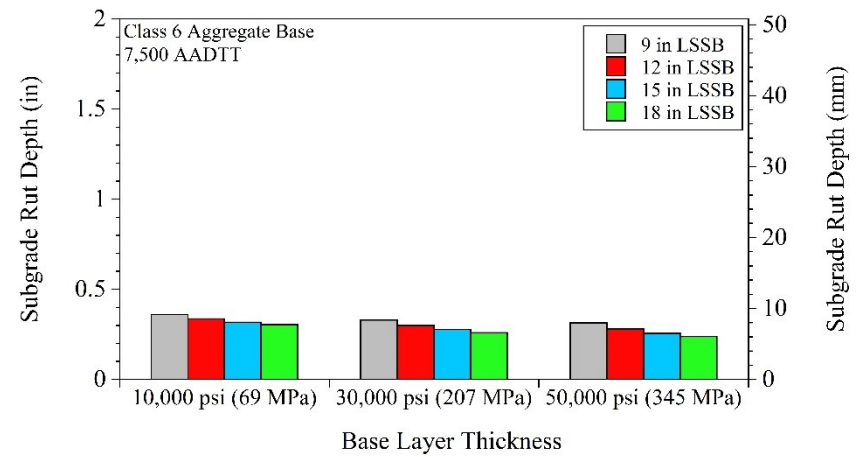
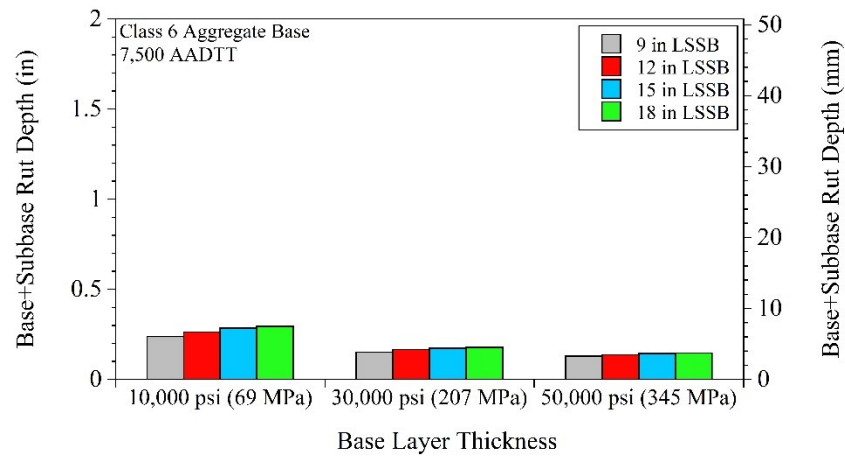
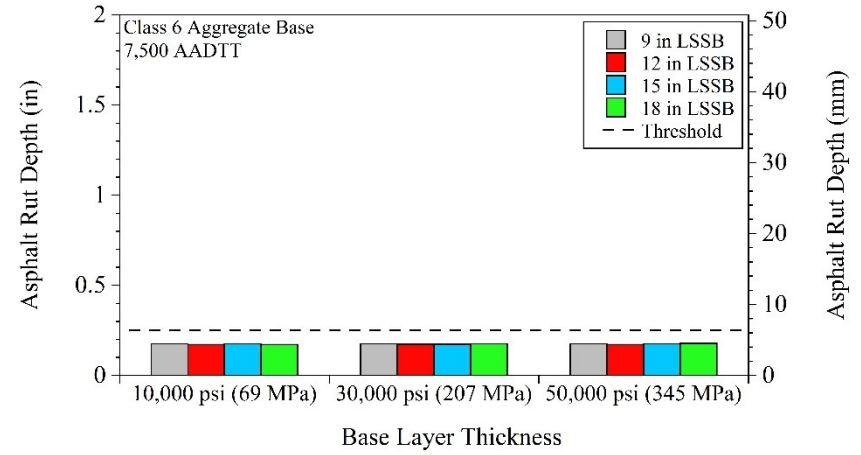
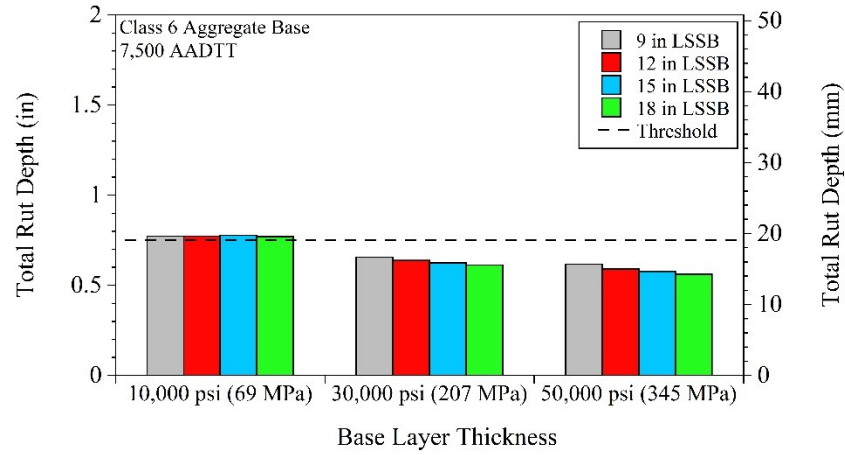
For pavements that contained Class 6 Aggregate - 100 AADTT:



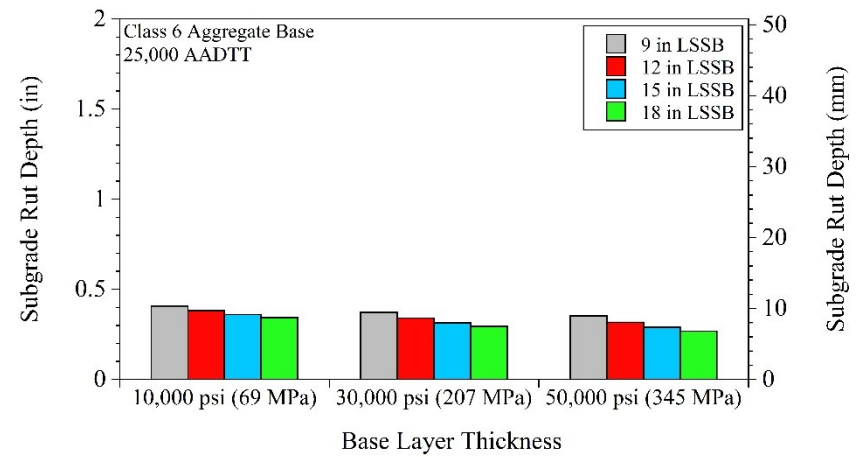
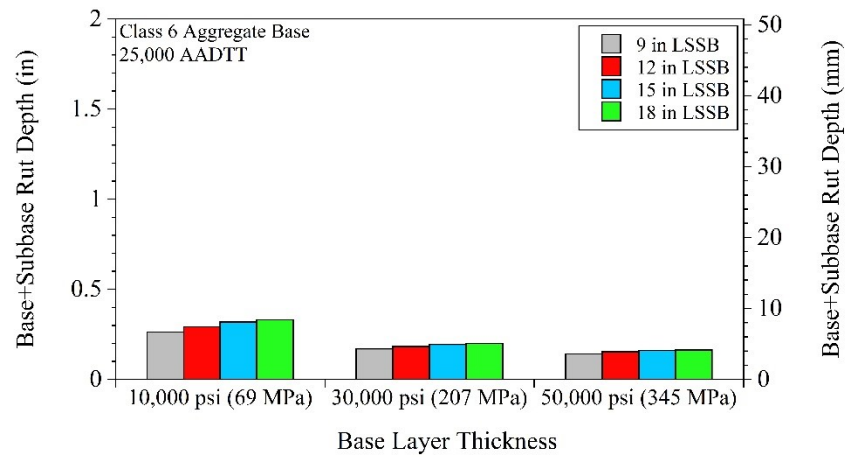
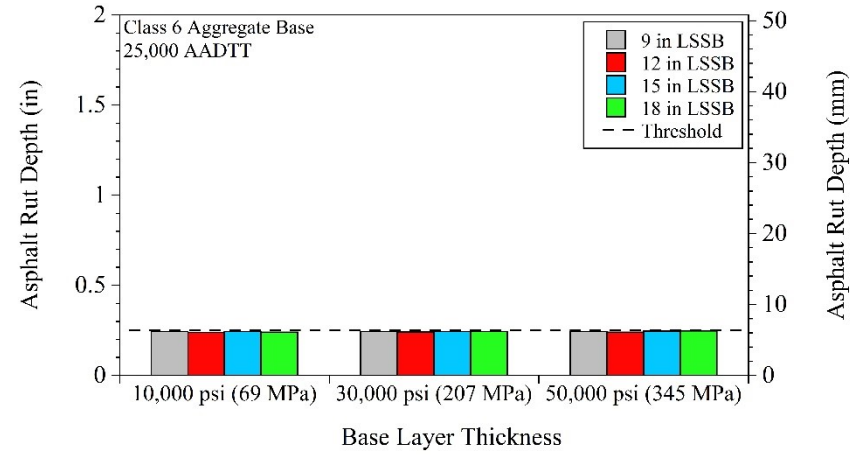
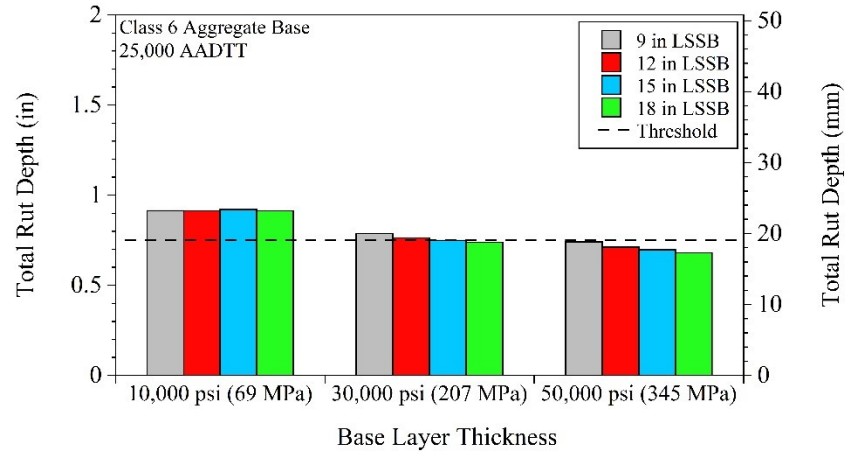
For pavements that contained Class 6 Aggregate - 500 AADTT:



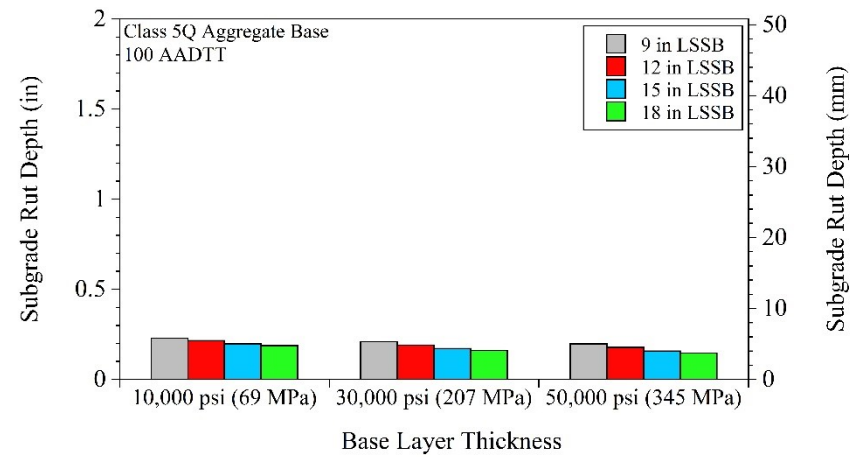
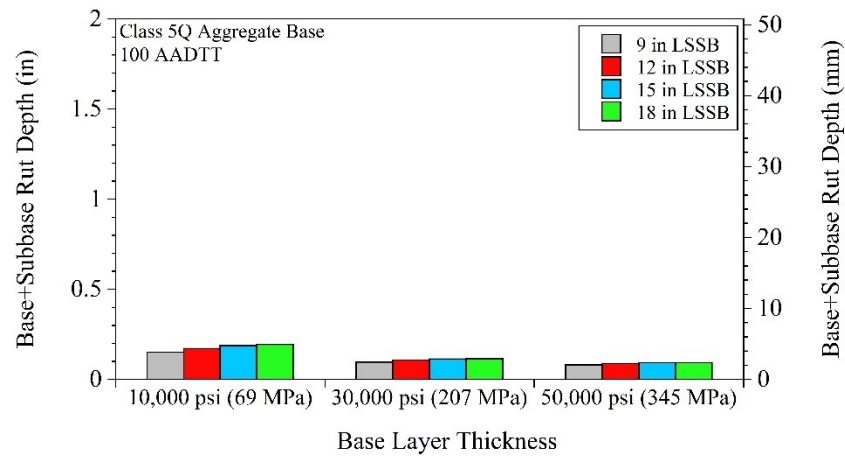
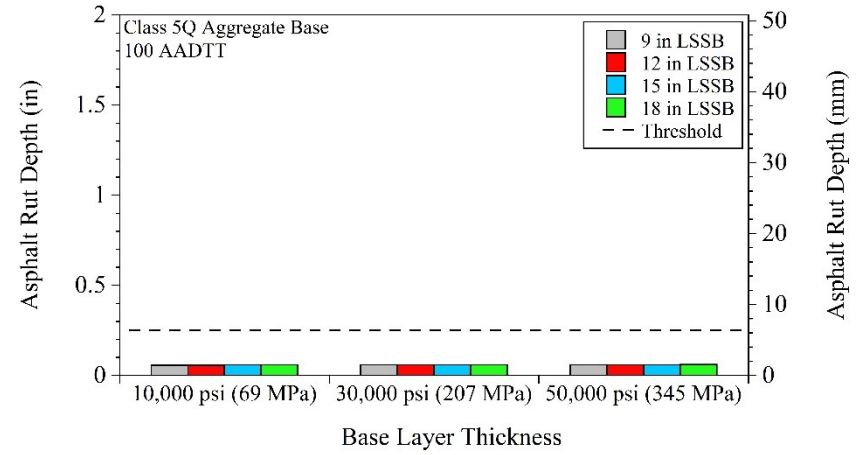
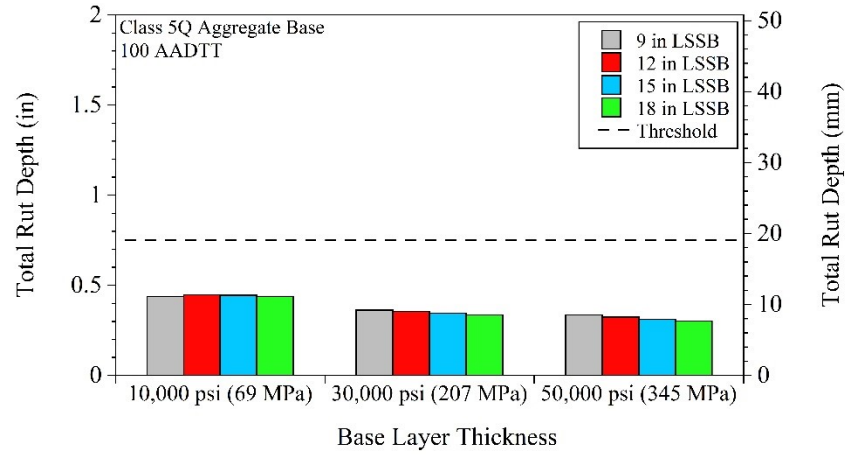
For pavements that contained Class 6 Aggregate - 7,500 AADTT:



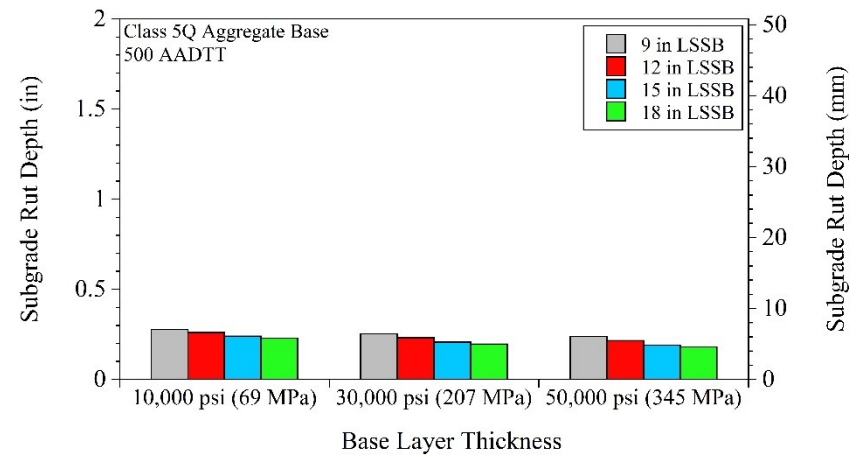
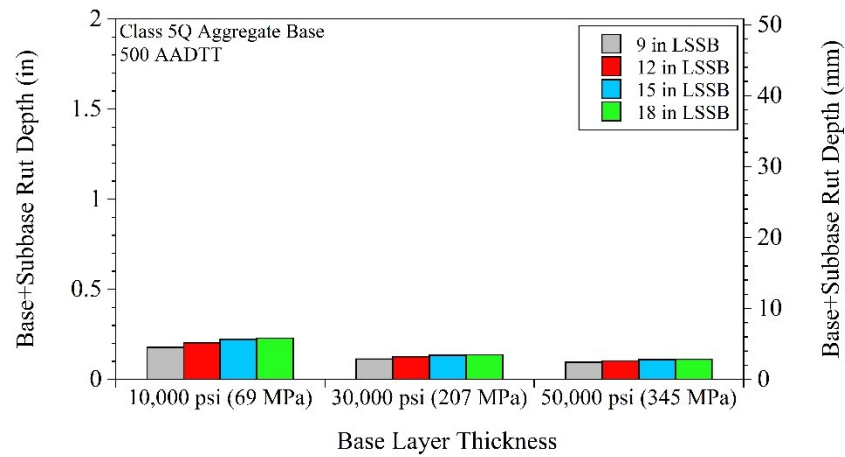
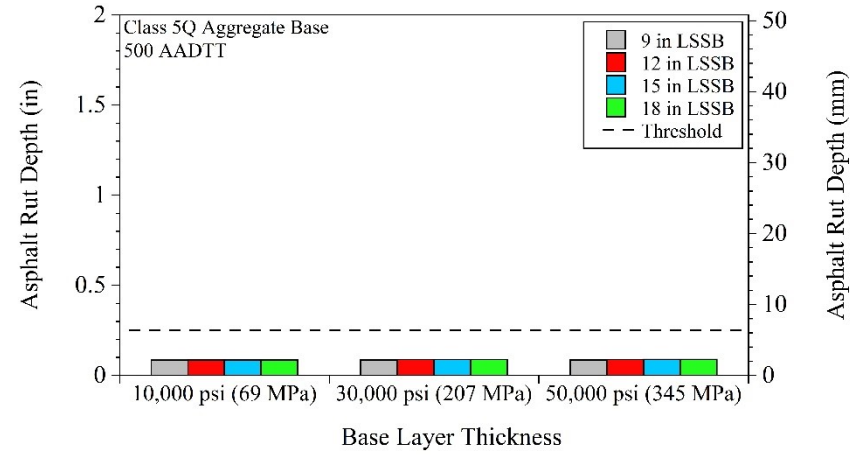
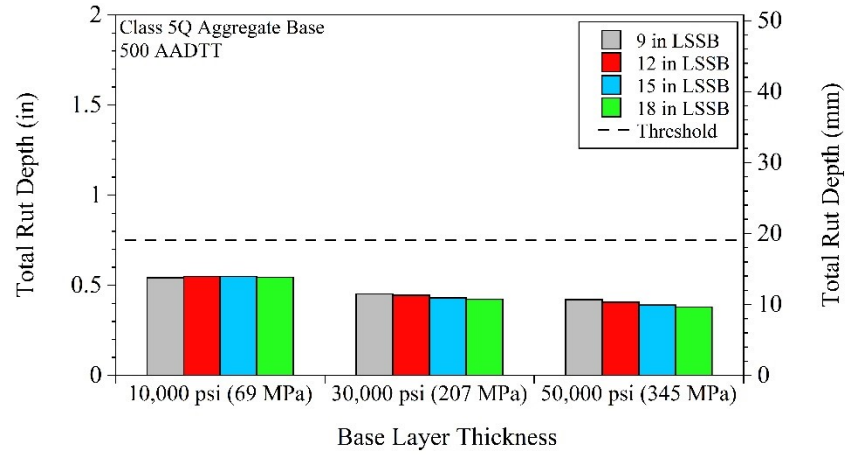
For pavements that contained Class 6 Aggregate - 25,000 AADTT:



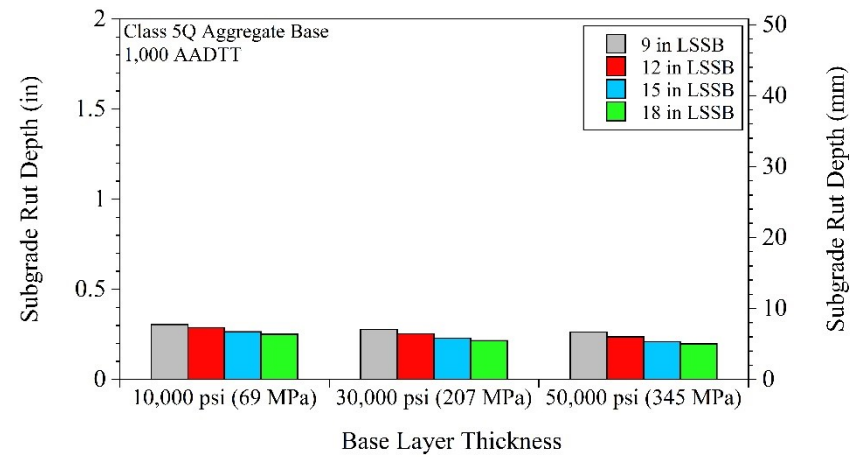
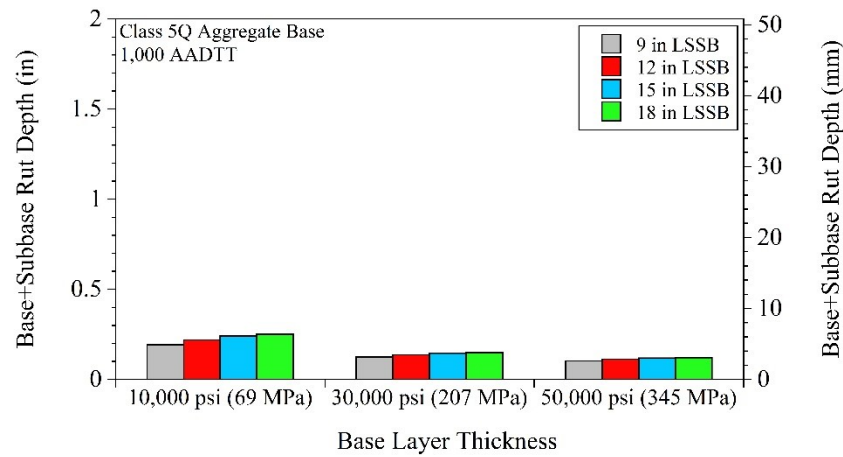
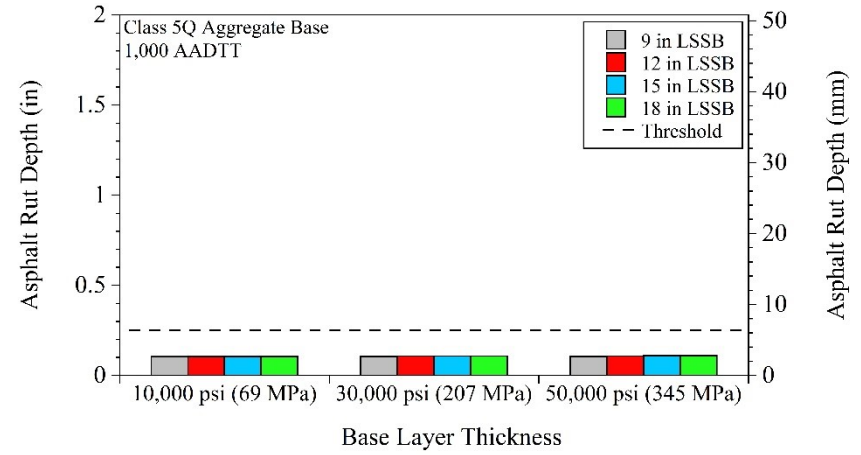
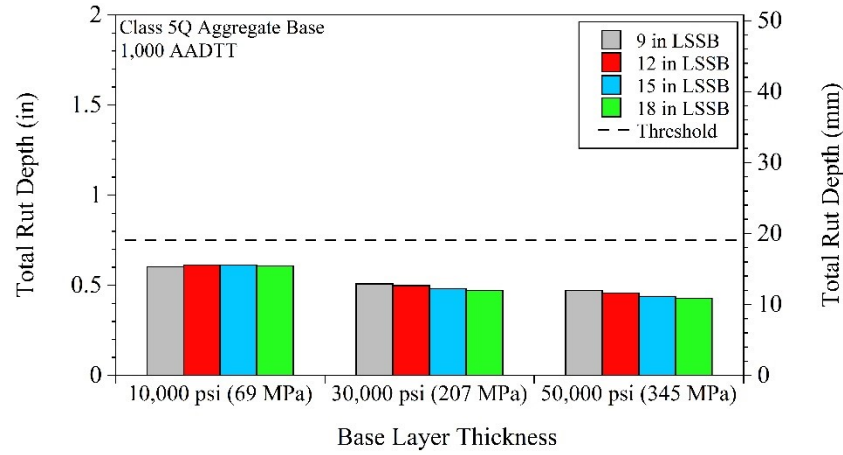
For pavements that contained Class 5Q Aggregate - 100 AADTT:



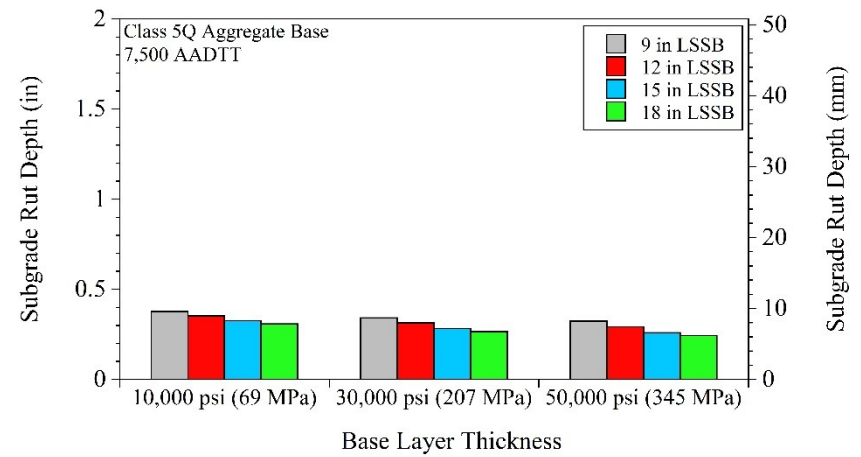
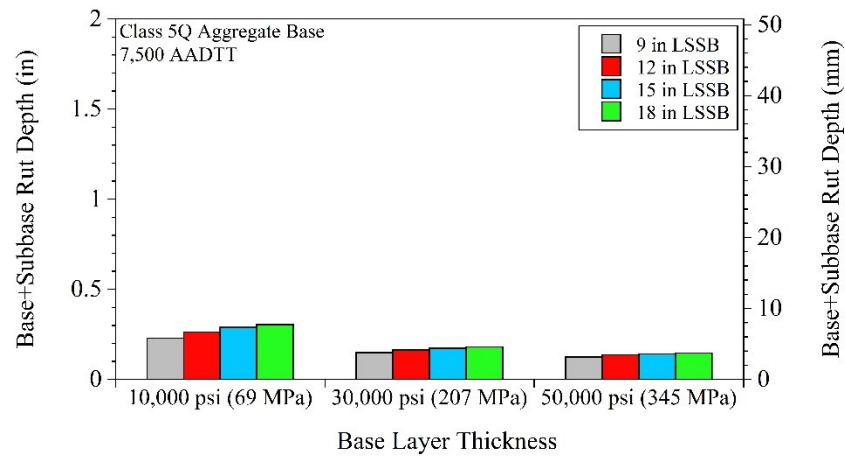
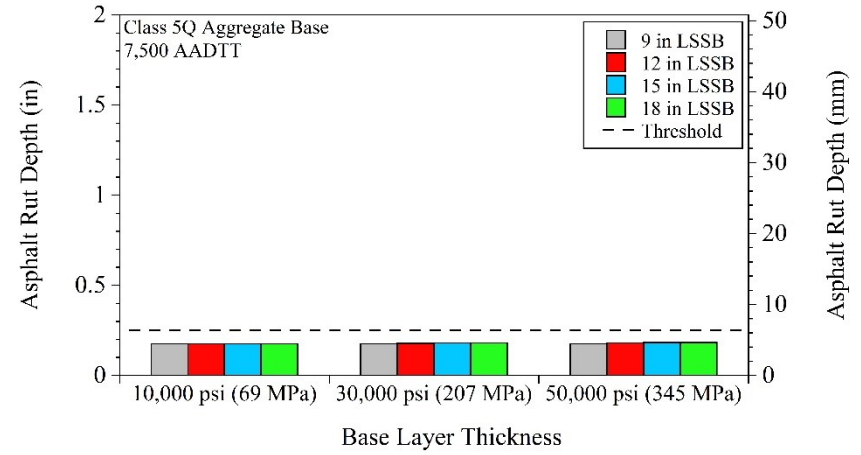
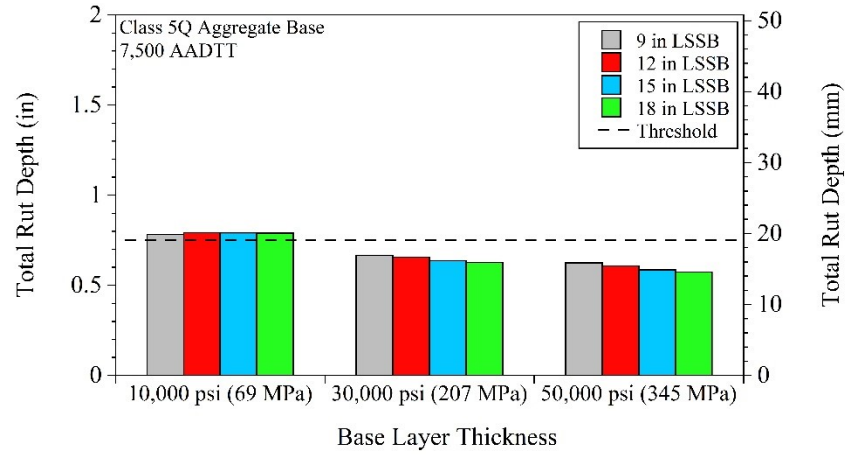
For pavements that contained Class 5Q Aggregate - 500 AADTT:



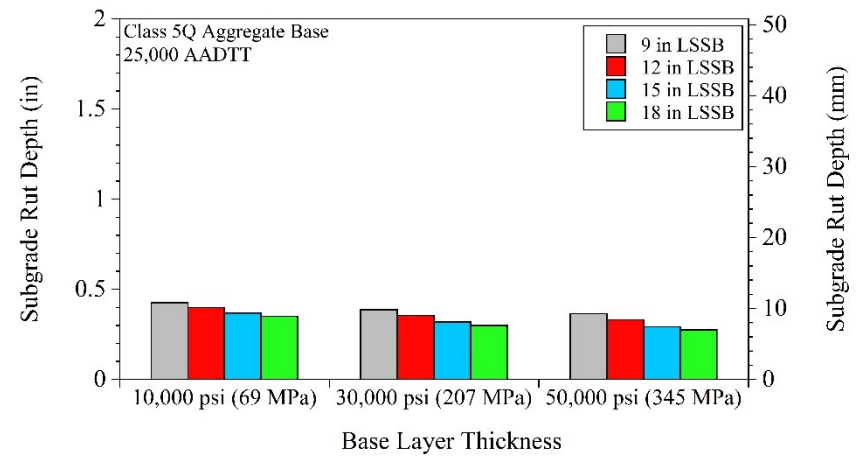
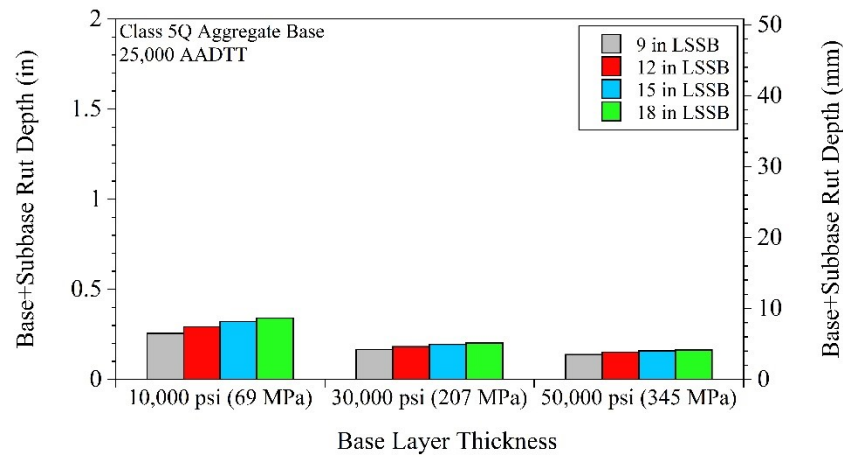
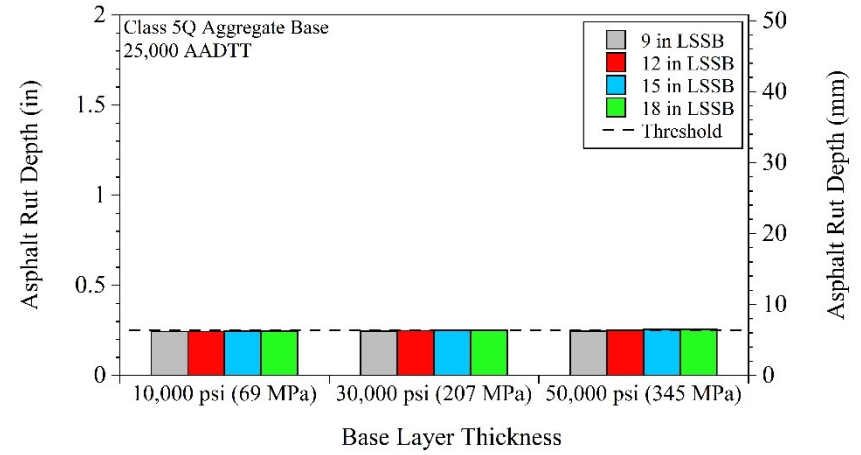
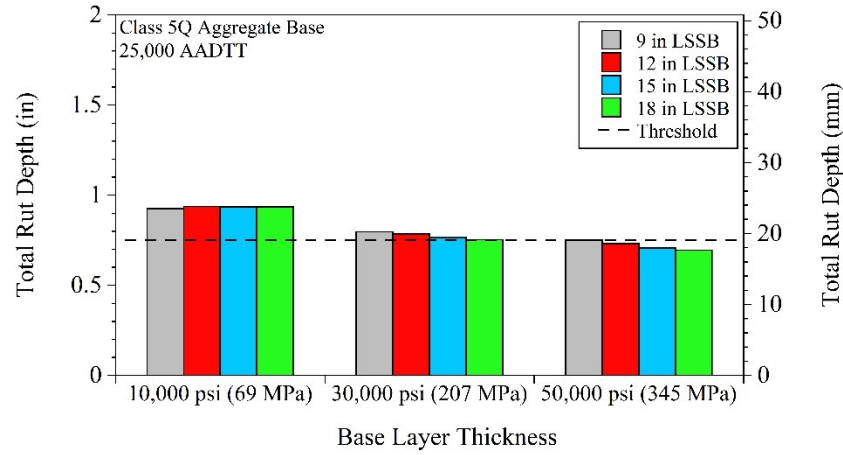
For pavements that contained Class 5Q Aggregate - 1,000 AADTT:



For pavements that contained Class 5Q Aggregate - 7,500 AADTT:



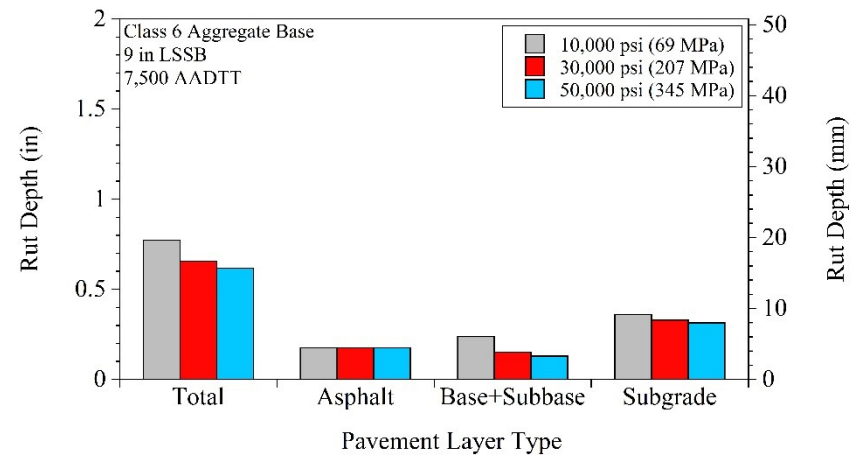
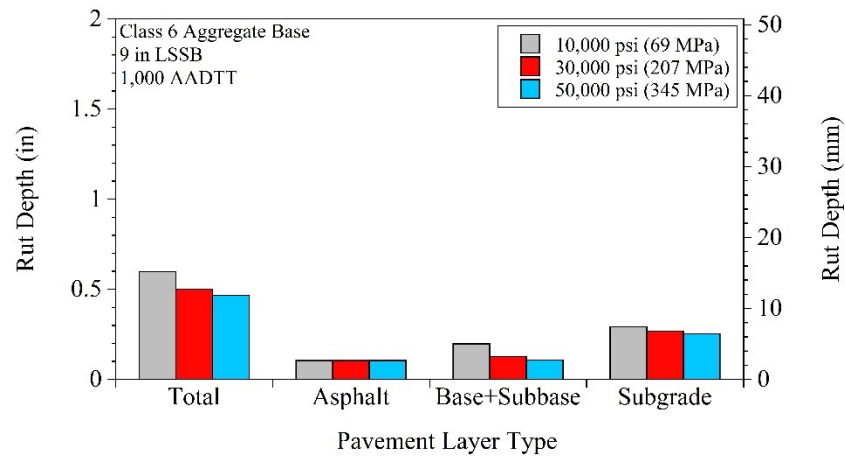
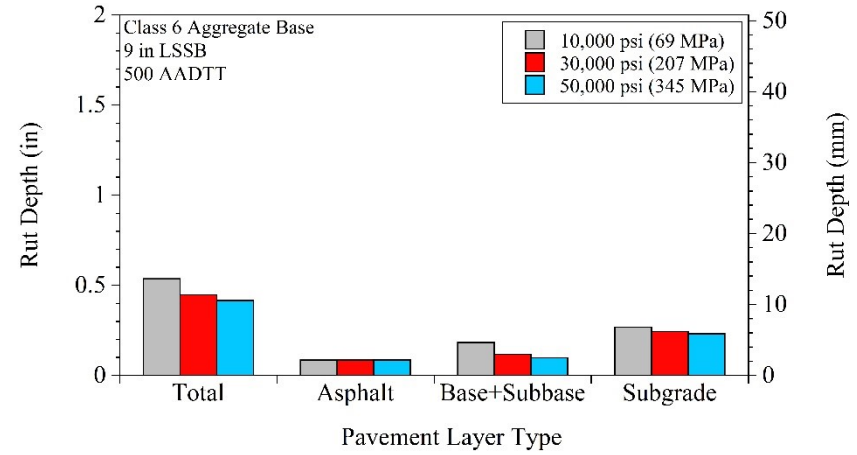
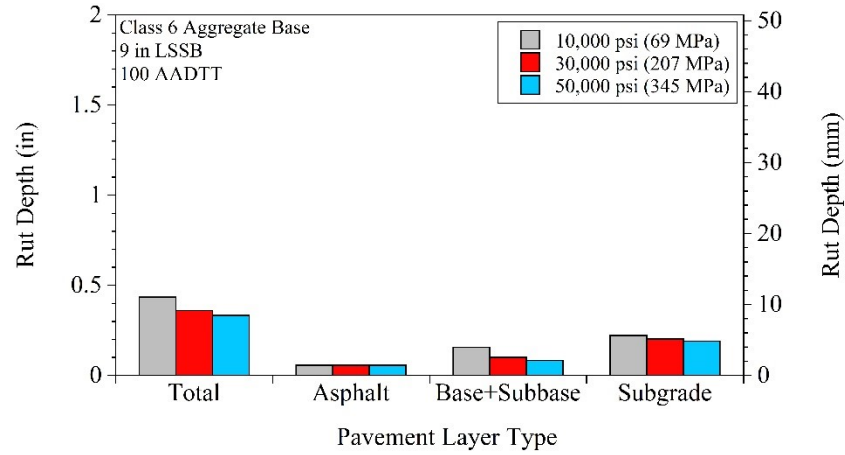
For pavements that contained Class 5Q Aggregate - 25,000 AADTT:

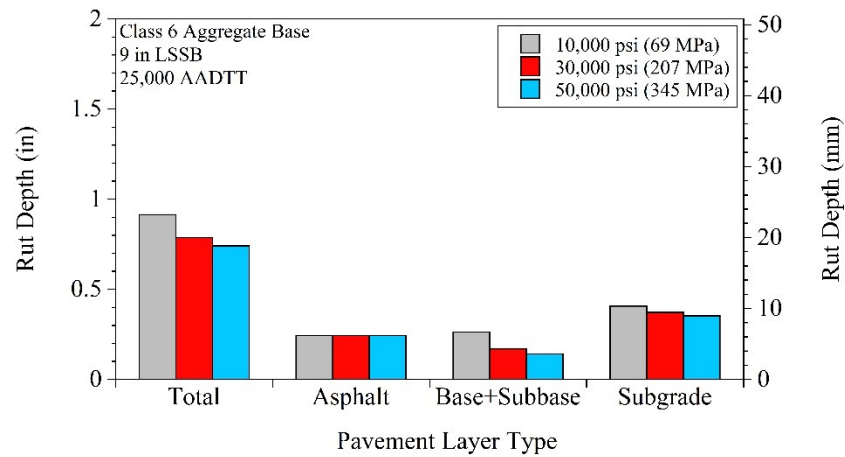


APPENDIX BJ

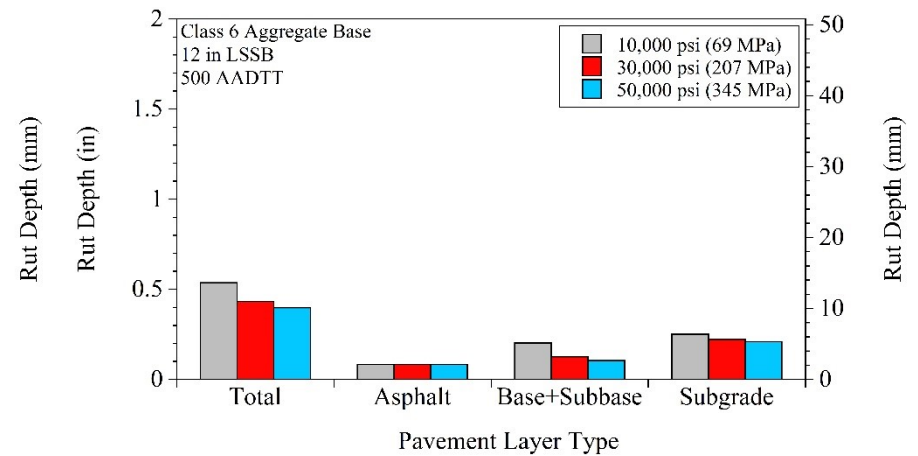
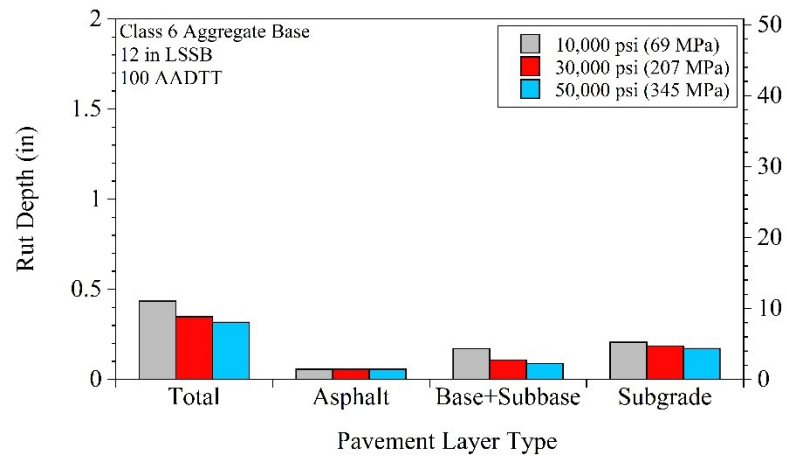
TOTAL AND LAYER RUTTING AT 50% RELIABILITY FOR LARGE STONE SUBBASE (LSSB) GROUPS

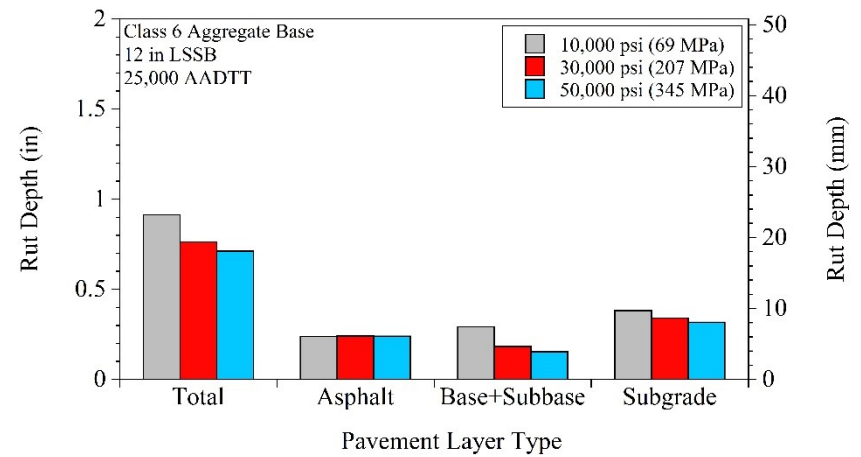
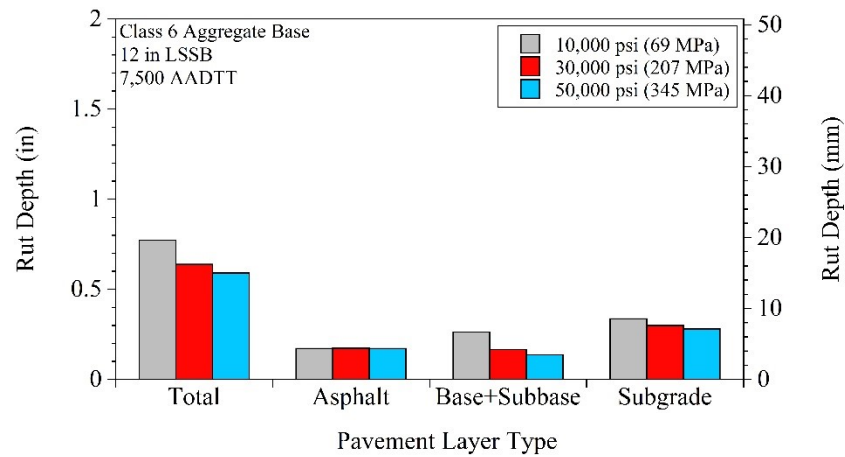
For pavements that contained Class 6 Aggregate and 9-in LSSB:



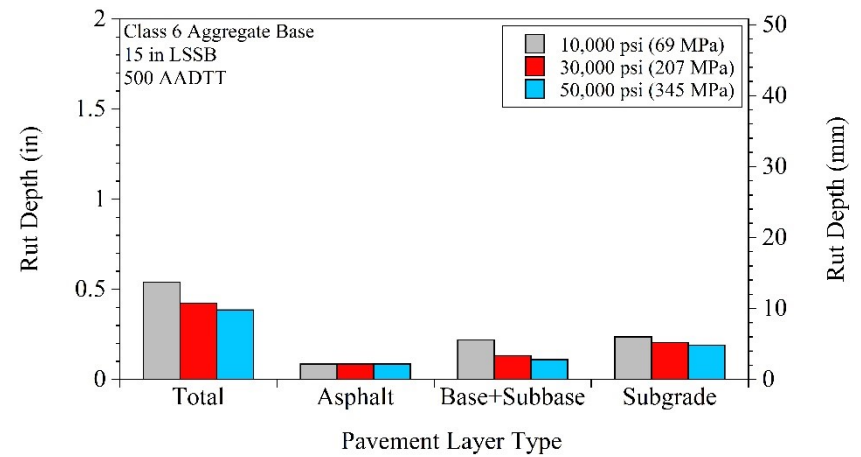
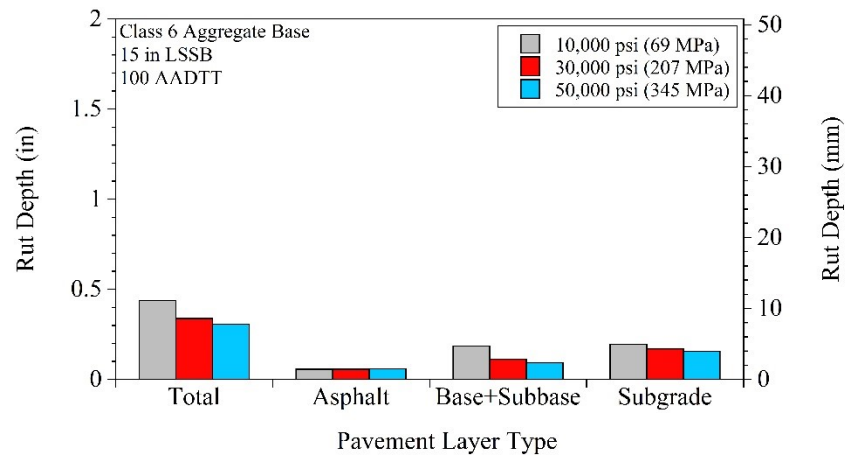


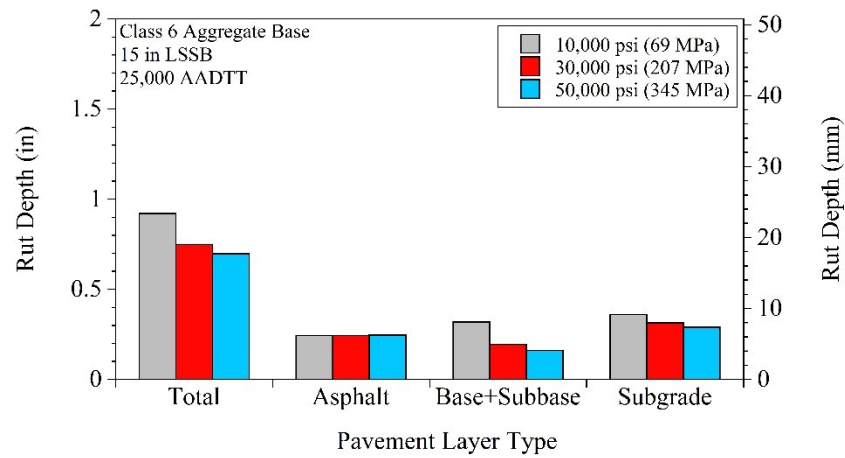
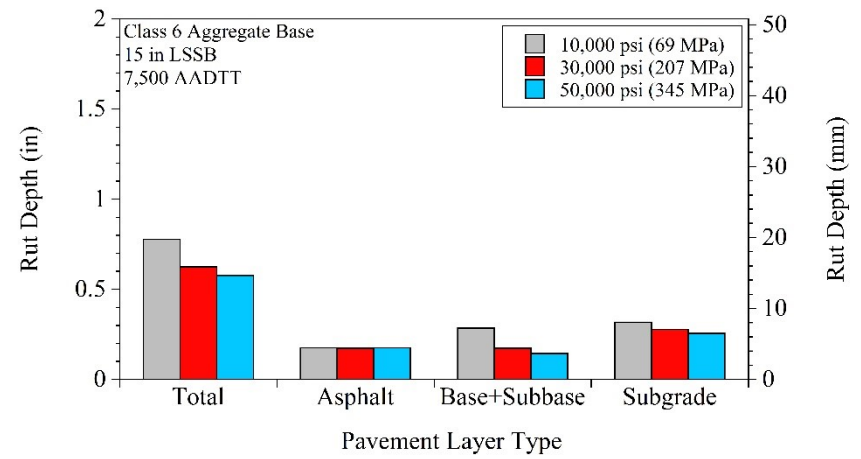
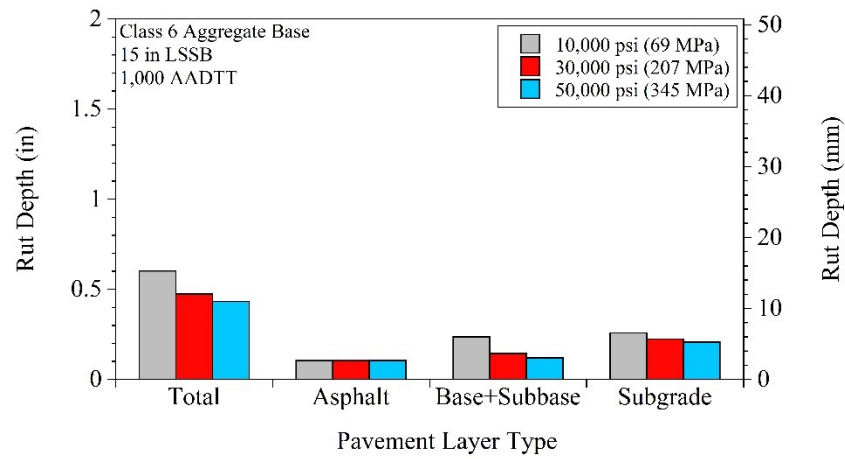
For pavements that contained Class 6 Aggregate and 12-in LSSB:



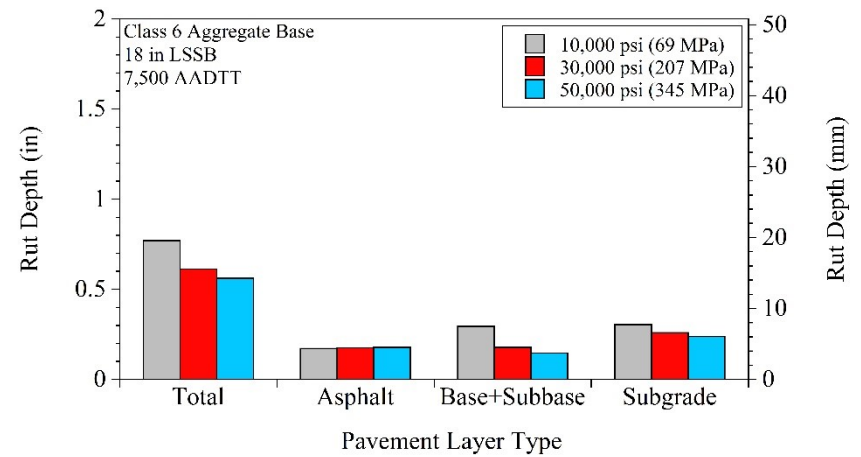
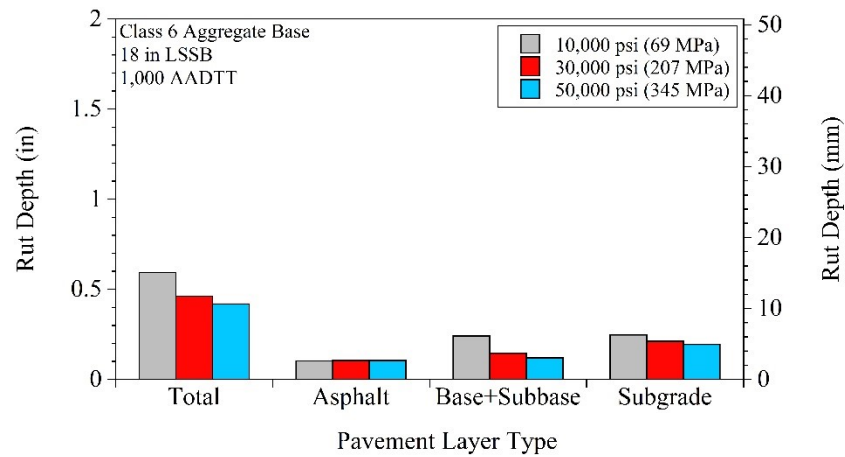
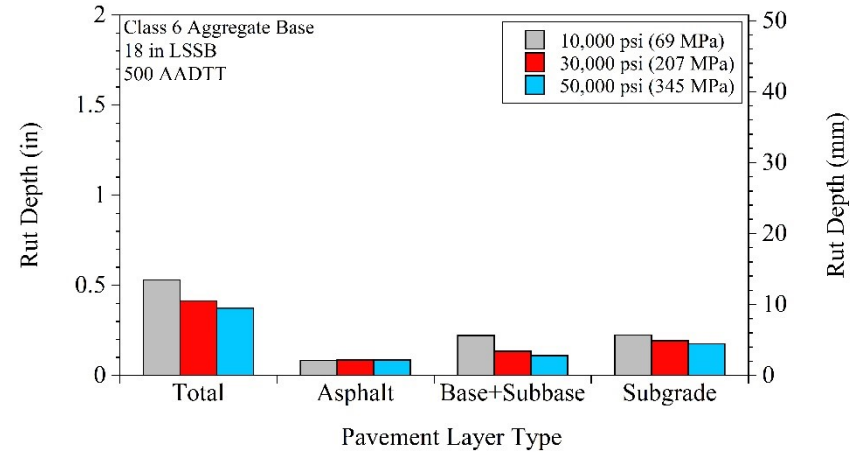
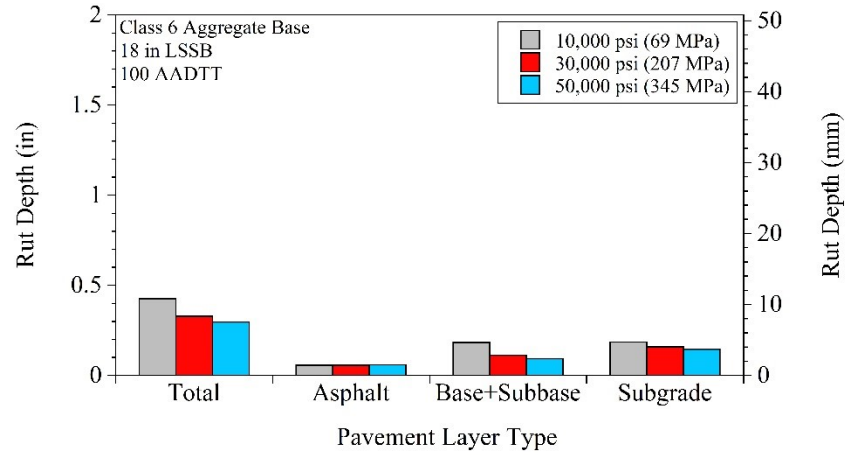


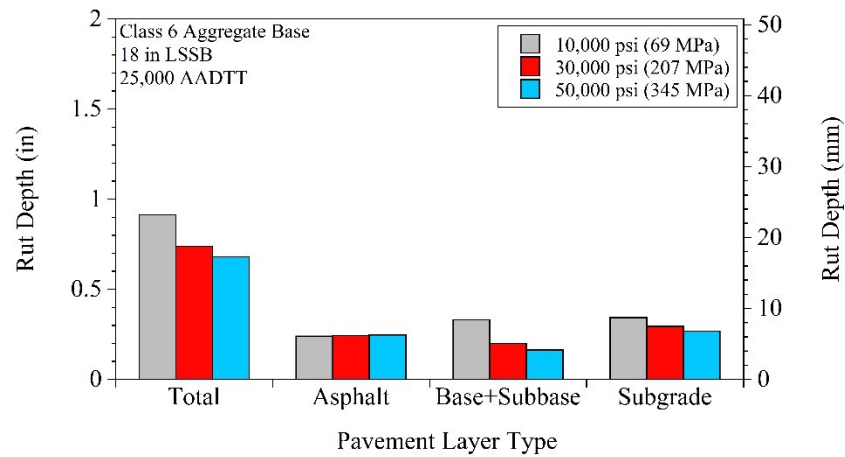
For pavements that contained Class 6 Aggregate and 15-in LSSB:



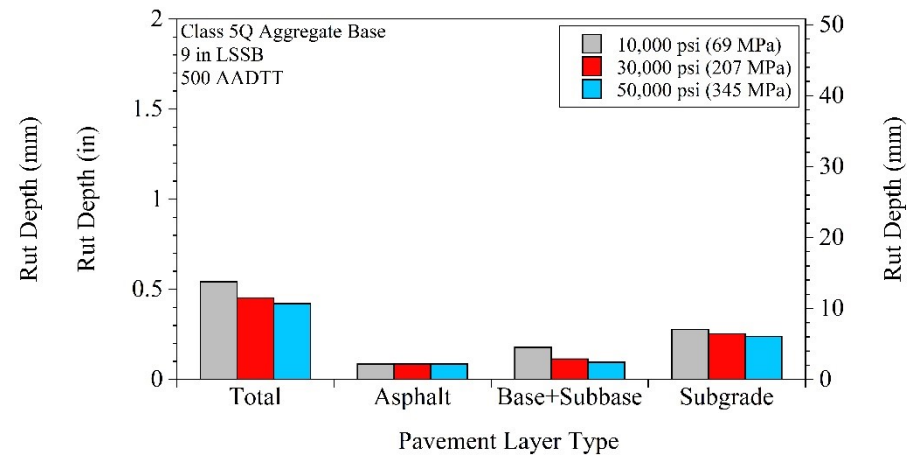
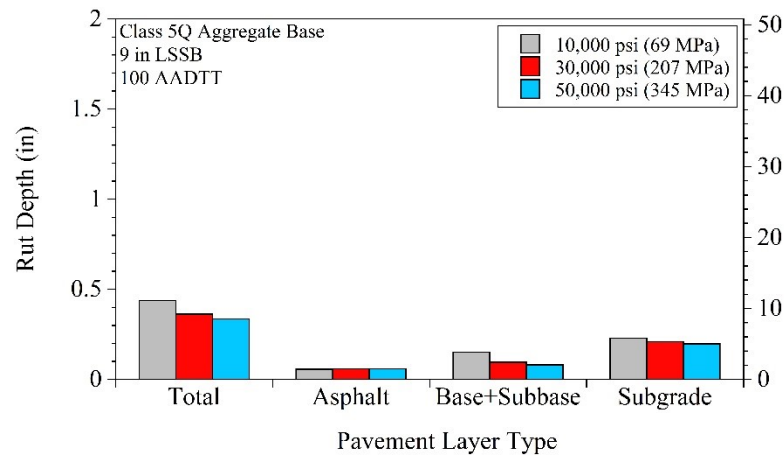


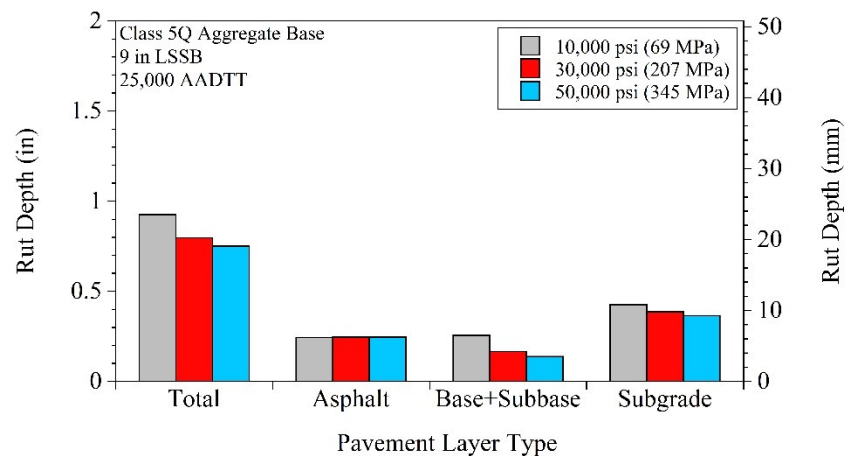
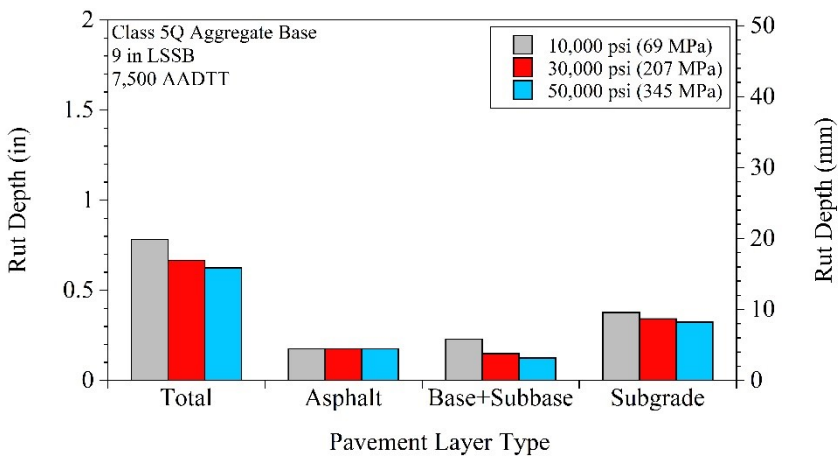
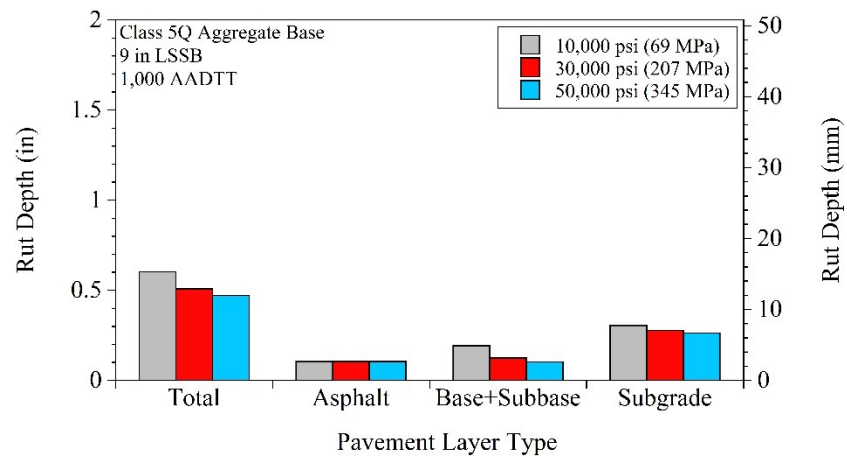
For pavements that contained Class 6 Aggregate and 18-in LSSB:



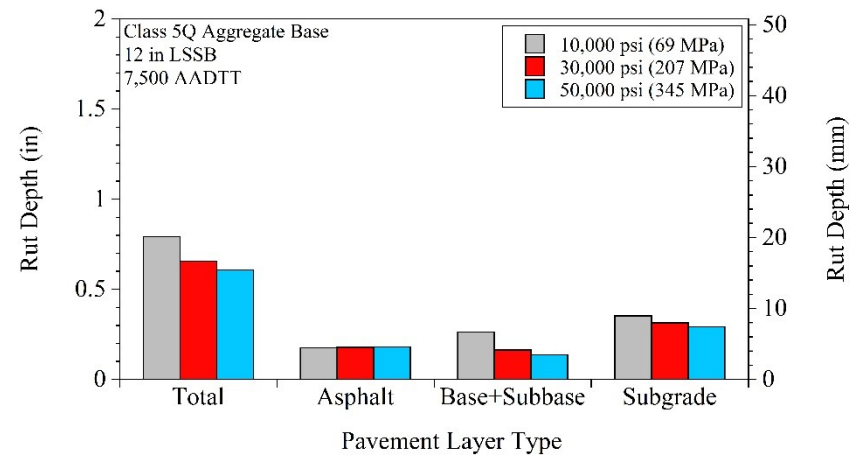
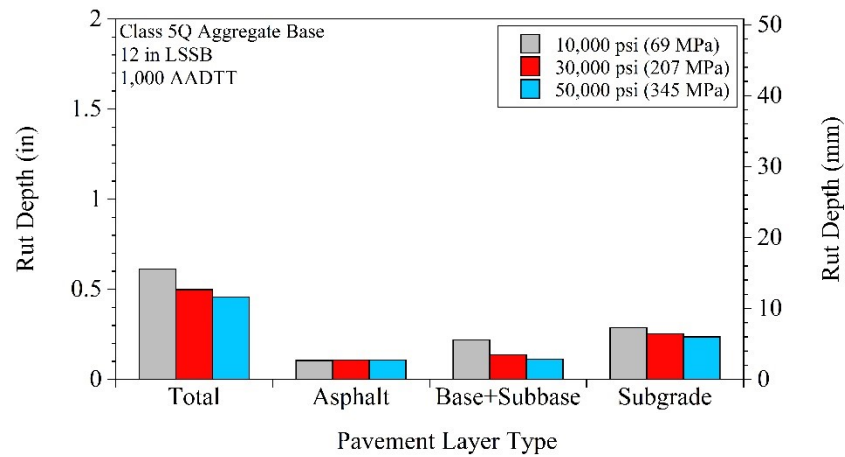
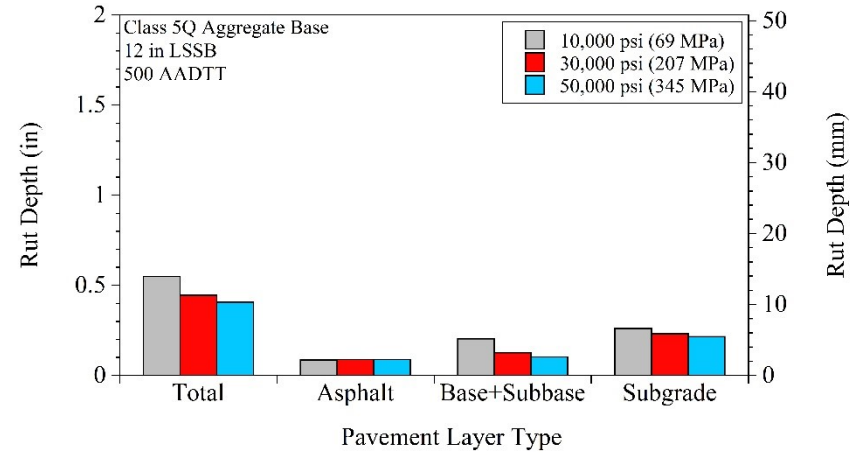
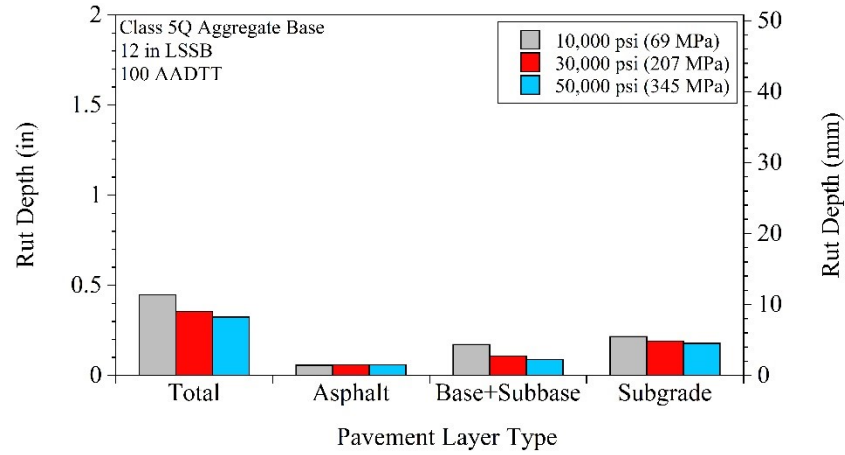


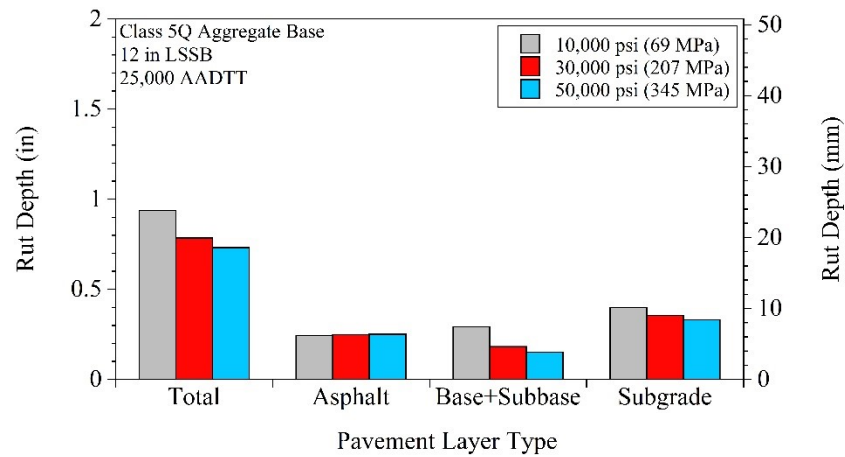
For pavements that contained Class 5Q Aggregate and 9-in LSSB:



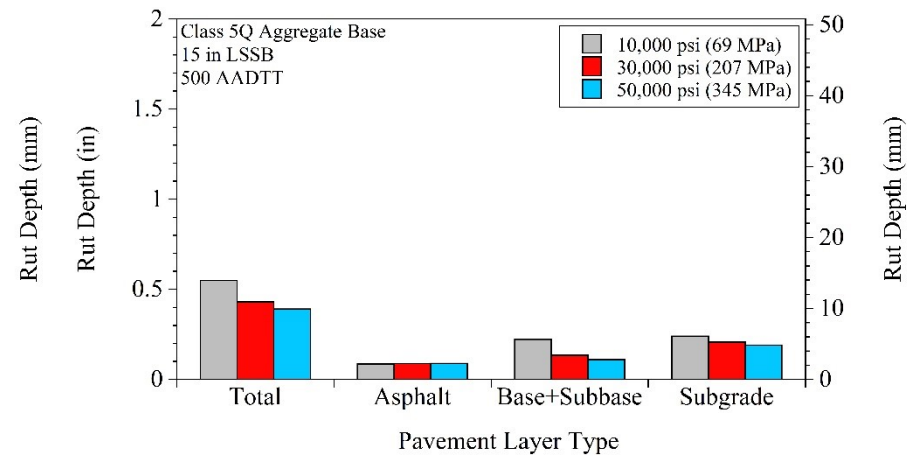
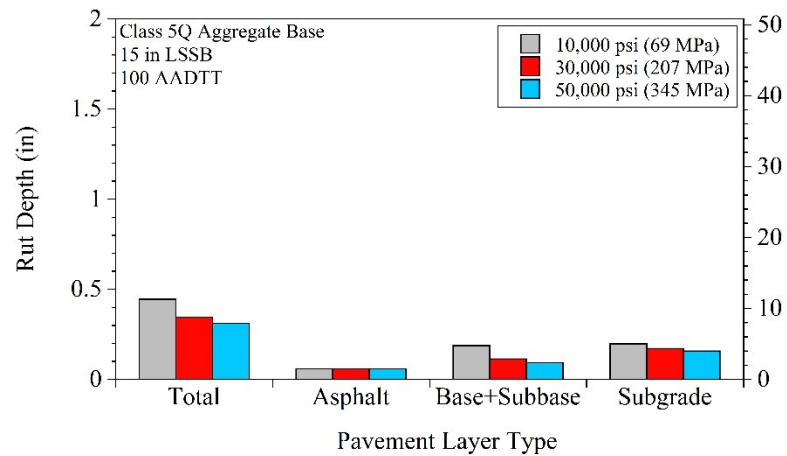


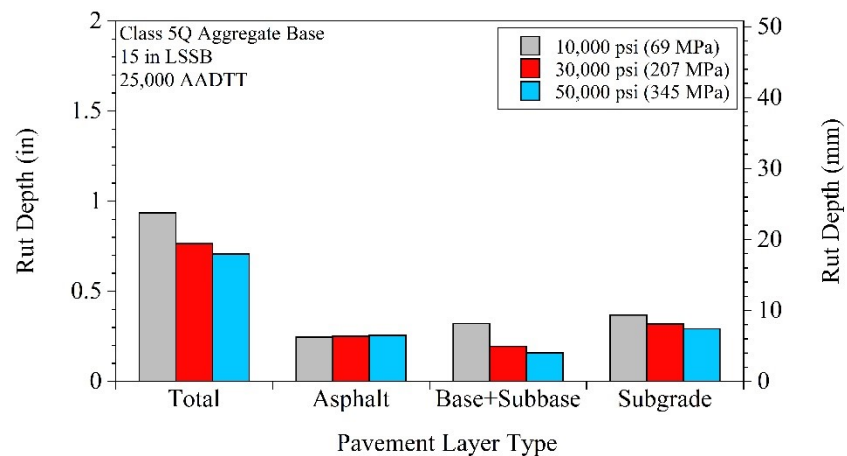
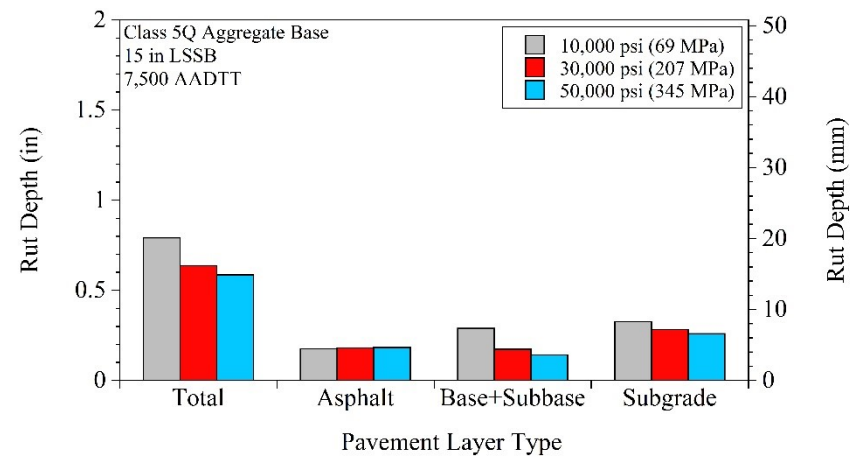
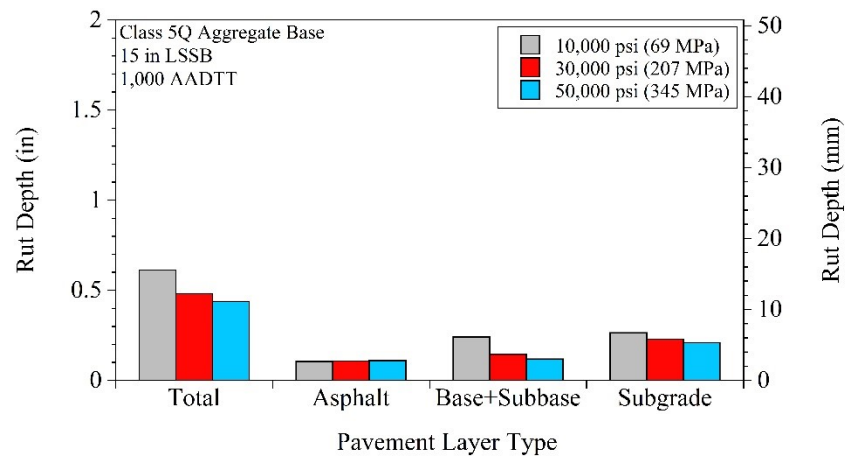
For pavements that contained Class 5Q Aggregate and 12-in LSSB:



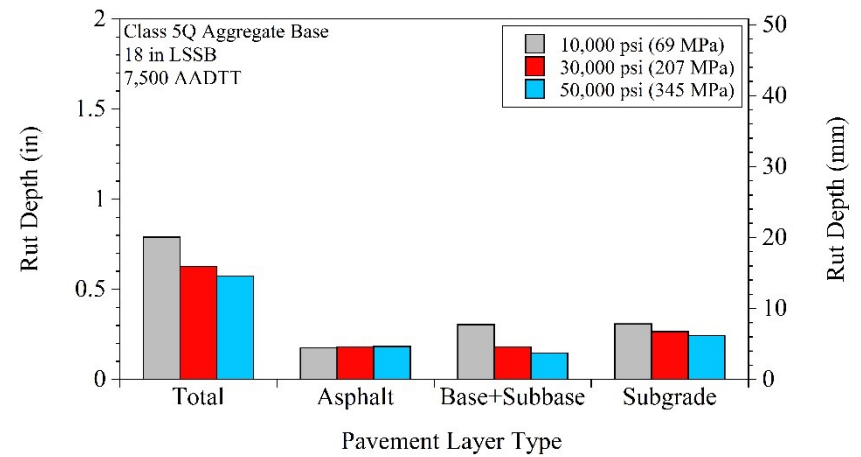
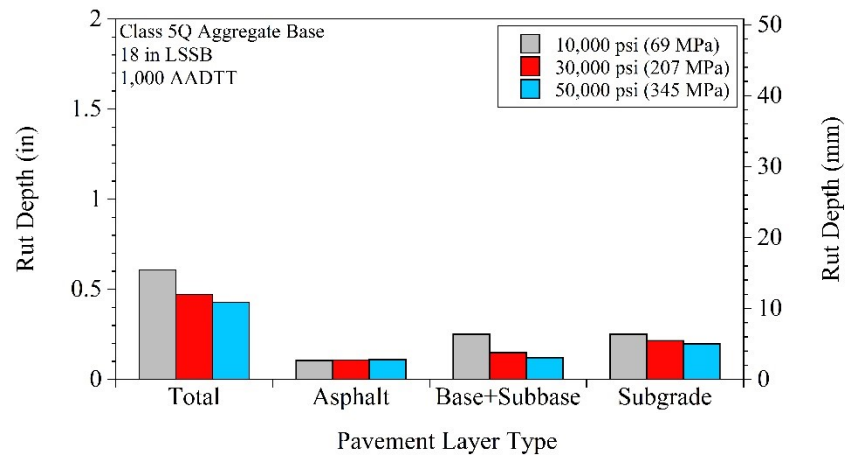
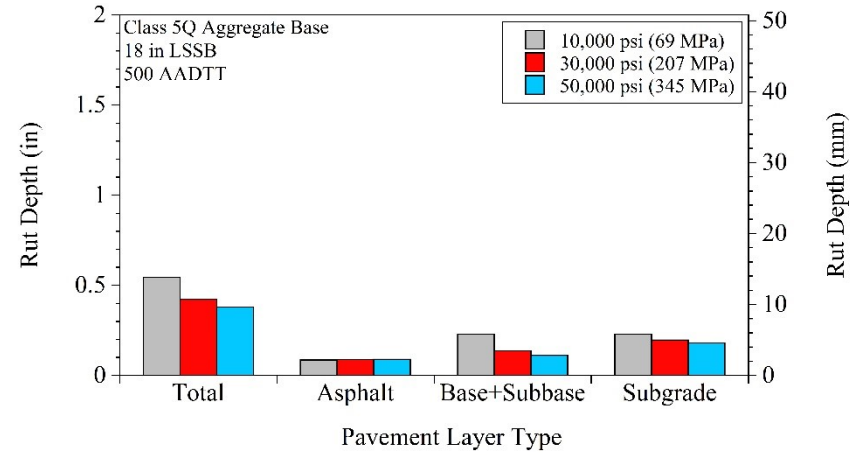
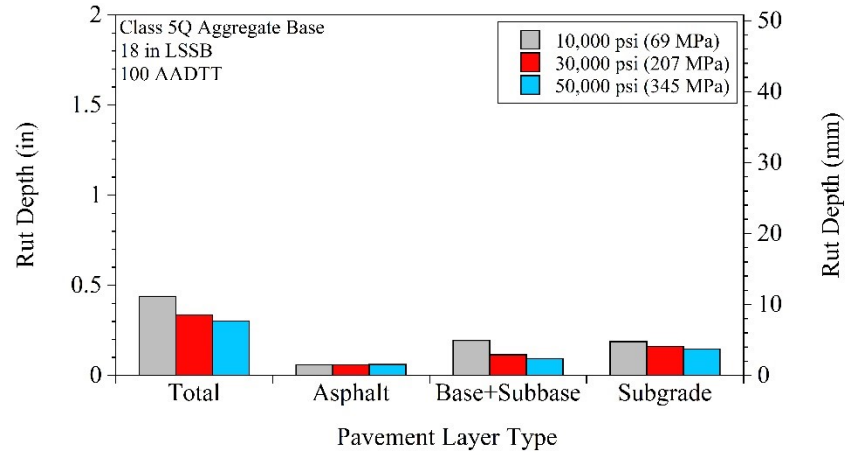


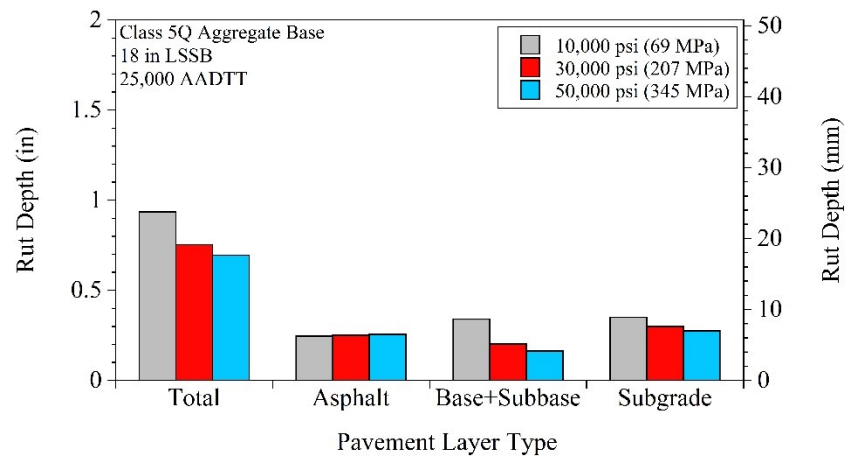
For pavements that contained Class 5Q Aggregate and 15-in LSSB:





For pavements that contained Class 5Q Aggregate and 18-in LSSB:

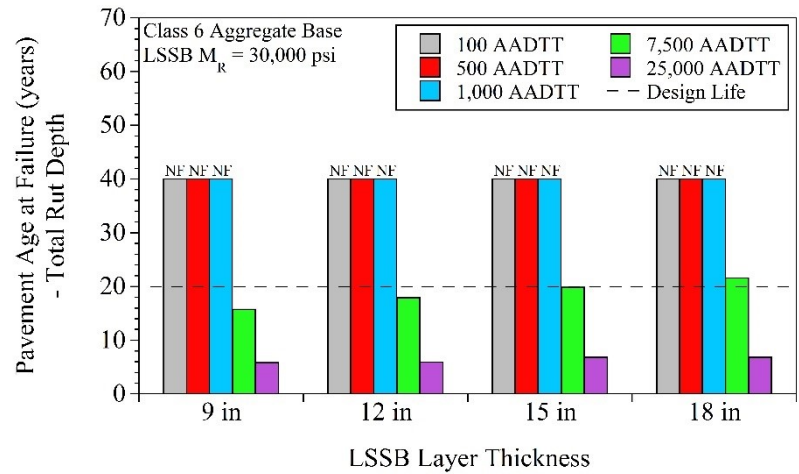
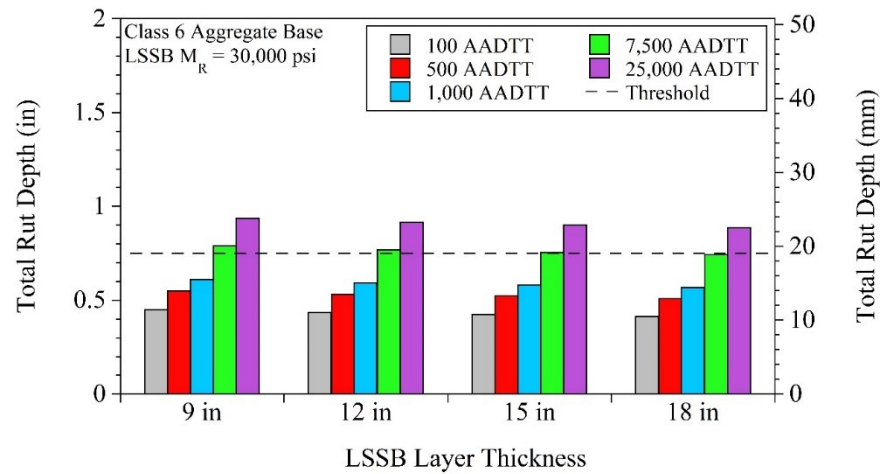
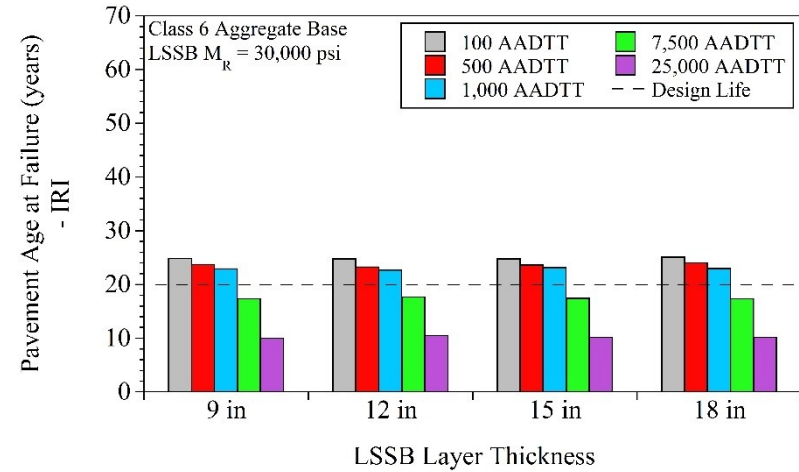
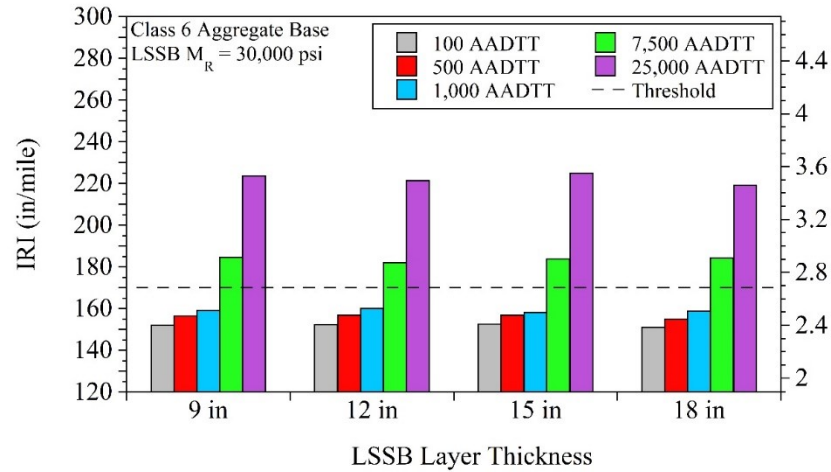


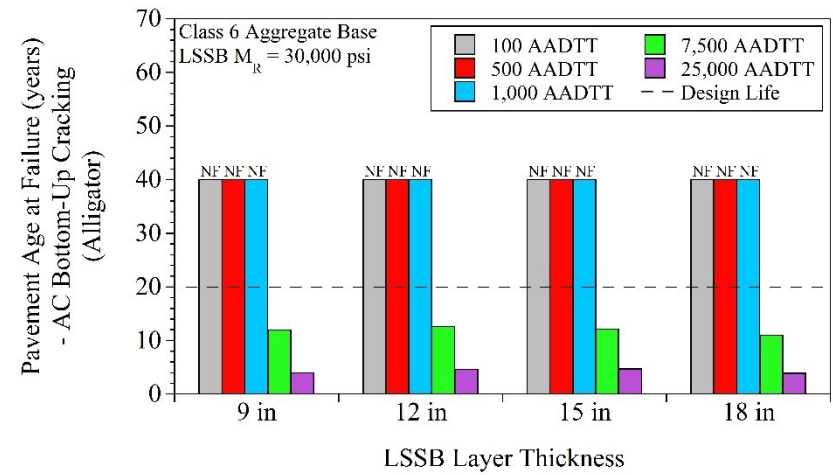
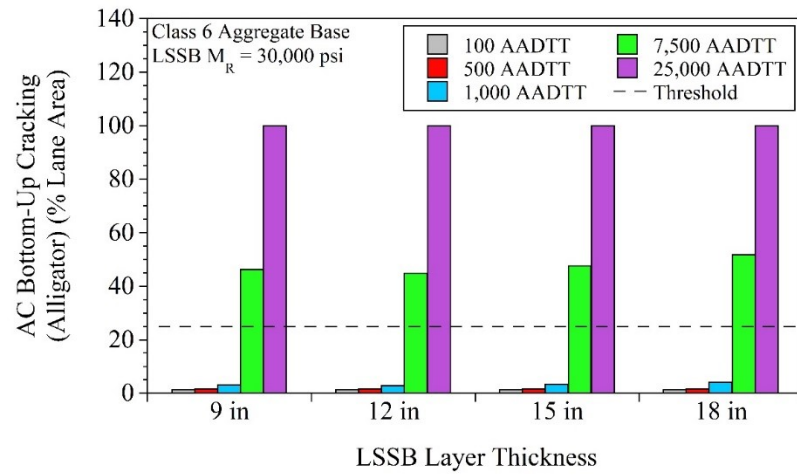


APPENDIX BK

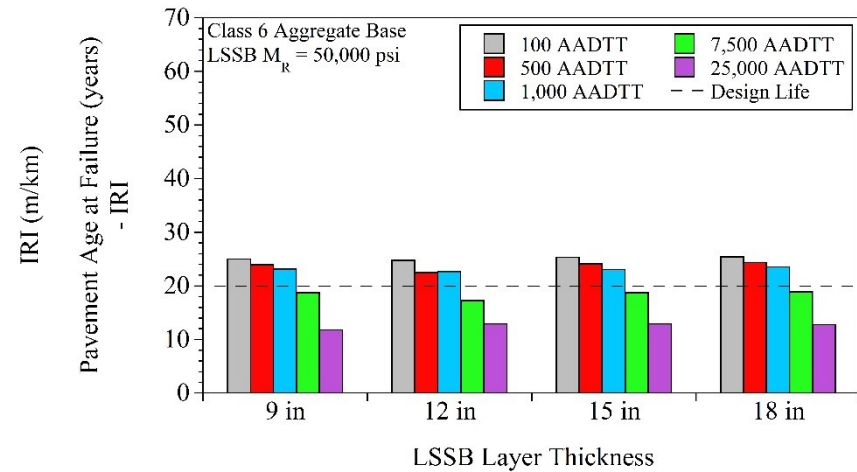
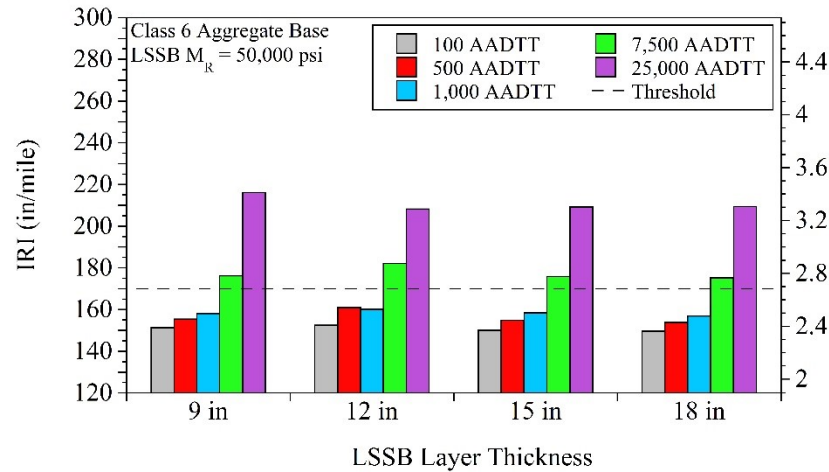
EFFECT OF TRAFFIC LEVEL ON PAVEMENT PERFORMANCE PREDICTIONS

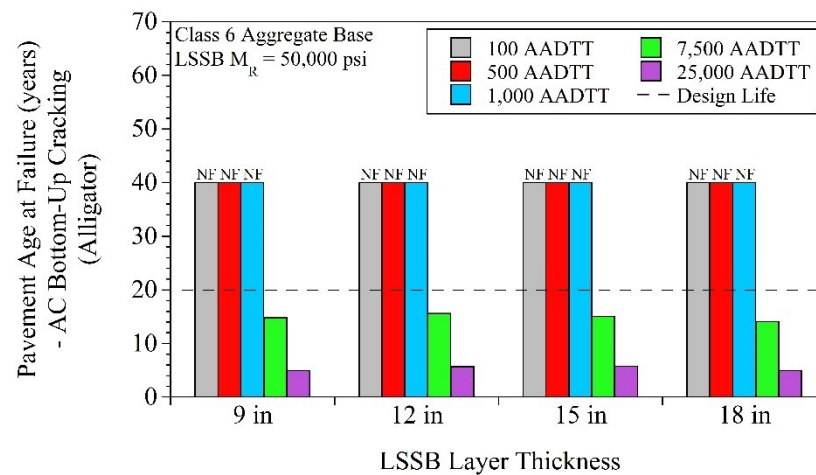
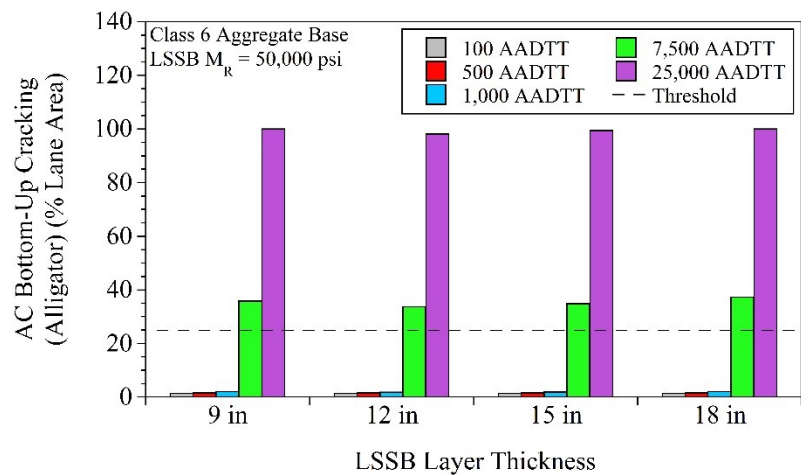
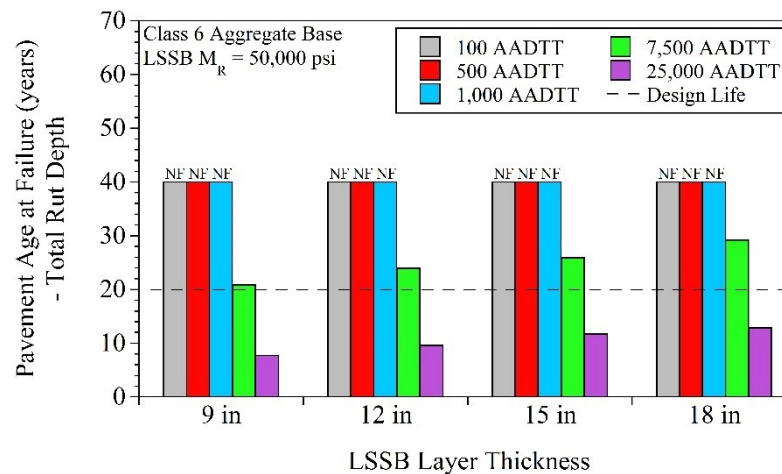
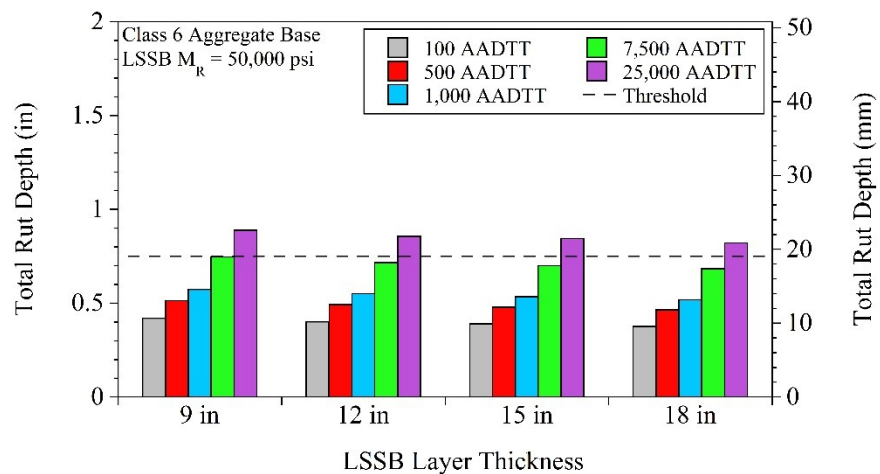
For pavements that contained Class 6 Aggregate and LSSB with $M_R = 30,000$ psi:



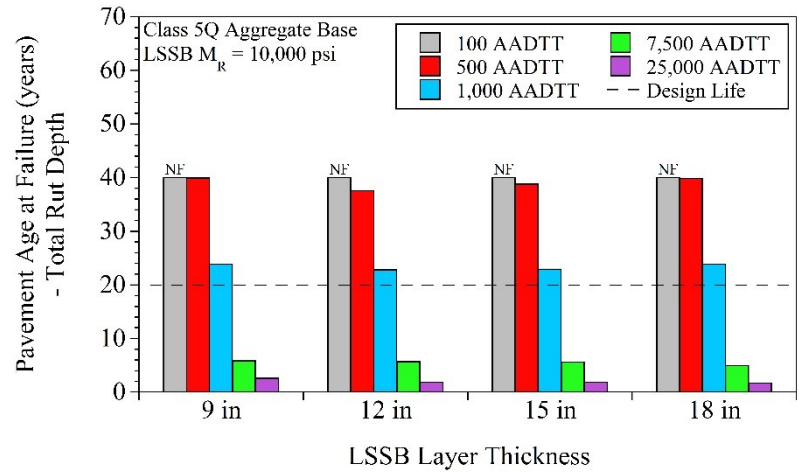
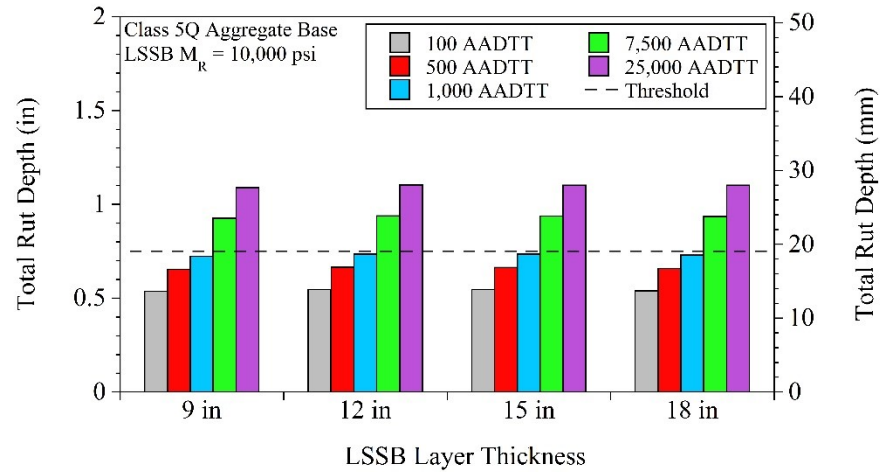
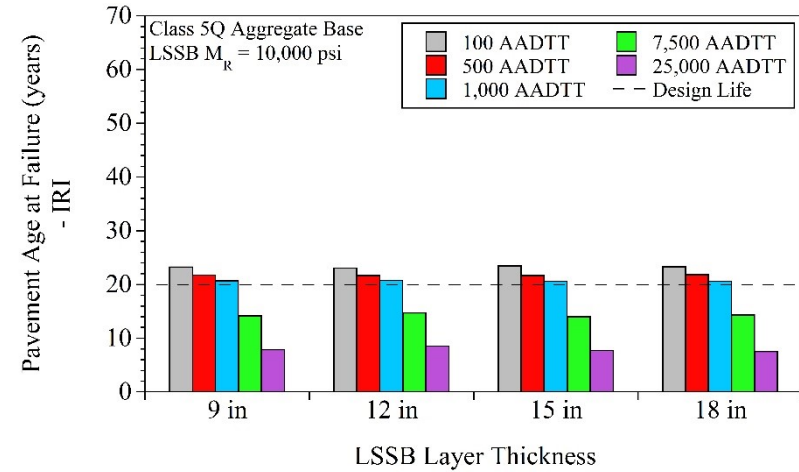
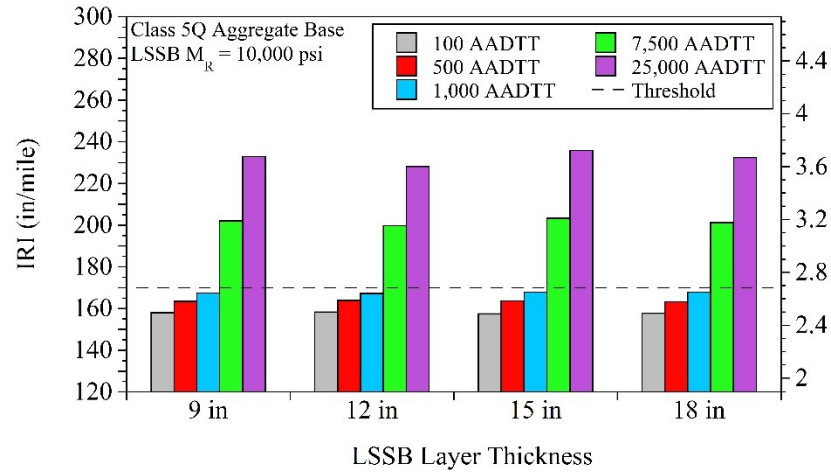


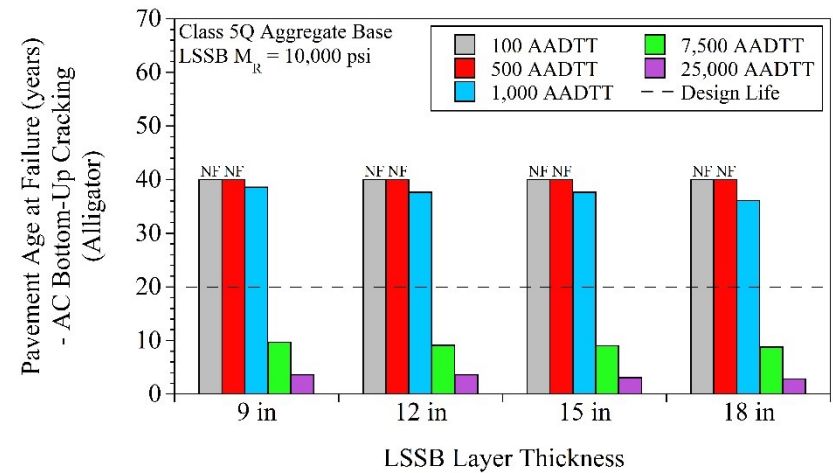
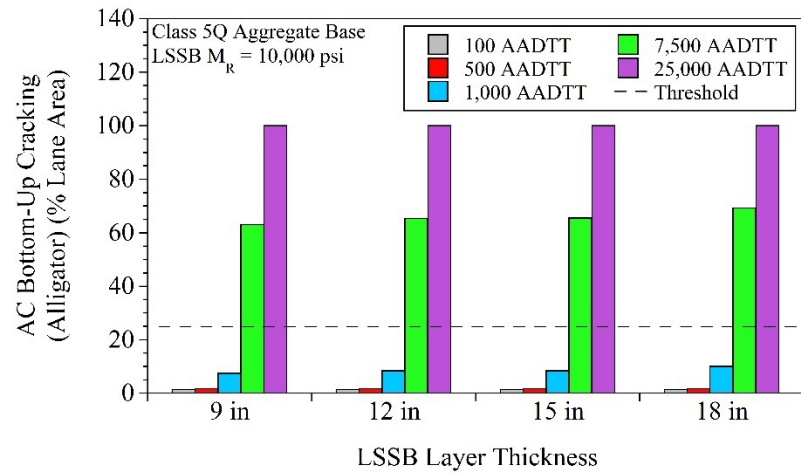
For pavements that contained Class 6 Aggregate and LSSB with $M_R = 50,000$ psi:



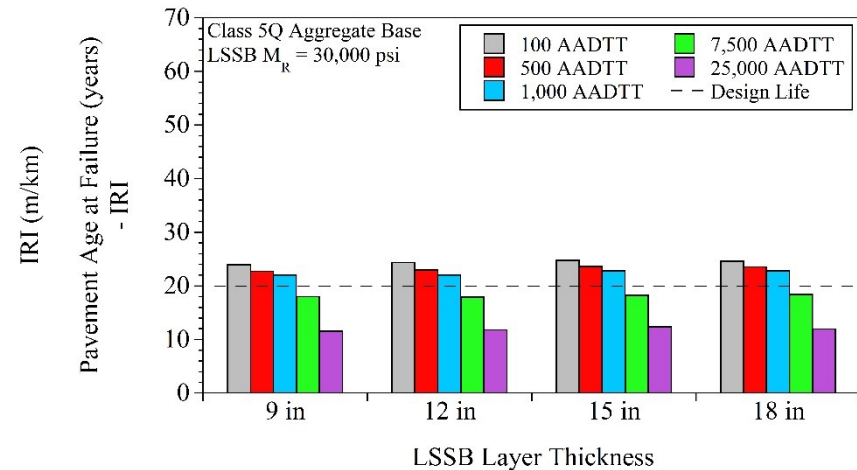
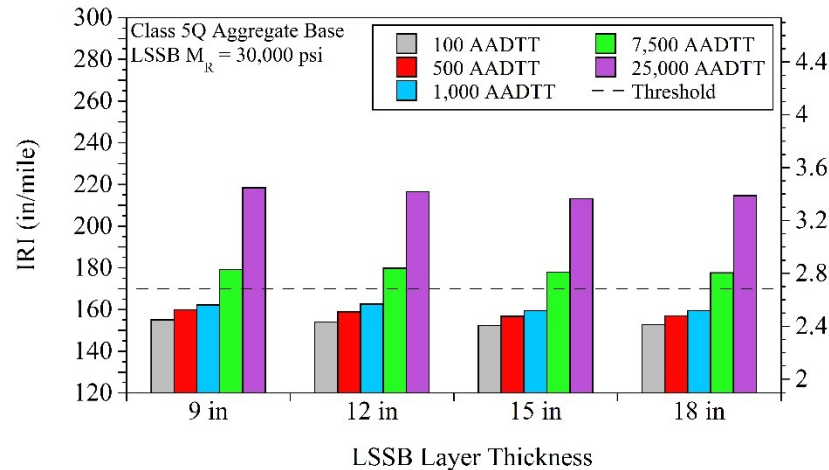


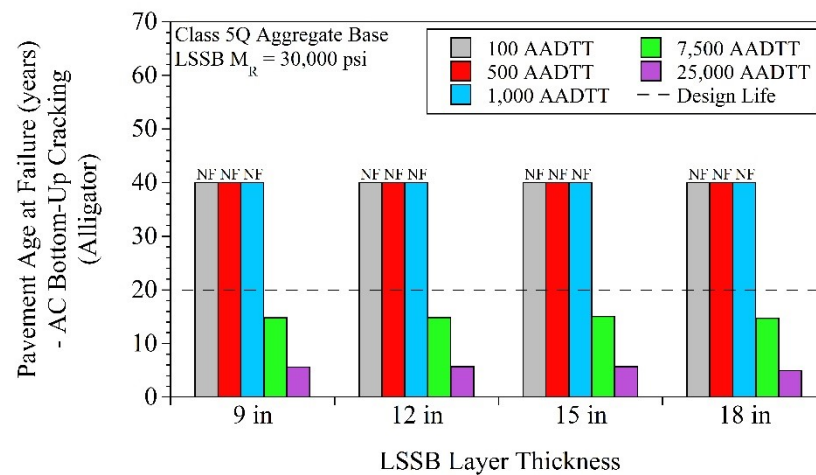
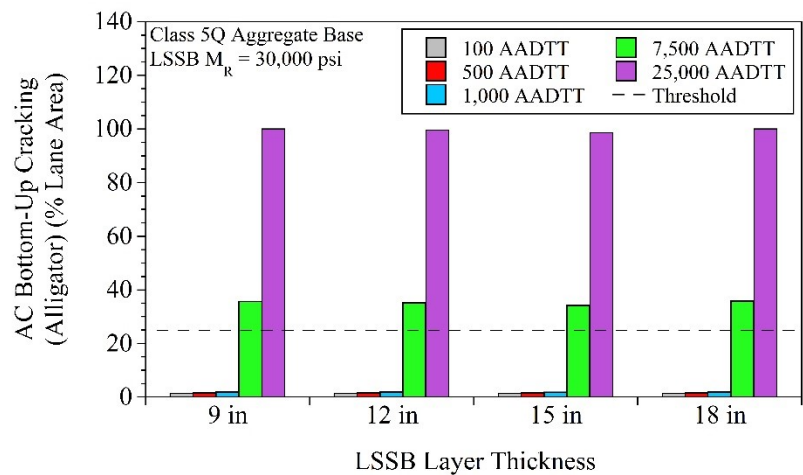
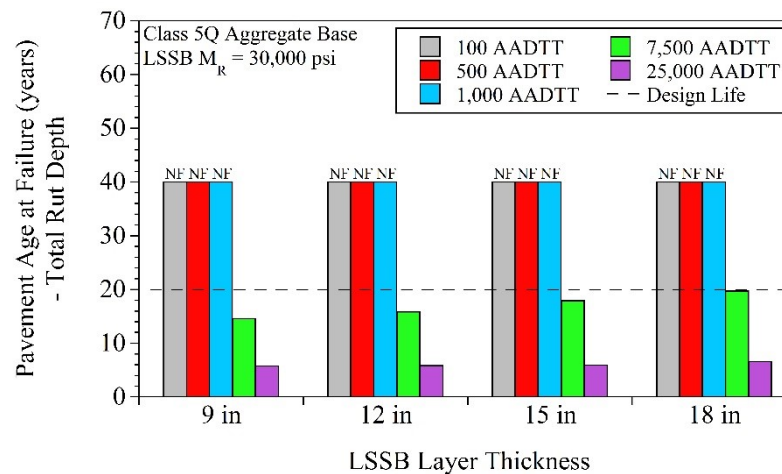
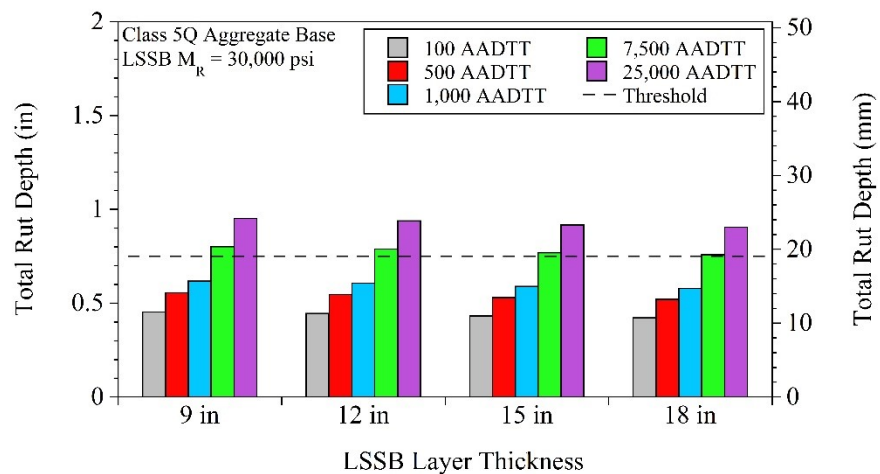
For pavements that contained Class 5Q Aggregate and LSSB with $M_R = 10,000$ psi:



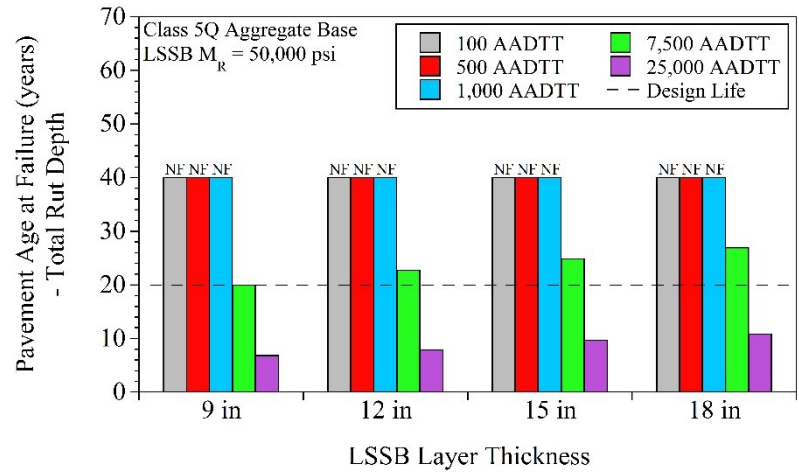
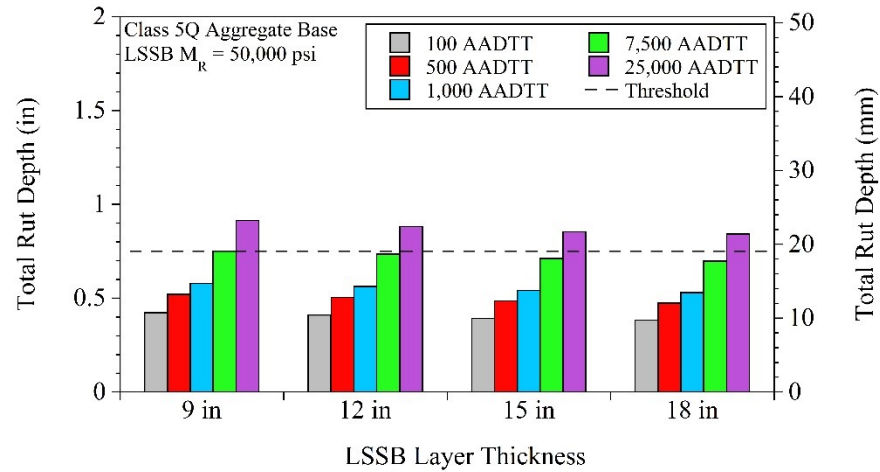
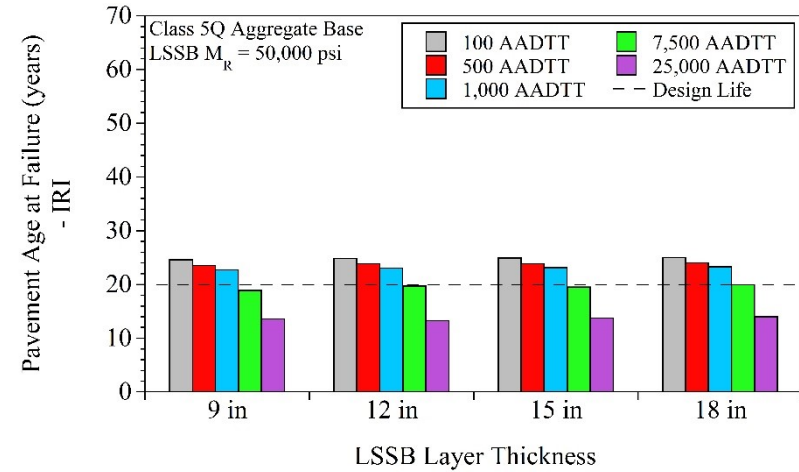
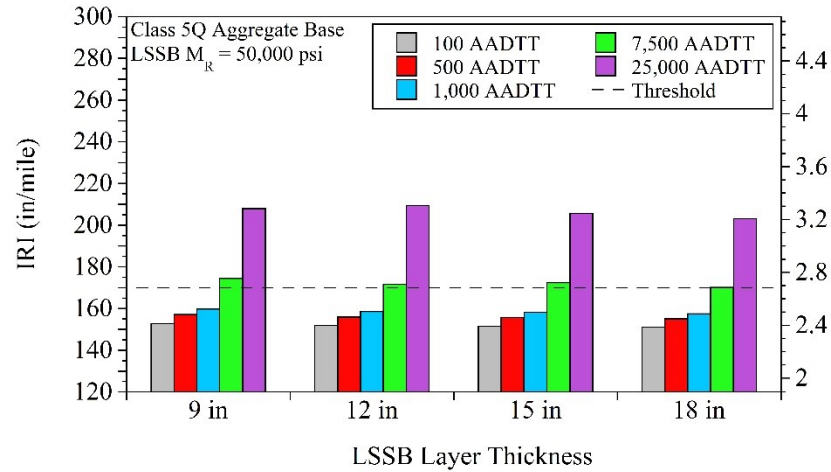


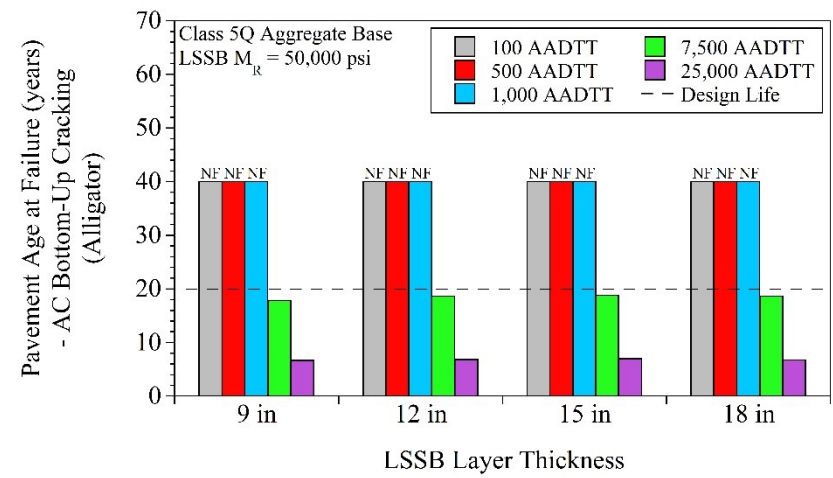
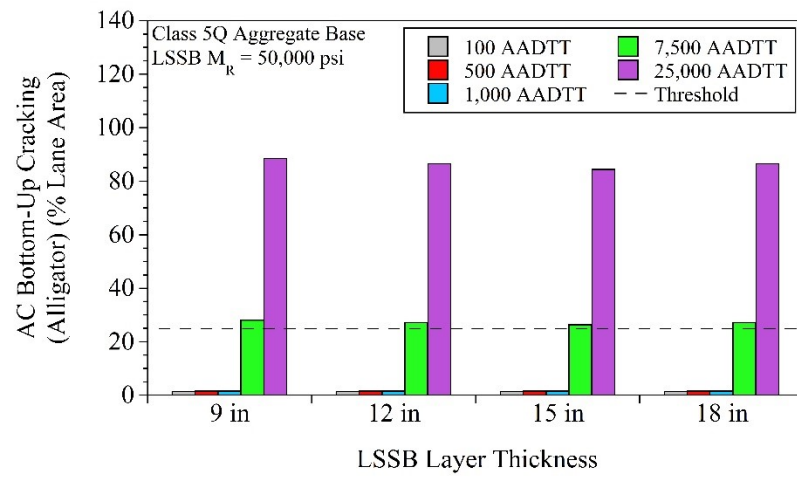
For pavements that contained Class 5Q Aggregate and LSSB with $M_R = 30,000$ psi:





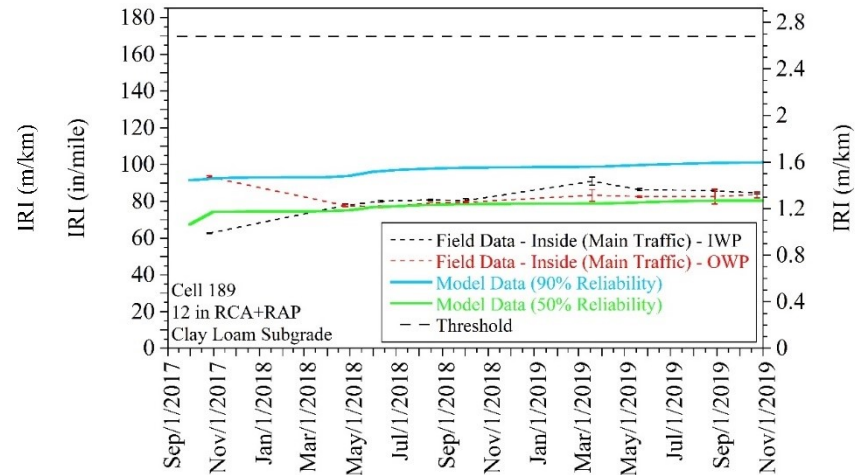
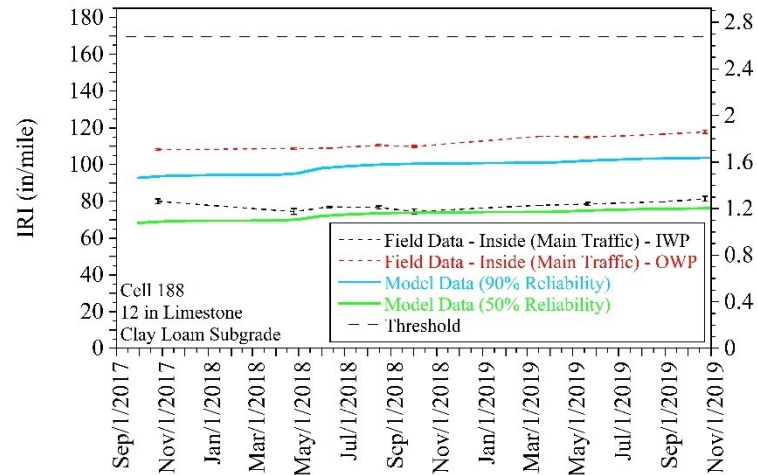
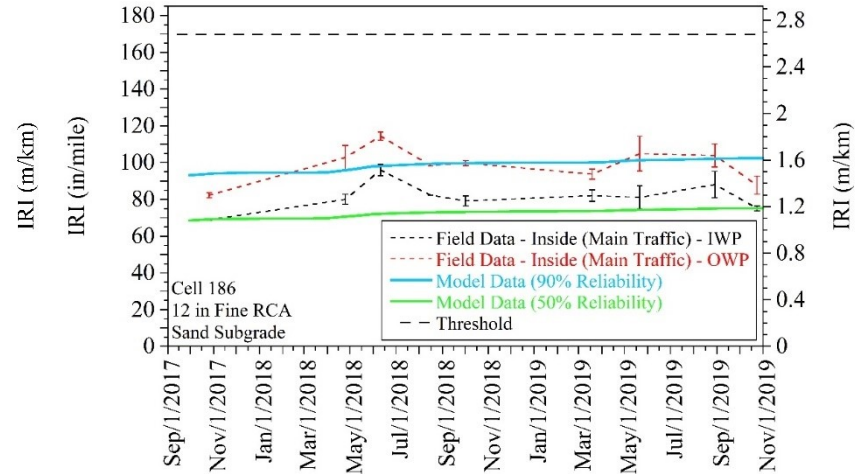
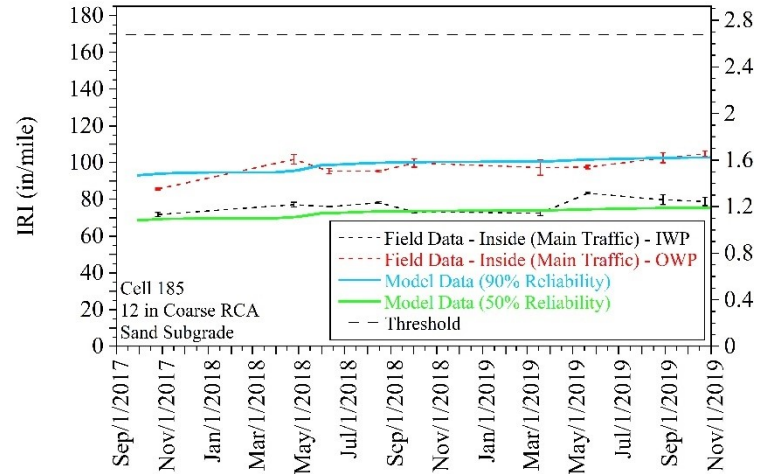
For pavements that contained Class 5Q Aggregate and LSSB with $M_R = 50,000$ psi:

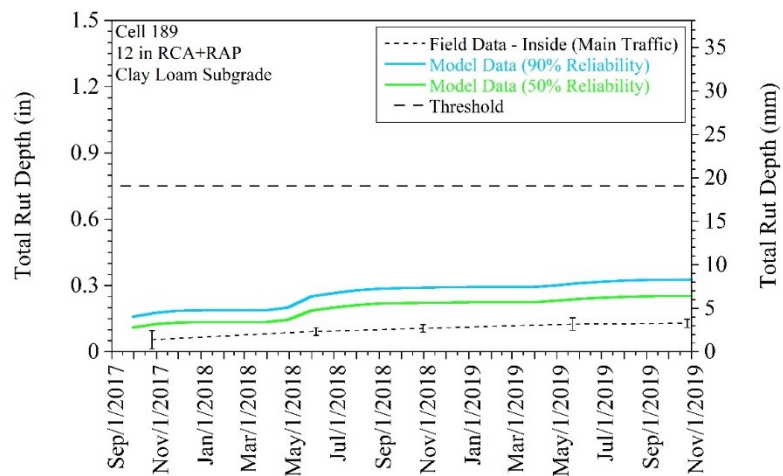
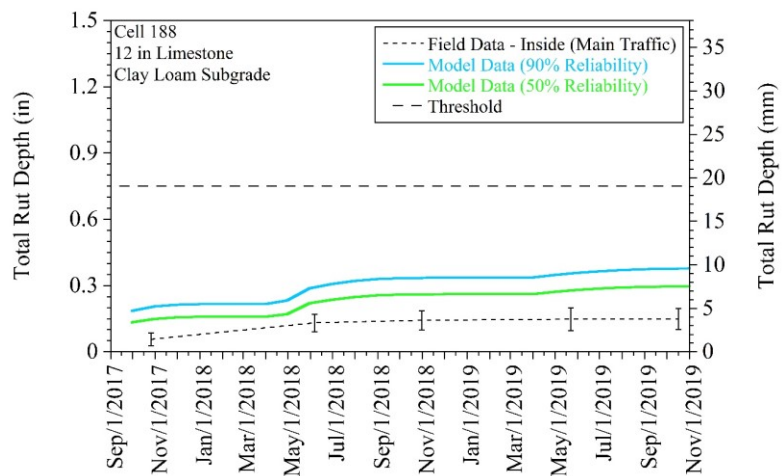
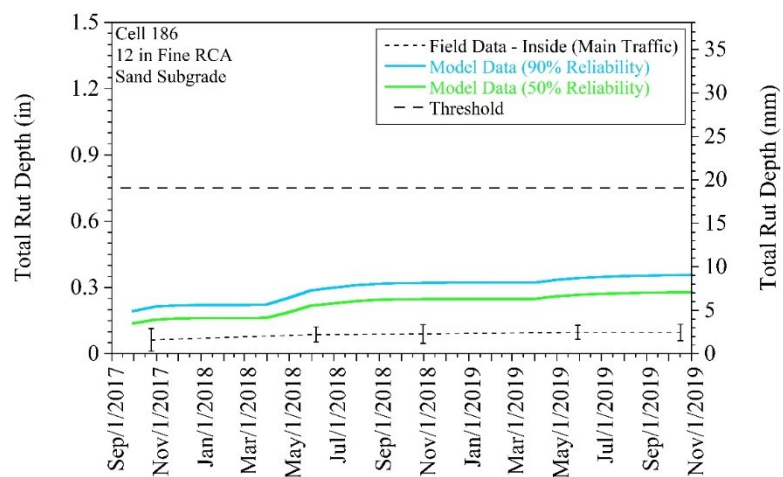
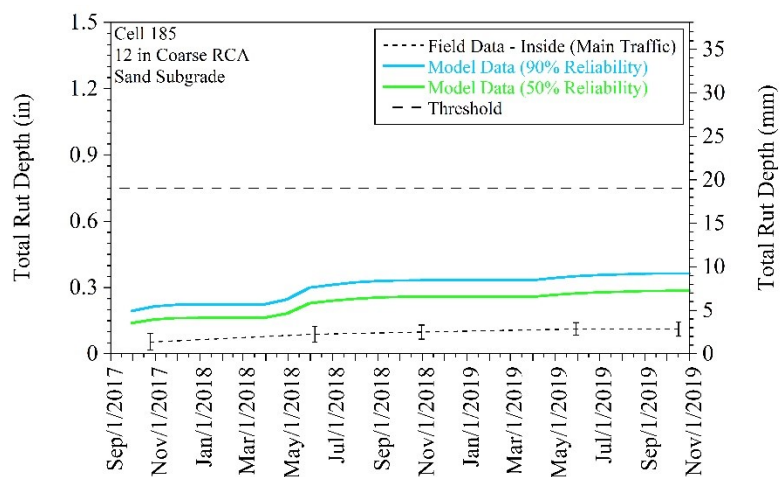


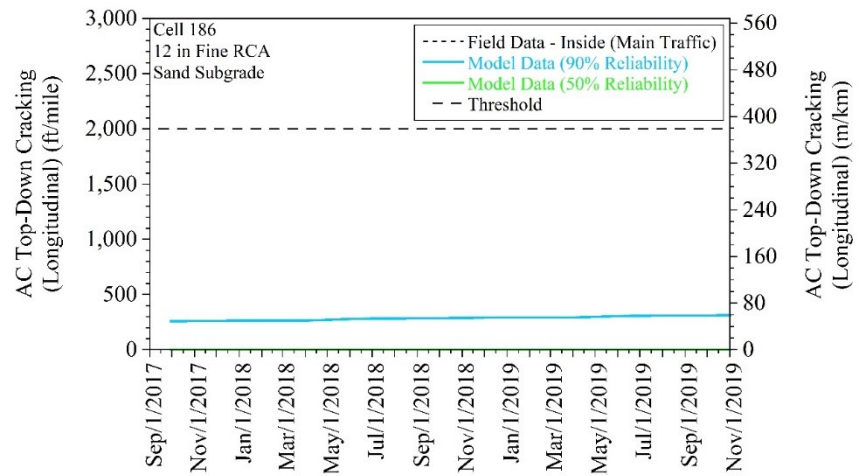
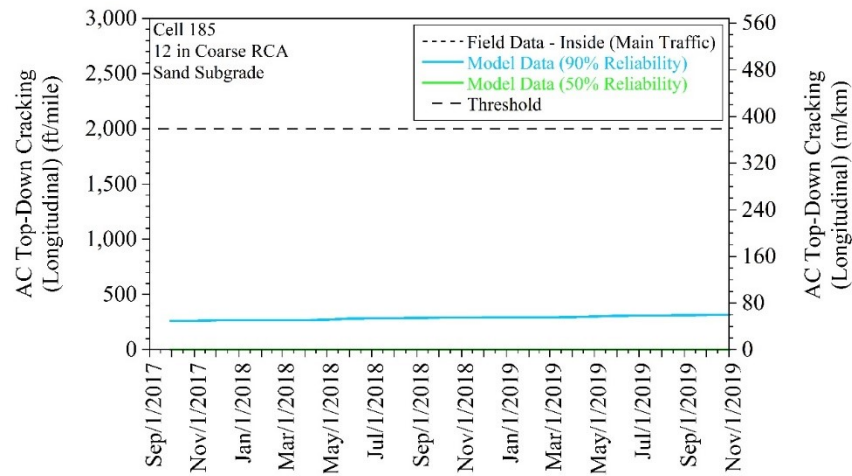


APPENDIX BL
COMPARISON BETWEEN FIELD DATA AND PAVEMENT ME
MODELS

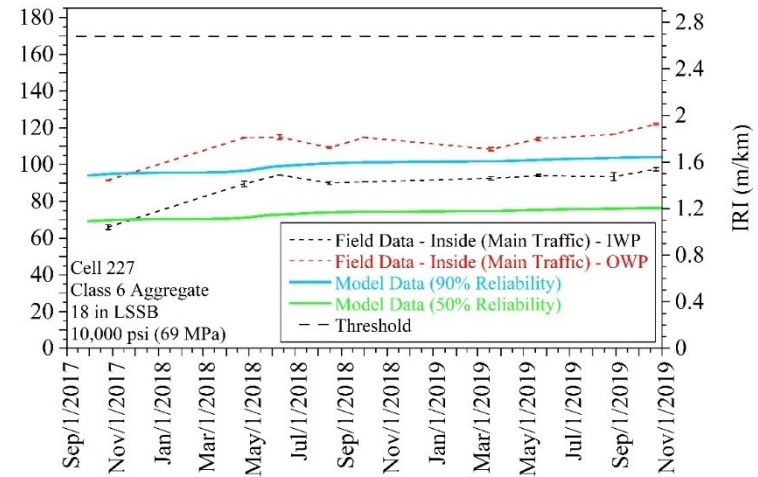
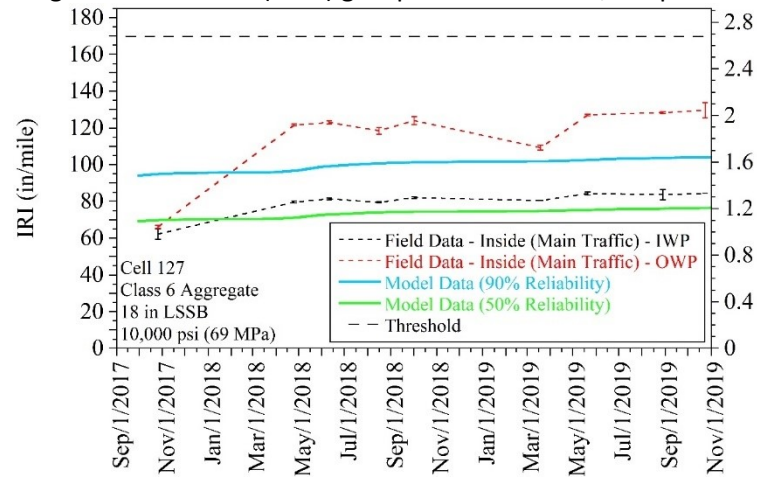
Recycled aggregate base (RAB) group:

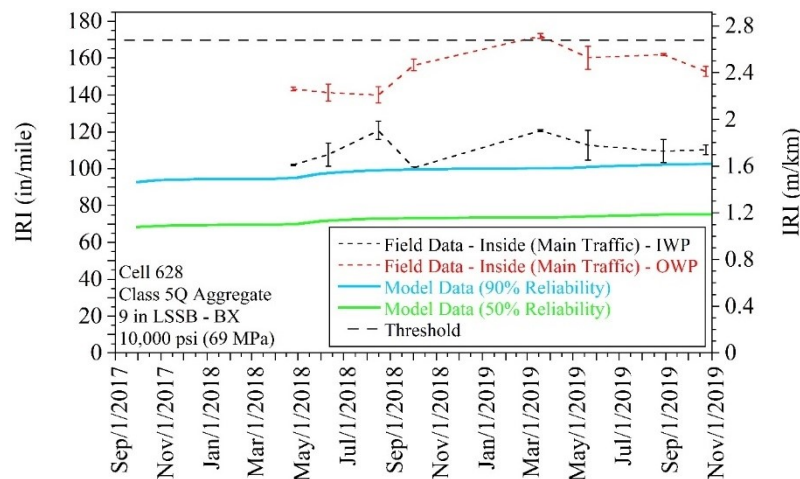
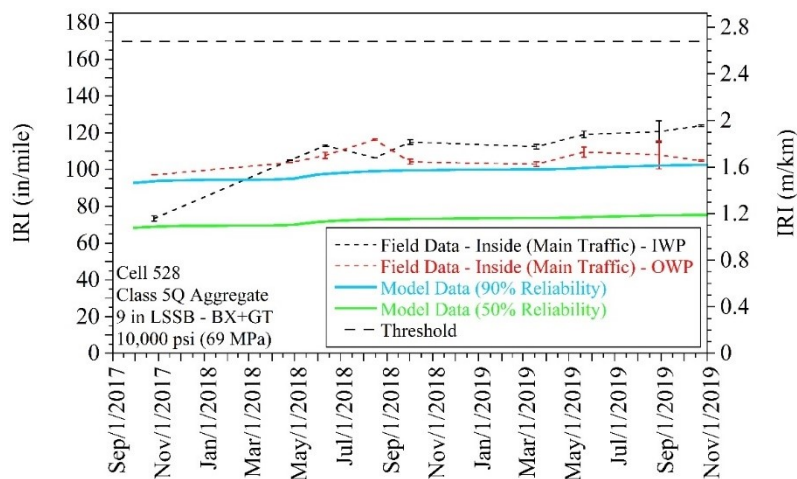
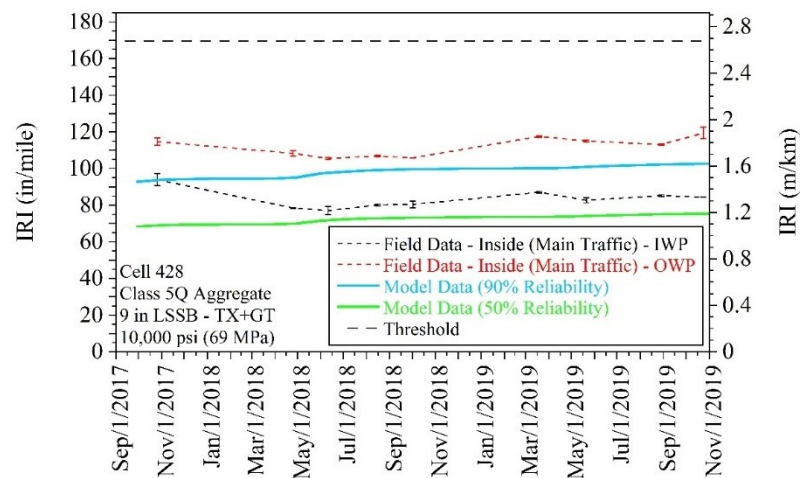
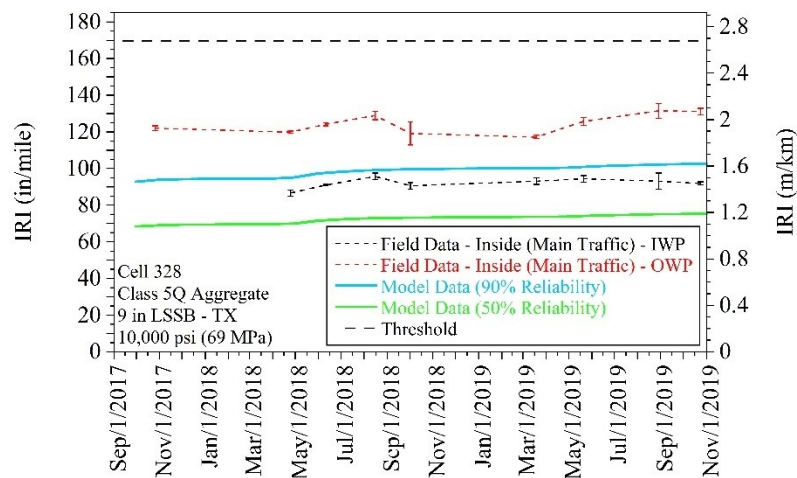


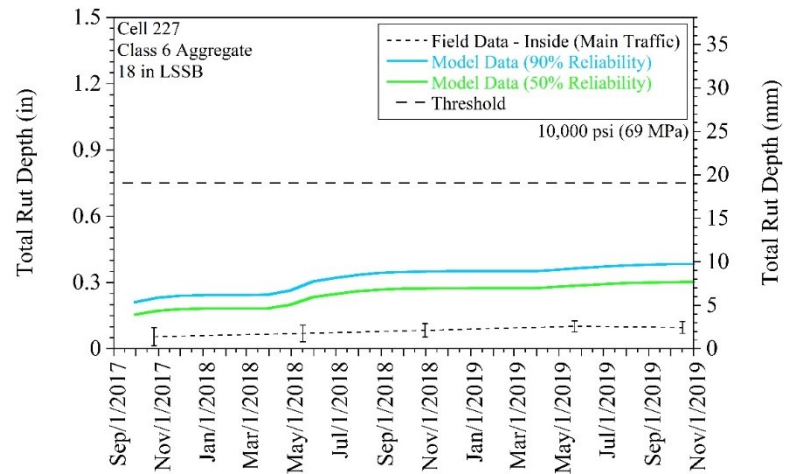
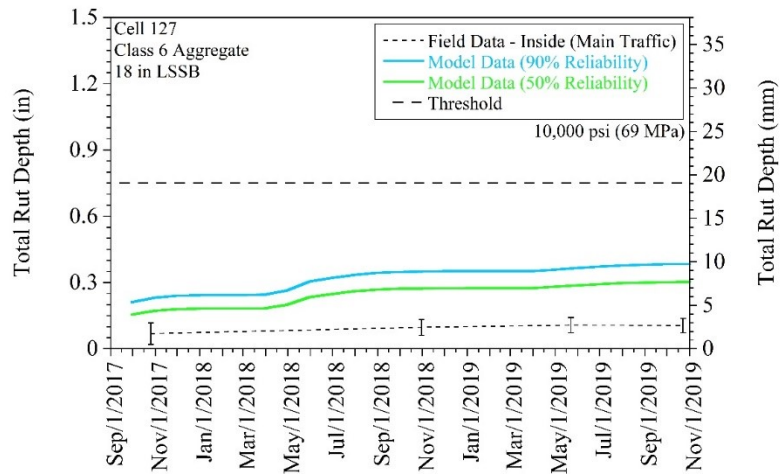
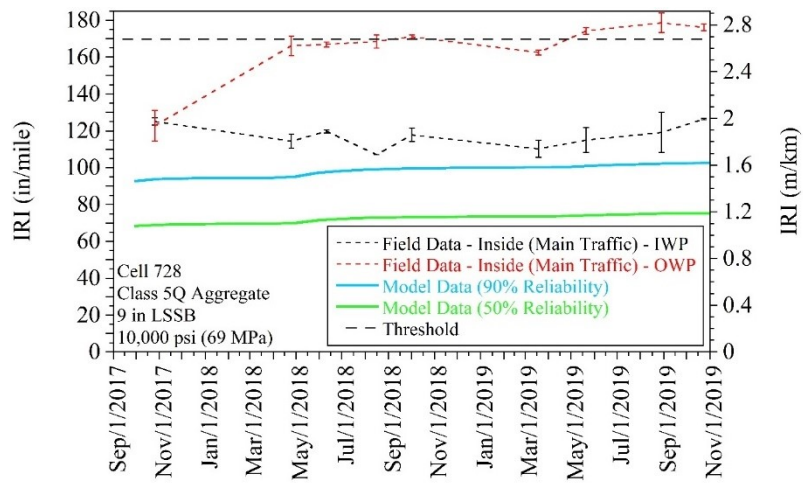


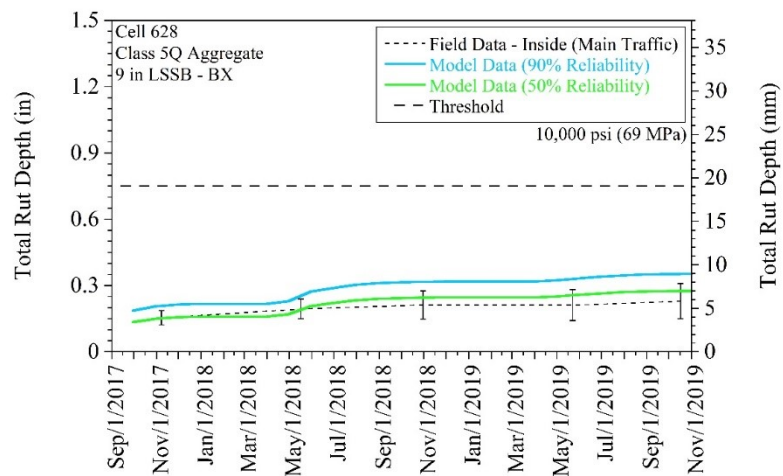
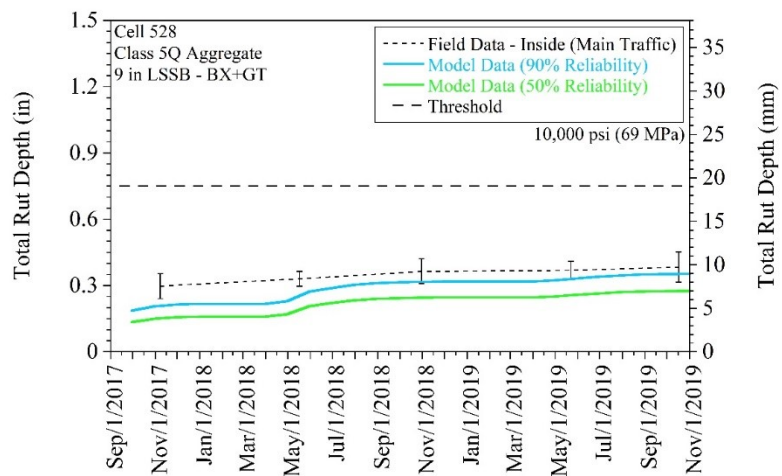
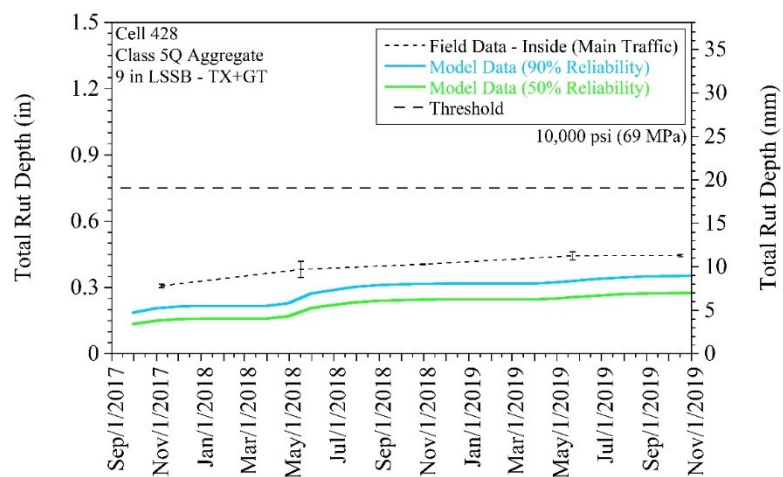
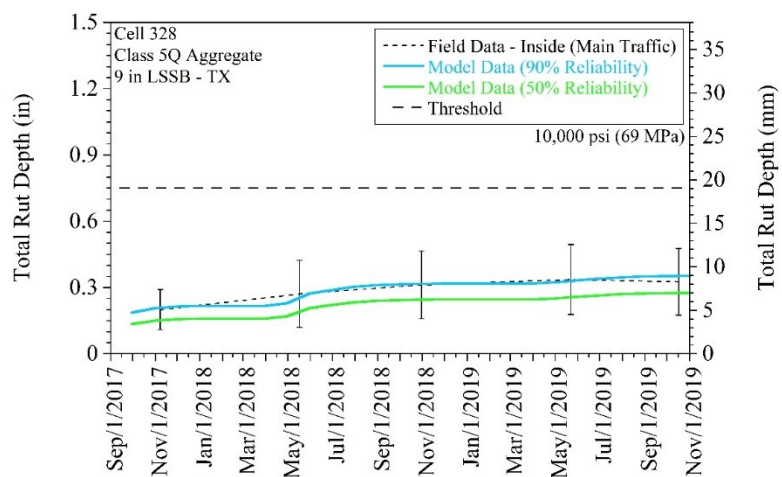


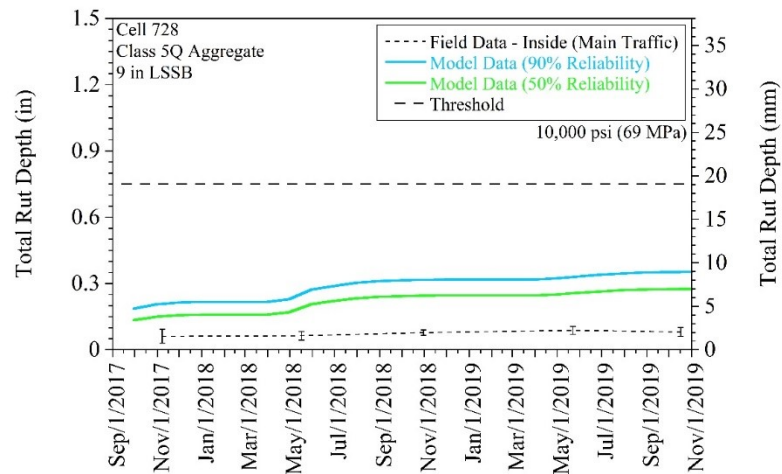
Large stone subbase (LSSB) groups - LSSB $M_R = 10,000$ psi:



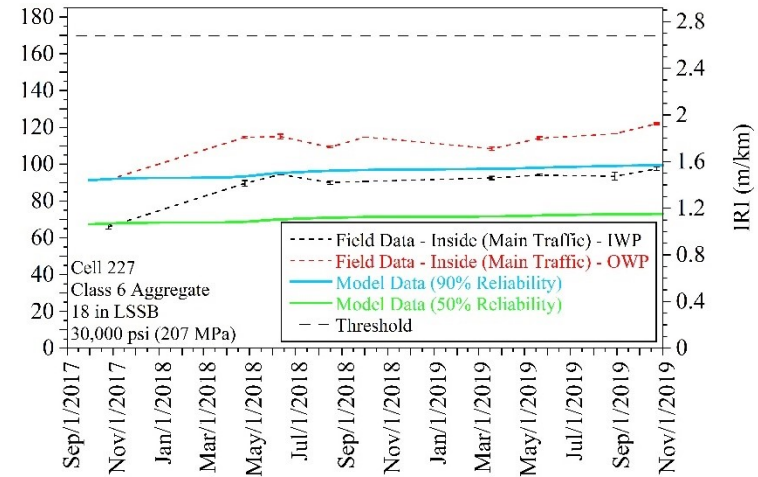
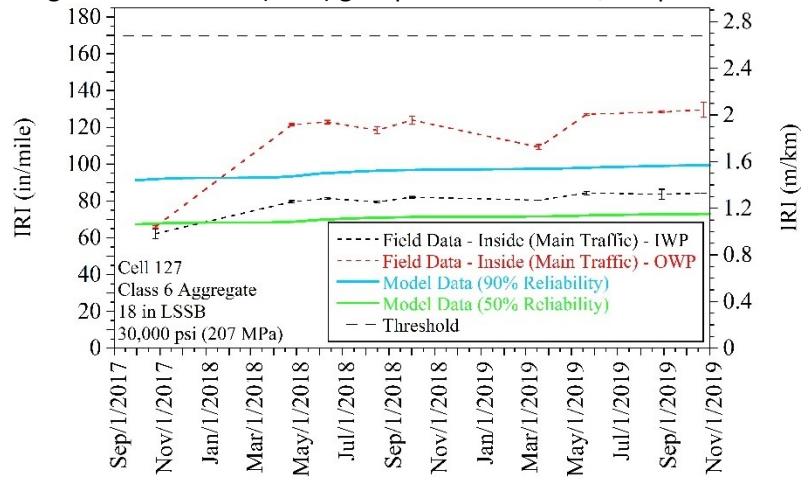


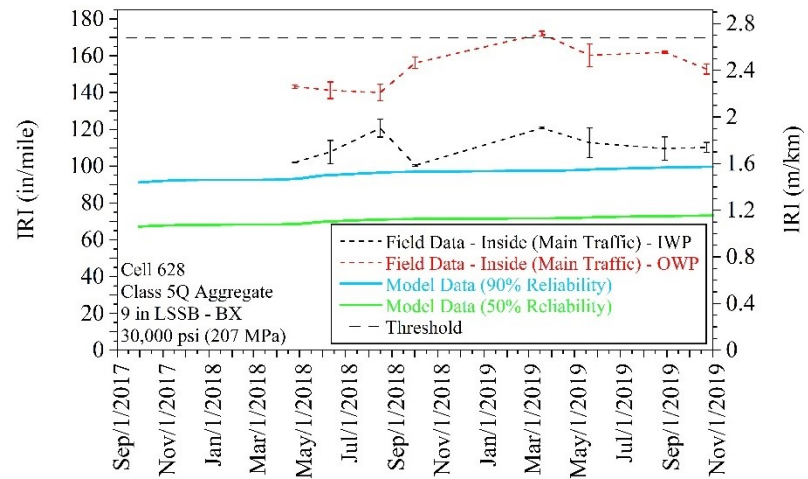
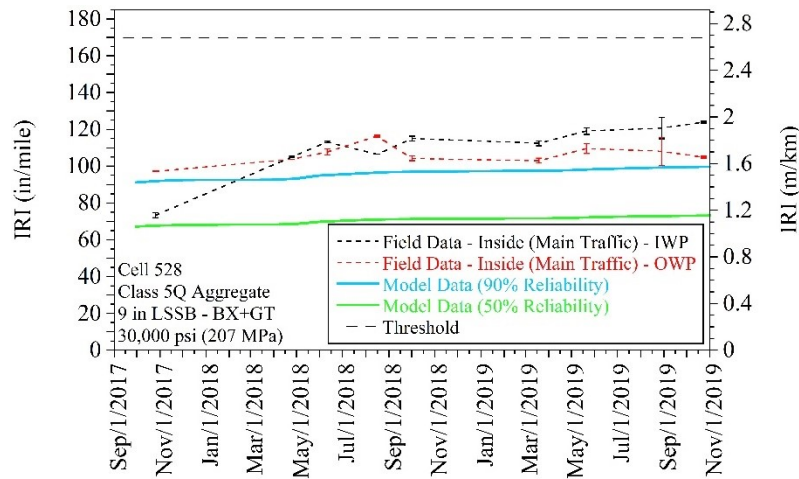
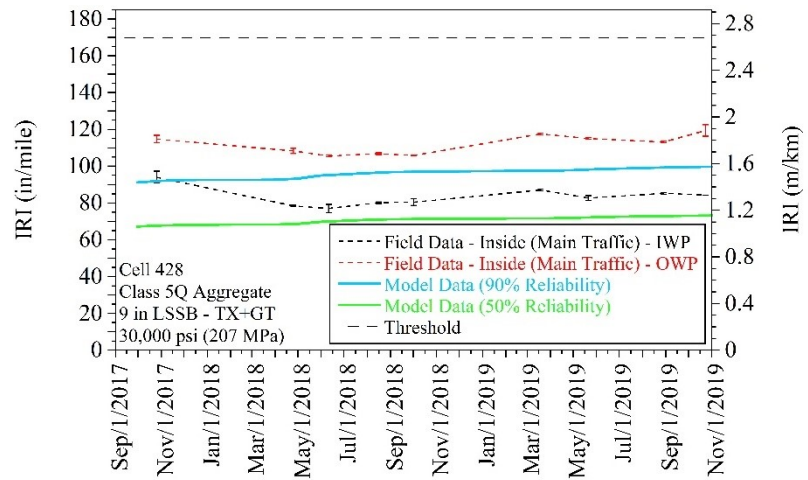
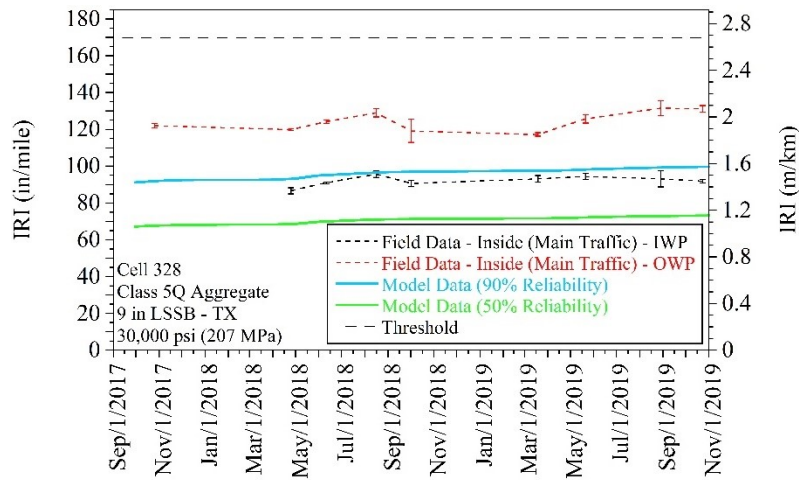


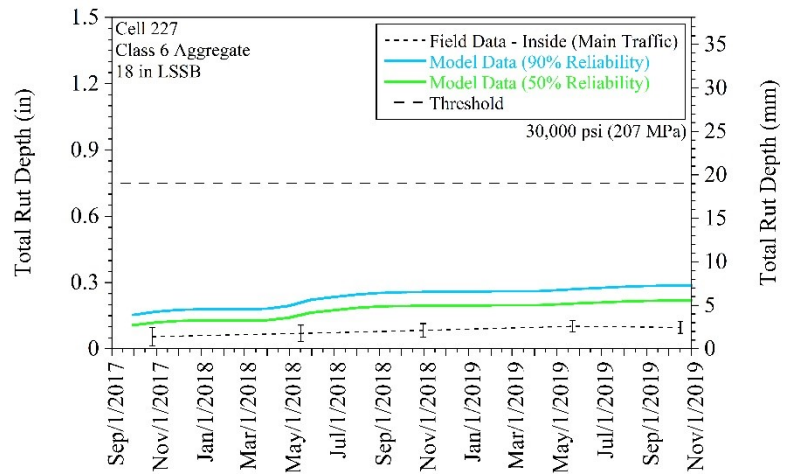
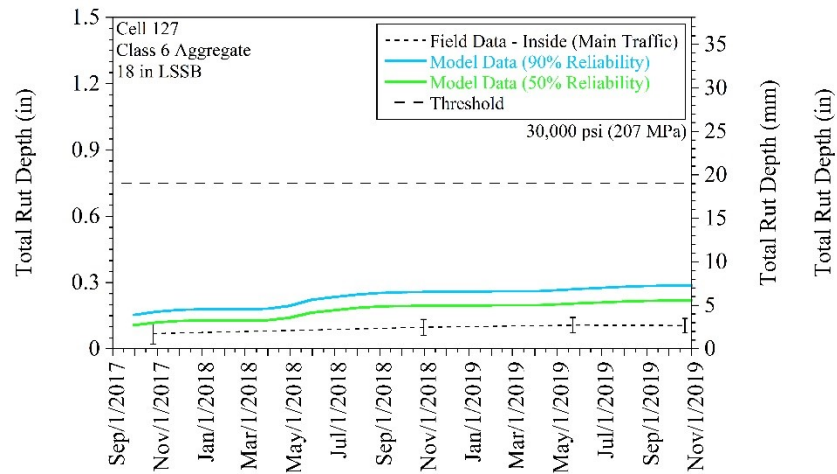
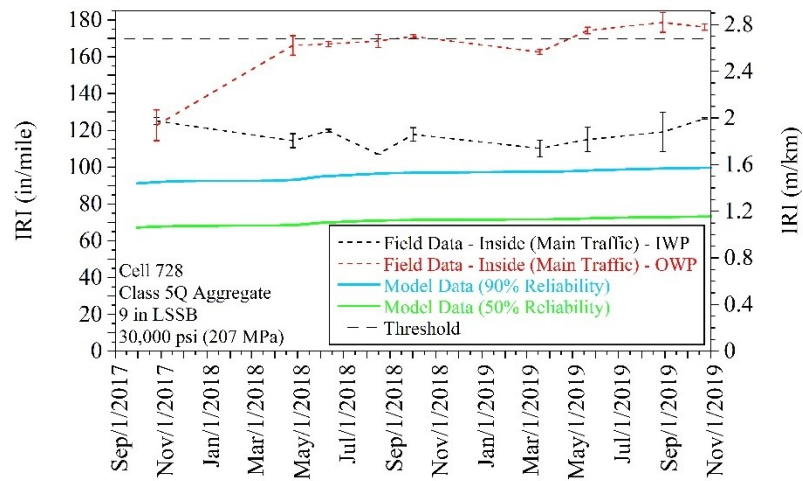


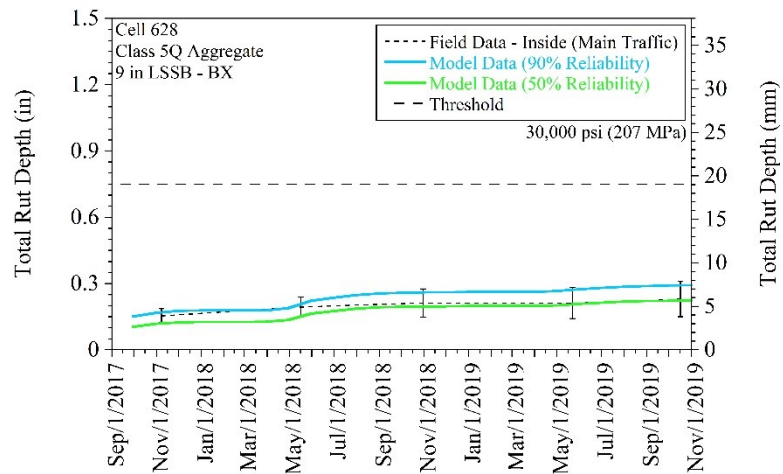
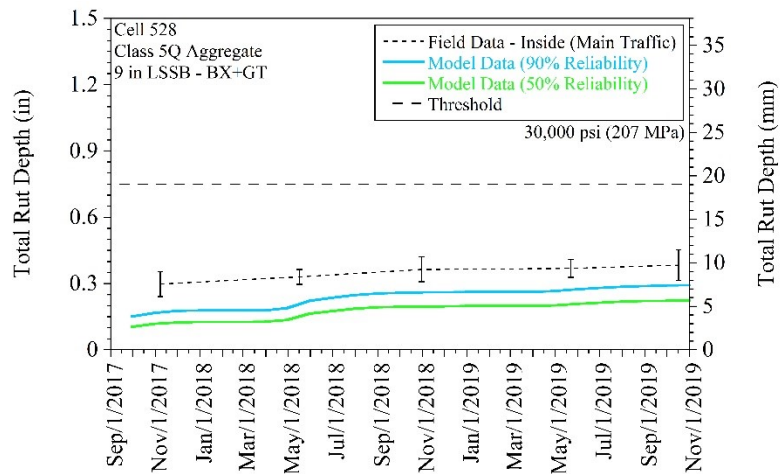
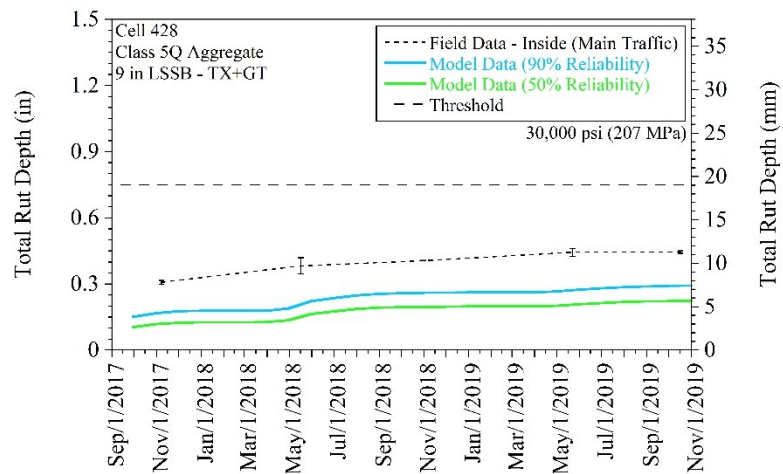
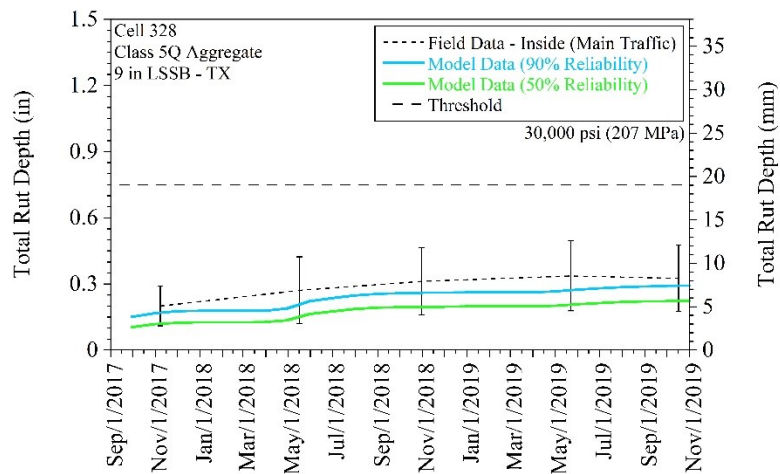


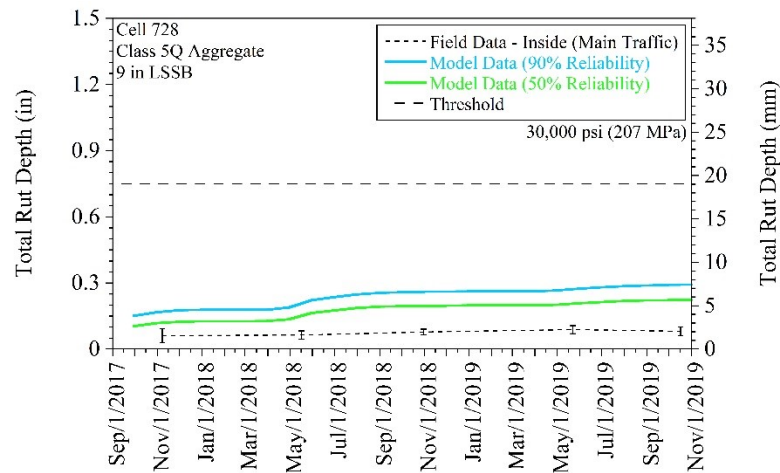
Large stone subbase (LSSB) groups - LSSB M_R = 30,000 psi:



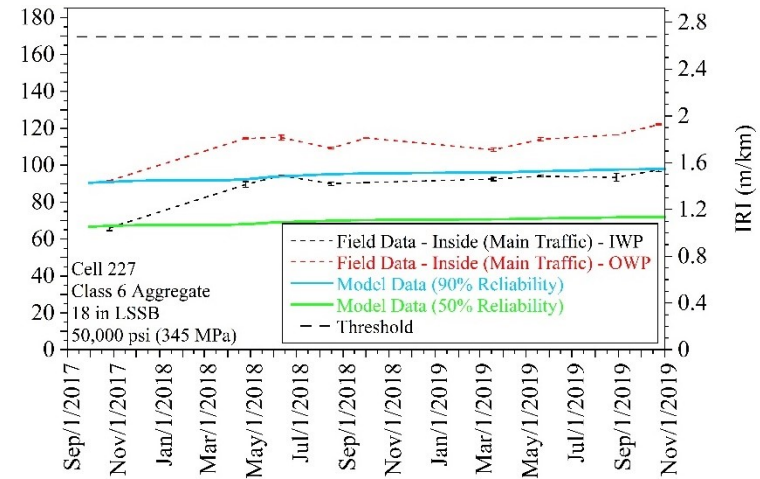
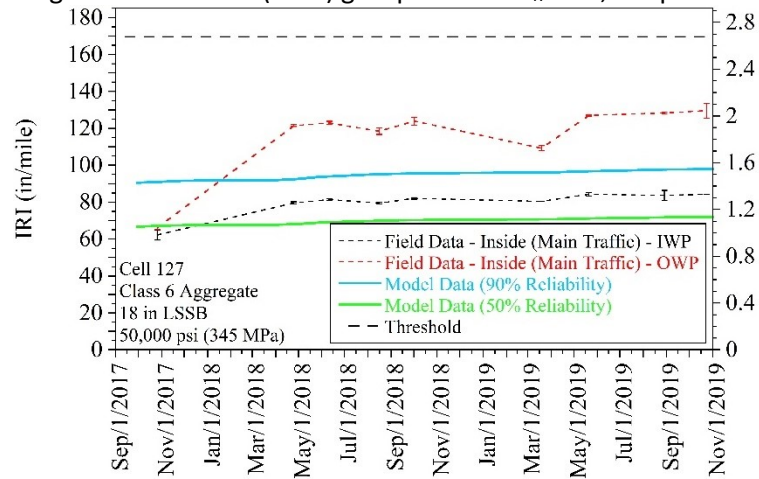


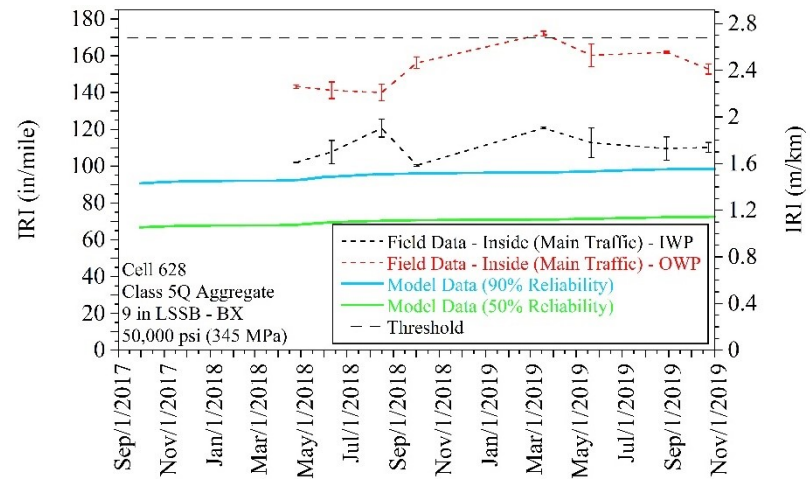
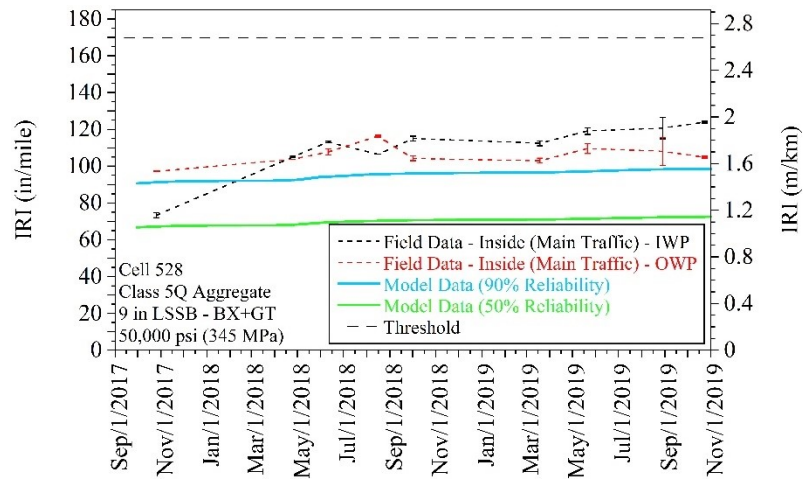
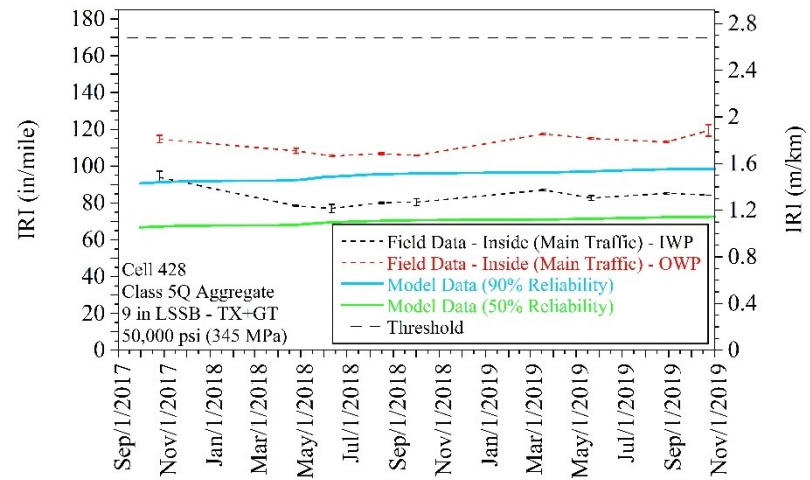
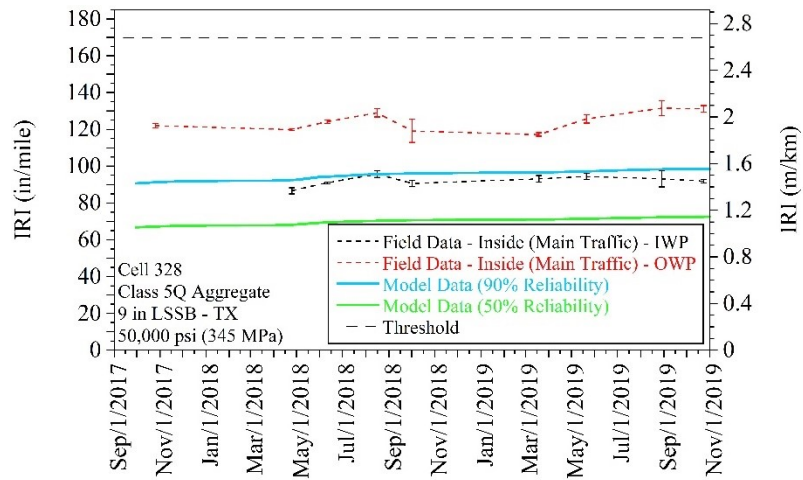


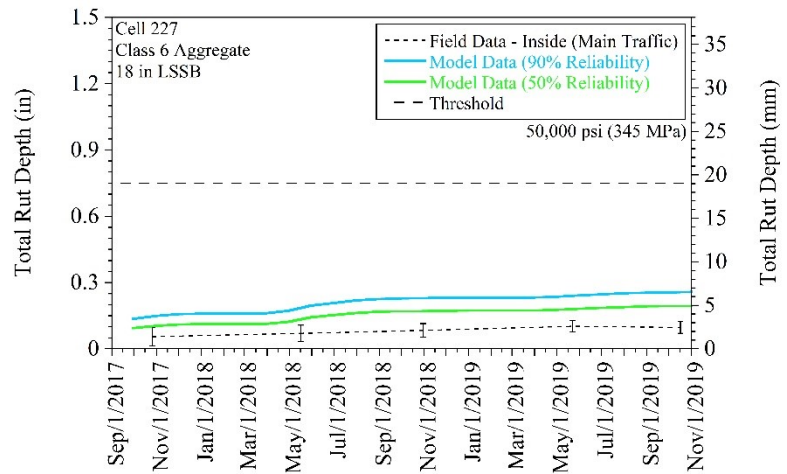
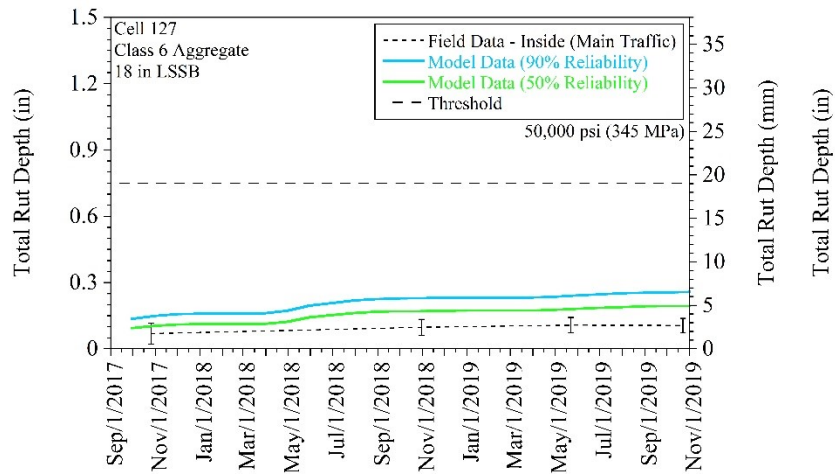
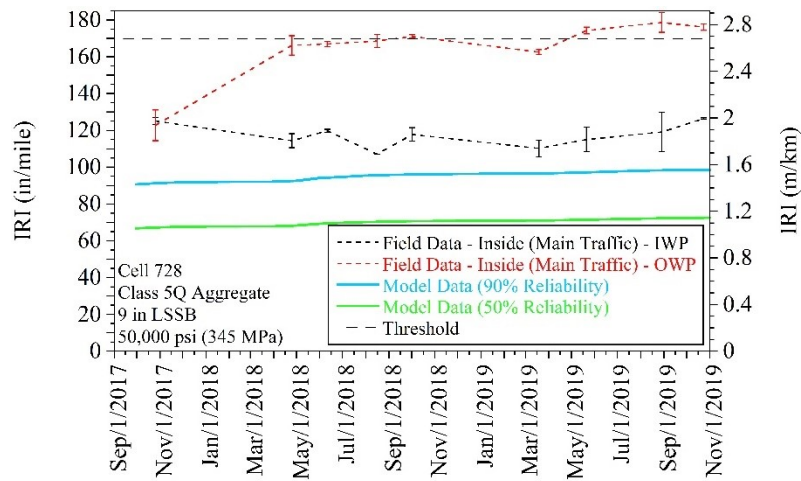


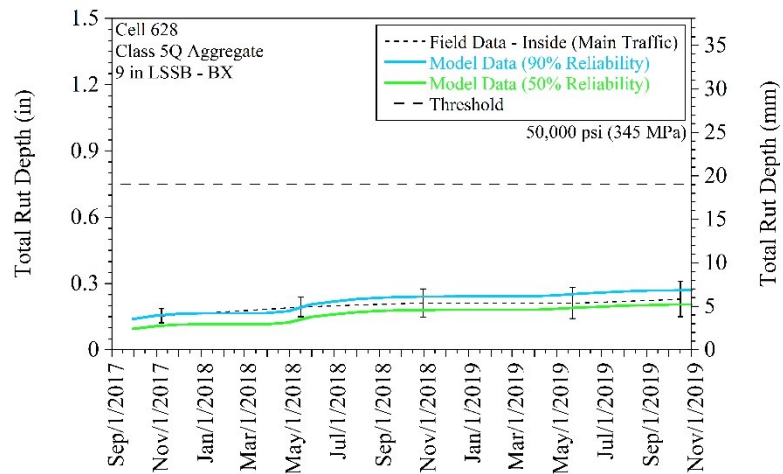
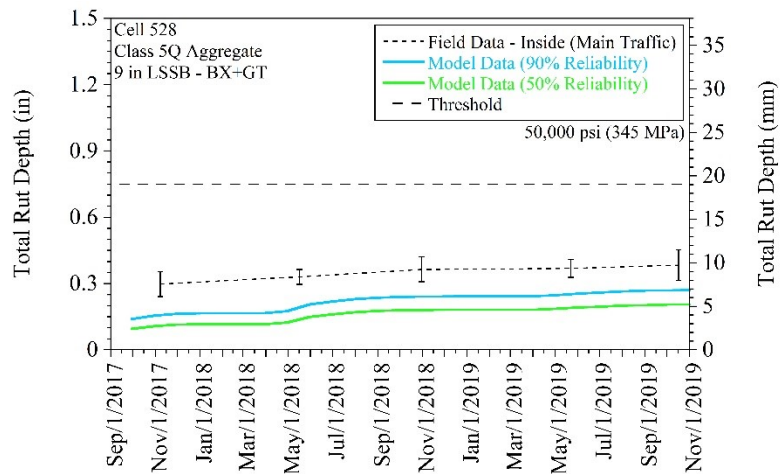
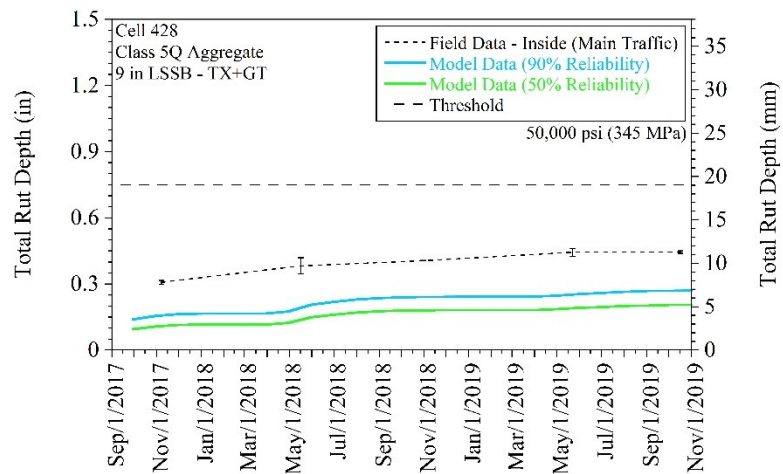
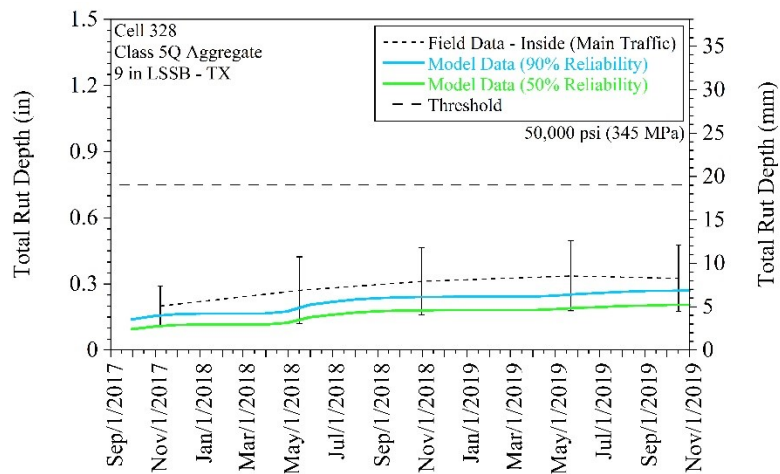


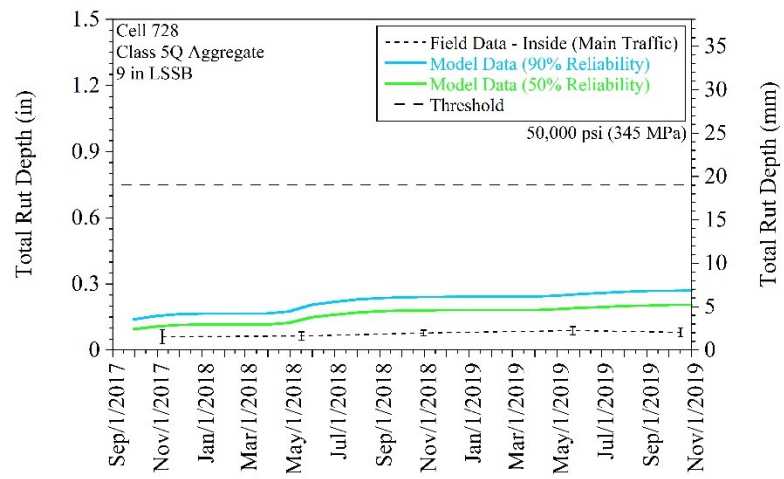
Large stone subbase (LSSB) groups - LSSB $M_R = 50,000$ psi:











APPENDIX BM

ASPHALT CONCRETE (AC) OVER AC OVERLAY DESIGNS

For Cell 185 (overlay asphalt binder = Superpave PG 58-34):

Design Inputs

Design Life: 40 years	Existing construction: August, 2017	Climate Data: 45.5, -93.75
Design Type: ACC_ACC	Pavement construction: September, 2018	Sources: 45, -93.75
	Traffic opening: September, 2018	45.5, -93.125
		45, -93.125
		45.5, -94.375
		45, -94.375

Design Structure

Layer type	Material Type	Thickness (in)
Flexible (OL)	Default asphalt concrete	4.0
Flexible (existing)	Default asphalt concrete	2.5
NonStabilized	A-1-a	12.0
NonStabilized	A-1-b	3.5
Subgrade	A-1-b	Semi-infinite

Volumetric at Construction:	
Effective binder content (%)	11.6
Air voids (%)	7.0

Traffic

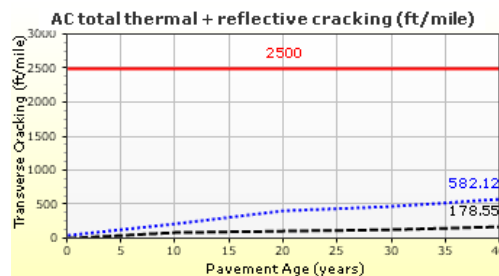
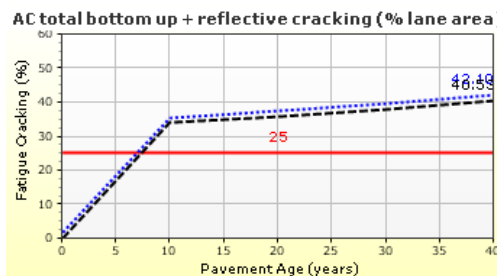
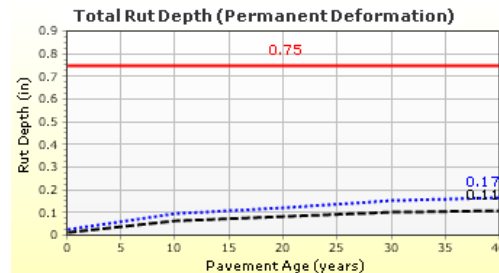
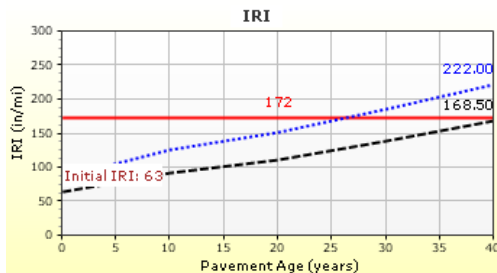
Age (year)	Heavy Trucks (cumulative)
2018 (initial)	1,000
2038 (20 years)	3,520,100
2058 (40 years)	8,683,820

Design Outputs

Distress Prediction Summary

Distress Type	Distress @ Specified Reliability		Reliability (%)		Criterion Satisfied?
	Target	Predicted	Target	Achieved	
Terminal IRI (in/mile)	172.00	222.01	90.00	53.33	Fail
Permanent deformation - total pavement (in)	0.75	0.17	90.00	100.00	Pass
AC total fatigue cracking: bottom up + reflective (% lane area)	25.00	42.10	90.00	0.00	Fail
AC total transverse cracking: thermal + reflective (ft/mile)	2500.00	582.12	90.00	100.00	Pass
Permanent deformation - AC only (in)	0.25	0.16	90.00	99.96	Pass
AC bottom-up fatigue cracking (% lane area)	25.00	0.00	50.00	100.00	Pass
AC thermal cracking (ft/mile)	1000.00	103.59	50.00	100.00	Pass
AC top-down fatigue cracking (ft/mile)	2000.00	4257.96	90.00	60.88	Fail

Distress Charts



HMA Rehabilitation (Input Level: 3)

Milled thickness (in)	1.00
Structural rating	Fair
Environmental rating	Good
Total rut depth (in)	0.70

For Cell 186 (overlay asphalt binder = Superpave PG 58-34):

Design Inputs

Design Life: 40 years
Design Type: ACC_ACC

Existing construction: August, 2017
Pavement construction: September, 2018
Traffic opening: September, 2018

Climate Data 45.5, -93.75
Sources 45, -93.75
45.5, -93.125
45, -93.125
45.5, -94.375
45, -94.375

Design Structure

Layer type	Material Type	Thickness (in)
Flexible (OL)	Default asphalt concrete	4.0
Flexible (existing)	Default asphalt concrete	2.5
NonStabilized	A-1-a	12.0
NonStabilized	A-1-b	3.5
Subgrade	A-1-b	Semi-infinite

Volumetric at Construction:	
Effective binder content (%)	11.6
Air voids (%)	7.0

Traffic

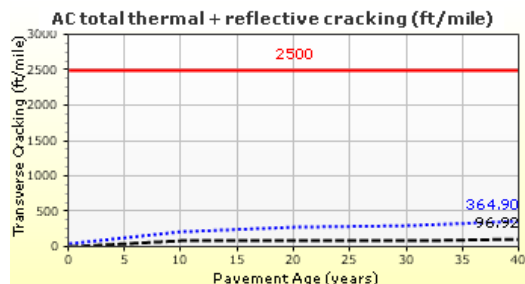
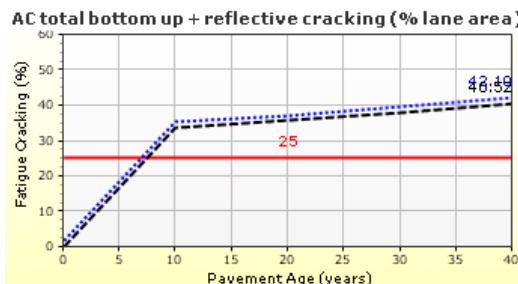
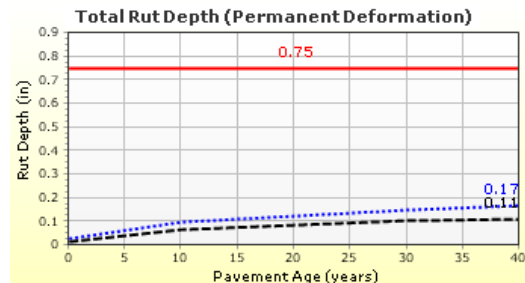
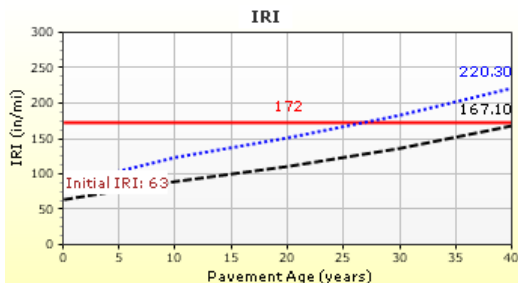
Age (year)	Heavy Trucks (cumulative)
2018 (initial)	1,000
2038 (20 years)	3,520,100
2058 (40 years)	8,683,820

Design Outputs

Distress Prediction Summary

Distress Type	Distress @ Specified Reliability		Reliability (%)		Criterion Satisfied?
	Target	Predicted	Target	Achieved	
Terminal IRI (in/mile)	172.00	220.28	90.00	54.71	Fail
Permanent deformation - total pavement (in)	0.75	0.17	90.00	100.00	Pass
AC total fatigue cracking: bottom up + reflective (% lane area)	25.00	42.10	90.00	0.00	Fail
AC total transverse cracking: thermal + reflective (ft/mile)	2500.00	364.90	90.00	100.00	Pass
Permanent deformation - AC only (in)	0.25	0.16	90.00	99.96	Pass
AC bottom-up fatigue cracking (% lane area)	25.00	0.00	50.00	100.00	Pass
AC thermal cracking (ft/mile)	1000.00	21.96	50.00	100.00	Pass
AC top-down fatigue cracking (ft/mile)	2000.00	2646.38	90.00	82.52	Fail

Distress Charts



— Threshold Value @ Specified Reliability --- @ 50% Reliability

HMA Rehabilitation (Input Level: 3)

Milled thickness (in)	1.00
Structural rating	Fair
Environmental rating	Good
Total rut depth (in)	0.70

For Cell 188 (overlay asphalt binder = Superpave PG 58-34):

Design Inputs

Design Life: 40 years
Design Type: ACC_ACC

Existing construction: August, 2017
Pavement construction: September, 2018
Traffic opening: September, 2018

Climate Data 45.5, -93.75
Sources 45, -93.75
45.5, -93.125
45, -93.125
45.5, -94.375
45, -94.375

Design Structure

Layer type	Material Type	Thickness (in)
Flexible (OL)	Default asphalt concrete	4.0
Flexible (existing)	Default asphalt concrete	2.5
NonStabilized	A-1-a	12.0
NonStabilized	A-1-b	3.5
Subgrade	A-6	Semi-infinite

Volumetric at Construction:	
Effective binder content (%)	11.6
Air voids (%)	7.0

Traffic

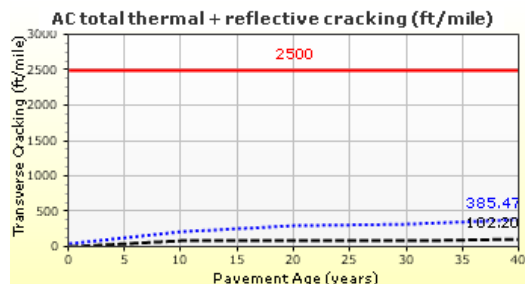
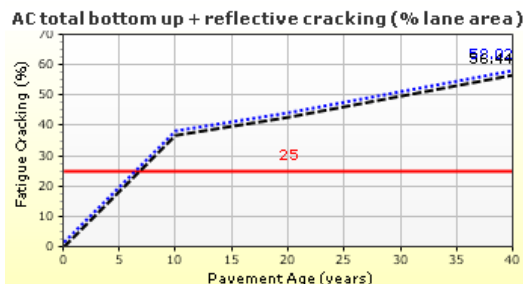
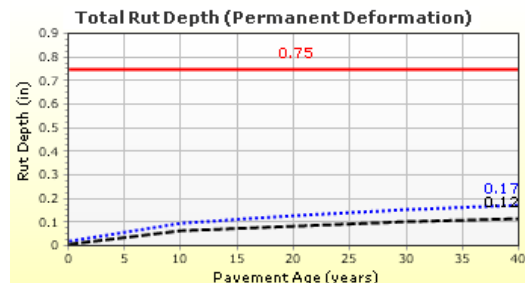
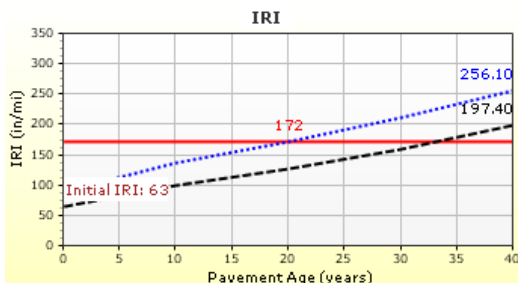
Age (year)	Heavy Trucks (cumulative)
2018 (initial)	1,000
2038 (20 years)	3,520,100
2058 (40 years)	8,683,820

Design Outputs

Distress Prediction Summary

Distress Type	Distress @ Specified Reliability		Reliability (%)		Criterion Satisfied?
	Target	Predicted	Target	Achieved	
Terminal IRI (in/mile)	172.00	256.08	90.00	28.97	Fail
Permanent deformation - total pavement (in)	0.75	0.17	90.00	100.00	Pass
AC total fatigue cracking: bottom up + reflective (% lane area)	25.00	58.02	90.00	0.00	Fail
AC total transverse cracking: thermal + reflective (ft/mile)	2500.00	385.47	90.00	100.00	Pass
Permanent deformation - AC only (in)	0.25	0.15	90.00	100.00	Pass
AC bottom-up fatigue cracking (% lane area)	25.00	0.00	50.00	100.00	Pass
AC thermal cracking (ft/mile)	1000.00	27.24	50.00	100.00	Pass
AC top-down fatigue cracking (ft/mile)	2000.00	13803.87	90.00	0.03	Fail

Distress Charts



— Threshold Value @ Specified Reliability --- @ 50% Reliability

HMA Rehabilitation (Input Level: 3)

Milled thickness (in)	1.00
Structural rating	Fair
Environmental rating	Good
Total rut depth (in)	0.70

For Cell 189 (overlay asphalt binder = Superpave PG 58-34):

Design Inputs

Design Life: 40 years
Design Type: ACC_ACC

Existing construction: August, 2017
Pavement construction: September, 2018
Traffic opening: September, 2018

Climate Data 45.5, -93.75
Sources 45, -93.75
45.5, -93.125
45, -93.125
45.5, -94.375
45, -94.375

Design Structure

Layer type	Material Type	Thickness (in)
Flexible (OL)	Default asphalt concrete	4.0
Flexible (existing)	Default asphalt concrete	2.5
NonStabilized	A-1-a	12.0
NonStabilized	A-1-b	3.5
Subgrade	A-6	Semi-infinite

Volumetric at Construction:	
Effective binder content (%)	11.6
Air voids (%)	7.0

Traffic

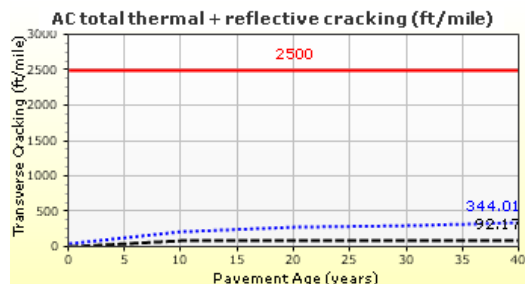
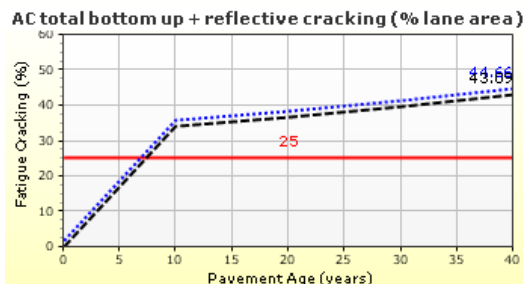
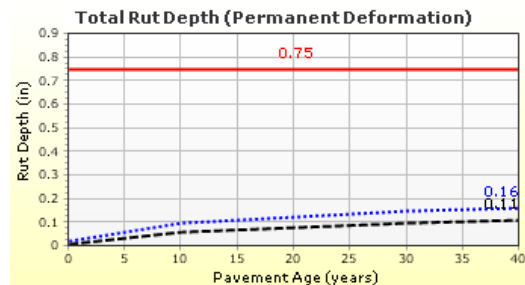
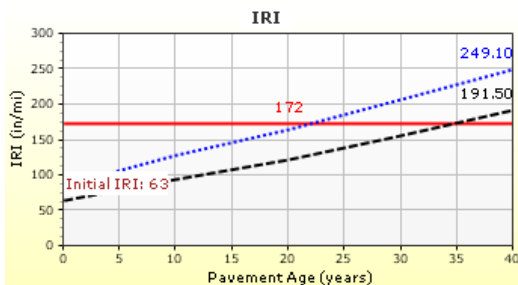
Age (year)	Heavy Trucks (cumulative)
2018 (initial)	1,000
2038 (20 years)	3,520,100
2058 (40 years)	8,683,820

Design Outputs

Distress Prediction Summary

Distress Type	Distress @ Specified Reliability		Reliability (%)		Criterion Satisfied?
	Target	Predicted	Target	Achieved	
Terminal IRI (in/mile)	172.00	249.07	90.00	33.17	Fail
Permanent deformation - total pavement (in)	0.75	0.16	90.00	100.00	Pass
AC total fatigue cracking: bottom up + reflective (% lane area)	25.00	44.66	90.00	0.00	Fail
AC total transverse cracking: thermal + reflective (ft/mile)	2500.00	344.01	90.00	100.00	Pass
Permanent deformation - AC only (in)	0.25	0.16	90.00	99.98	Pass
AC bottom-up fatigue cracking (% lane area)	25.00	0.00	50.00	100.00	Pass
AC thermal cracking (ft/mile)	1000.00	17.21	50.00	100.00	Pass
AC top-down fatigue cracking (ft/mile)	2000.00	13803.16	90.00	0.03	Fail

Distress Charts



— Threshold Value @ Specified Reliability --- @ 50% Reliability

HMA Rehabilitation (Input Level: 3)

Milled thickness (in)	1.00
Structural rating	Fair
Environmental rating	Good
Total rut depth (in)	0.70

For Cell 127/227 (overlay asphalt binder = Superpave PG 58-34) (LSSB M_R = 10,000 psi):

Design Inputs

Design Life: 40 years
Design Type: ACC_ACC

Existing construction: August, 2017
Pavement construction: September, 2018
Traffic opening: September, 2018

Climate Data 45.5, -93.75
Sources 45, -93.75
45.5, -93.125
45, -93.125
45.5, -94.375
45, -94.375

Design Structure

Layer type	Material Type	Thickness (in)
Flexible (OL)	Default asphalt concrete	4.0
Flexible (existing)	Default asphalt concrete	2.5
NonStabilized	A-1-a	6.0
NonStabilized	A-1-b	18.0
Subgrade	A-6	Semi-infinite

Volumetric at Construction:	
Effective binder content (%)	11.6
Air voids (%)	7.0

Traffic

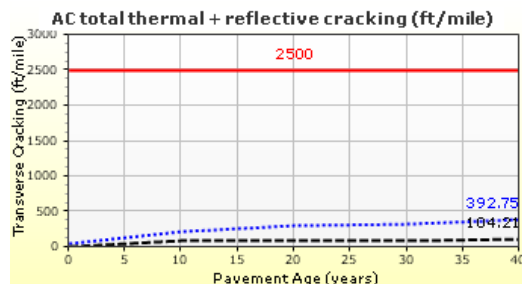
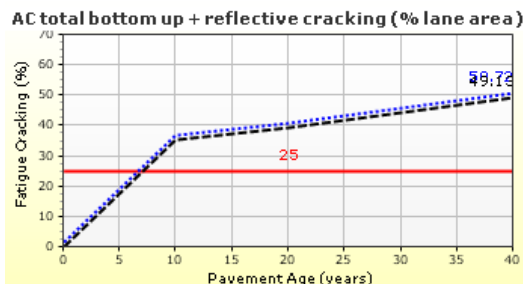
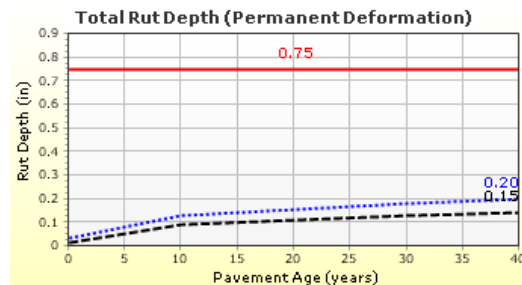
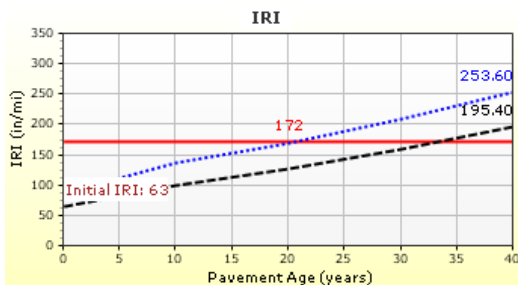
Age (year)	Heavy Trucks (cumulative)
2018 (initial)	1,000
2038 (20 years)	3,520,100
2058 (40 years)	8,683,820

Design Outputs

Distress Prediction Summary

Distress Type	Distress @ Specified Reliability		Reliability (%)		Criterion Satisfied?
	Target	Predicted	Target	Achieved	
Terminal IRI (in/mile)	172.00	253.65	90.00	30.33	Fail
Permanent deformation - total pavement (in)	0.75	0.20	90.00	100.00	Pass
AC total fatigue cracking: bottom up + reflective (% lane area)	25.00	50.72	90.00	0.00	Fail
AC total transverse cracking: thermal + reflective (ft/mile)	2500.00	392.75	90.00	100.00	Pass
Permanent deformation - AC only (in)	0.25	0.15	90.00	99.99	Pass
AC bottom-up fatigue cracking (% lane area)	25.00	0.00	50.00	100.00	Pass
AC thermal cracking (ft/mile)	1000.00	29.25	50.00	100.00	Pass
AC top-down fatigue cracking (ft/mile)	2000.00	13701.19	90.00	0.03	Fail

Distress Charts



— Threshold Value @ Specified Reliability --- @ 50% Reliability

HMA Rehabilitation (Input Level: 3)

Milled thickness (in)	1.00
Structural rating	Fair
Environmental rating	Good
Total rut depth (in)	0.70

For Cell 127/227 (overlay asphalt binder = Superpave PG 58-34) (LSSB M_R = 30,000 psi):

Design Inputs

Design Life: 40 years
Design Type: ACC_ACC

Existing construction: August, 2017
Pavement construction: September, 2018
Traffic opening: September, 2018

Climate Data 45.5, -93.75
Sources 45, -93.75
45.5, -93.125
45, -93.125
45.5, -94.375
45, -94.375

Design Structure

Layer type	Material Type	Thickness (in)
Flexible (OL)	Default asphalt concrete	4.0
Flexible (existing)	Default asphalt concrete	2.5
NonStabilized	A-1-a	6.0
NonStabilized	A-1-b	18.0
Subgrade	A-6	Semi-infinite

Volumetric at Construction:	
Effective binder content (%)	11.6
Air voids (%)	7.0

Traffic

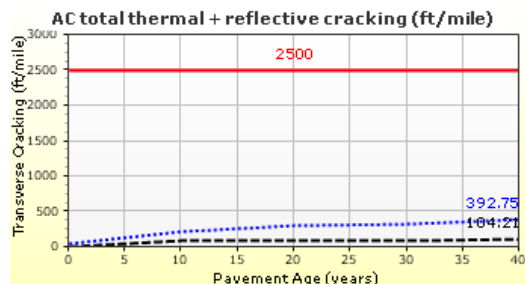
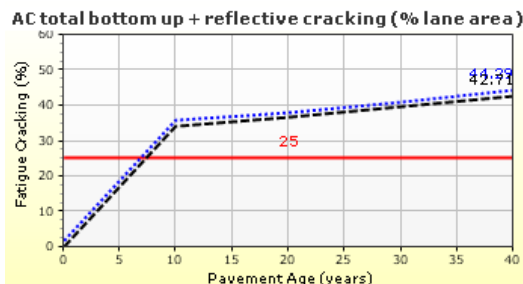
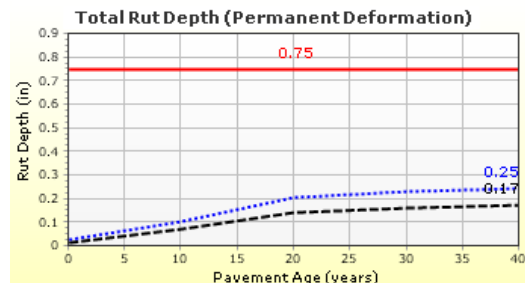
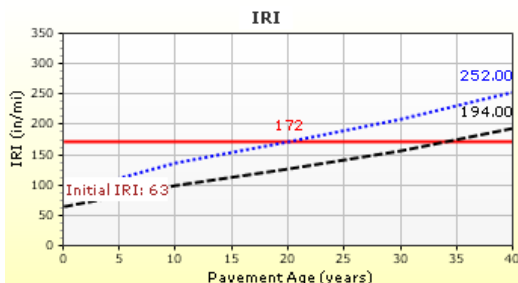
Age (year)	Heavy Trucks (cumulative)
2018 (initial)	1,000
2038 (20 years)	3,520,100
2058 (40 years)	8,683,820

Design Outputs

Distress Prediction Summary

Distress Type	Distress @ Specified Reliability		Reliability (%)		Criterion Satisfied?
	Target	Predicted	Target	Achieved	
Terminal IRI (in/mile)	172.00	251.95	90.00	31.30	Fail
Permanent deformation - total pavement (in)	0.75	0.25	90.00	100.00	Pass
AC total fatigue cracking: bottom up + reflective (% lane area)	25.00	44.29	90.00	0.00	Fail
AC total transverse cracking: thermal + reflective (ft/mile)	2500.00	392.75	90.00	100.00	Pass
Permanent deformation - AC only (in)	0.25	0.23	90.00	94.41	Pass
AC bottom-up fatigue cracking (% lane area)	25.00	0.00	50.00	100.00	Pass
AC thermal cracking (ft/mile)	1000.00	29.25	50.00	100.00	Pass
AC top-down fatigue cracking (ft/mile)	2000.00	13803.55	90.00	0.03	Fail

Distress Charts



— Threshold Value @ Specified Reliability --- @ 50% Reliability

HMA Rehabilitation (Input Level: 3)

Milled thickness (in)	1.00
Structural rating	Fair
Environmental rating	Good
Total rut depth (in)	0.70

For Cell 127/227 (overlay asphalt binder = Superpave PG 58-34) (LSSB M_R = 50,000 psi):

Design Inputs

Design Life: 40 years
Design Type: ACC_ACC

Existing construction: August, 2017
Pavement construction: September, 2018
Traffic opening: September, 2018

Climate Data 45.5, -93.75
Sources 45, -93.75
45.5, -93.125
45, -93.125
45.5, -94.375
45, -94.375

Design Structure

Layer type	Material Type	Thickness (in)
Flexible (OL)	Default asphalt concrete	4.0
Flexible (existing)	Default asphalt concrete	2.5
NonStabilized	A-1-a	6.0
NonStabilized	A-1-b	18.0
Subgrade	A-6	Semi-infinite

Volumetric at Construction:	
Effective binder content (%)	11.6
Air voids (%)	7.0

Traffic

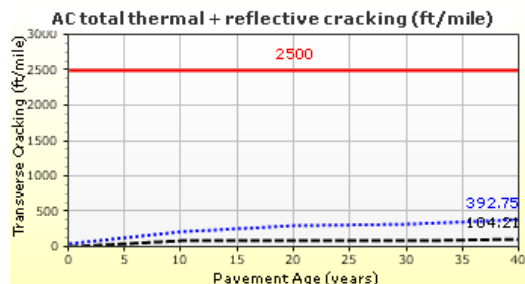
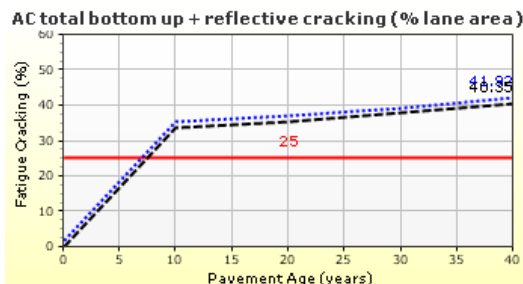
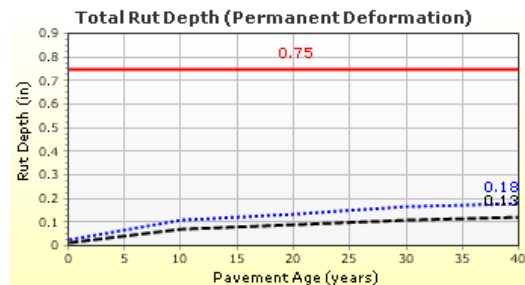
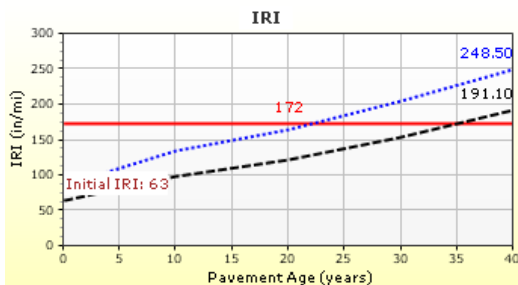
Age (year)	Heavy Trucks (cumulative)
2018 (initial)	1,000
2038 (20 years)	3,520,100
2058 (40 years)	8,683,820

Design Outputs

Distress Prediction Summary

Distress Type	Distress @ Specified Reliability		Reliability (%)		Criterion Satisfied?
	Target	Predicted	Target	Achieved	
Terminal IRI (in/mile)	172.00	248.52	90.00	33.49	Fail
Permanent deformation - total pavement (in)	0.75	0.18	90.00	100.00	Pass
AC total fatigue cracking: bottom up + reflective (% lane area)	25.00	41.92	90.00	0.00	Fail
AC total transverse cracking: thermal + reflective (ft/mile)	2500.00	392.75	90.00	100.00	Pass
Permanent deformation - AC only (in)	0.25	0.17	90.00	99.93	Pass
AC bottom-up fatigue cracking (% lane area)	25.00	0.00	50.00	100.00	Pass
AC thermal cracking (ft/mile)	1000.00	29.25	50.00	100.00	Pass
AC top-down fatigue cracking (ft/mile)	2000.00	13697.57	90.00	0.03	Fail

Distress Charts



— Threshold Value @ Specified Reliability --- @ 50% Reliability

HMA Rehabilitation (Input Level: 3)

Milled thickness (in)	1.00
Structural rating	Fair
Environmental rating	Good
Total rut depth (in)	0.70

For Cell 328/728 (overlay asphalt binder = Superpave PG 58-34) (LSSB M_R = 10,000 psi):

Design Inputs

Design Life: 40 years
Design Type: ACC_ACC

Existing construction: August, 2017
Pavement construction: September, 2018
Traffic opening: September, 2018

Climate Data 45.5, -93.75
Sources 45, -93.75
45.5, -93.125
45, -93.125
45.5, -94.375
45, -94.375

Design Structure

Layer type	Material Type	Thickness (in)
Flexible (OL)	Default asphalt concrete	4.0
Flexible (existing)	Default asphalt concrete	2.5
NonStabilized	A-1-a	6.0
NonStabilized	A-1-b	9.0
Subgrade	A-6	Semi-infinite

Volumetric at Construction:	
Effective binder content (%)	11.6
Air voids (%)	7.0

Traffic

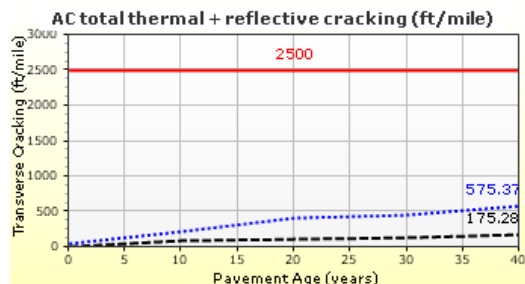
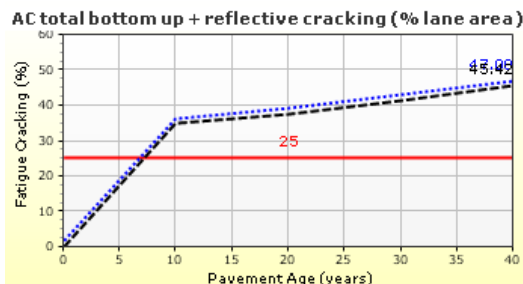
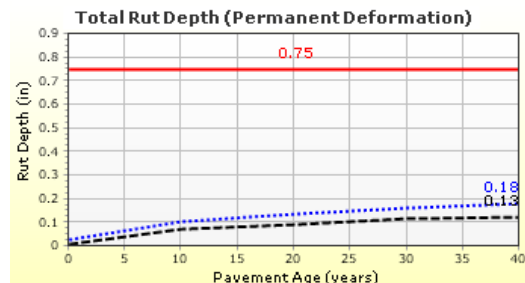
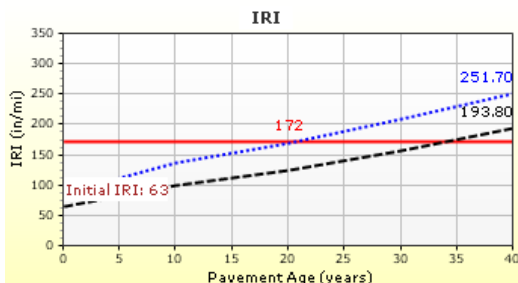
Age (year)	Heavy Trucks (cumulative)
2018 (initial)	1,000
2038 (20 years)	3,520,100
2058 (40 years)	8,683,820

Design Outputs

Distress Prediction Summary

Distress Type	Distress @ Specified Reliability		Reliability (%)		Criterion Satisfied?
	Target	Predicted	Target	Achieved	
Terminal IRI (in/mile)	172.00	251.71	90.00	31.52	Fail
Permanent deformation - total pavement (in)	0.75	0.18	90.00	100.00	Pass
AC total fatigue cracking: bottom up + reflective (% lane area)	25.00	47.00	90.00	0.00	Fail
AC total transverse cracking: thermal + reflective (ft/mile)	2500.00	575.37	90.00	100.00	Pass
Permanent deformation - AC only (in)	0.25	0.15	90.00	99.99	Pass
AC bottom-up fatigue cracking (% lane area)	25.00	0.00	50.00	100.00	Pass
AC thermal cracking (ft/mile)	1000.00	100.32	50.00	100.00	Pass
AC top-down fatigue cracking (ft/mile)	2000.00	13701.82	90.00	0.03	Fail

Distress Charts



— Threshold Value @ Specified Reliability --- @ 50% Reliability

HMA Rehabilitation (Input Level: 3)

Milled thickness (in)	1.00
Structural rating	Fair
Environmental rating	Good
Total rut depth (in)	0.70

For Cell 328/728 (overlay asphalt binder = Superpave PG 58-34) (LSSB M_R = 30,000 psi):

Design Inputs

Design Life: 40 years
Design Type: ACC_ACC

Existing construction: August, 2017
Pavement construction: September, 2018
Traffic opening: September, 2018

Climate Data 45.5, -93.75
Sources 45, -93.75
45.5, -93.125
45, -93.125
45.5, -94.375
45, -94.375

Design Structure

Layer type	Material Type	Thickness (in)
Flexible (OL)	Default asphalt concrete	4.0
Flexible (existing)	Default asphalt concrete	2.5
NonStabilized	A-1-a	6.0
NonStabilized	A-1-b	9.0
Subgrade	A-6	Semi-infinite

Volumetric at Construction:	
Effective binder content (%)	11.6
Air voids (%)	7.0

Traffic

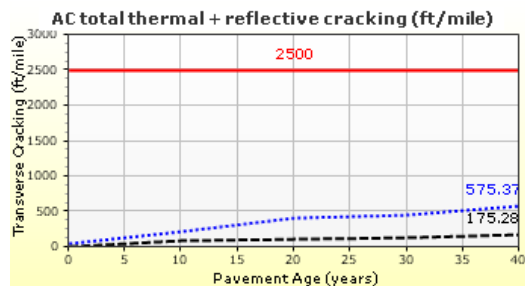
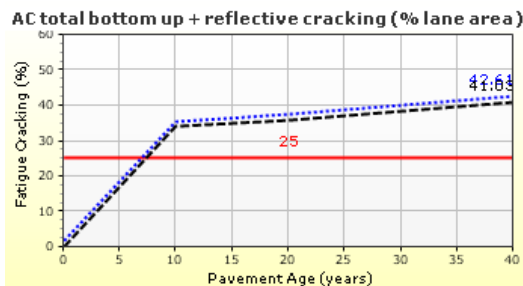
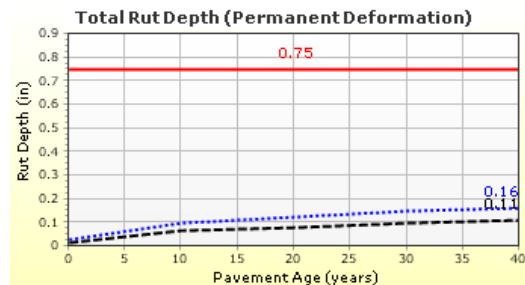
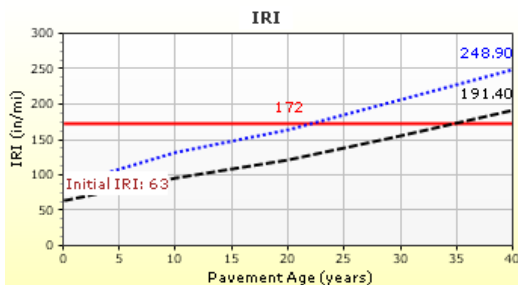
Age (year)	Heavy Trucks (cumulative)
2018 (initial)	1,000
2038 (20 years)	3,520,100
2058 (40 years)	8,683,820

Design Outputs

Distress Prediction Summary

Distress Type	Distress @ Specified Reliability		Reliability (%)		Criterion Satisfied?
	Target	Predicted	Target	Achieved	
Terminal IRI (in/mile)	172.00	248.89	90.00	33.29	Fail
Permanent deformation - total pavement (in)	0.75	0.16	90.00	100.00	Pass
AC total fatigue cracking: bottom up + reflective (% lane area)	25.00	42.61	90.00	0.00	Fail
AC total transverse cracking: thermal + reflective (ft/mile)	2500.00	575.37	90.00	100.00	Pass
Permanent deformation - AC only (in)	0.25	0.16	90.00	99.97	Pass
AC bottom-up fatigue cracking (% lane area)	25.00	0.00	50.00	100.00	Pass
AC thermal cracking (ft/mile)	1000.00	100.32	50.00	100.00	Pass
AC top-down fatigue cracking (ft/mile)	2000.00	13803.87	90.00	0.03	Fail

Distress Charts



— Threshold Value @ Specified Reliability --- @ 50% Reliability

HMA Rehabilitation (Input Level: 3)

Milled thickness (in)	1.00
Structural rating	Fair
Environmental rating	Good
Total rut depth (in)	0.70

For Cell 328/728 (overlay asphalt binder = Superpave PG 58-34) (LSSB M_R = 50,000 psi):

Design Inputs

Design Life: 40 years
Design Type: ACC_ACC

Existing construction: August, 2017
Pavement construction: September, 2018
Traffic opening: September, 2018

Climate Data 45.5, -93.75
Sources 45, -93.75
45.5, -93.125
45, -93.125
45.5, -94.375
45, -94.375

Design Structure

Layer type	Material Type	Thickness (in)
Flexible (OL)	Default asphalt concrete	4.0
Flexible (existing)	Default asphalt concrete	2.5
NonStabilized	A-1-a	6.0
NonStabilized	A-1-b	9.0
Subgrade	A-6	Semi-infinite

Volumetric at Construction:	
Effective binder content (%)	11.6
Air voids (%)	7.0

Traffic

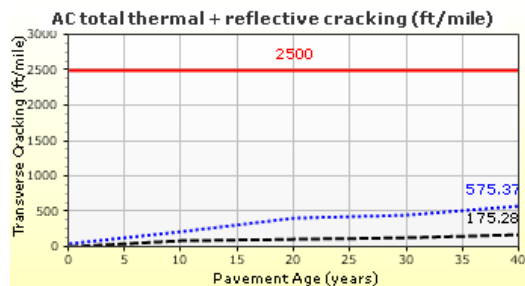
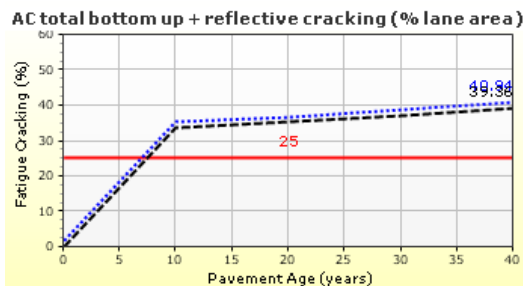
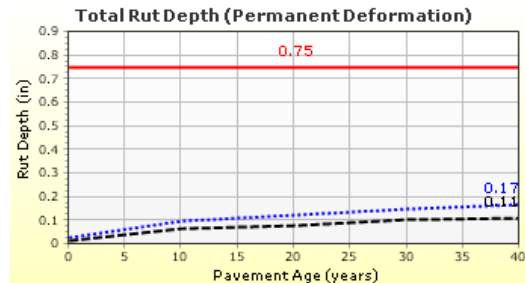
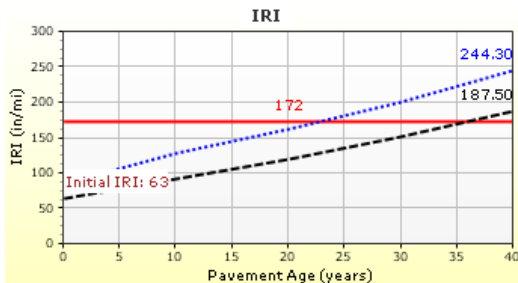
Age (year)	Heavy Trucks (cumulative)
2018 (initial)	1,000
2038 (20 years)	3,520,100
2058 (40 years)	8,683,820

Design Outputs

Distress Prediction Summary

Distress Type	Distress @ Specified Reliability		Reliability (%)		Criterion Satisfied?
	Target	Predicted	Target	Achieved	
Terminal IRI (in/mile)	172.00	244.29	90.00	36.37	Fail
Permanent deformation - total pavement (in)	0.75	0.17	90.00	100.00	Pass
AC total fatigue cracking: bottom up + reflective (% lane area)	25.00	40.94	90.00	0.00	Fail
AC total transverse cracking: thermal + reflective (ft/mile)	2500.00	575.37	90.00	100.00	Pass
Permanent deformation - AC only (in)	0.25	0.16	90.00	99.95	Pass
AC bottom-up fatigue cracking (% lane area)	25.00	0.00	50.00	100.00	Pass
AC thermal cracking (ft/mile)	1000.00	100.32	50.00	100.00	Pass
AC top-down fatigue cracking (ft/mile)	2000.00	8559.50	90.00	7.63	Fail

Distress Charts



— Threshold Value @ Specified Reliability --- @ 50% Reliability

HMA Rehabilitation (Input Level: 3)

Milled thickness (in)	1.00
Structural rating	Fair
Environmental rating	Good
Total rut depth (in)	0.70